UNIVERSIDAD COMPLUTENSE DE MADRID

FACULTAD DE CIENCIAS FÍSICAS

Departamento de Física de la Tierra, Astronomía y Astrofísica I (Geofísica y Meteorología) (Astronomía y Geodesia)

TESIS DOCTORAL

Tropical Atlantic influence on the Pacific: air-sea interactions and modulations

(Influencia del Atlántico tropical sobre el Pacífico: interacciones aire-océano y modulaciones)

MEMORIA PARA OPTAR AL GRADO DE DOCTOR

PRESENTADA POR

Marta Martín del Rey

Directoras

Belén Rodríguez de Fonseca
Irene Polo Sánchez

Madrid, 2015

UNIVERSIDAD COMPLUTENSE DE MADRID

FACULTAD DE CIENCIAS FÍSICAS

Departamento de Física de la Tierra, Astronomía y Astrofísica I (Geofísica y Meteorología) (Astronomía y Geodesia)

TROPICAL ATLANTIC INFLUENCE ON THE PACIFIC: AIR-SEA INTERACTIONS AND MODULATIONS

(INFLUENCIA DEL ATLÁNTICO TROPICAL SOBRE EL PACÍFICO: INTERACCIONES AIRE-OCÉANO Y MODULACIONES)

MEMORIA PARA OPTAR AL GRADO DE DOCTOR PRESENTADA POR

Marta Martín del Rey

Bajo la dirección de los doctores

Belén Rodríguez de Fonseca

Irene Polo Sánchez

Madrid, 2015

Universidad Complutense de Madrid

Facultad de Ciencias Físicas

Departamento de Física de la Tierra, Astronomía y Astrofísica I

TROPICAL ATLANTIC INFLUENCE ON THE PACIFIC: AIR-SEA INTERACTIONS AND MODULATIONS

(INFLUENCIA DEL ATLÁNTICO TROPICAL
SOBRE EL PACÍFICO:
INTERACCIONES AIRE-OCÉANO Y MODULACIONES)

Memoria para optar al grado de Doctor presentada por:

Marta Martín del Rey

Bajo la dirección de los doctores

Belén Rodríguez de Fonseca

Irene Polo Sánchez

Madrid, 2015

A mis padres, por dedicar su vida entera
a crear luz en cualquier oscuridad

Esta tesis ha sido financiada por los proyectos nacionales CGL2009-10285, CGL2011-13564-E and *CGL2012-38923-C02-01*, y también por el proyecto europeo *PREFACE, ref*.603521.

This thesis has been funded by the national projects CGL2009-10285, CGL2011-13564-E and *CGL2012-38923-C02-01*, and also by the European project *PREFACE, ref*.603521.

Agradecimientos

Soy lo que soy por nacer donde he nacido…

En primer lugar, como no podría ser de otro modo, me gustaría dar las gracias a mis padres, sin los cuales yo no estaría aquí.

Papá, Mamá … Gracias por la educación que me habéis dado, por ser mi referente, por inculcarme que nada es imposible y que puedo conseguir todo lo que me proponga. Gracias por apoyarme siempre en todas mis decisiones, las cuales me han llevado a convertirme en la mujer que hoy soy.

Gracias a mis hermanos …

A Ángel, por cuidarme y aconsejarme siempre, por ser mi ejemplo a seguir… por enseñarme que uno debe trabajar en aquello que le haga feliz.

A Raquel, por estar siempre ahí para mí, en los buenos y en los malos momentos. Gracias por escucharme, quererme y comprenderme … por nuestros ataques de risa entre vino y vino … porque estos últimos cinco años no habrían sido igual sin ti.

A María, por crecer siempre junto a mí, por entendernos con mirarnos, porque a pesar de la distancia siempre estamos cerca … por ser la otra mitad de mí.

A mi cuñada Yaiza, por quererme y apoyarme en todo momento, por ser en definitiva otra hermana más.

A mi cuñado Fran, por ofrecerme siempre su cariño y alegría contagiosa.

A mis cuquis, mis sobrinos Miguel y Nicolás. A Miguel, por su bondad y su nobleza, por mostrarme que con una sonrisa se puede iluminar el día más oscuro. A Nicolás, por ser un luchador y no rendirse nunca … por marcar mi sistema de referencia y recordarme que los imposible no existen.

La vida son instantes que se cruzan en el tiempo…

En segundo lugar, me gustaría dar las gracias a mis directoras de tesis Belén e Irene…

Belén, tengo grabado en mi mente la primera vez que te vi, sentada en tu despacho explicándome a toda velocidad el reciente descubrimiento que habíais hecho en el grupo TROPA y sobre el que trataría mi trabajo de máster: la conexión Atlántico-Pacífico. No sabía yo entonces, que aquel momento marcaría el punto de partida de estos últimos cinco años…

Gracias por poner todo tu conocimiento y tu tiempo a mi disposición, sin condiciones, sin límite… por entregarte en cuerpo y alma siempre y en cada momento, por transmitir el entusiasmo que solo alguien que ama su trabajo es capaz de hacer. Gente como tú es la que hace que las cosas funcionen y que el mundo siga girando. No creo que en estas líneas pueda agradecerte lo suficiente todo lo que has hecho (y sigues haciendo) por mí en estos años.

Irene, nos "conocimos" en la distancia y ella ha marcado nuestra relación durante estos años. Sin embargo, siempre has estado ahí para mí, desde Madrid o desde Reading. Gracias por nuestros chats, nuestros skypes… por descubrirme el maravilloso mundo del océano, por tener siempre unas palabras de ánimo en los momentos bajos, por tu paciencia y tu serenidad… Gracias por darme lo mejor de ti.

Belén, Irene… gracias por convertirme en la investigadora que hoy soy… o comienzo a ser. Habéis sido y sois el espejo en el que me miro. Pero, sobre todo, por encima de la investigación, están siempre las personas … GRACIAS por ser mucho más que mis directoras de tesis.

I would thank Alban Lazar to give me the opportunity to know the "NEMO world" ;-). Thank you for our fruitful conversations and discussions about oceanography… I hope to continue learning from you.

I would also thank Fred Kucharski to provide me the partially-coupled simulations used in this thesis and for our scientific discussions.

Me gustaría dar las gracias de manera especial a Jean-Marc Molines, por su paciencia, su ayuda incondicional y su apoyo. Gracias por poner todo tu conocimiento sobre el modelo NEMO a mi disposición, por hacerme fácil lo difícil…. Mil gracias.

La vida crece entre los matices…

En tercer lugar, me gustaría dar las gracias a las personas que han creado los matices de mi vida en estos cinco años.

Gracias a Elsa y Teresa por su ayuda en todo momento, por todas nuestras charlas, cafés y congresos… pero sobre todo, gracias por dejarme aprender de vosotras.

No puedo olvidarme de mis compañeros de laboratorio. Gracias a MIS CHICOS: Roberto, Julián, Jorge, Iñigo, Cahlo, Mariano y Jesús. Gracias por las risas compartidas, los momentos de agobio, los congresos, las comidas, los cafés … por aguantar mis órdenes siempre con la mejor de vuestras sonrisas y por crear el mejor ambiente de trabajo que se puede desear.

Gracias también a Ibrahima, Coumba, Ade, Cristina y Antonio, por formar parte de la familia UCM. No me olvido de los que han pasado por el laboratorio de Meteorología y de Geofísica y ya no están: Álvaro, Marta, Javi García, Javi Blanco, Sara, Juan y Javi Pavón. Muchas gracias por todos los momentos compartidos.

En especial, gracias a Blanca… porque empezaste siendo mi compañera de mesa pero unos cuantos daikiris de fresa nos llevaron irremediablemente a convertirnos en amigas. Gracias por ser mi confidente, mi consejera, por estar siempre ahí para mí, por coger aviones y plantarte donde haga falta, y sobre todo gracias por darme un abrazo siempre que lo he necesitado,… a pesar de lo que te cuesta… ;-P

Gracias a Fátima y Maurizio por escucharme, aguantar mis risas, mis lloros, mis agobios y mis enfados. Por su comprensión y sus consejos… por recordarme *Por qué he hecho lo que he hecho …* No puedo imaginarme estos últimos cinco años sin nuestros cafés…

Gracias a María y a Marta Domínguez, por compartir cafés y desayunos. Por estar siempre ahí para mí, por escucharme y aconsejarme con la mejor de sus sonrisas.

Gracias a todos los profesores del departamento y en especial a Carlos Yagüe por su ayuda y apoyo incondicionales. Gracias a Encarna, Ana, Luis Dinis y Luis Durán, por los momentos compartidos estos años.

Gracias a Salva y a Lucía por hacer más llevaderos los problemas informáticos y burocráticos… y por formar parte de mi familia de la UCM.

Gracias a Miriam y Diana, por llevar conmigo más de 12 años, por crecer juntas…por seguir compartiendo nuestros buenos y malos momentos desde donde quiera que nos encontremos.

Gracias a mis amigos de Madrid: Inés, Silvia, Marga, Gus y Gema y a mis amigos de Salamanca: Inesita, Ana, Alberto, Bea, Juan, Ana, Oscar, Carlos, Chuchi, Manuel, JuanCar… por seguir estando ahí.

Gracias a mis Parisinas: Cande, Noe, Isa y Raque… por ser mucho más que mi minipandi, por haberos convertido en mi familia.

A todas las personas que he nombrado y a las que no, a todos aquellos que de manera directa o indirecta han formado parte de mi camino en estos 5 años, todos sois un poco autores de esta tesis…

...GRACIAS DE CORAZÓN.

EXTENDED SUMMARY

1. INTRODUCTION

The Tropics confine regions that are determinant for the global climate, thus they receive a great amount of solar radiation, becoming storages of heat. This heat is released as energy within the ocean and to the atmosphere, originating oceanic and atmospheric circulations, which regulate the global climate.

In mean, over the tropical regions surface easterly winds converge in a thin band of convective systems named as Inter-Tropical Convergence Zone (ITCZ). As a consequence of the action of these winds, the warm waters are piled up in the western boundary, whilst the cooler waters from the bottom up-well in the eastern side. A Sea Surface Temperature (SST) gradient is established generating a zonal atmospheric circulation in the equator, the Walker Circulation. In the ocean, a see-saw of the thermocline, which is the zone in which the maximum vertical gradient of temperature takes place, is established at the equatorial band. Climate variability comprises the deviations respect to the mean of the variables that describe the behaviour of the components of the climate system. There are two phenomena controlling the tropical climate variability at inter-annual time-scales: El Niño-Southern Oscillation (ENSO) in the Pacific Ocean and the Atlantic Niño in the Atlantic Ocean.

El Niño-Southern Oscillation (ENSO) is a coupled phenomenon of inter-annual variability over the tropical Pacific [*Philander*, 1990], characterized by a warming (cooling) of the central-eastern equatorial Pacific. ENSO occurs during boreal winter and presents a periodicity between 2 and 7 years [*Trenberth*, 1997; *Federov and Philander*, 2000; *Wang and An*, 2002]. Changes in the associated SSTs are linked to anomalous Sea Level Pressure (SLP). For a warm event, the SLP pattern presents negative values in the warmer region of the tropical Pacific, and positive values in the western side. The originated dipolar SLP pattern is named as the Southern Oscillation (SO, *Walker* [1924]). For an ENSO event, anomalous westerly winds blow in the western equatorial Pacific piling up warm waters in the central-east of the basin, deepening the thermocline there. This anomalous heating enhances the convection, establishing a Walker anomalous cell

with descendant motions over Indonesia. At surface layers, this circulation influences the anomalous initial winds in a positive Bjerknes feedback that maintains the positive SST anomalies (Figure S1 left, *Bjerknes* [1969]).

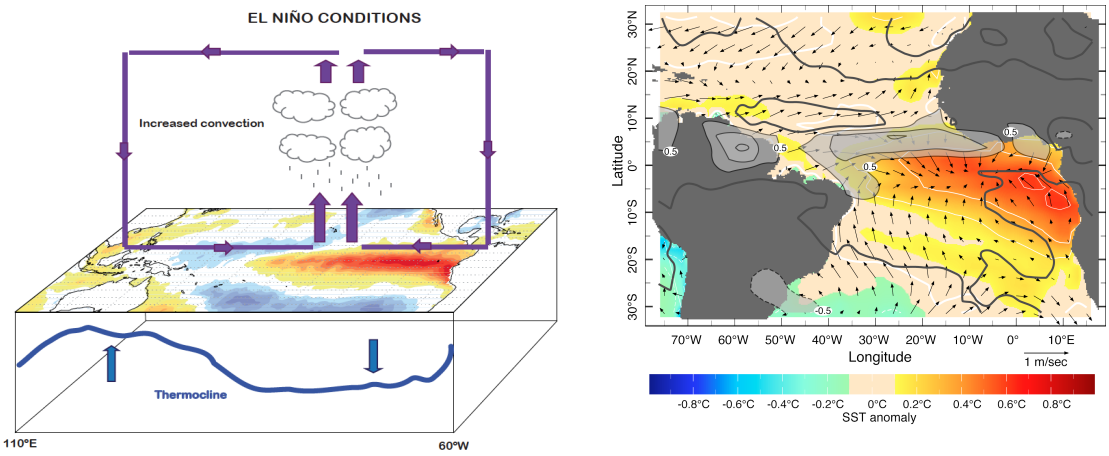

Figure S1. ENSO (left) and Atlantic Niño phenomenon (right, From *Kushnir et al.* [2003]).

ENSO is able to modulate the climate of the adjacent and remote areas through the so-called atmospheric teleconnections [*Klein et al.*, 1999; *Alexander et al.*, 2002]. Two of the most relevant theories explaining ENSO are the "delayed oscillator" [*McCreary*, 1983; *Battisti*, 1988; *Suarez and Schopf*, 1988] and the "recharge oscillator" [*Jin*, 1997], both highlighting the thermocline feedbacks in the growth of the SST anomalies. Other studies, however, have concluded that both, thermocline and zonal advective feedbacks contributing to ENSO development [*Jin and An*, 1999; *An and Jin*, 2001].

A coupled air-sea inter-annual mode of variability akin to ENSO, takes place in the tropical Atlantic, named as Atlantic Niño [*Merle*, 1980; *Zebiak*, 1993]. The Atlantic Niño is characterized by a weakening of the trade winds in the western equatorial Atlantic, associated with an anomalous warming at the eastern side of the basin (Figure S1, right). The Atlantic Niño peaks during boreal summer with a period of 2-4 years [*Latif and Grötzner*, 2000; *Ruiz-Barradas et al.*, 2000; *Kushnir et al.*, 2003]. This phenomenon impacts on climate of the adjacent and remote regions [*Ward*, 1998; *Cassou et al.*, 2005; *García-Serrano et al.*, 2008; *Kucharski et al.*, 2008; *Polo et al.*, 2008a; *Joly*

and Voldoire, 2010; *Mohino et al.*, 2011; *Rodríguez-Fonseca et al.*, 2011]. Recent studies have found a relation between the Atlantic Niño and ENSO phenomenon [*Keenlyside and Latif*, 2007; *Polo et al.*, 2008a; *Rodríguez-Fonseca et al.*, 2009; *Ding et al.*, 2012]. This finding is the principal motivation of the present Thesis (Figure S2). The above-mentioned authors put forward how, from the 1970s, the Atlantic Niño (Niña) seems to favour the development of La Niña (Niño) during the following winter [*Rodríguez-Fonseca et al.*, 2009; *Ding et al.*, 2012].

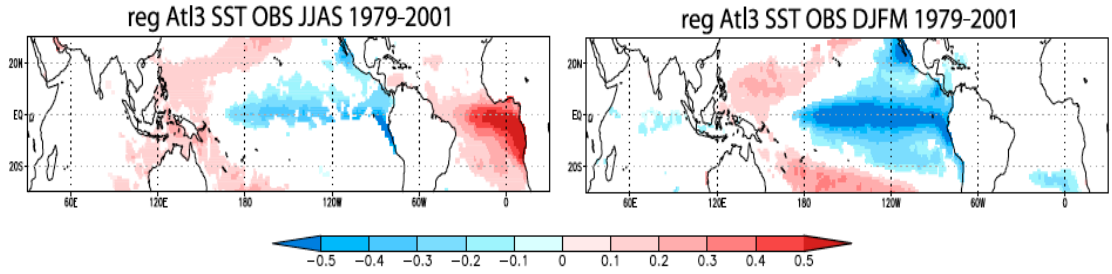

Figure S2. Connection between the Atlantic Niño and the Pacific Niña after the 1970s (from *Rodríguez-Fonseca et al.* [2009]). Regression of anomalous summer (JJAS, left) and winter (DJFM, right) SST anomalies over the summer (JJAS) Atl3 index for the period 1979-2001.

Nevertheless, there are still some open questions that need to be clarified. It is necessary to study how is the influence of tropical Atlantic SST onto ENSO and which are the processes involved in its development. A characterization of the Atlantic Niños that are able to impact on ENSO is required, together with the understanding of the air-sea interactions associated with the generation of those events. Finally, it is a must to address why the connection between these phenomena is only observed in the last decades of the XX century.

2. OBJECTIVES

- ***Objective 1***: To understand the contribution of the inter-annual variability of the tropical Atlantic on ENSO.

- ***Objective 2***: To study the stationarity of the Atlantic-Pacific connection, together with its possible multidecadal modulation.

- ***Objective 3***: To evaluate the predictive character of ENSO from tropical Atlantic SSTs.

- ***Objective 4***: To characterize the Atlantic Niño involved in the Atlantic-Pacific connection and compare with the canonical mode.

- ***Objective 5***: To study the air-sea interactions involved in the development of the different Atlantic Niños.

3. DATA & METHODS

3.1 Observations and Reanalysis

The present study uses data from observations and reanalysis. SST comes from HadISST [*Rayner et al.*, 2003] and also SST, thermocline depth, and wind-stress are taken from SODA reanalysis [*Giese and Ray*, 2011]. Atmospheric variables such as surface wind, 200 hPa and 925 hPa velocity potential and surface pressure from the 20th Century Reanalysis [*Compo et al.*, 2011]. Sea Level Pressure (SLP) from ERA-40 reanalysis [*Uppala et al.*, 2005] have been also used.

3.2 Coupled simulations

Partially coupled simulations have been used in the present study. On the one hand, **SPEEDY-RGO** considers SPEEDY global atmospheric circulation model [*Molteni*, 2003; *Kucharski et al.*, 2006b], with a T30 horizontal resolution and 8 levels in the vertical; coupled to a 1.5 reduced-gravity model [*Chang*, 1994] with an horizontal resolution of 2°x1°. Two experimental designs have been used. *SimAtlVar* [*Rodríguez-Fonseca et al.*, 2009], which is a simulation that considers the observed SSTs along the 20th century in the Atlantic and climatological SSTs elsewhere, except for the Indo-Pacific region, in which the atmosphere is coupled to the ocean. This experiment isolates the Atlantic influence on the tropical Pacific variability. Two simulations have been analysed, one for the period 1949-2002 and another for the period 1871 to 2002. The results from the simulations have been compared with a control simulation (*SimAtlCli*) in which climatological SSTs are prescribed in all the basins except for the Indo-Pacific region, in which the atmosphere is coupled to the ocean. Additionally, **SPEEDY-NEMO** partially coupled simulation has been also used, which considers the same SPEEDY atmospheric model but coupled to ocean NEMO model [*Madec et al.*, 1998]. This simulation covers the period

1945-2015 and presents the same experimental design than SPEEDY-RGO (*SimAtlVar*).

3.3 Ocean simulations

Finally, an OGCM simulation has been performed with the NEMO model in its tropical Atlantic configuration, NEMO-INTER simulation (http://forge.ipsl.jussieu.fr/nemo-atltrop). This model has a horizontal resolution of 0.25°x0.25° and 46 levels. NEMO is forced by inter-annual winds for the period 1960-2011.

3.4. Methods

Discriminant analysis techniques have been applied to study the tropical Atlantic and Pacific variability. Principal Component Analysis (PCA) and Maximum Covariance Analysis (MCA) are techniques to decompose an anomalous field into a number of modes, which maximize the covariance of the original field [*von Storch and Zwiers*, 2001; *Wilks,* 2005]. In the present work, the MCA technique has been adapted for the study of the Atlantic-Pacific connection considering only one predictor field and a set of different atmospheric and oceanic fields to be predicted. These predictand fields correspond to different variables at different seasons, being those involved in the mechanism that connect Atlantic and Pacific Niños [*Martín-Rey et al.*, 2014; *Polo et al.*, 2015a]. Inter-annual filters have been applied to the seasonal anomalies [*Butterworth*, 1930; *Stephenson et al.*, 2000] and the statistical significance of the results has been assessed using parametric (t-test, F-test) and also non-parametric tests (Monte Carlo test).

4. RESULTS AND CONCLUSIONS

4.1 Study of the influence of the Inter-annual Tropical Atlantic variability on ENSO after the 1970s [*Martín-Rey et al.*, 2012].

From *SimAtlVar* simulation, inter-annual modes of tropical Pacific SST variability before and after the 1970s have been studied and compared. It has been found how ENSO before 1970s are characterized by anomalous SSTs in the central-eastern of the tropical Pacific basin without significant changes in wind-stress and thermocline depth. These phenomena are not related with the SST anomalies in the equatorial Atlantic during the

previous summer and are similar to the internally generated ENSO. However, after the 1970s, simulated ENSO are characterized by an anomalous convergence (divergence) of the wind stress in the central Pacific during boreal summer, which generates SST and thermocline depth anomalies in the Tropical Pacific during winter months. These ENSO events, which development is associated with dynamical mechanisms, are strongly related with SST anomalies in the equatorial Atlantic during the previous summer.

4.2 Analysis of the oceanic processes associated with the development of ENSO induced by the equatorial Atlantic [*Polo et al.*, 2015a]

The atmospheric and oceanic processes associated with the Atlantic-Pacific connection have been studied from observations, reanalysis and *SimAtlVar* simulation. The results are focused on the oceanic processes that were lacking in *Rodríguez-Fonseca et al.* [2009]. When an Atlantic Niño occurs in the boreal summer, there is an enhancement of the convection over the equatorial Atlantic, which alters the Walker circulation generating an anomalous subsidence over the central Pacific. Surface wind divergence causes the thermocline to rise and the perturbation travels eastward as a Kelvin wave. As the wave propagates, the thermocline gets shallower, favouring the surface cooling. This cooling is due to temperature advection of anomalous stratification by mean vertical velocity and anomalous zonal currents under mean temperature gradient. An analogous mechanism, but with the corresponding change in sign, would take place for an Atlantic Niña.

4.3 Study of the non-stationarity of the Atlantic-Pacific connection and possible multi-decadal modulations [*Martín-Rey et al.*, 2014]

The Atlantic-Pacific connection appears as a coupled mode of the inter-annual tropical variability during the first decades of the XX century and from the 1970s. This mode involves all the atmospheric and oceanic variables related to the mechanism associated with the impact of the Atlantic Niño over the Pacific Niña (and vice versa). The periods in which the Atlantic-Pacific mode takes place coincide with negative phases of the Atlantic Multi-decadal Oscillation (AMO, *Knight et al.* [2006]). The AMO could be modulating this inter-basin connection at multi-decadal scales

through changes in the convection over the equatorial Atlantic and modifying the eastern equatorial Pacific variability.

4.4 Prediction of ENSO from equatorial Atlantic SSTs [*Martín-Rey et al.*, 2015a]

Taking into account the non-stationarity of the Atlantic-Pacific connection, a statistical prediction of boreal winter ENSO has been performed using anomalous SSTs in the tropical Atlantic during the previous summer as a predictor. The statistical hindcast model is based on the results of *Martín-Rey et al.* [2014] and is able to predict the principal variables associated with the Atlantic-forced ENSO events: SST, thermocline depth and surface winds. A good prediction is obtained for those periods in which the Atlantic-Pacific connection takes place, i.e. during the first and last decades of the XX century. This result entails that ENSO can be better predicted with the information of the Atlantic only during certain periods.

4.5 Characterization of the Atlantic Niños associated with ENSO [*Martin-Rey et al.*, 2015b]

The leading modes of the tropical Atlantic SST inter-annual variability during the boreal summer have been characterized in the periods in which the Atlantic-Pacific connection takes place. Two modes of variability emerge associated with an anomalous heating in the equatorial Atlantic. The first one is characterized by a warming (cooling) of the entire basin and is related to the next winter ENSO phenomena. It is preceded by a weakening of both subtropical High Pressure systems (Santa Helena and Azores) during the previous autumn and winter. This pressure weakening generates a reduction of the trade winds north and south of the tropical Atlantic, warming the underneath regions through turbulent heat fluxes. In the equatorial band, these surface pressure anomalies originate an anomalous wind convergence, which induces a convergence of the oceanic currents and a deepening of the thermocline, heating the equatorial region by vertical processes. The second mode of variability is characterized by an anomalous warming of the eastern equatorial Atlantic, surrounded by negative SST anomalies north and south of the equatorial Atlantic. This mode is preceded by an anomalous east-west surface pressure gradient, which give rises to anomalous westerly winds and a convergence of

currents that warms the equatorial region by vertical processes. This Atlantic Niño is unrelated to ENSO phenomena during next winter.

RESUMEN EXTENSO

1. INTRODUCCIÓN

Las regiones tropicales son de gran importancia para el clima global puesto que reciben una gran cantidad de radiación solar, convirtiéndose en depósitos de calor. La liberación de este calor en forma de energía dentro del propio océano y hacia la atmósfera origina circulaciones oceánicas y atmosféricas que regulan el clima global.

Climatológicamente, sobre las regiones tropicales aparecen unos vientos del este, denominados vientos alíseos, que convergen en una zona de convección profunda denominada Zona de Convergencia Intertropical (ITCZ). Como consecuencia de la acción de estos vientos, las aguas cálidas se acumulan en la parte occidental de las cuencas, mientras que las aguas frías procedentes del océano profundo emergen en la parte oriental. Se establece un gradiente de Temperatura de la Superficie del Mar (SST) que da lugar a la aparición de una circulación atmosférica zonal en el ecuador, la circulación de Walker. En el océano, aparece un dipolo este-oeste en la profundidad de la termoclina (que es la región donde se encuentra el mayor gradiente vertical de temperatura) a lo largo de la banda ecuatorial.

La variabilidad climática comprende el estudio de las desviaciones respecto de la media de las variables que describe los componentes del sistema climático. Existen dos fenómenos que controlan la variabilidad climática tropical a escalas interanuales: El Niño y la Oscilación del Sur (ENSO) en el océano Pacífico y el Niño Atlántico en el Atlántico tropical.

El Nino y la Oscilación del Sur (ENSO) es un fenómeno acoplado de variabilidad interanual del Pacífico tropical [*Philander*, 1990], caracterizado por un calentamiento (enfriamiento) del centro-este del Pacífico ecuatorial. El ENSO tiene lugar durante el invierno boreal y su periodo oscila entre 2 y 7 años [*Trenberth*, 1997; *Federov and Philander*, 2000; *Wang and An*, 2002]. Los cambios en la SST están relacionados con anomalías de la presión en superficie (SLP). Para un

evento cálido, la SLP presenta valores negativos sobre el calentamiento del este del Pacífico tropical, y anomalías positivas la parte occidental. El gradiente de SLP originado recibe el nombre de Oscilación del Sur (SO; *Walker* [1924]). Durante un ENSO, los vientos anómalos del oeste soplan en la parte occidental del Pacífico ecuatorial, apilando las aguas cálidas en el centro-este de la cuenca, profundizando la termoclina en dicha región. El calentamiento anómalo aumenta la convección, estableciéndose la circulación anómala de Walker con descensos sobre Indonesia. En superficie, esta circulación refuerza los vientos iniciales a través del mecanismo de realimentación positiva de Bjerknes (Figura S1 left, *Bjerknes* [1969]).

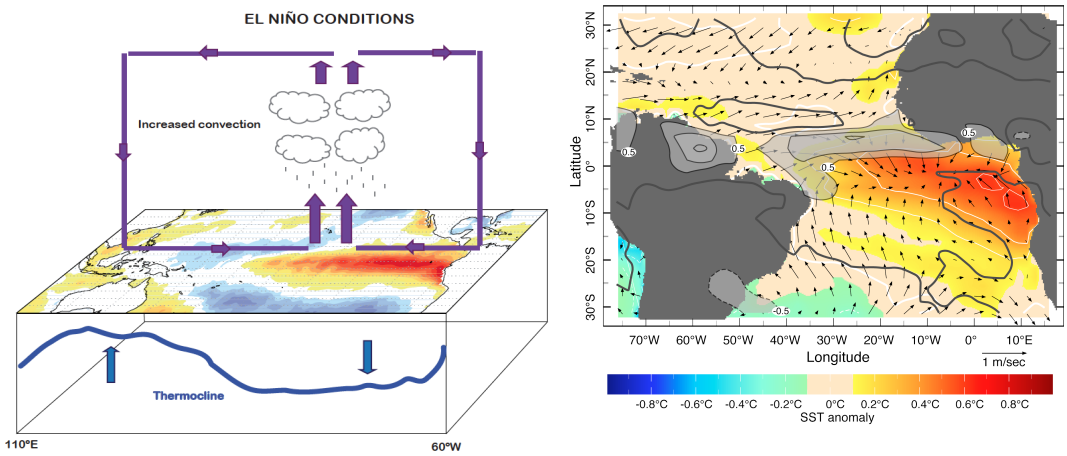

Figura S1. Los fenómenos ENSO (izquierda) y Niño Atlantico (derecha, procedente de *Kushnir et al.* [2003]).

El ENSO es capaz de modular el clima de las regiones adyacentes y también de áreas remotas, mediante las denominadas teleconexiones atmosféricas [*Klein et al.*, 1999; *Alexander et al.*, 2002]. Dos de las teorías más relevantes que intentan explicar el fenómeno ENSO son el "oscilador-retardado" [*McCreary*, 1983; *Battisti*, 1988; *Suarez and Schopf*, 1988] y el "oscilador-recargado" [*Jin*, 1997], destacando ambas el papel de los mecanismos de realimentación asociados con la termoclina en el desarrollo de las anomalías de SST. Sin embargo, otros estudios han indicado que tanto los mecanismos de realimentación relacionados con la termoclina, como los asociados

con procesos de advección zonal, juegan un papel muy importante en el desarrollo del ENSO [*Jin and An*, 1999; *An and Jin*, 2001].

Existe un modo de variabilidad interanual en el Atlántico tropical similar al ENSO, denominado Niño Atlántico [*Merle*, 1980; *Zebiak*, 1993]. El Niño Atlántico se caracteriza por un debilitamiento de los vientos alíseos en el oeste del Atlántico ecuatorial, asociados con un calentamiento anómalo en la parte oriental de la cuenca (Figura S1, derecha). El Niño Atlántico tiene lugar durante el verano boreal y su periodo oscila entre los 2 y 4 años [*Latif and Grötzner*, 2000; *Ruiz-Barradas et al.*, 2000; *Kushnir et al.*, 2003]. Este fenómeno impacta en el clima tanto de regiones próximas como de áreas remotas [*Ward*, 1998; *Cassou et al.*, 2005; *García-Serrano et al.*, 2008; *Kucharski et al.*, 2008; *Polo et al.*, 2008a; *Joly and Voldoire*, 2010; *Mohino et al.*, 2011; *Rodríguez-Fonseca et al.*, 2011]. Trabajos recientes han encontrado una relación entre el Niño Atlántico y el ENSO [*Keenlyside and Latif*, 2007; *Polo et al.*, 2008a; *Rodríguez-Fonseca et al.*, 2009; *Ding et al.*, 2012]. Este descubrimiento es la principal motivación de la presente Tesis Doctoral (Figura S2). Estos autores pusieron de manifiesto como a partir de los 1970s, un Niño (Niña) Atlántico favorece el desarrollo de la Niña (Niño) del Pacífico al invierno siguiente [*Rodríguez-Fonseca et al.*, 2009; *Ding et al.*, 2012].

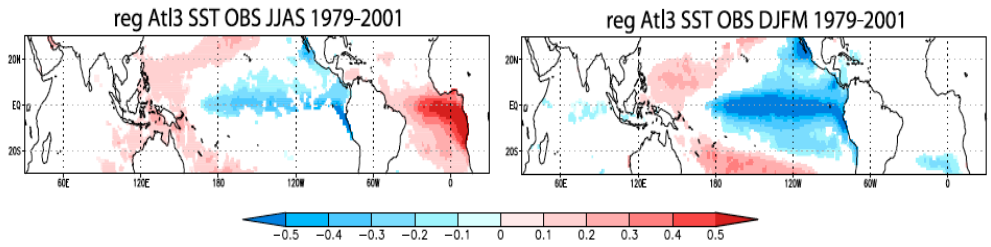

Figura S2. Conexión entre el Niño Atlántico y la Niña del Pacífico después de los 1970s (procedente de *Rodríguez-Fonseca et al.* [2009]). Regresión de las anomalías de SST en verano (JJAS, izquierda) e invierno (DJFM, derecha) sobre el índice del Atl3 en verano (JJAS) para el periodo 1979-2001.

Sin embargo, existen todavía preguntas abiertas que deben ser aclaradas. Es necesario estudiar cómo es la influencia de la SST del Atlántico tropical sobre el ENSO y cuáles son los procesos involucrados en su desarrollo. Es preciso caracterizar los Niños del Atlántico capaces de impactar en el ENSO, así como comprender los

procesos de interacción aire-océano asociados con su generación. Finalmente, se debe investigar por qué la conexión entre dichos fenómenos solamente se observa en las últimas décadas del siglo XX.

2. OBJETIVOS

Objetivo 1: Comprender la contribución de la variabilidad interanual del Atlántico tropical sobre el ENSO.

Objetivo 2: Estudiar la estacionariedad de la conexión Atlántico-Pacífico, además de su posible modulación multidecadal.

Objetivo 3: Evaluar la predictibilidad del ENSO a partir de la SST del Atlántico tropical.

Objetivo 4: Caracterizar el Niño Atlántico involucrado en la conexión Atlántico-Pacífico y compararlo con el modo canónico.

Objetivo 5: Estudiar los procesos de interacción aire-océano involucrados en el desarrollo de los diferentes Niños del Atlántico.

3. DATOS & METODOLOGÍA

3.1 Observaciones y Reanálisis

En el presente trabajo se han utilizado datos procedentes de observaciones y de reanálisis. La SST proviene de HadISST [*Rayner et al.*, 2003], pero también se ha considerado SST, profundidad de la termoclina y wind stress del reanálisis SODA [*Giese and Ray*, 2011]. Como variables atmosféricas se han usado el viento en superficie, el potencial de velocidad en 200 hPa y 925 hPa y la SLP del reanálisis del 20th century [*Compo et al.*, 2011]. La SLP procedente del reanálisis ERA-40 [*Uppala et al.*, 2005] también se ha utilizado.

3.2 Simulaciones acopladas

En el presente estudio se han utilizado simulaciones parcialmente acopladas. Por un lado, **SPEEDY-RGO** que considera el modelo global de circulación atmosférica SPEEDY [*Molteni*, 2003; *Kucharski et al.*, 2006b], con una resolución horizontal T30 y 8 niveles verticales. Este modelo se encuentra acoplado a un modelo de 1.5 capas, de gravedad reducida [*Chang*, 1994] con una resolución horizontal de 2°x1°. Dos diseños experimentales diferentes han sido utilizados. *SimAtlVar* [*Rodríguez-Fonseca et al.*, 2009], que considera la TSM observada en el Atlántico a lo largo del siglo XX y TSM climatológica en el resto de cuencas, excepto en el Indo-Pacífico donde la atmósfera se encuentra acoplada al océano. Este experimento permite aislar la influencia del Atlántico sobre la variabilidad del Pacífico Tropical. Dos simulaciones diferentes se han utilizado, una para el periodo 1949-2002 y otra para el periodo 1871-2002. Los resultados de ambas simulaciones se han comparado con una simulación de control (*SimAtlCli*) en la cual la TSM climatológica se prescribe en todas las cuencas oceánicas salvo en la región del Indo-Pacífico donde la atmósfera está acoplada al océano. De manera adicional se ha utilizado otra simulación parcialmente acoplada, **SPEEDY-NEMO** que considera el mismo modelo atmosférico SPEEDY, pero está acoplada al modelo de océano NEMO [*Madec et al.*, 1998]. Esta simulación cubre el periodo 1945-2015 y tiene el mismo diseño experimental que SPEEDY-RGO (*SimAtlVar*).

3.3 Simulaciones oceánicas

Finalmente, se ha realizado una simulación OGCM con la configuración del Atlántico tropical del modelo NEMO, la simulación NEMO-INTER (http://forge.ipsl.jussieu.fr/nemo-atltrop). Este modelo tiene una resolución horizontal de 0.25°x0.25° y 46 niveles en profundidad. NEMO ha sido forzado con vientos interanuales en el periodo 1960-2011.

3.4. Metodología

Se han aplicado técnicas de análisis discriminante para estudiar la variabilidad del Atlántico y Pacífico tropical. El Análisis de Componentes Principales (PCA) y el Análisis de Máxima Covarianza (MCA) son técnicas que descomponen un campo de anomalías en un número de modos de variabilidad que maximizan la covarianza del campo. En el presente trabajo, la técnica MCA se ha adaptado para el estudio de la conexión Atlántico-Pacífico, considerando solamente un campo predictor y un conjunto de campos atmosféricos y oceánicos a predecir. Estos campos se corresponden con las diferentes variables en distintas estaciones, asociadas con el mecanismo que conecta los Niños del Atlántico y del Pacífico [*Martín-Rey et al.*, 2014; *Polo et al.*, 2015a]. Además se ha aplicado un filtro interanual a las anomalías estacionales [*Butterworth*, 1930; *Stephenson et al.*, 2000] y la significación estadística de los resultados se ha evaluado mediante la aplicación de tests paramétricos, como el t-test ó F-test, y tests no paramétricos, como el test de Monte Carlo test.

4. RESULTADOS Y CONCLUSIONES

4.1 Estudio de la influencia de la variabilidad del Atlántico tropical en ENSO a partir de los 1970s [*Martín-Rey et al.*, 2012].

A partir de la simulación *SimAtlVar*, se han estudiado y comparado los modos de variabilidad interanual de la SST del Pacífico tropical antes y después de los 1970s. Se ha encontrado como los ENSO antes de los 1970s se caracterizaban por anomalías de SST en el centro-este de la cuenca del Pacífico sin cambios significativos en el wind stress o en la profundidad de la termoclina. Estos fenómenos no están relacionados con las anomalías de SST del Atlántico ecuatorial durante el verano previo y son similares a los eventos ENSO generados internamente. Sin embargo, a partir de los 1970s, los ENSO simulados se caracterizan por una convergencia (divergencia) anómala de viento en el Pacífico central durante el verano boreal, que genera anomalías en la SST y profundidad de la termoclina en el Pacífico tropical durante los meses de invierno. Estos fenómenos ENSO, cuyo

desarrollo está asociado a mecanismos dinámicos, están fuertemente relacionados con las anomalías de SST del Atlántico ecuatorial durante el verano previo.

4.2 Análisis de los procesos oceánicos asociados con el desarrollo del ENSO inducido por el Atlántico ecuatorial [*Polo et al.*, 2015a].

Los procesos atmosférico y oceánicos asociados con la conexión Atlántico-Pacífico han sido estudiados a partir de observaciones, reanálisis y de la simulación *SimAtlVar*. Estos resultados se centran en los procesos oceánicos, que eran los que no se habían analizado en el trabajo previo de *Rodríguez-Fonseca et al.* [2009].Cuando un Niño Atlántico tiene lugar durante el verano boreal, se produce un aumento de la convección sobre el Atlántico ecuatorial, que altera la circulación de Walker, generando una subsidencia anómala sobre el Pacífico central. La divergencia de viento en superficie en esta region levanta la termoclina y dicha perturbación se propaga hacia el este en forma de una onda de Kelvin. A medida que la onda se propaga, la termoclina se vuelve más somera, favoreciendo el enfriamiento de la superficie mediante advección de temperatura asociada con corrientes anómalas zonales y velocidades medias verticales. Un mecanismo similar, con el correspondiente cambio de signo, tiene lugar para una Niña del Atlántico.

4.3 Estudio de la no-estacionariedad de la conexión Atlántico-Pacífico y las posibles modulaciones multidecadales [*Martín-Rey et al.*, 2014]

La conexión Atlántico-Pacífico aparece como el principal modo acoplado de variabilidad interanual en las regiones tropicales durante las primeras décadas del siglo XX y a partir de los 1970s. Este modo involucra todas las variables atmosféricas y oceánicas asociadas con el mecanismo que describe el impacto del Niño del Atlántico sobre la Niña del Pacífico (y vice versa). Los periodos en los que el modo Atlántico-Pacífico aparece, coinciden con fases negativas de la Oscilación Multidecadal del Atlántico (AMO,*Knight et al.* [2006]). La AMO podría estar modulando esta conexión entre cuencas a escalas multidecadales mediante cambios en la convección sobre el Atlántico

ecuatorial y la modificación de la variabilidad oceánica en el este del Pacífico ecuatorial.

4.4 Predicción del ENSO a partir de la TSM del Atlántico ecuatorial [*Martín-Rey et al.*, 2015a]

Teniendo en cuenta la no-estacionariedad de la conexión Atlántico-Pacífico, se ha realizado una predicción estadística del ENSO en el invierno boreal utilizando las anomalías de SST del Atlántico tropical durante el verano previo como predictor. El modelo estadístico está basado en los resultados de *Martín-Rey et al.* [2014] y es capaz de predecir las principales variables asociadas con los eventos ENSO forzados por el Atlántico: SST, profundidad de la termoclina y vientos en superficie. La predicción es buena para los periodos en los que la conexión Atlántico-Pacífico tiene lugar, es decir, durante las primeras y últimas décadas del siglo XX. Este resultado sugiere que se puede predecir mejor el ENSO a partir de la información del Atlántico durante ciertos periodos.

4.5 Caracterización de los Niños del Atlántico asociados con el ENSO [*Martin-Rey et al.*, 2015b]

Se han caracterizado los principales modos de variabilidad interanual de la SST del Atlántico tropical durante el verano boreal en los periodos en los que la conexión Atlántico-Pacífico tiene lugar. Aparecen dos modos de variabilidad asociados con un calentamiento anómalo en el Atlántico ecuatorial. El primer modo se caracteriza por un calentamiento (enfriamiento) de toda la cuenca y está asociado con una Niña (Niño) en el Pacífico al invierno siguiente. Este modo está precedido por un debilitamiento de los sistemas de altas presiones subtropicales (el anticiclón de Sta Helena y el de Azores) durante el otoño e invierno previos. Estas anomalías negativas de presión originan una reducción de los vientos alíseos en el norte y sur del Atlántico tropical, calentando dichas regiones a través de flujos turbulentos de calor.

En la banda ecuatorial, estas anomalías de presión generan una convergencia anómala de viento que induce una convergencia de las corrientes oceánicas y una profundización de la termoclina que calienta la banda ecuatorial a través de procesos verticales. El segundo modo de variabilidad se caracteriza por un calentamiento anómalo del este del Atlántico ecuatorial, rodeado por anomalías negativas de TSM en el norte y sur del Atlántico ecuatorial. Este modo esta precedido por un gradiente este-oeste de presión en superficie que origina vientos anómalos del oeste y una convergencia anómala de las corrientes en el ecuador, calentándolo mediante procesos verticales. Este Niño Atlántico no se relaciona con el fenómeno ENSO al invierno siguiente.

1. MOTIVATION

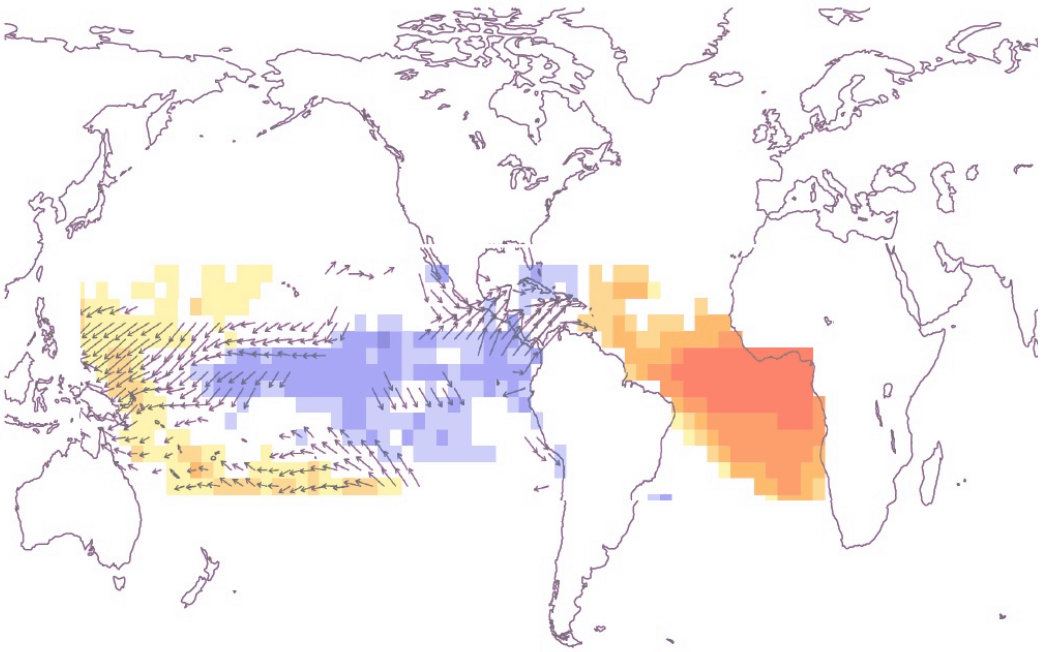

1. MOTIVATION

El Niño–Southern Oscillation (ENSO) is the most outstanding year-to-year climatic phenomenon on Earth [*Philander*, 1990]. ENSO takes place in the tropical Pacific, in which the seasonal cycle is characterized by an alternation of cooler and warmer conditions due to the interaction with the trade winds and the thermocline depth, through the so-called Bjerknes feedback [*Bjerknes*, 1969]. The maximum variability of the Sea Surface Temperature (SST) in this region occurs during winter months, when the trades are intensified, favouring the upwelling of deep cold waters to the surface, that bring great amounts of fish along the Peruvian coast.

During some years, the seasonal cycle is disrupted and ENSO phenomenon emerges. El Niño is characterized by a warming of the sea surface and a weakening of the trade winds in the central-east of the equatorial Pacific. As a consequence, a reduction of the coastal upwelling and a deepening of the thermocline depth take place in the eastern Pacific. The opposite phase of El Niño is named as La Niña and implies an intensification of the trades related to cooler SSTs and shallower thermocline depth in the central-east of the equatorial Pacific [*Philander*, 1985; *Philander*, 1990].

ENSO has a strong influence on the global climate and, due to its human, environmental and socio-economic impacts, research efforts have been made to forecast these events during the last decades. Moreover, the current seasonal prediction system is based on ENSO, which is considered as the leader engine of the seasonal forecast. In order to predict ENSO episodes and, therefore, to anticipate its associated impacts, several studies have analysed the ENSO precursors, firstly within the tropical Pacific [*Penland and Magorian*, 1993; *Barnston et al.*, 1999; *Clarke and Shu*, 2000; *Clarke and Van Gorder*, 2001; *Clarke and Van Gorder*, 2003] and, more recently, in other tropical and extra-tropical regions [*Frauen and Dommenget*, 2012; *Boschat et al.*, 2013; *Dayan et al.*, 2013; *Keenlyside et al.*, 2013].

Using this information, dynamical and statistical predictions for ENSO episodes have been performed obtaining good skills. Nevertheless, a realistic ENSO prediction still remains a challenge for the scientific community.

Recently, a new paradigm associated with this inter-annual phenomenon has arisen, highlighting the role of the Atlantic Ocean in modulating the tropical Pacific variability. On the one hand, several studies have indicated how changes in the Atlantic mean state associated with different phases of the Atlantic Multidecadal Oscillation, AMO [*Delworth and Mann*, 2000; *Knight et al.*, 2006] could induce a modification of the tropical Pacific background state and variability through atmospheric and oceanic teleconnections [*Dong et al.*, 2006; *Dong and Sutton*, 2007]. On the other hand, some authors put forward the possible connection between the tropical Atlantic inter-annual variability and ENSO phenomena, pointing out the leadership of the Atlantic Ocean [*Keenlyside and Latif*, 2007; *Polo et al.*, 2008a; *Jansen et al.*, 2009; *Rodríguez-Fonseca et al.*, 2009; *Ding et al.*, 2012]. The latter results have conformed the basis of this PhD Thesis and have motivated the research developed by TROPA group in the last years.

In this sense, in a former paper, *Keenlyside and Latif* [2007] found significant negative correlations between Atl3 [20°W-0°, 3°N-3°S] and Niño3 [150°W-90°W, 5°N-5°S] SST anomalies during the last decades of the 20th century, with the leadership of the Atlantic 6 months in advance (Figure Ia). After this work, *Polo et al.* [2008a] investigated the relationship between the leading modes of Tropical Atlantic SSTs and West African (WA) rainfall, concluding that an Atlantic Niño associated with increased precipitation over the Gulf of Guinea from late 1970s, was strongly anti-correlated with tropical Pacific SST anomalies during next winter (Figure Ib-c).

Similar results were obtained analysing the tropical Atlantic and Pacific variability using a recharge oscillator scheme, putting forward the existence of a feedback from the Atlantic on ENSO phenomenon, in a way that, warm Atlantic causes a cooling in Niño3 region and a shallowing of the equatorial Pacific thermocline (Figure Id; *Jansen et*

al. [2009]). Nevertheless, these studies did not give any special attention to the Atlantic-Pacific connection or the dynamical mechanisms at work.

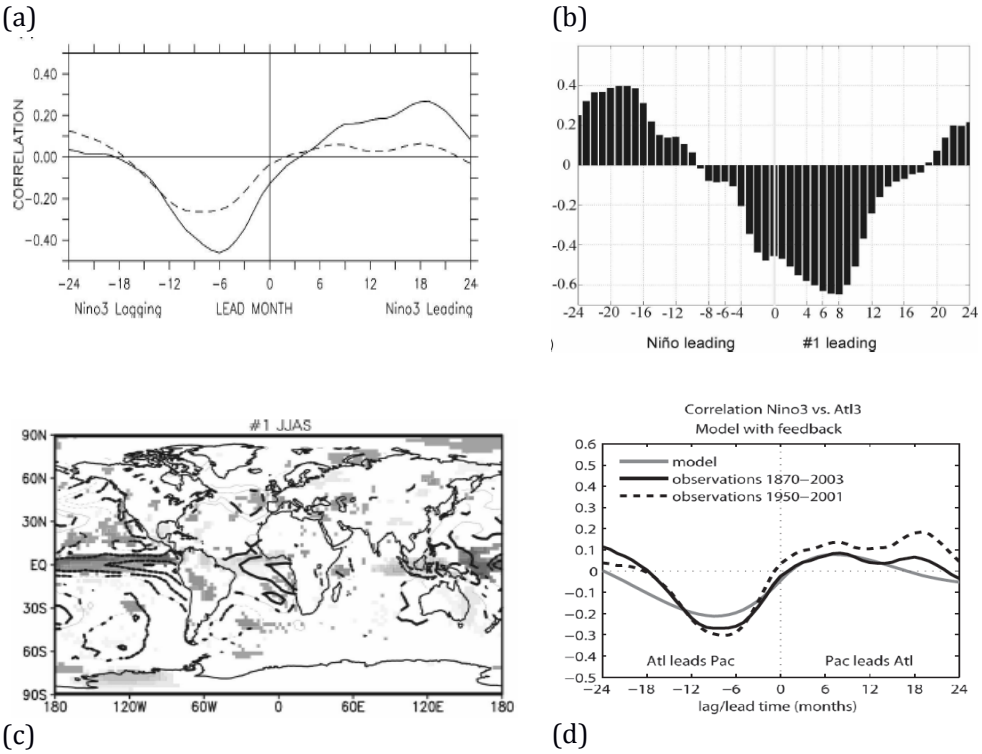

Figure I. Connection between the inter-annual Pacific and Atlantic variability. (a) Cross-correlation between Niño3 and Atl3 averaged SST anomalies. Solid lines are for the period 1970-2003 and dashed line are for the period 1870-2003. From *Keenlyside and Latif* [2007]. (b) Correlation coefficient between the leading tropical Atlantic SST expansion coefficient and Niño3 index, leading and lagging 24 months with respect to JJAS. (c) Regression of the total SST expansion coefficient associated with the leading EMCA mode onto the global SST (contours) and precipitation (shaded) anomalies. From *Polo et al.* [2008a]. (d) Cross-correlation between Niño3 and Atl3 SST anomalies for the Pacific-Atlantic Ocean coupled model compared to observational HadISST form the period 1870-2003(solid black) and 1950-2001 (dashed). From *Jansen et al.* [2009]

Rodríguez-Fonseca et al. [2009] analysed for the first time the active role of the Atlantic Niños in the enhancement of ENSO phenomena. These authors demonstrated that summer Atlantic Niños (Niñas) were able to favour the development of Pacific Niñas (Niños) during the following winter from the 1970s. The mechanism involved in the

connection was also investigated, concluding that when an Atlantic Niño takes place, the convection over the Atlantic is enhanced, altering the Walker circulation with an ascending branch over the Atlantic and subsidence over the central Pacific, linking in that way both tropical basins [*Rodríguez-Fonseca et al.*, 2009]. The descending motions over the central Pacific originate anomalous surface wind divergence, which, in turn, shallows the thermocline depth, contributing to the development of La Niña cold tongue (Figure IIc-h). The connection between Atlantic Niños and Pacific Niñas (and vice versa) was reproduced by partially coupled simulations that considered the observed Atlantic SSTs as the only external forcing, isolating in this way, the contribution of the Atlantic Ocean to the tropical Pacific variability [*Rodríguez-Fonseca et al.*, 2009]. These modelled results were confirmed by Atmospheric Global Climate Models (AGCMs, *Losada et al.* [2010b]) and by a more resolution coupled model [*Ding et al.*, 2012], given robustness to the Atlantic-Pacific Niños connection.

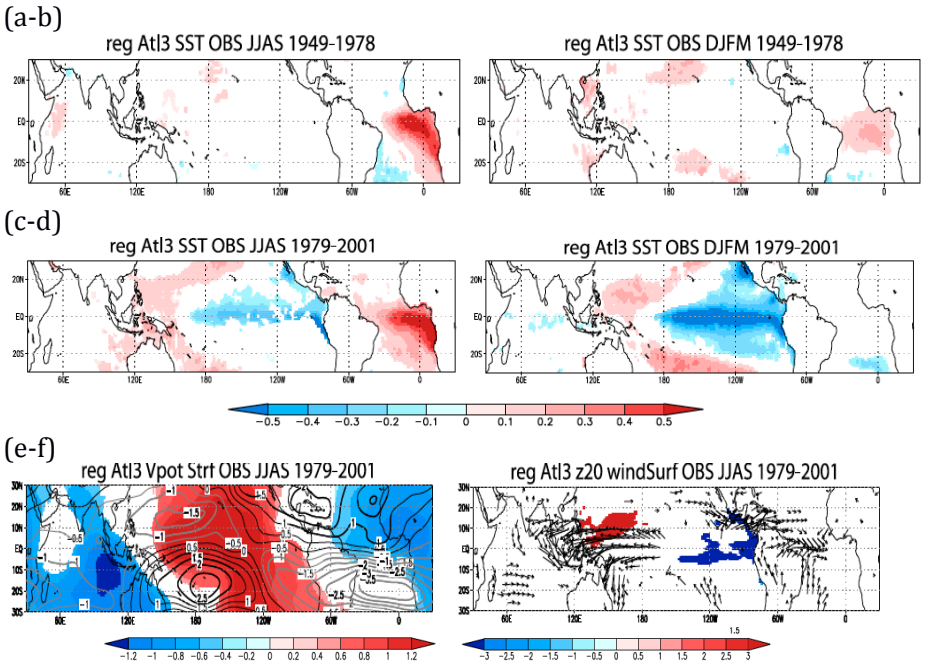

Figure II. Connexion between the Atlantic Niño-Pacific Niña after the 1970s (a-d). Observed anomalous SST regressed onto the boreal summer Atl3 index for the period 1949-1978 (a-b) and 1979-2001 (c-d) in summer and winter months. (e-f) Observed anomalous velocity potential (shaded in 10^{-6} m^2/s) and streamfunction (contours in 10^{-6} m^2/s) at 200 hPa regressed onto boreal summer Atl3 index in summer months for the period 1979-2001. From *Rodríguez-Fonseca et al.* [2009].

Rodríguez-Fonseca et al. [2009] proposed the alteration of the Walker circulation as the atmospheric mechanism to link Atlantic and Pacific Niños*. Nevertheless the oceanic dynamics involved in the development of ENSO phenomena associated with the remote Atlantic forcing are still unclear. Further research to determine the role of oceanic processes and also the possible contribution of oceanic waves is required.*

Although *Ding et al.* [2012] corroborated the finding of *Rodríguez-Fonseca et al.* [2009], the former authors posed that the Atlantic influence on ENSO was stationary on time and independent of the period considered (Figure III,right). On the contrary, Rodríguez-Fonseca et al. (2009) argued that the Atlantic-Pacific connection only occurred after the 1970s (Figure III,left). Parallel to these findings, some authors highlighted the role of the Atlantic background state in modulating the tropical Pacific variability. For negative phases of the Atlantic Multidecadal Oscillation (AMO), ENSO variability was increased due to a modification of the Pacific background state [*Dong et al.*, 2006; *Dong and Sutton*, 2007]. The meridional SST gradient in the Atlantic Ocean generates an atmospheric response, modifying the surface winds and the thermocline depth in the equatorial Pacific, enhancing the dynamical feedbacks and hence the ENSO variance [*Dong et al.*, 2006]. These results should be also taken into account in the analysis of the Atlantic-Pacific connection.

This is another motivating point to be explored: when does the Atlantic-Pacific Niños connection take place during the observational record?. The present work will shed light about the stationary or non-stationary behaviour of this inter-basin link and will look for possible modulators.

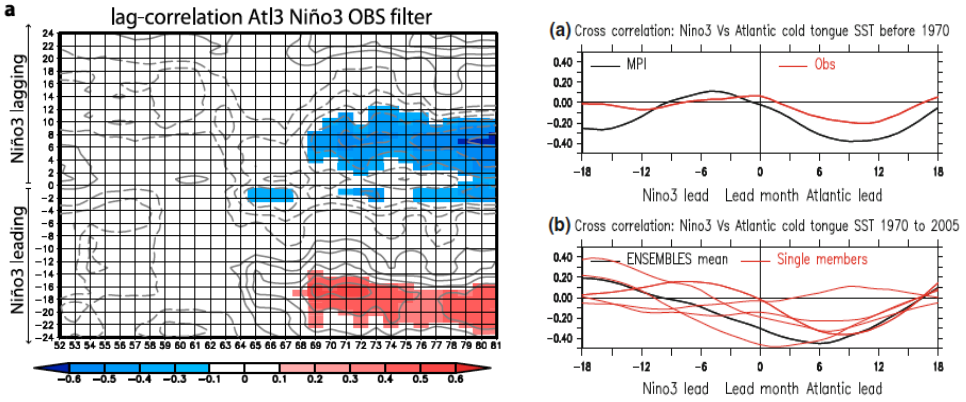

Figure III. Non-stationary relation between the Atlantic Niños and ENSO. (left) Twenty year lead-lag correlation, running one year from 1952–1972 to 1981–2001, between the observed summer (June–July–August–September) Atl3 and observed Niño3 SST anomalies for positive (from 0 to 24 months after summer) and negative (from 0 to 24 months before summer) lags. From *Rodríguez-Fonseca et al.* [2009]. (right) Cross-correlation between Niño3 and Atlantic cold tongue SST anomalies before and after the 1970s for observations and model simulations. From *Ding et al.* [2012].

In addition to the clarification of these scientific questions about the processes at work and the modulation of this inter-basin link, ENSO prediction based on the Atlantic inter-annual variability should be clarified, as the Atlantic Niño becomes a precursor of ENSO episodes. In this sense, *Jansen et al.* [2009], using a recharge oscillator scheme, proved that the ENSO prediction is enhanced when the Atlantic SST anomalies are considered. In the same line, *Frauen and Dommenget* [2012] reported that the initial conditions of the tropical Atlantic Ocean have a strong impact on ENSO predictability. The initialization of dynamical ENSO predictions from the information of the tropical Atlantic SSTs during previous months has been also investigated, obtaining a significant improvement in the skill when the model is initialized with equatorial Atlantic SSTs during boreal spring [*Keenlyside et al.*, 2013].

If the Atlantic-Pacific Niños connection only occurred after the 1970s, its occurrence would open windows of opportunity to predict ENSO episodes. A study of the predictive skill of the Atlantic SSTs on ENSO phenomena and its possible time-dependence is therefore required.

Focusing in the inter-annual tropical Atlantic variability, a key question about the different Atlantic-Pacific relationship before and after the 1970s is if the Atlantic Niño exhibits similar structure and/or dynamics for these two different periods. Historically, the Atlantic Niño has been considered as the response of weakened zonal winds over the western equatorial Atlantic [*Zebiak*, 1993]. More recently, some authors have suggested that the development of the Atlantic Niño is preceded by a weakening of Sta Helena High, which induces a reduction of the south-eastern trades and favours the warming of the equatorial Atlantic [*Polo et al.*, 2008a; *Lübbecke et al.*, 2010]. Moreover, in figure IIa-d (from *Rodríguez-Fonseca et al.* [2009]), different spatial configurations of Atlantic Niño phenomenon can be seen in the tropical Atlantic basin before and after the 1970s. Positive SST anomalies in the eastern equatorial Atlantic flanked by a horseshoe of negative ones are shown before the 1970s (figure IIa, hereafter Canonical Atlantic Niño), while an Atlantic Niño with positive SST anomalies covering the entire tropical Atlantic basin has been observed from the 1970s (Figure IIc, hereafter, Basin-Wide Atlantic Niño).

The reported changes in the Atlantic Niño impacts during the last decades [*Polo et al.*, 2008a; *Joly and Voldoire*, 2010; *Losada et al.*, 2010a; *Losada et al.*, 2010b; *Rodríguez-Fonseca et al.*, 2011] could be attributed to the modification of its spatial structure [*Losada and Rodriguez-Fonseca*, 2015], which could be suggesting that Canonical and the Basin-Wide Atlantic Niño have different atmospheric forcings which, in turn, activate diverse oceanic processes developing SST anomalies. *Further research about the origin of the Canonical and Basin-Wide Atlantic Niño, their precursors and air-sea mechanisms involved is needed.*

Figure IV presents a summary of the air-sea interactions associated with the Atlantic-Pacific connection that will be investigated in the present Thesis. To achieve it, an analysis of observational data and a set of modelled simulations from partially coupled models and Ocean General Circulation Models (OGCM), will be performed. The results of the present study can help to better understand the tropical Atlantic

and Pacific climate variability, as well as, to enhance the ENSO prediction which, in turn, will improve the current seasonal and decadal forecast systems.

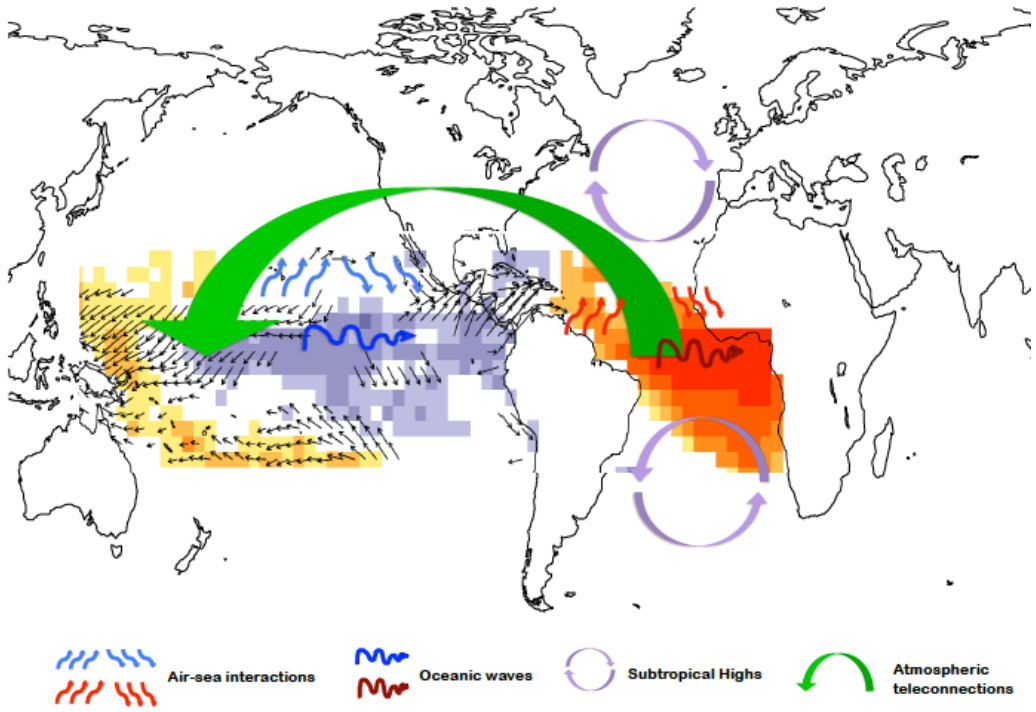

Figure IV. Air-sea interactions in the Atlantic-Pacific connection. Scheme of the air-sea interactions in the tropical Atlantic and Pacific oceans that will be studied in the present Thesis.

The present Thesis is structured as follows: the state of the art is presented in the first chapter of this study. The specific objectives of the present Thesis are described in chapter 3. The theorethical framework is described in chapter 4. Chapter 5 contains the methodology and data used throughout this study. The results are presented in the form of scientific publications in chapter 6. In sections 6.1 and 6.2, the influence of the tropical Atlantic inter-annual variability on the development of ENSO phenomena is investigated, through the analysis of the associated air-sea interactions. In Section 6.3 the possible non-stationarity behaviour of the Atlantic-Pacific connection is explored and its possible modulators are investigated. In section 6.4 the predictive skill of the tropical Atlantic SST in ENSO

episodes is assessed and the crucial variables in ENSO development associated with the Atlantic influence are determined. Section 6.5 is focused on the study of the Atlantic Niño phenomena able to impact on ENSO; the atmospheric forcings and the oceanic processes at work are investigated. The Finally, chapter 7 and 8 contain the integrating discussion and main conclusions of the present Thesis.

1. MOTIVACIÓN

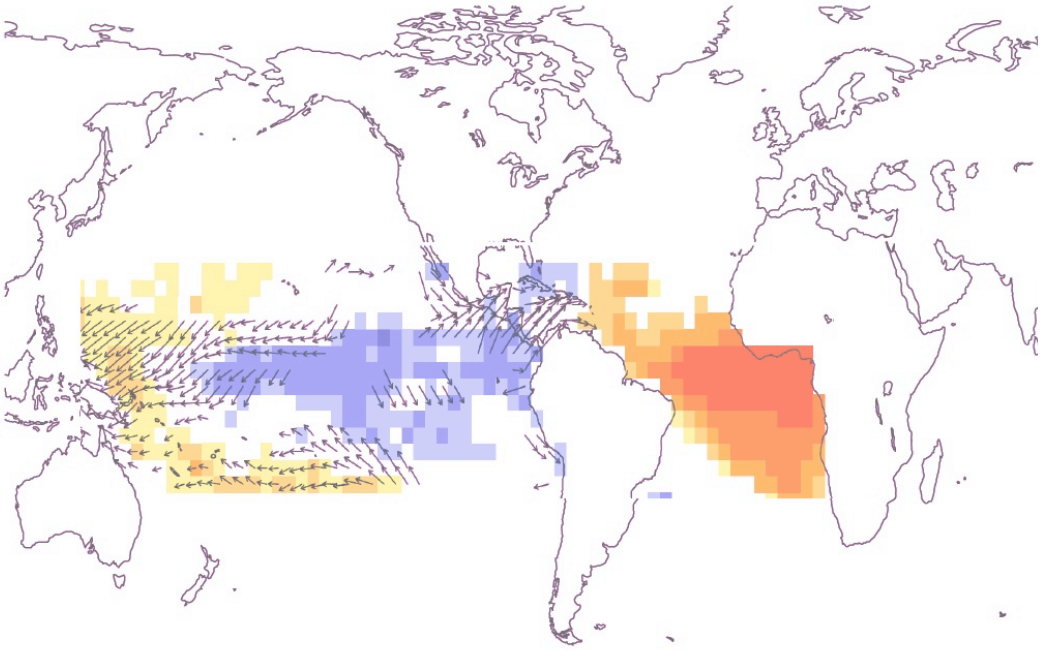

Motivación

El Niño y la Oscilación del Sur (ENSO) es el fenómeno climático más relevante a escala interanual [*Philander*, 1990]. El ENSO tiene lugar en el Pacífico tropical, cuyo ciclo estacional se caracteriza por una alternancia de temperaturas anómalamente frías o cálidas debido a la interacción con los vientos alíseos y la profundidad de la termoclina, mediante el mecanismo de realimentación de Bjerknes [*Bjerknes*, 1969]. La maxima variabilidad de la Temperatura de la Superficie del Mar (SST) tiene lugar durante los meses de invierno, cuando los vientos alíseos se intensifican, favoreciendo el afloramiento de aguas frías procedentes del océano profundo a la superficie, que origina la aparición de una gran cantidad de pesca a lo largo de la costa de Perú.

Durante ciertos años, el ciclo estacional se perturba y aparece el fenómeno del ENSO. El Niño se caracteriza por un calentamiento de la superficie del mar y un debilitamiento de los vientos alíseos en el centro-este del Pacífico ecuatorial. Como consecuencia, se reduce el afloramiento costero y se profundiza la termoclina en el este del Pacífico. La fase contraria al Niño se denomina La Niña y está asociada con una intensificación de los vientos alíseos, que genera SST anómalamente frías y una termoclina más somera en el centro-este del Pacífico [*Philander*, 1985; *Philander*, 1990].

ENSO tiene una gran influencia sobre el clima global y debido a sus impactos humanos, medioambientales y socio-económicos, se ha hecho un gran esfuerzo en las últimas décadas para predecir dichos fenómenos. Además, el sistema de predicción estacional actual está basado en ENSO, al cual se considera como el motor de la predicción estacional. Para predecir los episodios ENSO, y por tanto, anticiparse a sus impactos, ciertos estudios han analizado los precursores del ENSO, primeramente dentro del Pacífico tropical [*Barnston and Ropelewski*, 1992; *Penland and Magorian*, 1993; *Clarke and Shu*, 2000; *Clarke and Van Gorder*, 2001; *Clarke and Van Gorder*, 2003] y más recientemente, en otras regiones tropicales y extra-tropicales [*Frauen and Dommenget*, 2012; *Boschat et al.*, 2013; *Dayan et al.*, 2013; *Keenlyside et al.*, 2013]. A partir de esta información, se han realizado

predicciones dinámicas y estadísticas del ENSO, obteniéndose buenos resultados. Sin embargo, predecir de manera realista el fenómeno ENSO sigue siendo un desafío para la comunidad científica.

Recientemente, ha aparecido un nuevo paradigma asociado con este fenómeno interanual, que destaca el papel del océano Atlántico en modular la variabilidad del Pacífico tropical. Por un lado, ciertos estudios han indicado como los cambios en el estado medio del Atlántico, asociados con diferentes fases de la Oscilación Multidecadal del Atlántico, AMO [*Delworth and Mann*, 2000; *Knight et al.*, 2006] podrían producir una modification del estado medio y variabilidad del Pacífico a través de teleconexiones atmosféricas y oceánicas [*Dong et al.*, 2006; *Dong and Sutton*, 2007]. Por otro lado, otros autores han puesto de manifiesto la posible conexión entre la variabilidad interanual del Atlántico y el fenómeno ENSO, destacando el liderazgo del océano Atlántico [*Keenlyside and Latif*, 2007; *Polo et al.*, 2008a; *Jansen et al.*, 2009; *Rodríguez-Fonseca et al.*, 2009; *Ding et al.*, 2012]. Estos últimos resultados conforman las bases de la presente Tesis Doctoral y han motivado la investigación llevada a cabo por el grupo TROPA en los últimos años.

En este sentido, en un trabajo previo, *Keenlyside and Latif* [2007] se encontraron correlaciones negativas significativas entre las anomalías de SST de las regiones Atl3 [20°W-0°, 3°N-3°S] y Niño3 [150°W-90°W, 5°N-5°S] durante las últimas décadas del siglo XX, con el liderazgo del Atlántico con 6 meses de anterioridad (Figure Ia). Posteriormente, *Polo et al.* [2008a] investigó la relación entre los principales modos de variabilidad de la TSM del Atlántico tropical y la precipitación en África Occidental, concluyendo que un Niño Atlántico asociado con un aumento de precipitación sobre el Golfo de Guinea a partir de la década de los 1970s, se anticorrelaciona fuertemente con las anomalías de SST del Pacífico tropical durante el invierno siguiente (Figure Ib-c).

Resultados similares se obtuvieron analizando la variabilidad del Atlántico y Pacífico tropical usando un modelo de oscilador recargado, poniendo de manifiesto la existencia de un mecanismo de

realimentación del Atlántico sobre el fenómeno ENSO, de manera q ue un Atlántico cálido origina un enfriamiento en la región del Niño3 y una termoclina más somera en el Pacífico ecuatorial (Figure Id; *Jansen et al.* [2009]). Sin embargo, estos estudios no prestaron atención a la conexión Atlántico-Pacífico o a los mecanismos dinámicos involucrados.

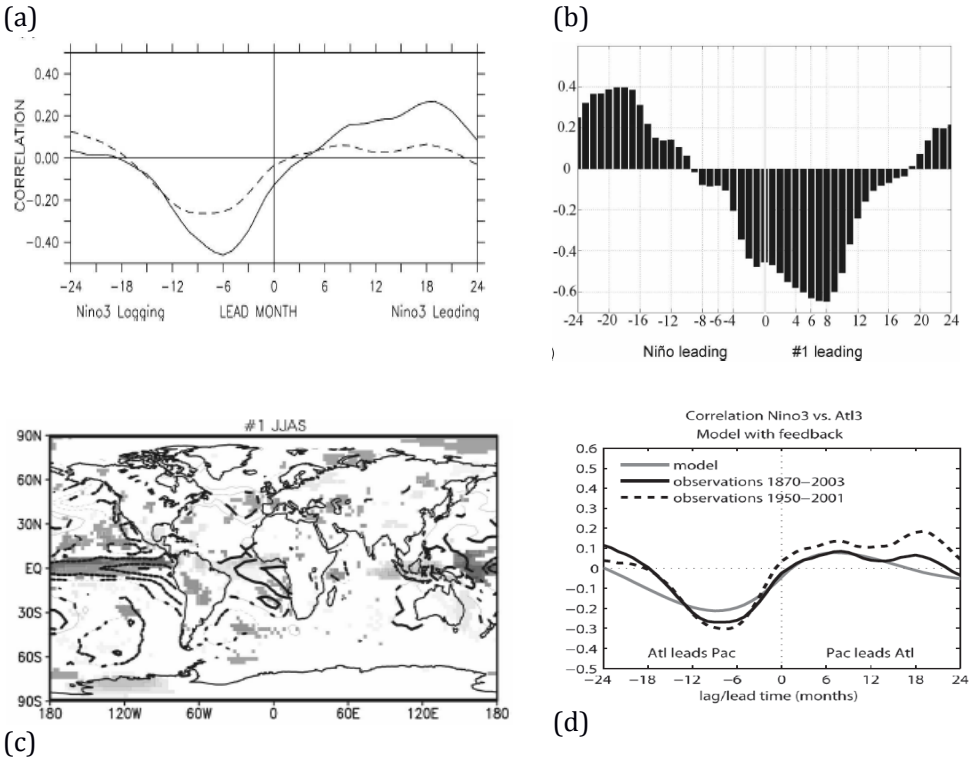

Figura I. Conexión entre la variabilidad interanual del Atlántico y del Pacífico.(a) Correlaciones cruzadas entre las anomalías promediasdas en las regiones Niño3 y Atl3. Las líneas continuas se refieren al periodo 1970-2003 y las líneas discontinuas están asociadas con el periodo 1870-2003 (procedente de *Keenlyside and Latif* [2007]). (b) Coeficiente de correlación entre el coeficiente de expansión del principal modo de variabilidad de la temperatura del Atlántico tropical y el índice Niño3, liderando y liderado 24 meses con respecto a JJAS. (c) Regresión del coeficiente total de expansión asociado con el principal modo de variabilidad de EMCA sobre las anomalías de TSM global (contornos) y precipitación (sombreado). Procedente de *Polo et al.* [2008a](d) Correlación cruzada entre el las anomalías de SST de Niño3 y Atl3 para el modelo acoplado Atlántico-Pacífico comparado con las observaciones de HadISST para el periodo 1870-2003 (línea continua) y 1950-2001 (línea discontínua). Procedente de *Jansen et al.* [2009].

Rodríguez-Fonseca et al. [2009] analizó por primera vez la contribución de los Niños del Atlántico en la amplificación de los fenómenos ENSO. Estos autores demostraron que los Niños (Niñas) del Atlántico eran capaces de favorecer el desarrollo de las Niñas (Niños) del Pacífico durante el invierno siguiente a partir de los 1970s. El mecanismo a través del cual se lleva a cabo la conexión también fue investigado, concluyéndose que cuando tiene lugar un Niño Atlántico, se aumenta la convección sobre el Atlántico, alterándose la circulación de Walker con una rama ascendente sobre el Atlántico y subsidencia sobre el Pacífico central, uniendo de esta manera ambas cuencas tropicales [*Rodríguez-Fonseca et al.*, 2009]. Los movimientos descendentes sobre el Pacífico central originan una divergencia anómala de viento en superficie, la cual produce un levantamiento de la termoclina, contribuyendo al desarrollo de la lengua fría de La Niña (Figure IIc-h). La conexión entre los Niños del Atlántico y las Niñas del Pacífico (y vice versa) se reprodujo con simulaciones parcialmente acopladas que consideraban las SST observadas en el Atlántico como único forzamiento externo, aislando de esta manera la contribución del océano Atlántico sobre la variabilidad del Pacífico tropical [*Rodríguez-Fonseca et al.*, 2009]. Estos resultados fueron confirmados con Modelos Atmosféricos de Circulación General (AGCMs, *Losada et al.* [2010b]) y por un modelo acoplado de mayor resolución [*Ding et al.*, 2012], dando solidez a la conexión Atlántico-Pacífico.

Rodríguez-Fonseca et al. [2009] propone una alteración de la circulación de Walker como el mecanismo atmosférico responsable de unir los Niños del Atlántico y del Pacífico. *Sin embargo los mecanismos oceánicos involucrados en el desarrollo de los fenómenos ENSO asociados con un forzamiento remoto del Atlántico aún se desconocen. Por tanto, es necesario determinar dichos procesos oceánicos así como la posible contribución de las ondas oceánicas en el desarrollo del fenómeno.*

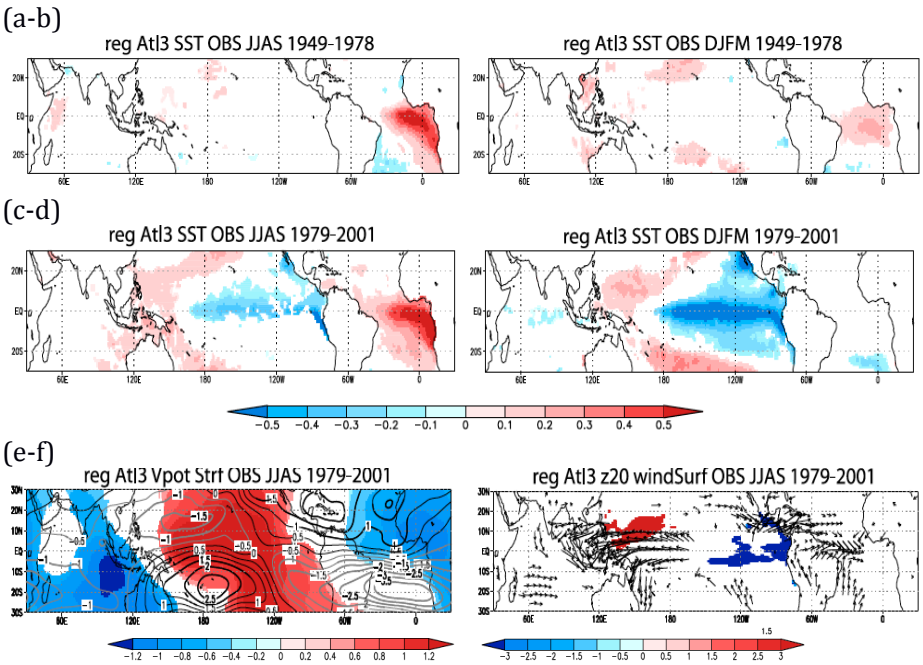

Figura II. Conexión entre el Niño Atlántico-La Niña del Pacífico a partir de los 1970s.(a-d). Anomalías observadas de SST proyectadas sobre el índice Atl3 en el verano boreal para el period 1949-1978 (a-b) y 1979-2001 (c-d) en verano e invierno. (e-f) Anomalías observadas de potencial de velocidad (sombreado en 10^{-6} m^2/s) y function de corriente (contornos in 10^{-6} m^2/s) en 200 hPa proyectada sobre el índice Atl3 en el verano boreal sobre los meses de verano para el period 1979-2001. Procedente de *Rodríguez-Fonseca et al.* [2009].

Aunque *Ding et al.* [2012] corroboró el descubrimiento de *Rodríguez-Fonseca et al.* [2009], estos autores propusieron que la influencia del Atlántico sobre el ENSO era estacionaria en el tiempo y que no dependía del periodo considerado (Figura III, derecha). Por el contrario, *Rodríguez-Fonseca et al.* [2009] sostenía que la conexión Atlántico-Pacífico solamente ocurría a partir de los 1970s (Figure III,left). De manera paralela a estos hallazgos, ciertos autores han puesto de manifiesto la contribución del estado medio del Atlántico en modular la variabilidad del Pacífico Tropical. Para fases negativas de la Oscillación Multidecadal del Atlántico (AMO), la variabilidad del ENSO se incrementaba debido a la modificación del estado medio del Pacífico [*Dong et al.*, 2006; *Dong and Sutton*, 2007]. El gradient meridional de SST en el océano Atlántico genera una respuesta atmosférica, modificando los vientos en superficie y la profundidad de la termoclina en el Pacífico ecuatorial, intensificando los procesos dinámicos de realimentación y por tanto la variabilidad del ENSO

[*Dong et al.*, 2006]. Estos resultados deberían tenerse en cuenta en el análisis de la conexión Atlántico-Pacífico.

Este es otro aspecto importante a ser investigado: ¿cúando tiene lugar la conexión entre los Niños del Atlántico y del Pacífico durante el periodo observacional? El presente trabajo arrojará luz sobre el comportamiento estacionario o no-estacionario de esta conexión y explorará sus posibles moduladores.

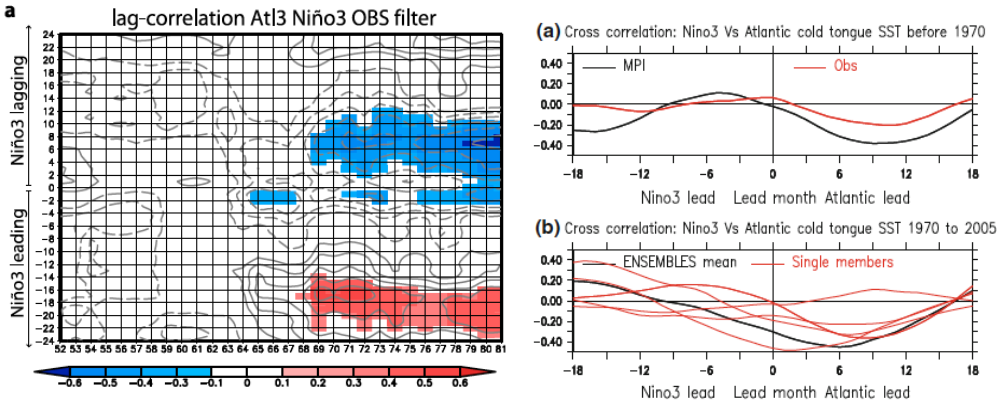

Figura III. Relación no-estacionaria entre el Niño Atlántico y ENSO. (izquierda) Correlación liderada-desfasada en ventanas de 20 años, moviendo 1 año desde 1952–1972 hasta 1981–2001, entre el indice de anomalías observadas de TSM para el indice Atl3 en verano (JJAS) y el Niño3 para desfases positivos (de 0 a 24 meses después del verano) y negativos (desde 0 a 24 antes del verano). Procedente de *Rodríguez-Fonseca et al.* [2009]. (derecha) Correlación cruzada entre el Niño3 y las anomalías de TSM de la lengua fría antes y después de los 1970s para observaciones y simulaciones. From *Ding et al.* [2012].

Además de aclarar estas cuestiones científicas sobre los procesos que están actuando en la modulación de la conexión entre cuencas, la predicción del ENSO a partir de la variabilidad interanual del Atlántico debe ser investigada, ya que el Niño Atlántico se convierte en un precursor de los eventos ENSO. En este sentido, *Jansen et al.* [2009], usando el modelo del oscilador recargado, demuestra que la predicción del ENSO se mejora cuando se consideran las anomalías de SST del Atlántico. En la misma línea, *Frauen and Dommenget* [2012] indicaron que las condiciones iniciales del Atlántico tropical tienen un gran impacto en la predictabilidad del ENSO. La inicialización de las predicciones dinámicas del ENSO a partir de la información de la SST

del Atlántico tropical durante los meses previos se ha evaluado, obteniéndose una mejora considerable en la predicción cuando se inicializa el modelo con TSM del Atlántico ecuatorial durante la primavera boreal [*Keenlyside et al.*, 2013].

Si la conexión Atlántico-Pacífico solamente tiene lugar después de los 1970s, su ocurrencia establecerá ventanas de oportunidad para predecir los eventos ENSO. Por tanto, es necesario realizar un estudio sobre el carácter predictivo de las TSM del Atlántico sobre el fenómeno del ENSO, así como su posible dependencia del periodo de tiempo.

Centrándose en la variabilidad interanual del Atlántico tropical, una cuestión clave en la diferente conexión Atlántico-Pacífico antes y después de los 1970s es si el Niño Atlántico presenta una estructura y dinámica similar para ambos periodos. Históricamente, el Niño Atlántico se ha considerado como la respuesta a un debilitamiento de los vientos zonales en el oeste del Atlántico ecuatorial [*Zebiak*, 1993]. Recientemente, ciertos autores han sugerido que el desarrollo del Niño Atlántico es precedido por un debilitamiento del Anticiclón de Sta Helena, que induce una reducción de los vientos alíseos del sureste y favorece el calentamiento del Atlántico ecuatorial [*Polo et al.*, 2008a; *Lübbecke et al.*, 2010]. Además, en la figura IIa-d (procedente de *Rodríguez-Fonseca et al.* [2009]), se aprecian diferentes configuraciones espaciales del Niño Atlántico antes y después de los 1970s. Anomalías positivas en el este del Atlántico ecuatorial, rodeadas por un patrón de anomalías frías en forma de herradura aparece antes de los 1970s (Figura IIa, de aquí en adelante Niño Atlántico Canónico), mientras que un Niño Atlántico con anomalías postivas de SST cubriendo toda la cuenca del Atlántico tropical se observa a partir de los 1970s (Figura IIc, de aquí en adelante Niño Atlántico "Basin-Wide").

Los cambios documentados de los impactos del Niño Atlántico en las últimas décadas [*Polo et al.*, 2008a; *Joly and Voldoire*, 2010; *Losada et al.*, 2010a; *Losada et al.*, 2010b; *Rodríguez-Fonseca et al.*, 2011] podrían ser debidos a una modificación de su estructura espacial [*Losada and Rodriguez-Fonseca*, 2015], lo cual podria sugerir que el

Niño Atlántico Canónico y el "Basin-Wide" tienen diferentes forzamientos atmosféricos, los cuales activan diferentes procesos oceánicos responsables de la generación de las anomalías de SST. *Por tanto, es necesario investigar el origen de los Niños Atlánticos Canónicos y "Basin-Wide", sus precursores y los procesos de interacción aire-océano involucrados.*

La figura IV muestra un resumen de los mecanismos de interacción aire-océano asociados con la conexión Atlántico-Pacífico que será investigada en la presente Tesis Doctoral. Para ello, se realizará un análisis de datos procedentes de observaciones y de un conjunto de simulaciones parcialmente acopladas y con Modelos de Circulación General del Océano (OGCM). Los resultados de la presente Tesis ayudarán a comprender mejor la variabilidad climática del Atlántico y Pacífico tropical, así como a mejorar la predicción del ENSO, y por tanto los sistemas actuales de predicción estacional y decadal.

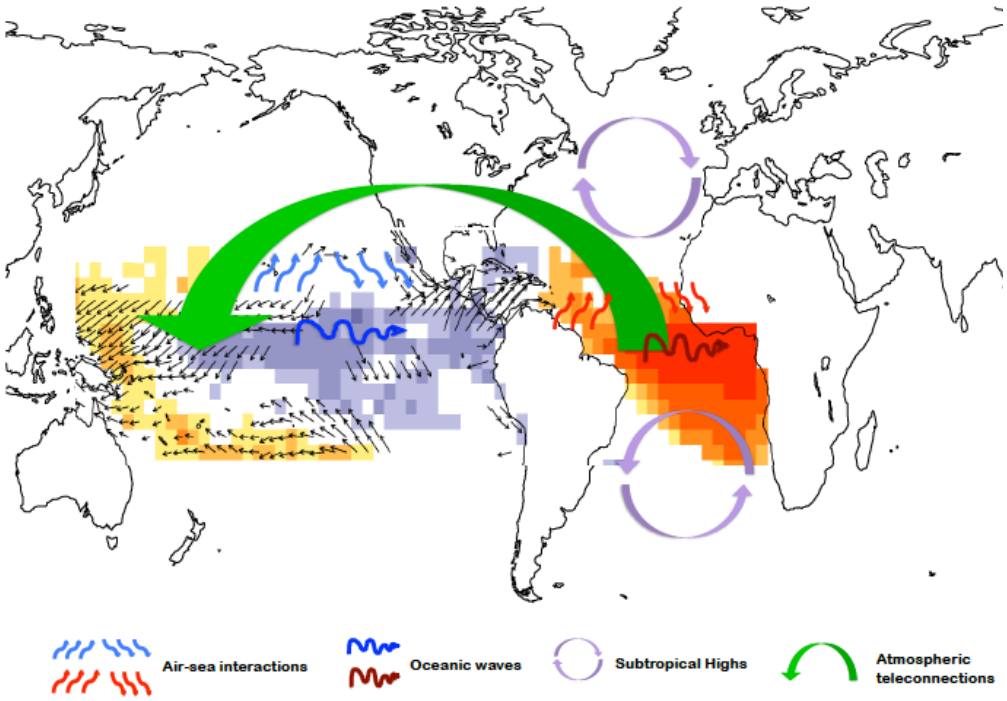

Figura IV. Interacciones aire-océano en la conexión Atlántico-Pacífico. Esquema de los procesos de interacción aire-océano en el Atlántico y Pacífico tropical que serán estudiados en la presente Tesis.

La presente Tesis está estructurada de la siguiente manera: el capítulo 2 describe el estado del arte del presente trabajo. Los objetivos específicos de la Tesis son enumerados en el capítulo 3. El marco teórico se describe en el capítulo 4. El capítulo 5 contiene la metodología y los datos utilizados en esta estudio. Los resultados se presentan en formato de publicaciones científicas en el capítulo 6. En las secciones 6.1 y 6.2 se investiga la influencia de la variabilidad interanual del Atlántico tropical en el desarrollo de los fenómenos ENSO, a través del análisis de los procesos de interacción aire-océano. En la sección 6.3, se analiza la posible no-estacionariedad de la conexión Atlántico-Pacífico así como sus posibles moduladores. En la sección 6.4., se estudia la capacidad predictiva de la SST del Atlántico tropical sobre los eventos ENSO y se determinan las variables fundamentales asociadas con el desarrollo de dicho fenómeno. En la sección 6.5 se analizan los Niños del Atlántico capaces de impactar en el ENSO, mediante el estudio de sus forzamientos atmosféricos y de los procesos oceánicos involucrados. Finalmente, los capítulos 7 y 8 contienen la discusión integradora y las principales conclusiones de la presente Tesis Doctoral.

2. STATE OF THE ART

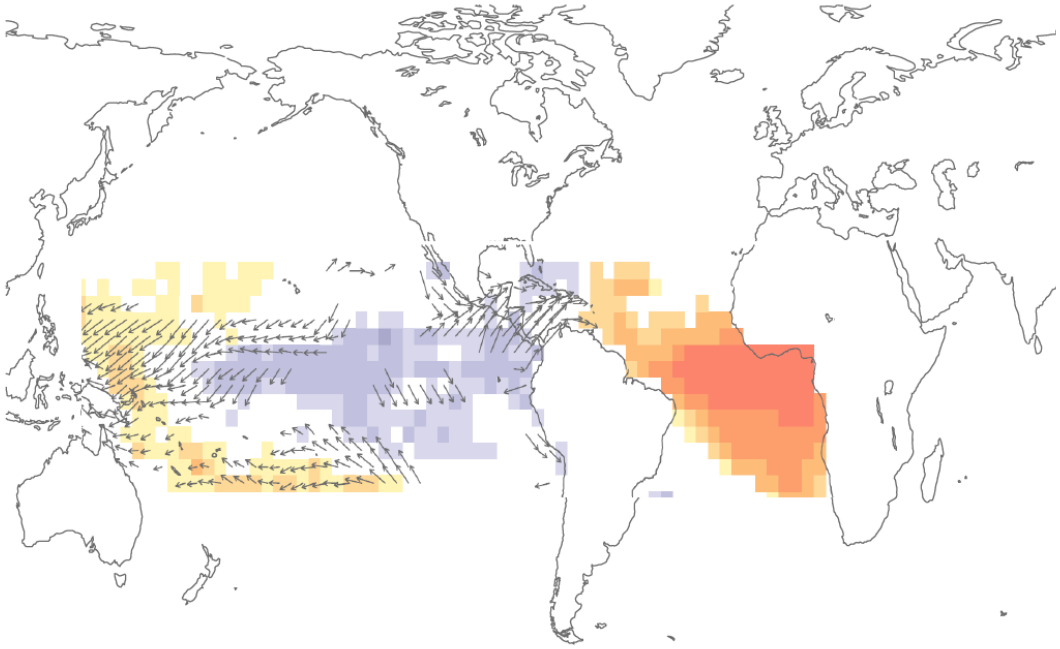

2. STATE OF THE ART

2.1. Tropical Climate Variability

The tropical regions are defined as the areas surrounding the Equator, limited by the Tropic of Cancer (23º27'N) in the northern hemisphere and the Tropic of Capricorn (23º27'S) in the southern hemisphere. The climate of these regions is closely linked to the huge amount of solar radiation received and stored in terms of heat content in the tropical oceans. The discharge of this energy within the own ocean and to the atmosphere drives the regional and global oceanic and atmospheric circulations, which, in turn, modify the climate of local and remote areas.

A great amount of the solar energy, around 50%, is absorbed by the oceans and temporarily stored near the surface. The transfer of this heat between the upper ocean and the atmosphere across the surface is called heat flux. The sum of the total heat fluxes into and out of a water volume is denoted as heat budget, and for a stable ocean, it must be balanced, otherwise the whole ocean would heat up or cool down. At the sea surface, the main terms of the heat budget are the insolation (flux of energy into the sea), the net infrared radiation (radiation emitted from the sea), the sensible heat flux (flux of heat out of the sea due to conduction), the latent heat flux (the flux of energy out of the sea, carried by evaporated water) and the advection (heat carried away by currents). Nevertheless, the contribution of these terms over the Earth is not homogenous, since the tropics receive a higher amount of solar energy than the poles. This asymmetric heat distribution tends to be equilibrated through meridional atmospheric cells. Although *Hadley* [1735] proposed a unique convection cell, the Earth's rotation and the conservation of the angular momentum require the existence of three meridional atmospheric cells: Hadley, Ferrel and Polar cells (*Ferrel* [1856]; *Bjerknes* [1921]; Figure 1a). The Hadley cell is a direct cell associated with the meridional thermal gradient established between the tropical band and higher latitudes. The air rises over the equator and displaces poleward, descending in mid-latitudes. At the surface, as a

consequence of the Earth rotation and thus, the Coriolis effect, north-east and south-east trade winds appear in the tropical regions [30°N-30°S] (red arrows, Figure 1a). On the contrary, the Ferrel cell is an indirect thermal cell, characterized by ascending motions around 60° and subsidence in mid-latitudes, given rise to surface westerly winds (yellow arrows, Figure 1a). Finally, in the polar regions the air flows poleward through the upper troposphere and comes back at surface levels, closing the polar cell and creating the surface easterly polar winds (white arrows, Figure 1a).

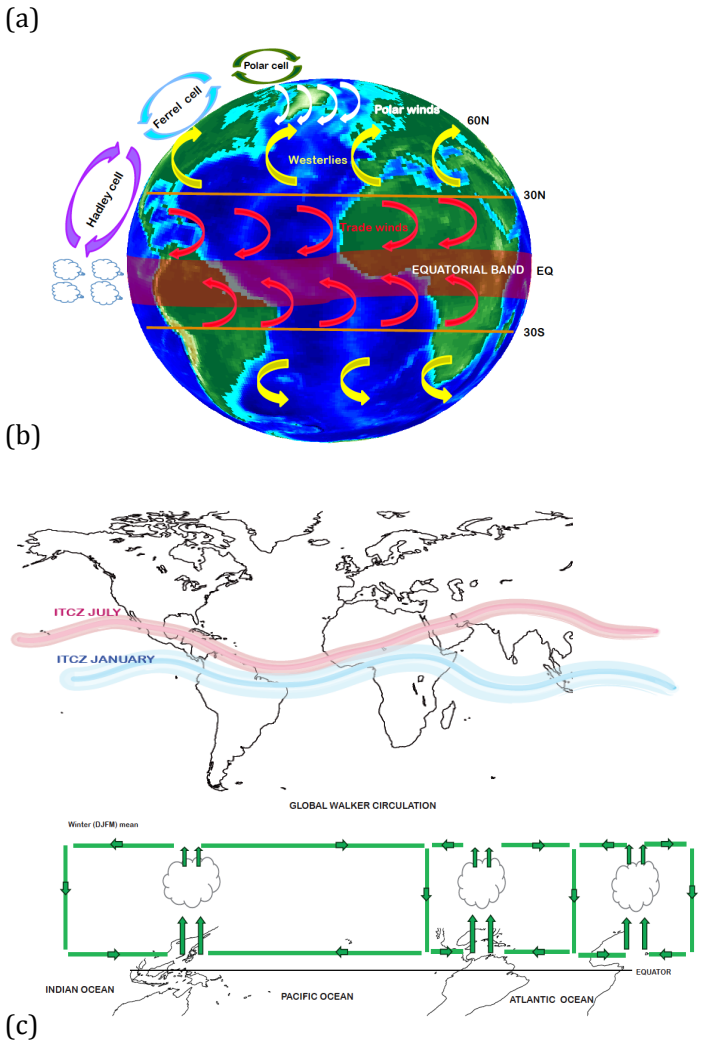

Figure 1. Scheme of the global mean atmospheric circulation. (a) Meridional circulation constituted by the Hadley, Ferrel and Polar cells. meridional circulation. (b) Meridional displacement of the Inter Tropical Convergence Zone (ITCZ). The ITCZ moves northward during boreal summer months and reaches its southernmost position in boreal winter months.(c)Walker circulation in winter months.

In the tropical regions, the convergence of the northern and southern trade winds generates an area of low atmospheric pressure, named as Inter Tropical Convergence Zone (ITCZ). This narrow zone of deep convection and precipitation is often called the 'climate equator' and it is located around 5°N-8°N of the geographical equator, although the ITCZ over land ventures farther north or south than the ITCZ over the oceans due to the variation in land temperatures [*Hastenrath*, 1991; *Mitchell and Wallace*, 1992]. The ITCZ displays meridional excursions across the tropical band along the year. It moves toward the Southern Hemisphere from September to February and reverses direction in preparation for the boreal summer (Figure 1b). The trade winds pile up the warm waters to the west and favour the upwelling of deep cold waters in the eastern side of the basins. As a consequence, the convection is enhanced over the warmest waters and descending motions appear in the east, establishing a zonal atmospheric circulation connecting all the tropical basins named as Walker circulation (Figure 1c; *Gill* [1982]; *Philander* [1990]; *Hartmann* [1994]).

Due to the interaction with the trade winds, a thin surface layer with almost constant temperature and salinity, denoted as mixed layer, is created in the upper ocean. It goes from the surface to 25-500 meters, although its depth varies with location and season (Figure 2, *Steward* [2008]). The warm surface waters of the mixed layer are separated from the colder waters of the deep ocean for a region in which the temperature and salinity decreases rapidly with depth. This region is called *thermocline* and its shape varies at seasonal time scales (Figure 2a). The thermocline can be quite shallow on average in the tropical regions, deeper in the west (around 150-200m) and closed to the surface in the eastern side of the basin (0-50m). The 20°C isotherm is located within this area of maximum vertical temperature gradient. Thus, it should be considered as a measure of the tropical thermocline depth [*Reverdin and McPhaden*, 1986].

(a)

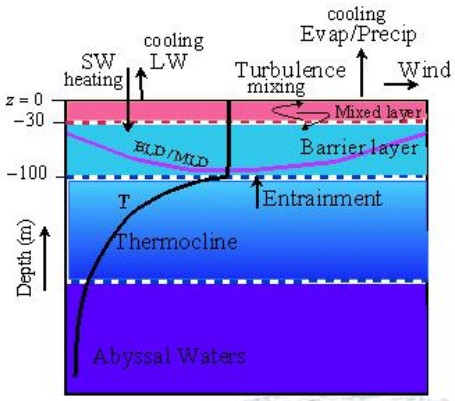

(b)

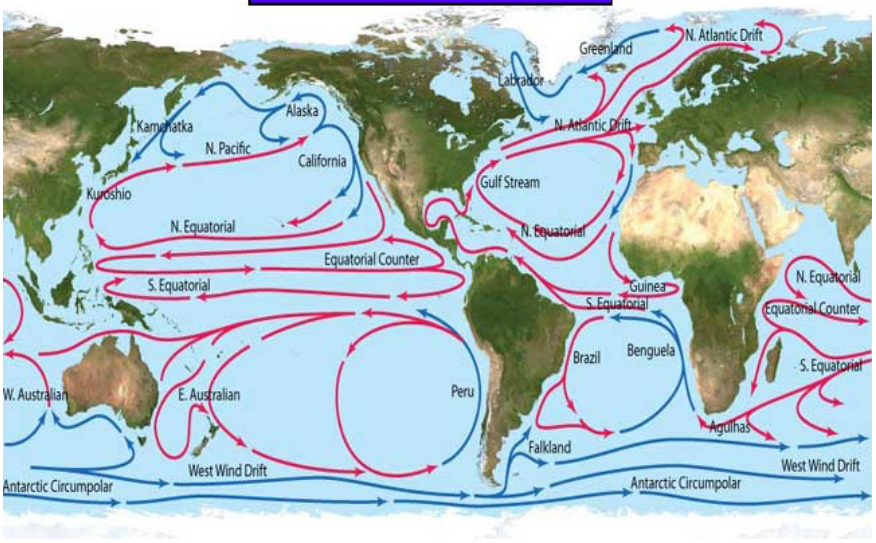

Figure 2. Vertical profile of the ocean and scheme of the oceanic currents. (a) Temperature profile, different layers of the ocean, surface and vertical processes are depicted here. The upper part of mixed layer is well mixed, but in the barrier layer part of the mixed layer, density gradients are dominant (from http://nptel.ac.in/courses/119102007/8). (b) Scheme of the main oceanic currents in the globe (from Bloom (2010) Global Climate Change: Convergence of Disciplines. Sinauer Associates.)

Similar to the atmosphere, the oceans distribute the heat stored in the tropical regions to other local and remote areas through oceanic currents. At the surface, two westward currents appear in the tropical band, the North Equatorial Current (NEC) and the South Equatorial Current (SEC). The accumulation of warm waters in the west is compensated by an Equatorial Under Current (EUC) flows eastward along the equator. From the tropics to higher latitudes, the heat is propagated through meridional currents, which, due to the Earth rotation and the Coriolis effect, are curved given rise to the oceanic gyres (Figure 2b).

The interaction between the trades and the mixed layer is carried out through thermodynamical and dynamical air-sea mechanisms, which control the tropical climate and variability. The climatological trade winds flow westward, pilling warm waters and deepening the thermocline in the west and induce shallower thermocline conditions in the eastern side, favouring the upwelling of cold waters. As a consequence of this zonal SST gradient, the Walker circulation is established, reinforcing the trades and activating the dynamical Bjerknes feedback [*Bjerknes*, 1969]. Another air-sea coupled mechanism operating at the tropical regions is the Wind Evaporation SST (WES) feedback [*Xie and Philander*, 1994; *Carton et al.*, 1996; *Chang et al.*, 1997]. This thermodynamical feedback is associated with the asymmetric meridional distribution of the ITCZ. If the north-eastern trade winds weaken, the heat loss is reduced generating an anomalous warming north of the equator. An inter-hemispheric Sea Level Pressure (SLP) gradient is created as the atmospheric response to these meridional SST pattern, reinforcing the initial wind anomalies [*Xie and Philander*, 1994; *Xie and Arkin*, 1996].

Other important drivers of the tropical climate are the oceanic waves, which appear as a natural adjustment of the ocean to the wind fluctuations and allow connecting the anomalies of different areas of the tropical basin. These waves propagate eastward (Kelvin waves) and westward (Rossby waves), modifying the vertical stratification of the ocean and activating the dynamical feedbacks involved in the development of the SST anomalies [*Matsuno*, 1966; *Moore*, 1968; *França et al.*, 2003; *Polo et al.*, 2008b]. Several studies have documented, the relevant role that oceanic waves have in the development and decay of tropical inter-annual variability modes [*Suarez and Schopf*, 1988; *Polo et al.*, 2008a; *Lübbecke et al.*, 2010].

The climate of the tropical regions has important environmental and socio-economical impacts, since the main economic sources of surrounding countries are based on agriculture and fisheries, which are highly climate-dependent. In particular, three of the main upwelling systems in the world (Mauritania, Benguela and Peru) are located in the tropical Atlantic and Pacific basins. Moreover, the

health and livelihood of millions of people, especially in the semiarid regions of Nordeste (Brazil) and West Africa, are particularly sensitive to inter-annual rainfall fluctuations associated with the intensity and position of the ITCZ [*Nobre and Shukla*, 1996; *Hurrell et al.*, 2005]. Zonal displacements of the convection over the tropical belt, modulates the precipitation regime of adjacent countries, affecting their agricultural production. The principal features of the tropical Pacific and Atlantic climate are described in the following sections.

2.1.1. Seasonal cycle

The seasonal cycle of the tropical regions is governed by the annual migration of the ITCZ. During summer months, when the ITCZ is further north, the trade winds are intensified favouring the upwelling and thus, the development of the equatorial cold tongue in the eastern side of the basin (Figure 3). These anomalous winds pile up the warm waters to the west, deepening the thermocline. A zonal SST gradient is created (shaded, Figure 3), which induces an alteration of the Walker circulation, which in turn, reinforces the original trades, establishing the Bjerknes feedback [*Bjerknes*, 1969].

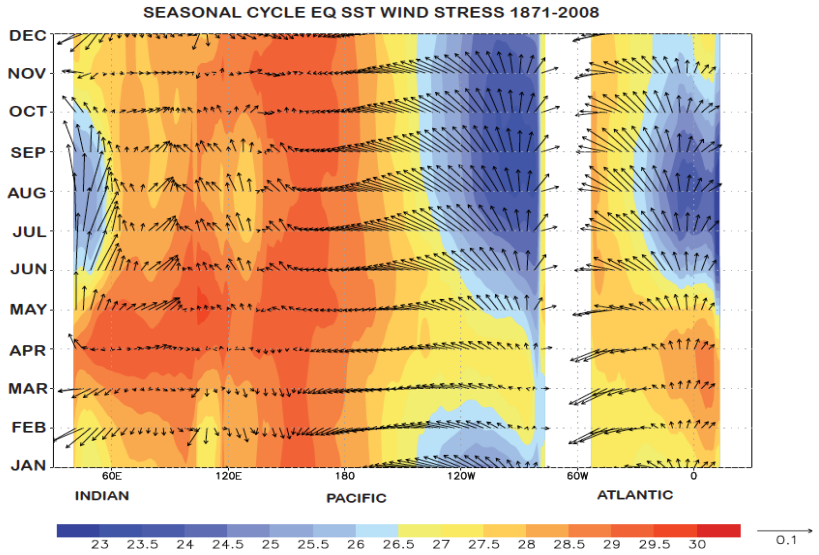

Figure 3. Equatorial seasonal cycle. Time-Longitude climatological SST and wind stress (vectors in m/s) at the Equator. The observations come from HadISST [*Rayner et al.*, 2003] and SODA reanalysis [*Giese and Ray*, 2011]. The period considered is from 1871-2008.

2.1.2. Inter-annual variability

During some years, the seasonal cycle is disrupted and climate anomalies appear in the tropical regions. These anomalous years constitute the inter-annual variability. In the tropics, the variability is governed by multiple influences at different time scales, given rise to variability modes. At inter-annual time scales, the principal modes of tropical Pacific and Atlantic variability are El Niño-Southern Oscillation (ENSO) and the Atlantic Niño, respectively. The main characteristics and impacts of these phenomena are described in the following sections.

2.2. Tropical Pacific inter-annual variability: El Niño-Southern Oscillation

2.2.1. Description of ENSO phenomenon

El Niño–Southern Oscillation (ENSO) is the leading air-sea coupled mode of inter-annual variability in the Tropical Pacific Ocean with worldwide impacts [*Bjerknes*, 1969; *Philander*, 1990]. The atmospheric component of ENSO is the Southern Oscillation (SO), which is defined as the inter-annual oscillation of the Sea Level Pressure (SLP) between the western and the eastern Tropical Pacific [*Walker*, 1924].

El Niño is characterized by a warming and a weakening of the trade winds in the centre-east of the equatorial Pacific. As a consequence, a reduction of the coastal upwelling and a deepening of the thermocline depth take place in the eastern equatorial Pacific. The heating of air masses in this region causes them to rise, leading to deep convection and strong rainfall above it and subsidence at both sides of the basin (Figure 4a). This alteration of the Walker circulation reinforces the initial SST and wind anomalies, activating the Bjerknes feedback [*Bjerknes*, 1969]. The opposite phase of El Niño is denoted as La Niña and implies an intensification of the trades, displacing the warm waters to the west and favouring the development of an anomalous cooling in the central-eastern tropical Pacific. Ascending motions over Indonesia and subsidence next to South American coast, close the anomalous Walker circulation (Figure 4b; *Philander* [1985]; [1990]).

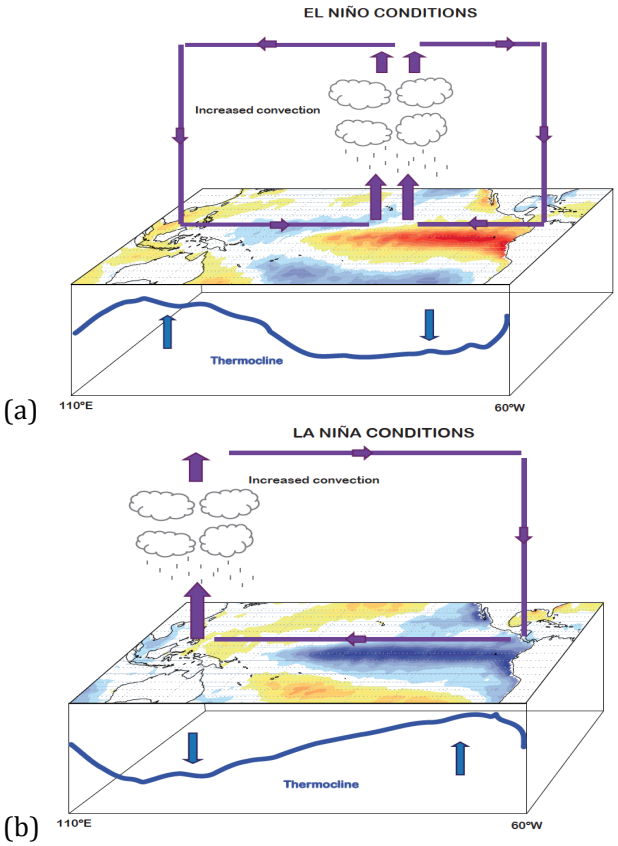

Figure 4. Scheme of El Niño and La Niña phenomenon. Warm, El Niño (a), and cold, la Niña (b), conditions in the tropical Pacific.

Although ENSO phenomenon occcurs in the tropical Pacific, it exerts a strong influence on the global climate (*Annamalai and Slingo* [2001]; *Alexander et al.* [2002]). During el Niño episode, the centre of atmospheric deep convection over the maritime continent is shifted to the central equatorial Pacific, originating an anomalous subsidence over the Indo-Pacific region. This zonal displacement of the convection alters the heat fluxes over the tropical oceans, changing the atmospheric circulation through atmospheric wave adjustment [*Lau and Nath*, 1996; *Klein et al.*, 1999]. An *"atmospheric bridge"* that involves a modification in the Hadley and Walker cells or the triggering of atmospheric Rossby waves, has been proposed as the mechanism to connect the Pacific basin to tropical and extra-tropical regions [*Klein et al.*, 1999; *Alexander et al.*, 2002].

From the early 1980s, a huge effort has been made in order to better understand ENSO phenomena: developing an ENSO observing system [*McPhaden*, 1999], investigating the mechanisms responsible for its development [*Wyrtki*, 1975; *McCreary*, 1983; *Suarez and Schopf*, 1988; *Jin*, 1997; *Neelin et al.*, 1998; *McPhaden*, 1999; *An and Jin*, 2001; *Wang and Fiedler*, 2006] and analysing its variability and global teleconnections [*Federov and Philander*, 2000; *Diaz et al.*, 2001; *Alexander et al.*, 2002; *Wang and An*, 2002; *Yeh et al.*, 2009; *Choi et al.*, 2011; *Yeh et al.*, 2011].

2.2.2. ENSO air-sea interactions

The positive feedback described by [*Bjerknes*, 1969] would lead the equatorial Pacific to a never-ending warm state during el Niño phenomenon. Nevertheless, a cold phase of ENSO, La Niña, is also observed [*Philander*, 1985; *Philander*, 1990]. The processes responsible for the transition between El Niño and La Niña phases are still unclear. Several theories have been proposed, grouped into two frameworks. Firstly, the ENSO can be explained as either a self-sustained oscillatory mode of the coupled ocean-atmosphere system, while, several studies consider ENSO as a stable mode triggered or interacting with stochastic forcing.

Following the first hypothesis, four different oscillatory modes have been proposed: *the delayed oscillator, the recharge oscillator, the western Pacific oscillator* and *the advective-reflective oscillator.*

The *delayed oscillator* considers the eastern Pacific as the only active region in the development and decay of ENSO phenomena. A positive atmospheric-oceanic feedback occurs in the eastern equatorial Pacific, creating the SST anomalies of El Niño. The delayed negative feedback is associated with oceanic Rossby waves, triggered in the east and propagated westward, reflecting in the western boundary. The downweling Rossby wave returns as an upwelling Kelvin wave responsible of reversing the SST anomalies and, in turn, finishing El Niño phenomenon (*McCreary* [1983]; *Suarez and Schopf* [1988]; Figure 5a).

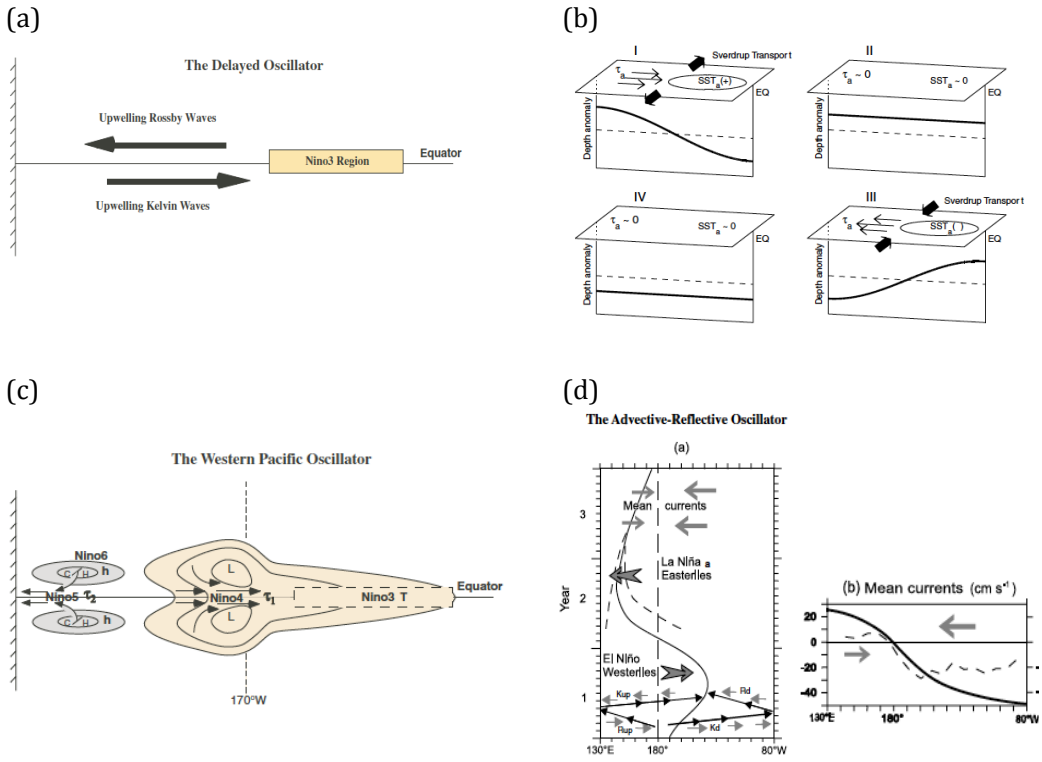

Figure 5. Schemes of the ENSO theories: delayed oscillator (a), the recharge oscillator (b), the western Pacific oscillator (c) and for the advective-reflective oscillator (d) (From *Wang and Fiedler* [2006])

The *recharged oscillator* scheme was described and formulated by *Jin* [1997]. Anomalous westerly winds in west Pacific pile up warm waters in the eastern side and charge gradually the entire tropical Pacific heat content during the onset of the El Niño [*Wyrtki*, 1975; *Wyrtki*, 1985]. A divergence of the Sverdrup transport[1] gives rise to a discharge of the tropical Pacific, reaching a transition phase, in which a shallower thermocline depth allows the pumping of the deep cold waters to the surface, leading the cold phase (Figure 5b).

Weisberg and Wang [1997] proposed a conceptual *western Pacific oscillator model*, highlighting the role of the western Pacific in the development of ENSO SST anomalies. Following the *Gill* [1980] theory, an anomalous equatorial heating induces two symmetric

[1] The Sverdrup transport is the mass transport within the upper ocean driven by the curl of the wind stress. For a stationary and baroclinic flow with small lateral friction and molecular viscosity, the northward mass transport of wind driven currents is equal to the curl of the wind stress

cyclones at both sides of the equator and anomalous westerlies in the equatorial band. These wind anomalies deepen the thermocline depth and warm the eastern equatorial Pacific. On the western side of the basin, the pair of cyclonic circulations originates anomalous easterlies that raise the thermocline depth, favouring the cooling of the off-equatorial western Pacific (Figure 5c). Furthermore, these winds trigger an oceanic Kelvin wave propagating eastward and acting as a negative feedback to El Niño episode [*McPhaden and Yu*, 1999; *Picaut et al.*, 2002; *Boulanger et al.*, 2003].

Finally, the *reflective-advective oscillator* model is based on the role of the zonal currents in the development and termination of ENSO phenomena. *Picaut et al.* [1996]; [1997] demonstrated that the Southern Oscillation is closely linked to the eastern displacement of the oceanic convergence zone in the eastern edge of the western Pacific warm pool. During El Niño event, anomalous westerlies in central Pacific trigger oceanic Kelvin and Rossby waves propagating eastward and westward respectively. The reflection of both waves at the boundaries of the Pacific basin, originates an upwelling Kelvin wave and downwelling Rossby waves accompanied by anomalous zonal currents. These currents are responsible of the termination of El Niño phenomenon, through the displacement of the warm pool to its original position (Figure 5d).

Another point of view for ENSO phenomenon is considering itself as a stable or damped mode, triggered by atmospheric or oceanic stochastic forcing [*Thompson and Battisti*, 2001; *Philander and Fedorov*, 2003]. This hypothesis provides a natural explanation for the irregular ENSO variability and the difficulty to predict those events. The ENSO, as a stable mode, could be perturbed by external atmospheric forcings as the Madden Julian Oscillation (MJO) or the westerly wind bursts or it could be also altered by oceanic perturbations as the tropical instability waves [*Eisenman et al.*, 2005; *Gebbie et al.*, 2007; *Kug et al.*, 2010b]. Despite the different conceptual model of ENSO phenomenon, the main characteristics prevailed: ENSO starts with warmer SSTs in the central Pacific related to a weakening of the trades. The termination of the phenomenon should

be associated with negative feedbacks as the previously ENSO models proposed.

2.2.3. Sources of ENSO and Predictability

Taking into account the influence of ENSO on the global climate and its human, environmental and socio-economic impacts, research efforts have been made to predict ENSO episodes during the last decades. On the one hand, classical ENSO precursors have been determined within the Tropical Pacific basin: the equatorial heat content and the surface winds in western Pacific during previous months are needed to trigger ENSO events, according to the recharge oscillator scheme [*Clarke and Shu*, 2000; *Clarke and Van Gorder*, 2001; 2003]. From this information, statistical ENSO predictions using linear models have been performed, obtaining significant correlation skills [*Barnston and Ropelewski*, 1992; *Latif and Barnett*, 1994; *Clarke and Van Gorder*, 2001; 2003; *Jin et al.*, 2008].

On the other hand, recent studies have put forward that other tropical and extra-tropical regions could also contribute to the development of ENSO episodes. Some authors have proposed a link between the mid-latitudes and equatorial Pacific SST [*Vimont et al.*, 2001; 2003]. An anomalous atmospheric circulation over the north Pacific during winter months, modifies the heat fluxes inducing a SST footprint in north and tropical Pacific that persists until summer months. The damping of the SST anomalies generates an atmospheric response, changing the wind stress[2] in western tropical Pacific and triggering an equatorial Kelvin wave responsible to the development of ENSO phenomenon (Figure 6a; *Vimont et al.* [2001];[2003]). Furthermore, *Anderson et al.* [2013] have indicated that these changes in North Pacific SLP also modify the equatorial heat content, triggering the ENSO episodes according the recharge oscillator theory described by [*Jin*, 1997].

[2] The wind stress is the shear stress exerted by the wind on the sea surface. It is expressed as a function of the wind speed at a certain height above the surface, and has the same direction than the surface wind.

Outside of the tropical Pacific, an important external precursor is the Indian Ocean. *Izumo et al.* [2010] have demonstrated that a negative phase of the Indian Ocean Dipole (IOD[3]) precedes the development of el Niño phenomenon by 14 months. The IOD modulates the Walker circulation in autumn and generates anomalous westerly winds in west Pacific, leading El Niño SST anomalies (Figure 6b). Moreover, *Terray and Dominiak* [2005] added that, apart from the anomalous surface winds in west Pacific, Indian SST anomalies could induce an anomalous Hadley cell in the south-western Pacific, which excites oceanic Rossby waves contributing to create the horseshoe SST pattern of El Niño phenomenon.

Regarding to extra-tropical forcings, *Terray* [2011] has put forward the possible influence of the southern hemisphere mid-latitude variability on ENSO. Subtropical SST anomalies propagate into the tropical Atlantic and Indian Oceans from boreal winter to spring, originating a subsequent dynamical atmospheric response linking the three tropical basins (Figure 6c). This atmospheric response is characterized by a weakening of the equatorial ITCZ, which forces an atmospheric Kelvin wave propagating to the Pacific basin and inducing anomalous surface winds in western Pacific that trigger El Niño episode.

The impact of the external precursors on ENSO predictability has been investigated in recent studies. It has been demonstrated how the inclusion of other tropical and extra-tropical regions improves the prediction of ENSO episodes (Figure 6d, *Dayan et al.* [2013]; *Boschat et al.* [2013]). This result highlights the important role of the external tropical and extra-tropical variability in ENSO forecast, which still remains a challenge for the scientific community.

[3] The Indian Ocean Dipole is an intrinsic mode of variability of the Indian Ocean, similar to ENSO. During a positive IOD, negative SST anomalies appear off Sumatra inducing weaker local convection and easterly winds, which reinforced the initial SST anomalies through the Bjerknes feedback.

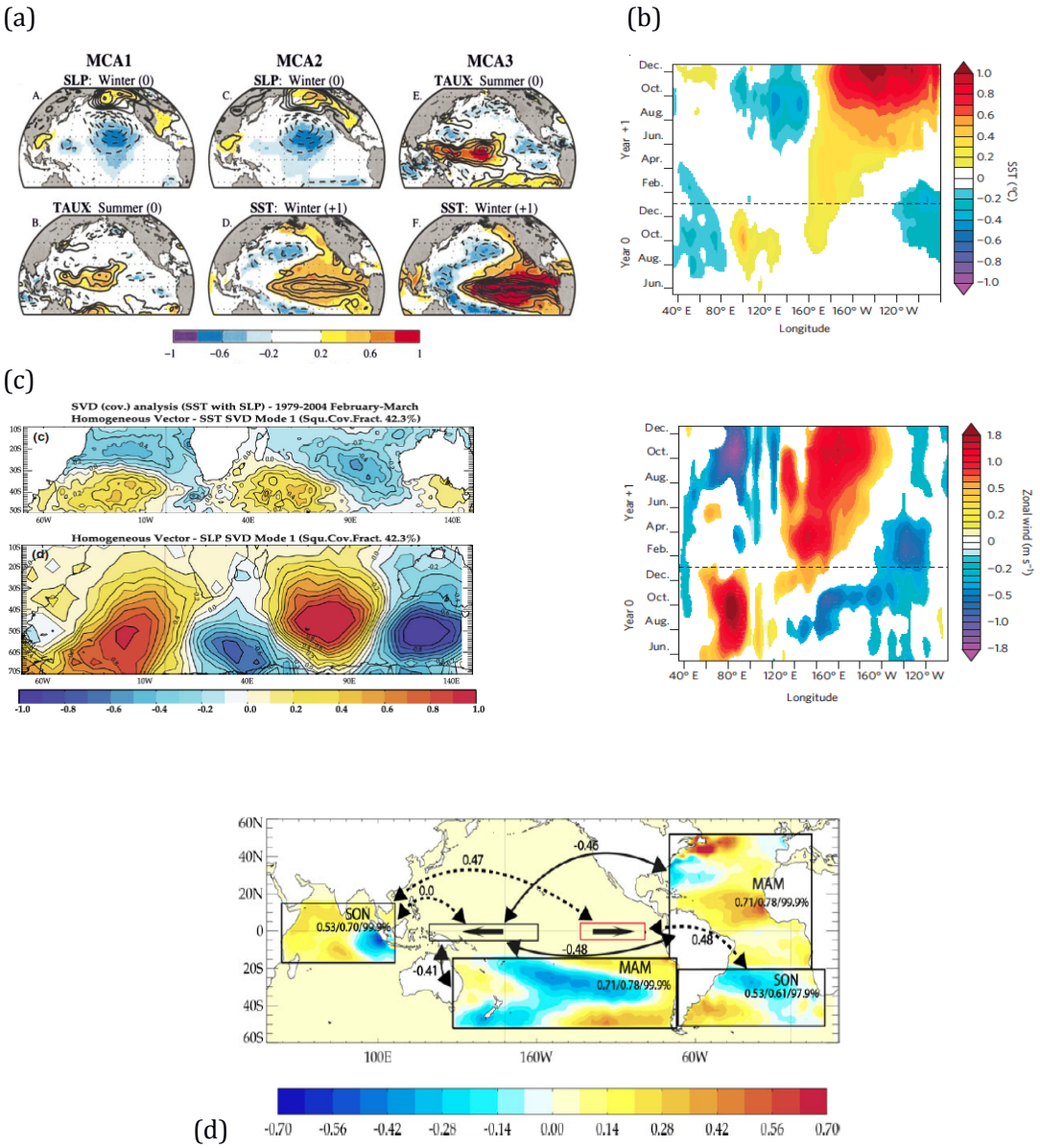

Figure 6. External precursors of ENSO phenomena. (a) Leading heterogeneous patterns for three separate Maximum Covariance Analysis between SLP and zonal wind stress, SLP-SST and taux. From *Vimont et al.* [2001].(b)Longitude-time section of Indo-Pacific observed SST (top) and zonal wind (bottom) over the equatorial Indo-Pacific during and after a negative IOD. From *Izumo et al.* [2010]. (c)Homogeneous maps of leading SVD paired with SLP in February-March for a combined South Atlantic-Indian domain for the period 1979-2004. From *Terray* [2011]. (d) Regression patterns of the first EOF of NTA SST anomalies in MAM over South Pacific SST anomalies in MAM, SA SST anomalies in SON and Tropical Indian SST anomalies in SON. From Dayan et al. 2013

.

2.2.4. ENSO teleconnections

Although ENSO phenomenon takes place in the tropical Pacific, it is able to modulate the global climate [*Slingo and Annamalai*, 2000; *Alexander et al.*, 2002]. In particular, the impact of ENSO on the tropical Atlantic variability has been widely investigated. On the one hand, a warming in North Tropical Atlantic (NTA) during boreal winter and spring is the common response to the previous El Niño episode. A weakening of the northeast trades in NTA reduces the heat loss due to evaporation and entrainment, inducing positive SST anomalies (Figure 7a, top; *Nobre and Shukla* [1996]; *Enfield and Mayer* [1997]; *Saravanan and Chang* [2000]). As a consequence, the ITCZ is shifted to the north, intensifying the southeast trades and favouring the cooling of the equatorial band, given rise to a meridional SST gradient [*Enfield and Mayer*, 1997; *Giannini et al.*, 2001; *Huang et al.*, 2002].

On the other hand, the influence of ENSO phenomena over the South Tropical Atlantic (STA) has been also explored without reaching a consensus [*Münnich and Neelin*, 2005; *Handoh et al.*, 2006b; *Rodrigues et al.*, 2011]. Several authours found that ENSO generates anomalous surface winds in western equatorial Atlantic, which contribute to the development of SST anomalies in the central-east of the equatorial band through equatorial wave dynamics [*Latif and Barnett*, 1994; *Münnich and Neelin*, 2005]. Nevertheless, *Rodrigues et al.* [2011] demonstrated that the characteristics of ENSO phenomena are decisive in the modulation of the tropical Atlantic SST anomalies. It is in agreement with *Handoh et al.* [2006b], who demonstrated that there exist tropical Atlantic SST events independent of ENSO phenomena.

The propagation of the ENSO signal to the Atlantic basin could be carried out through different atmospheric mechanisms. Extra-tropical wave trains, as the Pacific North American (PNA, *Amaya and Foltz* [2014]; *Nobre and Shukla* [1996]; *Handoh et al.* [2006a]) and the Pacific South American (PSA, *Handoh et al.* [2006b]) pattern, or an alteration of the Walker circulation (Figure 7b; *Latif and Barnett* [1994]; *Saravanan and Chang* [2000]; *Chiang and Kushnir* [2000];

Giannini et al. [2001]; *Münnich and Neelin* [2005]; *Wang and Zhang* [2002]) are proposed to link the tropical Atlantic and Pacific basins.

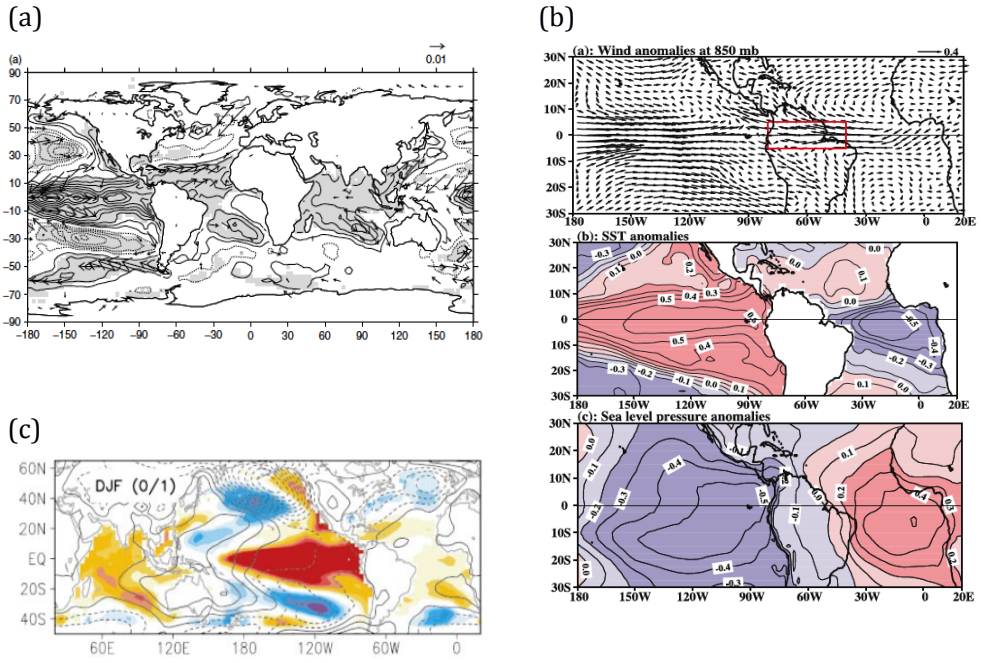

Figure 7. ENSO teleconnections. (a) Global composite anomaly maps for the NTA mode (top) and STA mode (bottom) of SST anomalies (shaded) and wind stress (vectors) for ENSO-associated events. From *Handoh et al.* [2006a](b) Correlation maps of wind anomalies at 850 mb (top), SST anomalies (middle), SLP anomalies (bottom). Positive (negative) correlation is in red (blue) color. From [*Wang*, 2006](c) Observed El Niño composite of SST (shaded) and SLP (grey contours) anomalies in DJFM. From *Alexander et al.* [2002]

The variability of the Indian Ocean is also modulated by ENSO (Figure 7c). El Niño alters the Walker circulation and generates anomalous surface winds in the Indo-Pacific region, which trigger oceanic Rossby waves that change the stratification of the upper ocean, favouring the development of positive SST anomalies [*Lau and Nath*, 1996; *Klein et al.*, 1999; *Lau and Nath*, 2000; *Venzke et al.*, 2000; *Alexander et al.*, 2002; *Lau and Nath*, 2003].

Outside the tropics, a relationship between ENSO and Euro-Mediterranean climate has been documented [*Fraedrich and Müller*, 1992; *Moron and Plaut*, 2003; *Gouirand et al.*, 2014]. The atmospheric ENSO signal propagates to the Euro-Atlantic sector through

atmospheric Rossby waves or the alteration of the Walker and Hadley circulations [*Wang and Zhang*, 2002; *Brönnimann et al.*, 2007]. Moreover, ENSO phenomenon also influences the West African Monsoon system: warmer SSTs in the equatorial Pacific are associated with a reduction of rainfall over the Sahel [*Ward*, 1998; *Janicot et al.*, 2001; *Giannini et al.*, 2003; *Joly et al.*, 2007]. In this sense, when el Niño takes place, the interaction of an atmospheric Kelvin wave propagating from the Pacific to the Atlantic, with a Rossby wave triggered by the anomalous west Pacific-Indian Ocean SST gradient, produce a large-scale subsidence over the Sahel, reducing the seasonal precipitation [*Ward*, 1998; *Janicot et al.*, 2001; *Rowell*, 2001; *Giannini et al.*, 2003; *Joly et al.*, 2007; *Mohino et al.*, 2011].

2.3. Tropical Atlantic inter-annual variability: The Atlantic Niño

The variability of the tropical Atlantic is strongly linked to changes in the location and intensity of the ITCZ [*Moura and Shukla*, 1981; *Hastenrath and Greischar*, 1993; *Nobre and Shukla*, 1996; *Servain et al.*, 1999; *Chiang et al.*, 2002; *Kushnir et al.*, 2003; *Hurrell et al.*, 2005]. The air-sea interactions control the tropical Atlantic variability, given rise to different variability modes. At inter-annual time scales, the leading mode is the Equatorial Mode or Atlantic Niño, nevertheless, the existence of other variability modes as the Meridional Mode, Benguela Niño and South Atlantic Ocean Dipole has been also reported.

2.3.1. Heat budget in the tropical Atlantic

Due to the wind variations or to the propagation of oceanic waves, different air-sea processes are activated in the tropical Atlantic basin, given rise to the development of the SST anomalies. A seasonal heat budget analysis of the tropical Atlantic mixed layer, from observations and modelled data, reveals that, out of the equator, the SST changes are mainly due to surface heat fluxes. Nevertheless, along the equatorial band, the mixed layer temperature change is the result of the balance between the net heat fluxes and the vertical processes [*Foltz et al.*, 2003; *Peter et al.*, 2006].

Regarding to the inter-annual variability, recent studies have put forward the important role of the dynamical oceanic processes in the development of the equatorial SST anomalies [*Vauclair and du Penhoat*, 2001; *Sterl and Hazeleger*, 2003; *Polo et al.*, 2015b], contrasting to the subtropical SST ones, controlled by turbulent fluxes. Nevertheless, *Richter et al.* [2013] demonstrated that during certain years, a 'non-canonical' Atlantic Niño event appears in the tropical Atlantic basin, characterized by warmer SSTs in the north tropical Atlantic, as a consequence of a reduction of the north-eastern trades, which propagate to the equator through meridional advection.

2.3.2. The Atlantic Niño

2.3.2.1 Atlantic Niño description

The Atlantic Niño is the leading air-sea coupled mode of variability akin to ENSO, which emerges in the tropical Atlantic basin at inter-annual time scales [*Merle*, 1980; *Zebiak*, 1993]. It is characterized by a relaxation of the climatological trade winds, which produces a zonal redistribution of the warm waters and heat content in the equatorial band, reducing the thermocline slope [*Carton and Huang*, 1994; *Carton et al.*, 1996; *Ruiz-Barradas et al.*, 2000; *Vauclair and du Penhoat*, 2001]. Warm SST anomalies appear on the eastern equatorial Atlantic, together with an anomalous convergence of the trade winds [*Zebiak*, 1993]. As a consequence, the ITCZ displaces southward generating an enhancement of the convection and rainfall over the entire equatorial band (Figure 8; *Kushnir et al.* [2003];*Carton and Huang* [1994]).

Despite its similarities with its Pacific counterpart, the Atlantic Niño takes place during boreal summer when the tropical Atlantic has its maximum variability [*Carton and Huang*, 1994; *Hurrell et al.*, 2005], contrasting with the winter peak of ENSO phenomena. Moreover, the Atlantic Niño has smaller amplitudes and periods (2-4 years) than ENSO (2-7 years) and it also accounts a minor fraction of the total variance [*Latif and Grötzner*, 2000; *Kushnir et al.*, 2003].

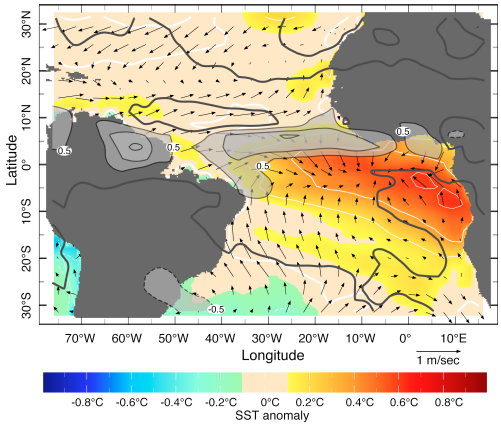

Figure 8. Atlantic Niño pattern. Dominant pattern of tropical Atlantic variability during boreal summer (June-August). It explains 23% of the seasonal variance. (From*Kushnir et al.* [2003]).

2.3.2.2 Atlantic Niño air-sea interactions

The air-sea interactions associated with the tropical Atlantic inter-annual SST variability have been the subject of a handful of studies in recent decades [*Ruiz-Barradas et al.*, 2000; *Keenlyside and Latif*, 2007; *Polo et al.*, 2008a]. The tropical Atlantic present similar characteristics than the tropical Pacific basin: westward surface winds, summer equatorial cold tongue and shallower thermocline in the east, which imply the existence of analogous coupled ocean-atmosphere feedbacks [*Keenlyside and Latif*, 2007].

a) Bjerknes feedback

A Bjerknes feedback mechanism akin to that acting in ENSO exists in the tropical Atlantic basin [*Houghton and Tourre*, 1992; *Zebiak*, 1993; *Carton and Huang*, 1994; *Chang et al.*, 2000; *Sutton et al.*, 2000; *Kushnir et al.*, 2003; *Keenlyside and Latif*, 2007]. Anomalous warm events emerge in the eastern tropical Atlantic, as a consequence of a weakening of the equatorial trades, which induce a deepening of the thermocline depth [*Houghton and Tourre*, 1992; *Zebiak*, 1993; *Carton and Huang*, 1994; *Chang et al.*, 2000; *Sutton et al.*, 2000; *Kushnir et al.*, 2003; *Keenlyside and Latif*, 2007]. The coupling between the wind variations and the oceanic dynamics is carried out through the

Bjerknes feedback (Figure 9; *Keenlyside and Latif* [2007]). Anomalous surface winds in western equatorial Atlantic induce Sea Level Anomalies (SLA), which favour the development of SST anomalies in the eastern side of the basin [*Servain et al.*, 1982; *Hirst and Hastenrath*, 1983; *Zebiak*, 1993]. However, the Bjerknes feedback in the tropical Atlantic is weaker and less dominant than in the Pacific basin, accounted only the 10% of the total variance, and seems to operate during boreal summer and fall [*Sutton et al.*, 2000; *Keenlyside and Latif*, 2007].

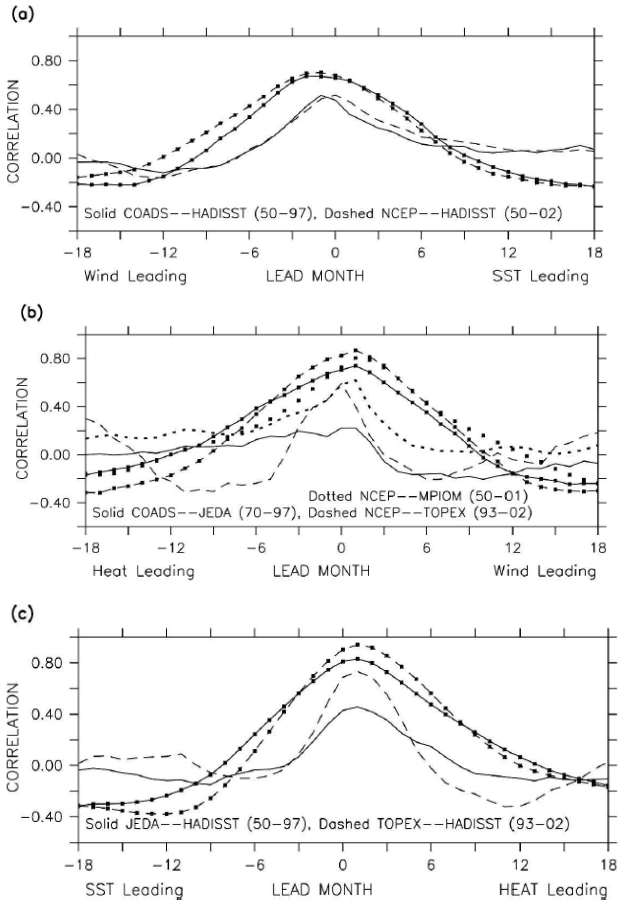

Figure 9. Bjerknes feedback in the tropical Atlantic. (a) Cross correlation between Atl3 SST anomalies and WAtl zonal wind (solid) and zonal surface wind stress (dashed); (b) between WAtl zonal wind speed with Atl3 400-m heat storage anomalies (solid), WAtl zonal surface stress with Atl3 SLA (dashed) and OGCM simulated 400-m average temperature anomalies (solid with square); (c) and between Atl3 400-m HST and Atl3 SST anomalies (SSTA, solid), Atl3 SLA and Atl3 SSTA (dashed). From *Keenlyside and Latif* [2007].

b) Equatorial oceanic waves

In addition to the air-sea interactions involved in the Bjerknes feedback, the oceanic waves could also play an important role in the tropical Atlantic variability [*França et al.*, 2003; *Polo et al.*, 2008b; *Hormann and Brandt*, 2009]. Wind stress variations in the western equatorial Atlantic could trigger oceanic Kelvin waves, which propagate eastward along the equator and poleward along the African coast, favouring the creation of the equatorial SST anomalies (Figure 10a; *Moore et al.* [1978]; *Servain et al.* [1982]; *Lübbecke et al.* [2010]).

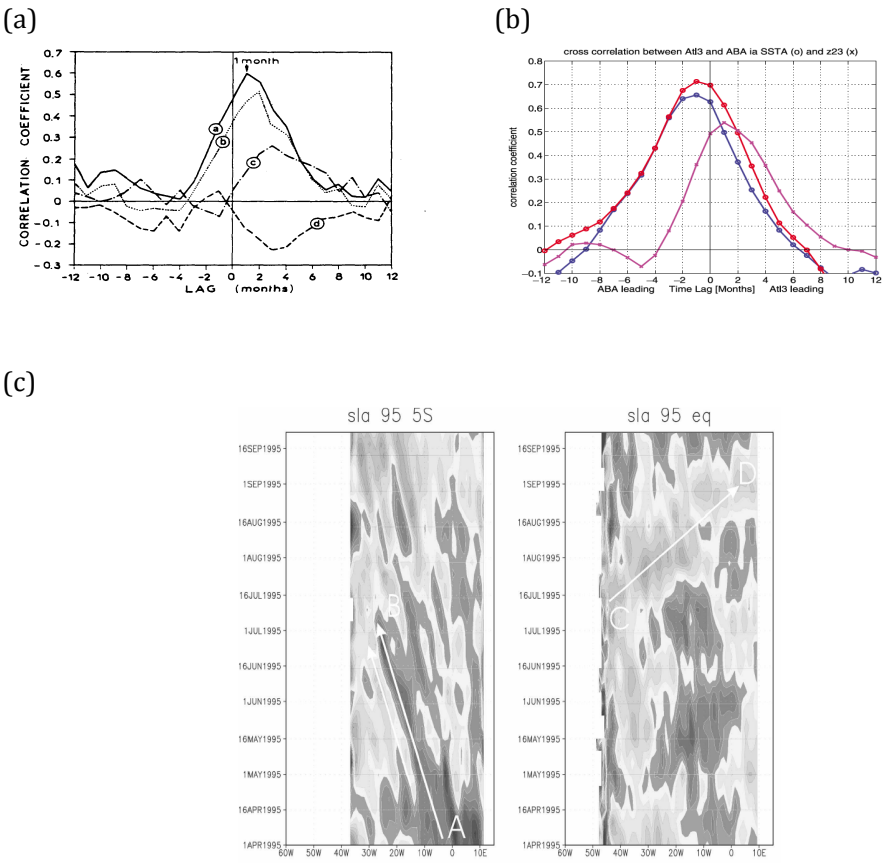

Figure 10. Role of the oceanic waves in the Atlantic Niño phenomenon.(a) Lead-Lad correlation between zonal wind stress next to Brazilian coast (BR) and SST in west Guinea (GW, curve a), zonal wind stress in BR with SST in north Guinea (GN,curve b), wind stress in GW and SST in GW (curve c) and meridional wind stress in GW and SST in GW (curve d). From *Servain et al.* [1982]. (b) Cross-correlation between Atl3 index and ABA SST and thermocline depth from model (red) and obs (blue). From *Lübbecke et al.* [2010]. (c) SLA from April to September along 5S (left) and the equator (right) for 1995. From *Polo et al.* [2008a].

Latif and Grötzner [2000] suggested that these anomalous winds in western equatorial Atlantic are forced by ENSO phenomena. Nevertheless, other authors indicated that these surface wind anomalies take part of a weakening of the Sta Helena High Pressure System [*Lübbecke et al.*, 2010]. Additionally, these authors suggested that the propagation of these equatorial Kelvin waves could also contribute to the development of SST anomalies in Benguela region, preceding by 3 months the equatorial ones (Figure 10b; *Lübbecke et al.* [2010]; *Florenchie et al.* [2003]). On the other hand, *Polo et al.* [2008a] demonstrated that local winds along Benguela coast could excite Rossby waves propagating westward and contributing to the development of the off-equatorial Atlantic Niño SST anomalies (Figure 10c).

2.3.3. Other Tropical Atlantic variability modes

2.3.3.1 Meridional Mode

The Meridional Mode (MM) or Inter-hemispheric Mode is characterized by a meridional SST gradient north and south of the equator. For a positive phase, warmer SSTs are located in NTA, while an anomalous cooling covers the equatorial and STA. This inter-hemispheric gradient is associated with a northward displacement of the ITCZ, which originates cross-equatorial surface wind anomalies and dry conditions in Northeast Brazil (Figure 11; *Moura and Shukla* [1981]; *Nobre and Shukla* [1996]; *Enfield and Mayer* [1997]; *Chiang et al.* [2002].

The Meridional Mode peaks in boreal spring when the NTA SST has its maximum variability and thus, can be forced externally, most prominently by the ENSO phenomenon and the North Atlantic Oscillation, NAO [*Czaja et al.*, 2002; *Czaja*, 2004]. The MM presents a strong decadal component [*Enfield and Mayer*, 1997; *Dommenget and Latif*, 2000] and seems to be developed by thermodynamic air-sea interactions [*Carton et al.*, 1996; *Ruiz-Barradas et al.*, 2000]. In particular, *Chang et al.* [1997] proposed that the MM is controlled by

the WES feedback. As a consequence of the anomalous meridional SST gradient, the ICTZ moves northward, intensifying the south-easterly winds in the STA and weakening the trades north of the equator. As a result, the surface heat flux is reduced and the initial SST gradient is reinforced [*Xie and Philander*, 1994; *Carton et al.*, 1996; *Chang et al.*, 1997].

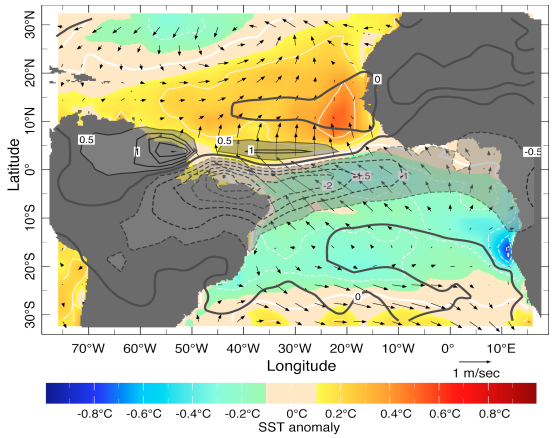

Figure 11. Meridional Mode. First mode of the tropical Atlantic variability during boreal spring. It explains the 33% of the seasonal variance (From *Kushnir et al.* [2003]).

2.3.3.2 Benguela Niño

Pronounced warm events have been also manifested off the coast of Angola, denoted as Benguela Niños (Figure 12; *Shannon et al.* [1986]). This phenomenon represents the most prominent mode of low frequency variability in the southeast Atlantic, with significant impacts on local fisheries and southern African rainfall [*Hirst and Hastenrath*, 1983; *Rouault et al.*, 2003; *Hurrell et al.*, 2005; *Rouault et al.*, 2007]. Inter-annual SST fluctuations in the Angola–Benguela Area (ABA) occurs during boreal spring and seem to be associated with the local [*Polo et al.*, 2008a; *Richter et al.*, 2010] or remote [*Lübbecke et al.*, 2010] wind forcing. *Polo et al.* [2008] showed that a weakening of the alongshore winds reduces the upwelling over the Benguela front, and, consequently, modifies the SST and the thermocline depth over

that region. In contrast, *Lübbecke et al.* [2010] proposed that the Benguela Niños are remotely forced by equatorial wind anomalies. Anomalous westerlies in western equatorial Atlantic could trigger an oceanic Kelvin wave, propagating along the equator and the south African coast, impacting in the thermocline depth and thus favouring the warming of Benguela area during the spring.

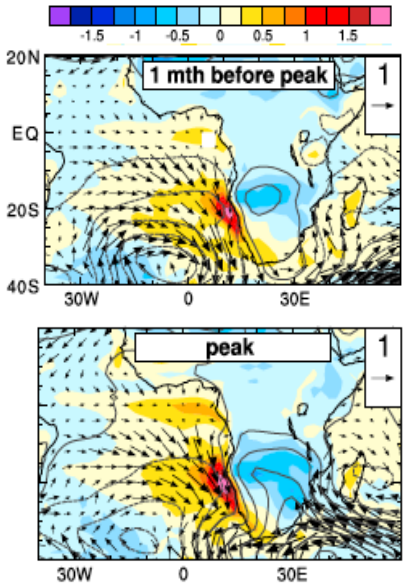

Figure 12. Benguela Niño. Horizontal maps of simulated anomalous SST (shaded), surface wind stress (arrows) and SLP (contours) composited on the ABA SST index. From *Richter et al.* [2010].

2.3.3.3 South Atlantic Ocean Dipole (SAOD)

Recent studies have documented the existence of a South Atlantic Ocean Dipole (SAOD), characterized by anti-correlated SST anomalies between the equatorial and the south-western south tropical Atlantic (Figure 13; *Nnamchi et al.* [2011a]). Warm SST anomalies first appear off the coast of Angola, while simultaneously an anomalous cooling emerges in the south-western STA. North-westerly winds emanating along the Argentina coast blow northward and converge at the equatorial band with the anomalous south-easterly winds, helping to develop the equatorial warm anomalies (arrows, Figure 13).

Although the SAOD has a life cycle of about eight months, its peak is observed during boreal summer, in which the SST anomalies are strongly coupled to atmospheric circulation and precipitation anomaly fields. In particular, the positive phase of the SAOD (warmer SSTs in the eastern equatorial Atlantic and negative ones in the south-western Atlantic) is related to an increase of precipitation in the Gulf of Guinea [*Nnamchi and Li*, 2011b; *Nnamchi et al.*, 2013].

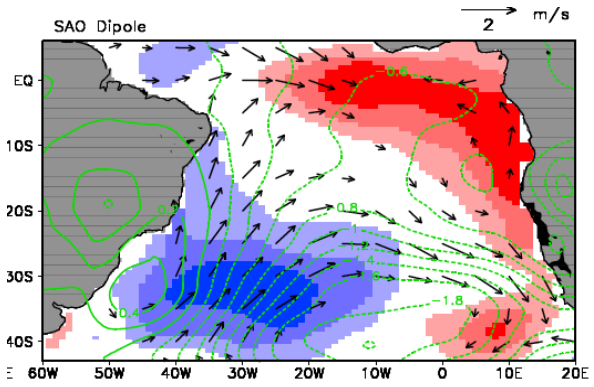

Figure 13. South Atlantic Dipole Ocean. (b) Composite averages of the SST, surface winds, and SLP anomalies illustrating the SAOD (1951, 1963, 1974,1996, and 1999). SAOD composites are based on Atl-3 index ≥0.5°C and SSTASWP ≤−0.5°C. From *Nnamchi et al.* [2011a]

2.3.4. Atlantic Niño teleconnections

The Atlantic Niño is highly coupled to the rainfall variability of adjacent areas. In particular, a strong impact over the West African Monsoon (WAM) system has been documented [*Lamb*, 1978; *Janicot*, 1992; *Wagner and da Silva*, 1994; *Rowell et al.*, 1995; *Ward*, 1998; *Polo et al.*, 2008a; *Losada et al.*, 2012a]. Warmer SSTs in the equatorial Atlantic produces lower meridional SST gradient that inhibits the northward displacement of the convection belt, weakening the monsoon circulation [*Losada et al.*, 2010a]. This modification in the atmospheric circulation gives rise to a dipolar precipitation pattern, with increased rainfall in the Gulf of Guinea (GG) and a reduction of the precipitation over the Sahel (Figure 14a; *Lamb* [1978]; *Janicot* [1992]; *Wagner and da Silva* [1994]; *Rowell et al.* [1995]; *Ward* [1998]; *Polo et al.* [2008a]; *Losada et al.* [2012a]).

On the other hand, the influence of the Atlantic Niño phenomenon on the Indian Monsoon has been also reported. Positive SST anomalies in the south tropical Atlantic excite an atmospheric Kelvin wave which originates descending motions over the Indian basin, reducing the Indian Monsoon rainfall during spring and summer months (Figure 14b; *Kucharski et al.* [2007]; [2008; 2009])

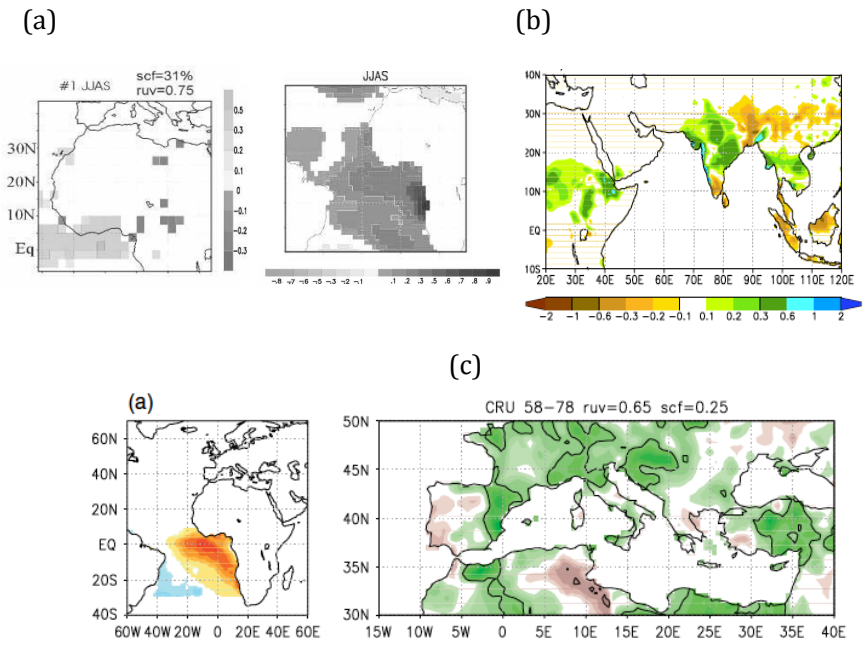

Figure 14. **Atlantic Niño teleconnections.** (a) First leading mode of Extended Maximum Covariance analysis between the Tropical Atlantic SSTs and the precipitation over the WAM (from *Polo et al.* [2008a]). (b) Regression onto the tropical Atlantic SST index over the CRU rainfall. (From *Kucharski et al.* [2008]). (c)Left: Homogeneous SST map for JAS season; Right: Heterogeneous precipitation map for JAS season (from *Losada et al.* [2012a]).

The climate of remote areas can be also modulated by the Atlantic Niño phenomenon, through climate teleconnections. In this sense, anomalous SSTs in the equatorial Atlantic during summer months could excite atmospheric Rossby waves from the western and central tropical Atlantic Ocean [*Peng et al.*, 2005; *García-Serrano et al.*, 2008], modifying the NAO pattern during the next autumn and winter [*Cassou et al.*, 2004; *Peng et al.*, 2005; *García-Serrano et al.*, 2008]. Moreover, a warming in tropical Atlantic is also associated with cold

and wet conditions in the central-western Mediterranean basin (Figure 14c; *Ward* [1998]; *Baldi et al.* [2004]. This teleconnection is carried out through an alteration of the Hadley cell, modulated by the WAM [*Baldi et al.*, 2004; *Gaetani et al.*, 2010], or by atmospheric Rossby waves triggered from the Caribbean region [*Cassou et al.*, 2004; *Peng et al.*, 2005; *García-Serrano et al.*, 2008].

2.3.4.1.1 Atlantic Niño forcings

The Atlantic Niño phenomenon is triggered by an anomalous relaxation of the tropical trade winds. Nevertheless, the origin of these anomalous winds remains unclear. Recent studies have put forward that this wind forcing could take part of a large-scale pattern associated with a weakening of Sta Helena High (Figure 15; *Lübbecke et al.* [2010]; *Richter et al.* [2010]; *Polo et al.* [2008a])..

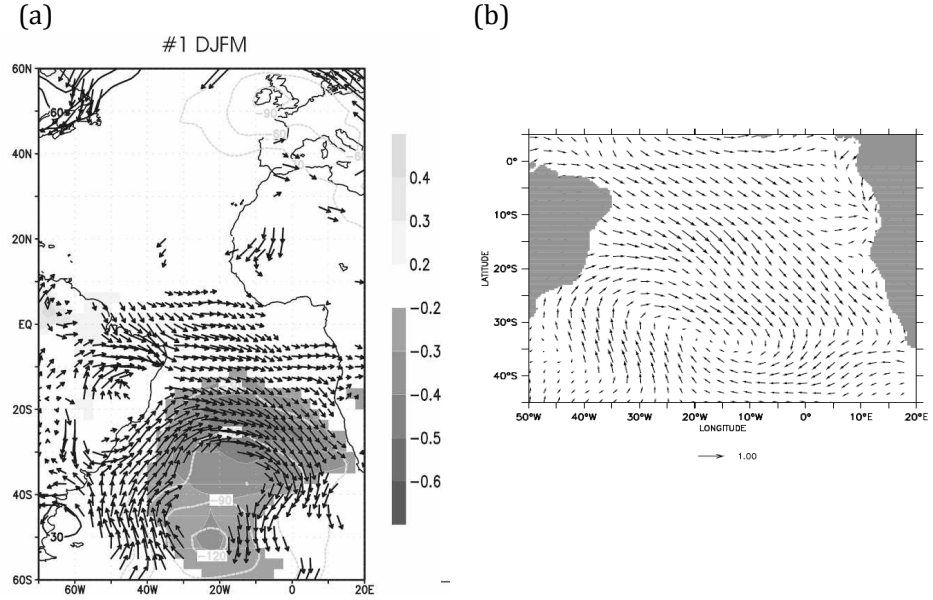

Figure 15. Subtropical atmospheric forcing of the Atlantic Niño.(a) Regression of the total SST expansion coefficient associated with the leading EMCA mode (Atlantic Niño) onto the surface wind anomalies (vectors) and the SLP (shaded) for December-January-February-March (DJFM). From *Polo et al.* [2008a]. (b)Correlation between the time series of April SST anomalies averaged over the ABA and wind stress in February from ORCA05-REF for the time period 1958-2000. From *Lübbecke et al.* [2010].

Nevertheless, other authors pointed out the role of external forcings as the North Atlantic Oscillation (NAO) and ENSO phenomena [*Latif and Grötzner*, 2000; *Saravanan and Chang*, 2000; *Okumura et al.*, 2001] in modulating the tropical Atlantic inter-annual variability

2.3.4.1.2 North Atlantic Oscillation (NAO)

The North Atlantic Oscillation (NAO) is the leading atmospheric mode of climate variability in the North Atlantic region and it is characterized by a see-saw pattern of SLP anomalies between Azores and Iceland [*Rogers*, 1984; *Hurrell*, 1995; 2001]. The fluctuations in the SLP field associated with the Azores High, induce changes in the surface winds, modulating the climate over the Euro-Mediterranean and North American region [*Marshall et al.*, 2001] as well as the variability of NTA SSTs [*Czaja et al.*, 2002; *Mélice and Servain*, 2003]. Nevertheless, *Okumura et al.* [2001] suggested that an inter-hemispheric dipole SST pattern in the tropical Atlantic could generate a NAO-like response, thus an interaction between the tropical and extra-tropical via Azores High variability seems to exist in the Atlantic basin [*Xie and Tanimoto*, 1998].

2.3.4.1.3 El Niño-Southern Oscillation (ENSO)

The ENSO influence on the north tropical Atlantic variability has been widely demonstrated. However, its contribution to equatorial and south tropical Atlantic SSTs is ambiguous and inconsistent. On the one hand, several studies suggested that ENSO originates anomalous surface winds in western equatorial Atlantic [*Latif and Grötzner*, 2000; *Münnich and Neelin*, 2005] through changes in the Walker circulation, modifying the location and strength of the ITCZ [*Chiang and Kushnir*, 2000; *Münnich and Neelin*, 2005; *Wang and Fiedler*, 2006]. These wind fluctuations favour the development of equatorial SST anomalies through the activation of oceanic dynamical mechanisms [*Latif and Grötzner*, 2000; *Keenlyside and Latif*, 2007]. Although the common atmospheric mechanism proposed to carry out this inter-basin teleconnection is the Walker circulation [*Wang and Zhang*, 2002; *Wang*, 2005; 2006], atmospheric wave trains emanating

from the central tropical Pacific, and travelling via South America, are also suggested as the mechanism responsible to connect the Pacific and the Atlantic basins [*Handoh et al.*, 2006b].

On the other hand, several discrepancies about the ENSO impact on the Atlantic Niño phenomenon have been documented. Some authors have indicated that the effectiveness of the ENSO influence on the tropical Atlantic variability depends on the interference between the ENSO atmospheric signal and the basic state of the equatorial Atlantic thermocline [*Chang et al.*, 2006]. In the same line, *Rodrigues et al.* [2011] have argued that the characteristics of ENSO phenomena are crucial to the establishment of the inter-basin connection. This inconsistent relationship has been attributable to the existence of a delayed negative feedback in the tropical Atlantic [*Lübbecke and McPhaden*, 2012]. In this way, a pronounced warming in the NTA, appeared as a response of the ENSO phenomena, would produce a stronger meridional SST gradient, which would lead wind stress anomalies north of the equator. These anomalous winds would trigger downwelling Rossby waves propagating westward, reaching the western boundary and reflecting into downwelling equatorial Kelvin waves. The propagation of the Kelvin wave along the equator counteracts the initial cooling due to the boreal winter wind stress response to El Niño. Nevertheless, for a weaker warming in NTA, the equatorial cooling associated with the northward displacement of the ICTZ, as a consequence of the ENSO impact, persists or is even amplified [*Rodrigues et al.*, 2011; *Lübbecke and McPhaden*, 2012].

2.4. The Atlantic influence on ENSO

2.4.1. Connection between the inter-annual tropical Atlantic and Pacific variability

During the last years, the role of the Atlantic Ocean in modulating the tropical Pacific variability has been highlighted [*Wright*, 1986; *Mélice and Servain*, 2003; *Keenlyside and Latif*, 2007; *Polo et al.*, 2008a; *Jansen et al.*, 2009; *Rodríguez-Fonseca et al.*, 2009; *Ding et al.*, 2012]. In a former paper, *Mélice and Servain* [2003] showed that SST anomalies of the STA lead the Southern Oscillation (SO) ones by 4

months (Figure 16a). Moreover, several studies reported a strong anti-correlation between the summer equatorial Atlantic SST anomalies and the tropical Pacific ones during next winter (Figure 16b-e; *Keenlyside and Latif* [2007]; *Polo et al.* [2008a]). Similar results were obtained by *Jansen et al.* [2009], using a recharge oscillator scheme to predict ENSO phenomena. Nevertheless, these studies did not give any special attention to the Atlantic-Pacific connection or the dynamical mechanisms at work.

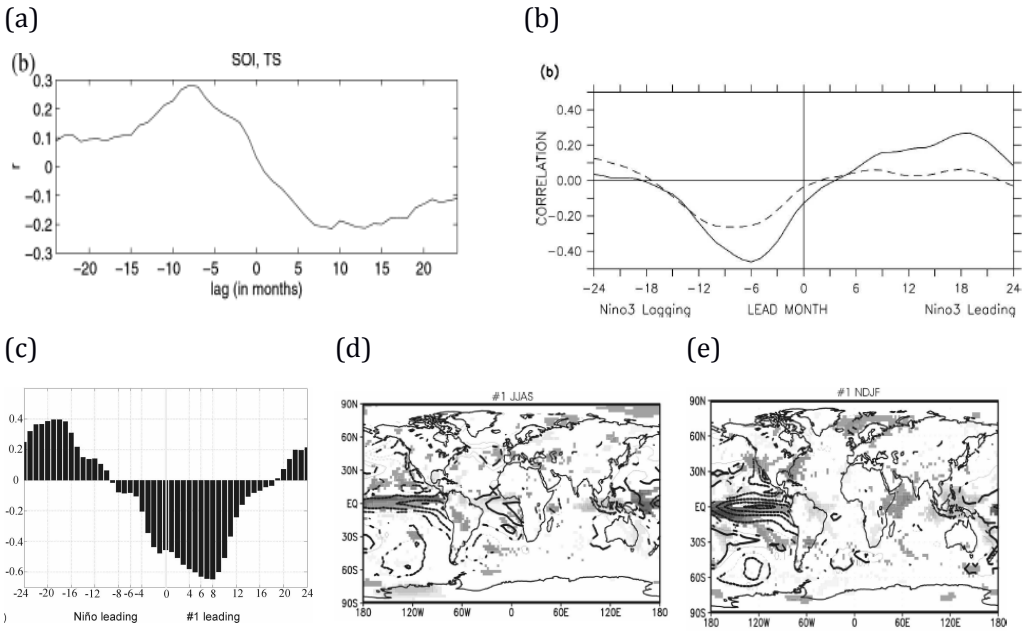

Figure 16. Connection between Atlantic and Pacific inter-annual variability. (a) Lagged correlation coefficient from -24 to 24 months between the Souther Oscillation index (SOI) and the Tropical South (TS) Atlantic SST anomalies. From *Mélice and Servain* [2003] (b) Cross-correlation between Niño3 and Atl3 averaged SST anomalies. Solid lines are for the period 1970-2003 and dashed line are for the period 1870-2003. From *Keenlyside and Latif* [2007]. (c) Correlation coefficient between the leading mode SST expansion coefficient and Niño3 index, leading and lagging 24 months. (d-e)Regression of the total SST expansion coefficient associated with the leading EMCA mode onto the global SST anomalies. From *Polo et al.* [2008a]

Rodríguez-Fonseca et al. [2009] analysed for the first time the active role of the equatorial Atlantic SSTs in triggering the ENSO phenomena. It was demonstrated, from observations and partially coupled simulations, that a summer Atlantic Niño (Niña) is able to favour the development of the Pacific La Niña (El Niño) during next winter from the 1970s (Figure 17). Before the 1970s, an Atlantic Niño characterized by a warming in the equatorial Atlantic and negative SST anomalies in north and south Tropical Atlantic, appeared alone in the tropical basin, without any associated SST signal in the Pacific Ocean (Figure 17a-b). Nevertheless, after the 1970s, an Atlantic Niño with positive SST anomalies covering the entire tropical Atlantic appears related to negative SST anomalies in the equatorial Pacific during summer months, which resemble a completely developed la Niña pattern during next winter (Figure 17c-d).

Rodríguez-Fonseca et al. [2009] also investigated the atmospheric mechanism involved in the inter-basin connection and proposed that when an Atlantic Niño takes place, the convection is enhanced over the equatorial Atlantic, modifying the Walker circulation and linking both tropical basins (Figure 17c-d). Anomalous subsidence in central Pacific could originate a surface wind divergence, altering the thermocline depth and thus favouring the development of La Niña cold tongue (Figure 17e-j ; *Rodríguez-Fonseca et al.* [2009]).

Nevertheless, several aspects about the role played by the Atlantic Niños in the modulation of the tropical Pacific variability are still unresolved. Further research about the oceanic processes at work in the development of ENSO phenomena associated with the remote Atlantic forcing is required.

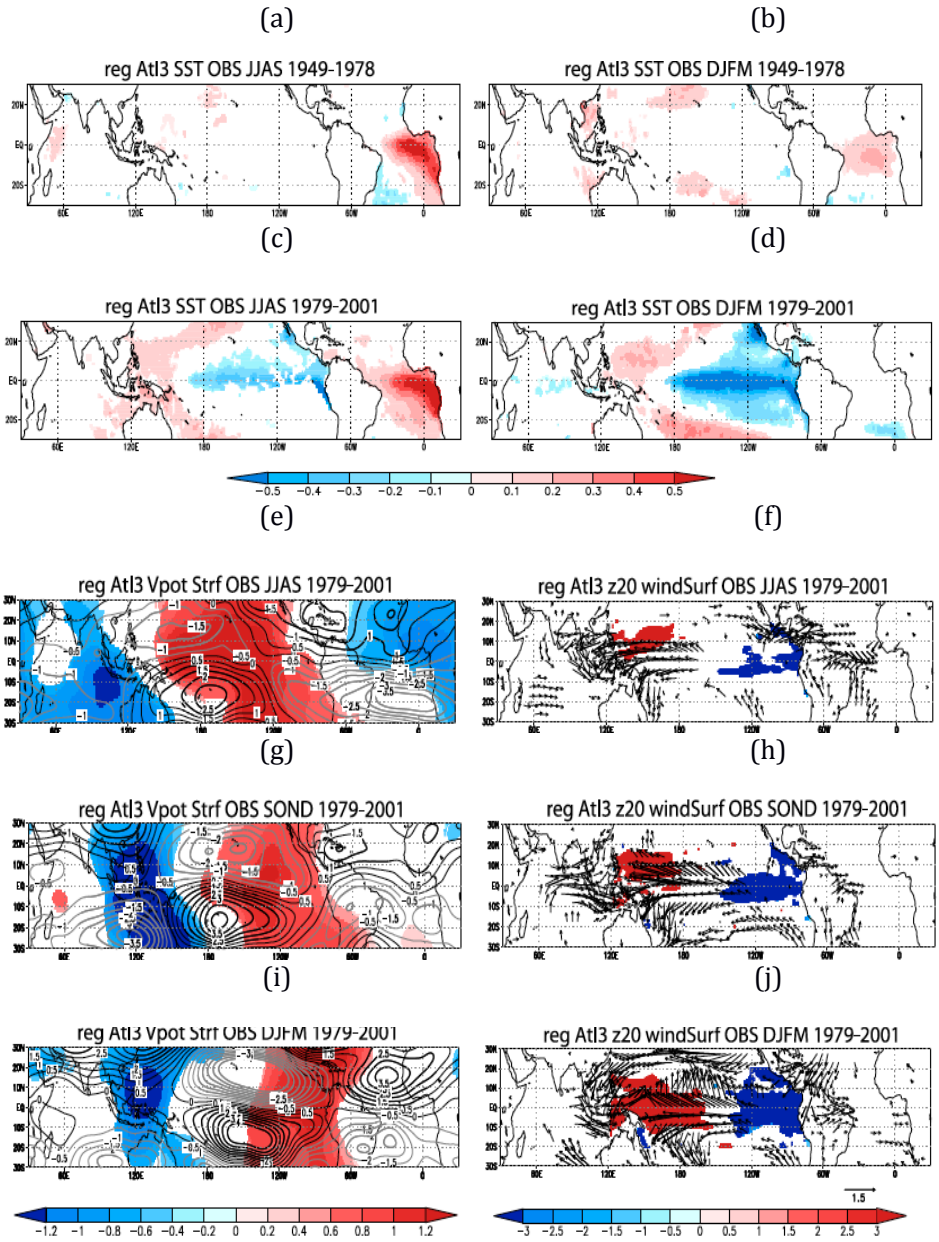

Figure 17. Atlantic Niños (Niñas) -Pacific Niñas (Niños) connection after the 1970s (a-d) Tropical Pacific SST response to summer Atlantic Niño for different time-periods. Observed anomalous SST (in C) regressed onto the boreal summer Atl3 index for the period 1949-1978 and 1979-2001 in summer and the following winter. (e-j) Dynamical response to summer Atlantic Niño. Observed anomalous velocity potential (shaded in 10^{-6} m^2/s) and streamfunction (contous in 10^{-6} m^2/s) at 200 hPa regressed onto boreal summer Atl3 index for the period 1979-2001. Only significant areas that exceed 95% confidence level are shown. From *Rodríguez-Fonseca et al.* [2009]

Recently, the connection between the Atlantic Niños (Niñas)-Pacific Niñas (Niños) has been confirmed by a more resolution-coupled model, given robustness to this finding (Figure 18a; *Ding et al.*, [2012]). Although *Ding et al.*, [2012] corroborated the results of *Rodríguez-Fonseca et al.* [2009], the former authors posed that the Atlantic influence on ENSO was stationary on time and independent on the period considered (Figure 18b), while *Rodríguez-Fonseca et al.* [2009] argued that the Atlantic-Pacific connection only occurred after the 1970s (Figure 18c).

To determine when the Atlantic-Pacific Niños connection takes place during the whole observational period is needed, in order to shed light about the stationary or non-stationary behaviour of this inter-basin link and its relation to the multidecadal variability.

During the last years, the possible contribution of NTA SST anomalies to the development ENSO phenomena has been also investigated. *Ham et al.* [2013a] have demonstrated that the NTA SSTs could trigger Central-Pacific (CP) ENSO episodes through a subtropical atmospheric teleconnection along the Pacific ITCZ. A warming (cooling) in NTA during the spring induces low-level anticyclonic (cyclonic) circulation over western Pacific, generating anomalous easterlies (westerlies) that contribute to cool (warm) the central Pacific during winter months (Figure 18d-e). This NTA-ENSO connection differs from the Atlantic Niño influence, since the latter one is carried out through an anomalous Walker circulation and tends to create Eastern-Pacific (EP) ENSO events (Figure 18f-g, *Ham et al.* [2013b]).

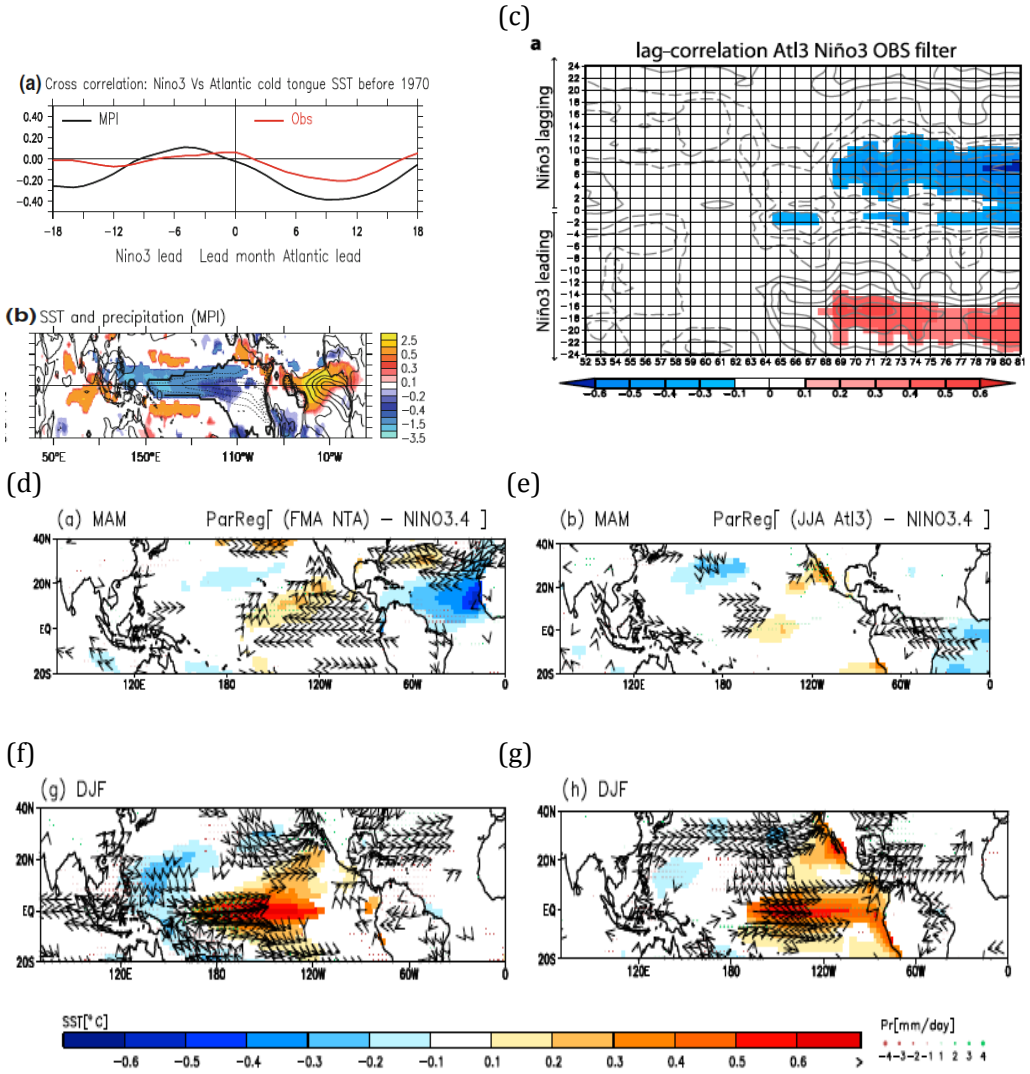

Figure 18. Non-stationary relationship between the tropical Atlantic variability and ENSO (a) Twenty year lead-lag correlation, running one year from 1952–1972 to 1981–2001, between the observed summer Atl3-index (JJAS) and Niño3-index, for positive (from 0 to 24 months after summer) and negative (from 0 to 24 months before summer) lags. From *Rodríguez-Fonseca et al.* [2009].(b) SST (contour) and precipitation (shaded) regressed onto boreal summer Atlantic cold tongue SST from model ensemble mean.(c) Cross-correlation between Niño3 and Atlantic cold tongue SSTs from HadISST (1900-1970, red line) and the ensemble mean (1955-1970) of MPI model simulations with the observed SST prescribed in the Atlantic. From *Ding et al.* [2012]. (d-g) Lagged regressions of 3 months averaged SST, wind vector at 850hPa and precipitation during MAM (d-e) and DJF (f-g) onto NTA SST [90-20E, 0-15N] averaged during FMA after excluding the impact of Niño3.4 SST [170-120W,5S-5N] during the previous DJF season from 1980 to 2010. From Ham et al. [2013b].

2.4.2. Influence of the tropical Atlantic variability on ENSO prediction

The connection between the inter-annual variability of the tropical Atlantic and Pacific basins gives a step forward in the current ENSO prediction system, since the Atlantic Niño becomes a precursor of ENSO episodes. Previous studies have investigated the role of the tropical Atlantic SSTs in predicting ENSO phenomena [*Jansen et al.*, 2009; *Frauen and Dommenget*, 2012; *Keenlyside et al.*, 2013]. *Jansen et al.* [2009] analysed the air-sea coupled interactions in the tropical oceans using a recharge oscillator scheme. These authors pointed out that ENSO predictability enhances due to a feedback between the equatorial Atlantic and Pacific SST anomalies (Figure 19a-b).

Furthermore, *Frauen and Dommenget* [2012] demonstrated that the initial conditions of the tropical Atlantic Ocean have little influence on ENSO characteristics (amplitude and frequency), but a strong impact on ENSO predictability (Figure 19c). *Keenlyside et al.* [2013] evaluated the importance of the initialization of dynamical ENSO predictions from the information of the previous tropical Atlantic SSTs. These authors concluded that a significant skill improvement is obtained when the model is initialized with equatorial Atlantic SSTs during boreal spring. According to this, a better prediction of ENSO events could be achieved using the information of the tropical Atlantic SSTs during previous seasons.

Nevertheless, the existence of the Atlantic-Pacific Niños connection only after the 1970s opens windows of opportunity to predict ENSO episodes. A study of the predictive skill of the Atlantic SSTs on ENSO phenomena and its possible time-dependence is needed.

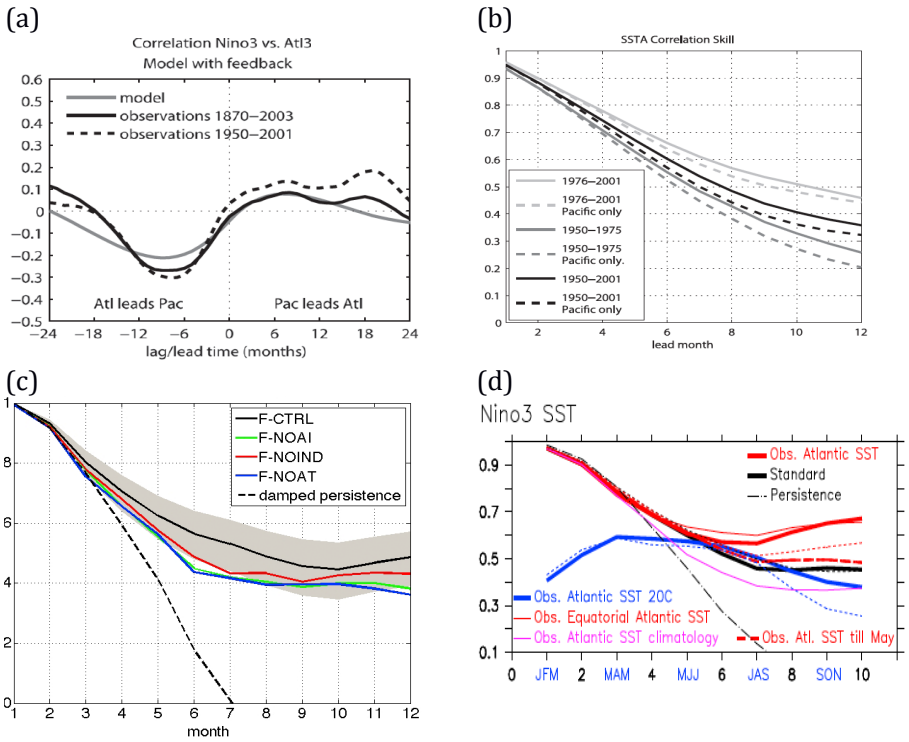

Figure 19. ENSO prediction from the Atlantic SSTs. Cross-correlation between Niño3 SST and Atl3 SSTA for the Pacific-Atlantic Ocean coupled model (grey line) compared to observational HadISST data from the period 1870-2003 (solid black line) and 1950-2001 (dashed line). (b) Forecast skill of the oscillator model for the Pacific-Atlantic Ocean coupled model. The anomaly correlation between the predicted and observed Niño3 SSTA is shown. From *Jansen et al.* [2009]. (c) Correlation of monthly mean NINO3 SST anomalies from the CTRL time series with monthly mean NINO3 SST anomalies from the F-NOAT experiment (blue), the F-NOIND experiment (red), the F-NOAI experiment (green), the F-CTRL experiment (black), and the persistence of the CTRL time series (dashed line). F-CTRL is a 500-year control run and F-NOAT, F-NOIND, F-NOAI are the sensitivity experiments with climatological SST prescribed in the tropical Atlantic (30N-30S), the tropical Indian (30S-northern boundary) and both tropical oceans respectively. From *Frauen and Dommenget* [2012]. (d) Anomaly correlation skill for the 3-month mean Niño3 averaged SST for the observed Atlantic SST and standard predictions as function of forecast lead-time. Also shown are skill of analogous predictions with either the observed SST prescribed only over the equatorial Atlantic (10N-20S) or observed SST monthly climatology prescribed over the Atlantic (60N-60S); skill of a 5-member 20th century climate simulations with observed SST prescribed over the Atlantic; and persistence skill. From *Keenlyside et al.* [2013].

2.4.3. Decadal modulation of the inter-annual tropical variability

2.4.3.1 Ocean Multidecadal Variability

Large-scale patterns of natural decadal variability, the Pacific Decadal Oscillation (PDO, *Mantua et al.* [1997]; *Mantua and Hare* [2002]) and the Atlantic Multidecadal Oscillation (AMO, *Kerr* [2000]; *Knight et al.* [2006]) emerge in the Pacific and Atlantic Oceans respectively. The positive phase of the PDO is defined by cooler SST anomalies in central north Pacific and warmer ones along the west coast of North America and equatorial Pacific region. The positive AMO phase is characterized by a warming in North Atlantic Ocean, contrasting with cooler SST anomalies south of the equator (Figure 20). The amplitude of the PDO has varied irregularly at inter-annual to inter-decadal time scales, while the AMO presents a quasi-cycle of roughly 70 years.

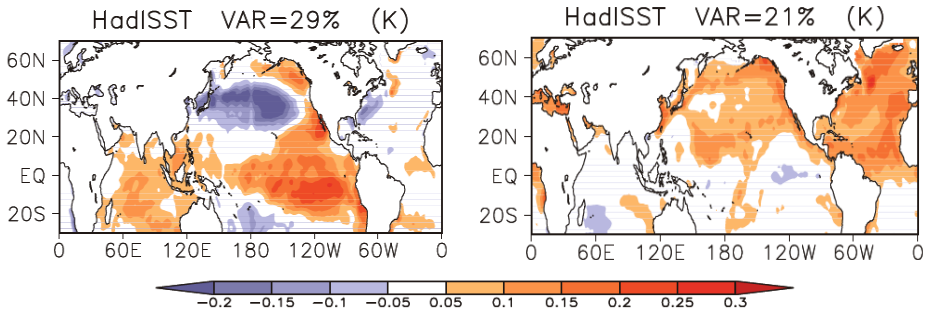

Figure 20. Decadal variability patterns. Spatial patterns of the Pacific Decadal Oscillation (PDO, left) and the Atlantic Multidecadal Oscillation (right). From *Liu and Sui* [2014]

The changes in the Atlantic Niño and ENSO patterns, as well as, their climate teleconnections could be attributed to a modification of the Atlantic and Pacific background states [*López-Parages and Rodríguez-Fonseca*, 2012; *L'Heureux et al.*, 2013; *McGregor et al.*, 2013; *Svendsen et al.*, 2014]. Moreover, the Global Warming (GW) could also contribute to the reported change of the background state of the global oceans during recent decades.

Variations in the mean SST conditions of the Atlantic Ocean could

impact on the tropical Atlantic variability. On the one hand, *Tokinaga and Xie* [2011] indicated that a warming in the tropical Atlantic associated with the GW produces a reduction of the zonal SST gradient, and consequently, a decreased of the inter-annual variability during summer months. On the other hand, *Polo et al.* [2013] showed that for warmer south Atlantic conditions (negative AMO phase comparing to positive AMO phase), the variability in the eastern equatorial Atlantic is enhanced during the autumn. *Despite, several changes have been reported, it is not clear how the AMO modulates the inter-annual tropical Atlantic variability.*

Although there is no consensous about the role of the Atlantic mean state in the tropical Atlantic variability, these anomalous warming is able to enhance the convection over the Atlantic, favouring the triggering of the climate teleconnections [*Kucharski et al.*, 2007; *García-Serrano et al.*, 2008; *Kucharski et al.*, 2008; *Losada et al.*, 2010b; *Kucharski et al.*, 2011; *Losada et al.*, 2012a; *McGregor et al.*, 2013; *Kucharski et al.*, 2014].

Regarding to the Pacific basin, a modification in the tropical and north Pacific mean state and variability, partly attributed to a PDO-like pattern, has been related to a modification of ENSO properties at multidecadal time scales [*Federov and Philander*, 2000; *Yeh and Kirtman*, 2005; *S Yeh et al.*, 2011]. Apart from the PDO pattern, *Dong et al.* [2006] demonstrated that for positive AMO phases, the westerlies in the eastern Pacific are strengthened and the thermocline is deepened, reducing the upwelling feedbacks and in turn the ENSO variance and amplitude [*Dong et al.*, 2006; *Timmermann et al.*, 2007; *Kang et al.*, 2014]. The influence of the AMO on the tropical Pacific background state could be carried out through large-scale atmospheric [*Dong and Sutton*, 2002; *Zhang and Delworth*, 2005; *Sutton and Hodson*, 2007] and oceanic mechanisms [*Timmermann et al.*, 2005].
Although the main changes in the Atlantic and Pacific background state are driven by the natural decadal variability patterns (PDO and the AMO), the contribution of the GW during recent decades should be also considered [*Sun et al.*, 2013; *Dong and Zhou*, 2014; *Kang et al.*,

2014]. In this sense, recent studies have evidenced a possible interaction between those patterns [*d'Orgeville and Peltier*, 2007; *Dong and Zhou*, 2014; *Liu and Sui*, 2014]. A warmer Atlantic could induce an trans-basin (Atlantic-Pacific) see-saw SLP pattern, intensifying the easterlies in the tropical Pacific and favouring the coupled processes responsible of the development of La Niña-like SST pattern [*Kucharski et al.*, 2011; *McGregor et al.*, 2013; *Kucharski et al.*, 2014]. These cooler conditions in the tropical Pacific basin could be associated with the strengthening of the Walker circulation during the last decades [*L'Heureux et al.*, 2013; *Dong and Zhou*, 2014]. Moreover, this negative SST trend in the tropical Pacific is consequence of a competition between the AMO, Interdecadal Pacific Oscillation (IPO) and Global Warming (GW). The SST cooling in the eastern Pacific is dominated by the phase transition of the IPO, from positive to negative phases in late 1990s, which overwhelms the global warming signal. In addition, the phase transition of the AMO during the 1990s, partially weakens the cooling of the equatorial Pacific [*Dong and Zhou*, 2014]. In this line, recent studies proposed a global oceanic forcing, characterized by an inter-hemispheric dipole-like pattern with centers of action in the Atlantic and Indian Ocean basins as a modulator of the tropical teleconnections at multidecadal time scales [*Fang et al.*, 2008; *Sun et al.*, 2013].

2.4.3.2 Multidecadal modulations

a) Changes in ENSO characteristics and impacts

ENSO properties (period, amplitude, structure and propagation) have changed in a coherent manner since late 1970s, due to a modification of the tropical Pacific background state [*Federov and Philander*, 2000; *Wang and An*, 2002; *S An et al.*, 2006; *Ye and Hsieh*, 2006; *Fang et al.*, 2008; *Borlace et al.*, 2013].

In particular, *Wang and An* [2002] have reported decadal changes in ENSO phenomena before and after the climate shift[4] (mid 1970s,

4 The climate shift is associated with a change in the tropical Pacific climate during 1976-1977

Graham [1994]; *Miller* [1994]). After the 1970s, an eastward displacement of the westerlies and the equatorial convection produces a reduction of the zonal advective currents and enhances the vertical advection processes, prevailing the eastward propagation of the SSTs in the equatorial Pacific. This structural change of ENSO phenomena implies an amplification of the seasonal cycle, which generates longer periods and higher amplitudes, through a strong instability coupling, which delays the transition between warm and cold ENSO phases [*Wang and An*, 2002].

S An et al. [2006] attributed the modification of ENSO characteristics to the existence of different ENSO modes before and after the 1970s. Before the mid-1970s, the ENSO resembles the "ocean-basin mode", which is produced by the equatorial trapped waves and destabilized by the zonal advective feedback. On the other hand, after the mid-1970s, the ENSO follows the "recharge-oscillator mode", in which the vertical advective feedbacks play a crucial role in the development of the SST anomalies. In the same line, the existence of different ENSO types, according to the spatial distribution of the SST and subsurface temperature anomalies, has been proposed [*Larkin and Harrison*, 2005a; *Larkin and Harrison*, 2005b; *Ashok et al.*, 2007; *Kao and Yu*, 2009; *Kug et al.*, 2009; *Yu et al.*, 2011]. The canonical El Niño, Eastern Pacific (EP) ENSO or Cold Tongue (CT) ENSO is characterized by maximum SST anomalies in Niño3 region [150W-90W, 5N-5S], while the "dateline El Niño", Central Pacific (CP) ENSO or "El Niño Modoki" presents higher SST anomalies in Niño4 region [160E-150W, 5N5S]. Hereafter, EP and CP ENSO will be used to denote the two different types of El Niño phenomenon (Figure 21).

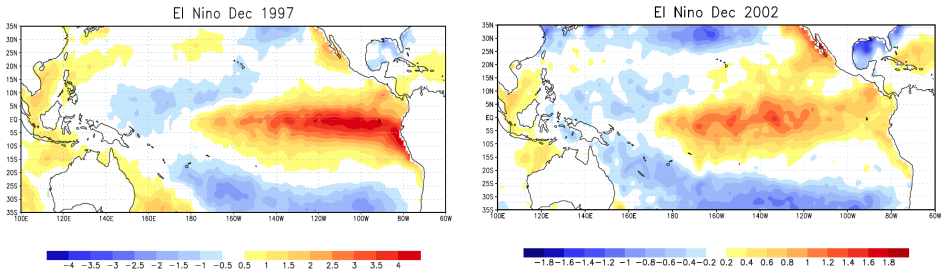

Figure 21. ENSO types. Eastern Pacific (EP) ENSO of 1997 (left) and Central Pacific (CP) ENSO of 2002 (right). Observed seasonal SST anomalies from December-January-February-March. (From *Rayner et al.* [2003])

CP ENSO present largest SST and wind anomalies in central Pacific, with no alteration of the thermocline depth. These events seem to be related to atmospheric forcing, which favours the zonal mean advection due to anomalous currents, responsible of the generation of SST anomalies. On the contrary, the EP ENSO show anomalous SSTs in the eastern Pacific, with a basin-wide alteration of the thermocline depth and its development and decay are mainly due to vertical advection processes [*Kao and Yu*, 2009; *Kug et al.*, 2009]. CP and EP ENSO have different periodicities, 2-yr *vs* 4-yr, suggesting that CP ENSO occurs more frequently than EP ones [*Kao and Yu*, 2009; *Yu et al.*, 2011]. During recent decades, an increase of the frequency of CP ENSO phenomena has been documented and attributed to changes in the mean state of the tropical Pacific [*Yeh et al.*, 2009; *Choi et al.*, 2011; *McPhaden et al.*, 2011; *S Yeh et al.*, 2011; *Chung and Li*, 2013]. Nevertheless, the role of the Pacific background state in favouring the occurrence of those phenomena still remains unclear since higher ratio between CP and EP ENSO have been reported for both warmer and cooler tropical Pacific conditions, associated with decadal variability patterns or the anthropogenic forcing [*Yeh et al.*, 2009; *Choi et al.*, 2011; *McPhaden et al.*, 2011; *McPhaden*, 2012; *Chung and Li*, 2013].

In addition to the modification in its characteristics the ENSO teleconnections have also changed during the last years. A non-stationary influence of ENSO over Euro-Atlantic region has been reported (Figure 22a; *López-Parages and Rodríguez-Fonseca* [2012]; *Greatbatch et al.* [2004]; *Mariotti et al.* [2002]; *Zanchettin et al.* [2008]). Oscillations of the decadal oceanic patterns, the PDO and the AMO, could modify the zonal mean flow at upper levels, favouring the propagation of atmospheric waves from the tropical to extra-tropical regions, modulating in this way the ENSO impact on Euro-Atlantic precipitation at multidecadal time scales (Figure 22b-c; *López-Parages and Rodríguez-Fonseca* [2012]; *López-Parages et al.* [2014]).

In the same line, the connection between West African (WA) rainfall and ENSO phenomenon has been strengthened during recent decades (*Trzaska et al.* [2007]; *Janicot et al.* [2001]; *Janicot et al.* [1996]; *Joly et al.* [2007]; *Mohino et al.* [2011]; *Rodríguez-Fonseca et al.* [2011];.

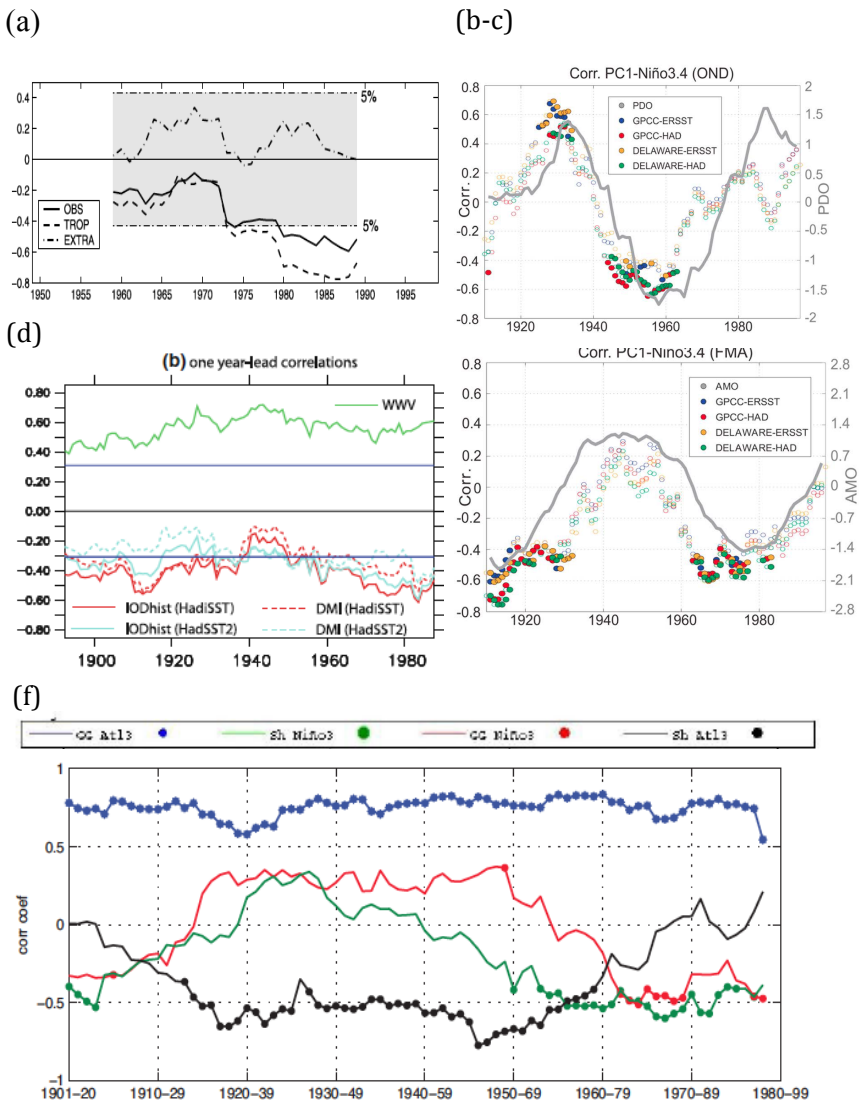

Figure 22(a). Multidecadal change in ENSO teleconnections. Running cross-correlation using 21-yr windows between the observed SOI and COWL (winter mean of Cold Ocean Warm Land pattern) index (solid line) and the ensemble mean tropical (dashed) and extratropical (dot-dash) forced model runs. From *Greatbach et al.* [2004]; (b) 21 year moving window correlations between the leading iEMedR PC1 and Niño3.4 index in OND (left) and FMA (right). In grey line, the standardized PDO (*Mantua et al.* [1997]) and AMO index [*Enfield et al.*, 2001] are presented. From *López-Parages and Rodríguez-Fonseca* [2012]. (e) Interdecadal variation of Indian Ocean Dipole (IOD)/Warm Water Volume (WWV)-ENSO relationships considering 1-year lead correlations of IOP/WWV with the following year's ENSO. From *Izumo et al.* [2014] (f) 20-yr running correlation from 1901–1920 to 1980–99, between observed JJAS Atl3 index and JJAS GG precipitation index (blue line), JJAS Atl3 index and Sahel rainfall index (black line), JJAS Niño3 index and JJAS GG rainfall index (red line) and JJAS Niño3 index and Sahel rainfall index (green line). From *Losada et al.* [2012b].

Losada et al. [2012b]). *Losada et al.* [2012b] have demonstrated that although the impact of the individual oceanic basins on WA rainfall seems to be relatively stationary on time, after the 1970s, interferences between the Atlantic Niño and ENSO impacts change the pattern of WA rainfall (Figure 22f).

Regarding to the influence of the Indian Ocean SSTs on ENSO evolution, changes in the oceanic heat content and wind anomalies in western Pacific have been only observed during the first decades of the 20th century and after the 1970s (Figure 22d). Furthermore, *Chakravorty et al.* [2014] pointed out that a stronger warming in the Indian Ocean following el Niño event is associated with ocean dynamics after the 1970s, contrasting with the main contribution of the heat fluxes in previous decades.

b) Changes in the Atlantic Niño characteristics and impacts

The Atlantic Niño pattern has also changed during last decades. Before the 1970s, a canonical Atlantic Niño, characterized by positive SST anomalies in the eastern equatorial Atlantic, flanked by negative ones in the north and south tropical Atlantic. Nevertheless, after the 1970s, the Atlantic Niños present a warming of the entire tropical Atlantic basin (Figure 17a-d).

The differences in the spatial structure of the Atlantic Niños could be attributed to different atmospheric and oceanic forcings during the recent decades. As it has been described in previous sections, the development of the Atlantic Niño is associated with a weakening of the equatorial trades. These anomalous winds could be due to local or remote atmospheric forcings [*Latif and Grötzner*, 2000; *Münnich and Neelin*, 2005; *Polo et al.*, 2008a; *Lübbecke et al.*, 2010; *Richter et al.*, 2010], which could trigger oceanic Rossby and Kelvin waves [*Polo et al.*, 2008a; *Lübbecke et al.*, 2010] or activate different air-sea mechanisms [*Keenlyside and Latif*, 2007; *Richter et al.*, 2013] responsible of the development of the equatorial SST anomalies. *Further research about the origin of the different Atlantic Niño*

patterns, their precursors and the atmospheric and oceanic mechanisms at work is required.

The change in the spatial configuration of the Atlantic Niños coincides with a modification of its climate teleconnections. After the 1970s, the characteristic dipole pattern of anomalous rainfall between the GG and the Sahel, associated with Atlantic SST anomalies, has disappeared and a monopolar structure emerges over West African region [*Polo et al.*, 2008a; *Rodríguez-Fonseca et al.*, 2009; *Mohino et al.*, 2011; *Rodríguez-Fonseca et al.*, 2011]. A similar rainfall pattern has been also found at the beginning of the 20th century [*Joly and Voldoire*, 2010; *Losada et al.*, 2012b], suggesting a possible multidecadal modulation of this teleconnection.

Moreover, the impact of the Atlantic Niño over the Mediterranean climate has been also modified in the last decades: the general enhancement of the precipitation over the Euro-Mediterranean area turns into a tripolar rainfall pattern attributed to the simultaneous contribution of the tropical Atlantic, Pacific and Indian basins [*Losada et al.*, 2012a]. More recently, *Losada and Rodriguez-Fonseca* [2015] demonstrated that the different Atlantic Niño configuration modify its impact over the Indo-Pacific climate.

Due to the above-mentioned results, the possible multidecadal modulation of Atlantic Niño and ENSO teleconnections through changes in the tropical Atlantic and Pacific background states, should be taking into account in the present Thesis.

2.5. Simulating the tropical climate

Due to the limited observational record, the study of climate variability requires the use of Coupled General Circulation Models (CGCMs). Nevertheless, most of the current CGCMs suffer from large errors in reproducing the seasonal cold tongue: warmer SSTs, around 2K-3K higher than the observed ones, are simulated in the eastern equatorial Atlantic and Pacific basins (Figure 23a; *Mechoso et al.* [1995]; *Davey et al.* [2002]; *Yu and Mechoso* [1999]; *De Szoeke and Xie*

[2008]; *Li and Xie* [2014]; *Wang et al.* [2014]). Atmospheric biases, as a southward shift of the ITCZ or westerly bias in the equatorial surface winds; or oceanic bias, as strong zonal currents and excessive oceanic upwelling are possible causes for the wrong reproduction of the seasonal cycle at the tropical band [*Breugem et al.*, 2006; *Stockdale et al.*, 2006; *Deser et al.*, 2006b; *Breugem et al.*, 2008; *Richter and Xie*, 2008].

Another important atmospheric bias present in the CGCMs is the simulation of a double ITCZ (Figure 23b). Several studies have hypothesized that a poor representation of the ocean-atmospheric feedbacks, unrealistic winds in the eastern Pacific warm pool, unrealistic SST threshold leading the onset of the convection, improper entrainment effect, unrealistic alongshore winds at Chile and Peru or cloud biases could be responsible of this error [*Lin*, 2007; *De Szoeke and Xie*, 2008; *Hirota et al.*, 2011; *Bellucci et al.*, 2012; *Hirota and Takayabu*, 2013; *Hwang and Frierson*, 2013]

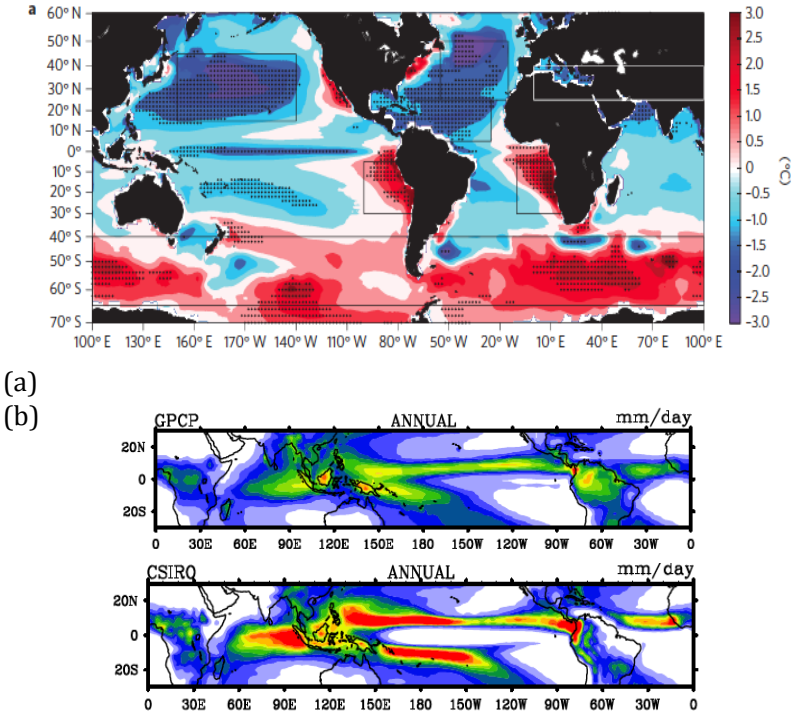

Figure 23. Atmospheric and oceanic biases present in current CGCMs. (a) The annual-mean SST bias averaged in CMIP5 models. The SST bias is calculated by the SST difference between the model SST and extended reconstructed SST. The dots denote where at least 18 of 22 models (82%) have the same sign in the SST bias. (from *Wang et al.* [2014]). (b) Observed (top) and modelled annual precipitation (bottom) (from *Oueslati and Bellon* [2014])

Although lots of efforts have been made in the last years, a realistic reproduction of the tropical climate variability still remains a challenge for the scientific community. On the one hand, the persistent systematic errors in the tropical Pacific basin (underestimation of the zonal advective feedback, thermocline feedback and thermodynamic damping terms) give rise to a cold tongue bias in the equatorial eastern Pacific, which causes a weaker atmospheric thermodynamical response to SST changes and a weaker oceanic response to wind fluctuations [*Kim and Cai*, 2014]. These biases have profound effects on the realistic representation of ENSO amplitude, spatial structure and the transition between phases [*Guilyardi et al.*, 2009; *Taschetto et al.*, 2014]. Major progresses in the simulation and seasonal prediction of ENSO and its global impacts have been made during the last decades [*Delecluse et al.*, 1998; *Davey et al.*, 2002; *Randall et al.*, 2007]. Due to the improvement in the parameterizations and model resolutions [*Guilyardi et al.*, 2004; *Roberts et al.*, 2009], as well as the use of oceanic observations in initializing seasonal forecasts, the CGCMs show a better representation of the SST anomalies in the eastern Pacific [*AchutaRao and Sperber*, 2006]. Furthermore, *Bellenger et al.* [2013] have demonstrated how the seasonal cycle, the mean state of the model and ENSO are intimately linked, in a way that, errors in the simulation of these phenomena share the same origin. Correcting the mean state and the seasonal cycle could improve the amplitude of SST inter-annual variability in the tropical Pacific and in turn the ENSO teleconnections [*Magnusson et al.*, 2013].

On the other hand, the correct simulation of the tropical Atlantic climate and variability is also needed, since the climatic variability of the Tropical Atlantic has a direct impact on the health and livelihood of millions of people living in equatorial West Africa and north-eastern South America. As it has been previously mentioned, many GCMs suffer serious biases in the tropical Atlantic, as a southward shift of the annual mean of ITCZ, a westerly bias in equatorial surface winds, and a failure to reproduce the eastern equatorial cold tongue in boreal summer (Figure 24a; *Richter and Xie* [2008]). Despite these

substantial mean state biases, several models are able to reproduce the observed equatorial variability: the spatial pattern, magnitude, occurrence and duration of the event (Figure 24b; *Richter et al.* [2012a]). Nevertheless, some deficiencies are still present in the CGCMs: the maximum variability is lagged 1-2 months respect to the observed one, as well as the seasonal cycle of the cold tongue thermocline depth. *Richter et al.* [2012a] indicated that the latitudinal displacement of the western equatorial Atlantic ITCZ is much pronounced in the models than in observations, which could contribute to the delayed onset of the equatorial cold tongue, and thus, the interannual variability (Figure 24c). *Doi et al.* [2012] suggested that a reduction in bias of the ITCZ improves the simulation of the precipitation over South America and Sahelian region.

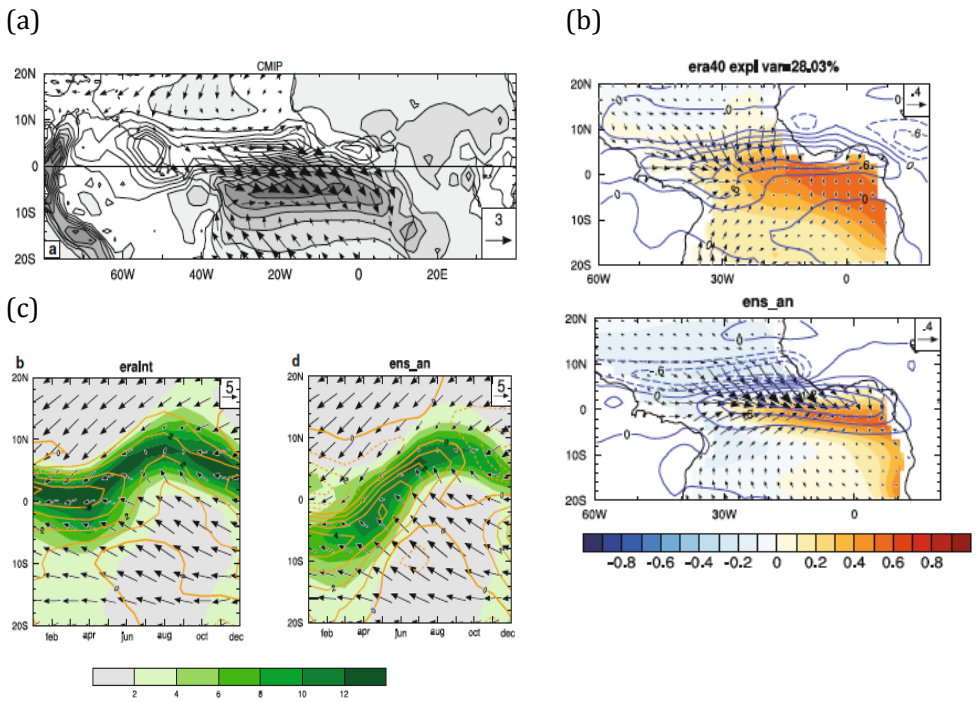

Figure 24. Bias in the tropical Atlantic. (a) MAM precipitation (shaded and contours) and surface wind (vectors) biases of CMIP ensemble means. From *Richter et al.* [2012a]. (b) First EOF of seasonally averaged JJA SST (shading) in ERA 40 (top) and ensemble CMIP5 models (bottom). The precipitation values (contours) and surface winds (vectors) are also plotted. (c) Latitude-time sections of climatological precipitation (shading) and surface wind stress (vectors) from ERA-INTERIM (left) and ensemble of CMIP5 models (right). From *Richter et al.* [2012a].

Despite this progress, simulating the mean properties in the tropics is still is a daunting task and remains as one of the main challenges for the scientific community [*Van Oldenborgh et al.*, 2005; *Capotondi et al.*, 2006; *Wittenberg et al.*, 2006; *Guilyardi et al.*, 2009]; In this context, a European project, PREFACE (Enhancing PREdiction oF tropical Atlantic ClimatE and its teleconnections, ref: 603521; http://preface.b.uib.no) has been recently funded to improve our understanding and capabilities to predict Tropical Atlantic climate and impacts. To achieve it, PREFACE project is focused on the analysis of the tropical Atlantic systematic errors, their causes and effects on the simulated climate.

3. OBJECTIVES

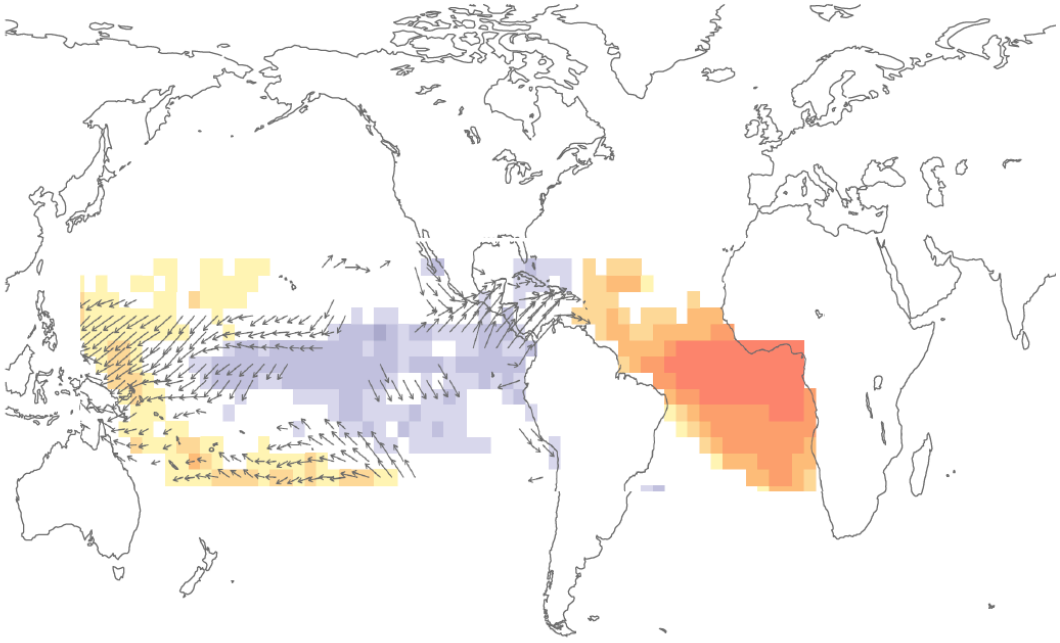

3. OBJECTIVES

The main objective of this thesis is

To study the air-sea interactions associated with the influence of the tropical Atlantic inter-annual variability on ENSO phenomena. In particular, the non-stationary behavior of the Atlantic Niños (Niñas)-Pacific Niñas (Niños) connection and its impact on the Atlantic predictive skill on ENSO episodes will be investigated, as well as the atmospheric and oceanic mechanisms involved in the development of these Atlantic Niños.

This main objective could be divided into several specific objectives:

Objective 1: To understand the contribution of the tropical Atlantic inter-annual variability on ENSO.

To this aim, observations and partially coupled simulations considering the observed Atlantic SSTs as the only external forcing will be used. These partially coupled simulations allow to isolate the Atlantic contribution to the tropical Pacific variability from other external forcings included in observations. The results of this objective will try to give answer to the following questions:

- *Is the Atlantic Niño able to modify the tropical Pacific oceanic variability?*

- *Which are the oceanic processes at work in the development of ENSO from a remote Atlantic influence?*

Objective 2: To understand the stationarity of the Atlantic-Pacific connection and to analyse possible multidecadal modulations.

In order to understand if this connection occurs along the whole observational record, multivariate discriminant analyses will be applied for different periods during the 20th century. Observations

and partially coupled simulations will be used, and the main drivers of the modulation of this inter-basin link will be determined. The results of this objective will give answer to the following questions:

- *Is the Atlantic-Pacific connection an internal mode of tropical variability?*

- *In which periods does the Atlantic-Pacific connection take place?*

- *Which is the modulator pattern for the Atlantic-Pacific connection?*

Objective 3: To assess the skill of the tropical Atlantic SSTs in predicting ENSO.

A statistical crossvalidated hindcast of ENSO, using the summer tropical Atlantic inter-annual variability as predictor, will be performed to assess its predictability. The results of this statistical prediction will be analysed in order to answer the following questions:

- *Which is the skill of the summer equatorial Atlantic SSTs in predicting ENSO phenomena?*

- *Which are the variables and processes involved in ENSO that are better predicted by the summer Atlantic SSTs?*

Objective 4: To characterize the Atlantic Niño involved in the Atlantic-Pacific connection and to compare it with the canonical mode.

Multivariate discriminant analyses will let determine the spatial configuration of the inter-annual tropical Atlantic SST variability related to ENSO in negative AMO periods. These results will try to answer the following questions:

- *How are the main modes of inter-annual tropical Atlantic SST during those decades?*

- *How are the atmospheric forcings of these inter-annual modes?*

Objective 5: To study the air-sea interactions involved in the development of different Atlantic Niños.

To this aim, an inter-annual experiment with the tropical Atlantic configuration of NEMO model will be performed. The model will be forced with observed surface winds along the period 1960-2011 and the heat budget terms associated with the Atlantic Niño development will be analysed in order to answer the following questions:

- *How is the wind and pressure forcing patterns associated with the development of the Atlantic Niños?*

- *Which are the oceanic processes involved in development of the Atlantic Niño patterns?*

- *Which processes control the development of the surface anomalous heating associated with the Atlantic Niños?*

3. OBJETIVOS

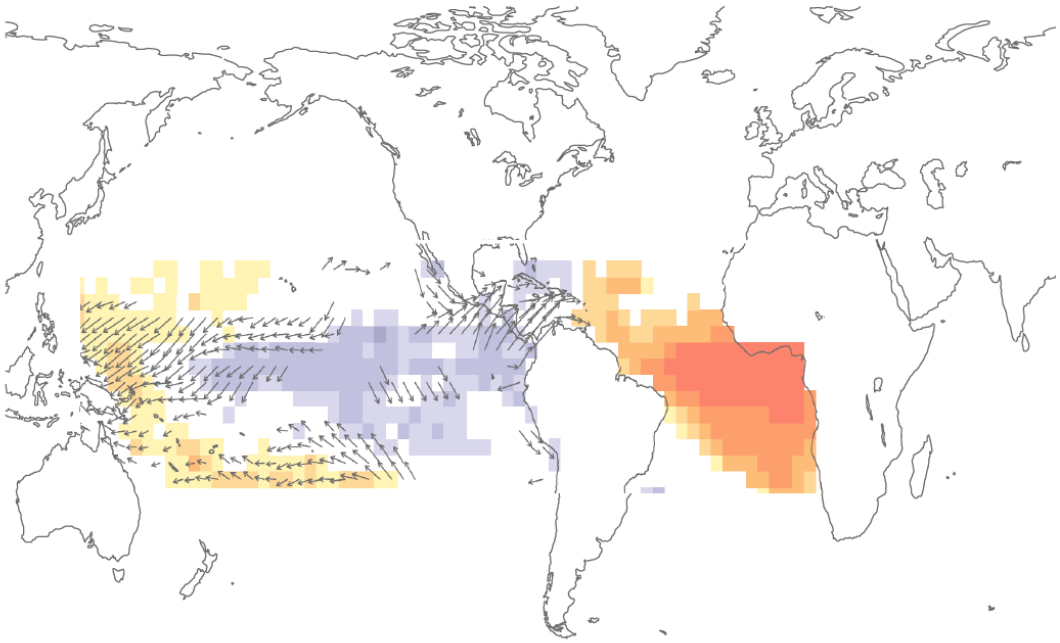

3. OBJETIVOS

El principal objetivo de esta tesis es

Estudiar los procesos de interacción aire-océano asociados con la influencia de la variabilidad interanual del Atlántico sobre el fenómeno del ENSO. En particular, se investigará la no-estacionariedad de la conexión entre Niños (Niñas) del Atlántico-Niñas (Niños) del Pacífico y su impacto la predictivilidad del Atlántico sobre los fenómenos ENSO. Además se analizarán los procesos atmosféricos y oceánicos involucrados en el desarrollo de estos Niños del Atlántico.

Este objetivo principal puede dividirse en los siguientes objetivos específicos:

Objectivo 1: Entender la contribución de la variabilidad interanual del Atlántico tropical en el fenómeno del ENSO.

Para ello, se usarán datos procedentes de observaciones y de simulaciones parcialmente acopladas que consideran la Temperatura de la Superficie del Mar observada en el Atlantico como único forzamiento externo. Estas simulaciones permiten aislar la contribución del Atlántico sobre la variabilidad del Pacífico tropical respecto de otros forzamientos externos presentes en las observaciones. Los resultados de este objetivo permitirán responder a las siguientes preguntas:

- *¿Es capaz el Niño Atlántico de modificar la variabilidad tropical oceánica del Pacífico tropical?*

- *¿Cuáles son los procesos oceánicos involucrados con el desarrollo de los fenómenos ENSO forzados por el Atlántico?*

Objectivo 2: Comprender la estacionariedad de la conexión Atlántico-Pacífico y analizar las posibles modulaciones multidecadales.

Para saber si esta conexión tiene lugar a lo largo de todo el periodo observacional, se aplica un análisis discriminante multivariante a diferentes periodos a lo largo del siglo XX. Se utilizarán datos procedentes de observaciones y simulaciones parcialmente acopladas y se identificarán los principales moduladores de esta conexión entre cuencas. Los resultados de este objetivo permitirán dar respuesta a las siguientes preguntas:

- *¿Es la conexión Atlántico-Pacífico un modo interno de variabilidad tropical?*

- *¿En que periodos tiene lugar la conexión Atlántico-Pacífico?*

- *¿Cuál es el patrón que modula dicha conexión?*

Objectivo 3: Evaluar la habilidad de la Temperatura de la Superficie del Mar del Atlántico tropical en predecir el fenómeno ENSO.

Se realizará un hindcast estadístico del fenómeno del ENSO, usando la variabilidad interanual de la Temperatura de la Superficie del Mar del Atlántico tropical como predictor. Los resultados de esta predicción estadística se analizarán para responder a las siguientes preguntas:

- *¿Cuál es la habilidad de la Temperatura de la Superficie del Mar del Atlántico tropical en verano para predecir el fenómeno del ENSO?*

- *¿Qué variables y procesos involucrados en el fenómeno ENSO predice mejor la Temperatura de la Superficie del Mar del Atlántico tropical en verano?*

Objectivo 4: Caracterizar el Niño Atlántico involucrado en la conexión Atlántico-Pacífico y compararlo con el Niño Atlántico canónico.

El análisis discriminante multivariante permitirá determinar la configuración espacial de la variabilidad interanual de la Temperatura de la Superficie del Mar del Atlántico tropical relacionada con el fenómeno del ENSO en periodos de AMO negativa. Estos resultados tratarán de dar respuesta a las siguientes preguntas:

- *¿Cómo son los principales modos de variabilidad interanual de la temperatura de la superficie del mar del Atlántico tropical durante esas décadas?*
- *¿Cómo son los forzamientos atmosféricos de estos modos interanuales?*

Objectivo 5: Estudiar los procesos de interacción aire-océano involucrados en el desarrollo de los diferentes Niños del Atlántico.

Para ello, se realizará una simulación interanual con la configuración del Atlántico tropical del modelo NEMO. El modelo se forzará con vientos observados en superficie durante el periodo 1960-2011. Además se analizarán los terminos del balance de calor asociados con el desarrollo del Niño Atlántico, con el fin de contestar a las siguientes preguntas:

- *¿Cómo es el forzamiento del viento y de la presión en superficie de los distintos patrones del Niño Atlántico?*
- *¿Cuáles son los procesos oceánicos involucrados en el desarrollo de los diferentes patrones del Niño Atlántico?*
- *¿Cuáles son los procesos que controlan el desarrollo del calentamiento superficial asociado con el Niño Atlántico?*

4. THEORETHICAL FRAMEWORK

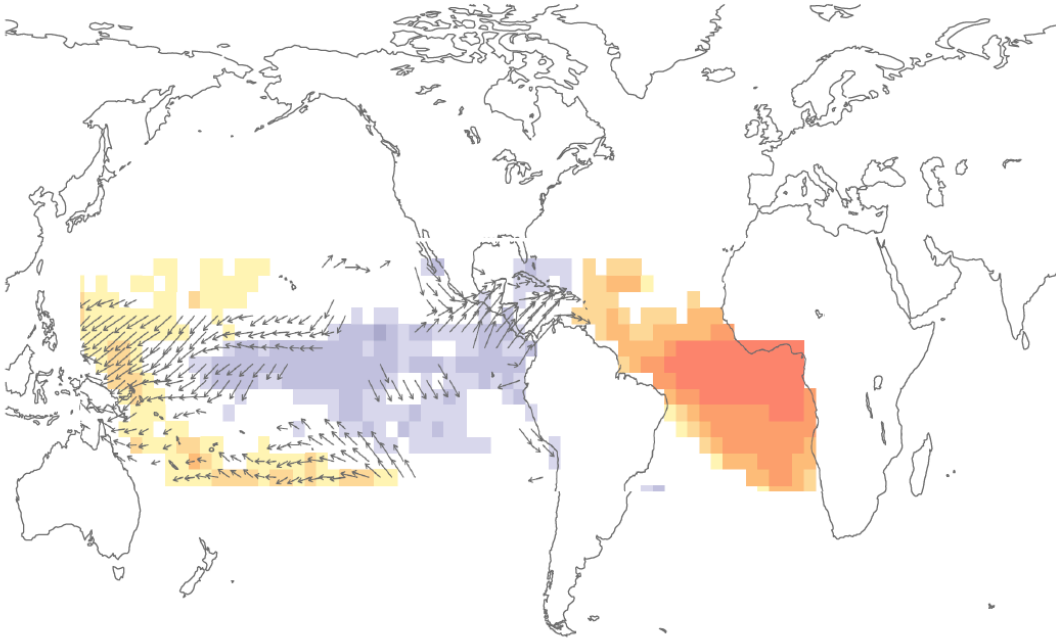

4. THEORETICAL FRAMEWORK

As it has been mentioned in previous sections, the present Thesis is focused on the analysis of the connection between the Atlantic Niño and ENSO. This relationship carries out through air-sea interactions in the tropical regions. Thus, in order to understand the underlying physical mechanisms, the atmospheric response associated with an equatorial warming, the oceanic response to a wind burst as well as the heat budget analysis of the upper ocean are described in the next sections.

4.1. Atmospheric response in the tropics

Equatorial waves

Close to the equator, due to the absence of rotational flow, tropical convection triggers atmospheric waves propagating eastward and westward, trapped in the equatorial band, which acts as a wave-guide. The atmospheric propagation of the equatorial waves lets communicate large longitudinal distances, producing remote responses associated with local heat sources [*Holton*, 2004]. The equatorial waves are classified in two types: Rossby waves and Kelvin waves and they will be briefly described as follows.

Equatorial Rossby waves

For the tropical band, the Coriolis parameter can be approximated by

$$f = \beta y \quad [1]$$

where $\beta = 2\Omega/a$ being Ω the angular velocity and a the radius of the Earth respectively. From this approximation, the linearized shallow-water equations for perturbations on a motionless mean state can be expressed as

$$\frac{\partial \Phi\prime}{\partial t} = -gh_e\left(\frac{\partial u\prime}{\partial x} + \frac{\partial v\prime}{\partial y}\right) \quad [2]$$

$$\frac{\partial u\prime}{\partial t} - \beta y v' = -\frac{\partial \Phi\prime}{\partial x} \quad [3]$$

$$\frac{\partial v\prime}{\partial t} + \beta y u' = -\frac{\partial \Phi\prime}{\partial y} \quad [4]$$

where *u* and *v* are the zonal and meridional velocities of the fluid, h_e is the depth of the fluid and Φ' is the perturbation of the geopotential ($\Phi' = gh'$).

In general three solutions verify the previous equation system and can be interpreted as equatorial gravity waves, equatorial Rossby waves and Rossby-gravity waves. Taking into account that the assumption $f \approx \beta y$ is not valid for latitudes higher than ± 30°, the solutions (waves) are trapped in the equatorial band. The dispersion diagram for the different oceanic waves is presented in Figure M1.

Equatorial Kelvin waves

Other important equatorial waves are the Kelvin waves, which verify that the perturbation in the meridional velocity is zero $v' = 0$. Thus, the equation system can be simplified

$$\frac{\partial \Phi\prime}{\partial t} = -gh_e\left(\frac{\partial u'}{\partial x}\right) \quad [5]$$

$$\frac{\partial u\prime}{\partial t} = -\frac{\partial \Phi\prime}{\partial x} \quad [6]$$

$$\beta y u' = -\frac{\partial \Phi\prime}{\partial y} \quad [7]$$

In this case, the solution of this equation system describes an equatorial wave propagating eastward, with zonal velocity and geopotential perturbations varying in latitude as Gaussian functions centered on the equator [*Holton*, 2004].

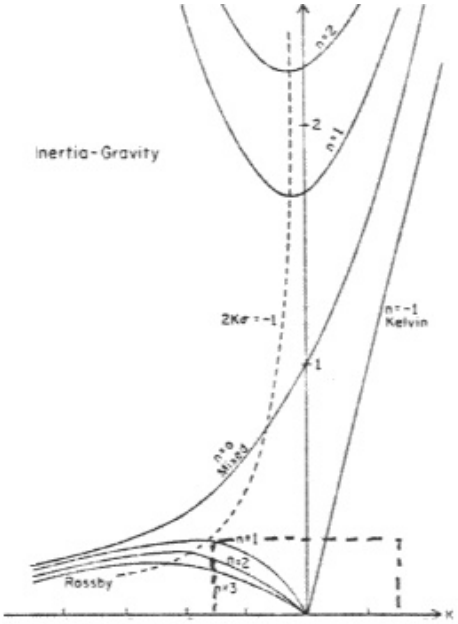

Figure M1. Equatorial waves. Dispersion diagram for modes of the linear shallow water equations. From *Cane and Sarachik* [1976]

4.2. Equatorial response to diabatic heating: Gill-Matsuno mechanism

The Gill-Matsuno mechanism proposes that an equatorial diabatic heating is able to excite atmospheric waves propagating eastward and westward trapped along the equatorial band [*Matsuno*, 1966; *Gill*, 1980]. The propagation of the equatorial Kelvin wave is accompanied by easterlies toward the heat source. The atmospheric response as equatorial Kelvin wave is symmetric respect to the equator and produces a modification of the Walker circulation, with easterlies flowing parallel to the equator over the forcing region, ascending motions over there and then flowing eastward in upper levels. West to the heat source, the perturbations propagate through Rossby waves associated with westerlies in the equatorial band and easterlies in higher latitudes. Two symmetric cyclonic circulations appear at both sides of the equator at the surface, with the respective two anticyclones in upper levels (Figure M2). Considering the faster propagation of the Kelvin wave respect to the Rossby wave (the velocity is around 3 times higher), it influences a larger spatial

domain. The Gill-Matsuno mechanism creates a similar reponse in the ocean.

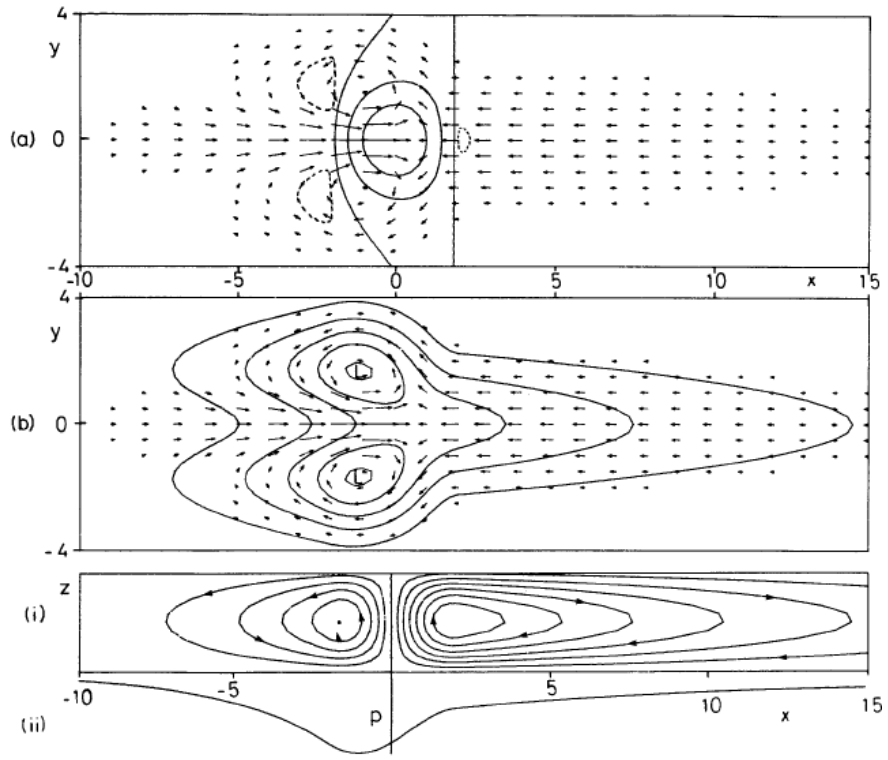

Figure M2. **Gill-Matsuno mechanism**. (a) Surface wind (vectors) and vertical velocity (contours). (b) Surface wind (vectors) and sea level pressure (SLP,contours). (Bottom) Stream function along the equatorial band. From *Gill* [1980]

4.3. Oceanic response to an equatorial wind burst

Similarly to the atmosphere, the equatorial ocean adjusts to a perturbation (i.e. Equatorial wind forcing) through Rossby and Kelvin waves [*Philander et al.*, 1984]. *Suarez and Schopf* [1988] introduced the oceanic response associated with anomalous surface winds in the western tropical Pacific in order to model ENSO in its known "delayed oscillator". It has been considered an idealised numerical experiment that uses the equations from a reduced-gravity model (*Philander* [1990], equations [8-10]). In this way, the ocean is considered to be formed by two inmiscible layers with constant density. The interface between these two inmiscible layers simulates the tropical thermocline that separates the surface warmer waters from the deep

ocean. Assuming that a fluid of constant density is incompressible (from the continuity equation), ignoring its density variations in the horizontal momentum equations (according to the Boussinesq approximation) and considering that the pressure does not depend on the depth (from the hydrostatic balance), the ocean equations can be expressed as,

$$\frac{\partial u}{\partial t} - fv + g' \frac{\partial \eta}{\partial x} = \frac{\tau_x}{H} \qquad [8]$$

$$\frac{\partial v}{\partial t} + fu + g' \frac{\partial \eta}{\partial y} = \frac{\tau_y}{H} \qquad [9]$$

$$g' \frac{\partial \eta}{\partial t} + c^2 \left(\frac{\partial u}{\partial x} + \frac{\partial v}{\partial y} \right) = 0 \quad [10]$$

where η is the displacement of the interface, u and v the zonal and meridional velocity components, t is the time; $f = 2\Omega sin\vartheta$ is the Coriolis parameter, being Ω the rotation of the Earth and ϑ the latitude; $g' = \frac{\rho_2 - \rho_1}{\rho_1}$ is the gravitational acceleration with ρ_1 and ρ_2 the density of the surface and bottom layer, respectively, and $c = \sqrt{gh}$ the gravity wave phase speed.

According to this idealised experiment, anomalous westerly winds in western side of the basin generate a deepening of the thermocline in the central Pacific, which propagate eastward as an downwelling Kelvin wave (KW) along the equator, and westward as off-equator upwelling Rossby waves (RW). As the KW and RW propagate, the vertical stratification of the upper ocean is modified, contributing to the development of the El Niño SST anomalies through thermocline feedbacks (Figure 3 left panels; *An and Jin* [2001]; *Jin and An* [1999]). When the waves reach the coast, they are reflected and the RW returns as an equatorial upwelling KW with a certain delay, responsible of the termination of El Niño phenomenon (Figure M3, right panels).

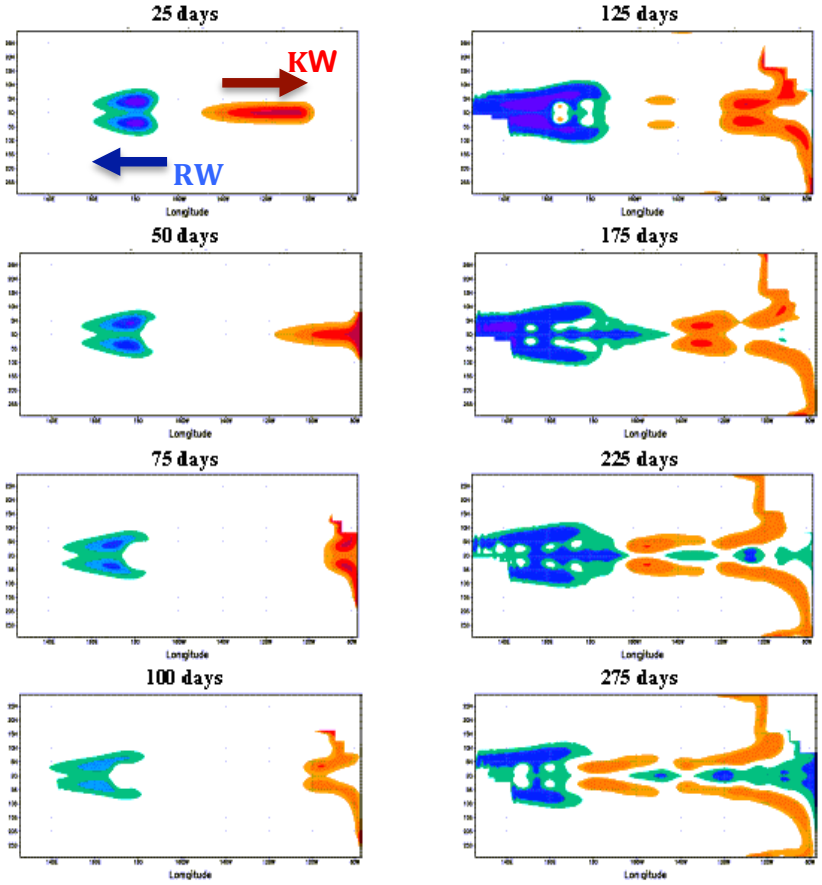

Figure M3. Scheme of the delayed-oscillator ENSO theory. Propagation of the positive thermocline anomalies as an eastward equatorial Kelvin wave and the negative ones as westward off-equator Rossby waves as the oceanic response to anomalous westerly winds in western Pacific.

4.4. Heat budget in the ocean

In order to investigate the oceanic processes involved in the development of the SST anomalies at inter-annual time-scales a heat budget analysis is computed.

Variations of the temperature in a single layer, the mixed layer, can be due to atmospheric and oceanic processes, which follow the thermodynamic equation

$$\frac{\partial T}{\partial t} + \vec{v}\nabla T = \nabla(\kappa \nabla T) \qquad [11]$$

where T is the temperature of the mixed layer, $\vec{v}$ is the fluid velocity and κ is the thermal diffusion. The evolution of the temperature T of a mixed layer with an h depth are given by a balance of several terms [*Vialard et al.*, 2001; *Peter et al.*, 2006; *Polo et al.*, 2015b],

$$\underbrace{\frac{\partial T}{\partial t} = \frac{-1}{h}\int_{-h}^{0} u\frac{\partial T}{\partial x}dz - \frac{1}{h}\int_{-h}^{0} v\frac{\partial T}{\partial y}dz - \frac{1}{h}\int_{-h}^{0} D_l}_{\mathbf{a}} \underbrace{- \frac{1}{h}(T - T_h)\left(\nabla hu + \frac{\partial h}{\partial z}\right) - \frac{1}{h}\left[\kappa_z \frac{\partial T}{\partial z}\right]_{-h}}_{\mathbf{b}}$$

$$\underbrace{\frac{-Q_{rad}(1-F_{-h})+Q_{tur}}{\rho_0 C_p h}}_{\mathbf{c}} \qquad [12]$$

where T_h is the temperature below the mixed layer; u,v and w are the zonal, meridional and vertical currents, respectively; D_l is the lateral diffusion and K_z the vertical mixing coefficient. The total net heat fluxes, Q_{net} , are divided in the radiative Q_{rad} and turbulent Q_{tur} heat fluxes, and F is the function that describes the fraction of shortwave fluxes penetrating in the mixed layer. Finally, ρ_0 is the seawater density and C_p is the seawater specific heat capacity coefficient.

According to equation [12], the trend of the temperature in the mixed layer (left) can be expressed as the sum of the contributions of oceanic and atmospheric components. The atmospheric forcings or air-sea fluxes are described by the term (c), on the right side of the equation; while the oceanic part is given by the terms (a) and (b), associated with the horizontal (horizontal advection and lateral diffusion) and vertical terms (turbulent mixing, vertical advection and entrainment), respectively.

This equation could be simplified according to the case considered. For the evaluation of the heat budget associated with the development of ENSO in partially coupled simulations, some simplifications have been done. The model considers an AGCM coupled to a 1.5-layer gravity model (*Chang* [1994]; for more details, see Sections 6.1 and 6.2), thus the ocean is simplified and it assumes

that the interactive mixed layer is the 1.5 layer, with constant depth H_s, which is also referred as the thermocline depth and thus, the thermodynamic equation is expressed as,

$$\frac{\partial T}{\partial t} = \frac{Q}{\rho_0 C_p H_s} - u_s \times \nabla \mathrm{T} - \frac{w_e H(w_e)(T - T_e)}{H_s} + \kappa \nabla^2 T \qquad [13]$$

where Q is net heat flux at the surface, u_s is horizontal velocity at the upper model's layer (surface current), w_e is vertical velocity of entrainment, H(w_e) is the Heaviside step function (unit for $w_e > 0$ and zero for $w_e < 0$), Te is temperature of entrained water beneath the base of the mixed layer, and κ is a diffusivity coefficient (*Chang* [1994]). According to equation [13] changes in temperature of the mixed layer (left-hand side term) are due to the net surface heat flux at the interface with the atmosphere, horizontal advection, vertical entrainment, and horizontal diffusion (right-hand side terms). In the ocean model the value of T_e carries the information on the change of the thermocline temperature through the entrainment parametrization.

Considering that each field can be decomposed as the sum of its mean value and its anomaly, and that the diffusion term is neglected since it is small compared to the other terms, the thermodynamic equation [13] is simplified in the following way

$$\frac{\partial T\prime}{\partial t} \approx \frac{Q'}{\rho_0 C_p H_s} - u_s' \cdot \nabla \bar{T} - \overline{u_s} \cdot \nabla T' - \frac{w_e \prime \Delta \bar{T}}{H_s} - \frac{\overline{w_e} \Delta T\prime}{H_s} \qquad [14]$$

From the equation [14] the different terms of the thermodynamic equation has been computed and are presented in section 6.2. The simulation provides the temperature of the layer (T), the zonal velocity of the oceanic currents (u_s), the net heat fluxes (Q), the entrainment velocity (w_e) and the temperature in the base of the mixed layer (T_e).

The temperature gradient of the sea surface can be expressed as,

$$\nabla T = \frac{\partial T}{\partial x}\vec{\imath} + \frac{\partial T}{\partial y}\vec{\jmath} \quad [15]$$

For the computation of the derivatives, a finite-difference scheme has been applied for the spatial dimensions x and y of the temperature field. As the change in temperature along the longitude and latitude should be calculated, according to the spatial grid, the derivates of equation [14] are decomposed as follows,

$$\frac{\partial T}{\partial lon} = \frac{\partial T}{\partial X} \cdot \frac{\partial X}{\partial lon} = \frac{\partial T/\partial X}{\partial lon/\partial X} \quad [16]$$

$$\frac{\partial T}{\partial lat} = \frac{\partial T}{\partial Y} \cdot \frac{\partial Y}{\partial lat} = \frac{\partial T/\partial Y}{\partial lat/\partial Y} \quad [17]$$

being $\frac{\partial T}{\partial X}$ and $\frac{\partial T}{\partial Y}$ the change in temperature in X and Y, longitude and latitude respectively.

For the boundaries of the domain, these terms have been computed from a lead or lagged finite-differences, while for the grid points inside the domain, the centered finite-differences scheme has been applied[5], for instance, for the term $\frac{\partial T}{\partial X}$,

Lead differences $\frac{T(i,j+1)-T(i,j)}{\Delta x}$ [18]

Centered differences $\frac{T(i,j+1)-T(i,j)}{\Delta x}$ [19]

Lagged differences $\frac{T(i,j+1)-T(i,j)}{\Delta x}$ [20]

[5] The function gradient from Matlab has been applied for the computation of these derivatives

For the *SimAtlVar*, H_s has been considered constant and equal to 50m in according to Chang et al. (1994). The zonal currents (u_s), velocity of entrainment (w_e) and net heat fluxes (Q) are provided by *SimAtlVar.* For the calculation of the heat budget for the observations and the SPEEDY-NEMO simulation, the H_s is considered to be the isotherm of 20C(z20), as a measure of the thermocline depth. Therefore, the terms have been evaluated over the layer above z20. To notice that, in the SPEEDY-NEMO simulation, only the zonal currents were available to us, thus the vertical terms were not calculated.

A heat budget analysis has been carried out with an Ocean General Circulation model (OGCM) and it will be described in detail in section 6.5.

5. METHODOLOGY

The main objective of this Thesis is the study of the air-sea interactions associated with the connection between the inter-annual variability modes of the tropical Atlantic and Pacific Oceans, including its stationarity.

The climate variability can be defined as the study of the climate anomalies of a specific physical field. Thus, statistical methods and tools are used to analyse the atmospheric and oceanic variability of the tropical Atlantic and Pacific regions, as well as, to understand the underlying physical mechanisms.

5.1. Data

The data of the atmospheric and oceanic fields used in the present Thesis comes from observations and reanalysis datasets. Additionally, to better understand the physical processes at work in the observational results, model simulations have been also considered.

5.1.1. Sources of data

5.1.1.1 Observations

HadISST

The HadISST dataset has been computed by the Met Office Hadley Centre. The SST data are taken from the Met Office Marine Data Bank (MDB) and from the Comprehensive Ocean-Atmosphere Data Set (COADS) (now ICOADS). Moreover, the sea ice data are provided by a variety of sources including digitized sea ice charts and passive microwave retrievals.

The HadISST data have a spatial resolution of 1°x1° and covers the period from 1870 up to now. These data are based on in-situ observations and are extended to more sparse oceanic regions through the application of a two stage reduced-space optimal interpolation procedure (RSOI, *Kaplan* [1997]) that uses EOF technique [*Rayner et al.*, 2003].

5.1.1.2 Reanalysis

Reanalysis is a scientific method to produce data sets for climate monitoring and research. Reanalyses are created through a "frozen" (unchanging) scheme of data assimilation, which considers all available observations every 6-12 hours over the period being analyzed. A reanalysis typically extends over several decades or longer, and covers the entire globe from the Earth's surface to well above the stratosphere. Reanalysis products are used extensively in climate research and services, including for monitoring and comparing current climate conditions with those of the past, identifying the causes of climate variations and change, and preparing climate predictions.

a) Atmospheric reanalysis

The atmospheric reanalyses are built from Atmospheric Global Coupled Model (AGCM) simulations, which consider the observed SST as a boundary condition and are constrained by the assimilation of meteorological observations. A reanalysis is forced to follow the

observed atmospheric variability, through the correction from the simulated to the observed variables every 6 hours.

ERA40 reanalysis

ERA-40 is an atmospheric reanalysis of meteorological observations created by the European Centre for Medium-Range Weather Forecasts (ECMWF) that goes from September 1957 to August 2002 [*Uppala et al.*, 2005] and has a spatial resolution of 2.5°x2.5° and 60 vertical levels (top in 0.1 hPa). The observations assimilated are air temperature, humidity, radiance, surface pressure, wind, oceanic wave height, among others, provided by satellite-borne instruments (from the 1970s onwards), aircraft, ocean-buoys and radiosondes (since the late 1980s).

The data assimilation system used for ERA-40 was based on the software version of the ECMWF data assimilation and forecasting system 3D-VAR [*Uppala et al.*, 2005], with a model resolution of T159 and 60 levels in the vertical. It is the first reanalysis to directly assimilate satellite radiance data and cloud motion winds are also used. Regarding to its limitations, the tropical moisture (precipitation, total column water vapor) is larger than the observed from 1991 onward. Moreover, the precipitation exceeds evaporation and spurious temperature trends appear in the Artic region.

NCAR 20th reanalysis

The NCAR 20th reanalysis is an atmospheric reanalysis performed with the Ensemble Kalman Filter as described in [*Compo et al.*, 2011] based on the method of [*Whitaker and Hamill*, 2002]. This reanalysis assimilates observations of surface pressure and SLP from the International Surface Pressure Databank station component version 2 [*Yin et al.*, 2008], ICOADS [*Woodruff et al.*, 2010], and the International Best Track Archive for Climatic Stewardship (IBTrACS, *Kruk et al.* [2010]) every 6 hours.

The model has a spatial resolution of 2°x2° and 28 levels in the vertical. The data are extended from 1871 up to the present. The specified boundary conditions of the model are taken from the time-evolving SST and sea ice concentration fields of the HadISST1.1 dataset [*Rayner et al.*, 2003].

b) Oceanic reanalysis

SODA reanalysis

The Simple Ocean Data Assimilation, SODA [*Carton et al.*, 2000; *Giese and Ray*, 2011] is an oceanic reanalysis that uses the model POP2.x to assimilate the variables provided by the NCAR 20th reanalaysis (*Whitaker et al.* [2004]; *Compo et al.* [2006]) and SST observations from ICOADS [*Giese and Ray*, 2011]. It has horizontal resolution of 0.5°x0.5° and 40 vertical levels levels, 10m top layer and covers the period 1871-2008. The reanalysis provides three types of variables, those well constrained by observations, those partly constrained by dynamical relationships to variables frequently observed, and those poorly constrained such as horizontal velocity divergence

5.1.1.3 Considerations about the variables

Thermocline depth (z20)

The 20ºC isotherm depth (z20) is considered as a proxy of the thermocline depth. The data of the upper ocean temperature come from SODA reanalysis.

Wind stress

The wind stress is the variable responsible of the transference of momentum from the atmosphere to the ocean, so it could be interpreted as the surface wind that is effective in modifying the surface ocean [*Steward*, 2008]. It is defined as the drag per unit of area caused by wind shear, so the wind stress applies a friction over

the sea surface that can drive the oceanic currents [*Gill*, 1982; *Pickard and Pond*, 1983]. The wind stress can be expressed as:

$$\tau = \rho_a c_D {U_{10}}^2 \qquad [21]$$

where $\rho_a = 1.3\ kg/m^3$ is the density of air, c_D is the empirical drag coefficient and U_{10} is the surface wind at 10 meters. The direction of the wind stress is the same as the surface wind [*Gill*, 1982; *Pickard and Pond*, 1983]. Monthly means of wind stress have been used in the present Thesis, from SODA reanalysis [*Giese and Ray*, 2011].

Velocity potential

Any flow can be expressed as the sum of a divergent and a rotational component,

$$\vec{v} = \vec{v}_\psi + \vec{v}_\phi \quad [22]$$

being $\vec{v}_\psi$ and $\vec{v}_\phi$ the divergent and rotational parts of the zonal wind $\vec{v}$ and ψ and ϕ the streamfunction and velocity potential, respectively, which verify

$$\vec{\nabla} \times \psi = \vec{v}_\psi \quad [23]$$

$$\vec{\nabla}\phi = \vec{v}_\phi \quad [24]$$

The velocity potential ϕ is defined as a scalar function that satisfies the basic laws of fluid mechanics: *conservation of mass and momentum*, assuming incompressible, inviscid and irrotational flow [*Lagrange*, 1788]. Thus, the velocity potential can be calculated from the Laplace equation,

$$\nabla^2 \Phi = 0 \quad [25]$$

since ϕ verifies that $u = \frac{\partial \Phi}{\partial x}$ and, $v = \frac{\partial \Phi}{\partial y}$, being u and v the zonal and meridional components of the surface wind.

The divergent part of the flow, the velocity potential, is associated with the convergence and divergence processes related to the vertical motions in the atmosphere [*Wang and Zhang*, 2002]. Thus, in the present Thesis, the velocity potential will provide information about the atmospheric circulation taking part in the tropical regions, induced by changes in the temperature.

Variable	**Description**	**Source**	**Reference**	**Frequency/ Period**
SST	Sea Surface temperature	HADISST SODA	*Rayner et al.* [2003] *Giese and Ray* [2011]	Monthy means 1870-2013 1871-2008
Z20	Thermocline depth	SODA	*Giese and Ray* [2011]	Monthly means 1871-2008
SSH	Sea Level Height	NEMO-INTER simulation	*Martín-Rey et al.* [2015b]	Monthly means 1960-2011
Wind stress	Wind stress	SODA	Giese and Ray [2011]	Monthly means 1871-2008
u,v	Surface wind	DFS4 NCAR-20th	*Brodeau et al.* [2010] *Compo et al.* [2011]	Monthly means 1960-2011 1871-2008
w	Vertical velocity	ERA-40	*Uppala et al.* [2005]	Monthly means 1957-2002
SLP	Sea Level Pressure	ERA-40 NCAR-20th	*Uppala et al.* [2005] *Compo et al.* [2010]	Monthly means 1957-2002 1871-2010
chi200 chi925	Velocity potential	NCAR-20th	*Compo et al.* [2011]	Monthly means 1871-2010
Q	Heat Fluxes	OAFlux	*Yu et al.* [2008]	Monthly means 1958-2013

Table M1. Summary of the atmospheric and oceanic variables from different data sets used in the present Thesis.

5.1.1.4 Model simulations

Modelled simulations with partially coupled models and Ocean General Circulation Models (OGCMs) have been also considered in the present work.

a) Partially coupled simulations

The partially coupled simulations are very useful since they allow to study the air-sea interactions in specific regions. Two different partially-coupled simulations have been used in the present Thesis, **SPEEDY-RGO** and **SPEEDY-NEMO**. In both cases, the atmospheric part is an Atmospheric Global Coupled Model (AGCM), with T30 horizontal resolution and 8 levels in the vertical, SPEEDY model [*Molteni*, 2003; *Kucharski et al.*, 2008]. For the **SPEEDY-RGO**, this AGCM is coupled to an extended 1.5-layer reduced-gravity model with a resolution of 2°x1° in longitude-latitude [*Chang*, 1994; *Kucharski et al.*, 2008]. In the oceanic part of the model only the top layer is dynamically active, with the interface between the upper and the deep ocean representing the thermocline and assuming the deep ocean as motionless and infinitely deep. The thermodynamic equation is also included to relate temperature variations with mixing, advection and surface heat fluxes [*Chang*, 1994]. A flux correction has been applied to the climatological surface heat fluxes and wind stress in order to reduce the model's drift [*Chang et al.*, 2006b].

Two different groups of simulations have been used:

– ***SimAtlVar*** simulations: fully coupled simulations in the tropical Indo-Pacific basin [30°N-30°S] and climatological SSTs elsewhere, except for the Atlantic Ocean [60°N-60°S], where observed monthly varying SSTs are used. The resulting SST for the tropical Pacific basin corresponds to an ensemble of nine runs for the total period 1949-2002. Additionally, these simulations were extended to the period 1871-2002.

– ***SimAtlCli*** simulations: fully coupled simulations in the tropical Indo-Pacific basin and climatological SSTs elsewhere. The resulting SSTs of the ensemble of five runs correspond to a total period of 132 years.

On the other hand, **SPEEDY-NEMO** has the same experimental design than **SPEEDY-RGO** in *SimAtlVar*, observed SSTs are prescribed in the Atlantic Ocean and it is fully coupled to the Indo-Pacific basin. Nevertheless, this set of simulations considered the version 3.0 of NEMO model [*Madec et al.*, 1998],which is a primitive equation z-level model that uses the hydrostatic and Boussinesq approximations. It has a tripolar ORCA2 configuration with horizontal resolution and a tropical refinement to 1/2. The model has 31 levels in depth with a thicknesses ranging from 10 m at the surface to 500 m at the ocean bottom. The simulated period goes from 1949 to 2015. Only one member of the ensemble was used.

The SPEEDY-RGO and SPEEDY-NEMO simulations have been used to investigate the impact of the tropical Atlantic variability in the development of ENSO phenomena (in Sections 6.1, 6.2 and 6.3).

b) OGCM simulations

In order to investigate the oceanic processes involved in the development of the Atlantic Niños, simulations with a regional configuration of NEMO (Nucleus for European Modelling of the Ocean) model, has been used.

The regional NEMO-ATLTROP configuration has been developed in LOCEAN laboratory (http://forge.ipsl.jussieu.fr/nemo-atltrop) from the NEMO OGCM [*Madec*, 2008] including the global "Océan Parralélisé" (OPA) module. OPA solves the primitive equations on an Arakawa C grid, with a second-order finite difference scheme. NEMO-ATLTROP is restricted the tropical Atlantic region, where the nominal horizontal resolution is 0.25°x 0.25° and the grid has been limited to 30°N and 30°S. The maximum depth of 5000 m is spanned by 46 z-

levels ranging from 5 m thickness in the upper 30 m to 200 m thickness at the bottom.

Surface boundary forcing is ensured by bulk formulas developed by [*Large et al.*, 1997]. Input surface variables needed to estimate air-sea fluxes are wind speed at 10m, air temperature and humidity, shortwave and long-wave radiations and precipitation. Global 6-hour variables from a combination of ECMWF analyses and reanalysis and observed flux data, called "DRAKKAR forcing sets" (DFS4,*Brodeau et al.* [2010]) are used as external forcings. The DFS4 data set includes corrections in the temporal discontinuities and yield better agreement with some recent high quality data. The use of this forcing set was shown to improve the representation of central features of the global ocean circulation.

Simulation	Model	Forcing	Use
SimAtlVar	SPEEDY-RGO	Observed Atlantic SSTs	Understand the contribution of the Atlantic to the inter-annual tropical Pacific variability
SimAtlCli	SPEEDY-RGO	Climatological SSTs	Compare the internal variability with the Atlantic-forced one
SPEEDY-NEMO	SPEEDY-NEMO	Observed Atlantic SSTs	Understand the contribution of the Atlantic to the inter-annual tropical Pacific variability
NEMO-INTER	NEMO-ATLTROP	Surface wind	Analyse the air-sea interactions involved in the inter-annual variability modes

Table M2. Summary of the different simulations used in the present study.

In the PhD Thesis an inter-annual simulation for the period 1958 to 2011 has been performed, hereinafter, NEMO-INTER simulation. In order to avoid the initial drift of the model, the first two years of the

simulation have not been considered. This simulation provides the heat budget terms of the mixed layer as output files, which will be used to analyse the oceanic processes involved in the development of the different Atlantic Niño phenomena, in a similar way than *Polo et al.* [2015a]. The modelled data used from NEMO-INTER goes from 1960 to 2011.

5.2. Methodology

The statistical analysis carried out starts with a pre-processing of the data in which the climate anomalies have been calculated for different frequencies, which are isolated through the application of statistical filters. The computation of climate indices or the determination of the running correlation between two fields, are also part of the pre-processing stage. Then, several multivariante discriminant techniques have been applied to determine the main directions of maximum variability of the oceanic or atmospheric field. Finally, the results are represented as different spatial maps, in which their significance is assessed through the application of statistical significant tests (Figure M1).

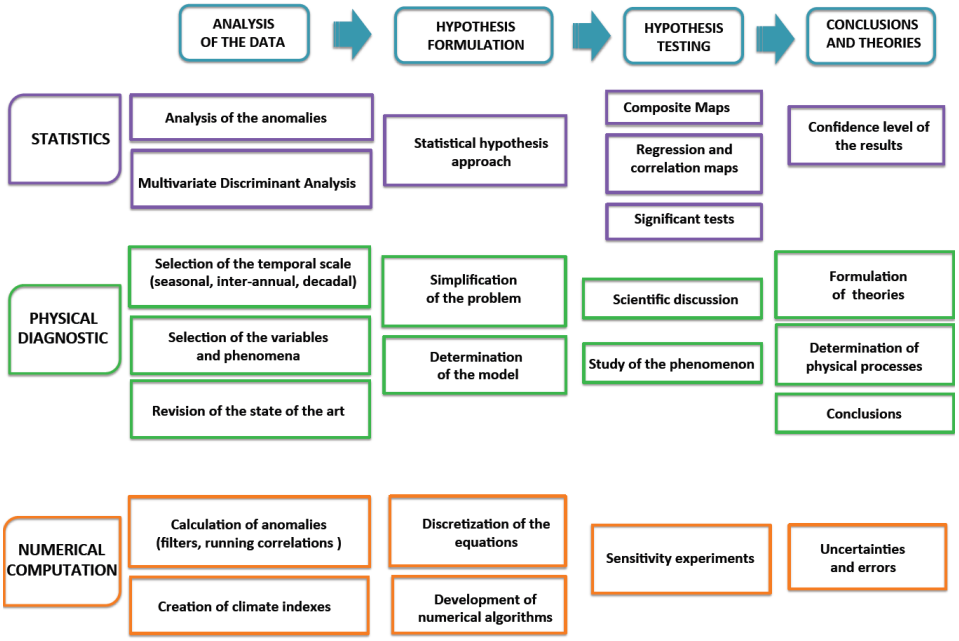

Figure M4. Scheme of the analysis of the data

5.2.1. Pre-processing of the data

5.2.1.1 Seasonal means and anomalies

In general, the absolute value of a climate variable in a particular time "t" can be described as the sum of its mean state and the deviation with respect that state (anomaly). The mean state is defined as the long-term mean of a specific atmospheric or oceanic field, while the deviations from that mean are denoted as anomalies. In this sense, any climatic field can be decomposed as:

$$Y = \bar{Y} + Y' \quad [26]$$

where Y' are the anomalies of the climatic field Y in a given region and during a certain period respect to the long-term mean value $\bar{Y}$. Different climatological means have been considered in the present work, associated with different periods of study, which should be taken into account in the interpretation of the results. The calculation of the anomalies depends on the temporal domain, in a way that weekly, monthly, seasonal or annual anomalies let study the climate variability from intra-seasonal to inter-annual or decadal time scales.

In the present Thesis, seasonal anomalies, computed by subtracting the seasonal cycle of the period of study, are considered as a measure of the inter-annual variability of a specific month or season. In particular, summer months from June to September (JJAS) and winter months from December to March (DJFM) have been considered for the study of the tropical Atlantic and Pacific respectively, because they correspond to seasons in which those oceans exhibit maximum variability. Furthermore, for the analysis of the wave activity, the intra-seasonal variability has been investigated from 5-day anomalies, calculated by subtracting the monthly means of the period of study.

5.2.1.2 Filtering the data.

The variability of a physical field is caused by diverse processes operating at different time scales [*Von Storch and Zwiers*, 2001]. Statistical filters are commonly used in climate variability, since they allow separating the variability associated with a specific phenomenon, according to its frequency or wavelength. In this sense, the time series of a selected field can be expressed as:

$$Y_t = Y_t^H + Y_t^L \qquad [27]$$

where Y_t^H and Y_t^L represents the stationary high and low variability components, respectively. The different filters used in the present Thesis are described as follows.

Running mean filter

The running mean is a simple filter to smooth a selected signal by removing the fast variations. This filter consists in replacing each value Y_t of the time series by a temporal mean in a specific time interval with a 2K+1 length [*Von Storch and Zwiers*, 2001]:

$$Z_t = \sum_{k=-K}^{K} \frac{1}{2K+1} Y_{t+K} \qquad [28]$$

Thus, the running mean is classified as a low-pass filter. In this manuscript, this technique is used to investigate the low-frequency changes in the mean state and variability of the tropical Atlantic and Pacific Oceans (see section 6.1).

Inter-annual filter

To isolate the shorter variations from those of lower frequencies, an inter-annual filter is applied to the data. This filter is based on the computation of the differences between the value of one year and the precedent one during the whole temporal domain,

$$\Delta Y = Y_t - Y_{t-1} \qquad [29]$$

highlighting in this way the atmospheric and oceanic inter-annual variations. This is a standard and widely used method for de-trending time series [*Bjerknes*, 1964; *Box and Jenkins*, 1976; *Stephenson et al.*, 2000]. This filter has been applied to the seasonal tropical Atlantic and Pacific SST anomalies to isolate the high frequency signal associated with the Atlantic Niño and ENSO phenomena (section 6.3).

Butterworth filter

A digital filter, the Butterworth filter [*Butterworth*, 1930], is also considered in the present Thesis. This filter uses the Laplace transform or Z transform (for continuous-time or discrete-time signals) to describe the relationship between the input *x(t)* and the output *y(t)* signals through the transfer function H(s). This transfer function H(s) can be expressed in the s-plane as

$$H(s) = \frac{Y(s)}{X(s)} \quad [30]$$

where s is the imaginary axis, X(s) and Y(s) the Laplace or Z transforms of x(t) and y(t) signals, respectively.

The design of the digital filters lets isolate the signal in a specific range of frequencies, named as *passband*. Depending on the temporal domain, from shorter to intermediate or longer time scales, the filters are denoted as low-pass, band-pass and high-pass filters. The range of frequencies attenuated by the filter is called *stopband*.

In particular, in the present Thesis, a high-pass Butterworth filter[6] with a cut-off frequency of 7 years has been applied to the seasonal anomalies of the tropical Atlantic SST, to isolate the inter-annual variability related to the Atlantic Niño phenomenon (see section 6.5). Furthermore, a band-pass Butterworth filter, with pass-band frequencies of 20-100 days is applied to the 5-day SSH anomalies to study of the wave activity associated with the development of the Atlantic Niño (see section 6.5).

[6] The Butterworth filter can be applied using the internal functions *butter* and *filtfilt* from the mathematical software Matlab.

5.2.1.3 Calculation of climate indices

Climate indices are useful indicators of the climate variations in selected regions. A climate index is defined as the area-averaged value of a physical field for each time step of the temporal domain, obtaining in this way, a time series of the original field. In this Thesis, several indices associated with the Atlantic and Pacific inter-annual variability have been considered. In particular, equatorial Atlantic and Pacific anomalous SSTs are used to characterize the Atlantic Niño and El Niño phenomena (Figure M5).

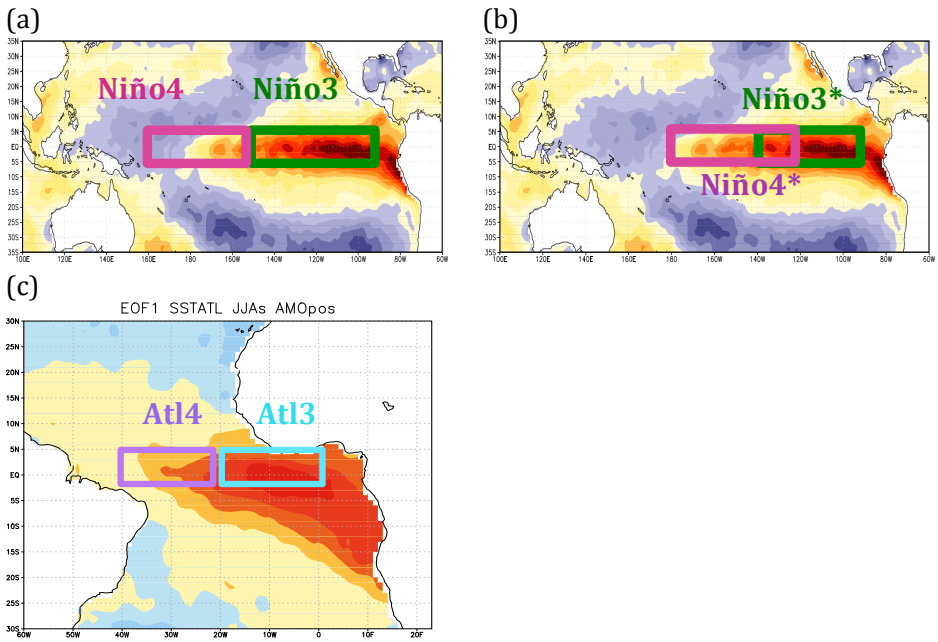

Figure M5. Climate indices in the tropical Atlantic and Pacific basins. (a) Regions used to compute Niño3 [150°W-90°W, 5°N-5°S] and Niño4 [160°E-150°W, 5°N-5°S] indices. (b) Same as (a) but for Niño3* [140°W-90°W; 5°N-5°S] and Niño4* [180°E-120°W, 5°N-5°S]. (c) Same as (a) but for Atl3 [20°W-0°E, 3°N-3°S] and Atl4 [40°W -20°W, 3°N-3°S] indexes.

Regarding the Pacific basin, Niño3-index is defined as the anomalous SSTs averaged over the central-eastern Pacific [150°W-90°W, 5°N-5°S], while Niño4-index contains averaged SST anomalies in the central Pacific [160°E-150°W, 5°N-5°S] (Figure M5a). Additionally, for the partially coupled simulations also considered in this Thesis (see section 5.1.1.4), a new definition of Niño3 and Niño4 indexes is

required: Niño3* is the anomalous SST averaged in the region [140°W-90°W; 5°N-5°S] and Niño4* is the averaged SST anomalies in the area [180°E-120°W, 5°N-5°S] (Figure M5b). In a similar way, the Atlantic Niño phenomenon is characterized by Atl3 and Atl4 indexes, associated with the averaged SST anomalies over the eastern [20°W-0°E, 3°N-3°S] and western [40°W -20°W, 3°N-3°S] equatorial Atlantic, respectively (Figure M5c).

The indices of the Inter-Decadal Pacific Oscillation (IPO), Atlantic Multidecadal Oscillation (AMO) and the Global Warming (GW), have been defined as in *Villamayor and Mohino* [2015].

5.2.1.4 Running correlation

One of the most common techniques to evaluate the relationship between two atmospheric or oceanic variables, X and Y, is to calculate the linear correlation between them. In the present Thesis, the Pearson correlation has been used,

$$r_{xy} = \frac{Cov(X,Y)}{s_x s_y} = \frac{\frac{1}{n-1}\sum_{i=1}^{n}[(x_i-\bar{x})(y_i-\bar{y})]}{\left[\frac{1}{n-1}\sum_{i=1}^{n}(x_i-\bar{x})^2\right]^{1/2}\left[\frac{1}{n-1}\sum_{i=1}^{n}(y_i-\bar{y})^2\right]^{1/2}} \quad [31]$$

where Cov(X,Y) is the covariance between both variables and s_x and s_y are their standard deviations [*Von Storch and Zwiers*, 2001]. In this sense, correlation scores close to ±1 indicate a higher connection between both fields, while correlation values near 0 implies the absence of relationship between them.

Furthermore, an important aspect to take into account in the study of climate variability is the possible time-dependence of the correlation between two fields. For this reason, the running-correlation or moving correlation is used. The running correlation explores how the correlation between two fields varies in time through the selection of *n*-size windows. The correlation is calculated in the window of the first *n* observations, then the window is moved by one position, and

the correlation is re-calculated. This procedure is repeated for the whole data series. Although the running correlation is a useful tool to evaluate the possible relationship between two fields, more sophisticated techniques using the covariance matrix, described in the following section, will provide a better understanding of the inter-relation between climate variables.

5.2.2. Discriminant analysis

The study of the climate variability involves the use of a huge amount of data, due to the large temporal and spatial extensions of the climatic regions. Thus, it is necessary to apply statistical discriminant analyses that help to determine the directions in which maximum variability is organised. The most useful statistical techniques are the Empirical Orthogonal Functions (EOF) and the Maximum Covariance Analysis (MCA, *Von Storch and Zwiers* [2001]).

On the one hand, the purpose of EOF analysis is to reduce the dimensions of a spatial-temporal field containing a large number of variables to a few dimensions or principal components that explain the maximum percentage of variance. These new variables are linear combinations of the original ones and are chosen to represent the maximum fraction of the variability of the original field [*Wilks*, 2005]. On the other hand, MCA technique looks for the linear combinations of the time series of each field that explain the maximum covariance between them [*Wallace and Gutzler*, 1981; *Bretherton et al.*, 1991; *Von Storch and Zwiers*, 2001; *Polo et al.*, 2008a]. In particular, in the present Thesis, an Extended Multiple Maximum Covariance Analysis (EMMCA) is designed and applied to the anomalies and it will be described in detail in next sections.

5.2.2.1 Empirical Orthogonal Functions (EOF)

The EOF analysis was firstly introduced by *Lorenz* [1956] and it is quite possibly the most widely used multivariate statistical technique in atmospheric and oceanic sciences. Principal Component Analysis (PCA) also refers to the same procedure.

Regarding to climate variability, EOF technique decomposes the anomalous field into a number of modes which maximize the variance of a two-dimensional space-time matrix $Y(n_s, n_t)$, being n_s the spatial dimension and n_t the temporal one. The application of the EOF analysis provides a set of spatial structures (EOFs) and associated temporal series (Principal Components, PCs), which together describe the *modes of variability* (Figure M6). Each variability mode explains a fraction of the total variance of the original field (Y).

From a mathematical point of view, for a given field $Y(n_s,n_t)$- being n_s and n_t the spatial and temporal domains respectively- the anomalies are calculated by subtracting the temporal mean $\bar{Y}$ to the original field (Y) for each point of the spatial domain,

$$Y'(t) = Y(t) - \bar{Y}(t) \quad [32]$$

The EOF analysis[7] consists on the eigenvalue decomposition of the covariance matrix, C, of the temporal anomalies,

$$C = \frac{1}{N}\sum_t Y'(t) * Y'(t)^T \quad [33]$$

which, for the case of a non-singular square matrix verifies:

$$C*E = L*E \quad [34]$$

The columns of the matrix E contain the so-called eigenvectors e_k (EOFs) of the covariance matrix and the elements of the diagonal of the matrix L constitute the eigenvalues λ_k of C, being k the number of modes. The eigenvalues give a measure of the variance explained by each pattern [*North*, 1984].

These EOFs represent the directions of maximum variability of the total field. Considering a number of K modes, the original field Y can

[7] This computation can be performed using internal functions of the mathematical software Matlab as *princomp*, *eig*, *pca* or *pcacov*.

be reconstructed as a linear combination of the orthogonal spatial patterns e^k (or EOFS) and their associated coefficients α_k (or PCs):

$$Y'(t) = \sum_{k=1}^{K} \alpha_k(t) * e^k \quad [35]$$

with a minimum root mean square error (RMSE),

$$RMSE = \sum_t \left[Y(t) - \sum_{k=1}^{K} \alpha_k(t) * e^k \right] \quad [36]$$

The time series or principal components α_k (PCs) are obtained by projecting their associated eigenvectors e^k (EOFs) over the initial anomalous field Y'

$$\alpha_k(t) = Y'(t) * e^k \quad [37]$$

For Gaussian distributions, the coefficients α_k (PCs) are statistically independent with respect to the others and spatially orthogonal to them. Thus, the total variance of the field Y' can be decomposed as independent contributions of the EOFs,

$$\sum_t |Y'(t)|^2 = \sum_{t,k} \alpha_k(t)^2 \quad [38]$$

with each k mode explaining a fraction of the total variance given by the expression,

$$f\ var_k = \left[\frac{\lambda_k}{\sum_{k=1}^{K} \lambda_k} \right] * 100 \quad [39]$$

where λ_k is the eigenvalue of each mode.

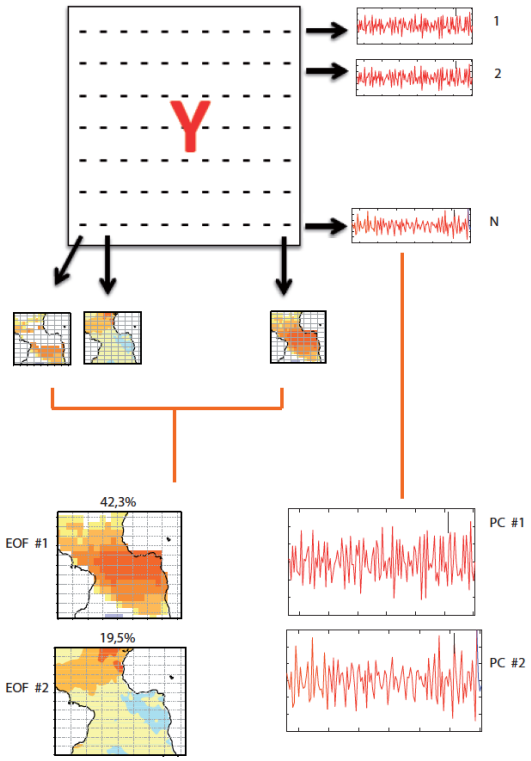

Figure M6. Scheme of the Empirical Orthogonal Function Analysis (From *Rodríguez-Fonseca* [2001] and *Polo* [2008]).

Selection of the optimal number of modes

To select the optimal number of modes that represent a higher fraction of the total variance, it should be taken into account the statistically significance of the EOFs, which depends on the separation between modes. *North et al.* [1982] proposed a diagnostic to determine the independence of the variability modes based on the slope of the estimated eigenvalue spectrum. Following the North criteria [40], if the sampling error of a particular mode is larger than the space between this mode and the precedent one, the mode is part of a degenerate multiplet.

$$\lambda_i - \lambda_{i+1} > \lambda_i * \sqrt{2/N} \quad [40]$$

The representation of the EOFs is carried out through the calculation of regression and correlation maps. These maps are calculated correlating or projecting the standardized PC associated with each mode over the time series of each grid point of the original anomalous field Y'(see section 5.2.4).

5.2.2.2 Maximum Covariance Analysis (MCA)

Another methodology of discriminant analysis involving the use of two or more fields is the Maximum Covariance Analysis (MCA[8]). The MCA calculates the principal directions of maximum covariance between a predictor Z and a predictand field, Y [*Bretherton et al.*, 1991; *Cherry*, 1997]. In fact, this methodology is an application of the Singular Value Decomposition (SVD), which is an algebraical technique to diagonalize non-squared matrices, as happens with the covariance matrix of two fields with different sizes [*von Storch and Frankignoul*, 1998]. SVD calculates linear combinations of the time series of Z and Y (named as expansion coefficients, hereinafter U and V) that maximize the covariance among them (Figure M7).

Mathematically, two spatio-temporal fields $Z(n_z,n_t)$ and $Y(n_y,n_t)$, with spatial dimensions n_z and n_y, and n_t as the temporal one, are considered as the predictor and predictand field, respectively. The time anomalies of both fields are calculated by removing the climatological seasonal cycle to the seasonal means,

$$Y' = Y - \bar{Y} \quad [41]$$
$$Z' = Z - \bar{Z} \quad [42]$$

In this way, the covariance matrix is defined as

$$C = \frac{1}{N}\sum_t \mathrm{Y}'(\mathrm{t}) * \mathrm{Z}'(t)^T \quad [43]$$

[8] To apply this discriminant technique, Matlab internal functions as *svd* are able to perform the computation of the leading modes of maximum covariance between two different fields.

Taking into account that C is non-squared, the diagonalization is done using a diagonal matrix $\Lambda(n_z, n_y)$ that verifies,

$$CC^T = R\Lambda Q^T Q \Lambda^T R^T = R\Lambda^2 R^T \quad [44]$$
$$C^T C = Q^T \Lambda^T R R^T \Lambda Q = Q^T \Lambda^{T^2} Q \quad [45]$$

where R and Q are the orthogonal eigenvectors corresponding to Y and Z respectively.

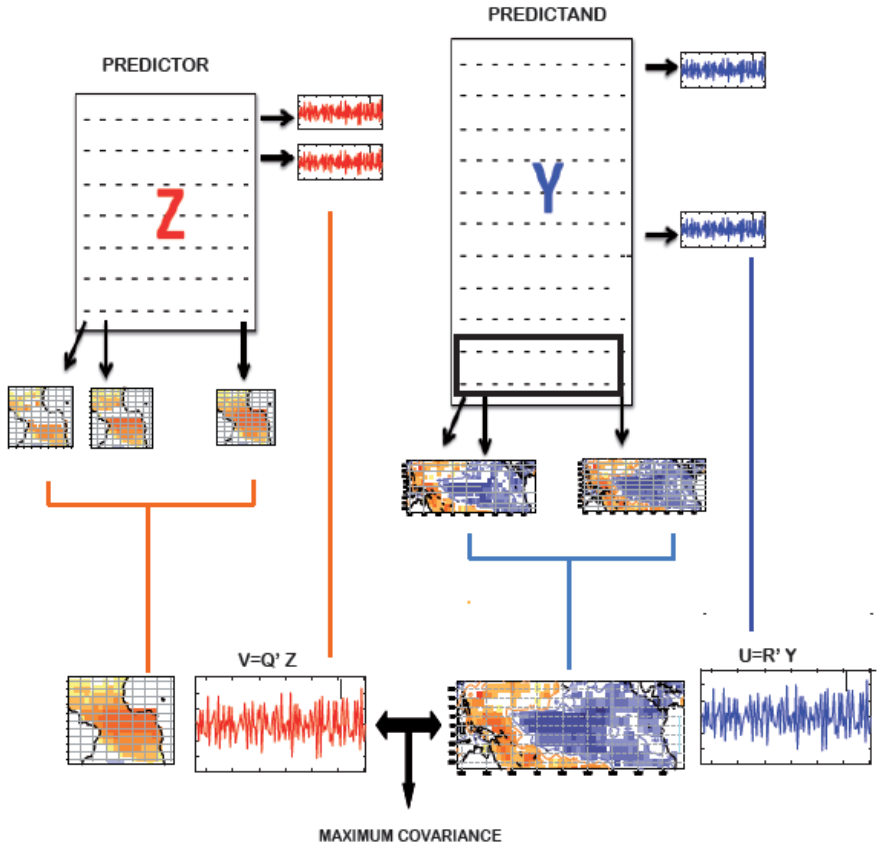

Figure M7. Scheme of the MCA technique (from *Rodríguez-Fonseca* [2001])

The singular vectors R and Q are the spatial configurations of the main mode of covariability, while the expansion coefficients, U and V, are obtained as linear combinations of the original predictor Z and

predictand field *Y*, verifying that the covariability among them is maximum.

$$U = R'^{T} * Y' \qquad [46]$$

$$V = Q'^{T} * Z' \qquad [47]$$

Finally, the eigenvalues λ_k are a measure of the percentage of variance explained by each mode *k*, given by the squared covariance fraction:

$$scf_k = \frac{\lambda_k^2}{\sum_{k=1}^{K} \lambda_k^2} \qquad [48]$$

To evaluate the relation between the expansion coefficients of the predictor (Z) and the predictand (Y) fields for a mode k, the Pearson correlation coefficient (see equation [31]) is calculated

$$r^2{}_k = (corr(u_k, v_k))^2 \qquad [49]$$

The variability modes obtained from the MCA are represented through regression and correlation maps (see section 5.2.4). These maps are computed regressing (correlating) the time series associated with the expansion coefficient onto the time series associated with each of the grid point of the spatial domain of the anomalous predictor (Y) or predictand field (Z). Heterogeneous and homogeneous spatial maps can be represented. The homogeneous maps are calculated by the correlation (projection) of the expansion coefficient with its associated space-time anomalous field. Nevertheless, the heterogeneous maps are calculated projecting or correlating the expansion coefficient of one variable over the anomalous field of another variable.

Both, predictor and predictand fields introduced in the analysis can be formed by one or more variables but also by the same variable in different lags (*Polo et al.* [2005]; [2008]; *García-Serrano et al*. [2008]). In the present Thesis, a new methodology named as Extended

Multiple Maximum Covariance Analysis (EMMCA) has been designed for the first time and it is described in detail in the next section.

Extended Multiple Maximum Covariance Analysis (EMMCA)

The MCA can de applied with one of the domains of the predictand (Y) and predictor matrices (Z) with a more complex dimension depending on the needs. In particular, the present Thesis is focused on the study of the interaction between the inter-annual variability modes of the tropical Atlantic and Pacific variability, which involves the connection of different atmospheric and oceanic fields. As the MCA is applied using multiple lags and variables, it has been named as Extended Multiple Maximum Covariance Analysis (hereafter EMMCA). The EMMCA calculation is a mix of the methodologies exposed in *Polo et al.* [2005] in which multiple variables are included in the analysis and in *Polo et al.* [2008a] in which multiple predictors are included in the analysis.

Nevertheless, in this work one variable has been considered as predictor field (similar to *García-Serrano et al.* [2008]) and multiple lags and variables have been used as predictand one. Thus, the predictor field (Z) has (n_z,n_t) dimensions, but the predictand field Y has dimensions (n_y^{vdl} , n_t) where *vdl* indicate the specific combinations of variables (v), lags (l) and spatial domains (d) for all the fields to predict, all having the same time length (Figure M8).

Once EMMCA is applied, the spatial and temporal patterns for the individual predictand fields are obtained projecting the original predictand matrix Y for the variable i, $Y(n_y^i,n_t)$ over the total expansion coefficient U_k obtained as outputs of the EMMCA:

$$r_{ik} = U_k * Y(n_y^i, n_t)^T \qquad [50]$$

This methodology can be applied to create a regression coefficient, ψ , which would contain the information of the relationship between the predictor and predictand fields. This regression coefficient could be used to predict ENSO phenomena from the tropical Atlantic SSTs.

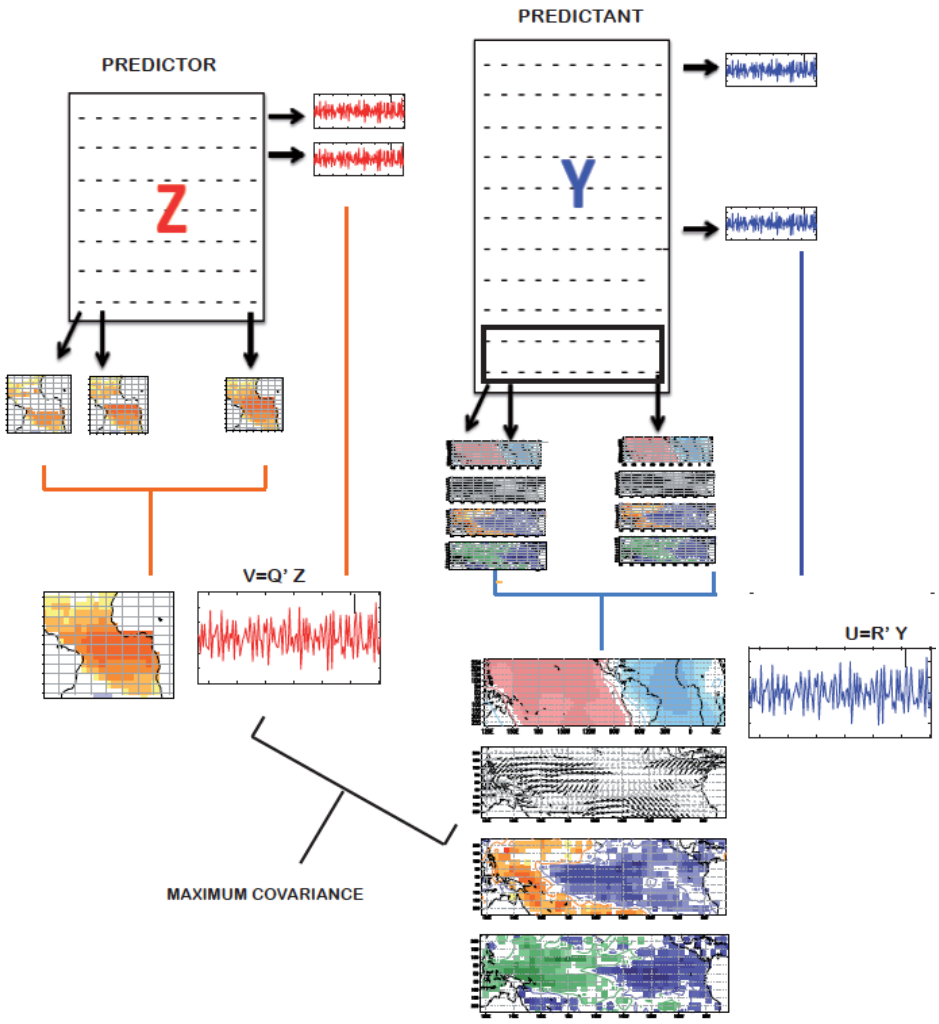

Figure M8. Scheme of the Extended Maximum Covariance Analysis (EMMCA) for a predictor (Z) and a set of predictand fields grouped into the matrix Y(*Martín-Rey et al.* [2014], section 6.3)

For the representation of the variability modes obtained from the EMMCA analysis, heterogeneous and homogeneous spatial maps are shown. The former ones are calculated by projecting or correlating the expansion coefficient of one variable over the anomalous space-time field of another variable (see section 5.2.4). Nevertheless, for homogeneous maps, the expansion coefficient used is the same as the anomalous field considered for the regression or correlation map. Commonly, it is represented the homogenous maps for the predictor field and the heterogeneous ones for the predictand field, in which the statistical significant areas are highlighted.

5.2.3. Hindcast

Using the information from EMMCA, a statistical hindcast of ENSO phenomena considering the Atlantic Niño as predictor is performed in section 6.4.

5.2.3.1 Cross-validated hindcast based on MCA

A statistical hindcast has been developed using the previously described EMMCA technique. In this case, the EMMCA considers an unique predictor field (*Z*) and a set of different variables in specific seasons and regions as predictand field (*Y*).

Firstly, in order to validate the model (EMMCA), a leave-one-out cross-validation method is used. This method consists on repeating the EMMCA procedure n_t times, excluding in each time step the year *i* that is going to be predicted from the original sample [*Dayan et al.*, 2013]. In this way, the covariance matrix used to predict the year *i*, can be expressed as follows:

$$C_i = Z_i(n_z, n_t - 1) * Y_i(n_y, n_t - 1) \quad [51]$$

where n_z, n_y are the spatial dimensions of the predictor (Z) and predictand field (Y) respectively, and n_t is the number of years considered in the analysis. Notice that, the time dimensions of the new samples, for the predictand (Y_i) and predictor fields (Z_i), have been reduced in one year, n_t-1.

Secondly, the EMMCA is applied to the new covariance matrix [26], obtaining a regression coefficient for each year i, $\psi_i(n_z, n_y)$. This regression coefficient contains the information about the relationship between the predictor and the predictand field in that year. The predictand field for the year *i*, is hindcasted from the regression coefficient (ψ_i) and the predictor field (Z_i), which have been constructed from the information given by the rest of the years of the sample, n_t-1:

$$Y_{pred,i}(n_y, n_t - 1) = \psi_i(n_y, n_z) * Z_i(n_z, n_t - 1) \quad [52]$$

Finally, the procedure is repeated n_t times omitting each of the years to be hindcasted until the end of the period of study.

5.2.3.2 Calculation of the skill and root mean square error

Several scores are frequently used to describe the skill of quantitative forecasts. These scores include the correlation skill score, the root mean square error (RMSE) and the proportion of explained variance [*Von Storch and Zwiers*, 2001].In particular, in the present Thesis, the Pearson correlation skill score is calculated to evaluate the goodness of the hindcast and it is defined as,

$$r_{YY_p} = \frac{Cov(Y_p,Y)}{\sqrt{Var(Y_p)Var(Y)}} \quad [53]$$

where $Cov(Y_p,Y)$ is the covariance between the predicted (Y_p) and the observed (Y) field and $Var(Y_p)$ and $Var(Y)$ are the variances of the original fields.

Additionally, the root mean square error (RMSE) of the predicted value respect to the observed one is also estimated as,

$$RMSE = \sqrt{\frac{\sum_{i=1}^{n}(Y_i - Y_{pred,i})^2}{n_t}} \quad [54]$$

where Y_i is observed values and $Y_{pred,i}$ is predicted values for the year i.

5.2.4. Representation of the results

The main results of the Thesis are plotted using different representations that will be described as follows.

5.2.4.1 Correlation and regression maps

Most of the results of this manuscript are presented as regression and correlation maps between climate anomalies and time series reflecting a specific direction of variability.

Correlation maps

The correlation maps are computed as the correlation between a particular time series (T) and each of the time series describing the evolution of a field (M) in each of the grid points (n_s) of a specific region,

$$C_m(n_{s,}1) = corr\ (T(1,n_t)^T, M(n_s,n_t)^T) \quad [55]$$

being n_s and n_t the spatial and temporal dimensions respectively [*Von Storch and Zwiers*, 2001].

The time series can be standardized and are associated with the atmospheric or oceanic anomalies in a selected region (for instance, Niño3 or Atl3 indices). Furthermore, it can be also the Principal Component or expansion coefficient obtained from the EOF or MCA analysis, respectively. A significance test should be applied in order to assess the significant influenced regions, which are those regions in which the evolution of a particular variable shows a significant relation with the time series under study.

Regression maps

Similarly to the correlation maps, the regression maps are calculated projecting each grid point (n_s) of an anomalous field (M) over a standardized time series (T_s),

$$R_m(n_{s,}1) = \frac{(M(n_s,n_t)*T_s(1,n_t)^T)}{(n_t-1)} \quad [56]$$

Only those areas in which the correlation maps are statistically significant can be interpreted. The resultant values indicate that the

change in the amplitude of one variable is associated with a change of 1 standard deviation in the index that has been projected [*Von Storch and Zwiers*, 2001].

5.2.4.2 Composite maps

Another important tool to identify and describe the processes associated with the climate variability is the calculation of composite maps [*Von Storch and Zwiers*, 2001]. The basic idea of composite maps is to construct a 'typical' sample of states of a given anomalous field (M). To this aim, a climate index, defined as the average anomalous field in a selected region, is computed (T_i). Those years in which the climate index is higher/lower than a critical value are chosen. The composite maps are calculated as the average of the anomalous space-time field during those years.

In order to highlight the linear contribution of the signal, for some cases, a high-minus-low composites have been performed as the difference between the composite maps from those associated with the climate index (T_i) higher and lower than a threshold,

$$COMP = \sum_k M(ns,k) - \sum_r M(ns,r) \quad [57]$$

where k and r are the number of 'high' and 'low' events, respectively and M the anomalous space-time field. The separate study of high and low composite maps allows to understand the non-linearities of the spatial pattern associated with the climate phenomenon.

5.2.4.3 Hövmoller diagrams

A hovmöller diagram is a commonly way of plotting atmospheric/oceanic data to emphasize the temporal propagation of climate anomalies. In particular, it is very useful for the study of oceanic waves [*Hovmöller*, 1949]. The axes of a Hovmöller diagram are typically longitude or latitude (in the x-axis) and time (in the y-axis). Moreover, hovmöller diagrams are also used to plot the time evolution of vertical profiles of scalar quantities such as temperature,

density, or concentrations of constituents in the atmosphere or ocean. In that case time is plotted along the abscissa and vertical position (depth, height, pressure) along the ordinate (Figure M9).

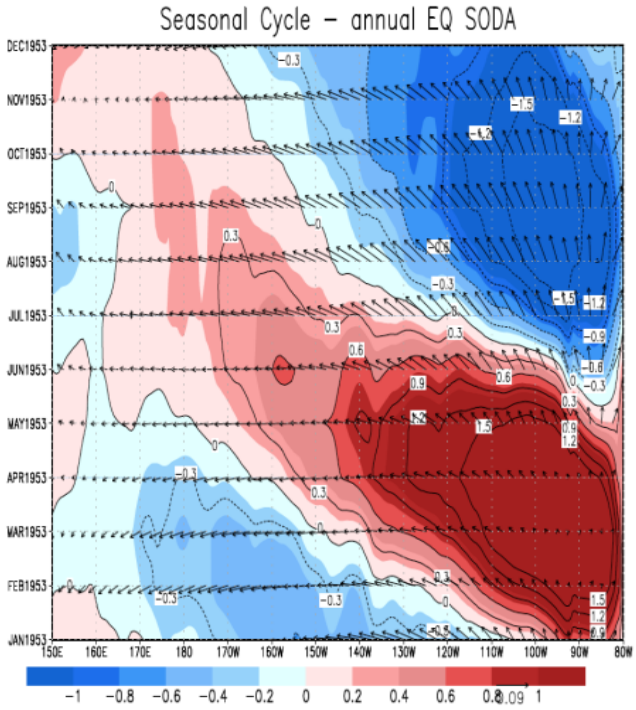

Figure M9. Hovmöller of the seasonal cycle of the SST (shaded), thermocline depth (contours) and surface wind (vectors) average over the equatorial band (5N-5S). From *Polo et al.* [2015a].

In the present Thesis, hovmöller diagrams have used to analyse the development of the Atlantic-forced ENSO phenomena (see section 6.2), the changes in the equatorial Atlantic and Pacific mean state and variability during the second half of the 20th century (see section 6.1) and the wave activity in the tropical Atlantic and Pacific basins during the development of the Atlantic and Pacific El Niño phenomenon (see section 6.5).

5.2.5. Significance tests

In climate research, due the limited number of samples, it is necessary to estimate the significance of the results. It allows us to avoid those non-robust patterns that are obtained by chance, as a consequence of mathematical artefacts. For this reason, statistical tests based on the

procedure called *hypothesis testing* are applied to the climate data [*Von Storch and Zwiers*, 2001]. The *hypothesis testing* considers an initial hypothesis, the null hypothesis H_0, which is accepted or rejected based on statistical methods applied for a sample of the population of study. The alternative hypothesis H_1 encompasses a range of possibilities that may be true if the H_0 is false. A *hypothesis testing* process can only have two outcomes: either H_0 is rejected or it is not rejected. The former does not imply acceptance of H_1, it simply means that there is strong evidence that H_0 is false. Failure to reject H_0 simply means that the evidence in the sample is not inconsistent with H_0 [*Von Storch and Zwiers*, 2001].

Different hypothesis tests are used depending on the probability distribution of the population for the variable considered and the null. A *test statistic* following a given probability distribution, named as the null distribution, is computed and, together with the significance level (1-α) determines the so-called *non-rejection region* of H_0. If the test statistic falls inside the non-rejection region of H_0, the null hypothesis is non-rejected with the chosen confidence level. On the contrary, if the test statistic is placed outside the non-rejection region of H_0, the alternative hypothesis is accepted with a significance level of α (Figure M10). Notice that the confidence level is crucial to define the width of the rejection region and thus, it drives the significance of the variable of study.

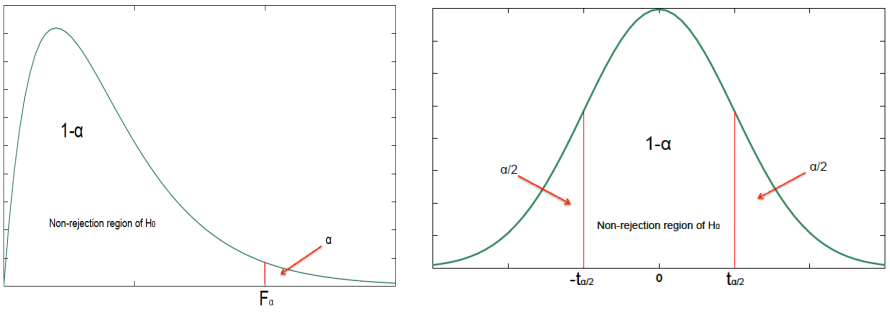

Figure M10. Probability density function of a statistic for a one-tailed (left) and two-tailed tests (right). The green lines represent the probability density function of the statistic when H_0 is true and the red lines limite the non-rejection region with a confidence level (1-α).

Two different hypothesis tests exist: parametric and non-parametric tests. The former ones are those that follow a particular theoretical distribution as an appropriate representation of the data, while the non-parametric test is not assumed to be driven by a specific distribution. The parametric test usually presents a normal distribution, but the null distribution should be built up for the non-parametric tests [*Wilks*, 2005].

Moreover, the hypothesis tests are also classified as one-tailed and two-tailed tests. One-tailed tests are used for asymmetric distributions that have a single tail, in which it is expected that violations of the null hypothesis will be associated with a test statistic located in a particular side of the null distribution (Figure M7, left). On the other hand, a two-tailed test is used when either a very large or very small values of the test statistic are unfavourable to the null hypothesis. The rejection region for two-tailed tests consists of both the extreme left and extreme right tails of the null distribution. These two portions of the rejection region are delineated in such a way that the sum of their two probabilities under the null distribution yields the level of the test (Figure M8,right; *Wilks* [2005]).

In the present Thesis, several parametric tests, as the Student's t-test for equal means or the Fisher test for equal variances, an non-parametric ones as a Monte Carlo test are used and will be described in the following sections.

5.2.5.1 Parametric tests

T-test of equal means

It is a parametric test that compares the mean of two samples x_1 and x_2 that are assumed to follow a normal distribution and which have equal but unknown variances. Thus, the null and alternative hypotheses are:

H_0: The means of the populations of the samples are equal: $\mu_1 = \mu_2$

H1: The means of the populations of the samples are different: $\mu_1 \neq \mu_2$

The test statistic is defined as:

$$t = \frac{\bar{x}_1 - \bar{x}_2}{\sqrt{\frac{s_1^2}{n_1} + \frac{s_2^2}{n_2}}} \quad [58]$$

where s_1,s_2 and n_1,n_2 are the variances and sizes of the original samples x_1 and x_2 respectively [*Von Storch and Zwiers*, 2001].

For a significance level α, the non-rejection region of H_0 is given by the interval $[-t_{d,\alpha/2}, t_{d,\alpha/2}]$, being *d* the number degrees of freedom, calculated as

$$d = \frac{\left(s_1^2/n_1 + s_2^2/n_2\right)^2}{\frac{(s_1^2/n_1)^2}{n_1 - 1} + \frac{(s_2^2/n_2)^2}{n_2 - 1}} \quad [59]$$

When the size of the samples is higher, $n_1+n_2 > 30$, the null distribution of a Student's t-distribution follows the normal distribution with *d* degrees of freedom.

In the present work, the Student's t-test of equal means is applied considering a significance level $\alpha=0.1$ or $\alpha=0.05$.

T-test of correlation

It is a parametric test that estimates the relationship between two samples, x_1 and x_2 through the calculation of the linear Pearson correlation (see equation [31]) between them:

$$r_{x_1 x_2} = \frac{cov_{x_1 x_2}}{s_{x_1} s_{x_2}} \quad [60]$$

where *cov* is the covariance between x_1 and x_2 and s_{x1} and s_{x2} the variance of each sample. The correlation coefficient goes from -1 to 1, indicating maximum correlation between x_1 and x_2 when $r= \pm 1$. On the contrary, r=0 implies that both samples are uncorrelated.

To evaluate if the correlation between both samples is significant, a t-test of correlation is applied considering as null and alternative hypothesis:

H_0: the samples x_1 and x_2 are independent, $r = 0$.

H_1: the samples are not independent, $r \neq 0$.

The null hypothesis will be rejected if the test statistic,

$$t = \frac{r\sqrt{N-2}}{\sqrt{1-r^2}} \quad [61]$$

Student's t-distribution with N-2 degrees of freedom, verifies $t > t_{\alpha/2}$. Along the present Thesis, the t-test of correlation is applied with significance levels $\alpha=0.1$ or $\alpha=0.05$.

Fisher F-test

Another non-parametric test considered in the present study is the Fisher test. This test determines if two populations with the same mean also share the same variance (σ^2). Thus, the null and alternative hypothesis are expressed as:

H_0: The samples x1 and x2 have the same variance, $\sigma_1^2 = \sigma_2^2$

H_1: The samples have different variances, $\sigma_1^2 \neq \sigma_2^2$

The test statistic is defined as:

$$F = \frac{s_1^2}{s_2^2} \quad [62]$$

following the F-Fisher distribution with n_1-1 and n^2-1 degrees of freedom under the null hypothesis. H_0 is rejected when F is not included in the interval $[F_{1-\frac{\alpha}{2},n_1-1,n_2-1}, F_{\frac{\alpha}{2},n_1-1,n_2-1}]$ for a significance level α. Significant levels $\alpha=0.1$ or $\alpha=0.05$ are considered in the present study.

5.2.5.2 Non-parametric tests

Not all the hypothesis tests follow theoretical distributions for the data or theoretical sampling distributions of the test statistics. It occurs when the parametric assumption required for a particular test is not met or the test statistic that is dictated by the physical problem is a complicated function of the data. The tests not requiring such assumptions are denoted as non-parametric tests [*Wilks*, 2005].

Monte Carlo test

It is a non-parametric test based on the procedures collectively called re-sampling tests. This procedure consists on the comparison between the test statistic associated with the null distribution built up in each of the *n* permutations of the initial time series and the test statistic computed from the original data set [*Wilks*, 2005] .

From the set of test statistics obtained in the *n* permutations of the sample, the probability density function is calculated. The location of the test statistic computed without permuting the sample over this curve gives the significance level of the result (Figure M11). The test statistic is significant with a confidence level 100(1-α)% if its position is prior to n(1- α) position.

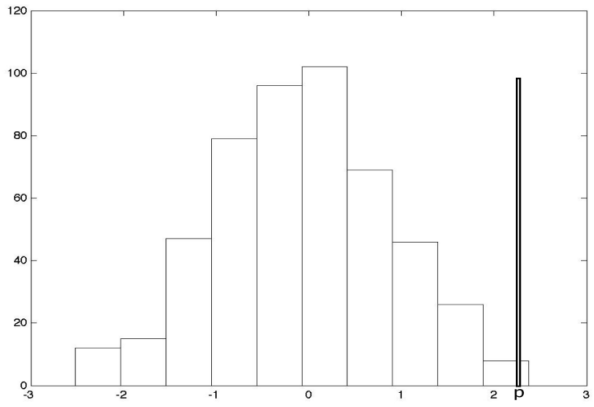

Figure M11. Histogram associated with 500 random permutations and the statistic value obtained. As a high number of permutations have been performed, the histogram can be considered as a probability density function (From *Losada* [2010]).

6. RESULTS

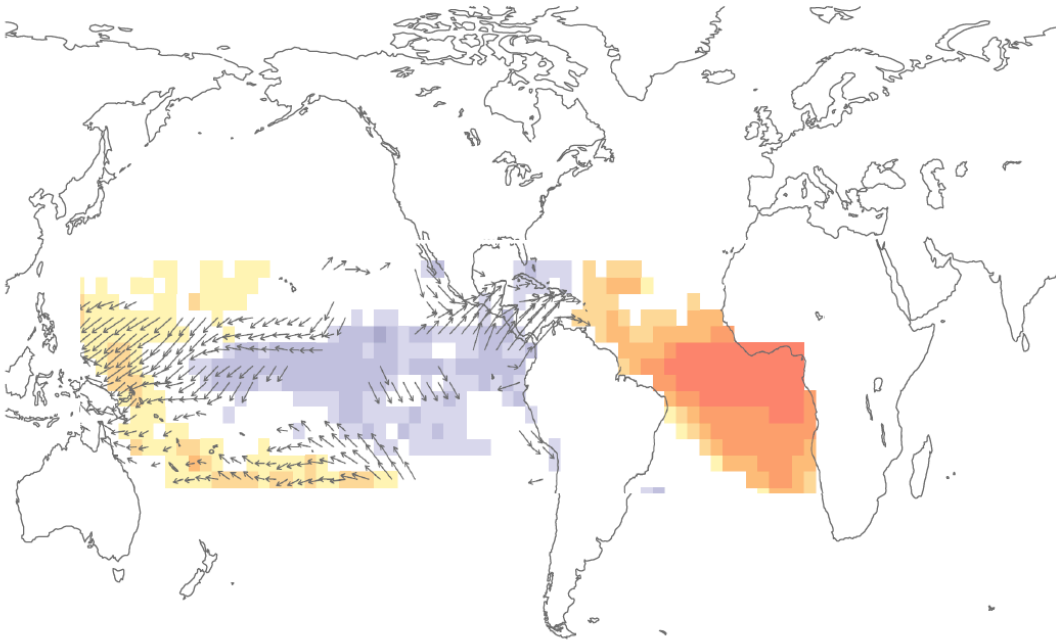

6.1. Study of the influence of the tropical Atlantic inter-annual variability on ENSO phenomena after the 1970s.

(Martín-Rey et al. 2012)

In this section, the ENSO phenomena related to the remote influence of the tropical Atlantic SSTs have been analysed. These results are associated with the Objective 1 of the present thesis.

A partially coupled simulation with observed SSTs prescribed in the Atlantic and coupled to the Indo-Pacific has been considered. The comparison of these results with those from a control simulation with climatological SSTs elsewhere allows isolating the Atlantic contribution in the tropical Pacific variability from the internal variability of the model.

The leading modes of tropical Pacific inter-annual SST variability show significant differences before and after the 1970s, providing a new evidence of the Atlantic influence on the Pacific Ocean. An anomalous cooling in the equatorial Atlantic induces anomalous surface winds in the central-eastern Pacific, modifying the thermocline depth and suggesting the contribution of vertical processes in the development of El Niño phenomenon after the 1970s. On the contrary, before the 1970s, El Niño episodes are only characterized by anomalous warming in the tropical Pacific basin, without changes in the thermocline depth, similar to those events created by internal variability. It indicates that the development of these phenomena could be associated with thermodynamical processes.

ADVANCES IN SPANISH PHYSICAL OCEANOGRAPHY
M. Espino, J. Font, J.L. Pelegrí, A. Sánchez-Arcilla (eds.)

Scientia Marina 76S1
September 2012, 105-116, Barcelona (Spain)
ISSN: 0214-8358
doi: 10.3989/scimar.03610.19A

Changes in the interannual variability of the tropical Pacific as a response to an equatorial Atlantic forcing

MARTA MARTÍN-REY [1,2], IRENE POLO [3], BELÉN RODRÍGUEZ-FONSECA [1,2] and FRED KUCHARSKI [4]

[1] Instituto de Geociencias, CSIC-UCM, Facultad de Ciencias Físicas, 28040 Madrid, Spain.
E-mail: mmartindelrey@fis.ucm.es
[2] Universidad Complutense Madrid, Departamento de Física de la Tierra Astronomía y Astrofísica I, 28040 Madrid, Spain.
[3] NCAS-Climate, University of Reading, Reading, United Kingdom.
[4] Abdus Salam International Centre for Theorical Physics (ICTP), Earth System Physics Section, Trieste, Italy.

SUMMARY: Previous studies have reported that the tropical Atlantic has had an influence on tropical Pacific interannual variability since the 1970s. This variability is studied in the present work, using simulations from a coupled model in the Indo-Pacific but with observed sea surface temperature (SST) prescribed over the Atlantic. The interannual variability is compared with that from a control simulation in which climatological SSTs are prescribed over the Atlantic. Differences in the Pacific mean state and in its variability are found in the forced simulation as a response to a warming in the equatorial Atlantic, characterized by a cooler background state and an increase in the variability over the tropical Pacific. A striking result is that the principal modes of tropical Pacific SST interannual variability show significant differences before and after the 1970s, providing new evidence of the Atlantic influence on the Pacific Ocean. Significant cooling (warming) in the equatorial Atlantic could have caused anomalous winds in the central-easter Pacific during the summer since 1970s. The thermocline depth also seems to be altered, triggering the dynamical processes involved in the development of El Niño (La Niña) phenomenon in the following winter. An increase in frequency of Niño and Niña events favouring the Central Pacific (CP) ones is observed in the last three decades. Further analyses using coupled models are still necessary to help us to understand the causes of this inter-basin connection.

Keywords: Tropical Atlantic variability, Atlantic-Pacific connection, ENSO.

RESUMEN: Cambios en la variabilidad interanual del Pacífico Tropical como respuesta a un forzamiento del Atlántico Ecuatorial. – Trabajos previos han puesto de manifiesto como el Atlántico Tropical influye en la variabilidad interanual del Pacífico a partir de los años 70. El presente trabajo estudia la variabilidad del Pacífico Tropical a partir de simulaciones realizadas con un modelo acoplado en el Indo-Pacífico que considera la Temperatura de la Superficie del Mar (TSM) observada en el Atlántico como forzamiento externo. Los resultados de esta simulación son comparados con los obtenidos en una simulación de control, con TSM climatológicas en el Atlántico. La simulación forzada muestra cambios en el estado base y la variabilidad del Océano Pacífico relacionados con un calentamiento en el Atlántico ecuatorial, destacando un aumento de la variabilidad y un enfriamiento del Pacífico ecuatorial. Además, los principales modos de variabilidad del Pacífico antes y después de los 70 son diferentes, reafirmándose la influencia del Atlántico sobre el Océano Pacífico. Un enfriamiento (calentamiento) en el Atlántico ecuatorial podría generar vientos anómalos en el centro-este de la cuenca del Pacífico durante el verano desde dicha década. La profundidad de la termoclina también se modificaría, desencadenándose los procesos dinámicos involucrados en el desarrollo de El Niño (La Niña) en el invierno siguiente. Los resultados muestran un aumento de la frecuencia de Niños y Niñas, favoreciéndose los eventos del Centro del Pacífico (CP) en las últimas décadas. Estudios adicionales mediante el uso de modelos acoplados serían necesarios para poder comprender las causas de la conexión entre cuencas.

Palabras clave: variabilidad del Atlántico Tropical, conexión Atlántico-Pacífico, ENSO.

INTRODUCTION

Atlantic and Pacific Tropical basins have similar interannual variability modes referred to as the Atlantic Niño and El Niño-Southern Oscillation (ENSO), peaking in the boreal summer and winter respectively. Both of them are characterized by an anomalous warming in the east of the basin, associated with a weakening of the climatological trades and supported by the Bjerknes positive feedback (Bjerknes 1969, Zebiak 1993). Although ENSO impacts are larger, both are known to have worldwide impacts (Philander 1990, Polo *et al*. 2008, García-Serrano *et al*. 2008, Losada *et al*. 2010a,b, López-Parages and Rodríguez-Fonseca 2012).

Previous papers have studied the possible relationship between the Atlantic and Pacific Niños, suggesting a lack of connection (Wang *et al*. 2006) or a fragile relationship between them (Chiang *et al*. 2000, Chang *et al*. 2006). However, recent studies report an increase in the correlation between the Atlantic and Pacific SST interannual variability (Münnich and Neelin 2005, Keenlyside and Latif 2007), highlighting the leadership of the tropical Atlantic in the interbasin connection since the early 1970s (Rodríguez-Fonseca *et al.* 2009). Several model studies have also suggested the impact of the Atlantic SST on the Pacific basin via atmospheric teleconnections (Dommenget *et al*. 2006, Sutton and Hodson 2007, Rodriguez-Fonseca *et al.*, 2009; Losada *et al.* 2010a, Wang *et al*. 2010).

Recently, Ding *et al*. (2011) replicated the experiment of Rodríguez-Fonseca *et al*. (2009) with a more resolved coupled model, finding good agreement between the model and the observations and confirming this leadership of the Atlantic during the last few decades. The former authors claimed that the relationship between basins is stationary, whereas Rodríguez-Fonseca *et al*. (2009) claim that the relation does not hold before the 1970s.

Significant anti-correlations have been found between the summer (JJAS) Atl3 index and the next winter's (DJFM) Niño3 index since the late 1960s and not before, in observations and modelled data (Fig. 1). These correlations support the result of Rodríguez-Fonseca *et al.* (2009): a summer Atlantic Niño could favour the development of a Pacific Niña during the next winter. However, the lack of significant correlation between Atl3 and modelled Niño3 in the summer months (Fig. 1) suggests that other processes could be contributing to the development of the thermal anomalies in the Pacific Ocean.

Using the same simulations as Rodríguez-Fonseca *et al*. (2009), recent studies have tried to characterize the oceanic processes involved in the development of ENSO due to the Atlantic influence in the last few decades (Martín-Rey *et al*. 2010). Different mechanisms seem to be contributing to the heat balance of the tropical Pacific before and after the 1970s, but further analyses are needed to understand the influence of the Atlantic on the Pacific Ocean.

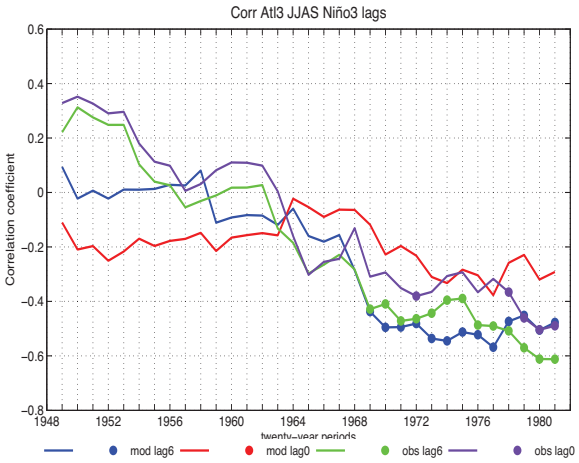

FIG. 1. – Running correlation of 20-year windows, from 1950-1969 to 1981-2000 between summer (JJAS) observed Atl3 index and Niño3 index in lag 0 (JJAS) and lag +6 (DJFM) from model (*SimAtlVar*) and observations. A Monte Carlo test has been applied and significant values at 90% confidence level are represented in dots. The observations come from HadISST1 (Rayner *et al.* 2003). A colour version of this figure may be found in the online electronic manuscript.

According to previous studies, a remarkable change has taken place in the last few decades, in both the characteristics and development of the ENSO phenomena (An and Wang, 2000, Federov and Philander 2000, An 2008, Choi *et al.* 2010, Yeh *et al*. 2011). Alterations of the intensity, frequency and type of the ENSO have also been observed in recent decades (Kao and Yu 2009, Lee and McPhaden 2010). This shift could be associated with changes in the Atlantic (Dong *et al.* 2006) and/or Pacific background state (Moon *et al*. 2004), since an alteration of the mean sea surface temperature (SST), thermocline depth (z20) and zonal wind can modify the ENSO characteristics (Federov and Philander 2000). In addition, a "feedback-like mechanism" between the mean state and the interannual events has been documented, so warm (cold) ENSO events seem to increase (decrease) the SST of the equatorial region, changing, in turn, the background state (Kug *et al*. 2009, Lee and McPhaden 2010).

Regarding the variability of the ENSO phenomenon, several authors have reported the different ENSO "flavours", eastern Pacific (EP) and central Pacific (CP), in the last century, suggesting great differences in their sources and impacts (Kug *et al*. 2009, Kao and Yu 2009, Yeh *et al*. 2009, Choi *et al.* 2010). The origin of the CP and EP ENSO is associated with different forcings, so EP ones are highly dependent on thermocline variations, while CP ones are mainly influenced by atmospheric forcing (Kug *et al*. 2009, Choi *et al*. 2010). Likewise, other studies have shown the importance of the mean state in favouring EP or CP ENSO (Yeh *et al.* 2009, 2011, Choi *et al*. 2010, Yeh *et al*. 2011).

Although previous studies have pointed out the connection between the tropical Atlantic and Pacific Ocean and the leadership of the Atlantic in this connection (Rodríguez-Fonseca *et al.* 2009, Ding *et al.* 2011); and others have indicated the modification of

the oceanic and atmospheric processes involved in the development of the ENSO since the early 1970s (Martín-Rey *et al*. 2010), changes in the principal modes of variability and in the type, frequency and phase of the ENSO events have not yet been studied. Furthermore, the previous studies were very restricted to Atl3 and Niño3 regions and not to the entire tropical basins

The aim of the present work is to clarify whether the Pacific SST interannual variability has really changed due to the Atlantic Ocean forcing in the last decades of the 20th century. To this end, here we describe the first variability mode for the forced simulation, comparing this mode with that from an unforced simulation in order to isolate the mode due to the Atlantic influence. Two different periods were chosen in order to verify the non-stationary impact of the Atlantic over the Pacific.

The paper is organized as follows: First, the data and methodology are described. Then the main results are presented, focusing on: i) the analysis of the modification of the Pacific variability since the 1970s and the possible alteration of the Pacific and Atlantic mean states; ii) the analysis of changes in the interannual variability of the tropical Pacific due to Atlantic forcing; and iii) classification of ENSO events. Finally, a discussion and the conclusions are presented.

MATERIALS AND METHODS

Data and model

This study was carried out using both observed and modelled data. The observational SST came from the HadISST1 (Rayner *et al*. 2003) dataset of the UK Metoffice (http://hadobs.metoffice.com/hadisst/). The observed wind stress was obtained from the Simple Ocean Data Assimilation (Carton *et al*. 2000). The modelled SST, thermocline depth and wind stress outputs came from coupled model simulations. The atmospheric component of the model was the ICTP General Circulation Model (Kucharski *et al*. 2008) version 40, with T30 horizontal resolution and 8 levels in the vertical. The oceanic part was an extended 1.5-layer reduced-gravity model with a resolution of 2°×1° longitude-latitude (Chang 1994). Two different groups of simulations were used:

– Fully-coupled simulations in the tropical Indo-Pacific basin and climatological SSTs elsewhere, except for the Atlantic Ocean, where observed monthly varying SSTs were used. The resulting SST for the tropical Pacific basin corresponds to an ensemble of nine runs for the total period 1949-2002 (as in Rodríguez-Fonseca *et al*. 2009). Hereafter this simulation will be named *SimAtlVar*.

– Fully-coupled simulations in the tropical Indo-Pacific basin and climatological SSTs elsewhere. The resulting SSTs of the ensemble of five runs corresponded to a total period of 132 years. Hereafter this simulation will be named *SimAtlCli*.

The ability of the model to reproduce the connection between the interannual events of the Atlantic and Pacific Oceans was demonstrated by Rodríguez-Fonseca *et al.* (2009). Both the model and the observations show the beginning of this interbasin connection in the late 1960s and the model also confirms the alteration of Walker circulation as the responsible mechanism for this connection in the last few decades.

It is important to analyse the reliability of the model in simulating the equatorial Pacific seasonal cycle and its variability (Fig. 2). The observed seasonal cycle is relatively well captured by the model (solid lines) although the amplitude of the simulated annual mean SSTs is higher than that of the observed ones, exhibiting a warm SST bias in the eastern equatorial Pacific, which is a common feature of most coupled models (Lin *et al*. 2010, Zhao *et al*. 2011, Mechoso *et al*. 1995).

Regarding the standard deviation, the model shows an increase in the variability in the Niño3 region during the summer, coinciding with the maximum variability of the tropical Atlantic (not shown). The Pacific variability peaks in July in both *SimAtlCli* and *SimAtlVar*, showing higher values in the latter, which could be associated with Atlantic forcing (Fig. 2). On the other hand, the observations indicate maximum variability of the Niño3 region in winter when this phenomenon peaks (dotted line).

Although it is known that the seasonal cycle of the tropical Pacific is mainly due to internal variability (Xie 1994), the significant differences obtained between the seasonal cycle of *SimAtlVar* and *SimAtlCli* (Fig. 2, stars) could be due to the Atlantic influence, because it is the only external forcing. This fact should

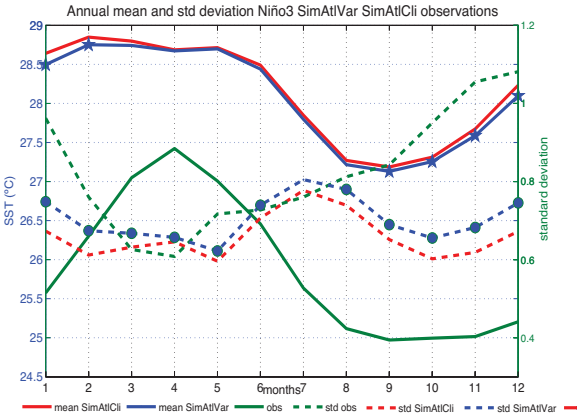

FIG. 2. – Seasonal cycle and standard deviation of Niño3 index from *SimAtlVar*, *SimAtlCli* and observations. Solid lines are associated with y-axis on the left (in °C) and dotted ones with the y-axis on the right side. The observations come from HadISST1 (Rayner *et al*. 2003). The difference between the seasonal cycle and standard deviation from *SimAtlVar* respect *SimAtlCli* has been calculated and a t-test of equal means and a F-test have been applied. Significant differences at 95% confidence level are shown in stars and dots for seasonal cycle and standard deviation respectively over *SimAtlVar* lines. A colour version of this figure may be found in the online electronic manuscript.

be also taken into account in the comparison with observations, since the lack of agreement could be associated with other external contributions such as the impact of the Indian Ocean (Izumo *et al*. 2010) and global warming (Kucharski *et al*. 2011), not taken into account in the present work.

Three indexes were used in this study to characterize Pacific El Niño, the Atlantic Niño and the western equatorial Atlantic. Niño3 is defined as the SST anomalies averaged over the area 150°W to 90°W and 5°N to 5°S; Atl3 index is defined as the SST anomalies averaged over the area 20°W to 0°E and 3°N to 3°S; finally, Atl4 is defined as the SST anomalies averaged over the area 40°W to 20°W and 3°N to 3°S.

Methods

Most of the analyses performed in this study are based on statistical comparisons of both the background state and the variability of the Pacific due to the Atlantic influence before and after the 1970s, considering the seminal work of Rodríguez-Fonseca *et al.* (2009).

The analyses concerning changes in the background state and decadal variability of the Pacific Ocean include statistical tests of significance. Two different tests were used, a *t* test and an *F* test. The *t* test is a parametric test applied under the equal means null hypothesis. The *F* test is a two-tailed test that considers the equal variances as the null hypothesis. Significant values at the 90% and 95% confidence level are shown in the present study. In the significance tests for the set of simulations in the equatorial Pacific (Figs. 2 and 3), all members of the ensemble were taken into account instead of the ensemble mean.

The analysis related to the determination of modes of SST interannual variability was based on the empirical orthogonal functions (EOF) technique, which was applied to the total period 1949-2002. The EOF analysis (von Storch and Frankignoul 1998) is used to decompose the anomalous field into a number n of modes which maximize the variance of a two-dimensional space-time matrix $Y(n_s, n_t)$ being n_s the spatial dimension and n_t the temporal one. The solution of the eigenvalue problem for the variance matrix

$$C(n_s, n_t) = Y \times Y^T \quad (1)$$

provides n principal eigenvectors, EOF (n_s, n), and n eigenvalues λ_n, indicating the explained variance for each EOF. These EOFs represent the directions of maximum $Y(n_s, n_t)$ variability of the total field. The time series or principal components (PC) associated with these spatial patterns are obtained by projecting the EOF over the initial matrix Y

$$PC_k(1, n_t) = EOF_k{}^t\,(1, n_s) \times Y(n_s, n_t) \quad (2)$$

where k corresponds to the number associated with each of the eigenvectors, k=1,..,n.

In the present study, the monthly SST anomalies from December to March (DJFM) were chosen for the period 1949-2002. In order to isolate interannual variations from those of lower frequencies, the difference between the values of each two consecutive years was computed, giving a new field $\Delta y = y_k - y_{k-1}$. This is a standard and widely-used method for filtering time series (Bjerknes 1964, Stephenson *et al*. 2000). The EOF analysis for the set of simulations takes into account all members of the ensemble instead of the ensemble mean.

To assess the robustness of the results, a Monte Carlo non-parametric significance test was performed. This methodology creates a random distribution of the sample, permuting the original time series and analysing the non-shuffled results with those obtained by chance. Significant values at the 90% confidence level are shown according to this test.

El Niño types were classified as Eastern Pacific (EP) and Central Pacific (CP) according to the location of the maximum SST, which placed them in Niño3 [150°W-90°W;5°N-5°S] or Niño4 [160°E-150W°, 5°N-5°S] regions (Kao and Yu 2009, Kug *et al*. 2009, Yeh *et al*. 2009). The ENSO events created by the model show their SST anomalies slightly displaced eastward, so a new definition of Niño3 and Niño4 regions is necessary: Niño3* [140°W-90°W; 5°N-5°S] and Niño4* [180°E-120°W, 5°N-5°S]. CP (EP) Niños satisfy the condition $\overline{SST}_{Niño4*} > \overline{SST}_{Niño3*}$ ($\overline{SST}_{Niño4*} < \overline{SST}_{Niño3*}$). On the other hand, CP (EP) Niñas satisfy the condition $\overline{SST}_{Niño4*} < \overline{SST}_{Niño3*}$ ($\overline{SST}_{Niño4*} > \overline{SST}_{Niño3*}$).

RESULTS

Changes in the mean state and decadal variability

As stated above, Atl3 interannual variability has been significantly correlated with Niño3 variability since the late 1960s (Fig. 1). Although this result was also shown in Rodríguez-Fonseca *et al*. (2009), the changes in the background state or climatological mean of the tropical Atlantic and Pacific basins were not discussed in that work. To tackle this problem, alterations in the Pacific and Atlantic mean and standard deviation during the period 1950-2000 were analysed. Figure 2 shows significant differences in the seasonal cycle (stars) and standard deviation (dots) over the eastern Pacific in *SimAtlVar* in comparison with *SimAtlCli*.

The mean SST over the eastern Pacific is cooler in winter months for *SimAtlVar* than for *SimAtlCli* (Fig. 2), while relatively high variability is shown in the forced simulation (dotted lines). A comparison between the simulations forced by the Atlantic and the control simulations suggests that the addition of the Atlantic Ocean seems to cool the Pacific mean SST during the winter and enhance its variability in all seasons.

Using 20-year windows (Fig. 3), the changes in the Pacific mean state during the study period were evaluated by subtracting the total mean of *SimAtlCli* from each 20-year mean of *SimAtlVar*. Two months were

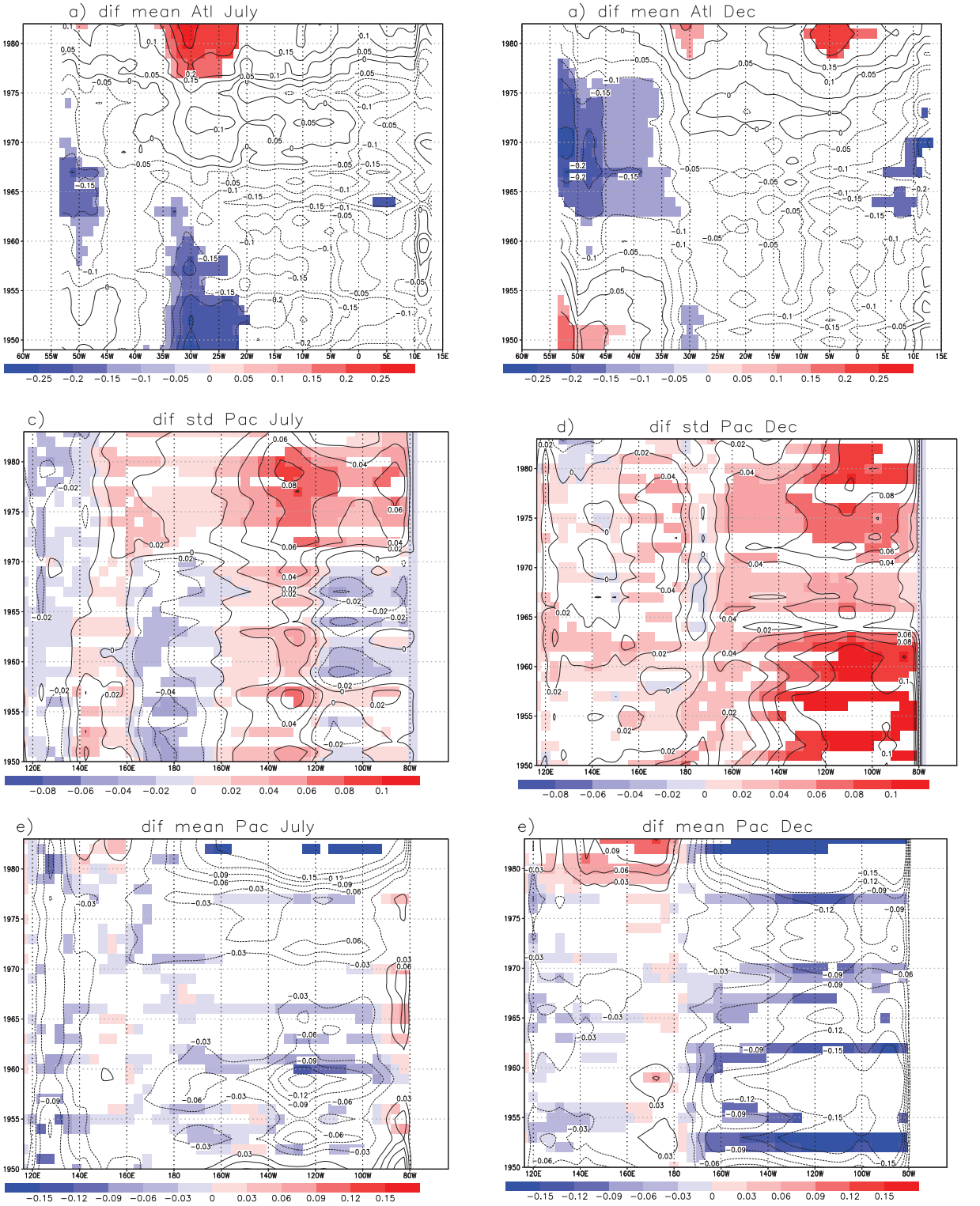

FIG. 3. – (a-b) Differences between mean observed equatorial Atlantic SST from 1950-69 to 1981-2000 in July (left) and December (right, in °C). (e-f) As (a-b) but for the mean simulated (from *SimAtlVar*) equatorial Pacific SST; *SimAtlCli* for the total period are used as a reference value. A t-test of equal means has been applied and significant values at 90% confidence level are presented. (c-d) Differences between the standard deviation of the equatorial Pacific SST, considering all the members for *SimAtlVar*, with respect to the standard deviation of the total period from *SimAtlCli*. A F-test of equal variances has been applied and significant values at 90% confidence level are shown. The observations come from HadISST1 (Rayner *et al*. 2003). In order to isolate interannual variations from those of lower frequencies, the difference between the values of each two consecutive years is computed for all data. A colour version of this figure may be found in the online electronic manuscript.

selected, July and December, according to the maximum variability shown in observations and modelled data (Fig. 2).

A shift in the equatorial Atlantic mean state is observed in July since the late 1960s, so a previous cooling of the Atlantic turns into a warming from the mid-1960s. In particular, a significant warming appears in the Atl4 region (40°W-20°W, 3°N-3°S) since the mid-1970s (Fig. 3a), persisting through the seasons (not shown). The modification of the mean state of the eastern equatorial Atlantic is restricted to winter months and only occurs after the 1980s. This result suggests a modification of the western Atlantic SST during summers of the last three decades of the 20th century. The homogeneous warming of the entire equatorial Atlantic in this period has also been reported in previous studies as a reduction of the observed zonal gradient of tropical Atlantic SST (Tokinaga and Xie 2011).

The observed warming of the summer equatorial Atlantic since the 1970s could be affecting the Pacific Ocean, increasing equatorial Pacific variability in the central and eastern part of the basin during summer months (Fig. 3c). The summer Pacific variability forced by the Atlantic could therefore have become higher than the internal variability in the last three decades. Regarding winter months, a constant increase in the Pacific variability is shown during the entire period 1950-2001 (Fig. 3d). Nevertheless, maximum anomalies in the centre and east of the Pacific, similar to the summer pattern (Fig. 3c), are observed since 1970s. Therefore, the Atlantic influence on Pacific variability in summer seems to persist through the seasons. Regarding the Pacific background state, no relevant changes are observed in summer, but an east-west SST gradient following a La Niña-like pattern, with negative anomalies in the centre-east (170°W-80°W) and positive ones in the west of the basin is observed in winter since the early 1980s (Fig. 3f).

The connection between the interannual processes established since 1970 (Fig. 1) could be related to the change of the Pacific background state in the early 1980s (Fig. 3f). A hypothesis is proposed: *a warmer tropical Atlantic could have altered Walker circulation and have linked the Atlantic Niños (Niñas) with the Pacific Niñas (Niños) since the 1970s. Finally, these phenomena could have been gradually modifying the Pacific mean state, becoming statistically significant several years later*. This proposed hypothesis will be tested in a future study with sensitivity experiments with partially coupled models considering different background states of the Atlantic.

Modification of the interannual Pacific variability due to the Atlantic influence

Because the tropical Pacific variability is modified at decadal timescales under an Atlantic forcing, a study of the changes in the interannual variability with and without an Atlantic influence must be considered. To this end, an EOF analysis for winter (DJFM) Pacific SST was performed for both *SimAtlVar* and *SimAtlCli* SST outputs for the total period of the simulation. Figure 4 presents the corresponding correlation maps for anomalous SSTs, z20 and wind stress in JJAS and DJFM for the tropical Pacific for *SimAtlVar* (where the Atlantic SSTs are observed).

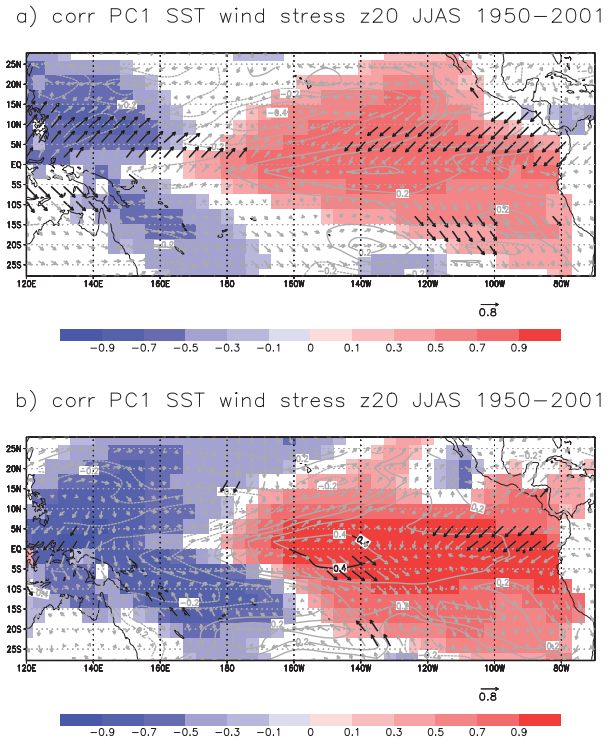

FIG. 4. – (a) Correlation between the first PC of the tropical Pacific SST in DJFM from *SimAtlVar* and the modelled seasonal SST (shaded), thermocline depth (contour) and windstress (vector) anomalies in the previous summer (JJAS). (b) Same as (a) but for the winter (DJFM). A Monte Carlo test has been applied to obtain significant values at 90% confidence level. The correlation with thermocline depth is presented in thin contour lines and significant areas are bolded. Only significant areas have been shaded for SST and plotted for vectors. In order to isolate interannual variations from those of lower frequencies, the difference between the values of each two consecutive years is computed for all data. A colour version of this figure may be found in the online electronic manuscript.

The leading mode of variability is characterized as an El Niño–like pattern with positive values in the central-east of the basin and a horseshoe-like structure of negative ones in the western Pacific for both *SimAtlVar* (Fig. 4) and *SimAtlCli* (not shown). The first mode associated with the Atlantic influence (*SimAtlVar*) explains 37.7% of the total variance, whereas the mode associated with the internal variability (*SimAtlCli*) explains only 35.9%. Thus, the Atlantic Ocean seems to increase the interannual variability of the tropical Pacific in comparison with the internal interannual variability, coherently with the results presented in Figures 2 and 3.

Figure 4 (a-b) presents the correlation maps of the leading principal component onto SST, thermocline

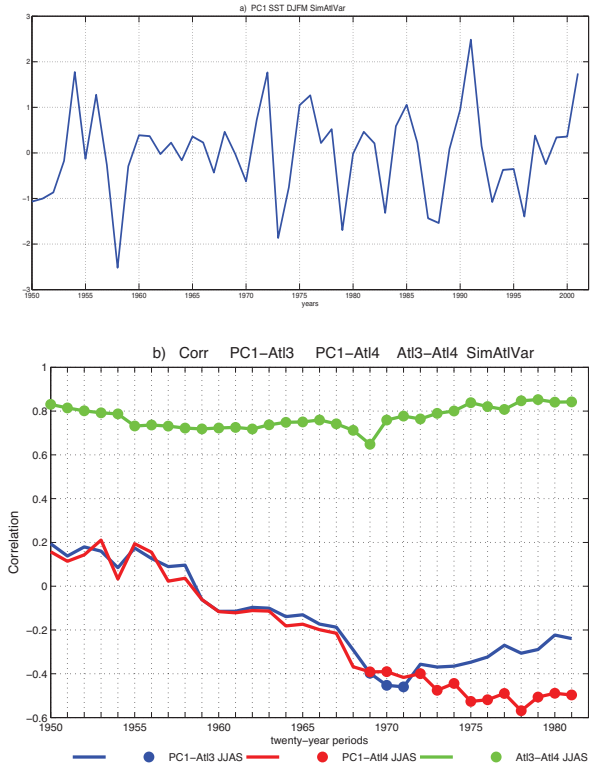

FIG. 5. – (a) Leading PC of the Tropical Pacific SST in DJFM for the period 1950-2001. The nine simulations of *SimAtlVar* have been used instead of the ensemble mean to compute the PC. It explains 37.7 % of the total variance. (b) Twenty-year correlation between the PC1 and summer observed Atl3 index (black line) and Atl4 index (grey line) in JJAS. Twenty-year correlation between Atl3 and Atl4 indexes is shown as a light grey line. A Monte Carlo test has been applied and significant values at 90% confidence level are shown in dots. The observations come from HadISST1 (Rayner *et al*. 2003). In order to isolate interannual variations from those of lower frequencies, the difference between the values of each two consecutive years is computed for all data. A colour version of this figure may be found in the online electronic manuscript.

depth (z20) and wind stress anomalies for the whole period, considering the simulations with the Atlantic forcing (*SimAtlVar*). These figures show anomalous winds and warming in the central-east (160°W-140°W) of the equatorial Pacific in summer with no significant anomalies in the thermocline depth (Fig. 4a). However, more intense El Niño configuration related to a deeper significant thermocline is observed in winter months (*SimAtlVar*, Fig. 4b). Thus, the summer anomalous winds could also modify the thermocline depth, triggering the oceanic processes involved in the development of ENSO phenomena during the next few months. It is important to note that the leading mode of variability obtained from *SimAtlCli* has no significant signal in z20, which means that less active thermocline feedbacks are involved (not shown). The results presented in Table 1 show how the Atlantic Ocean could favour the creation of less frequent but more intense and dynamic ENSOs, which explain a higher percentage of the Pacific variability (37.7% versus 35.9%).

The results presented in Figure 4 take into account the influence of the Atlantic during the whole period, considering a stationary influence of this basin. However, the observations and Figure 1 show that the Atlantic influence has become significant since the 1970s. In order to study the non-stationarity of this contribution, a 20-year moving correlation between the PC1 (from *SimAtlVar*) and Atl3 and Atl4 indexes, from 1950-69 to 1981-2000, was calculated (Fig. 5). Significant negative correlations are obtained since the late 1960s and early 1970s for Atl4 and Atl3, respectively. Additional calculations show how these anti-correlations do not depend on the window length (not shown).

It is interesting to note that the correlation values between the Atl3 and Atl4 indexes reach 0.8 in the last three decades. The simultaneous contribution of the Atl3 and Atl4 regions suggests the influence of the entire equatorial Atlantic on the Pacific variability since the 1970s, highlighting the leadership of the western equatorial Atlantic region. Previous studies have already reported the role of anomalous winds in the western equatorial Atlantic in the connection between the Atlantic and Pacific Niños (Münnich and Neelin 2005, Mélice and Servain 2003). However, these authors suggested the influence of ENSO in the creation of anomalous westerlies in the western tropical Atlantic, triggering the eastward propagation of oceanic Kelvin waves responsible for developing the Atlantic Niño. Conversely, the present study points out the leadership of the Atlantic in the connection between these tropical basins, as well as the presence of an equatorial pattern that covers not only Atl3 but also Atl4 (Fig. 5b).

With the aim of understanding the change in the role of the Atlantic SST variability on the Pacific SST interannual leading mode, the correlation of PC1 onto the SST, z20 and wind stress before and after the 1970s is presented in Figure 6. The periods 1950-69 (absence of correlation in Fig. 5) and 1971-90 (significant correlation in Fig. 5) are chosen as reference periods. In Figure 6c significant wind convergence in the central-eastern Pacific is shown in summer after the 1970s, with a significant signal on z20. In the next winter, significant anomalies of z20 covering the eastern Pacific arise. Therefore, summer anomalous wind could be affecting the ocean surface, perturbing the thermocline depth, triggering active thermocline feedbacks and enhancing the winter SST in the eastern basin (Fig. 6d). On the other hand, weaker ENSO are shown in the period 1950-69, only characterized by a warming in the eastern Pacific, without modifying wind stress or z20 (Fig. 6a-b). Internal ENSO could be associated with more advective feedbacks according to previous studies (Martín-Rey *et al*. 2010), while the role of vertical processes in the development of ENSO has been greater in the last two decades, in agreement with other authors (An 2008).

El Niño phenomenon in *SimAtlVar* before and after the 1970s has also been compared with the variability in the unforced simulation *SimAtlClim* (not shown).

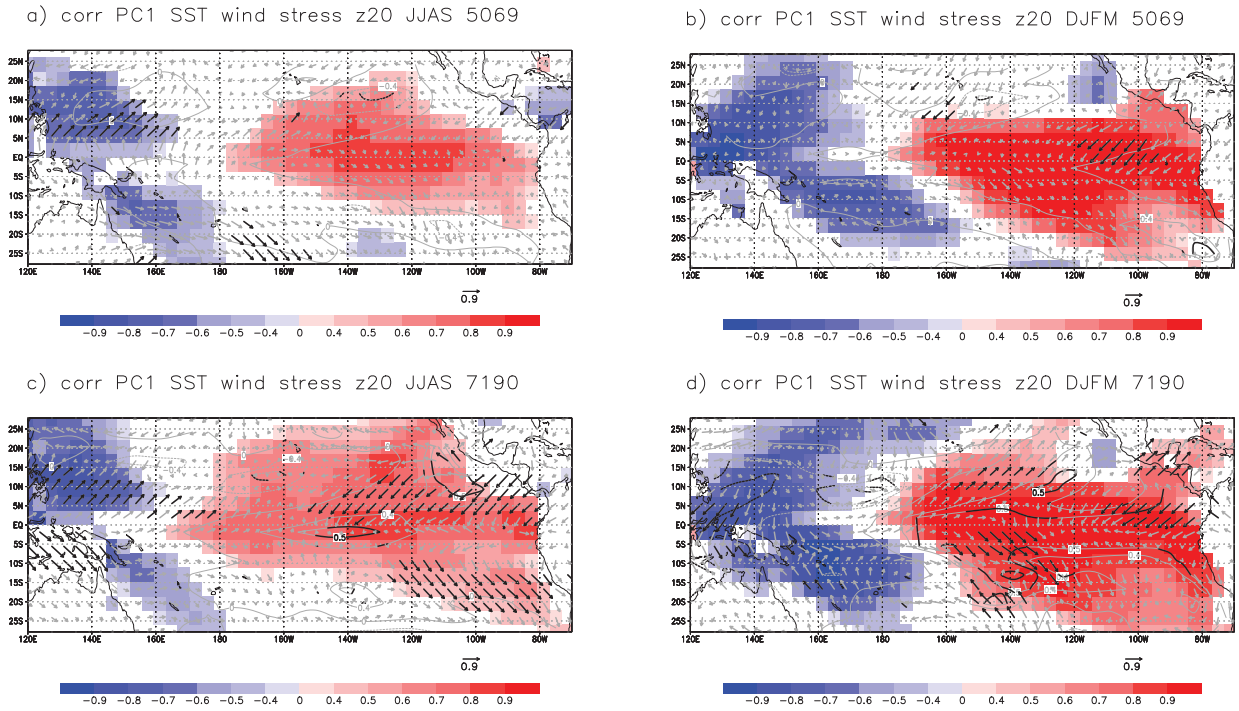

FIG. 6. – Correlation between PC1 of tropical Pacific SST in winter (DJFM) over the modelled seasonal SST (shaded), thermocline depth (contour) and windstress (vector) anomalies in summer (JJAS, left) and winter (DJFM, right) for the periods 1950-69 (top) and 1971-1990 (bottom). A Monte Carlo test has been applied to obtain significant values at 90% confidence level. The correlation with thermocline depth is presented in thin contour lines and significant areas are bolded. Only significant areas have been shaded for SST and plotted for vectors. In order to isolate interannual variations from those of lower frequencies, the difference between the values of each two consecutive years is computed for all data. A colour version of this figure may be found in the online electronic manuscript.

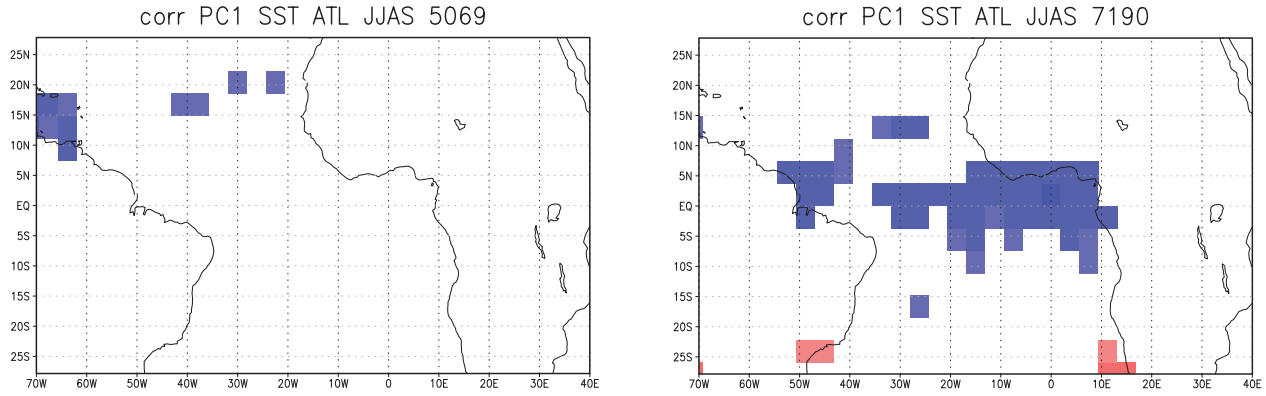

FIG. 7. – Correlation between PC1 of tropical Pacific SST in winter (DJFM) over the observed summer SST for the periods 1950-69 (right) and 1971-1990 (left). A Monte Carlo test has been applied and significant values at 90% confidence level are shaded. The observations come from HadISST1 (Rayner *et al.* 2003). In order to isolate interannual variations from those of lower frequencies, the difference between the values of each two consecutive years is computed for all data. A colour version of this figure may be found in the online electronic manuscript.

The difference between these patterns highlights the important role played by wind stress in the tropical Pacific in summer, creating a perturbation in thermocline depth that alters the dynamic ocean processes involved in the ENSO development.

In order to determine the Atlantic pattern affecting the leading equatorial Pacific variability mode after the 1970s, the regression of the first PC1 onto the observed Atlantic SST during the previous summer is shown in Figure 7. For the positive phase of the Pacific leading EOF, an equatorial cooling that covers not only the eastern but also the western side of the Atlantic basin is observed since 1970, but not in previous decades (Fig. 7a-b), confirming the anti-correlation found in Rodríguez-Fonseca *et al.* (2009) and later in Ding *et al.* (2011).

This result indicates that the Atlantic has been able to modify the main variability modes of the tropical Pacific since the 1970s, so that an anomalous cooling over the equatorial Atlantic is related to a warming of the equatorial and eastern Pacific. The mechanism

TABLE 1. – Statistical analysis of the ENSO phenomena from Principal Components created from *SimAtlVar* (all the 9 members are considered) for the total periods 1950-69 (P1) and 1971-90 (P2) and from *SimVarClim* (all the 5 members are considered).

	SimAtlVar (9 members)			SimAtlCli (5 members)	Forced simulation vs control
	P1	P2	1950-2001	130 years	
Ratio Niños/Niñas	0.88	0.95	0.97	1.06	Increase of Niñas
Ratio EP/CP	6.25	3.11	3.81	4.01	Increase of CP
Skewness	0.33	-0.019	0. 01	0.25	Increase of symmetry
Related to TA		Atl3-Atl4	Atl4	No related	Atl-Pac connection
Variance explained (DJFM)			37.7%	35.9%	Increase variability specially DJFM
Periodicity (from peaks of power spectrum)			[6 8] years	[6 7] years	Increase periodicity in 4-5 years
			[4-5] years	3.5; 5.5 years	band

involves anomalous winds in the central Pacific during the summer, and a modification of the thermocline depth in this region. This perturbation could propagate eastward, creating more intense ENSOs in the last three decades. This is in agreement with the more active dynamic feedbacks since the 1970s from an Atlantic forcing (Martín-Rey *et al.* 2010).

Classification of ENSO events

The CP and EP phenomena generated by the model (from *SimAtlVar* and *SimAtlCli*) are analogous to those shown in observations (Kao and Yu 2009, Kug *et al*. 2009, Lee and McPhaden 2010). The CP Niños (Niñas) have a dipolar structure formed by positive (negative) anomalies in the central-eastern (120°W-180°W) and negative (positive) ones in the western equatorial Pacific (not shown). The maximum central SST anomaly is restricted to the equatorial band, reaching the dateline. On the other hand, EP ENSOs are similar to CP ones, but the maximum SST anomalies are placed in the eastern Pacific (150°W-100°W).

Although modelled Niños are mainly EP (more than 70%), the ratio between EP and CP events is slightly reduced in *SimAtlVar* (Table 1), suggesting an increase in CP ENSOs due to the Atlantic influence. Regarding the ENSO phase, an increase in the occurrence of La Niña phenomenon is also observed in *SimAtlVar*. The tropical Atlantic Ocean therefore seems to favour the negative phase of ENSOs. Furthermore, the internal variability shows a strong asymmetry of ENSO events with a stronger positive phase of ENSO, skewness 0.25 in the *SimAtlCli* versus 0.01 in the *SimAtlVar*. Atlantic forcing seems to rectify this bias of the internal variability by given more weight to La Niña events.

In order to study the modification of the ENSO phenomena due to the Atlantic contribution, a statistical analysis of the interannual processes of the tropical Pacific was performed in the selected periods, 1950-69 and 1971-90 (from *SimAtlVar).* The ENSO events were identified and classified according to their positive (El Niño) or negative (La Niña) phase and their type (CP or EP, Table 1). An increase in the number of events is shown after the 1970s, most of all in the positive phase, so the ratio between Niños and Niñas is close to 1. The number of CP ENSOs has doubled since 1970. This increase in CP events has been also reported in previous studies (Ashok *et al*. 2007, Yeh *et al.* 2009, Lee and McPhaden 2010) but the causes of this change are still unresolved. Yeh *et al*. (2009) suggest the contribution of anthropogenic forcing in favouring CP ENSOs. Finally, decadal and multidecadal variability could also play an important role in the type of ENSO phenomena (McPhaden and Zhang 2002, Lee and McPhaden 2008, Yu *et al.* 2010, Yeh et al. 2011).

DISCUSSION AND CONCLUSIONS

This paper analyses the changes in the mean state, variability and modes of variability in the tropical Pacific, using a coupled simulation with the observed SST in the Atlantic as external forcing, as in Rodríguez-Fonseca *et al*. (2009). This analysis shows that the connection established between the Atlantic Niños (Niñas) and the Pacific Niñas (Niños) since the early 1970s may have contributed not only to the interannual events but also to the change in the Pacific variability and background state in the last three decades.

This study uses different simulations in order to address different features not shown in Rodríguez-Fonseca *et al*. (2009): 1) the *SimAtlVar* simulation in comparison with the *SimAtlCli* control simulation demonstrates the clear influence of the Atlantic on the Pacific; and 2) the differences between the same *SimAtlVar* simulation for the period before the 1970s and after the 1970s demonstrate that the Atlantic-Pacific connection is non-stationary and thermocline feedbacks have been more active in the Pacific El Niño development in the last three decades.

On the basis of these results, a preliminary hypothesis is posed: a warmer Atlantic could have altered the Walker circulation, linking the two tropical oceans since the late 1960s, increasing Pacific variability and connecting the interannual events of the two basins. Because of the Atlantic contribution, these ENSO phenomena could have gradually changed the Pacific background state, highlighting a significant cooling since the late 1970s. However, to test this hypothesis, partially coupled simulations are needed.

The Tropical Pacific SST variability shows an El Niño-like leading pattern, significantly anti-correlated with the Atl4 and Atl3 indexes since the late 1960s and early 1970s, respectively. The significant correlation between Atl4 and PC1 suggests that the western

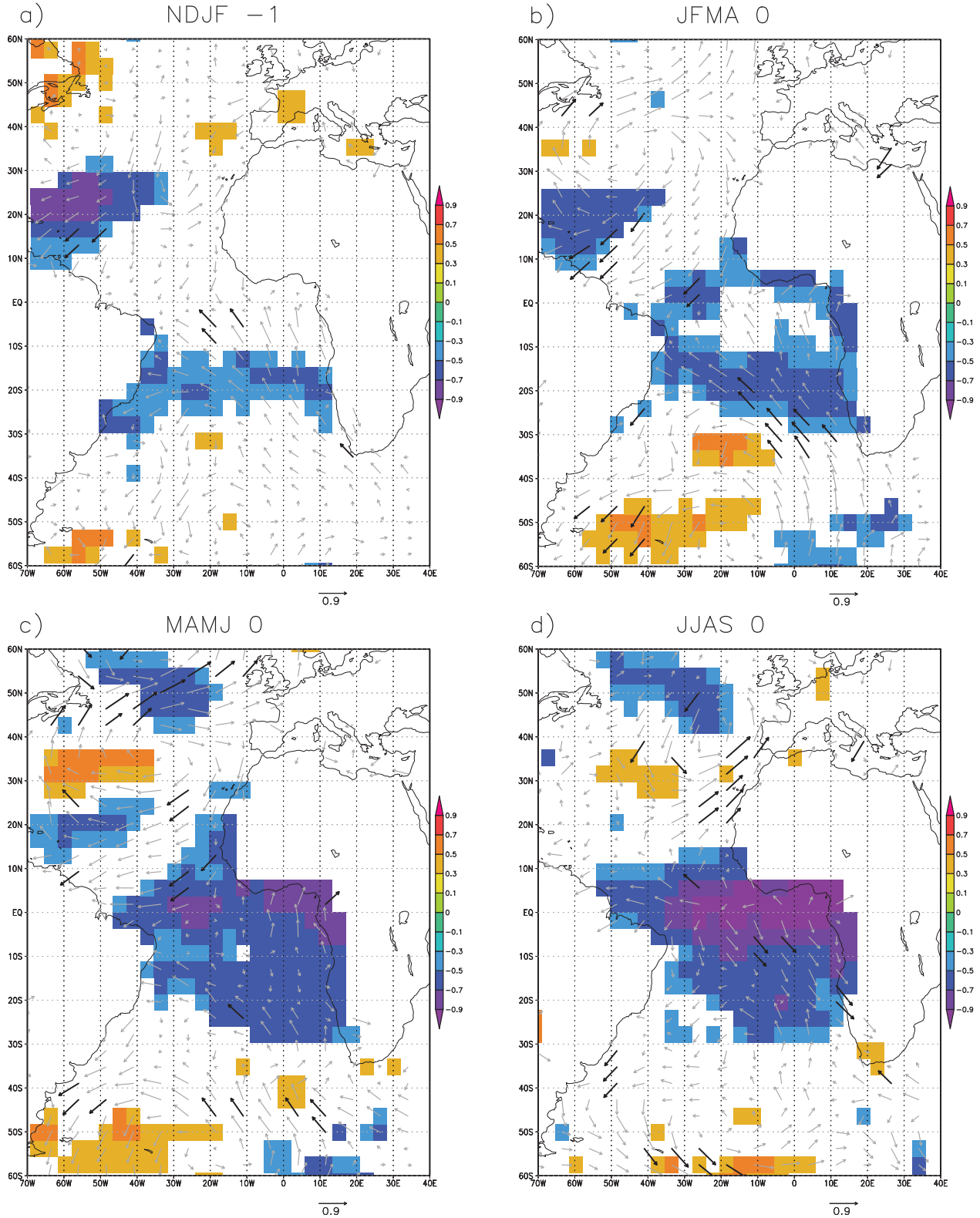

FIG. 8. – Correlation between the time series of the summer (JJAS) equatorial Atlantic SST pattern (where the time series has been calculated by regressing the SST pattern from Figure 6c map over the time-space matrix of anomalous SST in JJAS in the equatorial Atlantic) and the observed anomalous SST (multiplied by –1 for consistency with the rest of the article) and wind stress from NDJF (year –1) to JJAS (year 0) in the Atlantic Ocean for the period 1971-90. A Monte Carlo test has been applied and significant values at 90% confidence level are shown in shaded (SST) and black vectors (wind stress). The observations come from HadISST1 (Rayner *et al*. 2003). In order to isolate interannual variations from those of lower frequencies, the difference between the values of each two consecutive years is computed for all data. A colour version of this figure may be found in the online electronic manuscript.

tropical Atlantic has played a determinant role in the inter-basin connection in recent decades. The simultaneous contribution of the Atl3 and Atl4 indexes in Pacific variability since the 1970s suggests that the entire equatorial band in the Atlantic Ocean must have been involved.

The understanding of the origin and development of the Atlantic SST pattern related to the ENSO mode since the 1970s is beyond the scope of this study and will be the aim of a future one. However, here we present a preliminary attempt to discern the observed wind stress and SST anomalous patterns over the tropical Atlantic that can force El Niño during the following winter in the last few decades (Fig. 8). Anomalous easterly winds south of the equator (10°S-20°S), associated with a strengthening of the St. Helena High (Figure 8a), could favour the upwelling in the Benguela area, cooling this region in the following months (Fig. 8b). On the other hand, the subtropical high in the North Atlantic seems to also be altered in spring, contributing to the cooling of the western and northern tropical Atlantic (Fig. 8c). The contribution of the St. Helena Subtropical High was studied previously in Lübbecke *et al.* (2010) and Richter *et al*. (2010), but these authors did not deal with the contribution of the Azores High, which is a novelty of this work and requires further analysis. The alteration of the St. Helena High seems to favour the development of the SST anomalies in the eastern Atlantic (Lübbecke *et al*. 2010, Richter *et al*. 2010), but the Atlantic SST pattern related to Pacific Niños since the 1970s shows a westward extension (Fig. 8d) that could be due to the additional contribution of the Azores High. Finally, an equatorial SST pattern covering the entire equatorial basin (60°W-10°E, 10°N-30°S) is developed. This result suggests the possible contribution of the subtropical highs of both hemispheres in the development of Atlantic Niños since the 1970s.

The correlation patterns of the PCs before and after the 1970s show anomalous cooling in the equatorial Atlantic associated with anomalous winds over the central tropical Pacific in summer months. These wind anomalies could also create a perturbation in z20 in the central Pacific, propagating eastward and generating more intense ENSO phenomena since the 1970s. The Atlantic thus seems to alter the dynamic processes associated with the development of ENSO in the last decades. This result agrees with Martín-Rey *et al.* (2010), who suggest the important role of the vertical processes in the creation of ENSO events in the last few decades from an Atlantic forcing. However, further analysis of the changes in the oceanic processes due to the Atlantic contribution before and after the 1970s are needed.

The Atlantic forcing is able to explain some of the recent changes in the ENSO variability since the 1970s, such as the increase in the intensity of the events, the increase in CP Niños, the increase in frequency in the band of 1/[4-5] years^{-1}, and more active thermocline feedbacks. However, it fails to explain the great asymmetry of Niños since the 1970s, which has been related to more non-linear processes and stronger thermocline feedbacks (An 2008). This failure could be due to some limitation in the coupled model but more research into the sources of decadal variability of ENSO phenomena is also needed.

All these changes (summarized in Table 1) suggest that the Atlantic mean state and its associated interannual variability make an important contribution to understanding the recent changes over the tropical Pacific basin in last decades. Further research is necessary to understand the development of Atlantic Niños since the 1970s, in order to determine the causes of the Atlantic-Pacific connection established in the last few decades.

ACKNOWLEDGEMENTS

This study was supported through the Spanish MICINN projects TRACS (CGL2009-10285) and MOVAC (ref. 200800050084028). We would like to thank the anonymous reviewers, in particular reviewer 3, for their useful comments, which helped to improve the manuscript. Also, we would like to thank Alan Lounds for his corrections and suggestions in the English revision. We are very grateful to the editor for making very encouraging and helpful suggestions and helping in the whole process.

REFERENCES

An S.I. and Wang B. 2000. Interdecadal change of the structure of the ENSO mode and its impact on the ENSO frequency. *J. Clim.* 13: 2044-2055.

An S.I. 2008. A review of interdecadal changes in the nonlinearity of the El Niño-Southern Oscillation. *Theor. Appl. Climatol*. 97: 29-40.

Ashok K., Behera S.K., Rao S. A., Weng H., Yamagata T. 2007. El Niño Modoki and its possible teleconnections. *J. Geophys. Res*. 112: C11007.

Bjerknes J. 1964. Atlantic air-sea interaction. *Adv. Geophys.* 10: 10-82.

Bjerknes J. 1969. Atmospheric teleconnections from the equatorial Pacific. *Mon. Weather Rev.* 97: 163-72.

Carton J.A., Chepurin G., Cao X.H., Giese B.S. 2000. A Simple Ocean Data Assimilation analysis of the global upper ocean 1950–95. Part I: Methodology. *J. Phys. Oceanogr.* 30: 294-309.

Chang P. 1994. A study of the seasonal cycle of sea surface temperature in the tropical Pacific Ocean using reduced gravity models. *J. Geophys. Res.* 99: 7725-7741.

Chang P., Fang Y., Saravannan R., Ji L., Seidel H. 2006. The cause of the fragile relationship between the Pacific El Niño and the Atlantic Niño. *Nature* 443: 324-328.

Chiang J.C.H., Kushnir Y. 2000. Interdecadal changes in the eastern Pacific ITCZ variability and its influence on the Atlantic ICTZ. *Geophys. Res. Lett.* 27: 3687-3690.

Choi J., An S., Kug J.-S., Yeh S.W. 2010. The role of mean state on changes in El Niño's flavor. *Clim. Dyn*. 37: 1205-1215.

Ding H., Keenlyside N.S., Latif M. 2011. Impact of the Equatorial Atlantic on the El Niño Southern Oscillation. *Clim. Dyn*. doi: 10.1007/s00382-011-1097-y.

Dommenget D., Semenov V., Latif M. 2006. Impacts of the tropical Indian and Atlantic Oceans on ENSO. *Geophys. Res. Lett.* 33: L11701.

Dong B., Sutton R.T., Scaife A.A. 2006. Multidecadal modulation of el Niño-Southern Oscillation (ENSO) variance by Atlantic Ocean sea surface temperatures. *Geophys. Res. Lett.* 33: L08705.

Federov A., Philander S.G. 2000. Is El Niño changing? *Science* 288: 1997-2002.

García-Serrano J., Losada T., Rodríguez-Fonseca B., Polo I. 2008. Tropical Atlantic variability modes (1979–2002). Part II: Time-evolving atmospheric circulation related to SST-forced tropical convection. *J. Clim.* 21: 6476-6497.

Kao H.-Y., Yu J.-Y. 2009. Contrasting Eastern-Pacific and Central-Pacific Types of ENSO. *J. Clim*. 22: 616-632.

Keenlyside N.S., Latif M. 2007. Understanding Equatorial Atlantic interannual variability. *J. Clim*. 30: 131-142.

Kucharski, F., Bracco A., Yoo J.H., Molteni F. 2008. Atlantic forced component of the Indian monsoon interannual variability. *Geophys. Res. Lett.* 35: L04706.

Kucharski F., Kang I.-S., Farneti R., Feudale L. 2011. Tropical Pacific response to 20th Century Atlantic Warming. *Geophys. Res. Lett.* 38: L03702.

Kug J.-S., Jin F.F., An S.I. 2009. Two types of El Niño Events: Cold tongue El Niño and Warm Pool El Niño. *J. Clim*. 22: 615-636.

Izumo T., Vilard J., Lengaigne M., Montegut C.D.B., Behera S.K., Luo J.J., Cravatte S., Masson S., Yamagata T. 2010. Influence of the state of the Indian Ocean dipole of the following year's El Niño. *Nature* 3: 168-172.

Lee T., McPhaden M.J. 2010. Increasing intensity of El Niño in the central-equatorial Pacific. *Geophys. Res. Lett*. 37: L14603.

Lee T., McPhaden M.J. 2008. Decadal phase change in large-scale sea level and winds in the Indo Pacific region at the end of the 20th century. *Geophys. Res. Lett.* 35: L01605.

Lin P.-F., Liu H.-L., Li C., Zhang X.-H. 2010. Spring Cold Bias of SST and Minimal Wind Mixing in the Equatorial Pacific Cold Tongue. *Atmos. Oceanic. Sci. Lett*. 3: 342-346.

López-Parages J., Rodríguez-Fonseca B. 2012. Multidecadal Modulation of El Niño influence on the Euro-Mediterranean rainfall. *Geophys. Res. Lett*. 39: L02704.

Losada T., Rodríguez-Fonseca B., Janicot S., Gervois S., Chauvin F., Ruti P. 2010a. A multimodel approach to the Atlantic equatorial mode. Impact on the West African monsoon. *Clim. Dyn*. 35: 29-43.

Losada T., Rodríguez-Fonseca B., Polo I., Janicot S., Gervois S., Chauvin F., Ruti P. 2010b. Tropical response to the Atlantic Equatorial mode: AGCM multimodel approach. *Clim. Dyn*. 5: 45-52.

Lübbecke J.F., Böning C.W., Keenlyside N.S., Xie S. 2010. On the connection between Benguela and equatorial Atlantic Niños and the role of the South Atlantic Anticyclone. *J. Geophys. Res.* 115: C09015.

Martín-Rey M. 2010. *Estudio del océano superior del Pacífico Tropical y su relación con un forzamiento del Atlántico*. Master Thesis, Universidad Complutense de Madrid.

McPhaden M.J., Zhang D. 2002. Slowdown of the meridional overturning circulation in the upper Pacific Ocean. *Nature* 415: 603-608.

Mechoso C.R., Robertson A.W., Barth N., Davey M.K., Delecluse P., Gent P.R., Ineson S., Kirtman B., Latif M., Le Treut H., Nagai T., Neelin J.D., Philander S.G.H., Polcher J., Schopf P.S., Stockdale T., Suarez M.J., Terray L., Thual O., Tribbia J.J. 1995. The seasonal cycle over the Tropical Pacific in Coupled Ocean-Atmosphere General Circulation Models. *Mon. Weather Rev*. 123: 2825-2838.

Melice J.L., Servain J. 2003. The tropical Atlantic meridional SST gradient index and its relationships with the SOI, NAO and Southern Ocean. *Clim. Dyn*. 20: 447-464.

Moon B.K, Yeh S.W., Dewitte B., Jhun J.G., Kang I.S., Kirtman B.P. 2004. Vertical structure variability in the equatorial Pacific before and after the Pacific climate shift of the 1970s. *Geophys. Res. Lett.* 31: L03203.

Münnich M., Neelin J. D. 2005. Seasonal influence of ENSO on the Atlantic ITCZ and equatorial South America. *Geophys. Res. Lett*. 32: L21709.

Philander S.G. 1990. *El Niño, La Nina, and the Southern Oscillation*. Academic Press, San Diego, 293 pp.

Polo I., Rodríguez-Fonseca B., Losada T., García-Serrano J. 2008. Tropical Atlantic variability modes (1979–2002). Part I: Time-evolving SST modes related to West African rainfall. *J. Clim*. 21: 6457-6475.

Rayner, N.A., Parker D.E., Horton E.B., Folland C.K., Alexander L.V., Rowell D.P., Kent E.C., Kaplan A. 2003. Globally complete analyses of sea surface temperature, sea ice and night marine air temperature, 1871-2000. *J. Geophys. Res.* 108, 4407.

Richter I., Behera S., Masumoto Y., Taguchi B., Komori N., Yamagata T. 2010. On the triggering of Benguela Niños: Remote equatorial versus local influences, *Geophys. Res. Lett*. 37: L20604.

Rodríguez-Fonseca B., Polo I., García-Serrano J., Losada T., Mohino E., Mechoso C.R., Kucharski F. 2009. Are Atlantic Niños enhancing Pacific ENSO events in recent decades? *Geophys. Res. Lett*. 36: L20705.

Stephenson D.B., Pavan V., Bojariu R. 2000. Is the North Atlantic oscillation a random walk? *Int. J. Climatol*. 20: 1-18.

Sutton R.T., Hodson D.L.R. 2007. Climate Response to Basin-Scale Warming and Cooling of the North Atlantic Ocean. *J. Clim*. 20: 891-907.

Tokinaga H., Xie S.P. 2011. Weakening of the equatorial Atlantic cold tongue over the past six decades. *Nature Geosci.* 4: 222-226.

Von Storch H., Frankignoul C. 1998. Empirical Modal Decomposition in coastal oceanography. In: Brink K.H., Robinson A.R. (eds.) *The Sea: Vol. 10, the Global Coastal Ocean.* John Wiley, p. 419-455.

Wang C. 2006. An overlooked feature of tropical climate: Inter-Pacific-Atlantic variability. *Geophys. Res. Lett*. 33: L12702.

Wang C.S., Lee K., Mechoso C.R. 2010. Interhemispheric Influence of the Atlantic Warm Pool on the Southeastern Pacific. *J. Clim.* 23: 404-418.

Xie S.-P. 1994. On the genesis of the equatorial annual cycle. *J.Clim.* 7: 2008-2013.

Yeh S.-W., Kirtman B. Kug J-S, Park W., Latif M. 2011. Natural variability of the central Pacific El Niño event on multi-centennial timescales. *Geophys. Res. Lett*. 38: L15709.

Yeh S.-W., Kug J.-S., Dewitte B., Kwon M.-H., Kirtman B., Jin F.-F. 2009. Recent changes in El Niño and its projection under global warming. *Nature* 461: 511-515.

Yu J.-Y., Kao H.-Y., Lee T. 2010. Subtropics-related interannual sea surface temperature variability in the central Equatorial Pacific. *J. Clim*. 23: 2869-2884.

Zebiak S.E. 1993. Air-sea interaction in the equatorial Atlantic region. *J. Clim*. 6: 1567-1586.

Zhao M., Wang G., Hendon H.H., Alves O. 2011. Impact of including surface currents on simulation of Indian Ocean variability with the POAMA coupled model. *Clim. Dyn*. 36: 1291-1302.

Received March 4, 2011. Accepted January 27, 2012.
Published online August 5, 2012.

6.2. Analysis of the oceanic processes associated with the development of Pacific La Niña triggered by an Atlantic Niño.

(Polo et al. 2015)

This section is focused on the analysis of the oceanic mechanisms at work in the onset and development of the Pacific La Niña triggered by an Atlantic Niño phenomenon. These results are associated with the Objetive 1 of the present memory.

Observations and partially coupled simulations that considered the observed Atlantic SSTs as the only external forcing, reveal that an Atlantic Niño phenomenon enhances the convection over the equatorial Atlantic, altering the Walker circulation and inducing anomalous subsidence in central Pacific. The associated surface wind divergence generates anomalous easterlies in west Pacific, pilling up warm waters in the west and triggering an upwelling Kelvin wave that propagates eastward from autumn to winter months. The thermocline depth shallows as the wave propagates, favouring the cooling of the sea surface through anomalous temperature advection by anomalous currents and by mean vertical entrainment velocity. The zonal advective and thermocline feedbacks reinforce the surface wind anomalies over the central-eastern Pacific, establishing the Bjerknes feedback and setting up the oceanic conditions needed for the development of La Niña cold tongue.

Clim Dyn (2015) 44:115–131
DOI 10.1007/s00382-014-2354-7

Processes in the Pacific La Niña onset triggered by the Atlantic Niño

Irene Polo · Marta Martin-Rey · Belen Rodriguez-Fonseca · Fred Kucharski · Carlos Roberto Mechoso

Received: 3 May 2013 / Accepted: 25 September 2014 / Published online: 7 October 2014

Abstract Previous observational and model studies have shown that a warm (cold) event in the equatorial Atlantic during the boreal summer are related to the development of a Pacific La Niña (El Niño) event, that is fully developed in the following winter. Although the connection takes place via atmospheric bridge, the processes at work have not been clarified for such a remote and lagged relationship. The present paper uses a partially coupled atmosphere–ocean model to infer a mechanism by which a Pacific El Niño event can be developed. In this way, enhanced equatorial convection in the equatorial Atlantic during a warm event results in enhanced subsidence and surface wind divergence over the equatorial Pacific around the dateline. This wind anomaly contributes to pile up water in the western equatorial Pacific, triggering a perturbation in the depth of the oceanic thermocline, which propagates eastward as an equatorial Kelvin wave from autumn to winter. The thermocline shallowing as the wave propagates allows for cooling of the oceanic mixed layer through anomalous temperature advection by anomalous zonal currents and by mean vertical entrainment velocity. Zonal advective and thermocline feedbacks reinforce the surface winds anomalies over the central eastern equatorial Pacific setting up the conditions for the development of a cold event in this ocean. The sequence during an Atlantic cold event is similar with the appropriate change in signs. These findings are relevant to ENSO predictability at seasonal timescales.

Keywords El Niño–Southern Oscillation (ENSO) · Atlantic Niño · Kelvin wave · Walker circulation

I. Polo (✉)
NCAS-Climate, Department of Meteorology, University of Reading, Earley Gate, P.O. Box 243, Reading RG6 6BB, UK
e-mail: i.polo@reading.ac.uk

M. Martin-Rey · B. Rodriguez-Fonseca
Meteorology and Geophysics Department, Universidad Complutense de Madrid (UCM), Plaza de las Ciencias, 28040 Madrid, Spain

F. Kucharski
The Abdus Salam International Centre for Theoretical Physics, P.O. Box 586, 34100 Trieste, Italy

F. Kucharski
Department of Meteorology, Center of Excellence for Climate Change Research, King Abdulaziz University, Jeddah, Saudi Arabia

C. R. Mechoso
Department of Atmospheric and Oceanic Sciences, University of California, Los Angeles (UCLA), 7127 Math Sciences Building 405 Hilgard Avenue, Los Angeles, CA, USA

1 Introduction

El Niño–Southern Oscillation (ENSO) refers to interannual, quasi-periodic events of strong air–sea coupled interactions in the Tropical Pacific. ENSO represents the strongest interannual disruption of the tropical Pacific climate system with worldwide impacts through teleconnection processes (Bjerknes 1969; Philander 1990). The existence of specific perturbations able to trigger ENSO events remains controversial. Possible candidates for such a role are intraseasonal atmospheric events in the tropical Pacific, such as westerly wind-bursts and Madden–Julian oscillation episodes (Kessler et al. 1995; McPhaden et al. 2006).

Our current understanding of ENSO is based on the growth of unstable perturbations in the ocean–atmosphere system through the so-called positive Bjerknes feedback (Bjerknes 1966; Philander 1990). Wyrtki (1975) described El Niño as the release of warm water from the western

equatorial Pacific after a build-up due to stronger trades in the central part of the basin. A number of fundamental studies using a hierarchy of models gave a strong impetus to El Niño research in the 1980s. The transition between the warm and cold ENSO phases (El Niño and La Niña) has been described to occur through a delayed negative feedback of ocean dynamic adjustment (Cane and Zebiak 1985; Suarez and Schopf 1988; Zebiak and Cane 1987; Battisti and Hirst 1989), according to which the classical positive feedback mechanism (Bjerknes 1966) is kept in check by nonlinearities in the system and by delayed effects associated with equatorially trapped waves reflecting at the basin's boundaries: equatorial Rossby waves reflect off the western as negative anomaly Kelvin waves that provide a negative feedback. Jin (1997a, b) described ENSO in the framework of a "recharge–discharge" oscillator theory, in which the charge and discharge refer to the build-up and release of equatorial heat content, respectively, by the non-equilibrium between the zonal-mean ocean heat content and wind stress at the equator. This recharge oscillator model leaves implicit the role of wave propagation and reflection. Mechoso et al. (2003) suggested that the model could be made substantially more complete by including the adjustment time between wind stress and eastern Pacific Sea Surface Temperature (SST). Several authors have investigated ENSO's phase locking to the seasonal cycle (e.g., Galanti and Tziperman 2000; Heng and Mechoso 2009a, b). Former conceptual models of ENSO tended to emphasize the thermocline feedback. The importance of zonal advective processes for SST anomalies to develop in the central to eastern Pacific during the El Niño events, however, has also been demonstrated (Picaut et al. 1997; An et al. 1999).

Variations in time of El Niño amplitude, period, skewness, and even structure have been reported in a number of studies (e.g., Trenberth and Shea 1987; Gu and Philander 1995; Cane et al. 1997; An and Wang 2000; Federov and Philander 2000; An 2009; Ashok et al. 2007).

The role of tropical and extratropical regions on ENSO development and prediction have been analysed (Luo et al. 2010; Boschat et al. 2013; Dayan et al. 2013; Izumo et al. 2010, 2014). In particular, the contribution of the Indian Ocean cannot be neglected. The decoupling of the Indian basin has a strong impact on ENSO dynamics (Yu et al. 2002; Frauen and Dommenget 2012). The Indian Ocean seems to modify the wind anomalies in the western Pacific 14 months in advance, changing the warm water volume (WWV) and triggering, in this way, the development of ENSO following the recharge oscillator scheme (Izumo et al. 2010, 2014).

Our concern, however, in the present paper is the link between the interannual variability in the tropical Pacific and Atlantic reported in several recent studies (Mo and Häkkinen 2000; Chiang et al. 2000; Münnich and Neelin 2005; Keenlyside and Latif 2007; Polo et al. 2008a; Rodríguez-Fonseca et al. 2009, hereafter RF09; Ding et al. 2012; Martín-Rey et al. 2012; Ham et al. 2013a, b). The tropical Atlantic also shows episodes of equatorial interannual variability with strongest amplitudes during the boreal summer (Zebiak 1993). These episodes are commonly referred to as "Atlantic Niños" (Ruiz-Barradas et al. 2000; Polo et al. 2008a; Losada et al. 2009, 2010). RF09-in agreement with Wang (2006)—has shown observational evidence on the Atlantic Niños are able to alter the dynamics of the central Pacific via anomalies in the Walker circulation, favouring the development of a Pacific La Niña during the following winter. RF09 also demonstrated that such Atlantic–Pacific connection could be captured in idealized experiments with a model of the coupled atmosphere–ocean system (CGCM; Kucharski et al. 2007, 2008) in which Atlantic SSTs are restored to observations. Ding et al. (2012) have reproduced RF09 results using a coupled GCM with finer resolution in both its ocean and atmosphere components. The agreement between the results obtained by RF09 and Ding et al. (2012) gives confidence to the Atlantic–Pacific connection at interannual time scales as conjectured by the former authors. RF09 have proposed, however, that this connection is non-stationary and takes place since the late 1960s, while Ding et al. (2012) consider the interbasin link to be time-independent. More recently, Martín-Rey et al. (2012) compared the simulations performed by RF09 with others using the same CGCM, but in which SSTs in the tropical Atlantic are prescribed according to an observed, time-varying climatology. They concluded that including interannual variability in the Atlantic SSTs (as in RF09) results in increased ENSO variability with more active thermocline feedbacks, especially after the late 1960s.

The findings on influence of Atlantic Niños on ENSO have opened a new paradigm, according to which the skill of ENSO predictions would be higher if the tropical Atlantic variability were considered (Jansen et al. 2009; Frauen and Dommenget 2012; Keenlyside et al. 2013). Frauen and Dommenget (2012) have argued that, although the decoupling of the tropical Atlantic has a little influence on the amplitude and frequency of ENSO, the initial conditions of the tropical Atlantic have a strong impact on ENSO predictability. Moreover, Keenlyside et al. (2013) indicate the importance of the initial Atlantic conditions during boreal spring to improve ENSO forecast.

Although there is already a substantial body of literature on the links between the Atlantic Niños and Pacific Niñas (and vice versa), the processes at work for these links remain to be clarified. The present study fills this gap using data from those simulations performed by RF09, together with another coupled simulation and also from reanalysis data, focusing on the time-period when the inter basin

links have been reported (1979–2002). The aim of the present study is to provide an in-depth analysis of the oceanic mechanisms for the Pacific La Niña/o development in response to the Atlantic Niño/a that have been only partly suggested in RF09. Our method is based on the regression of different oceanic and atmospheric variables, together with the terms of the heat budget equation, onto the time series of SST anomalies in the equatorial Atlantic (Atl3 index).

The manuscript is organized in the following way. In Sect. 2, the observed and modelled data as well as the experiments are described together with a brief assessment of the model's ability to reproduce the seasonal cycle of those variables used to describe tropical variability. The evidence of the Atlantic–Pacific connection is shown from observed and simulated SST. In Sect. 3, the simulated responses from observed Atlantic SST are quantitatively analysed and the mechanisms responsible for generating the remote climate impacts over Tropical Pacific are considered in more detail. The conclusions and implications of our findings are presented in Sect. 4.

2 Data and methods

2.1 Data and model experiments

The observational fields for the atmosphere are represented by the ERA-40 reanalysis (Uppala et al. 2005). Zonal and meridional winds and vertical velocity at 13 pressure levels have been considered. SSTs correspond to the HadISST1 dataset compiled at the UK-Metoffice (Rayner et al. 2003). The upper ocean data is taken from the latest version of SODA reanalysis (version, 2.2.4, Giese and Ray 2011). In particular, wind stress, temperature at 5 m (as SST) and depth of 20 °C isotherm (D20), as a proxy of the equatorial thermocline depth, are used. Finally, the surface fluxes are taken from the OAFlux project dataset (Yu et al. 2008).

The simulations in RF09 were performed with an atmospheric global circulation model coupled to a 1.5 layer ocean model (hereafter SPEEDY-RGO) in selected regions. The model's atmospheric component is the ICTP Atmosphere General Circulation Model (AGCM; Kucharski et al. 2007, 2008, 2013), version 40. This AGCM is a balanced complexity model based on a spectral primitive-equation core and a set of simplified parametrization schemes. The horizontal resolution is T30 and there are eight levels in the vertical. The model's oceanic component is a shallow-water reduced-gravity model with a resolution of 2° in longitude by 1° in latitude. This intermediate ocean model has proved useful in ENSO research (Cane and Zebiak 1985; Zebiak and Cane 1987; Anderson and McCreary 1985; Battisti and Hirst 1989; Jin and Neelin 1993; Sheinbaum 2003). In the model, only the top layer is dynamically active, the interface between the upper and the deep ocean represents the thermocline, and the deep ocean assumed motionless and infinitely deep. The thermodynamic equation is also included to relate temperature variations with mixing, advection and surface heat fluxes (Chang 1994). A flux-correction is applied to climatological surface heat fluxes and wind stresses to reduce the model's drift (Chang et al. 2006).

In the selected configuration, the AGCM and ocean model were run fully coupled in the Tropical Indo-Pacific basin (between 30°S and 30°N), while observed monthly-mean SSTs were prescribed in the Atlantic, with climatological SSTs elsewhere. RF09 performed a set of nine simulations with different initial conditions. The initial conditions were created by starting the atmospheric and oceanic simulations from restarts of previous long runs and perturbing the randomly the atmospheric initial conditions. Since the simulations are starting in 1948, but are analysed from 1979, this leaves a spin-up period of 32 years, which is more that sufficient for equatorial Pacific thermocline variability. The results shown in the present work correspond to the ensemble mean of the nine runs for the period 1979–2002.

In addition to RF09 simulations, the mechanisms have been checked using an available simulation with a more resolved ocean model using the same experimental design (hereafter SPEEDY-NEMO). The ocean model is based on NEMO v.3.0 (Madec et al. 1998) which is a primitive equation z level model making used of the hydrostatic and Boussinesq approximations. The version used has a tripolar ORCA2 configuration with horizontal resolution and a tropical refinement to 1/2. The model has 31 vertical levels with a thicknesses ranging from 10 m at the surface to 500 m at the ocean bottom.

For consistency with previous works, our analysis is based on mean fields over four consecutive months.

2.2 Model validation and methodology

2.2.1 Model validation

Figure 1 shows the seasonal cycle of the SST, D20 and wind stress over the equatorial Pacific for the observations and the simulations. From the observations the development of the upwelling season is highlighted from August to September (Fig. 1a). The SPEEDY-RGO simulation shows a weakening of the eastern Pacific upwelling compared with observations, as is common to many state-of-the-art coupled models (Mechoso et al. 1995). The simulated eastern Pacific pattern of thermocline depth, which reflects dynamical ocean processes, presents an overestimation of the annual cycle and it seems to be linked to the

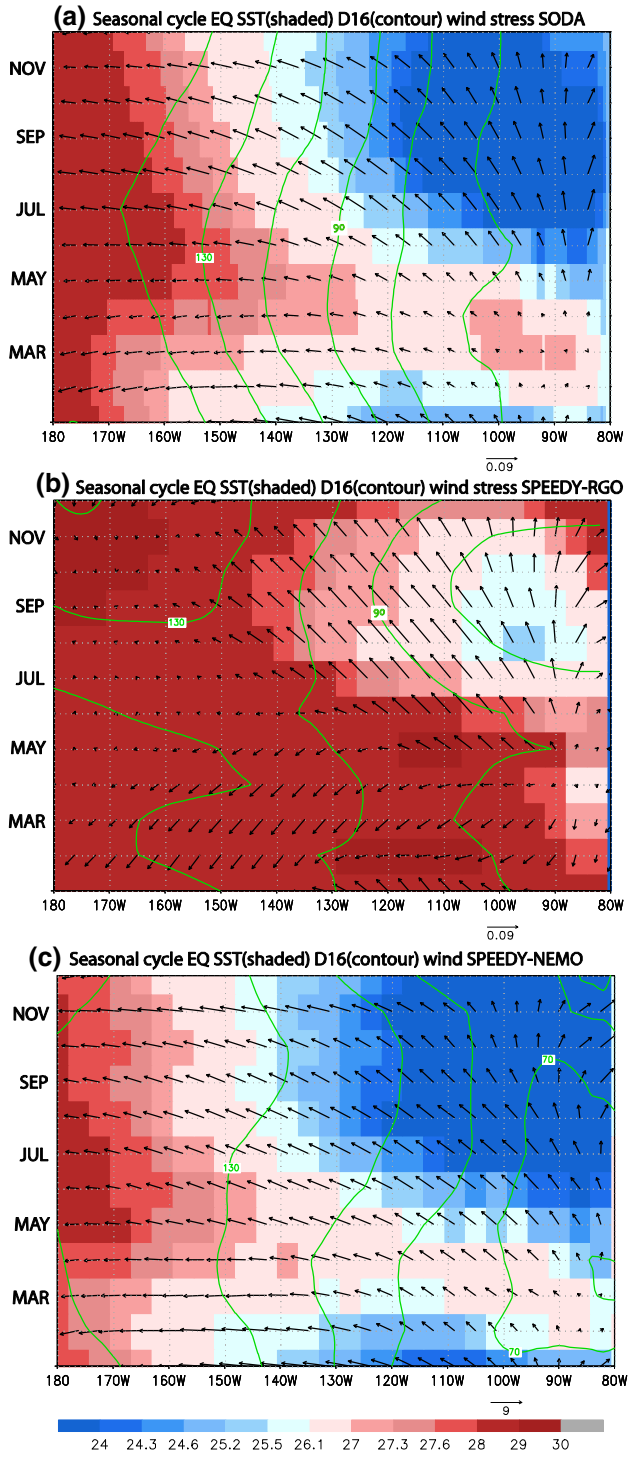

Fig. 1 Seasonal cycle at the equatorial Pacific. **a** Seasonal cycle averaged over 3°N–3°S of the sea surface temperature (*shaded*, in C) 16 °C isotherm depth D20 (*contour*, in m) and wind stress (*vectors*, N/m^2) from the SODA reanalysis. **b** Same as **a** but for the SPEEDY-RGO simulations outputs. **c** Same as **a** but for the SPEEDY-NEMO simulation outputs

SST seasonal cycle, suggesting a strong coupling between D20 and SST. The simulation shows a marked zonal thermocline gradient along the year, peaking in the upwelling season from July to November.

Wind amplitudes are weaker than in the observation over the central part of the Pacific. The model is more successful in simulating the thermocline variations in the eastern Pacific. Note the agreement for all variables, SST, D20 and wind in 160°W–140°W in summer months (June–July) when the Tropical Atlantic has its maximum variability and influences the Pacific Ocean.

Finally, the SPEEDY-NEMO simulation shows an improvement in simulating the seasonal cycle over the equatorial Pacific especially for the upwelling season. However, there is a SST bias present with a westward extension of the cool waters (Fig. 1c).

Figure 2 shows the seasonal cycle of the Niño3 index from the simulations and the observation and Atl3 index from the observations. Those indexes are defined, respectively, as the SST anomaly in the eastern equatorial Pacific (5°S–5°N; 150°W–90°W) and in the central-eastern equatorial Atlantic (3°S–3°N; 20°W–0°E). According to Fig. 2, the mean SST simulated in Niño3 has a warm bias along the whole annual cycle. The simulations captures reasonably well the seasonal deviations of SST from the annual mean (Fig. 2b), especially SPEEDY-NEMO. The standard deviation (Fig. 2c) in the simulations is lower than in the observation in the boreal winter months, suggesting that simulated Niño events have weak amplitude. An interesting feature in Fig. 2 is the increase of the simulated SST variability in the eastern Pacific from May to August in SPEEDY-RGO, which coincides with the maximum of variability for the observed SST in the Tropical Atlantic (red line). Although there is a bias in the seasonality of Niño3 variability, the summer peak could be attributed in part to the inclusion of the Atlantic as the only model's boundary condition with (prescribed) interannual variability in agreement with Martín-Rey et al. (2012). In SPEEDY-NEMO simulation there is not seasonality in the interannual variability for Nino3 index (Fig. 2c).

2.2.2 *Methodology*

We analyse in the present paper the processes involved in the observed Atlantic influence on the Pacific by examining regression and correlation maps between selected atmospheric and oceanic fields along the development of ENSO and the June to September (JJAS) Atl3 index. To assess the robustness of the results a Monte Carlo test is applied. This is a nonparametric test that consists in shuffling time series

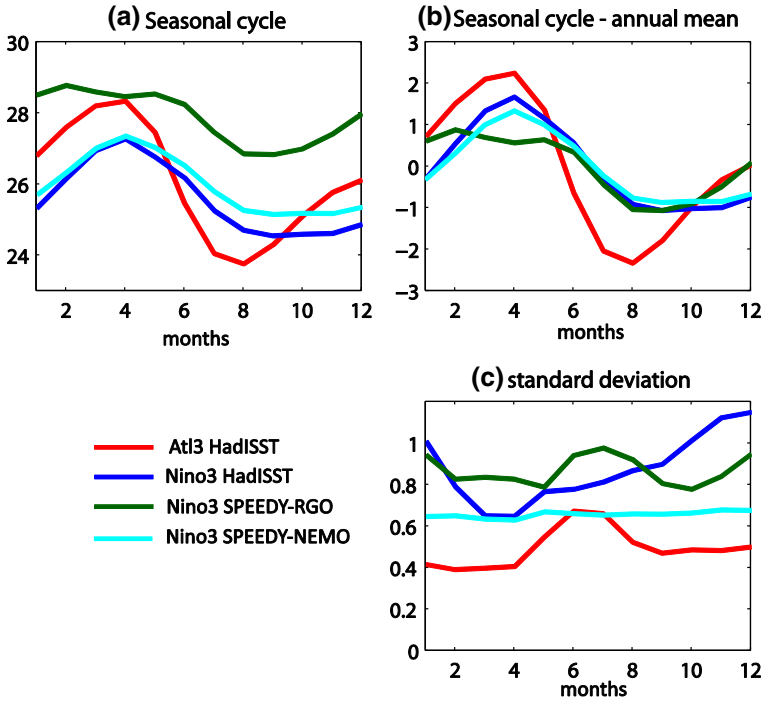

Fig. 2 Seasonal cycle of the indexe. **a** Mean SST as a function of months to illustrate the seasonal cycle of the Atl3 index (*red*) Niño3 index from the HadISST observational dataset (*blue*) and Niño3 index from the SPEEDY-RGO simulations (*green*) and Nino3 index from the SPEEDY-NEMO simulation (*cyan*) for the period 1979–2001. **b** Same as **a** but with the annual mean removed to highlight the seasonal cycle. **c** Standard deviation of SST as a function of months to illustrate seasonality of the interannual variability for the same indexes. The interannual variability has been computed as the average of the standard deviation of each member of the ensemble for the case SPEEDY-RGO

and performing their correlation for a large number of times and therefore constructing a distribution function of the permutations. Significant results at the 90 % confidence level according to the test are shown in the figures.

The amplitude of the SPEEDY-RGO simulated ensemble mean anomalies is about 3 times smaller than in the observations. Nevertheless, magnitudes are still significant in reference to the model's intrinsic variability. The amplitude of anomalies in individual ensemble members (not shown) can be double those in the mean however. This discrepancy could be due to the biases in the relatively simple coupled model that we use however, it could be also in part because the modeled ensemble mean is representing the purely forced signal, whereas the observed regressions contain contributions that are not entirely forced by the tropical Atlantic. Nonetheless, it is beyond the scope of this paper to identify the magnitude of the purely Atl3 forced signal, which would require partially coupled multi-model ensembles. In order to take into account the difference between the variability in the observation and simulation, we divide the regression maps by the corresponding standard deviations, thus showing correlation maps.

We have chosen for the study the 1979–2002 period, when the correlation between the variability in the tropical Atlantic and Pacific is significant. This choice allows us to make direct comparisons with the results of previous studies (RF09; Ding et al. 2012; Martín-Rey et al. 2012). Although the interbasin relationships start to be significant at the end of the 1960s, we have also selected this period to have more homogeneous observational data in both, time and spatial coverage due to the introduction of satellite information.

In the SPEEDY-RGO simulations, for the ocean heat budget analysis we evaluate the different terms in the ocean model's thermodynamic equation, expressed in the following way,

$$\frac{\partial T}{\partial t} = \frac{Q}{\rho_0 C_p H_s} - u_s \times \nabla T - \frac{w_e H(w_e)(T - T_e)}{H_s} + \kappa \nabla^2 T \qquad (1)$$

where T is temperature of the mixed layer assumed to have constant depth Hs, ρ_0 is ocean water density, C_p is specific heat capacity, Q is net heat flux at the surface, u_s is horizontal velocity at the upper model's layer (surface current), w_e is vertical velocity of entrainment, $H(w_e)$ is the Heaviside step function (unit for $w_e > 0$ and zero for $w_e < 0$), T_e is temperature of entrained water beneath the base of the mixed layer, and κ is a diffusivity coefficient (Chang 1994). According to Eq. (1), changes in temperature of the mixed layer (left-hand side term) are due to the net surface heat flux at the interface with the atmosphere, horizontal advection, vertical entrainment, and horizontal diffusion (right-hand side terms). In the ocean model we use, the value of T_e carries the information on the change of the thermocline temperature through the entrainment parametrization. The linearised version of Eq. (1), with diffusion term neglected because it is small compared with the other terms, is,

$$\frac{\partial T'}{\partial t} \approx \frac{Q'}{\rho_0 C_p H_s} - \mathbf{u}'_s \times \nabla \overline{T} - \overline{\mathbf{u}_s} \times \nabla T' - \frac{w'_e \Delta \bar{T}}{H_s} - \frac{\overline{w_e} \Delta T'}{H_s} \qquad (2)$$

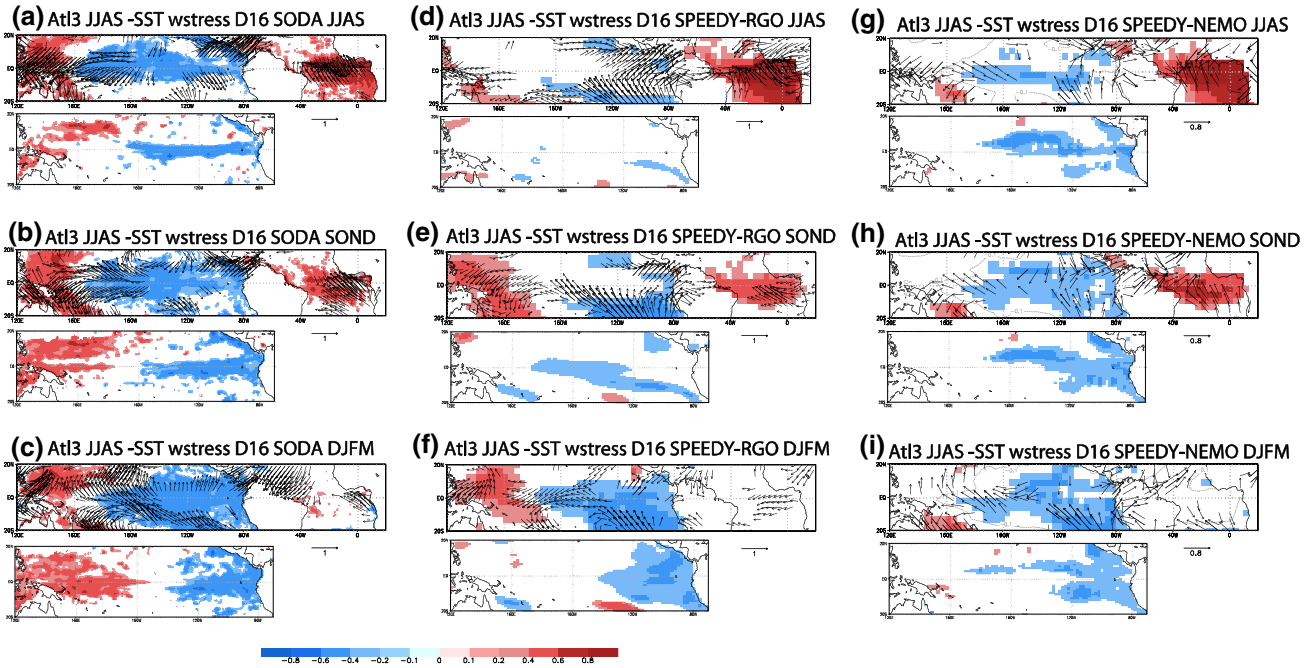

Fig. 3 Evolution of the spatial correlation maps related to Atl3. **a–c** Correlation maps between summer (JJAS) Atl3 index and the SST (*top shaded*), wind stress (*top vectors*) and thermocline depth (*bottom*) for summer JJAS season (**a**), autumn season (**b**) and winter DFJM season (**c**) for SODA reanalysis. Only significant areas have been plotted from a Montecarlo test with 500 permutation at 90 % of confidence level. **d–f** Same as **a–c** but for the SPEEDY-RGO simulations outputs. **g–i** Samea as **a–c** but for the SPEEDY-NEMO simulation outputs

where over bars indicate long-term climatology and primes denote deviation from the mean. In the present study, we work with expression (2).

For the sake of simplicity, in the calculation of the heat budget for the observations and the SPEEDY-NEMO simulation, the H_s is considered to be D20. Therefore, the terms has been evaluated over the layer above D20. To notice that, in the SPEEDY-NEMO simulation, only the zonal currents were available to us, thus the vertical terms were not calculated.

3 Results

3.1 Evidence of the Atlantic Ocean interannual variability altering the Pacific circulation

In order to analyse the processes involved in the Atlantic–Pacific connection, we focus on the period during which this interbasin link is significant. We start by inspecting correlation maps between the anomalous SST in Atl3 region during summer and wind stress, D20 and SST in the Pacific from summer to winter from observations (Fig. 3a–c). The results show a simultaneous relation in summer together with a reinforcement of La Niña event in the following winter. The observed wind stress anomalies related to the Atl3 index display a strengthening of the divergence in the central Pacific in JJAS which lead to a reinforcement of the trades, from summer to winter, over the western equatorial Pacific (west of 160°W). The off-equatorial wind stress curl (not shown) has a maximum value west of 160°W on both sides of the equator, with two positive D20 anomalies associated with a Rossby wave response to surface wind divergence (Matsuno 1966) (see red shadings in the D20 correlation maps in Fig. 3a–c). The anomalous divergence in the central Pacific (150°E–150°W) results in a decrease of sea surface height (i.e. shallower thermocline). The associated negative anomalies in D20 propagate eastward east of 160°W as a Kelvin wave (see blue shadings in D20 correlation maps in Fig. 3a–c), reaching the eastern part of the basin 3 months later. The Bjerknes mechanism seems to be also at work in the development of La Niña: as the thermocline shallows in the equatorial band, the SST decreases reinforcing the easterlies (Fig. 3a–c).

In the SPEEDY-RGO simulation (Fig. 3d–f), the Atl3 index in boreal summer is significantly and positively correlated with positive SST anomalies over the Atlantic, negative SST anomalies over the southeast tropical Pacific, and a stronger South Pacific Subtropical High (Fig. 3d). Later, in autumn, easterlies wind stress over the equator and western dateline imprint an anomalous D20 shoaling and cooling the central Pacific (Fig. 3e). The perturbation of D20

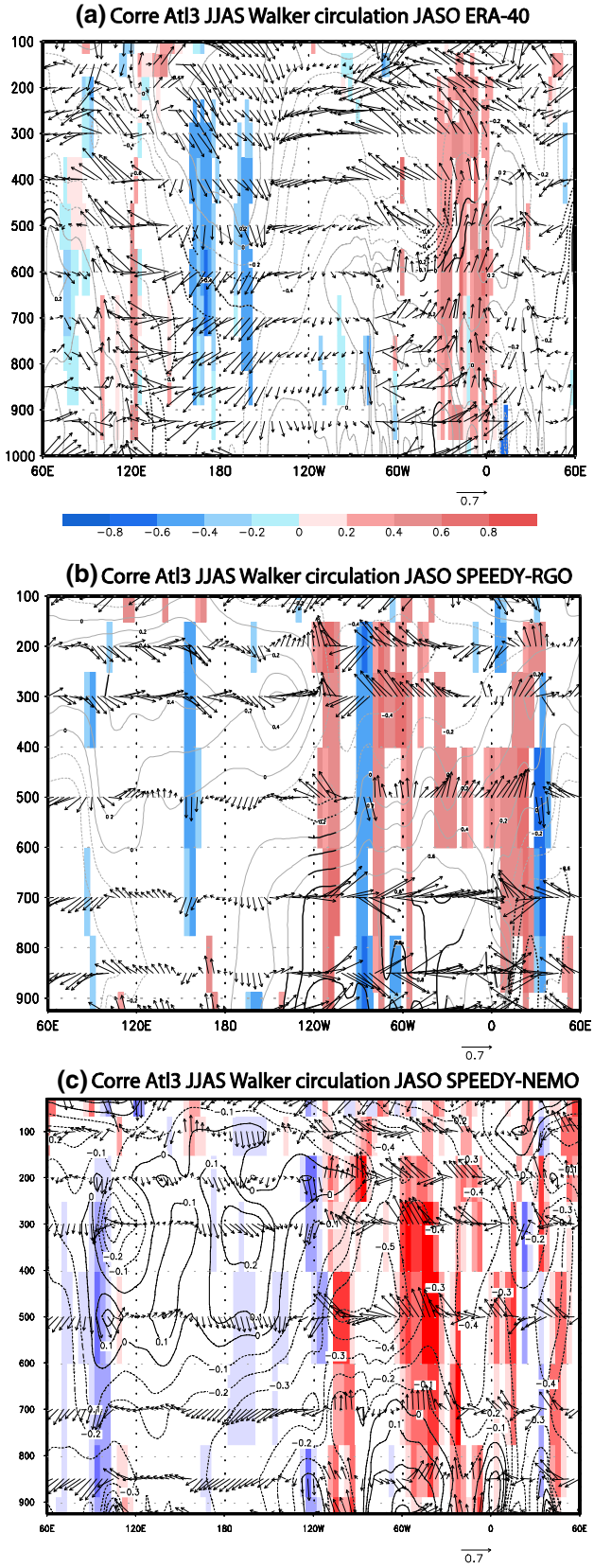

Fig. 4 Anomalous Walker circulation related to Atl3. **a** Correlation ▶ maps between JJAS Atl3 index and JASO wind field along the troposphere and averaged over the equatorial band (5°N–5°S) for observations (ERA-40). Correlations of zonal and vertical movements are represented as *vectors*. *Shaded areas* corresponds to significant correlation with vertical movement and the *contours* are correlation with zonal winds. **b** Same as **a** but for the SPEEDY-RGO simulations outputs. **c** Same as **a** but for the SPEEDY-NEMO simulation outputs

propagates eastward during the following months. Thus, in the winter season, the thermocline is shallower next to the South American coast, in association with an equatorial band of cold SST anomalies accompanied by enhanced easterlies in the central and west equatorial Pacific (Fig. 3f). The model captures the dynamical chain of events shown in the observations.

Finally in the SPEEDY-NEMO simulation, the anomalous westerly winds appears west of the dateline from an increase of SST over the Equatorial Atlantic in summer similar to the observations (Fig. 3g), cooling the surface and shallowing the thermocline east of the dateline (Fig. 3g). As the anomalous thermocline depth anomalies propagate eastward the development of La Nina is presented from autumn to winter (Fig. 3h, i).

Taking into account all these results, we can formulate a plausible hypothesis in the following way: The Atlantic and Pacific Niños could be connected through changes in the Walker circulation. Changes in surface winds in the central Pacific produces the piling up of water in the western Pacific that modifies the thermocline depth and triggers a Kelvin wave during summer. The wave would propagate eastward, changing the thermocline and then the SST in the following winter. A mechanism of this kind would be in accordance with classic ENSO models, and could be captured by our very simple ocean model (RGO) coupled to an AGCM. The following sections are devoted to discuss the viability of such a hypothesis

In the following section we explore in detail the processes responsible for the SST anomalies from summer to winter in the Tropical Pacific.

3.2 Interaction mechanisms

3.2.1 Atmospheric bridge

We start by examining the anomalies in the Walker circulation associated with the SST variability in the equatorial Atlantic in the simulation and the observation. Figure 4 shows the correlation between the Atl3 index in summer (JJAS) and the wind field in the tropospheric column averaged over the equatorial band (5°N–5°S) for July to

October (JASO). In the observations (Fig. 4a), positive SST anomalies in the Atlantic [30°W–0°E] are associated with ascending motions in the overlying atmospheric column and enhanced convection, and with anomalous subsidence and suppressed convection over the Pacific basin east and west of the dateline. As the maps are shown in terms of linear correlation scores, the opposite takes place for a cooling in the tropical Atlantic. The SPEEDY-RGO simulation (Fig. 4b) produces a similar pattern of anomalous Walker circulation anomalies formed by an ascending branch in the eastern Tropical Atlantic and descending motions over the central Pacific (west of the dateline). The atmospheric Gill-type response to an Atlantic heating (not shown) consists of two cyclones (anticyclones) west to the perturbation region (120°W–0°E) and two anticyclones (cyclones) in the west Pacific (120°E–120°W) in surface levels (upper levels), as it is shown in RF09.

The SPEEDY-RGO simulation captures the tropical response to variations in Atlantic SSTs observed albeit with weaker magnitudes. There is also a difference in the longitude where subsidence over the central Pacific occurs: west of the dateline in the simulation but also east of the dateline in the observation. This difference could influence the triggering of La Niña events in the simulation and the observation.

The SPEEDY-NEMO simulation also captures the ascending motions over the equatorial Atlantic with subsidence over central equatorial Pacific east of the dateline (Fig. 4c). Although the amplitude of the correlation related to the subsidence is small, the easterly wind anomalies in the lower levels of the atmosphere are very well simulated.

Despite the different of the location of the subsidence between the observation and the simulations, the sinking air over the central Pacific creates a surface divergence wind area, which is translated into a divergence of the Ekman transport and a shallowing of the thermocline and, as a consequence, deep cold water upwells. These associated oceanic processes are addressed in the next section.

3.2.2 Oceanic processes

Figure 5 shows the seasonal evolution of the thermocline depth, SST and wind over the equatorial Pacific in terms of correlation maps with the summer (JJAS) Atl3 index. The results are shown for both observations (first row) and simulations (second and third rows).

In the observation (Fig. 5a–c), the easterly wind stress anomalies over the central-west equatorial Pacific associated to a warming in the equatorial Atlantic, grow and propagate eastward from summer to winter as La Niña develops. From JASO to JFMA, the anomalous D20 in 160°W is displaced eastward suggesting a propagating feature associated with a Kelvin wave (Fig. 5a). As the Kelvin-like wave propagates, the thermocline becomes shallower along the eastern basin, allowing anomalous zonal advection to effectively cool the SST during the autumn–winter months (September to January, Fig. 5b). The Bjerknes feedback is also at work in the development of La Niña event, and an intensification of the surface divergence is observed in autumn and winter months as a result of the surface cooling (Fig. 5c).

In the SPEEDY-RGO simulation (Fig. 5d–f), the negative zonal wind stress anomalies in west-central Pacific in ASON-SOND perturb the sea surface generating significant negative D20 anomalies around dateline-160°W, which propagate eastward as an equatorial Kelvin wave (Fig. 5d). The first baroclinic mode, the only one present in the ocean component of the model, has a phase speed of about ~2 m/s (i.e. Kessler et al. 1995), and hence it usually take 3–5 months to reach the American coast from Maritime continent (from 120°E to 80°W). Estimates of the phase speed from the satellite observations confirm that the first baroclinic mode is present in the tropical oceanic basins although with a lower than theoretical speed of 1.5–1.7 m/s (Chelton and Schlax 1996; Polo et al. 2008b).

As the Kelvin wave propagates, the thermocline shallows from the central to the eastern equatorial Pacific. This shallowing makes more effective the advection of cool water by horizontal currents and vertical motion, which is translated into a cooling from November (Fig. 5e). The simulation also captures the Bjerknes feedback; the surface winds strengthen as the zonal surface temperature gradient increases. The zonal wind anomalies follow the atmospheric anomalous pressure gradient, which help to increase the cooling in the eastern Pacific (Fig. 5f). The intensification of anomalous easterly winds and the eastward shallowing of the thermocline are consistent with the presence of westward surface current anomalies, which become more and more significant from the coast of Peru to dateline from ASON to DJFM (not shown).

Finally, the warming in the western Pacific precedes La Niña development in the SPEEDY-RGO simulation (Fig. 5f). It will be shown that this warming is mainly due to heat fluxes (see Fig. 7d and discussion in the next section) and could also further increase the easterly wind stress to the east of the warming in the region 160°E–160°W. The warming in the western Pacific is also seen in the observations (Fig. 5c), where persistent positive SST anomalies are present west of 160°E from May to December. The response to the west Pacific warming (which is relatively large in the SPEEDY-RGO simulation) would also explain why the wind stress anomalies have the same magnitude as in the observation, whereas the SST anomalies in the eastern Pacific and D20 anomalies are much smaller.

In the SPEEDY-NEMO simulation (Fig. 5g–i), the eastward propagation of the D20 anomalies associated

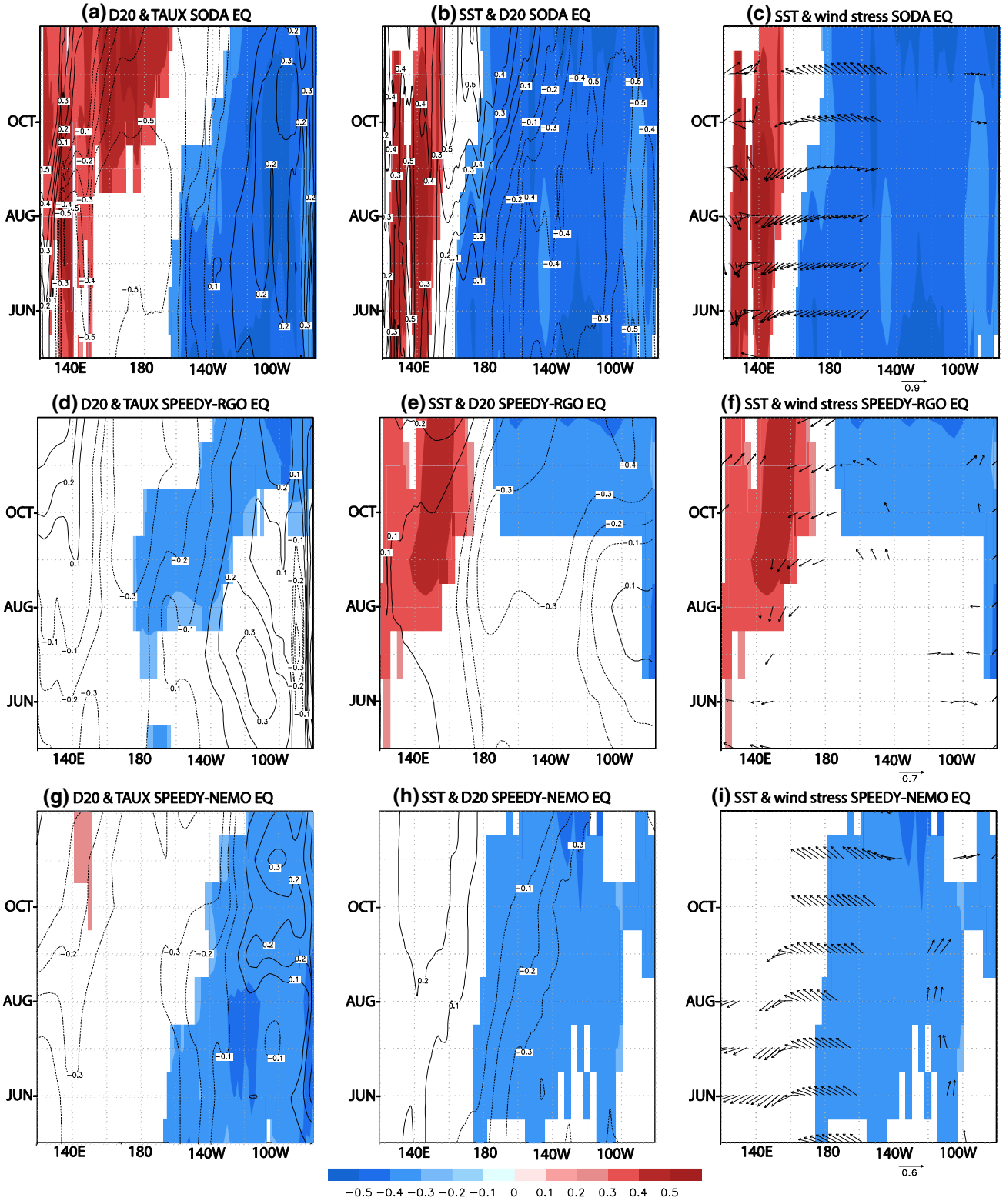

Fig. 5 Hovmuller diagrams of equatorial Pacific related to Atl3. **a–c** Hovmoller diagrams of D20, SST and wind stress from SODA reanalysis regressed onto summer (JJAS) Atl3 index from May–June–July–August (year 0) to December–January–February–March (year +1). The variables are represented in pairs in order to illustrate the relationship between the Bjerknes feedback's components. **a** D20 (*shaded*) and zonal wind (*contour*), **b** SST (*shaded*) and D20 (*contour*), **c** SST (*shaded*) and wind stress (vectors, zonal and meridional components are plotted with y-axis illustrating the northward component). Only statistically significant areas have been plotted with 90 % confidence level for shading and vectors. **d–f** Same as **a–c** but for the SPEEDY-RGO simulations outputs. **d–f** Same as **a–c** but for the SPEEDY-NEMO simulation outputs

with Atl3 index is well reproduced and it is related to an increase of the easterly wind anomalies in the central equatorial Pacific and the cooling of the surface from summer season in agreement with the observations.

3.3 SST tendencies

In this subsection we analyse separately the terms of the SST tendency equation in the observations and the simulations in order to arrive to a more quantitative understanding of the processes responsible for the SST changes over the eastern equatorial Pacific associated with the Atlantic warming.

Figure 6 shows the heat budget analysis for the observations. Figure 6 shows the effective contribution of the different terms to the SST tendency (dT'/dt, Fig. 6a, b): Net heat fluxes (Qnet, Fig. 6c, d), horizontal advection by anomalous ($u'gradT$, Fig. 6e, f) and mean currents ($ugradT'$, Fig. 6g, h); and vertical advection by mean ($we\Delta T'$, Fig. 6i, j) and anomalous ($we'\Delta T$, Fig. 6k, l) entrainment for the summer and autumn seasons JJAS (Fig. 6, left) and SOND (Fig. 6, right). Units in all cases are degree per month.

The change of the temperature occurs in the observations from the central to east Pacific from summer to autumn (Fig. 6a, b). The net surface fluxes tend to damp the surface cooling in SOND (Fig. 6d). The horizontal advection due to anomalous zonal velocities above the thermocline seems to cool the surface in the eastern part of the basin in SOND (Fig. 6f). However the most important term responsible for cooling the equatorial surface is due to the mean vertical velocity in an anomalous vertical stratification over central-east Pacific (Fig. 6l).

Figure 7 shows the heat budget analysis for the SPEEDY-RGO simulation. In the summer season (Fig. 7, left), the stronger SST changes in the SPEEDY-RGO simulation occur in the southeastern Pacific (Fig. 7a). In this location, anomalies in the atmospheric heat flux are the dominant term for creating negative SST anomalies (Fig. 7c). The anomalous heat fluxes are consistent with the existence of anomalous wind stress in the southeastern region (Fig. 3c), which favors the evaporative cooling. This anomalous turbulent heat fluxes could explain the main role of the net heat flux in the initial negative anomalies of SST in the region 120°W–80°W, 10°S–25°S. The anomalous cooling is advected through mean horizontal currents over 10°S–15°S (Fig. 7g). The anomalous wind stress over the southeastern Pacific also favours upwelling over the edge of the region (Fig. 7i). Finally, the mean upwelling over the southeast Pacific, although less important, also contributes to the cooling in summer (Fig. 7k). Therefore, net heat fluxes at the surface and horizontal advection are responsible for cooling the subtropical Pacific.

In the autumn SOND season (Fig. 7, right), the temperature change is important over the equatorial band (Fig. 7b), imprinting a La Niña pattern in the SST field in winter (Fig. 3f). As the horizontal currents have changed, the associated anomalous horizontal advection is important over the equatorial band (Fig. 7f). As the thermocline is shallower, the zonal advection is expected to produce a more effective cooling at the equator. Mean currents also contribute to cool the eastern equatorial region, although the cooling pattern is noisy (Fig. 7h). Nevertheless, anomalous entrainment by changes in the stratification (i.e. changes in the thermocline depth) by mean vertical velocity is the main responsible for the creation of the anomalous equatorial cold tongue in autumn (Fig. 7l) together with a minor contribution from anomalous upwelling (Fig. 7j). Net heat fluxes seem to contribute to the cooling in the southern part of the cold tongue; however they tend to damp the negative SST anomalies at the equator (Fig. 7d). The role of the atmospheric fluxes is consistent with previous works (Barnett et al. 1991; Kleeman et al. 1994; Wang and McPhaden 2001; Huang et al. 2011).

Finally, for the SPEEDY-NEMO simulation (Fig. 8), only some of the terms were available. We can conclude that the main change in the surface temperature occurs from central to east equatorial Pacific from summer to autumn (Fig. 8a, b) in agreement with the observations. The surface cooling in summer is due, in part, to the anomalous zonal velocities over an anomalous horizontal temperature gradient (Fig. 8e), while the surface heat fluxes are always acting to damp the anomalous negative SST (Fig. 8c). Since the cooling related to anomalous horizontal advection (Fig. 8e, f) is not able to explain the total cooling (Fig. 8a, b), we speculate that, as in the observations and the SPEEDY-RGO simulation, the anomalous vertical advection is having an important role cooling the surface.

The dominant term cooling the equatorial surface in La Niña event related to Atlantic Niño is the vertical temperature advection due to the mean vertical velocity for both, observations and SPEEDY-RGO simulation (Figs. 6l, 7l). The anomalous vertical stratification is key for the anomalous SST growth, which is therefore an evidence of Kelvin wave propagation in the development of La Niña.

The sequence of the processes in the development of La Niña in relation to an Atlantic Niño is illustrated in Fig. 9 and summarised in the next section.

4 Discussion and conclusions

We have analysed from observations and partially coupled simulations the different processes involved in the development of Pacific La Niña (El Niño) events associated with Atlantic El Niño (La Niña) ones for the period 1979–2002.

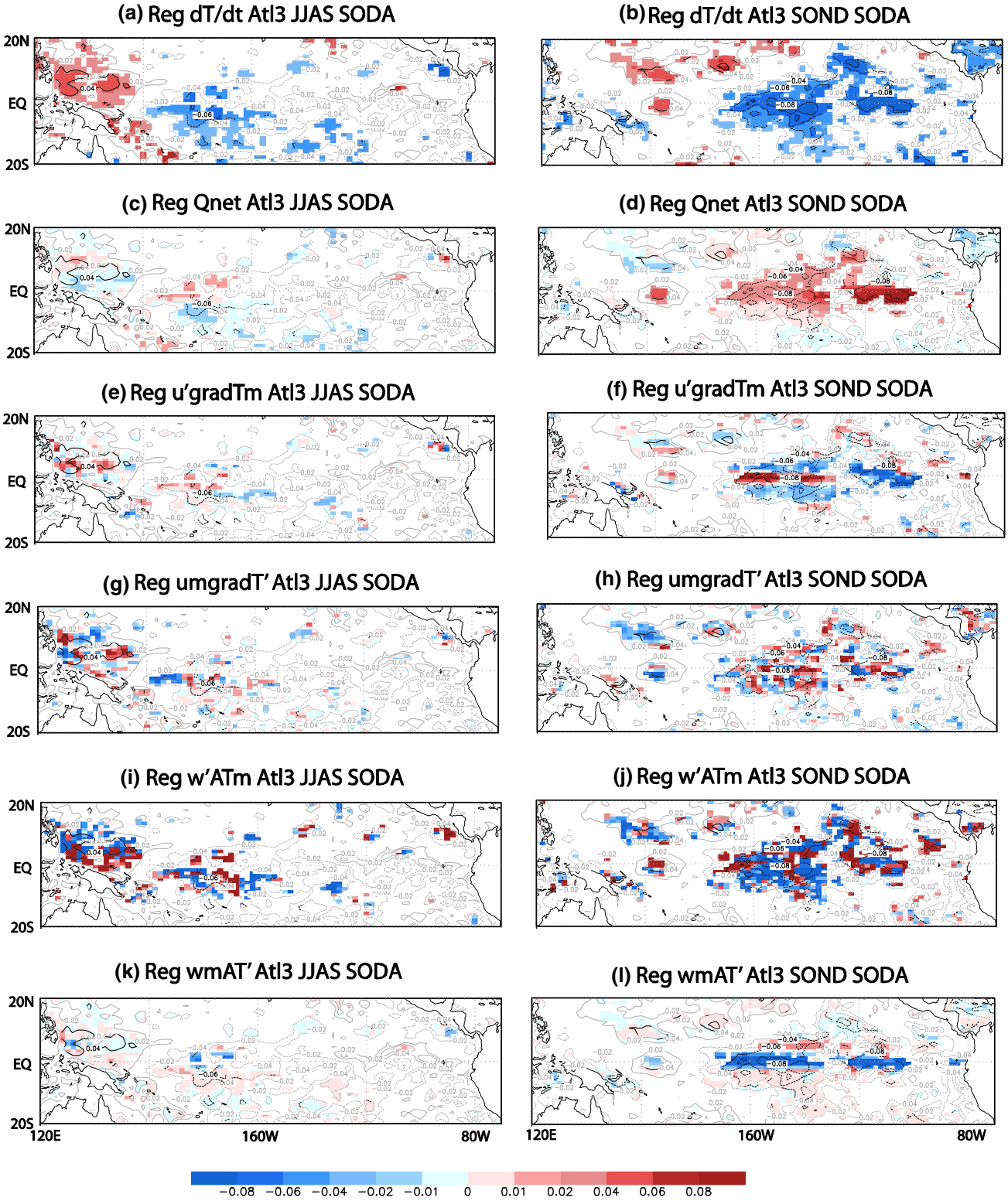

Fig. 6 Heat budget related to Atl3 in SODA. Regression maps of the terms in the heat budget onto JJAS Atl3 index. Different terms of the SST tendencies are *shaded* (in C/month) from top to bottom: tendency of the temperature of the mixed layer (**a**, **b**), net surface heat fluxes (**c**, **d**), mean temperature advection by anomalous horizontal currents (**e**, **f**), anomalous temperature advection by mean horizontal currents (**g**, **h**), mean vertical advection by anomalous upwelling (**i**, **j**) and anomalous vertical advection by mean upwelling (**k**, **l**) for summer (JJAS, *left*) and autumn months (SOND, *right*). The total change of temperature of the mixed layer is plotted in contours for all the maps (in C/month, *bold line* for significant areas exceeding 90 % confidence level, CI = 0.01)

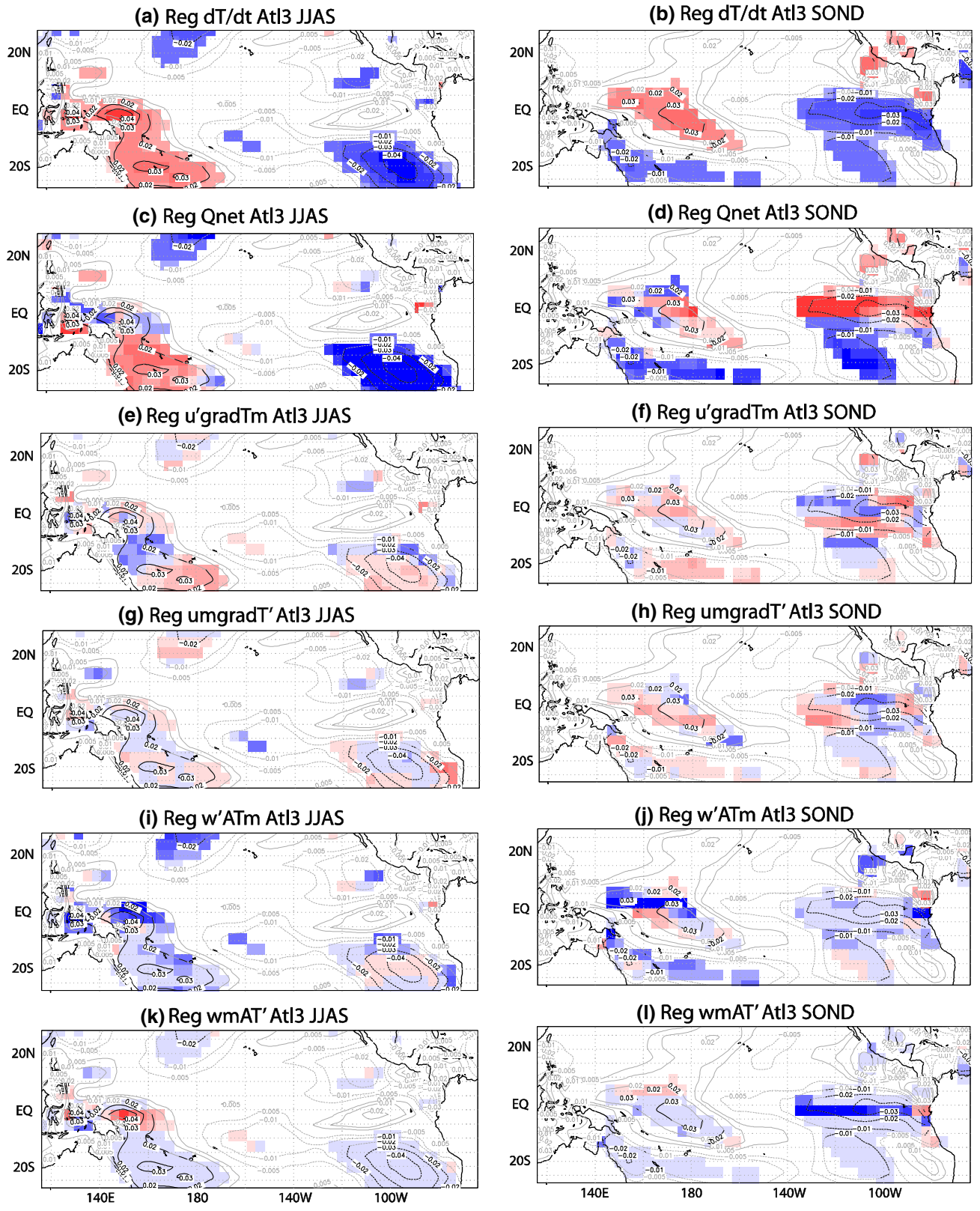

Fig. 7 Heat budget related to Atl3 in SPEEDY-RGO. Same as Fig. 6 but for the SPEEDY-RGO simulation. *Contour interval* is now 0.005

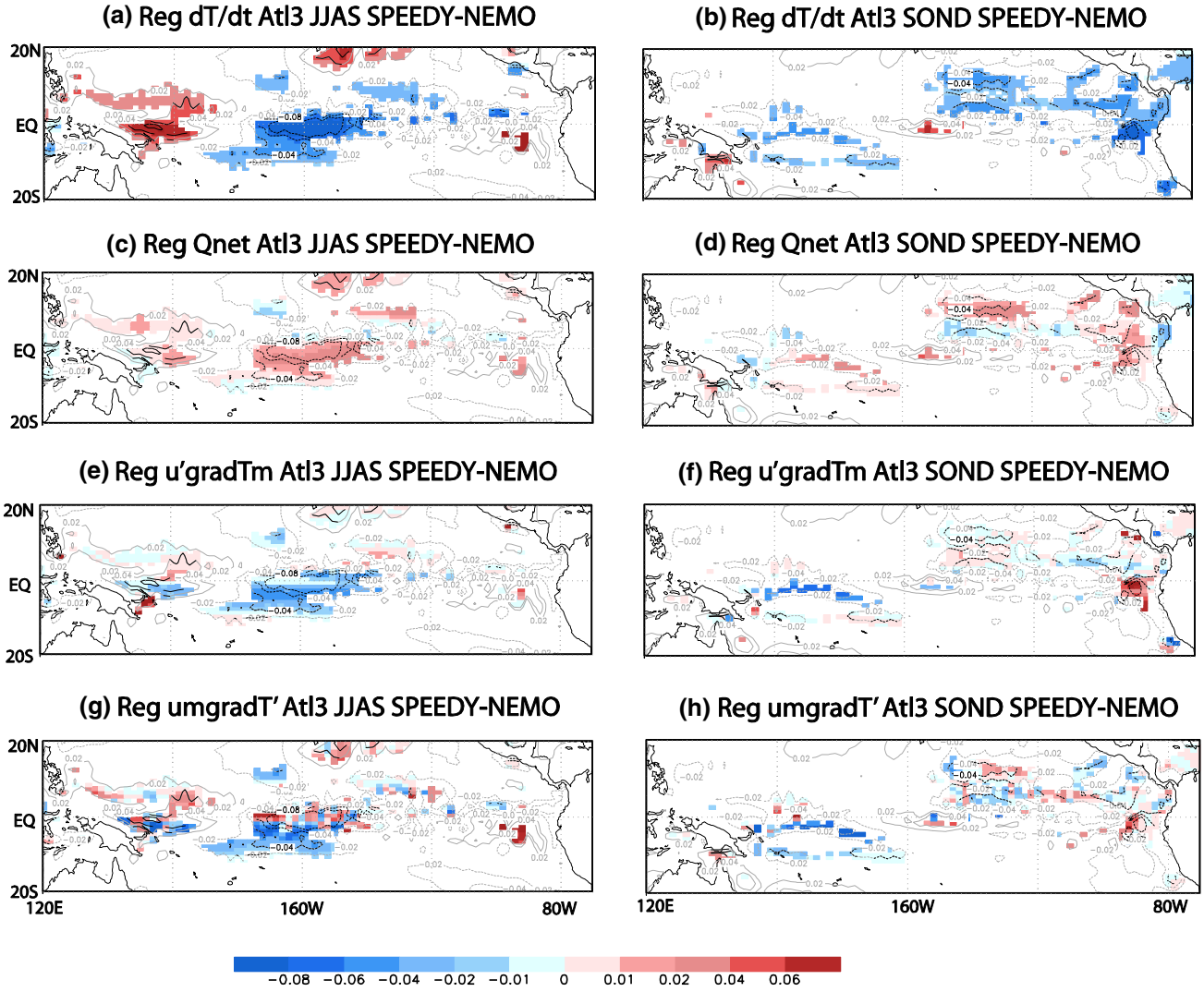

Fig. 8 Heat budget related to Atl3 in SPEEDY-NEMO. Same as Fig. 6 but for the SPEEDY-NEMO simulation outputs. *Contour interval* is now 0.01. The terms related to the vertical advection are missed due to lack of data available in the simulation

The main conclusions achieved in this paper are summarised as follows:

- An Atlantic Niño in the northern summer (JJAS) can enhance the convection in the equatorial Atlantic, altering the Walker circulation and inducing anomalous subsidence and surface divergence in the central Pacific during the period JASO (Fig. 9, **1**). As a consequence of the anomalous subsidence, anomalous easterly winds pile up the water in the western Pacific, where the thermocline becomes shallower (Fig. 9, **2**). The associated perturbation in the thermocline propagates eastward as a Kelvin wave from autumn to winter (Fig. 9, **3**) and westward as an off-equatorial Rossby wave. This result agrees with the "delayed-oscillator" theory (Suarez and Schopf 1988) and the "recharge-discharge oscillator" theory of ENSO proposed by Jin (1997a, b) and based in Cane and Zebiak (1985) and Wyrtki (1986) hypothesis: anomalous winds in the western equatorial Pacific modify the sea level high, triggering a Kelvin wave propagating eastward and impacting in the SST of the eastern Pacific. These SST anomalies reinforce the initial winds, through the Bjerknes feedback. Previous works considering this conceptual model also evidence the importance of the Atlantic Ocean in the predictability of ENSO phenomena (Frauen and Dommenget 2012).
- A heat balance analysis (in the observation and SPEEDY-RGO simulation) reveals that a shallower thermocline contributes to both processes: the advection of temperature by anomalous horizontal currents and the anomalous entrainment by mean vertical velocity, in

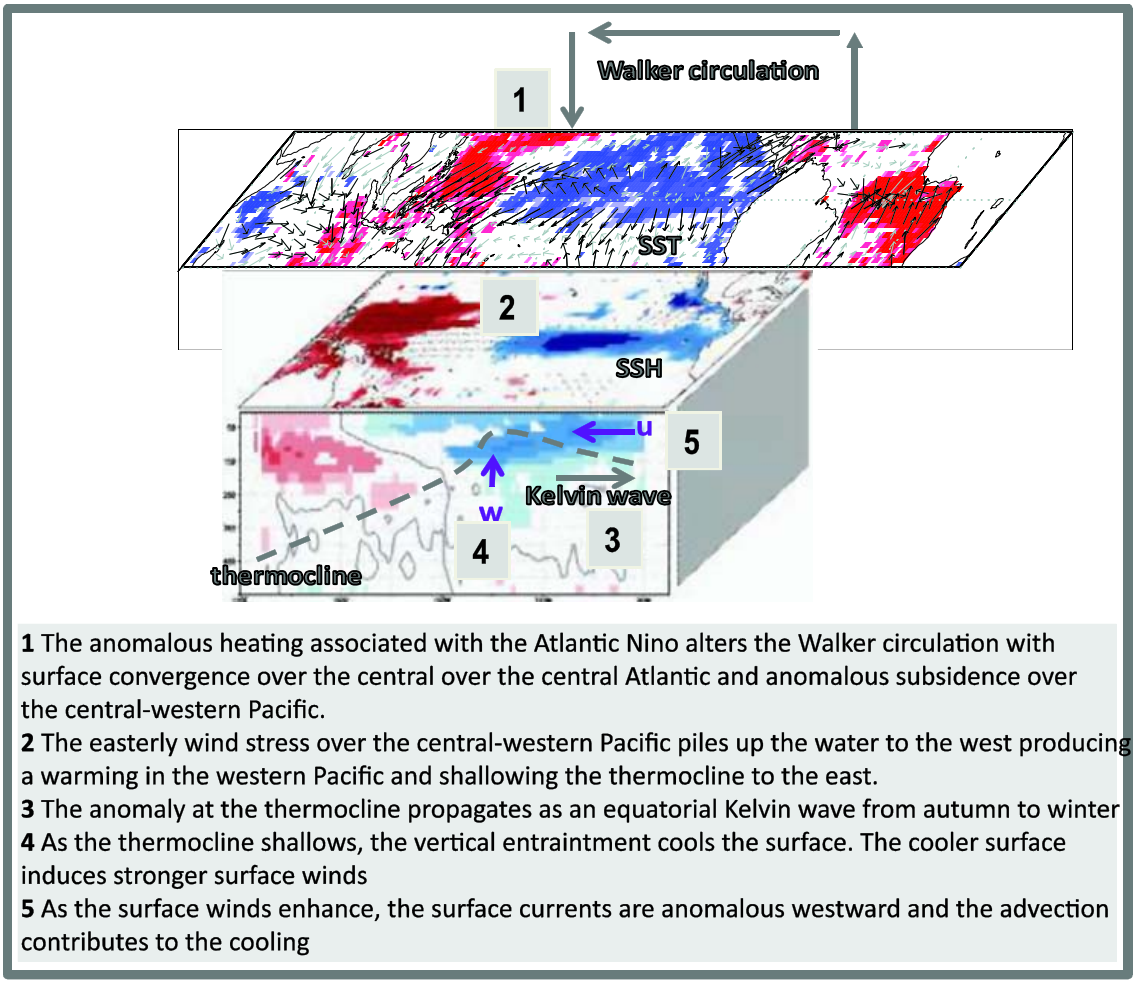

Fig. 9 Scheme of the dynamical mechanism of the Atlantic–Pacific connection for a warm phase of Atlantic Niño

agreement with previous studies (An et al. 1999; Moon et al. 2004). This result is also in agreement with Martín-Rey et al. (2012), who have shown how the model creates their own internal El Niño events but the processes at work, when no influence from the Atlantic is considered, do not alter the thermocline depth and are more thermodynamically driven.

- In the SPEEDY-RGO simulation, the dominant processes in changing the SST are seasonally dependent; (1) in summer, surface heat fluxes are the main responsible for the cooling over the south-east Pacific, (2) in autumn, the main change in SST occurs over the eastern equatorial Pacific by horizontal advection of SST by anomalous currents and vertical advection by mean vertical velocity which is the most important contribution (Fig. 9, **4**, **5**).
- As the SST cools over the eastern equatorial Pacific, the wind stress enhances (Fig. 9, **5**), establishing the Bjerknes feedback from ASON to DJFM, in which the thermocline depth, the winds and the SST are interacting in a positive way maintaining the anomalous state of the ocean.

An issue of concern in this study is the weak amplitude of the SPEEDY-RGO simulated anomalies, which are smaller than in the observations. The RGO model may be too simple to capture in depth seasonal variation in the mixed layer (Chang 1994). Ding et al. (2012) with a higher resolution model have found that amplitudes of the SST over the Pacific in relation to the equatorial Atlantic are closer to the observations. We also found better amplitudes in the SPEEDY-NEMO simulation (not shown). However, even the weak anomalies are able to trigger the feedback mechanisms. In our case, and taking into account the variability of the model, the standardised anomalies are realistic and in agreement with the observations, in a way that an anomaly of 1 standard deviation in the SST coming from the Atl3 region can impact on the anomalous D20 altering its amplitude in half standard deviation.

Although the model we use (RGO) is only of intermediate complexity, it still helps us to understand the growth and decay of La Niña associated with an Atlantic Niño. The mechanisms that we have found to be dominant for

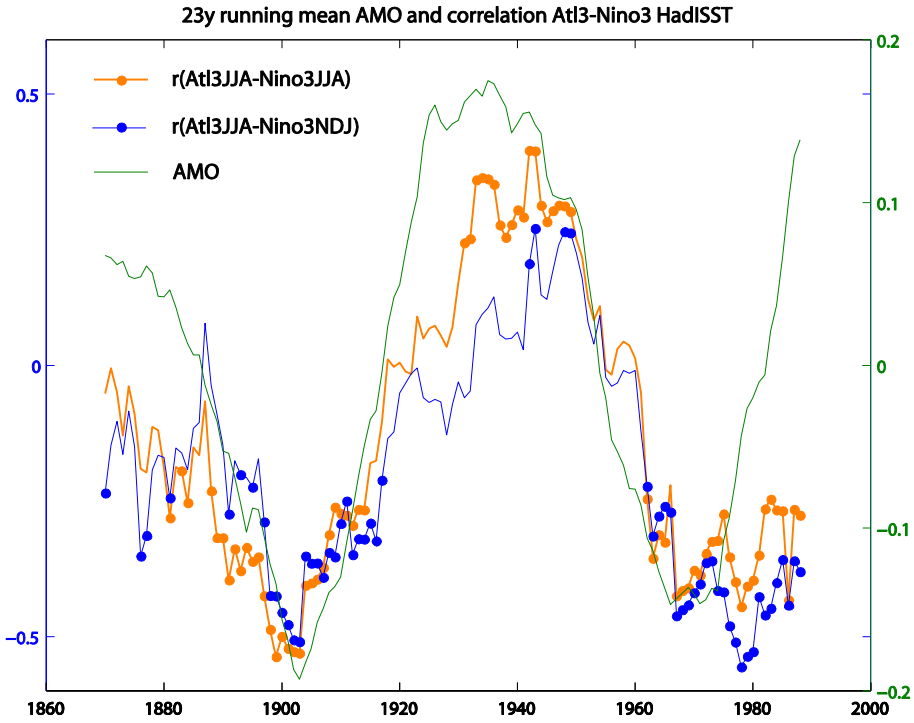

Fig. 10 Decadal modulation of the Atlantic–Pacific connection. 23-year running mean for the Atlantic multidecadal oscillation (*green line*, *right hand y-axis*, SST averaged over 0–70°N; 70°W–7°E). 23-year running correlation (*left hand y-axis*) between Atl3 index (region 20°W–0°E; 3°N–3°S) in June–July–August (JJA) and Nino3 (region 150°W–90°W; 5°N–5°S) in JJA (*orange line*) and 23-year running correlation between Atl3 JJA and Nino3 the following winter season November–December–January (NDJ) (*blue line*). *Dots* highlight the significant correlation following a Montecarlo test for 90 % confidence level

the Atlantic forced part of ENSO are consistent with the observational studies (An et al. 1999; Dewitte et al. 2009), which have reported that u′gradT and wgradT′ are the most important ENSO feedbacks from the 1970s.

In this work, we have discerned the ocean mechanism behind the development of Pacific La Niña from the Atlantic Niño forcing which was only partly suggested by RF09. However, the Atlantic is only able to explain part of the air–sea interaction in the ENSO development for a particular period, other basins as the Indian Ocean and extra-tropics could also be playing a substantial role in the ENSO growth and decay. Despite the limitations, since the analyzed simulation has the Atlantic as the only external forcing, this suggests that the Atlantic is an important key in determining the processes over the equatorial Pacific in the last three decades. This non stationarity in the Atlantic–Pacific relation deserves further and deeper investigation. Using HadSST observational data, Fig. 10 shows 23-year running correlation between Nino3 and Atl3 indexes along for the whole 20th century in order to identify possible modulations. It is shown how at the beginning of the twentieth century and after the 1970s the Atlantic and Pacific are significantly anticorrelated while in the rest of periods the correlation is positive but not statistically significant. Similar results have been found for ERSST dataset (not shown). An important feature is that the evolution of the correlation goes in phase with the Atlantic Multidecal Oscillation (Knight et al. 2006) pointing to modulations in the connection by changes in the slowly variant background SSTs. This modulation has already been shown in Losada et al. (2012) when correlating the Guinean rainfall (which is highly coupled to SSTs in the Equatorial Atlantic) and Niño3 index. Longer simulations restoring the observed SSTs over the Atlantic are needed in order to identify and corroborate the presence of internal multidecadal modulator factors. Due to the decadal and seasonal dependence of ENSO prediction skill, understanding of the multidecadal modulation of this interannual teleconnection between basins is crucial in order to improve ENSO forecast system.

Acknowledgments Irene Polo has been supported by a postdoctoral fellowship funded by the Spanish Government. This work has been also possible thanks to the Spanish Projects: Tropical Atlantic Variability and the Climate Shift (TRACS-CGL2009-10285), MOVAC and MULCLIVAR.

References

An SI (2009) A review of interdecadal changes in the nonlinearity of the El Niño–southern oscillation. Theor Appl Climatol 97:29–40. doi:10.1007/s00704-008-0071-z

An SI, Wang B (2000) Interdecadal change of the structure of the ENSO mode and its impact on the ENSO frequency. J Clim 13:2044–2055

An SI, Jin FF, Kang IS (1999) The role of zonal advection feedback in phase transition and growth of ENSO in the Cane–Zebiak model. J Meteor Soc Jpn 77:1151–1160

Anderson DLT, McCreary JP (1985) Slowly propagating disturbances in a coupled ocean–atmosphere model. J Atmos Sci 42:615–628

Ashok K, Behera SK, Rao SA, Weng H, Yamagata T (2007) El Niño Modoki and its possible teleconnection. J Geophys Res 112:C11007. doi:10.1029/2006JC003798

Barnett TP, Latif M, Kirk E, Roeckner E (1991) On ENSO physics. J Clim 5:487–515
Battisti DS, Hirst AC (1989) Interannual variability in a tropical atmosphere-ocean model: influence of the basic state, ocean geometry and nonlinearity. J Atmos Sci 46:1687–1712
Bjerknes J (1966) A possible response of the atmospheric Hadley circulation to equatorial anomalies of ocean temperature. Tellus 18:820–829
Bjerknes J (1969) Atmospheric teleconnections from the equatorial Pacific. Mon Weather Rev 97:163–172. doi:10.1175/1m520
Boschat G, Terray P, Masson S (2013) Extratropical forcing of ENSO. Geophys Res Lett 40:1605–1611
Cane MA, Zebiak SE (1985) A theory for El Niño and the southern oscillation. Science 228(4703):1085–1087. doi:10.1126/science.228.4703.1085
Cane MA, Clement AC, Kaplan A, Kushnir Y, Pozdnyakov D, Seager R, Zebiak SE, Murtugudde R (1997) Twentieth-century sea surface temperature trends. Science 275(5302):957–960. doi:10.1126/science.275.5302.957
Chang P (1994) A study of the seasonal cycle of sea surface temperature in the tropical Pacific Ocean using reduced gravity models. J Geophys Res 99:7725–7741
Chang P, Fang Y, Saravannan R, Ji L, Seidel H (2006) The cause of the fragile relationship between the Pacific El Niño and the Atlantic Niño. Nature 443:324–328. doi:10.1038/nature05053
Chelton DB, Schlax MG (1996) Global observations of oceanic Rossby waves. Science 272:234–238
Chiang JCH, Kushnir Y, Zebiak SE (2000) Interdecadal changes in the eastern Pacific ITCZ variability and its influence on the Atlantic ICTZ. Geophys Res Lett 27:3687–3690
Dayan H, Vialard J, Izumo T, Lengaigne M (2013) Does sea surface temperature outside the tropical Pacific contribute to enhanced ENSO predictability? Clim Dyn. doi:10.1007/s00382-013-1946-y
Dewitte B, Thual S, Yeh SW, An SI, Moon BK, Giese BS (2009) Low-frequency variability of temperature in the vicinity of the equatorial pacific thermocline in SODA: role of equatorial wave dynamics and ENSO asymmetry. J Clim. doi:10.1175/2009JCLI2764.1
Ding H, Keenlyside NS, Latif M (2012) Impact of the equatorial Atlantic on the El Niño southern oscillation. Clim Dyn. doi:10.1007/s00382-011-1097-y
Federov A, Philander SG (2000) Is el Niño changing? Science 288:1997–2002
Frauen C, Dommenget D (2012) Influences of the tropical Indian and Atlantic Oceans on the predictability of ENSO. Geophys Res Lett 39:L02706. doi:10.1029/2011GL050520
Galanti E, Tziperman E (2000) ENSO's phase locking to the seasonal cycle in the fast-SST, fast-wave, and mixed-mode regimes. J Atmos Sci 57:2936–2950
Giese BS, Ray S (2011) El Niño variability in simple ocean data assimilation (SODA), 1871–2008. J Geophys Res Oceans (1978–2012) 116. doi:10.1029/2010JC006695
Gu D, Philander SGH (1995) Secular changes of annual and interannual variability in the Tropics during the past century. J Clim 8:864–876
Ham YG, Kug JS, Park JY, Jin FF (2013a) Sea surface temperature in the north tropical Atlantic as a trigger for El Nino/southern oscillation events. Nat Geosci. doi:10.1038/NGEO1686
Ham YG, Kug JS, Park JY (2013b) Two distinct roles of Atlantic SSTs in ENSO variability: north tropical Atlantic SST and Atlantic Niño. Geo Res Lett 40:4012–4017
Heng X, Mechoso CR (2009a) Correlative evolutions of ENSO and the Seasonal cycle in the tropical Pacific Ocean. J Atmos Sci 66:1041–1049
Heng X, Mechoso CR (2009b) Seasonal Cycle—El Niño relationship: validation of hypotheses. J Atmos Sci 66:1633–1653
Huang B, Xue Y, Wang H, Wang W, Kumar A (2011) Mixed layer heat budget of the El Niño in NCEP climate forecast system. Clim Dyn. doi:10.1007/s00382-011-1111-4
Izumo T, Vilard J, Lengaigne M, Montegut CDB, Behera SK, Luo J-J, Cravatte S, Masson S, Yamagata Y (2010) Influence of the state of the Indian Ocean dipole of the following year's El Niño. Nat Geosci 3:168–172. doi:10.1038/ngeo760
Izumo T, Lengaigne M, Vialard J, Luo JJ, Yamagata T, Madec G (2014) Influence of Indian Ocean Dipole and Pacific recharge on following year's El Niño: interdecadal robustness. Clim Dyn 42:291–310
Jansen MF, Dommenget D, Keenlyside N (2009) Tropical atmosphere-ocean interactions in a conceptual framework. J Clim 22:550–567. doi:10.1175/2008JCLI2243.1
Jin FF (1997a) An equatorial recharge paradigm for ENSO. Part I: conceptual model. J Atmos Sci 54:811–829
Jin FF (1997b) An equatorial recharge paradigm for ENSO. Part II: a stripped-down coupled model. J Atmos Sci 54:830–847
Jin F-F, Neelin JD (1993) Modes of interannual tropical ocean–atmosphere interaction -a unified view. Part I: numerical results. J Atmos Sci 50:3477–3503
Keenlyside NS, Latif M (2007) Understanding equatorial Atlantic interannual variability. J Clim 30:131–142
Keenlyside NS, Ding H, Latif M (2013) Potential of equatorial atlantic varaibility to enhance El Nino prediction. Geophys Res Lett 40:2278–2283
Kessler WS, McPhaden MJ, Weickmann KM (1995) Forcing of intraseasonal Kelvin waves in the equatorial Pacific. J Geophys Res 100:10613–10632. doi:10.1029/95JC00382
Kleeman R, McAvaney BJ, Balgovind RC (1994) Analysis of the interannual heat flux response in an atmospheric general circulation model in the tropical Pacific. J Geophys Res 99:5539–5550
Knight JR, Folland CK, Scaife AA (2006) Climate impacts of the Atlantic multidecadal oscillation. Geophys Res Lett 33(17):L17706
Kucharski F, Bracco A, Yoo JH, Molteni F (2007) Low-frequency variability of the Indian monsoon–ENSO relationship and the tropical Atlantic: the ''weakening'' of the 1980s and 1990s. J Clim 20:4255–4266. doi:10.1175/JCLI4254.1
Kucharski F, Bracco A, Yoo JH, Molteni F (2008) Atlantic forced component of the Indian monsoon interannual variability. Geophys Res Lett 35:L04706. doi:10.1029/2007GL033037
Kucharski F, Molteni F, King MP, Farneti R, Kang I-S, Feudale L (2013) On the need of intermediate complexity general circulation models. BAMS 94:25–30. doi:10.1175/BAMS-D-11-00238.1
Losada T, Rodriguez-Fonseca B, Janicot S, Gervois S, Chauvin F, Ruti P (2009) A multimodel approach to the Atlantic equatorial mode. Impact on the West African monsoon. Clim Dyn 35:29–43. doi:10.1007/s00382-009-0625-5
Losada T, Rodriguez-Fonseca B, Polo I, Janicot S, Gervois S, Chauvin F, Ruti P (2010) Tropical response to the Atlantic equatorial mode: AGCM multimodel approach. Clim Dyn 5:45–52. doi:10.1007/s00382-009-0624-6
Losada T, Rodriguez-Fonseca B, Mohino E, Bader J, Janicot S, Mechoso CR (2012) Tropical SST and Sahel rainfall: a non-stationary relationship. Geophys Res Lett 39:L12705. doi:10.1029/2012GL052423
Luo J-J, Zhang R, Behera SK, Masumoto Y, Jin FF, Lukas R, Yamagata T (2010) Interaction between El Nino and extreme Indian ocean dipole. J Clim 23:726–742
Madec G, Delecluse P, Imbard M, Levy C (1998) OPA 8.1 general circulation model reference manual. Notes du pole de modelisation IPSL, University P. et M. Curie, B102 T15- E5, No. 11, Paris
Martín-Rey M, Polo I, Rodriguez-Fonseca B, Kucharski F (2012) Changes in the interannual variability of the tropical Pacific

as a response to an equatorial Atlantic forcing. Sci Mar 76:S1. doi:10.3989/scimar.03610.19A

Matsuno T (1966) Quasi-geostrophic motions in the equatorial area. J Meteo Soc Jpn 44:25–43

McPhaden JM, Zhang X, Hendon HH, Wheeler MC (2006) Large scale dynamics and MJO forcing of ENSO variability. Geophys Res Lett 33:L16702. doi:10.1029/2006GL026786

Mechoso CR, Robertson AW, Barth N, Davey MK, Delecluse P, Gent PR, Ineson S, Kirtman B, Latif M, Le Treut H, Nagai T, Neelin JD, Philander SGH, Polcher J, Schopf PS, Stockdale T, Suarez MJ, Terray L, Thual O, Tribbia JJ (1995) The seasonal cycle over the tropical Pacific in coupled ocean–atmosphere general circulation models. Mon Weather Rev 123:2825–2838

Mechoso C, Neelin J, Yu J-Y (2003) Testing simple models of ENSO. J Atmos Sci 60:305–318

Mo KC, Häkkinen S (2000) Interannual variability in the tropical Atlantic and linkages to the Pacific. J Clim 14:2720–2762

Moon BK, Yeh SW, Dewitte B, Jhun JG, Kang IS, Kirtman BP (2004) Vertical structure variability in the equatorial Pacific before and after the Pacific climate shift of the 1970s. Geophys Res Lett 31. doi:10.1029/2003GL018829

Münnich M, Neelin JD (2005) Seasonal influence of ENSO on the Atlantic ITCZ and equatorial South America. Geophys Res Lett 32:L21709. doi:10.1029/2005GL023900

Philander SG (1990) El Niño, La Niña, and the southern oscillation. Academic Press, San Diego. Ix. ISBN 0125532350

Picaut J, Masia F, du Penhoat Y (1997) An advective-reflective conceptual model for the oscillatory nature of the ENSO. Science 277:663–666

Polo I, Rodríguez-Fonseca B, Losada T, García-Serrano J (2008a) Tropical Atlantic variability modes (1979–2002). Part I: time-evolving SST modes related to West African rainfall. J Clim 21:6457–6475. doi:10.1175/2008JCLI2607.1

Polo I, Lazar A, Rodriguez-Fonseca B, Arnault S (2008b) Oceanic Kelvin waves and tropical Atlantic intraseasonal variability: 1. Kelvin wave characterization. J Geophys Res 113:C07009. doi:10.1029/2007JC0044951

Rayner NA, Parker DE, Horton EB, Folland CK, Alexander LV, Rowell DP, Kent EC, Kaplan A (2003) Globally complete analyses of sea surface temperature, sea ice and night marine air temperature, 1871–2000. J Geophys Res 108:4407. doi:10.1029/2002JD002670

Rodríguez-Fonseca B, Polo I, García-Serrano J, Losada T, Mohino E, Mechoso CR, Kucharski F (2009) Are Atlantic Niñosenhacing Pacific ENSO events in recent decades? Geophys Res Lett 36:L20705. doi:10.1029/2009GL040048

Ruiz-Barradas A, Carton JA, Nigam S (2000) Structure of interannual-to-decadal climate variability in the tropical Atlantic sector. J Clim 13:3285–3297

Sheinbaum J (2003) Current theories on El Niño–southern oscillation: a review. GeofísicaInternacional 42(3):291–305

Suarez MJ, Schopf PS (1988) A delayed action oscillator for ENSO. J Atmos Sci 45:3283–3287

Trenberth KE, Shea DJ (1987) On the evolution of the southern oscillation. Mon Weather Rev 115:3078–3096

Uppala SM et al (2005) The ERA-40 re-analysis. Q J R Meteorol Soc 131(612):2961–3012

Wang C (2006) An overlooked feature of tropical climate: inter-Pacific–Atlantic variability. Geophys Res Lett 33:L12702. doi:10.1029/2006GL026324

Wang W, McPhaden MJ (2001) The surface-layer heat balance in the equatorial Pacific Ocean. Part II: interannual variability. J Phys Oceanogr 30:2989–3008

Wyrtki K (1975) El Niño—the dynamic response of the equatorial Pacific Oceanto atmospheric forcing. J Phys Oceanogr 5:572–584

Wyrtki K (1986) Water displacements in the Pacific and the genesis of El Niño cycles. J Geophys Res 91:7129–7132

Yu J-Y, Mechoso CR, McWilliams JC, Arakawa A (2002) Impacts of the Indian Ocean on the ENSO cycle. Geophys Res Lett 29:46-1–46-4

Yu L, Jin X, Weller RA (2008) Multidecade global flux datasets from the objectively analyzed air–sea fluxes (OAFlux) project: latent and sensible heat fluxes, ocean evaporation, and related surface meteorological variables. WHOI technical report (OA-2008-01). http://oaflux.whoi.edu/

Zebiak SE (1993) Air–sea interaction in the equatorial Atlantic region. J Clim 6:1567–1586

Zebiak SE, Cane MA (1987) A model El Niño–southern oscillation. Mon Weather Rev 115:2262–2278. doi:10.1175/15200493(1987)

6.3. Study of the non-stationary behaviour of the Atlantic Niño influence on the tropical Pacific variability and its possible multidecadal modulation.

(Martín-Rey et al. 2014)

In this section, the connection between the inter-annual variability of the tropical Atlantic and Pacific Oceans has been investigated along the 20th century. These results are in the framework of the Objective 2 of the present thesis.

Observations and partially coupled simulations indicate that the Atlantic-Pacific connection appears as the leading air-sea coupled mode of tropical variability for the period 1870-2002. Nevertheless, the running correlation between the expansion coefficients of the tropical Atlantic SSTs and the Pacific variables put forward that the impact of the Atlantic on ENSO is non-stationary, since the air-sea coupled mode only shows up during the first decades of the 20th century and after the 1970s. These periods coincide with negative phases of the Atlantic Multidecadal Oscillation (AMO), suggesting the possible contribution of this large-scale pattern in the modulation of the Atlantic-Pacific connection.

Under negative AMO phases, the atmospheric divergence in upper levels over the western equatorial Atlantic is enhanced, at the same time that the eastern Pacific SST variability increases. These multidecadal changes in the Atlantic and Pacific mean states could favour the establishment of the connection between the inter-annual variability of both tropical basins.

Clim Dyn
DOI 10.1007/s00382-014-2305-3

On the Atlantic–Pacific Niños connection: a multidecadal modulated mode

Marta Martín-Rey · Belén Rodríguez-Fonseca · Irene Polo · Fred Kucharski

Received: 27 January 2014 / Accepted: 16 August 2014

Abstract Atlantic and Pacific El Niño are the leading tropical oceanic variability phenomena at interannual timescales. Recent studies have demonstrated how the Atlantic Niño is able to influence on the dynamical processes triggering the development of the Pacific La Niña and vice versa. However, the stationarity of this interbasin connection is still controversial. Here we show for the first time that the Atlantic–Pacific Niños connection takes place at particular decades, coinciding with negative phases of the Atlantic Multidecadal Oscillation (AMO). During these decades, the Atlantic–Pacific connection appears as the leading coupled covariability mode between Tropical Atlantic and Pacific interannual variability. The mode is defined by a predictor field, the summer Atlantic Sea Surface Temperature (SST), and a set of predictand fields which represent a chain of atmospheric and oceanic mechanisms to generate the Pacific El Niño phenomenon: alteration of the Walker circulation, surface winds in western Pacific, oceanic Kelvin wave propagating eastward and impacting on the eastern thermocline and changes in the Pacific SST by internal Bjerknes feedback. We suggest that the multidecadal component of the Atlantic acts as a switch for El Niño prediction during certain decades, putting forward the AMO as the modulator, acting through changes in the equatorial Atlantic convection and the equatorial Pacific SST variability. These results could have a major relevance for the decadal prediction systems.

Keywords ENSO · Atlantic · Pacific · Prediction · Tropical variability · Atlantic Multidecadal Oscillation · Sea surface temperature

1 Introduction

El Niño-Southern Oscillation (ENSO) is the leading mode of interannual variability in the Tropical Pacific Ocean with

This paper is a contribution to the special issue ontropical Atlantic variability and coupled model climate biases thathave been the focus of the recently completed Tropical Atlantic Climate Experiment (TACE), an international CLIVAR program (http://www.clivar.org/organization/atlantic/tace). This special issue iscoordinated by William Johns, Peter Brandt, and Ping Chang,representatives of the TACE Observations and TACE Modeling andSynthesis working groups.

M. Martín-Rey · B. Rodríguez-Fonseca
Instituto de Geociencias, IGEO, Centro Mixto UCM-CSIC, Madrid, Spain

M. Martín-Rey (✉) · B. Rodríguez-Fonseca
Departamento de Física de la Tierra, Astronomía y Astrofísica I (Geofísica y Meteorología), 4 planta, Facultad de C.C. Físicas, UCM, Pza de las Ciencias, Av/Complutense, 28040 Madrid, Spain
e-mail: mmartindelrey@fis.ucm.es

I. Polo
NCAS-Climate, Department of Meteorology, University of Reading, Earley Gate, PO Box 243, Reading RG6 6BB, UK

F. Kucharski
The Abdus Salam International Centre for Theoretical Physics, ICTP, Trieste, Italy

F. Kucharski
Department of Meteorology, Center of Excellence for Climate Change Research, King Abdulaziz University, Jeddah, Saudi Arabia

Published online: 31 August 2014

worldwide impacts (Philander 1990; Bjerknes 1969). An analogous air-sea coupled mode takes place in the Tropical Atlantic basin, named as Equatorial Mode, zonal mode or Atlantic Niño (Zebiak 1993). These modes peak in different seasons, winter and summer respectively. Previous studies have demonstrated the connection between the interannual variability of the Atlantic and Pacific basins. Some authors have suggested the leadership of the Pacific Ocean, modifying the tropical Atlantic variability through Walker circulation or wave trains emanating from the equatorial Pacific (Saravanan and Chang 2000; Sutton et al. 2000; Huang et al. 2002; Münnich and Neelin 2005; Handoh et al. 2006a, b). On the other hand, the Atlantic Ocean also seems to influence the Tropical Pacific variability through an atmospheric bridge (Keenlyside and Latif 2007; Polo et al. 2008; Rodríguez-Fonseca et al. 2009; Wang et al. 2010; Kayano et al. 2011; Ding et al. 2012; Martín-Rey et al. 2012; Ham et al. 2013; Polo et al. 2014). Furthermore, Indian Ocean is also proposed as a precursor of ENSO development through changes in the winds over the western equatorial Pacific (Annamalai et al. 2005; Terray and Dominiak 2005; Kug and Kang 2006; Izumo et al. 2010; Luo et al. 2010). Additionally, the contribution of extratropical regions to ENSO prediction has also been analysed (Terray 2011; Boschat et al. 2013; Dayan et al. 2013).

Regarding the tropical Pacific response to Atlantic SST, observational results and partially-coupled simulations, in which the observed Atlantic Sea Surface Temperature (SST) is the only external forcing, show that a summer Atlantic Niño (Niña) precedes the development of a Pacific La Niña (El Niño) during the boreal winter after the late 1960s (Rodríguez-Fonseca et al. 2009). For an Atlantic warm (cold) event, an alteration of the Walker circulation with anomalous ascending branch (descending motions) over the Atlantic and anomalous subsidence (ascending motions) over the Pacific is proposed as the atmospheric bridge connecting both basins. Sensitivity experiments with atmospheric general circulation models (AGCMs) and fully coupled general circulation models have confirmed this hypothesis (Losada et al. 2010; Ding et al. 2012 respectively).

More recently, using the simulated Pacific outputs of a partially coupled run with prescribed SSTs in the Atlantic, Martín-Rey et al. (2012) have demonstrated the existence of a leading SST variability mode in the Tropical Pacific in winter, which is forced by the equatorial Atlantic anomalous SSTs during the previous summer. This mode, which appears from the 1970s, coincides with the Pacific pattern associated with the Atlantic–Pacific Niños connection. In turn, its development is related to dynamical processes triggered by the Atlantic and in which the thermocline feedbacks are enhanced. Moreover, the ENSO events, which are not modulated by the Atlantic, appear to be more associated with thermodynamical processes.

A conceptual dynamical scheme of the Atlantic–Pacific connection is very important for its correct modelling and, thus, its correct prediction. For this reason, the oceanic mechanisms at work in the Tropical Pacific associated with the Atlantic influence, have been recently investigated by Polo et al. (2014). According to the former authors, for an Atlantic Niño (Niña) the Walker circulation is altered linking both basins. The subsidence (ascending motions) over the Pacific creates surface wind divergence (convergence) around the dateline, strengthening (weakening) the trades to the west, in the warm pool region, and shallowing (deepening) the thermocline east of the divergence (convergence). This perturbation propagates to the east as a Kelvin wave, following the Gill-Matsuno mechanism (Matsuno 1966; Gill 1980; Suarez and Schopf 1988), favouring (inhibiting) the vertical entrainment and cooling (warming) the sea surface. Finally, the Bjerknes feedback is established intensifying the westward (eastward) currents and maintaining the cooling (warming) in the eastern equatorial Pacific (Bjerknes 1969).

Several recent studies have put forward the importance of the Atlantic for the correct ENSO forecast (Frauen and Dommenget 2012; Dayan et al. 2013; Boschat et al. 2013; Keenlyside et al. 2013). Furthermore, the Atlantic–Pacific connection involves changes in the global climate variability since, in summer, both basins act together to modify the climate teleconnections (Losada et al. 2010, 2012; Rodríguez-Fonseca et al. 2011; Mohino et al. 2011).

Nevertheless, although some authors have indicated that this relation is stationary on time (Ding et al. 2012), other studies have only found the link after the 1970s (Rodríguez-Fonseca et al. 2009; Martín-Rey et al. 2012). This absence of stationarity has been observed using the summer Atl3 [20°W–0°; 3°N–3°S] and winter Niño3 [150°W–90°W; 5°N–5°S] indices for the whole twentieth century, showing high correlation scores during the first and last decades of the twentieth century (Polo et al. 2014). Also, Guinean rainfall variability, which is highly coupled with the Atlantic Niño, is related to ENSO phenomena only at the beginning and end of the twentieth century (Joly and Voldoire 2010; Losada et al. 2012). These decades coincide with negative phases of the Atlantic Multidecadal Oscillation (AMO, Delworth and Mann 2000; Knight et al. 2006), suggesting the possible role of this decadal variability pattern in triggering the connection (Polo et al. 2014).

The influence of the AMO-like pattern on the Pacific mean state and variability has been already documented using General Circulation Models (GCMs, Dong et al. 2006; Fang et al. 2008; Hong et al. 2013). Furthermore, the Atlantic Ocean response from a substantial change in the Atlantic Meridional Overturning Circulation (AMOC) has also been investigated. In this way, from a weakening of the AMOC, a negative AMO-like SST pattern in the Atlantic appears together with changes in the tropical variability

(Dong and Sutton 2007; Timmermann et al. 2007; Haarsma et al. 2008; Polo et al. 2013). Negative SST anomalies in the North Atlantic associated with a negative phase of the AMO seem to alter the large-scale tropical atmospheric circulation, changing the basic state in the tropical Pacific Ocean. This change is associated with a shallower thermocline depth and activates the thermocline and upwelling feedbacks, increasing ENSO variability (Federov and Philander 2000; An and Jin 2001; Dong and Sutton 2007). Similar analyses of the influence of a weakening of the AMOC onto the Atlantic basin have revealed a mean deepened equatorial thermocline, which leads to a decreasing in the Atlantic Niño variance (Haarsma et al. 2008; Polo et al. 2013). Additionally, the enhancement of the ENSO teleconnection onto the tropical Atlantic increases the tropical Atlantic variability in spring (Polo et al. 2013). Conversely, other recent study considering a weakening of the AMOC shows changes in the Atlantic mean state but not in the Pacific background state, which increases the Atlantic equatorial variability during summer months, strengthening the Atlantic–Pacific connection (Svendsen et al. 2013). Thus, it is not clear how the changes in the tropical basins are connected in the real world.

Taking into account the current state of the discussion, we pose the following questions: Is the Atlantic–Pacific connection a mode of variability? If so, is this mode modulated at multidecadal timescales?

In case of finding positive answers, opportunity windows for the correct prediction of ENSO will be opened, enhancing the importance of the correct simulation of the tropical Atlantic climate variability (Richter and Xie 2008, Richter et al. 2012; Wahl et al. 2011; Toniazzo and Woolnough 2013; Voldoire et al. 2014).

Therefore, the aim of this study is to test if this Atlantic–Pacific connection is an internal mode of climate variability within the tropical regions, and to shed light on when does this pattern take place and how this connection appears or not modulated at multidecadal time scales.

The present study is divided in five sections. Section 2 describes the data and the methodology used in this study. The main results are presented in Sect. 3. In Sect. 3.1 we identify the coupled variability modes between the Tropical Atlantic and Pacific. In Sect. 3.2, the Atlantic influence on the coupled mode is investigated. Finally, the discussion and conclusions are displayed in Sects. 4 and 5 respectively.

2 Data and methodology

2.1 Observations and reanalysis

The observed tropical Pacific SST, wind stress and thermocline depth come from SODA reanalysis (Giese and Ray 2011). The 20 °C isotherm depth has been considered as a proxy for the thermocline depth (z20). We have also used the observed tropical Atlantic SST from HadISST dataset (Rayner et al. 2003). The velocity potential at 200 and 950 hPa (hereafter, chi200 and chi950) has been calculated from the zonal and meridional wind obtained from twentieth century reanalysis (Compo et al. 2011) using the Laplace equation, $\nabla^2\Phi = 0$ where Φ is the velocity potential and verifies $\mathrm{u} = \frac{\partial \Phi}{\partial \mathrm{x}}$ and $\mathrm{v} = \frac{\partial \Phi}{\partial \mathrm{y}}$ being u and v the zonal and meridional components of the surface wind. The period of study goes from 1871 to 2002. Questions about the reliability of the data during the first decades of the twentieth century remains a caveat. In early years, the observed SST is very sparse since the majority of the measures come from ships, which changed their commercial shipping routes along the time. North Atlantic, western South Atlantic and North Indian Oceans are the regions with more density of measures. Nevertheless, the spatial coverage of tropical Atlantic and Pacific data is completed around the 1960s (Deser et al. 2010). SST data comes from million of observations which have been carefully checked in order to generate corrected datasets. However, corrections prior to about 1900 are less well known because of uncertainties in the mix of wooden and canvas buckets. Nevertheless, even in the 1870s, SST was little biased relative to land-surface air temperatures globally. Since 1941, observations mainly come from ship engine intake measurements, better insulated buckets and, latterly, from buoys (IPCC WG1). Therefore, SST data should be regarded as more reliable, also useful for projections at multi-decadal time-scales.

In particular, in the present study we have used Tropical Atlantic SST from HadISST dataset, which are based on in situ observations and extend the data to more sparse oceanic regions applying reduced space optimal interpolation (RSOI, Kaplan et al. 1997) which uses EOF technique (Rayner et al. 2003).

Also, SST data from version 2.2.4 of SODA reanalysis has been used for Pacific basin. This reanalysis considers for the boundary conditions and for the variables in the bulk formula, a new data set designed as 20CRv2 (Whitaker et al. 2004; Compo et al. 2006, 2008), hydrographic profiles from de Boyer et al. (2009) and SST observations from ICOADS (Woodruff et al. 2011). The variability of ENSO is well reproduced in the reanalysis although with stronger amplitude (Giese and Ray 2011).

2.2 Modelled data

The model used is SPEEDY model (Molteni 2003; Kucharski et al. 2006) coupled to an extended 1.5-layer reduced-gravity model (Kucharski et al. 2008; Chang 1994) and the simulations are the same as in previous studies (Rodríguez-Fonseca

et al. 2009; Martín-Rey et al. 2012; Polo et al. 2014) but extended from 1871 to 2002. The simulations consider the observed Atlantic SSTs (HadISSTs between 60°N and 60°S) as the only external forcing and they are fully coupled in the tropical Indo-Pacific region [30°N–30°S], with climatological SST elsewhere being named as *SimAtlVar*. For the comparison analysis, the oceanic and atmospheric variables previously mentioned for observations and reanalysis are considered, being also the period of study 1871–2002.

2.3 Seasonal cycle and variability of the equatorial Pacific SST

Both, modelled and observed seasonal cycle of the equatorial Pacific SST are characterized by the development of a cold tongue in the eastern basin during summer months (June-October), peaking in July–August for the whole period 1871–2002 (Fig. 1a, b). Despite of the lower amplitude of the simulated SST, a good agreement between model and observations is shown in the offshore eastern equatorial Pacific (140°–80°W) during this peak. Nevertheless, *SimAtlVar* presents an alteration of the seasonal cycle in comparison with the observations in the central-eastern part of the basin (Fig. 1b). Figure 1c presents the difference between the observed and modelled seasonal cycle, which reveals the typical SST bias present in most climate models characterized by warmer SST anomalies in the central-east and cooler ones in the west Pacific from August to December (Fig. 1c; Davey et al. 2002). The bias shows the opposite sign that the observed seasonal cycle, indicating how the observed seasonal cycle is damped in the simulation. An interesting feature is the lower changes between modelled and observed SST in the region 180°E–100°W in July (Fig. 1c), suggesting the reduction of the bias in this region during the peak of the cold tongue.

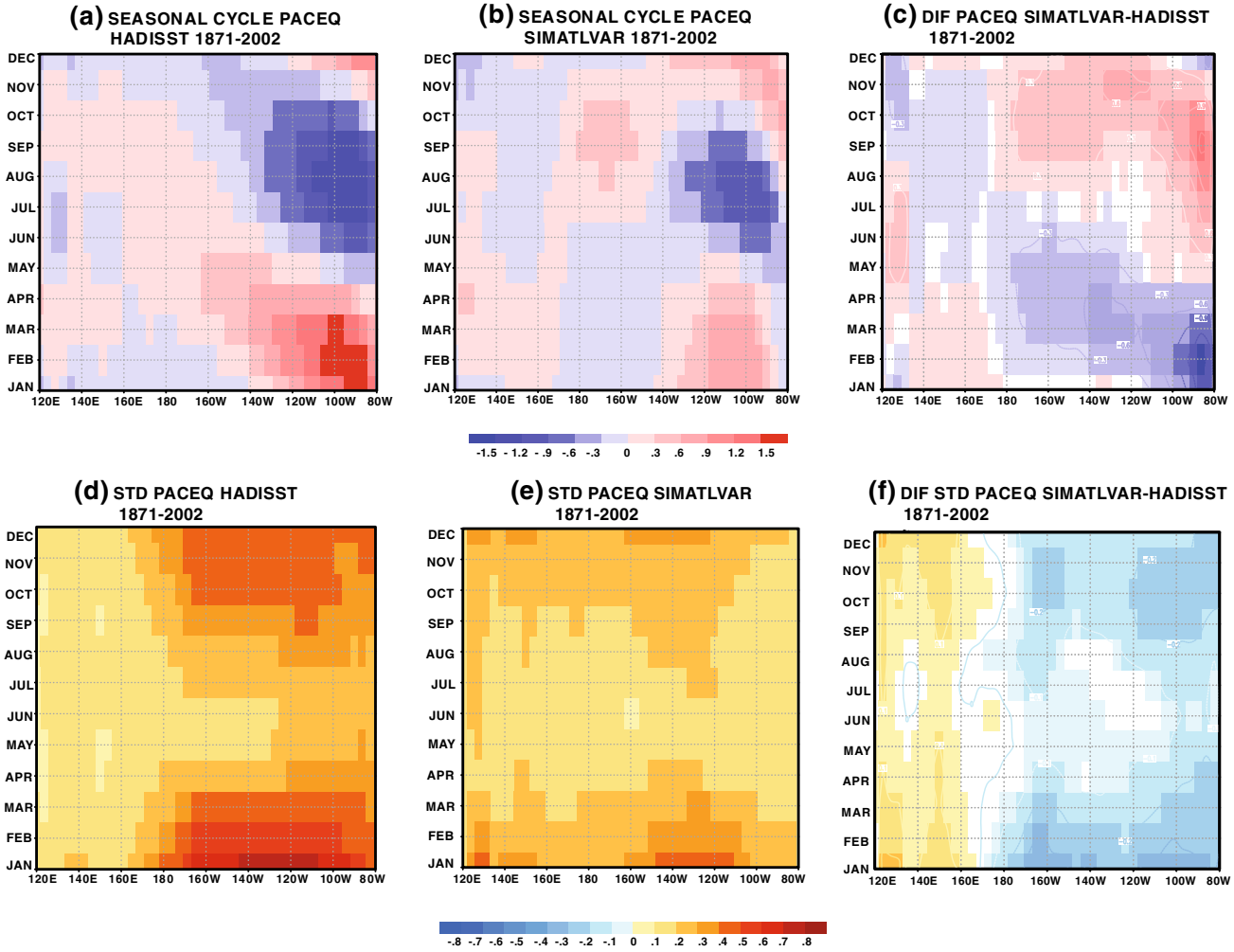

Fig. 1 Seasonal cycle and standard deviation of the equatorial Pacific SST for HadISST and SIMATLVAR from 1871 to 2002. **a**, **b**, **d**, **e** Seasonal cycle and standard deviation of the equatorial Pacific SST for observations (HadISST) and model simulations (*SimAtlVar*). The monthly means (in °C) have been detrended. **c**, **f** Difference between the simulated and observed seasonal cycle and standard deviation of the equatorial Pacific SST. A test of equal means/variances has been applied and the values exceeding 90 % confidence level are shown

Regarding variability, maximum values are located in the eastern equatorial Pacific (180°–100°W) for observations and model simulations during boreal autumn–winter (October to March, Fig. 1d, e). However, *SimAtlVar* also shows higher variability in western equatorial Pacific (120°–160°E) along the year, peaking in late boreal autumn and winter (Fig. 1e). Despite the lower amplitude, the model is able to capture the basic changes in the observed variability in the equatorial Pacific SST. Figure 1f indicates how the bias in variability is reduced in the western equatorial Pacific (west of the dateline) for the whole year. The results suggest that the simulation considering only the external Atlantic influence presents a reduction in the bias during the summer and also in its variability in the western Pacific along the whole year.

Thus, the next step is to compute for both models and observations, the Tropical Atlantic variability modes and study if these modes exert influences on the Pacific together with their associated modulations. The methodology is explained in the next section.

2.4 Methodology

Seasonal anomalies of 4-consecutive months, from January–February–March–April (JFMA) to December-January–February–March (DJFM), are computed subtracting the seasonal cycle of the total period of study. An interannual filter is applied in order to isolate the interannual variations from the low frequency ones (Bjerknes 1964; Stephenson et al. 2000). The filter consists in calculating the difference between two consecutive years, highlighting in this way the high frequency signal of the field.

Maximum Covariance Analysis (MCA) is used as the statistical discriminant analysis methodology to calculate the principal directions of maximum covariance between the predictor (SSTs) and the variables to predict (Bretherton et al. 1992; Cherry 1997). MCA considers two fields, X and Y, named as predictor and predictand field respectively, and applies a Singular Value Decomposition (SVD) to the covariance matrix. SVD calculates linear combinations of the time series of X and Y (named as expansion coefficients, hereinafter U and V) that maximize the covariance among them. U and V are computed by the diagonalization of the covariance matrix $C = X \times Y^T$ by SVD. The singular vectors R and Q are the resultant eigenvectors from the diagonalization, which are the spatial configurations of the main mode of covariability. The associated loadings on the time domain are the expansion coefficients U and V respectively. Finally, the eigenvalues are a measure of the percentage of variance explained by each mode. The percentage of explained covariance for each mode k is given by the square covariance fraction, calculated as a function of the eigenvalues. Additionally, to evaluate how much the expansion coefficients U and V are related to each other, we calculate the correlation coefficient for each mode.

In the meteorological context, the two matrices associated to the predictand and predictor fields (X and Y respectively) are dimensioned in the time (n_t) and space domain (n_x and n_y for X and Y respectively), although the spatial domain can be more complex depending on the needs, as it is the case of the present study. In this case, the study involves atmospheric and oceanic mechanisms in which more than two variables are connected. In particular, we want to analyse the Atlantic influence on the Pacific variability, in which, as indicated by a set of papers (Polo et al. 2008; Rodríguez-Fonseca et al. 2009; Ding et al. 2012; Martín-Rey et al. 2012; Ham et al. 2013) the summer Tropical Atlantic SST appears as the predictor field. As proposed by Polo et al. (2014), this predictor connects both basins through changes in the Walker circulation, impacting on tropical Pacific wind stress, thermocline depth and SST through an atmospheric bridge. For this reason, we consider that the predictand field X includes, in one matrix, all the fields involved in the connection, which in turn act at different lags. Thus, the MCA is applied using multiple lags and variables, so we have named it as Extended Multiple Maximum Covariance Analysis (hereafter EMMCA). The variables involved in the interbasin connection are Tropical Atlantic SSTs in summer (JJAS) as predictor field and the following predictand fields: Tropical velocity potential fields at the surface (925 or 950 hPa) and upper levels (200 hPa) in summer and winter months (JJAS–DJFM), tropical Pacific wind stress in summer (JASO), thermocline depth from summer to winter (JASO–SOND–DJFM) and Tropical Pacific SST in winter (DJFM).

A scheme of the EMMCA calculation is presented in Fig. 2, as a mix of the methodologies exposed in Polo et al. (2005) in which multiple variables are included in the analysis and Polo et al. (2008) in which multiple predictors are included in the analysis. Nevertheless, in this work, we just include one variable as predictor field and multiple lags (similar to García-Serrano et al. 2008) and variables as predictand ones. Thus, the X matrix is the predictor and has (n_x,n_t) dimensions, but the Y matrix has dimensions (n_y^{vdl}, n_t) where *vdl* indicate the specific combinations of variables (v), lags (l) and spatial domains (d) for all the variables to predict, all having the same time length, in agreement with the mechanism described in Polo et al. (2014).

Once EMMCA is applied, the spatial and temporal patterns for the individual Pacific variables are obtained projecting the original predictand matrix Y for the variable i, $Y(n_y^i, n_t)$ over the total expansion coefficient U_k obtained as outputs of the EMMCA:

$$r_i = U_k * Y\left(n_y^i, n_t\right)^T \quad (1)$$

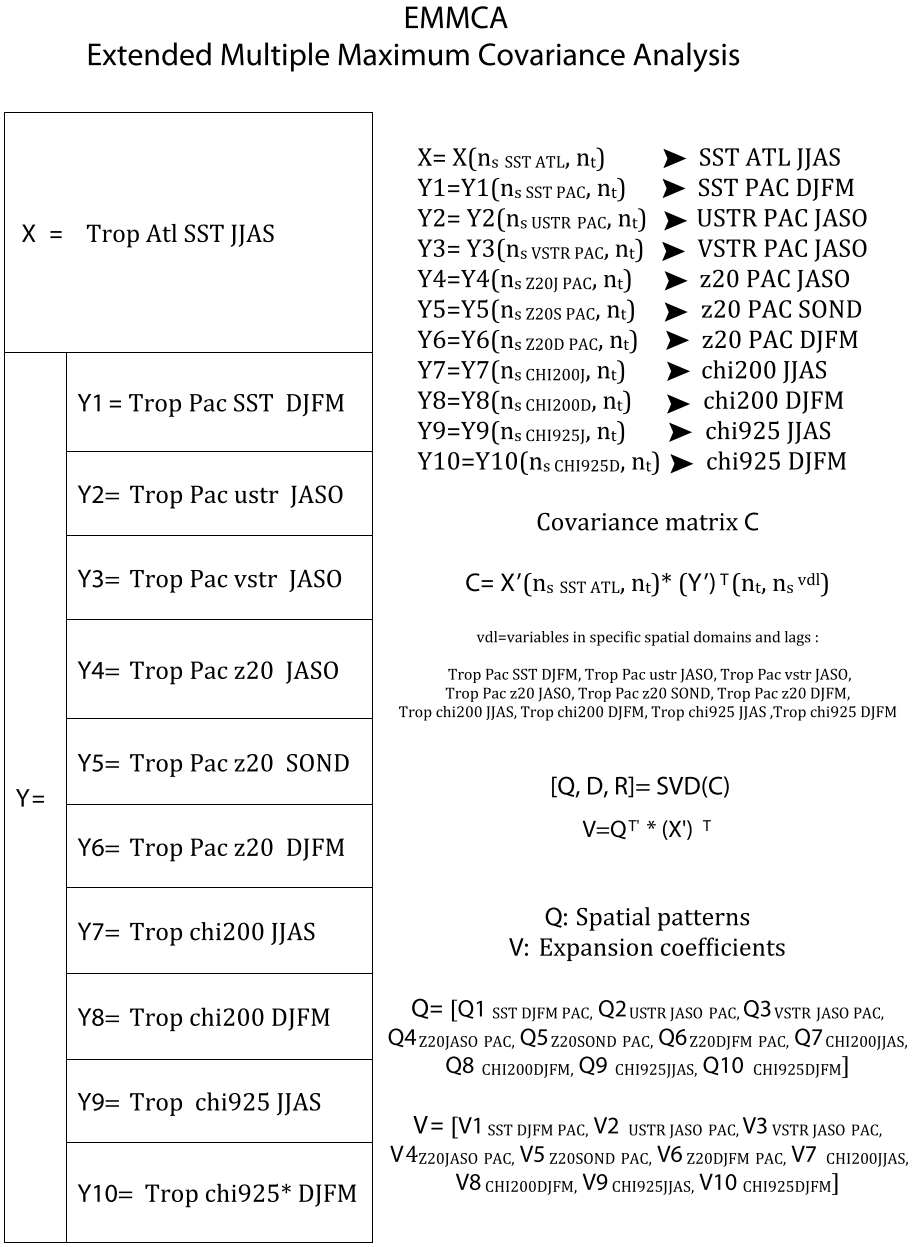

Fig. 2 Schematic of the EMMCA applied in the present study. (*Left*) Scheme of the arrays for the predictor (*X*) and the set of predictand fields (*Y*) used in the Extended Multiple Maximum Covariance analysis (EMMCA). (*Right*) Description of the different variables considered as predictor (summer Tropical Atlantic SST) and predictand fields (tropical velocity potential, Pacific wind stress, thermocline depth and SST) in specific lags and the methodology of the EMMCA

The robustness of the results is assessed by applying a Monte Carlo test. It is a non-parametric test, which consists in permuting the initial time series to create a random distribution of the sample. The results are compared with those obtaining by chance and significant values that exceed 90 % confidence level are shown in this paper. We have also used a parametric test, F-test, which considers the equality of variances as the null hypothesis. Significant values at 90 % confidence level are also shown.

In the next section, the results obtained when EMMCA is applied are described for both model and observations. Notice that a simple correlation of the Atl3 index onto the variables would lead to similar results, although with lower correlation scores, especially in the observations (not shown). However, the EMMCA methodology allows us to express the pattern as a robust climate coupled covariability mode and to perform a Niño3 hindcast from the output parameters in order to assess the predictability of the ENSO from the equatorial Atlantic SST (see later in the results).

3 Results

3.1 Identification of the leading covariability mode and analysis of its stationarity

Firstly, the whole available time period of data (1871–2002) is considered in the EMMCA analysis. The leading

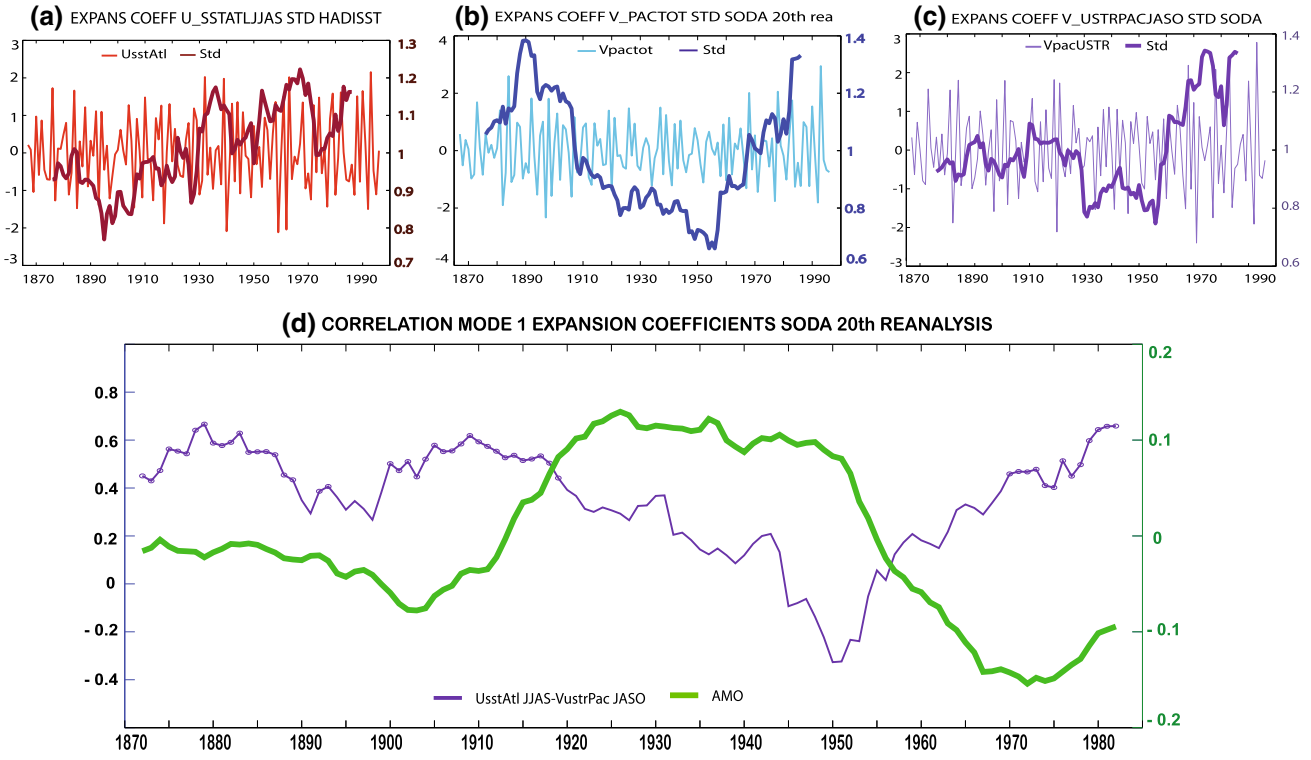

Fig. 3 Expansion coefficients of the leading mode of interannual variability from observations for the period 1872–2001. **a**–**c** Expansion coefficients and their 20-year running standard deviation (*thick line*) of the leading mode obtained applying the EMMCA to the total period 1872–2001 for the predictor field, the summer (JJAS) tropical Atlantic SSTs, the set of the predictand fields and the tropical Pacific zonal wind in summer (JASO). **d** Running correlation in 20-year windows between the expansion coefficient of the predictor and the expansion coefficient of the Pacific zonal wind stress (*purple line*). The statistical significant correlation exceeding 90 % confidence level, according to a Monte Carlo test, is presented in *dots*. The 20-year running mean of the Atlantic Multidecadal Oscillation index is also presented (*green line*)

covariability mode explains 35.2 % of the total variance and shows the link between the Tropical Atlantic and Pacific interannual variability, in particular summer Atlantic Niño (Niña) and a winter Pacific Niña (Niño). The results show how the summer Atlantic Niño appears associated with an alteration of the Walker circulation, with ascending branch over the Atlantic and descending motions over the central Pacific in relation to an Atlantic warming, creating surface wind divergence in summer months over this Pacific region (not shown). The evolution of the z20 suggests that the anomalous surface wind could trigger an oceanic Kelvin wave propagating eastward and impacting on the Pacific SST in winter months, according to the mechanism proposed by Polo et al. (2014).

The existence of this mode and the relation found between the predictand variables and the predictor could be indicating the presence of the Atlantic–Pacific connection (Rodríguez-Fonseca et al. 2009) during the whole century and, thus, a stationary behaviour. Nevertheless, it has been found how the amplitude of the standardized expansion coefficients varies on time, indicating the different loading amplitudes of the mode in some decades than in the others (Fig. 3). In particular, the variability of the expansion coefficient (thick line) for tropical Atlantic SST seems to be modulated by a positive decadal trend that could be associated with the global warming (Fig. 3a; Kucharski et al. 2011). Nevertheless, the expansion coefficient for the set of Pacific variables involved in the mode shows a multidecadal modulation with higher loadings during the first decades of the twentieth century and after the 1970s (Fig. 3b).

Additionally, the 20-year running correlation between the expansion coefficients for the summer Atlantic SST and the predictand fields also exhibits a multidecadal modulation with significant correlations at the beginning and end of the twentieth century (not shown). In particular, the moving correlation in 20-year windows is presented for the summer Atlantic SST and zonal Pacific wind stress expansion coefficient in Fig. 3d. Significant correlation seems to occur under negative phases of the Atlantic Multidecadal Oscillation (AMO), suggesting the non-stationary behaviour of the interbasin connection. The correlation score between AMO and running correlation curve, in Fig. 3d, reaches −0.52.

To corroborate the possible non-stationarity of the mode, the EMMCA analysis has been computed separately for periods associated with positive (1934–1969) and negative (1871–1933 and 1970–2001) phases of the AMO (Fig. 4a–r).

The results reveal how the Atlantic Niño–Pacific Niña mode (and vice versa, Fig. 4a–f, m–r) appears as the leading coupled covariability mode at the beginning and end of the twentieth century (explaining the 36.84 and 36.79 % of the total variance), but not in the decades in-between (Fig. 4g–l). Thus, for negative phases of the AMO, when the connection takes place, the Atlantic SST anomalies (Fig. 4a, m) cover the entire tropical basin [20°N–20°S, 70°W–20°E], enhancing the deep convection over the equatorial Atlantic (Fig. 4b, n), modifying the Walker circulation and impacting on the Pacific Ocean during summer season (Fig. 4b, c, n, o). The anomalous surface wind divergence peaks in the central Pacific (160°–120°W), shallowing the thermocline depth and triggering the Kelvin wave which impacts on the SST during winter months (Fig. 4d–f, p–r), according to the mechanism proposed by Polo et al. (2014). A Pacific La Niña-like pattern is completely developed in DJFM (Fig. 4f, r) and it is associated with a see-saw pattern in the velocity potential field (not shown).

However, for the period 1934–1969 and coinciding with a positive AMO phase, an Atlantic Niño appears associated with no defined SST pattern in the Tropical Pacific basin (34.06 % of the total variance, Fig. 4g–l). Also, the associated Atlantic Niño presents a different spatial configuration, with positive anomalies in the eastern side and negative ones in the subtropical South Atlantic (Fig. 4g). The change in the spatial structure of this mode, as well as, in its impacts, has also been documented in previous studies (Losada et al. 2010, 2012; Mohino et al. 2011). Nevertheless, during the positive AMO years, the Atlantic Niño does not appear associated with Walker circulation changes and interbasin atmospheric teleconnections. Although an atmospheric response to the equatorial warming is observed over the Atlantic, it does not modify the atmospheric circulation over the Pacific region (Fig. 4h). Significant wind convergence is presented at surface levels but it is independent of Atlantic forcing and is not able to impact on the winter Pacific SST (Fig. 4h, l).

3.2 The Atlantic influence in the Pacific variability

In this section, the real influence of the Atlantic on this mode is checked by repeating the analysis of Sect. 3.1 with the simulated data obtained when prescribing the observed SST over the Atlantic and coupling the Indo-Pacific basin.

To evaluate the Atlantic contribution to ENSO development, the EMMCA has also been performed for model simulations, *SimAtlVar,* considering the observed Atlantic SST as the only external forcing (Rodríguez-Fonseca et al. 2009; Martín-Rey et al. 2012). Model results reproduce the leading Atlantic–Pacific mode, explaining 26.52 % of the total variance, for the entire period 1871–2002 and the multidecadal modulation of the amplitude of the expansion coefficients (Fig. 5). The running correlation between the expansion coefficients of the predictor and predictand fields presents higher values at the beginning and end of the twentieth century (not shown). Indeed, the correlation between summer Atlantic SST and zonal Pacific wind stress suffers a sharp decrease during the 1910s–1940s from correlation scores of 0.8–0.2 suggesting the weakening of the Atlantic–Pacific mode in this period (Fig. 5d).

Validation of the model EMMCA shows that almost all expansion coefficients are significantly similar than the observational ones, with significant correlation scores of 0.97 and 0.33 between the expansion coefficients for the Tropical Atlantic SSTs and total Tropical Pacific variables respectively.

The correlation maps show the Atlantic–Pacific mode during the first and last decades of the twentieth century (explaining 29.68 and 29.82 % of the total variance, respectively), giving robustness to the observational finding (Fig. 6a–r vs Fig. 4a–r). Our model results confirm the alteration of the Walker circulation as a response of an Atlantic Niño (Niña) during those decades, coinciding with negative AMO phases (Fig. 6b, n). Nevertheless, the subsidence (ascending motions) over the central Pacific is displaced westward with respect to the observations, showing the surface wind divergence (convergence) around 180°–150°W (Fig. 6b, n), where the thermocline shallows (deepens) and triggers the upwelling (downwelling) Kelvin wave propagating to the east, reaching the South American coast in winter months (Fig. 6c–e, o–q). The zonal displacement of the surface divergence (convergence) originates a lag in the impact on the SST with respect to the wind forcing: significant cooling (warming) only appeared in the southeastern Pacific, while the warm (cold) horseshoe is already developed in winter months (Fig. 6f, r). This delay in the creation of the cold (warm) tongue has also been documented in previous studies, suggesting that although the wind anomalies in the western Pacific contributes to generate the warming (cooling) in this region, the feedbacks

Fig. 4 Leading Mode of the EMMCA for observations. **a–r** Homogeneous and Heterogeneous correlation maps for summer (JJAS) Tropical Atlantic SST and the expansion coefficients of the Tropical Atlantic SST in JJAS (in °C, *shaded*), tropical velocity potential at 200 hPa in JJAS (in m^2/s, *shaded*) and Tropical Pacific wind stress in JASO (in m/s, *vectors*), summer to winter (JJAS–SOND–DJFM) thermocline depth and Tropical Pacific SST in winter months, DJFM (in °C) for the periods 1872–1933 (**a–f**), 1934–1969 (**g–l**) and 1970–2001 (**m–r**). Only significant values at 90 % confidence level according to a Monte Carlo test are presented

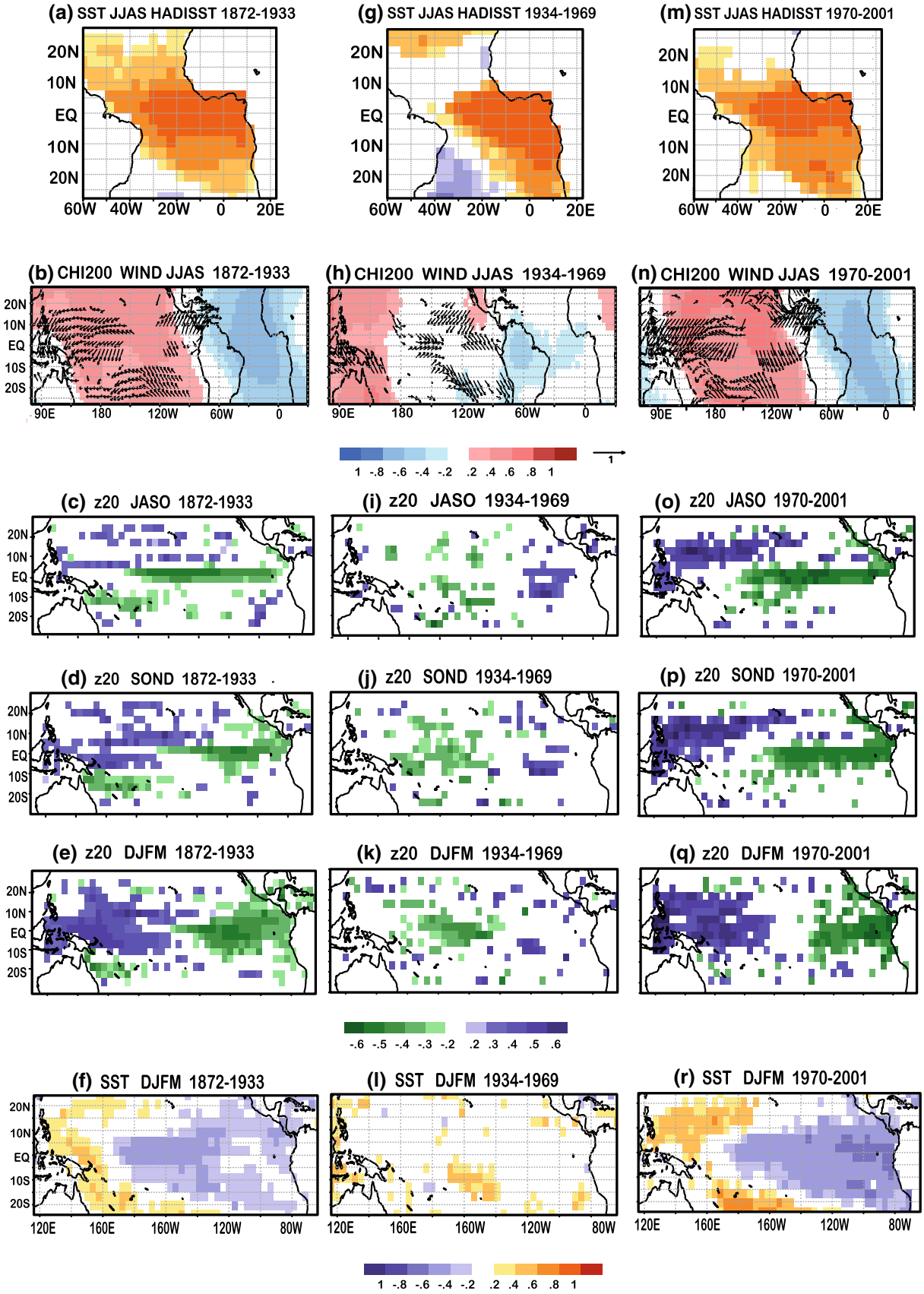
(a) SST JJAS HADISST 1872-1933
(g) SST JJAS HADISST 1934-1969
(m) SST JJAS HADISST 1970-2001
20N
10N
EQ
10N
20N
60W 40W 20W 0 20E
(b) CHI200 WIND JJAS 1872-1933
(h) CHI200 WIND JJAS 1934-1969
(n) CHI200 WIND JJAS 1970-2001
20N
10N
EQ
10S
20S
90E 180 120W 60W 0
1 -.8 -.6 -.4 -.2 .2 .4 .6 .8 1
1
(c) z20 JASO 1872-1933
(i) z20 JASO 1934-1969
(o) z20 JASO 1970-2001
(d) z20 SOND 1872-1933
(j) z20 SOND 1934-1969
(p) z20 SOND 1970-2001
(e) z20 DJFM 1872-1933
(k) z20 DJFM 1934-1969
(q) z20 DJFM 1970-2001
-.6 -.5 -.4 -.3 -.2 .2 .3 .4 .5 .6
(f) SST DJFM 1872-1933
(l) SST DJFM 1934-1969
(r) SST DJFM 1970-2001
120E 160E 160W 120W 80W
1 -.8 -.6 -.4 -.2 .2 .4 .6 .8 1

processes in the simulation are not so effective to cool (warm) the eastern Pacific, resulting in a slower Bjerknes feedback mechanism (Polo et al. 2014).

On the contrary, under positive AMO phases the Atlantic Niño is able to alter the Walker circulation over the tropical Atlantic basin with a descending branch over the Indian Ocean but with no impact on the Pacific basin, in agreement with observations (33.18 % of the total variance, Figs. 4h, 6h). Surface wind convergence is located around the dateline and significant warm SST anomaly pattern appears in the central-eastern Pacific during winter months (Fig. 6l). As no significant changes are observed in the thermocline depth and neither in the Walker circulation over the Pacific, the anomalous wind stress and SST development could be associated with a local forcing (Fig. 6h–k).

Despite its simplicity, the model is able to simulate the atmospheric and oceanic processes at work in this connection. The good agreement between modelled and observational results could be due to the fact that the Atlantic influence on ENSO development is based on equatorial dynamics associated with thermocline feedbacks, which are well resolved in the model (Polo et al. 2014). Additionally, the Atlantic modulated -ENSO phenomena seem to follow Wyrtki's (1975) theory: a wind perturbation in the central-western equatorial Pacific builds up water in the western Pacific which propagates eastward as a Kelvin wave favouring the creation of SST anomalies in the eastern equatorial Pacific.

Therefore, an AGCM coupled to a simplified 1.5 layer ocean model is able to simulate the change in the thermocline depth, as a consequence of the anomalous winds coming from the Atlantic, which in turn, propagates to the east as a Kelvin wave reaching the coast and favouring the SST anomalies related to ENSO phenomena (Fig. 6), according to the Wyrtki's hypothesis.

4 Discussion

Our study evidences that, during certain decades, there is a leading tropical coupled covariability mode that links the Atlantic and Pacific interannual variability. Thus, a summer Atlantic Niño is associated with a Pacific La Niña during the next winter, and vice versa. This relation is found using both observations and model simulations with prescribed Atlantic SSTs and coupled over the Indo-Pacific region. Although the relation between the Atlantic–Pacific Niños has been demonstrated in previous studies (Keenlyside

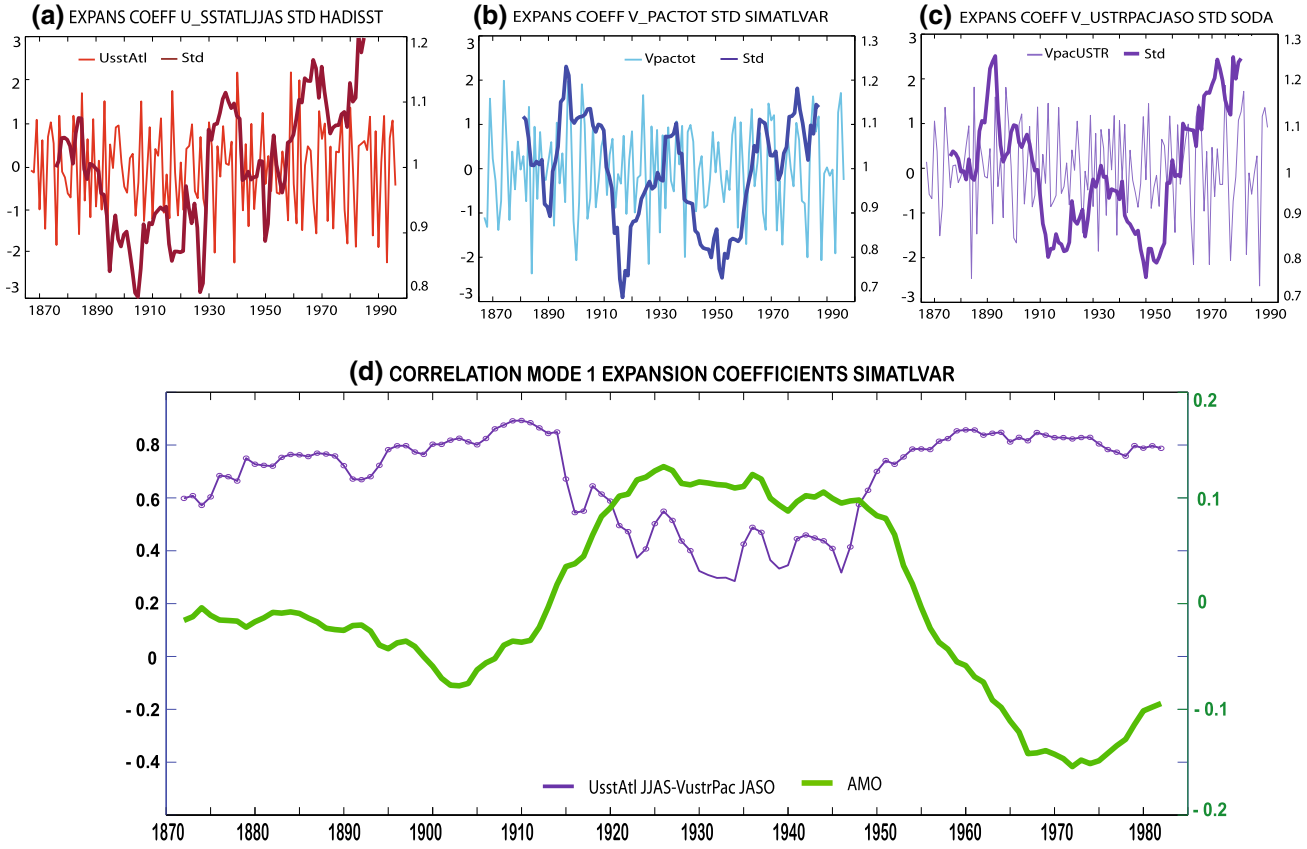

Fig. 5 Expansion coefficients of the leading mode of interannual variability from *SimAtlVar* for the period 1872–2001. Same as Fig. 3 but for *SimAtlVar*

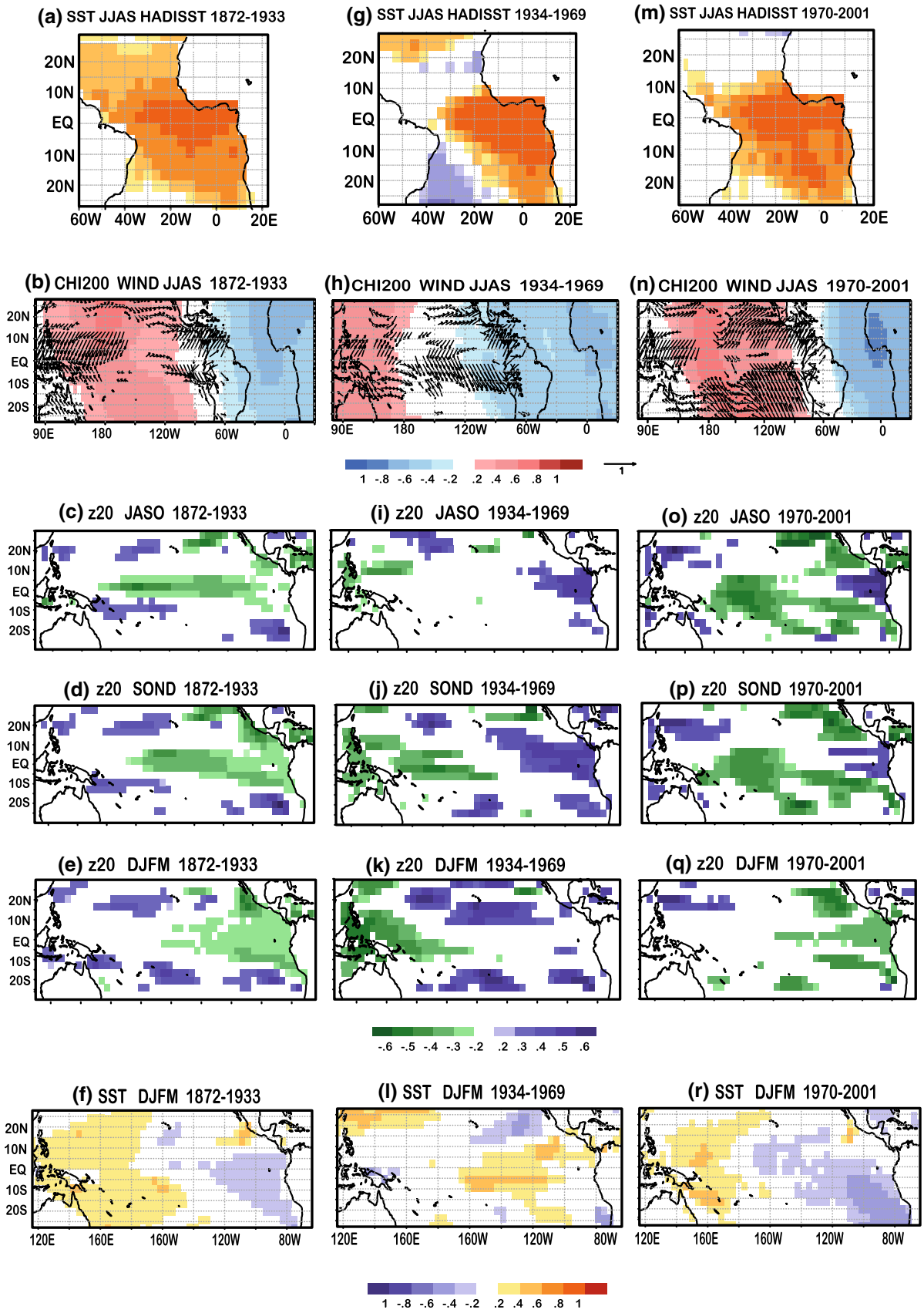

Fig. 6 Leading Mode of the EMMCA for *SimAtlVar*. Same as Fig. 4 but for *SimAtlVar*

and Latif 2007; Rodríguez-Fonseca et al. 2009; Ding et al. 2012; Martín-Rey et al. 2012), here, for the first time the Atlantic–Pacific connection is presented as a leading mode of coupled covariability, which appears modulated at multidecadal timescales. The decades in which the mode shows up coincide with negative phases of the Atlantic Multidecadal Oscillation (AMO), putting forward the possible modulation of this mode by this multidecadal variability pattern.

4.1 Multidecadal modulation

In order to shed light on the role of the AMO in the tropical Atlantic and Pacific variability, the multidecadal changes of the variability in winter equatorial Pacific SST (Niño3 region) and summer western equatorial Atlantic convergence at upper levels (in terms of the velocity potential) are computed using model simulations which consider the observed Atlantic SSTs as the only external forcing (Fig. 7a).

As the main difference between the Atlantic SST pattern related and unrelated with ENSO (Fig. 4b vs Fig. 4a, c) is located in the western equatorial Atlantic, we have analysed the changes in the divergent component of the upper-level flow in this region. These changes are significant during negative phases of the AMO, suggesting how the AMO is able to modify the amplitude of the anomalous convection and, thus, impacting on the Pacific SSTs (Fig. 7). Figure 7a shows how this enhancement (weakening) of Niño3 variability takes place during the first and last (middle) decades of the twentieth century, coinciding with negative (positive) AMO phases in which the South Atlantic is warmer (cooler) than normal. Indeed, the correlation map obtained between the time evolution of the curves from Fig. 7a and the anomalous global SSTs resembles clearly an AMO-like pattern: the inter-hemispherical pattern associated with the AMO (Fig. 7b, shaded) is well reproduced when using the time series obtained by the model (purple and red lines) over the global SSTs (Fig. 7b, dotted areas). This similarity corroborates the AMO influence on the Pacific SST variability reported in previous studies (An and Jin 2001; Dong et al. 2006; Timmermann et al. 2007; Hong et al. 2013; Polo et al. 2013). Additionally, for the first time, we suggest that the changes in the mean state of the Atlantic Ocean as an AMO response could modify the convergence at the upper levels of the western equatorial Atlantic, favouring and changing the variability of the atmospheric bridge which links the Atlantic and Pacific basins (red line, Fig. 7a, c).

Nevertheless, the role of the mean state and variability of the Atlantic SST in the Atlantic–Pacific connection remains unclear. On the one hand, some authors suggest that changes in the Atlantic mean state could enhance the equatorial Atlantic SST variability in summer, strengthening the Atlantic–Pacific connection (Svendsen et al. 2013). Also, modifications of the Atlantic and Pacific mean state associated with the global warming could also contribute to favour the interbasin connection (Kucharski et al. 2011). On the other hand, a mean deepened thermocline depth, which implies a decrease of the Atlantic variance, has been reported in recent studies (Haarsma et al. 2008; Polo et al. 2013). Additionally, spatial pattern of the Equatorial mode changes depending on the period considered (Fig. 4, 5, 6, first row) with different impacts on the ENSO phenomenon and coinciding with opposite phases of the AMO. Further sensitivity studies must be done in order to isolate the role of the mean state on the interannual variability and the interannual variability of the Atlantic Ocean and their impact on the Pacific basin.

4.2 Statistical hindcast of Niño3 SST

One way to examine to the role of the Atlantic in the Pacific is to test the ENSO prediction using the information from EMMCA (Fig. 8). A statistical hindcast is calculated for each of the three periods of study: 1871–1933, 1934–1969 and 1970–2001, associated with positive and negative phases of the AMO. The selected year *i* to predict is previously removed from the sample, and the EMMCA is applied to the new sample with dimensions:

X (n_x, $n_t - i$) and Y(n_y, $n_t - i$) for predictor and predictand fields respectively. A *Psi* function, which contains the information between the predictor (X) and predictand fields (Y), has been obtained. The Psi function and the predictor are used to hindcast the predictand fields:

$$Y(n_y, n_t) = Psi(n_y, n_x) * X(n_x, nt) \quad (2)$$

Here, we show the hindcast for Niño3 SST in winter months for periods of negative AMO phases, coinciding with the appearance of the Atlantic–Pacific mode, and period of positive AMO phase (Fig. 8). The observed SST is well predicted in the first and last decades of the twentieth century, showing significant correlation scores at 90 % confidence level (Fig. 8a, c), while this value decreases to almost zero in AMO positive decades (Fig. 8b). This result evidences that the AMO negative periods are opportunity windows for ENSO forecast using the summer tropical Atlantic SST as the predictor field.

5 Summary and conclusions

The present study has demonstrated, for the first time, that the Atlantic–Pacific Niños connection is a leading mode of interbasin covariability, which appears modulated at

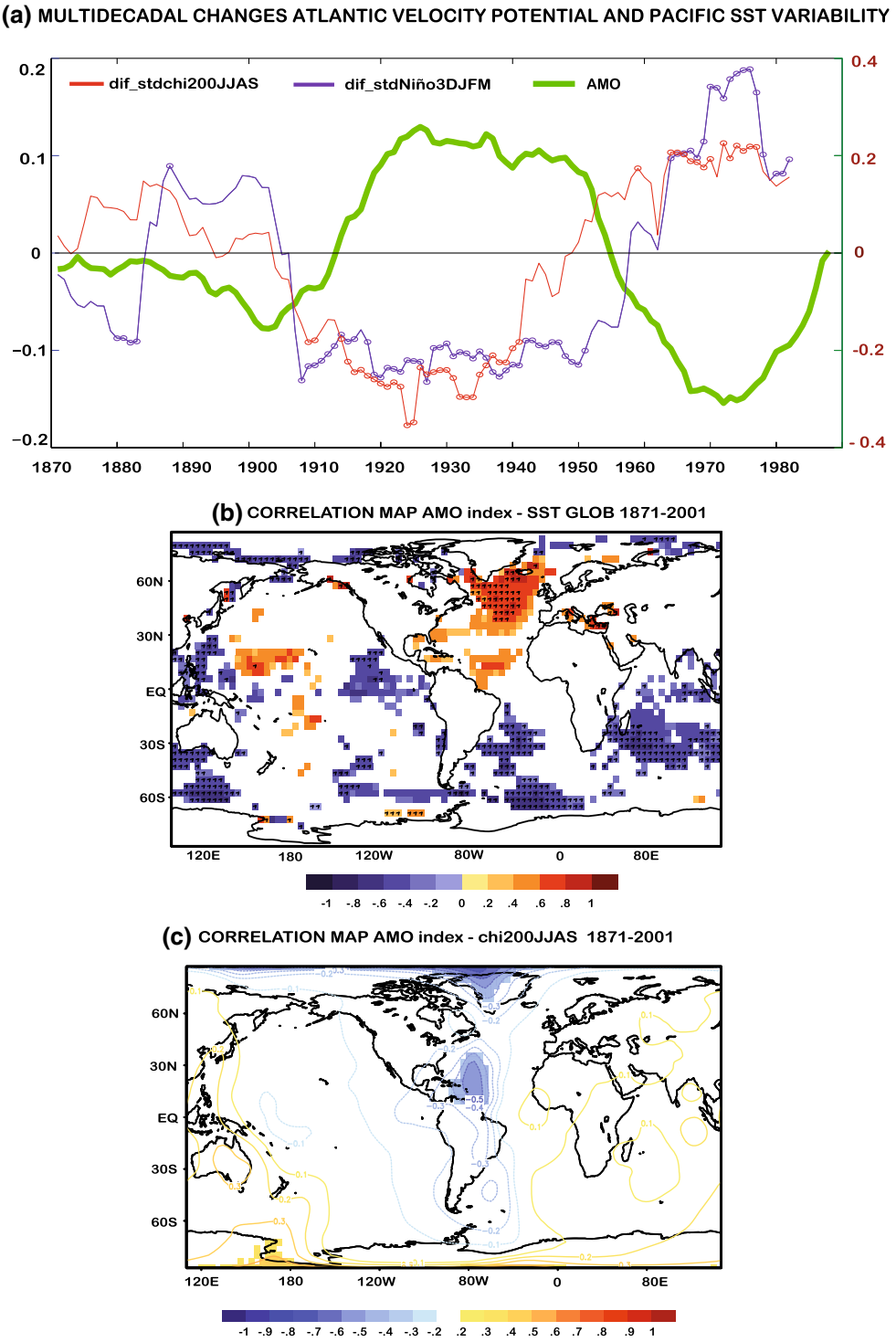

Fig. 7 Multidecadal changes in the equatorial Atlantic velocity potential and Pacific SST variability. **a** *Purple line* changes in the standard deviation of Niño3 index in winter (DJFM) months with respect to the whole period. 20-year running differences are computed and a F-test is applied to highlight the windows in which the differences are statistically significant at 90 % confidence level (*dots*). *Red line* the same as the purple line but for the summer (JJAS) velocity potential at 200 hPa (chi200) in the western equatorial Atlantic (70°W–35°W, 5°N–5°S) from *SimAtlVar*. *Green line* Atlantic Multidecadal Oscillation time series (defined as the annual SST anomalies averaged in North Atlantic region. The global warming signal has been previously removed; Villamayor and Mohino 2012). **b** Correlation map between the running 20-year differences for AMO index [*green line* in (**a**)] and the global SST anomalies in 20-year windows. **c** Same as (**b**) but for the running 20-year differences for the chi200 in JJAS [*red line* in (**a**)]. Significant values at 90 % confidence level according to a Monte Carlo test have been in *shaded*. Additionally, significant region which coincides in sign with those regions obtained correlating the *red* and *purple lines* from (**a**) over the global SST are also indicated with *black markers*

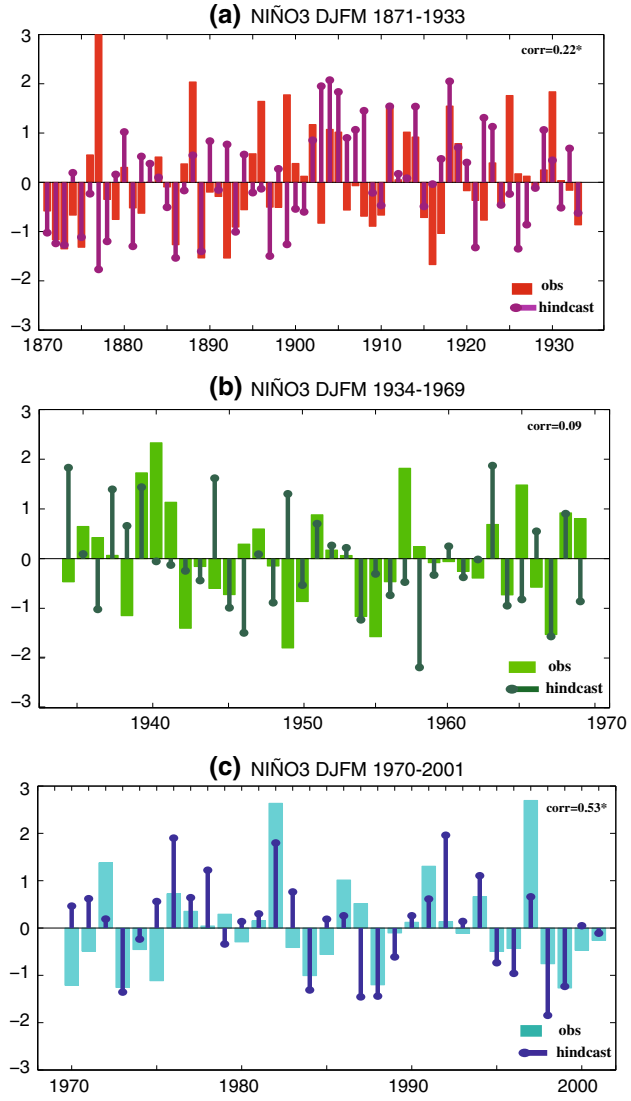

Fig. 8 Hindcast for the observed Niño3 SST in winter months (DJFM) for the periods 1871–1933, 1934–1969 and 1970–2001. *Bars* observed equatorial Pacific SST in Niño 3 region. *Stems* predicted equatorial Pacific SST in Niño3 region using the statistical hindcast from EMMCA information. *Stars* years in which there is a summer Atlantic Niño (Niña, expansion coefficient for Atlantic SST higher than ±1 std) followed by observed and predicted Pacific La Niña (El Niño, Niño3 index higher than ±0.5)

multidecadal timescales coinciding with negative phases of the AMO.

Warm (cool) SST anomalies over the equatorial Atlantic in summer are related to ascending (descending) motions over the Atlantic and subsidence over the Pacific, where an upwelling (downwelling) Kelvin wave is generated propagating eastward and impacting on the Pacific SST in winter months, favouring the development of La Niña (El Niño). This mechanism, which has been reported by Polo et al. (2014) is a mode of interbasin variability and has been isolated in this work, explaining almost the 30 % of the total variance.

The associated leading mode of the Tropical Atlantic SST variability, the Atlantic Niño, presents different spatial patterns depending on the decades considered: anomalous SSTs covering the entire Tropical Atlantic basin are observed under negative AMO phases, while a dipolar structure is presented for AMO positive periods (Figs. 4a, g, m, 6a, g, m). The main difference between them is located in the western Equatorial Atlantic (70°–35°W, 20°N–20°S); it is warmer during the first and last decades of the twentieth century (Figs. 4a, m, 6a, m). These decades coincide with negative AMO periods, where the southern Atlantic is warmer than normal, the western equatorial Atlantic atmosphere is more perturbed and could help to connect the Atlantic and Pacific basins at multidecadal time scales. Also, there is an increase of Pacific SST variability during these periods, favouring the occurrence of the Atlantic–Pacific Niños mode.

We suggest that the multidecadal internal variability of the ocean is able to modulate the Atlantic–Pacific connection through changes in the western equatorial Atlantic convection and Pacific SST variability (Fig. 7). This finding provides a step forward in the improvement of the seasonal and decadal forecast. The statistical hindcast of the Niño3 SST from the mode information has revealed that the Pacific SST can be reproduced with the information of the Tropical Atlantic SST in negative AMO periods (Fig. 8).

On the one hand, the Atlantic–Pacific connection increases ENSO predictability (Frauen and Dommenget 2012; Dayan et al. 2013; Boschat et al. 2013). But, on the other hand, the correct simulation of the AMO could in turn favour the periods in which this predictability is observed. Further analyses with coupled models are needed in order to check the modulation role of the Atlantic mean state in triggering the Atlantic–Pacific connection.

Acknowledgments This study was supported by the European project PREFACE (ref.603521) the Spanish MINNECO projects CGL2009-10295, CGL2011-13564-E and CGL2012-38923-C02-01 and for the Spanish Public Employment Service (SEPE). The authors want to thank the editor for his help during the whole process of submission and also the useful and constructive comments of the two anonymous referees, which have been considerably improved the manuscript.

References

An SI, Jin FF (2001) Collective role of thermocline and zonal advective feedbacks in the ENSO mode. J Clim 14:3421–3432

Annamalai H, Xie SP, McCreary JP, Murtugudde R (2005) Impact of Indian Ocean sea surface temperature on developing El Niño. J Clim 18:302–319

Bjerknes J (1964) Atlantic air-sea interaction. Adv Geophys 10:10–82

Bjerknes J (1969) Atmospheric teleconnections from the equatorial Pacific. Mon Wea Rev 97:163–172

Boschat G, Terray P, Masson S (2013) Extratropical forcing of ENSO. Geophys Res Lett 40(8):1605–1611. doi:10.1002/grl.50229
Boyer TP et al (2009) WorldOcean database 2009. In: Levitus S (ed) NOAA Atlas NESDIS, 66, US Govt Print Off, Washington, DC, p 216
Bretherton CS, Smith C, Wallace JM (1992) An intercomparison of methods for finding coupled patterns in climate data. J Clim 5:541–560
Chang P (1994) A study of the seasonal cycle of sea surface temperature in the tropical Pacific Ocean using reduced gravity models. J Geophys Res 99:7725–7741
Cherry S (1997) Some comments on singular value decomposition analysis. J Clim 10:1759–1761
Compo GP, Whitaker JS, Sardeshmukh PD (2006) Feasibility of a 100-year reanalysis using only surface pressure data. Bull Am Meteorol Soc 87:175–190. doi:10.1175/BAMS-87-2-175
Compo GP, Whitaker JS, Sardeshmukh PD (2008) The 20th century reanalysis project, paper presented at 3rd WCRP international conference on reanalysis. University of Tokyo, Tokyo, 28 Jan to 1 Feb
Compo GP et al (2011) The twentieth century reanalysis project. Q J R Meteorol Soc 137:1–28
Davey MK et al (2002) STOIC: a study of coupled model climatology and variability in tropical ocean regions. Clim Dyn 18:403–420
Dayan H, Vialard J, Izumo T, Lengaigne M (2013) Does sea surface temperature outside the tropical Pacific contribute to enhanced ENSO predictability? Clim Dyn. doi:10.1007/s00382-013-1946-y
Delworth TL, Mann ME (2000) Observed and simulated multidecadal variability in the Northern Hemisphere. Clim Dyn 16(9):661–676
Deser C, Alexander MA, Xie SP, Phillips AS (2010) Sea surface temperature variability: patterns and mechanisms. Annu Rev Marine Sci 2:115–143
Ding H, Keenlyside NS, Latif M (2012) Impact of the Equatorial Atlantic on the El Niño Southern Oscillation. Clim Dyn 38(9–10):1965–1972. doi:10.1007/s00382-011-1097-y
Dong B, Sutton RT (2007) Enhancement of ENSO variability by a weakened Atlantic thermohaline circulation in a coupled GCM. J Clim 20(19):4920–4939
Dong B, Sutton RT, Scaife AA (2006) Multidecadal modulation of El Nino-Southern Oscillation (ENSO) variance by Atlantic Ocean sea surface temperatures. Geophys Res Lett 33(8):L08705. doi:10.1029/2006GL025766
Fang Y, Chiang JC, Chang P (2008) Variation of mean sea surface temperature and modulation of El Niño-Southern Oscillation variance during the past 150 years. Geophys Res Lett 35(14):L14709. doi:10.1029/2008GL033761
Federov A, Philander SG (2000) Is El Niño changing? Science 288:1997–2002
Frauen C, Dommenget D (2012) Influences of the tropical Indian and Atlantic Oceans on the predictability of ENSO. Geophys Res Lett 39:L02706
García-Serrano J, Losada T, Rodríguez-Fonseca B, Polo I (2008) Tropical Atlantic variability modes (1979–2002). Part II: time-evolving atmospheric circulation related to SST-forced tropical convection. J Clim 21:6476–6497
Giese BS, Ray S (2011) El Niño variability in simple ocean data assimilation (SODA), 1871–2008. J Geophys R Oceans (1978–2012) 116:C2
Gill A (1980) Some simple solutions for heat-induced tropical circulation. Q J R Meteor Soc 106:447–462
Haarsma RJ, Campos E, Hazeleger W, Severijns C (2008) Influence of the meridional overturning circulation on tropical Atlantic climate and variability. J Clim 21:1403–1416
Ham YG, Kug JS, Park JY, Jin FF (2013) Sea surface temperature in the north tropical Atlantic as a trigger for El Niño/Southern Oscillation events. Nat Geosci 6:112–116
Handoh IC, Matthews AJ, Bigg GR, Stevens DP (2006a) Interannual variability of the tropical Atlantic independent of and associated with ENSO: part I. The North Tropical Atlantic. Int J Clim 26(14):1937–1956
Handoh IC, Bigg GR, Matthews AJ, Stevens DP (2006b) Interannual variability of the Tropical Atlantic independent of and associated with ENSO: part II. The South Tropical Atlantic. Int J Clim 26(14):1957–1976
Hong S, Kang IS, Choi I, Ham YG (2013) Climate responses in the tropical Pacific associated with Atlantic warming in recent decades. Asia–Pacific J Atmos Sci 49(2):209–217
Huang B, Schopf PS, Pan Z (2002) The ENSO effect on the tropical Atlantic variability: a regionally coupled model study. Geophys Res Lett 29(21):35-1
Izumo T, Vialard J, Lengaigne M, Montegut CDB, Behera SK, Luo JJ, Cravatte S, Masson S, Yamagata T (2010) Influence of the state of the Indian Ocean dipole of the following year's El Niño. Nature 3:168–172
Joly M, Voldoire A (2010) Role of the Gulf of Guinea in the interannual variability of the West African monsoon: what do we learn from CMIP3 coupled simulations? Int J Clim 30(12):1843–1856
Kaplan A, Kushnir Y, Cane MA, Blumenthal MB (1997) Reduced space optimal analysis for historical data sets: 136 years of Atlantic sea surface temperatures. J Geophys Res Oceans (1978–2012), 102(C13): 27835–27860
Kayano MT, Andreoli RV, Ferreira de Souza RA (2011) Evolving anomalous SST patterns leading to ENSO extremes: relations between the tropical Pacific and Atlantic Oceans and the influence on the South American rainfall. Int J Clim 31(8):1119–1134
Keenlyside NS, Latif M (2007) Understanding equatorial Atlantic interannual variability. J Clim 20(1):131–142
Keenlyside NS, Ding H, Latif M (2013) Potential of equatorial Atlantic variability to enhance El Niño prediction. Geophys Res Lett 40(10):2278–2283
Knight JR, Folland CK, Scaife AA (2006) Climate impacts of the Atlantic multidecadal oscillation. Geophys Res Lett 33(17):L17706. doi:10.1029/2006GL026242
Kucharski F, Molteni F, Bracco A (2006) Decadal interactions between the western tropical Pacific and the North Atlantic Oscillation. Clim Dyn 26:79–91
Kucharski F, Bracco A, Yoo JH, Molteni F (2008) Atlantic forced component of the Indian monsoon interannual variability. Geophys Res Lett 35:L04706
Kucharski F, Kang IS, Farneti R, Feudale L (2011) Tropical Pacific response to 20th century Atlantic warming. Geophys Res Lett 38(3):L03702. doi:10.1029/2010GL046248
Kug JS, Kang IS (2006) Interactive feedback between ENSO and the Indian Ocean. J Clim 19(9):1784–1801
Losada T, Rodríguez-Fonseca B, Polo I, Janicot S, Gervois S, Chauvin F, Ruti P (2010) Tropical response to the Atlantic Equatorial mode: AGCM multimodel approach. Clim Dyn 5:45–52
Losada T, Rodriguez-Fonseca B, Mohino E, Bader J, Janicot S, Mechoso CR (2012) Tropical SST and Sahel rainfall: a non-stationary relationship. Geophys Res Lett 39:12
Luo JJ, Zhang R, Behera SK, Masumoto Y, Jin FF, Lukas R, Yamagata T (2010) Interaction between El Niño and extreme Indian Ocean Dipole. J Clim 23:726–742
Martín-Rey M, Polo I, Rodríguez-Fonseca B, Kucharski F (2012) Changes in the interannual variability of the tropical Pacific as a response to an equatorial Atlantic forcing. Sci Mar 76, S1. doi:10.3989/scimar.03610.19A
Matsuno T (1966) Quasi-geostrophic motions in the equatorial area. J Meteor Soc Japan 44:24–42
Mohino E, Rodríguez-Fonseca B, Losada T, Gervois S, Janicot S, Bader J, Ruti P, Chauvin F (2011) Changes in the interannual

SST-forced signals on West African rainfall. AGCM intercomparison. Clim Dyn 37(9–10):1707–1725
Molteni F (2003) Atmospheric simulations using a GCM with simplified physical parametrizations. I. Model climatology and variability in multi-decadal experiments. Clim Dyn 20:175–191
Münnich M, Neelin JD (2005) Seasonal influence of ENSO on the Atlantic ITCZ and equatorial South America. Geophys Res Lett 32:L21709
Philander SG (1990) El Niño, La Niña, and the Southern Oscillation, Academic Press, San Diego. 46. ISBN 0125532350
Polo I, De Fonseca BR, Sheinbaum J (2005) Northwest Africa upwelling and the Atlantic climate variability. Geophys Res Lett 32(23):L23702
Polo I, Rodríguez-Fonseca B, Losada T, García-Serrano J (2008) Tropical Atlantic variability modes (1979–2002). Part I: time-evolving SST modes related to West African rainfall. J Clim 21:6457–6475
Polo I, Dong BW, Sutton RT (2013) Changes in tropical Atlantic interannual variability from a substantial weakening of the meridional overturning circulation. Clim Dyn 41(9–10):2765–2784
Polo I, Martín-Rey M, Rodríguez-Fonseca B, Kucharski F, Mechoso CR (2014) Processes in the Pacific La Niña onset triggered by the Atlantic Niño, Clim Dyn (under revision)
Rayner NA, Parker DE, Horton EB, Folland CK, Alexander LV, Rowell DP, Kent EC, Kaplan A (2003) Globally complete analyses of sea surface temperature, sea ice and night marine air temperature, 1871–2000. J Geophys Res 108:4407
Richter I, Xie SP (2008) On the origin of equatorial Atlantic biases in coupled general circulation models. Clim Dyn 31(5):587–598
Richter I, Xie SP, Behera SK, Doi T, Masumoto Y (2012) Equatorial Atlantic variability and its relation to mean state biases in CMIP5. Clim Dyn 42(1–2):171–188
Rodríguez-Fonseca B, Polo I, García-Serrano J, Losada T, Mohino E, Mechoso CR, Kucharski F (2009) Are Atlantic Niños enhancing Pacific ENSO events in recent decades? Geophys Res Lett 36:L20705
Rodríguez-Fonseca B et al (2011) Interannual and decadal SST-forced responses of the West African monsoon. Atmos Sci Lett 12(1):67–74
Saravanan R, Chang P (2000) Interaction between tropical Atlantic variability and El Niño-Southern oscillation. J Clim 13:2177–2194
Stephenson DB, Pavan V, Bojariu R (2000) Is the North Atlantic oscillation a random walk? Int J Clim 20:1–18
Suarez MJ, Schopf PS (1988) A delayed action oscillator for ENSO. J Atmos Sci 5(45):3283–3287
Sutton RT, Jewson SP, Rowell DP (2000) The elements of climate variability in the tropical Atlantic region. J Clim 13(18):3261–3284
Svendsen L, Gunnar N, Keenlyside N (2013) Weakening AMOC connects Equatorial Atlantic and Pacific variability. Clim Dyn. doi:10.1007/s00382-013-1904-8
Terray P (2011) Southern Hemisphere extra-tropical forcing: a new paradigm for El Niño-Southern Oscillation. Clim Dyn 36(11–12):2171–2199
Terray P, Dominiak S (2005) Indian Ocean Sea Surface Temperature and El Niño–Southern Oscillation: A New Perspective. J Clim 18(9):1351–1368
Timmermann A et al (2007) The influence of a weakening of the Atlantic meridional overturning circulation on ENSO. J Clim 20(19):4899–4919
Toniazzo T, Woolnough S (2013) Development of warm SST errors in the southern tropical Atlantic in CMIP5 decadal hindcasts. Clim Dyn 1–25. doi:10.1007/s00382-013-1691-2
Villamayor J, Mohino E (2012) *Variabilidad de la baja frecuencia de la precipitación de Sahel y su relación con la variabilidad multidecadal de las temperaturas de la superficie del mar en las simulaciones de CMIP5.* Master Thesis, Universidad Complutense de Madrid
Voldoire A, Claudon M, Caniaux G, Giordani H, Roehrig R (2014) Are atmospheric biases responsible for the tropical Atlantic SST biases in the CNRM-CM5 coupled model? Clim Dyn 1–22. doi:10.1007/s00382-013-2036-x
Wahl S, Latif M, Park W, Keenlyside N (2011) On the tropical Atlantic SST warm bias in the Kiel Climate Model. Clim Dyn 36(5–6):891–906
Wang C, Lee SK, Mechoso CR (2010) Interhemispheric Influence of the Atlantic Warm Pool on the Southeastern Pacific. J Clim 23(2):404–418
Whitaker JS, Compo GP, Wei X, Hamill TM (2004) Reanalysis without radiosondes using ensemble data assimilation. Mon Wea Rev 132:1190–1200
Woodruff SD et al (2011) ICOADS release 2.5: extensions and enhancements to the surface marine meteorological archive. Int J Clim 31(7):951–967
Wyrtki K (1975) El Niño-the dynamic response of the Equatorial Pacific Ocean to Atmospheric Forcing. J Phys Oceanogr 5:572–584
Zebiak SE (1993) Air-sea interaction in the equatorial Atlantic region. J Clim 6:1567–1586

6.4. Analysis of the predictive skill of the tropical Atlantic SSTs in ENSO development.

(Martín-Rey et al. 2015a)

The skill of the tropical Atlantic SSTs in predicting the ENSO phenomena along the 20th century is explored in this section, and these results are in the framework of the Objetive 3 of the present thesis.

The multidecadal modulation of the Atlantic-Pacific Niños connection puts forward that, during these decades, the ENSO phenomena could be predicted through the knowledge of the tropical Atlantic SSTs 6-months in advance. A statistical cross-validated hindcast of El Niño episodes along the 20th century is calculated, considering the Atlantic Sea Surface Temperatures as the unique predictor field, and a set of atmospheric and oceanic variables related to the Atlantic-Pacific mechanism as the predictand field. During negative AMO phases, ENSO predictive skill is enhanced and the hindcast reproduces quite well the observed ENSO episodes. Moreover, the summer surface wind in the western Pacific seems to be the key variable in the development of ENSO events associated with the remote Atlantic forcing. On the other hand, the hindcast fails in simulating the Pacific variables under positive AMO phases, pointing out the lack of ENSO predictability from the tropical Atlantic SSTs during those decades.

Atlantic opportunities for ENSO prediction

MARTA MARTÍN-REY

IGEO (UCM-CSIC)

Departamento de Geofísica y Meteorología, UCM, Madrid,Spain

BELÉN RODRÍGUEZ-FONSECA

IGEO (UCM-CSIC)

Departamento de Geofísica y Meteorología, UCM, Madrid,Spain

IRENE POLO

Department of Meteorology, University of Reading, UK

(Geophysical Research Letters, under review)

Abstract

El Niño-Southern Oscillation (ENSO) is the dominant mode of inter-annual climate variability with worldwide impacts. The knowledge of ENSO drivers and the underlying mechanisms is crucial to improve ENSO prediction, which still remains a challenge. The recently discovered connection between an Atlantic Niño (Niña) and a Pacific Niña (Niño), through an air-sea coupled mechanism during the first and last decades of the 20th century, highlights an opportunity for ENSO prediction. Here, a statistical cross-validated hindcast of ENSO along the 20th century is presented, considering the Atlantic Sea Surface Temperatures as the unique predictor field, and a set of atmospheric and oceanic variables related to the Atlantic-Pacific connection as the predictand field. The observed ENSO phase is well reproduced and the skill is enhanced at the beginning and the end of the 20th century. This multidecadal modulation of ENSO predictability related to sea surface temperatures over the tropical Atlantic could be crucial to improve its seasonal-to-decadal forecast and associated impacts.

1. Introduction

El Niño-Southern Oscillation (ENSO) is the dominant air-sea coupled mode of global inter-annual climate variability [Philander 1990]. ENSO phenomenon is

characterized by fluctuations between unusually warm (El Niño) and cold (La Niña) conditions in the Tropical Pacific Ocean, associated with an atmospheric seesaw pressure pattern, the Southern Oscillation (SO), and closely linked to the trade winds through the so-called Bjerknes feedback [Walker, 1924; Bjerknes, 1969]. The ENSO signal can be felt worldwide through atmospheric teleconnections, impacting in the livelihood of millions of people [Klein et al., 1999; Alexander et al., 2002; McPhaden et al., 2006]. Thus, a huge effort has been made from early 1980s to improve ENSO research, developing an ENSO observing system [McPhaden et al., 1998], investigating and modelling the mechanisms responsible for ENSO development [Wyrtki, 1975; 1985; McCreary, 1983; Suarez and Schopf, 1988; Jin, 1997a; 1997b] and analysing its variability and global teleconnections.

In particular, lots of efforts have been made to forecast ENSO phenomena during the last decades. On the one hand, classic ENSO precursors are found within the Tropical Pacific basin: western Indo-Pacific winds and equatorial heat content during previous months are crucial for triggering those episodes [*McPhaden et al*., 2006a; *McPhaden et al*., 2006b], according to the recharge oscillator scheme [Jin, 1997a; 1997b]. From this information, statistical predictions have been performed, obtaining significant correlation skills [Latif et al., 1994; Clarke and Van Gorder, 2003]. More recently, several studies have shown that the inclusion of other tropical and extra-tropical regions enhances ENSO predictability and improves the amplitude of these events [Jansen et al., 2009; Frauen and Dommenget, 2012; Dayan et al., 2013; Boschat et al., 2013; Keenlyside et al., 2013].

In particular, during the last years, several studies have highlighted the important contribution of the inter-annual equatorial Atlantic Sea Surface Temperature (SST) on the Tropical Pacific one [Keenlyside and Latif, 2007; Polo et al., 2008, 2015; Rodríguez-Fonseca et al., 2009; Ding et al., 2012; Martín-Rey et al., 2012, 2014; Ham et al., 2013a, 2013b]. In this sense, the leading mode of Tropical Atlantic SST variability, named as Atlantic Niño [Zebiak, 1993], has been found to precede the development of a winter Pacific La Niña after the 1970s [Rodríguez-Fonseca et al. 2009]. This inter-basin connection is established through an air-sea coupled mechanism: an anomalous equatorial warming enhances the convection, modifying the Walker circulation with an ascending branch over the Atlantic and subsidence over the central Pacific [Rodríguez-Fonseca et al., 2009; Losada et al., 2010; Ding et al., 2012]. Martín-Rey et al. [2012] and more recently Polo et al. [2015] have shed light about the associated atmospheric and oceanic processes. According to these authors, the anomalous surface wind divergence in the central Pacific piles up the warm waters to the west, triggering an equatorial upwelling Kelvin wave, which propagates eastward from boreal summer (JJAS) to winter (DJFM) months. As the Kelvin wave propagates to the east, the vertical stratification is modified and the thermocline feedbacks are activated, favouring the development of La Niña cold tongue. The opposite occurs for an Atlantic Niña event. Accordingly, the initial conditions of the tropical Atlantic have a strong impact on ENSO predictability

[Frauen and Dommenget, 2012], showing a considerable improvement of the skill when the model is initialized with equatorial Atlantic SSTs in boreal spring [Keenlyside et al., 2013].

Nevertheless, the equatorial Atlantic influence on ENSO development is not stationary on time [*Martín-Rey et al*., 2014]. The Atlantic-Pacific Niños connection appears as the leading co-variability mode of tropical variability only during the first decades of the 20th century and after the 1970s, which suggests opportunities for ENSO forecast.

The present study wants to do a step forward in the current ENSO prediction system by understanding the skill of ENSO statistical hindcast using only the Tropical Atlantic SSTs as the predictor field. Tackling with the non-stationarities, the time periods in which the inter-annual tropical Atlantic variability enhances ENSO prediction will be assessed. A linear statistical model has been developed and a cross-validated hindcast of ENSO has been performed for three different periods of study, from 1870 up to the present, according to the results from Martín-Rey et al. (2014).

2. Data and Methods

Monthly means of the observed tropical Atlantic SSTs from HadISST dataset [Rayner et al. 2003] and tropical Pacific wind stress, SST and thermocline depth, from the latest version of SODA reanalysis, version 2.2.4 [Giese and Ray, 2011] have been used. Thermocline depth (z20) is defined as depth of the 20°C isotherm. The velocity potential at 200 hPa and 950 hPa (chi200 and chi950, hereafter) has been computed from zonal and meridional wind from the NCAR 20th century reanalysis [Compo et al., 2011], being a variable related to the divergence at upper and lower levels respectively. De-trended 4-months seasonal anomalies have been calculated by subtracting the seasonal cycle and the linear trend from 1871 to 2007.

A statistical cross-validated hindcast of ENSO phenomena has been developed using the same methodology as Martín-Rey et al. [2014]: Extended Multiple Maximum Covariance Analysis (EMMCA). This technique considers the summer (JJAS) Atlantic SSTs as the unique predictor field (X) and a set of different variables in specific seasons and regions as predictand fields compiled in a matrix Y. These predictand variables are representative of the processes involved in the air-sea mechanism of the Atlantic-Pacific Niños connection: boreal summer (JJAS) and boreal winter (DJFM) tropical chi200 and chi950 as indicative of the upper level anomalous divergence (convergence) associated with the Atlantic warming (cooling) and the Pacific Southern Oscillation; boreal summer (JASO) tropical Pacific wind stress, boreal summer to winter (JJAS-SOND-DJFM) tropical Pacific z20 and boreal winter (DJFM) Tropical Pacific SST.

Firstly, to validate the model (EMMCA), a leave-one-out cross-validation method is used, excluding the year *i* that is going to be predicted from the original sample [Dayan et al., 2013]. In this way, the covariance matrix to predict the year *i* can be expressed as:

$$C_i = X_i(n_x, n_{t-1}) * Y_i(n_y, n_{t-1}) \quad [1]$$

where n_x, n_y are the spatial dimensions of the predictor (X) and predictand field (Y) respectively and n_t is the number of years considered in the analysis. Notice that the time dimensions of the new samples, for the predictand (Y_i) and predictor fields (X_i), have been reduced in one year, n_{t-1}. Secondly, we have applied the EMMCA to the new covariance matrix [1], obtaining a regression coefficient for the year i, $\psi_i(n_x, n_y)$. This regression coefficient contains the information about the relationship between the predictor and the predictand field in that year. The predictand field for the year i is predicted from the regression coefficient (ψ_i) and the predictor field (X_i), which have been constructed from the information given by the rest of the years of the sample, n_{t-1}:

$$Y_{pred,i}(n_y, n_{t-1}) = \psi_i(n_y, n_x) * X_i(n_x, n_{t-1}) \quad [2]$$

Finally, the procedure is repeated omitting each of the years to be predicted until the end of the period of study. The cross-validation method is performed for three selected periods, 1871-1938, 1939-1966 and 1967-2007. Although it has been considered the set of atmospheric and oceanic variables involved in the Atlantic-Pacific connection in the EMMCA, the present study is only focused on the tropical Pacific variables associated with ENSO: surface wind, thermocline depth and SST.

To select the Atlantic and Pacific Niño events, the expansion coefficient of Tropical Atlantic SST in JJAS obtained from the EMMCA (from Martín-Rey et al. [2014]) and Niño3 index [150°W-90°W; 5°N-5°S] in DJFM for the total period 1871-2007 have been considered. Significant values exceeding 90% or 95% confidence level according to a Monte Carlo test are presented.

3. Results

Figure 1 shows significant correlations between tropical Atlantic SSTs in JJAS (predictor, purple line) and Tropical Pacific wind stress one month later (JASO, predictand green line) only during the first and last decades of the 20th century (orange line). This result suggests that tropical Atlantic SSTs only act as a predictor of ENSO during those periods, in agreement with Martín-Rey et al. [2014]. Thus, three different periods are used to evaluate the ability of the Tropical Atlantic SSTs to predict ENSO phenomena along the 20th century: 1871-1938,1939-1966 and 1967-2007.

The correlation maps between the observed and predicted tropical Pacific variables involved in ENSO development (SST, zonal wind stress and z20) reveal a good prediction skill at the beginning of the 20th century and also after the 1970s (left and right panels in figure 2). In particular, a good agreement between the observed and cross-validated zonal wind stress is shown in western Pacific [120°E-160°W; 15°N-15°S], reaching correlation scores of 0.4-0.6 (Figure 2a,c). For a warming in the equatorial Atlantic, these wind anomalies are related to the anomalous surface wind divergence in the central Pacific, as a consequence of the descending branch of the Walker circulation, following the atmospheric mechanism proposed to link the tropical Atlantic and Pacific basins [Rodríguez-Fonseca et al., 2009; Losada et al., 2010; Ding et al., 2012; Polo et al., 2015]. The perturbation of

the thermocline depth in the central Pacific [180°-130°W, 5°N-5°S] during JASO season is also well reproduced by the hindcast, with correlation scores of 0.4 (Figure 2d,f). Finally, the model simulates quite well the eastward and westward propagation of z20 anomalies, according to the equatorial Kelvin and Rossby waves respectively following the ENSO theory [*Neelin et al*., 1998; *Suarez and Schopf*, 1988]

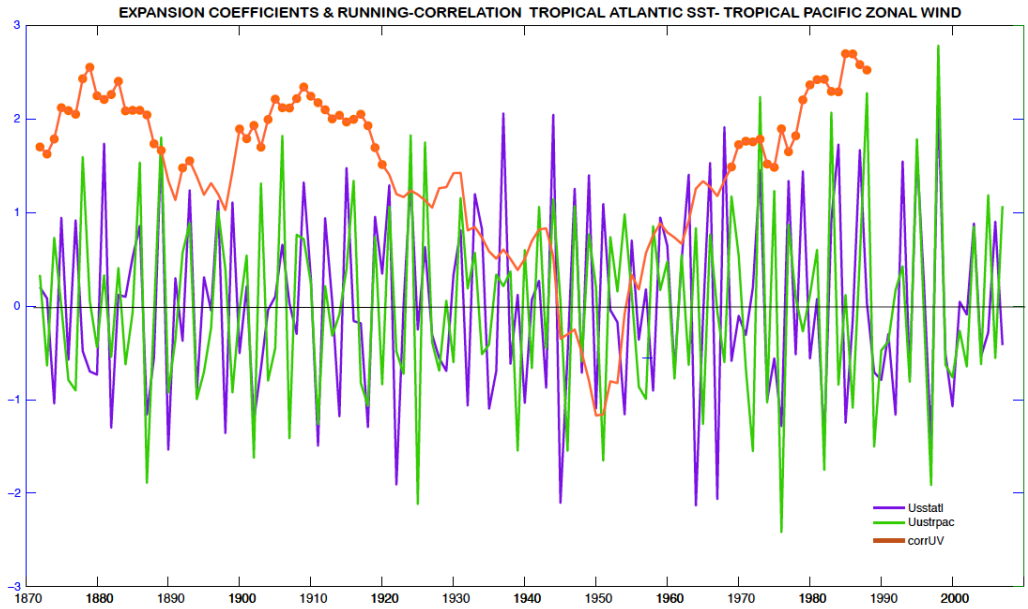

Figure 1. Modulation of the ENSO prediction skill from Tropical Atlantic SST Expansion coefficients of the observed anomalous tropical Atlantic SST in JJAS (purple) and tropical Pacific zonal anomalous wind stress in JASO (green) from the Extended Maximum Covariance Analysis (EMMCA) applied for the total period 1872-2001 (from Martín-Rey et al. 2014). The 20-yr moving correlation between both coefficients is also presented, (orange line), in which significant correlation scores are shown in dots.

These anomalous changes in z20 would modify the vertical stratification and favour the development of the SST anomalies (Figure 2g,i). The hindcast is also able to reproduce an ENSO-like pattern during DJFM season, characterized by the central-eastern equatorial tongue (Figure 2j,l). On the contrary, for the period 1939-1966 (central panels in figure 2), no significant correlation scores are found between observed and predicted tropical Pacific variables, thus there is not ENSO predictability from Tropical Atlantic SST for those years. These results imply that the Tropical Atlantic SST in JJAS is able to predict wind stress over western and eastern Pacific in JASO, which in turn will transfer this variability to the thermocline depth and SST in DJFM at the beginning and end of the 20th century, but not in the decades in-between. After describing the good skill of the hindcast in

reproducing the spatial structure of the variables involved in the Atlantic-forced ENSO, the time evolution of the observed and predicted Pacific variables is also evaluated (Figure 3). According with Polo et al. [2015], anomalous surface wind in western Pacific is crucial for triggering the Kelvin wave, which propagates eastward changing the vertical structure of the ocean and activating the thermocline feedbacks responsible for the creation of ENSO SSTs anomalies. For this reason, the following key variables for the development of the Atlantic-forced ENSO have been chosen in specific regions: zonal wind stress in western Pacific [120°E-160W°, 15°N-15°S], central Pacific z20 [180°-130°W; 5°N-5°S] and SST in the central-eastern equatorial Pacific [180°-80°W, 5°N-5°S] (yellow boxes in Figure 2). The time evolution of the anomalous zonal wind stress and thermocline depth during JASO season is well reproduced by the cross-validated hindcast for the first and last decades of the 20th century (Figure 3a-b and Tables S1-S2 in the supplementary material). Notice that, despite the model's ability to simulate the amplitude of the JASO zonal wind stress and thermocline depth for the three periods, the correlation scores rise and become significant only during 1871-1938 and 1967-2007, with small root mean square errors (Figure 3 and Tables S2-S4). For the equatorial SST, the predicted amplitude and time evolution coincides with the observed one in the period 1970-2001, nevertheless the correlation score decreases during the first decades of the 20th century (Figure 3c and Tables S1-S2 from the supplementary material). These results indicate that JASO wind stress is the key variable for the understanding of the Pacific response to the tropical Atlantic influence. An important aspect to take into account is that the RMSE decreases for all the predicted variables during the first decades of the 20th century and after the 1970s (Figure 3 and Table S4), indicating the goodness of the hindcast to simulate ENSO-associated variables during those periods. For the period 1939-1966, the prediction fails: higher discrepancies are found between the time evolution and amplitude of the predicted and observed variables, given rise to no significant correlation scores (solid black and green lines, Figure 3 and Table S1 from the supplementary material). In summary, the tropical Pacific wind stress, thermocline depth and SST related to the Pacific response from an Atlantic influence are well simulated by the model during the first and last decades of the 20th century, but not during the period 1939-1966, confirming the non-stationarity influence of the Tropical Atlantic SSTs on ENSO. For this reason, hereafter, we will focus on those periods with significant correlation skill, in which the Atlantic SSTs can act as a precursor of ENSO.

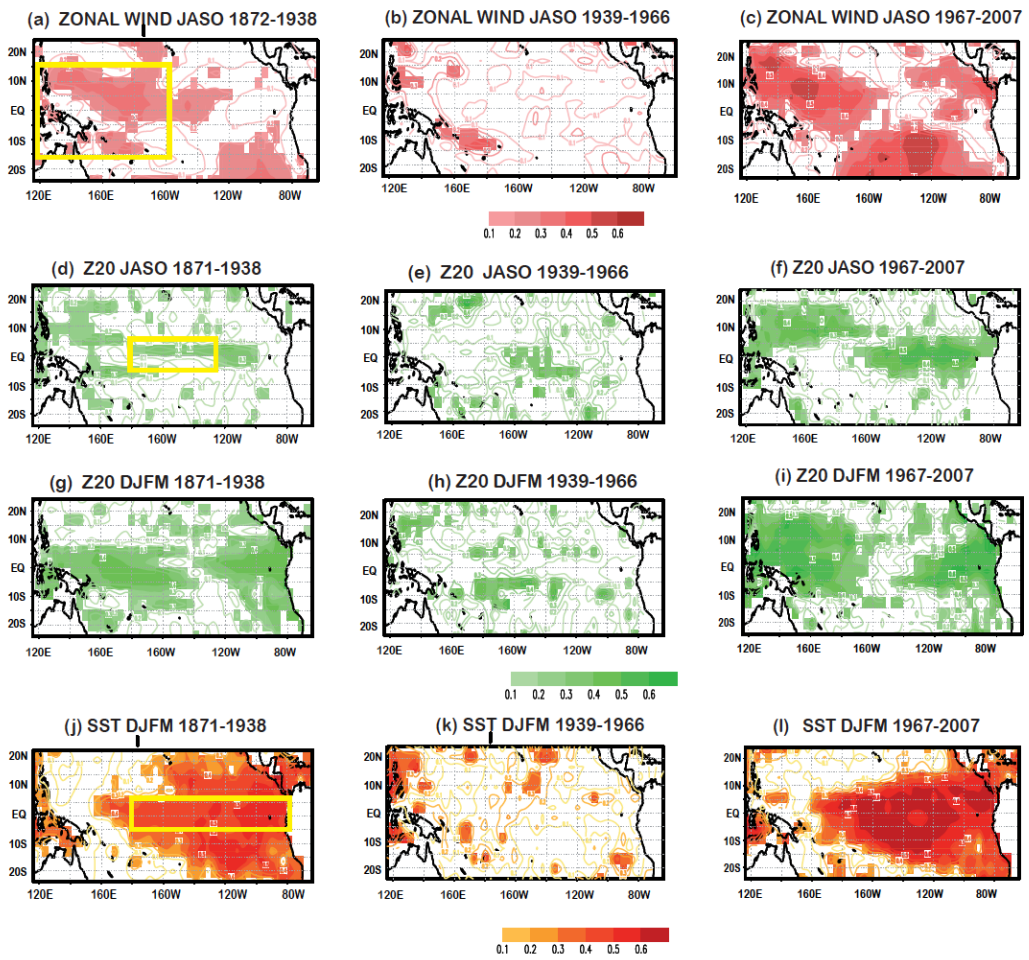

Figure 2. Correlation maps between observed and predicted variables over Tropical Pacific (a-l) Correlation maps between the observed and predicted zonal wind stress in JASO (a-c), JASO-DJFM thermocline depth (d-i) and DJFM SST (j-l); for the periods 1871-1933 (left pannels), 1934-1969 (central pannels) and 1970-2001 (right pannels). Significant values exceeding 90% confidence level according to a Monte Carlo test are presented in shaded.

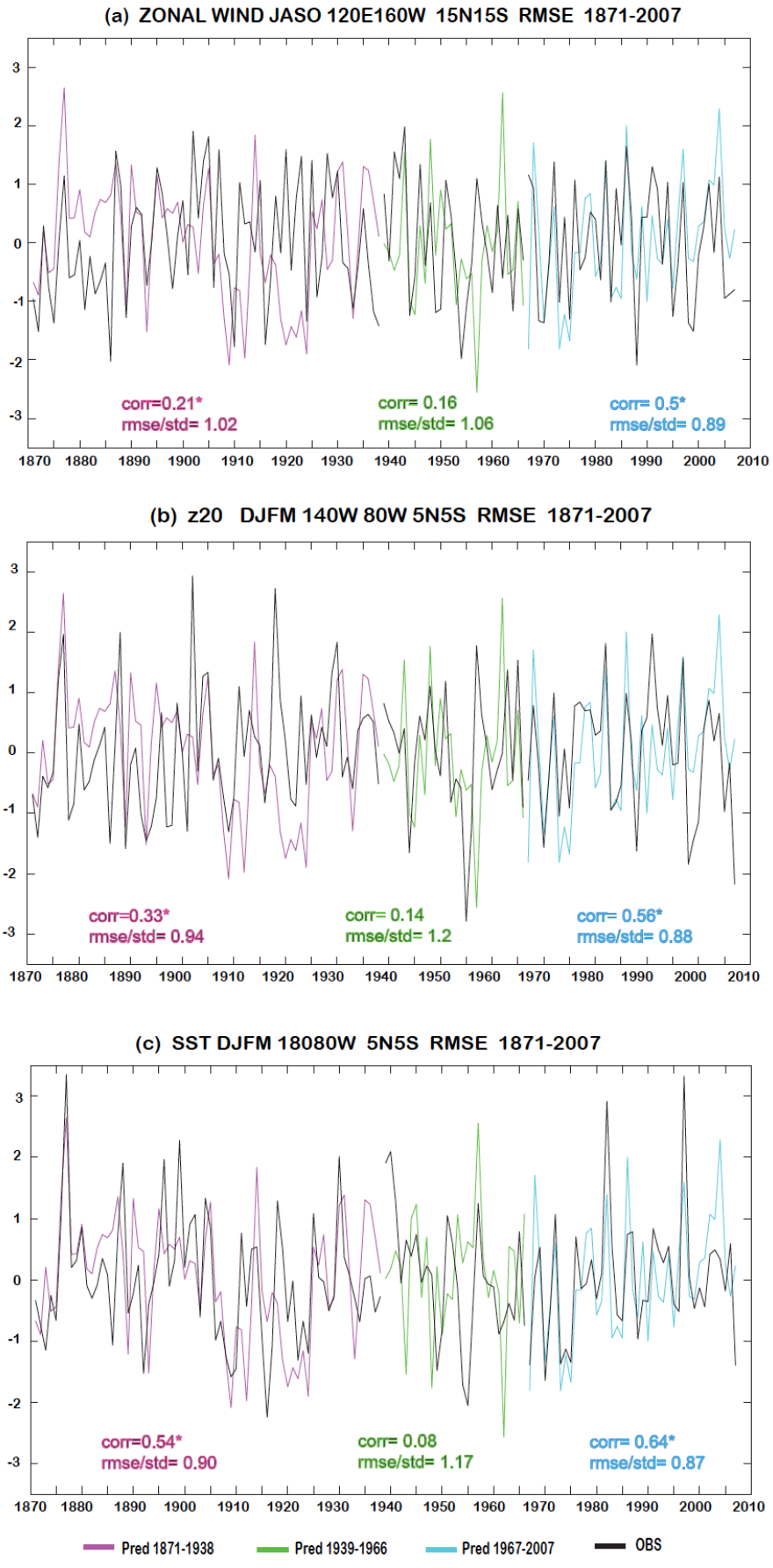
(a) ZONAL WIND JASO 120E160W 15N15S RMSE 1871-2007
corr=0.21*
rmse/std= 1.02
corr= 0.16
rmse/std= 1.06
corr= 0.5*
rmse/std= 0.89
(b) z20 DJFM 140W 80W 5N5S RMSE 1871-2007
corr=0.33*
rmse/std= 0.94
corr= 0.14
rmse/std= 1.2
corr= 0.56*
rmse/std= 0.88
(c) SST DJFM 18080W 5N5S RMSE 1871-2007
corr=0.54*
rmse/std= 0.90
corr= 0.08
rmse/std= 1.17
corr= 0.64*
rmse/std= 0.87
Pred 1871-1938
Pred 1939-1966
Pred 1967-2007
OBS

Figure 3: Temporal evolution of the predicted ENSO (a-c) Observed and predicted zonal wind in JASO ofwestern Pacific [120E-160W, 15N15S], z20 in JASO in central Pacific [180°-130°W; 5°N-5°S and SST in DJFM in central-eastern equatorial Pacific [180°-80°W, 5°N-5°S] for the period 1871-2001. Observations are plotted in black lines and the predicted variables have been calculated using the regression coefficient of the model (Psi) for each of the three periods of study: 1871-1933 (pink line), 1934-1969 (green line) and 1970-2001 (blue line). The correlation scores and RMSE/std for each period is also indicated.

Atlantic and Pacific El Niño events have been selected from the standardized expansion coefficient of tropical Atlantic SST in JJAS months and the observed and predicted Niño3 index in DJFM (Figure S1, supplementary material). The impact of Atlantic Niñas and Niños on ENSO phenomena have been analysed separately to investigate possible non-linearities in the inter-basin connection.

The following observed Pacific La Niña events (Niño3 index lower than -0.5 std) preceded by an Atlantic Niño during previous JJAS season, and also predicted by the model, have been selected for the composite: 1889, 1893, 1909, 1912, 1924, 1933, 1973, 1983, 1984, 1995 and 1998. Notice that, only those episodes occurred during the first and last decades of the 20th century, when the Atlantic-Pacific connection is established, have been chosen (Figure S1a). The Atlantic Niños are characterized by an extended band of positive SST anomalies covering the entire equatorial Atlantic region [40°W-20°E, 5°N-5°S] during JJAS (Figure 4a-h). Associated with this Atlantic warming, anomalous easterlies appear in western Pacific as part of the surface wind divergence in the centre of the basin (Figure 4a,e). As a result of these anomalous winds, a shallower z20 in the central Pacific [150°W-120°W] appears during JASO season, propagating eastward in agreement with a Kelvin wave, resembling a zonal seesaw pattern of z20 anomalies in the equatorial Pacific during DJFM (Figure 4b-c and 4f-g). This spatial configuration is associated with the eastward upwelling Kelvin wave and westward downwelling Rossby wave propagation from JASO to DJFM seasons . Finally, the characteristic cold tongue of La Niña event [180°-90°W, 5°N-5°S] is completely developed during DJFM months (Figure 4d,h) through the activation of the thermocline feedbacks (according with Polo et al. [2015]). Following the same criteria as for the selection of Atlantic Niños, 10 Atlantic Niña-Pacific El Niño years have been chosen: 1880, 1882, 1887, 1890, 1902, 1914, 1922, 1982, 1989, 1994 and 1997. Notice that the strongest El Niño events, which occurred during the last 20 years (1982 and 1997) are well captured by the hindcast (Figure S1b). Anomalous cooling over equatorial Atlantic is associated with an anomalous wind convergence in the central-east Pacific [140°W-120°W] in JASO (Figure 4i,m), which is able to trigger a Kelvin wave propagating eastward during the following months (Figure 4j,n). El Niño-like pattern of SST anomalies, together with an east-west gradient of anomalous z20 is shown DJFMs (Figure 4k-l, o-p).

Almost half of the events (5 over 11, for predicted and observed positive Atlantic events and 5 over 11 for negative Atlantic events) resemble the mechanism of the Atlantic-Pacific

connection described in Polo et al. [2015]. For the periods with significant correlation skill, the hindcast shows that around 40% of the Atlantic Niños (Niñas) impact on the Pacific La Niña (El Niño) episodes during the next winter. (Table S5-S8, supplementary material). Moreover, the number of Atlantic-Pacific episodes simulated by the hindcast is higher than those shown in observations, suggesting that, a percentage of the observed Atlantic-forced ENSO phenomena can be also influenced by other external contributions. In this sense, extra-tropical atmospheric and oceanic variability from North Pacific and north tropical Atlantic SSTs could modulate the wind variability in western equatorial Pacific, favouring the development of ENSO phenomena [Vimont et al., 2001, 2003; Ham et al., 2013a; Boschat et al., 2013] and enhancing their prediction [Dayan et al., 2013]. The influence of the Indian Ocean on ENSO phenomena has been also reported [Terray and Dominiak, 2005; Izumo et al., 2010, 2014]. The previously mentioned extra-tropical and tropical contributions could be interfering with the Atlantic forcing in the tropical Pacific basin, modulating the occurrence of ENSO episodes.

Notice that, although the running-correlation between the expansion coefficients of the predictor and predictand files indicate that the Atlantic-Pacific connection is active from the late 1960s (orange line, Figure 1), the analysis of the individual events reveals that during the period 2000-2007, the tropical Atlantic SSTs is not able to predict the ENSO phenomena (Figure S1). The Atlantic influence on ENSO verifies the "recharge-oscillator" and the "delayed-oscillator" theories, since it involves the pilling of warm waters to the west due to anomalous winds in the central Pacific, which trigger a oceanic Kelvin wave propagating to the east. This lack of predictability during recent decades is in agreement with McPhaden et al. (2012), which have demonstrated the weakened relationship between the Warm Water Volumen (WWV) and ENSO in the 21st century.

4. Summary and discussion

The potential role of the Tropical Atlantic SST in predicting ENSO phenomena has been investigated, based on previous studies showing the enhancement of ENSO development due to the inter-annual Atlantic variability. The results shed light on the decadal differences in the statistical prediction due to the modulation of the inter-basin relationship discussed in Martín-Rey et al. [2014].

In the present study it has been demonstrated that:

- A statistical hindcast for ENSO phenomena that considers the boreal summer (JJAS) tropical Atlantic SSTs as the predictor field is able to reproduce the Pacific variables involved in ENSO development. This is in agreement with the proposed air-sea mechanism of the Atlantic-Pacific connection [Rodríguez-Fonseca et al. 2009; Ding et al. 2012; Martín-Rey et al. 2014; Polo et al. 2015].

- The Atlantic SSTs act as a precursor for ENSO episodes only during the first and last decades of the 20th century.

- The hindcast fails in simulating the Pacific variables during the period 1939-1966, putting forward the lack of ENSO predictability from Tropical Atlantic SST during those decades.

- For those periods with a predictive skill, the statistical hindcast tends to predict larger SST anomalies in ENSO phenomena than in observations, showing also a stronger signal in the wind stress and thermocline depth fields.

- Summer (JASO) surface wind in the western Pacific seems to be the key variable in the development of ENSO events associated with the Atlantic remote forcing.

The present study implies a step forward in the understanding of ENSO predictability. Firstly, a new methodology has been applied to predict ENSO phenomena. Secondly, it has been demonstrated for the first time that the skill of the ENSO forecast based on the tropical Atlantic SSTs depends on the decades considered. The skill of ENSO prediction, using the JJAS tropical Atlantic SSTs as predictor, increases and becomes significant during the first and last decades of the 20th century, when the Atlantic-Pacific connection takes place. This multidecadal modulation could be associated with decadal patterns of oceanic variability, which in turn, modify the background state of the Atlantic and Pacific Oceans, favouring the inter-basin link. In this sense, previous studies have suggested that the Atlantic Multidecadal Oscillation (AMO) could modulate the Atlantic-Pacific connection through the enhancement of the convection over the western equatorial Atlantic and the increase of the oceanic variability in the eastern equatorial Pacific (Martín-Rey et al. 2014; Polo et al. 2015). Furthermore, López-Parages and Rodríguez-Fonseca (2012) proposed that apart from the AMO, the Pacific Decadal Oscillation (PDO) could drive the changes in ENSO teleconnections at multidecadal time scales. Additionally, Kucharski et al. (2011) relied on that the global warming (GW) induces a warmer tropical Atlantic that could alter the Walker circulation, modifying the oceanic feedbacks in the tropical Pacific, given rise to a La Niña-like SST pattern.

Following the above mentioned studies, the running correlation of the expansion coefficients for the tropical Atlantic SST and tropical Pacific zonal wind (as an indicator of the Atlantic-Pacific connection) has been compared with AMO, Intertropical Pacific Oscillation (IPO) and GW indexes (Figure S2). The Atlantic-Pacific mode appears during negative phases of the AMO, these decades also coincide with positive IPO phases.

Figure 4: Spatial structure of the Atlantic-forced ENSO.(a-h) Composite of the observed Atlantic Niño events and observed and predicted Pacific variables related to a Pacific La Niña: wind stress in JASO (a, e), z20 in JASO-DJFM (b-c,f-g) and SST in DJFM (d,h). Regions where 12 of the 15 events agree in sign are presented in black vectors and shaded. **(i-p)** Same as (a-h) but for the Atlantic Niña events and observed and predicted Pacific variables for a Pacific El Niño. Regions where 8 of the 10 events agree are shown in black vectors and shaded areas.

Atlantic Niños -Pacific Niñas

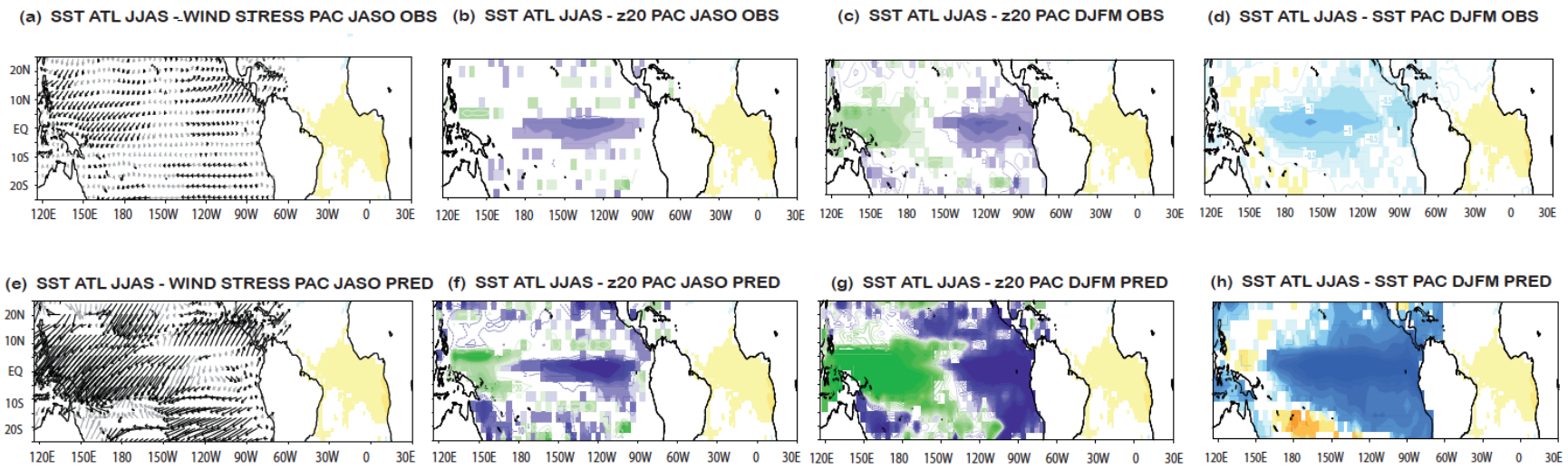

Atlantic Niñas -Pacific Niños

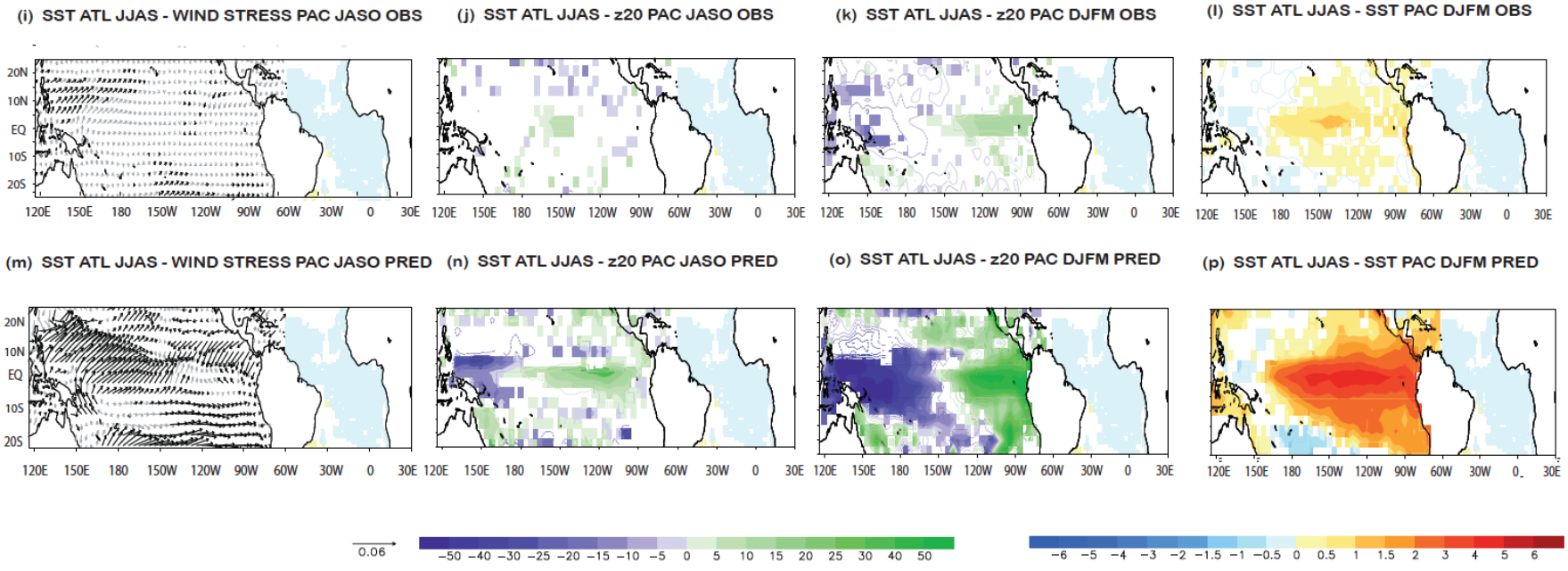

This result suggests that warmer SST conditions in the southern oceans could favour the inter-basin link. Furthermore, the positive temperature trend of the GW during the last decades could enhance the warming in the tropics, setting up the oceanic conditions needed to trigger the Atlantic-Pacific connection.

The forecast of ENSO still remains a challenge for the scientific community, since the current state-of-the-art coupled models are not able to show a realistic representation of ENSO amplitude, spatial structure and transition between phases (Guilyardi 2004; 2009). The present results put forward that the correct simulation of the Atlantic variability, from seasonal to decadal time scales, is crucial for a realistic ENSO prediction. Nevertheless, General Circulation Models (GCMs) have important biases in reproducing the tropical Atlantic climate. Current deficiencies of most of the state-of-the-art climate models in forecasting ENSO events could be associated with the equatorial Atlantic bias. In this sense, a European Project PREFACE (Enhancing PREdiction oF tropical Atlantic ClimatE and its impacts) has been funded with the aim of enhancing the prediction of tropical Atlantic and its impacts by reducing the bias of current state of the art coupled models. Finally, further investigation would be needed in order to properly attribute ENSO predictors during positive AMO phases.

Acknowledgements

The data for this paper come from different datasets: the wind stress and oceanic variables are taken from version 2.2.4 of SODA reanalysis (http://iridl.ldeo.columbia.edu/SOURCES/.CARTON-GIESE/.SODA/.v2p0p2-4/) and from the MetOffice dataset (HadISST, http://www.metoffice.gov.uk/hadobs/). The atmospheric variables come from the 20th reanalysis (http://www.esrl.noaa.gov/psd/data/20thC_Rean/).

This study was supported by the European project PREFACE (ref.603521) and the Spanish MINNECO project CGL2012-38923-C02-01.

References

Alexander, M. A., I. Bladé, M. Newman, J.R. Lanzante, N. C. Lau and J. D. Scott (2002), The atmospheric bridge: The influence of ENSO teleconnections on air-sea interaction over the global oceans, J. Clim., 15(16), 2205-2231.

Bjerknes, J. (1969), Atmospheric teleconnections from the equatorial Pacific, Mon. Weather Rev., 97,163-72

Boschat, G., P. Terray and S. Masson (2013), Extratropical forcing of ENSO. Geophys. Res. Lett., 40(8),1605-1611, doi: 10.1002/grl.50229

Clarke, A. J., and S. Van Gorder (2003), Improving El Niño prediction using a space-time integration of Indo-Pacific winds and equatorial Pacific upper ocean heat content, Geophys. Res. Lett., 30(7), doi: 10.1029/2002GL016673

Compo, G. P., et al. (2011), The Twentieth Century Reanalysis Project, Q. J. R. Meteorol. Soc. 137,1–28.

Dayan, H., J. Vialard, T. Izumo and M. Lengaigne (2013), Does sea surface temperature outside the tropical Pacific

contribute to enhanced ENSO predictability?, Clim. Dyn., 43(5-6), 1311-1325, doi: 10.1007/s00382-013-1946-y

Ding, H., N. S. Keenlyside and M. Latif (2012) Impact of the Equatorial Atlantic on the El Niño Southern Oscillation, Clim. Dyn., 38(9-10), 1965-1972, doi: 10.1007/s00382-011-1097-y.

Frauen, C., and D. Dommenget (2012), Influences of the tropical Indian and Atlantic Oceans on the predictability of ENSO, Geophys. Res. Lett., 39, L02706, doi:10.1029/2011GL050520.

Giese, B. S., and S. Ray (2011), El Niño variability in simple ocean data assimilation (SODA), 1871–2008, J. Geophys. R. Oceans (1978–2012), 116(C2), doi: 10.1029/2010JC006695.

Guilyardi, E., et al. (2004), Representing El Niño in coupled ocean-atmosphere GCMs: the dominant role of the atmospheric component, J. Climate, 17(24), 4623-4629.

Guilyardi, E., P. Braconnot, F. F. Jin, S. T. Kim, M. Kolasinski, T. Li, and I. Musat (2009), Atmosphere feedbacks during ENSO in a coupled GCM with a modified atmospheric convection scheme, J. Clim., 22(21), 5698-5718.

Ham, Y. G., J. S. Kug, J. Y. Park and F. F. Jin (2013a), Sea surface temperature in the north tropical Atlantic as a trigger for El Niño/Southern Oscillation events, Nature Geoscience, 6,112–116.

Ham, Y. G., J. S. Kug and J. Y. Park (2013), Two distinct roles of Atlantic SSTs in ENSO variability: north Tropical Atlantic SST and Atlantic Niño, Geophys. Res. Lett., 40(15), 4012-4017.

Izumo, T., et al. (2010), Influence of the state of the Indian Ocean Dipole on the following year's El Niño, Nature Geoscience, 3(3), 168-172.

Izumo, T., M. Lengaigne, J. Vialard, J. J. Luo, T. Yamagata and G. Madec (2014), Influence of Indian Ocean Dipole and Pacific recharge on following year's El Niño: interdecadal robustness, Clim. Dyn., 42(1-2), 291-310.

Jansen, M. F., D. Dommenget, and N. Keenlyside (2009), Tropical atmosphere-ocean interactions in a conceptual framework, J. Clim., 22(3), 550-567.

Jin, F. F. (1997a), An equatorial recharge paradigm for ENSO. Part I: Conceptual model, J. Atmos. Sci., 54,811-829.

Jin, F. F. (1997b), An equatorial recharge paradigm for ENSO. Part II: A stripped-down coupled model, J. Atmos. Sci., 54, 830–845.

Keenlyside, N. S., and M. Latif (2007), Understanding equatorial Atlantic interannual variability, J. Clim., 20(1), 131-142.

Keenlyside N. S., H. Ding and M. Latif (2013), Potential of equatorial atlantic variability to enhance El Niño prediction, Geophys. Res.Lett., 40(10), 2278-2283, doi : 10.1002/grl.50362

Klein, S. A., B. J. Soden and N. C. Lau (1999), Remote sea surface temperature variations during ENSO: Evidence for a tropical atmospheric bridge, J. Clim., 12(4), 917-932.

Latif, M., et al. (1994). A review of ENSO prediction studies. Clim. Dyn., 9(4-5), 167-179.

Losada, T., B. Rodríguez-Fonseca, I. Polo, S. Janicot, S. Gervois, F. Chauvin, P. Ruti (2010), Tropical response to the Atlantic Equatorial mode: AGCM multimodel approach, Clim. Dyn., 5, 45-52.

Martín-Rey, M., I. Polo, B. Rodríguez-Fonseca and F. Kucharski (2012), Changes in the interannual variability of the tropical Pacific as a response to an equatorial Atlantic forcing, Sci. Mar., 76 (S1), doi: 10.3989/scimar.03610.19A

Martín-Rey, M., B. Rodríguez-Fonseca, I. Polo and F. Kucharski (2014), On the Atlantic-Pacific Niños connection: A multidecadal modulated mode, Clim. Dyn., doi: 10.1007/s00382-014-2305-3.

McCreary, J. P. (1983), A model of tropical ocean-atmosphere interaction, Mon. Wea. Rev., 111(2), 370-387.

McPhaden, M. J., et al. (1998), The Tropical Ocean-Global Atmosphere observing system: A decade of progress, J. Geophys.Res.Oceans (1978–2012), 103(C7), 14169-14240.

McPhaden, M. J., S. E. Zebiak and M. H. Glantz (2006a). ENSO as an integrating concept in earth science, Science, 314(5806), 1740-1745.

McPhaden, M., X. Zhang, H. Hendon, and M. Wheeler (2006b), Large scale dynamics and MJO forcing of ENSO variability, Geophys. Res. Lett., 33 L16702.

Neelin, J. D., D. S. Battisti, A. C. Hirst, F. F. Jin, Y. Wakata, T. Yamagata, and S. E. Zebiak (1998), ENSO theory, J. Geophys. Res. Ocea. (1978–2012), 103(C7), 14261-14290.

Philander, S. G. (1990), El Niño, La Niña, and the Southern Oscillation, Academic Press, San Diego, 46, ISBN 0125532350.

Polo, I., B. Rodríguez-Fonseca, T. Losada, and J. García-Serrano (2008), Tropical Atlantic Variability modes (1979-2002), Part I: time-evolving SST modes related to West African rainfall, J. Clim., 21(24), 6457-6475.

Polo I., M. Martín-Rey, B. Rodríguez-Fonseca, F. Kucharski and C. R. Mechoso (2015) Processes in the Pacific La Niña onset triggered by the Atlantic Niño, Clim.Dyn., 44, 115–131 DOI 10.1007/s00382-014-2354-7.

Rayner, N. A., D. E. Parker, E. B. Horton, C. K. Folland, L. V. Alexander, D. P. Rowell, E. C. Kent, A. Kaplan (2003), Globally complete analyses of sea surface temperature, sea ice and night marine air temperature, 1871-2000, J. Geophys. Res., 108, 4407.

Rodríguez-Fonseca, B., I. Polo, J. García-Serrano, T. Losada, E. Mohino, C. R. Mechoso and F. Kucharski (2009), Are Atlantic Niños enhancing Pacific ENSO events in recent decades?, Geophys. Res. Lett., 36, L20705.

Sasaki, W., T. Doi, K. J. Richards and Y. Masumoto (2014), Impact of the equatorial Atlantic sea surface temperature on the tropical Pacific in a CGCM, Clim. Dyn., 1-14.

Suarez, M. J., and P. S. Schopf (1988), A delayed action oscillator for ENSO, J. Atmos. Sci.,5 (45), 3283-3287.

Terray, P., and S. Dominiak (2005). Indian Ocean sea surface temperature and El Nino-Southern Oscillation: A new perspective, J. Clim., 18(9), 1351-1368.

Vimont, D. J., D. S. Battisti, and A. C. Hirst, A. C. (2001), Footprinting: A seasonal connection between the tropics and mid-latitudes, Geophys. Res. Lett., 28(20), 3923-3926.

Vimont, D. J., Wallace, J. M. And D. S. Battisti (2003), The seasonal footprinting mechanism in the Pacific: implications for ENSO*, J. Clim., 16(16), 2668-2675.

Walker, G. T. (1924), World Weather II, .Mem.Indian Meteorol Dep, 24,275-332

Wyrtki, K. (1975). El Niño-The dynamic response of the equatorial Pacific oceanto atmospheric forcing, J. Phys. Ocea., 5(4), 572-584.

Wyrtki, K. (1985). Water displacements in the Pacific and the genesis of El Niño cycles, J. Geophys. Res. Ocea. (1978–2012), 90(C4), 7129-7132.

Zebiak, S. E. (1993), Air-sea interaction in the equatorial Atlantic region, J. Clim., 6,1567-1586.

6.5. Study of the air-sea interactions associated with the development of the Atlantic Niño

(Martín-Rey et al. 2015b; Martín-Rey et al. 2015c)

In this section the air-sea processes involved in the development of the Atlantic Niño pattern have been explored, in the framework of the Objectives 4 and 5 of the present thesis.

Taking into account the possible modulation of the Atlantic Niño teleconnections due to the AMO, different periods of study associated with positive and negative AMO phases has been considered. A unique Atlantic Niño pattern appears as the leading mode of the tropical Atlantic SST variability during positive AMO periods. However, two different Atlantic Niño patterns co-exist in the tropical Atlantic basin during negative phases of the AMO. The first mode presents a general warming of the entire tropical Atlantic, denoted Basin-Wide (BW-) Atlantic Niño, while the second mode is characterized by an equatorial warming flanked by negative SST anomalies in north and south tropical Atlantic. It is denoted as Canonical (C-) Atlantic Niño. The BW- and C- Atlantic Niño coincide with those patterns associated with different climate teleconnections during the last decades.

An inter-annual simulation with the tropical Atlantic configuration of NEMO model, shows that the BW-Atlantic Niño is preceded by a weakening of both Azores and Sta Helena High during previous winter and spring that induce a reduction of the northern and southern trades, together with an anomalous wind convergence at the equatorial band. On the other hand, an initial strengthening of Azores and Sta Helena High evolves into a zonal SLP gradient, which reinforces the north-eastern and south-eastern trades and creates anomalous westerly winds along the equator.

These anomalous wind forcings activate different oceanic mechanisms. For a BW- Atlantic Niño, the net heat fluxes and vertical terms contribute to generate the subtropical SST anomalies during

winter months, while the anomalos convergence of the currents at the equator in spring, deepen the thermocline, activating the vertical terms and thus warming the equatorial band.

The development of the cold horseshoe of the C-Atlantic Niño during winter months is entirely attributed to the net heat fluxes. Strong westerly winds from winter to spring induce an anomalous convergence of the currents, deepening the thermocline and reducing the entrainment and vertical advection, contributing in this way to warm the equatorial band. Equatorial wave activity also seems to exist during the onset and development of the BW- and C-Atlantic Niño phenomena, associated with local wind forcing or the reflection of Rossby waves triggered out of the equator.

Two different configuration of the Atlantic Niño phenomenon under negative AMO phases

MARTA MARTÍN-REY
IGEO (UCM-CSIC)
Departamento de Geofísica y Meteorología, UCM, Madrid,Spain

IRENE POLO
Department of Meteorology, University of Reading, UK

BELÉN RODRÍGUEZ-FONSECA
IGEO (UCM-CSIC)
Departamento de Geofísica y Meteorología, UCM, Madrid,Spain

ALBAN LAZAR
LOCEAN-IPSL, UPMC, Paris,France

(to be submitted)

Abstract

An air-sea coupled mode of inter-annual variability akin to ENSO emerges in the tropical Atlantic basin, named as Atlantic Niño. Although the Atlantic Niño is considered as the oceanic response of weakened zonal winds over western equatorial Atlantic, some studies have highlighted the important role of Sta Helena High and oceanic waves in triggering this phenomenon. Here, we demonstrate that two different Atlantic Niño patterns coexist in the tropical Atlantic basin during some decades characterized by a negative phase of the Atlantic Multidecadal Oscillation (AMO): one characterized by positive SST anomalies covering the entire tropical Atlantic (Basin Wide mode), and another one characterized by an equatorial warming flanked by negative SST anomalies in north and south Tropical Atlantic. The BW-Atlantic Niño is preceded by a weakening of both Azores and Sta Helena High, inducing a general reduction of the tropical trades and anomalous wind convergence in the equatorial band. The C-Atlantic Niño is associated with a strengthening of Azores and Sta Helena High during previous autumn that evolves in a zonal equatorial Sea Level Pressure (SLP) gradient, generating anomalous westerlies in the equatorial band. For both phenomena, the subtropical SST anomalies are created by net heat fluxes, although the vertical terms also contribute for a BW-Atlantic Niño pattern. The development of the equatorial warm tongue is mainly attributed to vertical terms, activated by different wind forcings for the C- and BW-Atlantic Niño events. Additional Turbulent heat fluxes are contributing to the warming in BW-Atlantic in previous winter. Propagation of Kelvin waves along the equatorial band, forced by local winds or subtropical Rossby waves could be playing a role in the development of BW- and C-Atlantic Niños
.

1. Introduction

An air-sea coupled mode of inter-annual variability akin to El Niño-Southern Oscillation (ENSO) emerges in the tropical Atlantic basin, named as Atlantic Niño [*Merle*, 1980; *Zebiak*, 1993]. This mode is characterized by a relaxation of the climatological trade

winds, which produces a zonal redistribution of the warm waters and heat content in the equatorial band, reducing the thermocline slope [*Carton and Huang*, 1994; *Carton et al*., 1996; *Ruiz-Barradas et al*., 2000; *Vauclair and du Penhoat*, 2001]. Warm SST anomalies are developed along the equator, on the eastern side of the basin, together with an anomalous convergence of the trade winds over the warmest region [*Zebiak*, 1993]. The ITCZ shifts southward, enhancing the convection and rainfall over the entire equatorial band [*Carton and Huang*, 1994]. Contrasting to ENSO, the Atlantic Niño peaks in boreal summer [*Carton and Huang*, 1994; *Hurrell et al*., 2006] and has smaller amplitudes and periods than its Pacific counterpart [*Latif*, 2001; *Kushnir et al*., 2003;].

Atlantic Niño seems to be developed and maintained by the Bjerknes feedback although weaker than ENSO [*Bjerknes*, 1969; Zebiak, 1993; *Keenlyside and Latif*, 2007]. However, other processes such as oceanic waves and heat fluxes could be also playing a role [*Latif*, 2001; Hormann and Brandt, 2009; *Polo et al*., 2008a;b; *Lübbecke et al*., 2010; Namchi et al. 2011].

The Atlantic Niño phenomenon is able to modulate the climate of adjacent and remote areas through atmospheric teleconnections. The Atlantic Niño has a strong impact on the West African Monsoon (WAM) system. Thus, a warming in the equatorial Atlantic produces lower ocean-land SLP gradient that inhibits the northward displacement of the ITCZ, weakening the monsoon circulation [*Losada et al*., 2010a]. This modification of the atmospheric circulation gives rise to a dipolar precipitation pattern over WA, characterized by increased rainfall over the Gulf of Guinea (GG) and a reduction of the precipitation in the Sahelian region [*Janicot*, 1992; *Lamb*, 1978; *Losada et al*., 2010b; *Polo et al*., 2008a; *Rowell et al*., 1995; *Wagner and da Silva*, 1994; *Ward*, 1998].

The Atlantic Niño has also a strong impact on the rainfall variability over Brazil (*Kushnir et al*., 2003). Together with the impacts in the surrounding areas, teleconnections with the Indian Ocean and the Indo-Pacific thought changes in the walker circulation (*Kucharski et al*., 2009; Rodriguez-Fonseca et al., 2009) and extratropical teleconnections through Rossby waves have been also reported (Garcia-Serrano et al., 2008; Losada et al., 2012; Garcia-Serrano et al., 2013)

Teleconnections of the Atlantic Niño phenomenon have been found to be stronger over the last decades: The inter-annual variability of the tropical Atlantic and Pacific SSTs are connected after the 1970s, in a way that, a summer Atlantic Niño favours the development of a Pacific La Niña during next winter [*Keenlyside and Latif*, 2007; *Polo et al*., 2008a; *Rodríguez-Fonseca et al*., 2009] through an alteration of the Walker circulation [*Rodríguez-Fonseca et al*., 2009; *Losada et al*., 2010b; *Ding et al*., 2012; Polo et al., 2015a]. Recently, *Martín-Rey et al*. [2014] have demonstrated that this Atlantic-Pacific Niños connection takes part of an air-sea coupled mode of tropical variability that only shows up during negative phases of the Atlantic Multidecadal Oscillation (AMO). This multidecadal modulation has opened windows of opportunity to predict El Niño episodes from the tropical Atlantic SSTs during previous summer [*Martín-Rey et al*., 2015a].

A striking point in the recent modification of the Atlantic Niño impacts is the concomitant alteration of its spatial structure. Before the 1970s, the Atlantic Niño is characterized by an anomalous warming in the eastern equatorial Atlantic flanked by a horseshoe of negative SST anomalies in north and south tropical Atlantic [*Rodríguez-Fonseca et al*., 2009; *Losada et al*., 2012]. Nevertheless, after the 1970s, the Atlantic Niño presents a general warming covering the entire tropical Atlantic basin [*Polo et al*., 2008a; *Rodríguez-Fonseca et al*., 2009; *Losada et al*., 2010b; *Mohino et al*., 2011; *Losada et al*., 2012a; *Martín-Rey et al*., 2012; *Martín-Rey et al*., 2014; *Polo et al*., 2015a]. Impacts associated with this different configuration have been addressed in a recent study in which changes in the associated teleconnections have been determined [*Losada and Rodriguez-Fonseca*, 2015]. The change in the Atlantic Niño pattern suggests that different atmospheric forcings and oceanic processes could contribute to its development. Previous studies have demonstrated that a weakening of Sta Helena High precedes an Atlantic Niño episode. Negative Sea Level Pressure (SLP) anomalies induce a reduction of the south tropical trades, modifying the air-sea processes and favouring the warming of the equatorial Atlantic [Polo et al., 2008a; Lübbecke et al., 2010; Richter et al., 2010; Lübbecke and McPhaden, 2013]. Furthermore, these authors have indicated that oceanic waves could modify both, the zonal currents and the vertical stratification of the equatorial Atlantic, activating the oceanic processes relevant for the development and decay of the Atlantic Niño [Florenchie et al., 2003; Polo et al., 2008a; Hormann and Brandt, 2009; Lübbecke et al., 2010;]. On the one hand, *Polo et al*. [2008a] showed that the Atlantic Niño SST pattern is originated in the Angola-Benguela upwelling area due to alongshore winds, while the Kelvin waves could play an important role in the decay of the Atlantic Niño phenomenon. On the other hand, *Lübbecke et al*. [2010] in agreement with Florenchie et al. (2003) pointed out that the development of the Atlantic Niño is driven by the propagation of a Kelvin wave along the equator and South African coast triggered by anomalous westerly winds in west equatorial Atlantic. In contrast, other authors have suggested that the Atlantic Niño pattern could be also carried out through the advection of warmer SST anomalies from north tropical Atlantic to the equatorial band [*Richter et al*., 2014]. Thus, the air-sea interactions and oceanic wave activity associated with the development of the Atlantic Niño events remain unclear.

The present study will study the oceanic and atmospheric processes involved in the different Atlantic Niño patterns during recent decades. The possible contribution of the oceanic waves will be also evaluated.

The manuscript is organized in the following way. In Sect. 2 data and methodology used are described. The main results are presented in Sect. 3. In Sect. 3.1 the dominant modes of tropical Atlantic inter-annual SST variability are determined. The atmospheric forcings and the oceanic processes related to the development of these modes are analysed in Sect. 3.2 and Sect. 3.3. In Sect. 3.4 the possible role of the oceanic waves in triggering the Atlantic Niño is explored. Finally, the discussion and conclusions are presented in Sect. 4.

2. Data and methodology

Observations and reanalysis

In the present study data from observations and reanalysis have been used. The observed SSTs come from the HadISST dataset [*Rayner et al*., 2003], while the SLP is taken from the NCAR 20th century reanalysis [*Compo et al*., 2011]. The period considered goes from 1960 to 2011.

Model simulations

In order to investigate the air-sea interactions associated with the development of the Atlantic Niños, an inter-annual simulation with a regional configuration of NEMO (Nucleus for European Modelling of the Ocean) model has been used. The NEMO OGCM [*Madec*, 2008] is adapted to the tropical Atlantic basin [30°N-30°S], gives rise to the regional configuration NEMO-ATLTROP (http://forge.ipsl.jussieu.fr/nemo-atltrop). NEMO-ATLTROP has a horizontal resolution of 0.25°x 0.25° (Arakawa C-type grid), with a maximum depth of 5000 m spanned by 46 z-levels ranging from 5 m thickness in the upper 30 m to 200 m thickness at the bottom. Atmospheric parameters as wind speed at 10 m, air temperature, humidity, shortwave and long-wave radiations and precipitation from the called DRAKKAR forcing sets (DFS4, *Brodeau et al*. [2010]) are considered as external forcings. In the present study, an inter-annual simulation for the period 1960-2011 has been performed, hereinafter, NEMO-INTER simulation.

Observed surface winds from DFS4 data set, as well as the simulated SST, Sea Surface Height (SSH) and thermocline depth have been used. The depth of the 20C (D20) isotherm has been considered as a proxy of the thermocline depth.

Processing data

Seasonal anomalies have been computed by subtracting the seasonal cycle from 1960 to 2011. In order to isolate the inter-annual and intra-seasonal variability, a high-pass Butterworth filter [*Butterworth*, 1930; *Von Storch and Zwiers*, 2001] has been applied to the anomalies.

Discriminant Analysis Techniques

The calculation of the dominant modes of Tropical Atlantic SST variability has been done applying the Principal Component Analysis (PCA) or Empirical Orthogonal Functions (EOF) method [*Von Storch and Zwiers*, 2001]. The EOF technique consists on the decomposition of an anomalous space-time field $Y(n_s,n_t)$ into a number of modes which maximize its variance, being n_s the spatial dimension and n_t the temporal one. The application of the EOF analysis provides a set of spatial structures (EOFs) and temporal series (Principal Components, PCs), related between them and describing *modes of variability*. Each variability mode explains a fraction of the total variance of the original field (Y, von Storch and Zwiers 1999).

Heat Budget Analysis

To investigate the oceanic processes involved in the development of the Atlantic Niño SST anomalies, a closed heat budget analysis is computed in the mixed layer. The temporal variations of the mixed layer temperature are given by a balance of several terms (according to *Peter et al*. [2006] and *Vialard et al*. [2001]) as it has been shown in equation [1],

$$\frac{\partial T}{\partial t} = \underbrace{-\frac{1}{h}\int_{-h}^{0} u\frac{\partial T}{\partial x}dz - \frac{1}{h}\int_{-h}^{0} v\frac{\partial T}{\partial y}dz}_{\mathbf{a}} - \underbrace{\frac{1}{h}\int_{-h}^{0} D_l - \frac{1}{h}(T - T_h)\left(\nabla hu + \frac{\partial h}{\partial z}\right)}_{\mathbf{b}} - \underbrace{\frac{1}{h}\left[\kappa_z \frac{\partial T}{\partial z}\right]_{-h}}_{\mathbf{c}} - \frac{Q_{rad}(1-F_{-h})+Q_{tur}}{\rho_0 C_p h} \quad [1]$$

where h and T are the depth and temperature of the mixed layer; T_h is the temperature below the mixed layer; u,v and w are the zonal, meridional and vertical currents, respectively; D_l is the lateral diffusion and K_z the vertical mixing coefficient. The total net heat fluxes, Q_{net} are divided in the radiative Q_{rad} and turbulent Q_{tur} heat fluxes, and F is the function that describes the fraction of shortwave fluxes penetrating in the mixed layer. Finally, ρ_0 is the seawater density and C_p is the seawater specific heat capacity coefficient.

According to equation [1], the trend of the temperature in the mixed layer (left) can be expressed as the sum of the contributions of oceanic and atmospheric components. The atmospheric forcings or air-sea fluxes are described by the term (c), on the right side of the equation; while the oceanic part is given by the terms (a) and (b), associated with the horizontal (horizontal advection and lateral diffusion) and vertical terms (turbulent mixing, vertical advection and entrainment), respectively.

Terms from equation [1] have been considered from NEMO-INTER simulation for the period 1960-2011. The simulation has the benefit of allowing outputs to close the heat budget over the mixed layer. Similar approach was also used in Polo et al. (2015a;b) to understand oceanic processes related to the formation of El Niño and Atlantic Niño respectively and it has been shown to be straightforward and useful method.

Analysis of the wave activity

Additionally, NEMO-INTER simulation will be used to analyse the possible wave activity associated with the development of the Atlantic Niño phenomenon. We have followed methodologies (i.e. filtering) that come from previous results reporting equatorial and coastally-trapped waves over the Atlantic (Polo et al., 2008b). To this aim, a wave track has been defined along the equator and the south-African coast following the model grid (ORCA025, Arakawa type C). The high resolution of NEMO-ATLTROP simulation (the distance between two grid points is around 26 Km at the Equator) allows to study in detail the wave propagation in the tropical Atlantic basin. The wave track follows the equatorial band and goes poleward along the south-African coast up to 31S as it is shown in Figure 1. Additional analysis of the SSH signals along 4N and 4S are also shown.

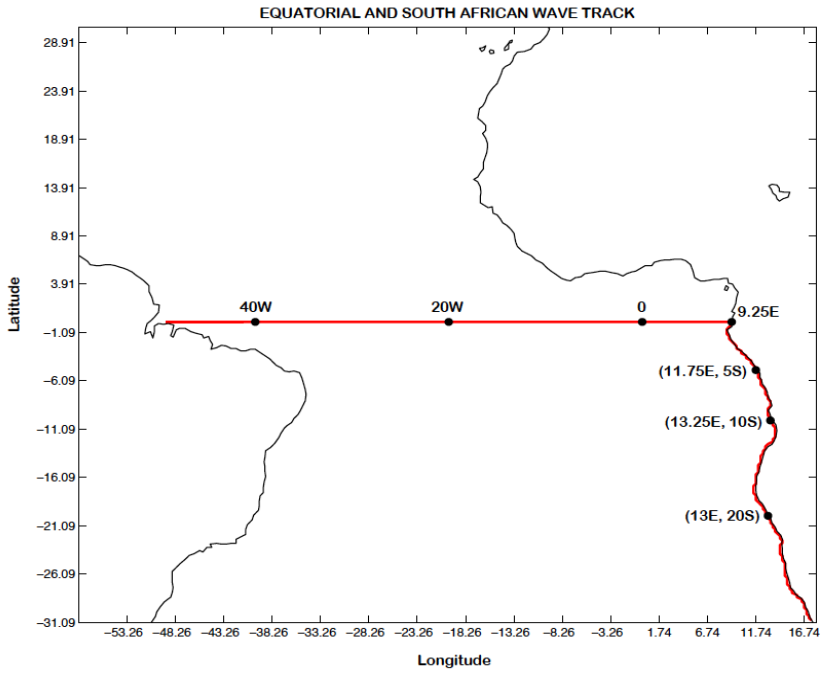

Figure 1. Map of the grid points along the equator and the south African coast used in the study of Kelvin wave tracks

The results are illustrated regressing the PC onto the different fields. To assess the robustness of the results, two different tests of significance have been applied: a T-test and a Monte Carlo test. Significant results at the 90 % confidence level according to the previous tests are shown in the present study.

Two different periods of study: 1960-1964 & 1996-2011 on the one hand and 1965-1995 on the other hand have been chosen as they are associated with positive and negative AMO phases respectively; according with observed changes in the Atlantic Niño teleconnection with the Pacific (Martin-Rey et al., 2015)

3. Results

3.1 Determination of the dominant modes of tropical Atlantic SST variability in different AMO phases

Inter-annual variability in the observations

Figure 2a-d shows the first two modes of observed Tropical Atlantic SST variability for positive and negative AMO phases. During positive AMO phases, the leading mode resembles the Atlantic Niño pattern characterized by an anomalous warming in the central-east equatorial Atlantic (Figure 2a), while the second mode presents a meridional SST gradient (Figure 2b), similar to the inter-hemispheric mode [Servain et al., 1992; Chang et al., 1997; *Ruiz-Barradas et al*., 2000]. Both modes account for the 42.3% and 14.9% of the total variance, respectively. However, under negative AMO periods, the first two modes are associated with an Atlantic Niño-like phenomenon (Figure 2c-d), explaining 35.1% and 20.3% of the total variance respectively. The leading mode shows an anomalous warming in a wider extension of the equatorial Atlantic basin [60W-20E, 15N-30S] with maximum SST anomalies in the central-east and south tropical Atlantic (Figure 2c). The second mode is characterized by positive SST anomalies restricted to the equatorial band, flanked by negative ones in north (NTA) and south tropical Atlantic (STA) (Figure 2d). This mode has also some characteristic of inter-hemispheric pattern (i.e. Wind-Evaporation-SST feedback could be operating) but with a center over the equator. Hereafter, they will be denoted as basin-wide (BW) and canonical (C) Atlantic Niño, respectively.

This result puts forward the co-existence of two different configurations of the Atlantic Niño phenomenon during negative AMO phases. These SST patterns coincide with those reported in previous works, associated with different Atlantic Niño teleconnections [*Polo et al*., 2008a; *Rodríguez-Fonseca et al*., 2009; *Losada et al*., 2010a,b; *Mohino et al*., 2011; *Martín-Rey et al*., 2012; *Martín-Rey et al*., 2014; *Polo et al*., 2015a]. The different spatial structure of BW- and C-Atlantic Niño suggests that different atmospheric forcings and oceanic mechanisms are involved in the development of those events. In order to explore the origin of these Atlantic Niños, an inter-annual simulation with the tropical Atlantic configuration of NEMO model, NEMO-INTER simulation, has been performed for the period 1960-2011.

Inter-annual variability model validation

First of all, the ability of NEMO-INTER simulation in reproducing the tropical Atlantic variability has been evaluated. Figure 2e-f shows that the model is able to simulate the inter-annual SST variability and its changes on time. The simulated SSTs present an unique Atlantic Niño pattern during positive AMO periods, explaining the 36.5% of the total variance. Nevertheless, the model does not simulate all the variability, as the second mode of the simulated SST does not resemble an inter-hemispheric-like pattern like in observations (Figure 2f).

.

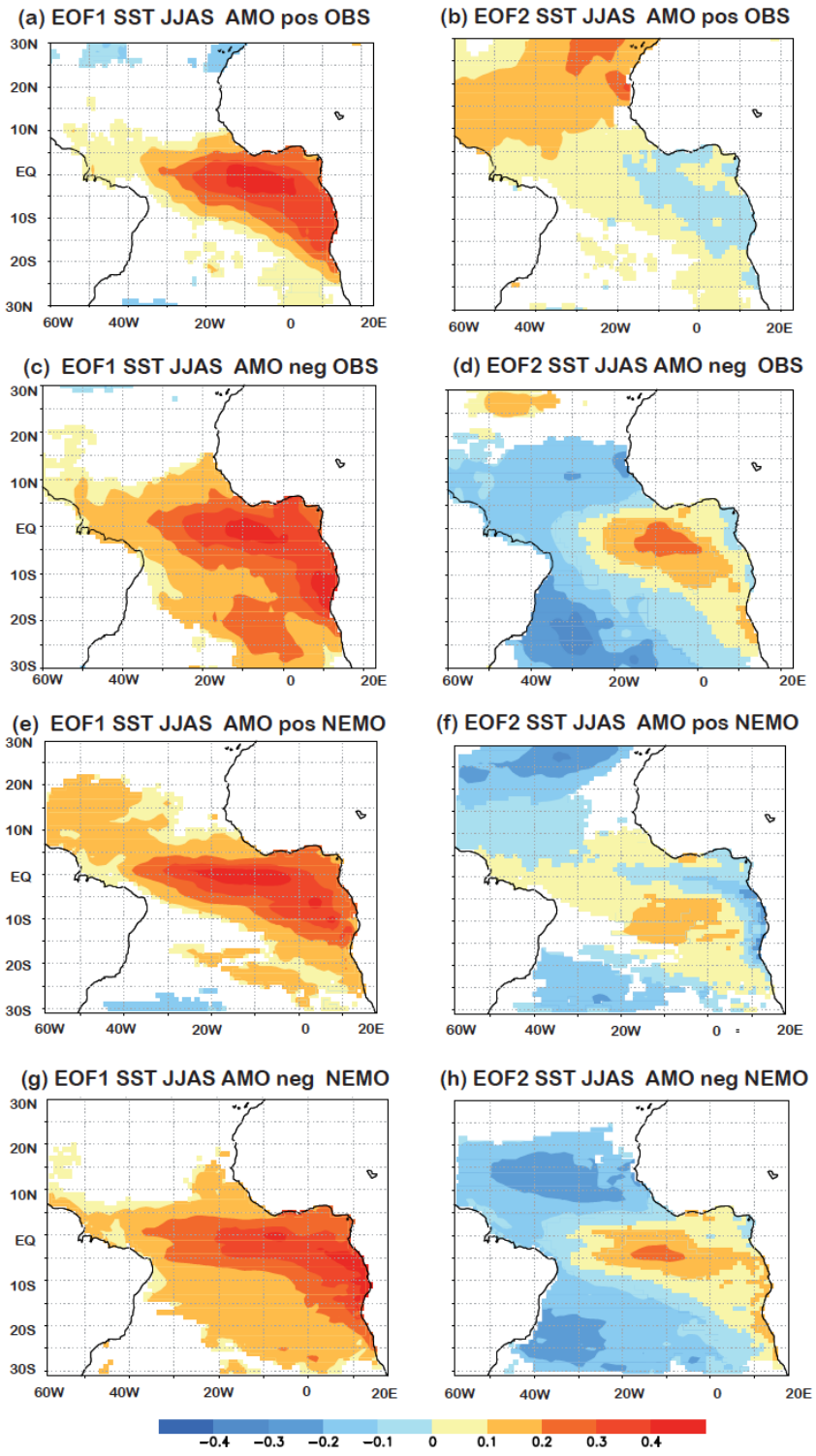

Figure 2. **Tropical Atlantic variability modes** (a-d) First and second modes (EOF1 and EOF2) of observed tropical Atlantic SST variability for positive (1960-1964 & 1996-2011) and negative (1965-1995) AMO periods. (e-h) Same as (a-d) but for the SST from the NEMO-INTER simulation. Significant values at 90% according to a Monte Carlo test are shown.

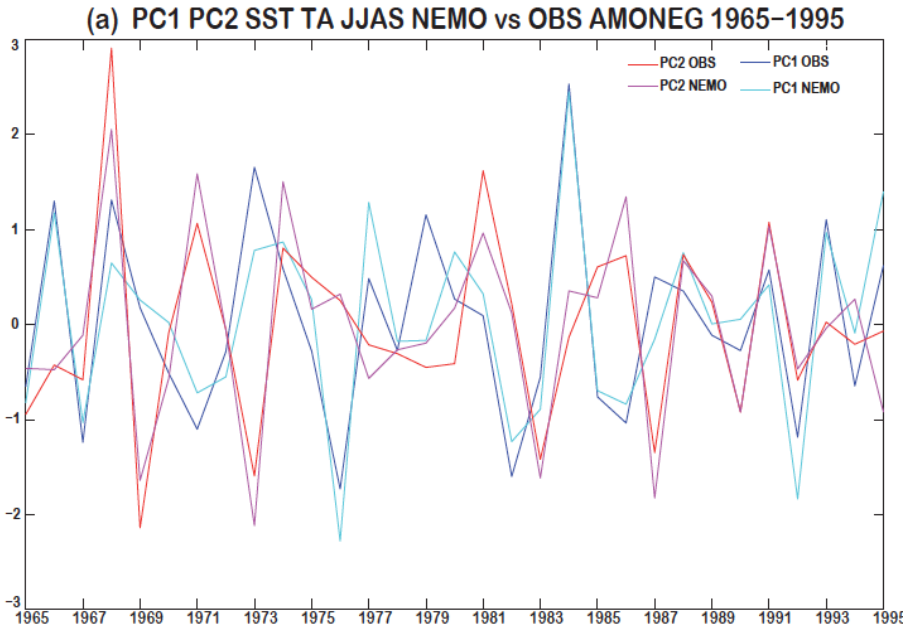

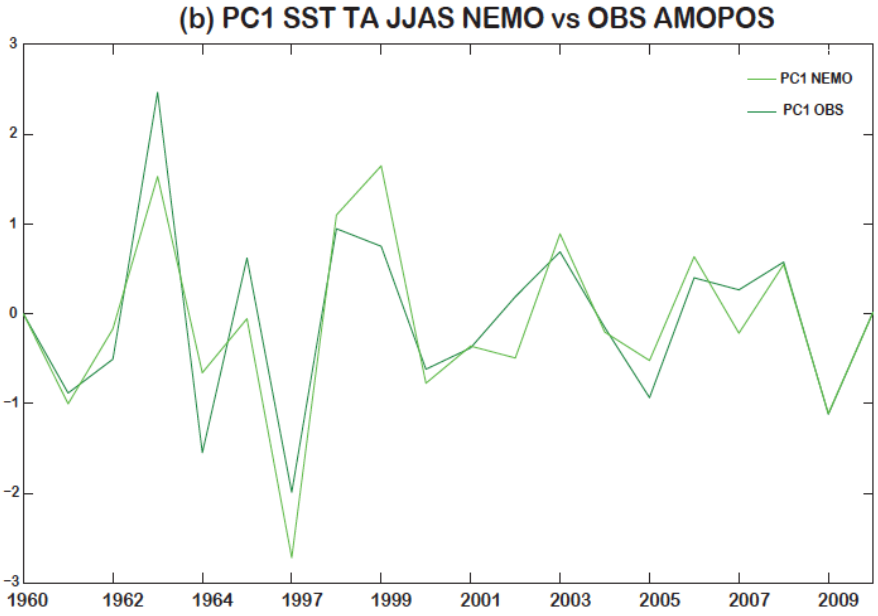

Figure 3. Time-series of the Tropical Atlantic variability modes (a) Principal Components of the first (PC1) and second mode (PC2) of tropical Atlantic SST variability for negative AMO period (1965-1995) from observations and NEMO-INTER simulation. (b) Same as (a) but for the leading mode of tropical Atlantic variability in a positive AMO phase (1960-1964 & 1996-2011).

On the other hand, under negative AMO phases, the variability of the simulated SST is comprised in two leading mode that resemble the observed BW- and C-Atlantic Niño patterns (Figure 2g-h), accounting for the 30.1% and 19.5% of the total variance respectively. Furthermore, the temporal evolution of these modes is also well captured by NEMO-INTER simulation (Figure 3), obtaining significant correlation scores of 0.87 for the positive AMO periods and 0.87 (BW-Atlantic Niño) and 0.9 (C-Atlantic Niño) for negative AMO phases.

Notice that during positive AMO periods, the observed Atlantic Niño pattern and the one captured by the simulated SSTs explain around 40% of the total variance. However, during negative AMO phases, a large fraction of the total variance is shared between the BW- and C-Atlantic Niño (around 30% and 20% respectively), putting forward that both phenomena drive the inter-annual variability of the tropical Atlantic Ocean during those decades (Figure 2). As the model is able to reproduce the existence of the BW- and C-Atlantic Niño during negative AMO phases, hereafter the PCs from the NEMO-INTER simulation will be used to investigate the origin of these two modes. Also, the atmospheric forcings associated with these Atlantic Niño phenomena are explored in next section

3.2 Atmospheric forcings of the Basin-Wide and Canonical Atlantic Niño

The characterization of the atmospheric pattern associated with these two Atlantic Niños can shed light about its forcings and predictability. To calculate them, regression maps between surface winds and SST fields and the Principal Components (PCs) of the BW- and C-Atlantic Niño from NEMO-INTER simulation, are presented in Figure 4 and Figure 5 respectively.

The evolution of the BW-Atlantic Niño shows anomalous westerly winds in the central part of the basin, south of the equator [30W-0, 5S-15S] during ONDJ (Figure 4a). These anomalous winds are intensified, taking part of a large-scale weakening of the southern tropical trades during the following seasons (Figure 4b-f), which could favour the development of positive SST anomalies in the south tropical Atlantic (STA, Figure 4b-f). Additionally, anomalous south-westerly winds are also observed in north tropical Atlantic (NTA) from late winter (Figure 4d), which could contribute to warm the north-western side [15N-30N, 60W-20W] of the basin (Figure 4d-f). The simultaneous weakening of the north and south tropical trades induces an anomalous equatorial wind convergence during the spring, helping to develop the warm tongue of the BW-Atlantic Niño (Figure 4f-h). On the other hand, the C-Atlantic Niño development starts in the NTA region, since an anomalous intensification of the north-eastern trades appears next to Mauritanian coast [35W-15W, 10N-20N] in early winter (NDJF, Figure 5b). A general strengthening of the trades in NTA from DJFM to MAMJ and anomalous south-easterly winds in the southern STA [40W-0, 20S-30S] from ONDJ to DJFM could contribute to cool then subtropical regions (Figure 5d-f). The intensification of the northern and southern trade winds, produces cross-equatorial winds which enhance westerly winds at the equatorial Atlantic from JFMA to JJAS (Figure 5d-h), favouring the development of the equatorial SST anomalies of the C-

Atlantic Niño pattern (Figure 5d-h).

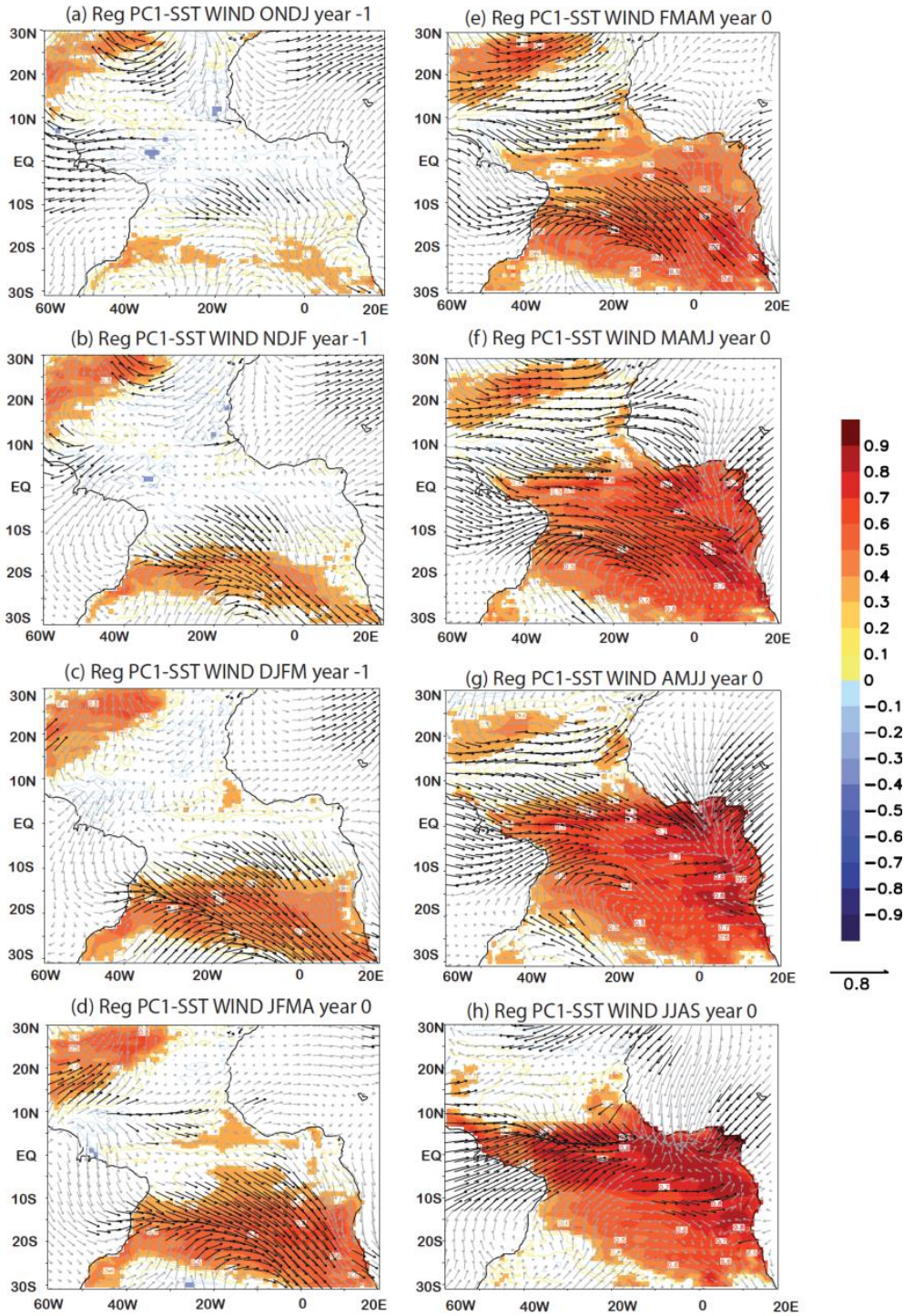

Figure 4. Basin-Wide Atlantic Niño evolution: (a-h) Regression maps between the PC of the Basin-Wide Atlantic Niño (PC1 for negative AMO periods) over the anomalous seasonal anomalies of surface wind (vectors) and modelled SST (shaded) from ONDJ to JJAS. Significant values exceeding 90% of the confidence level according to a t-test are shown.

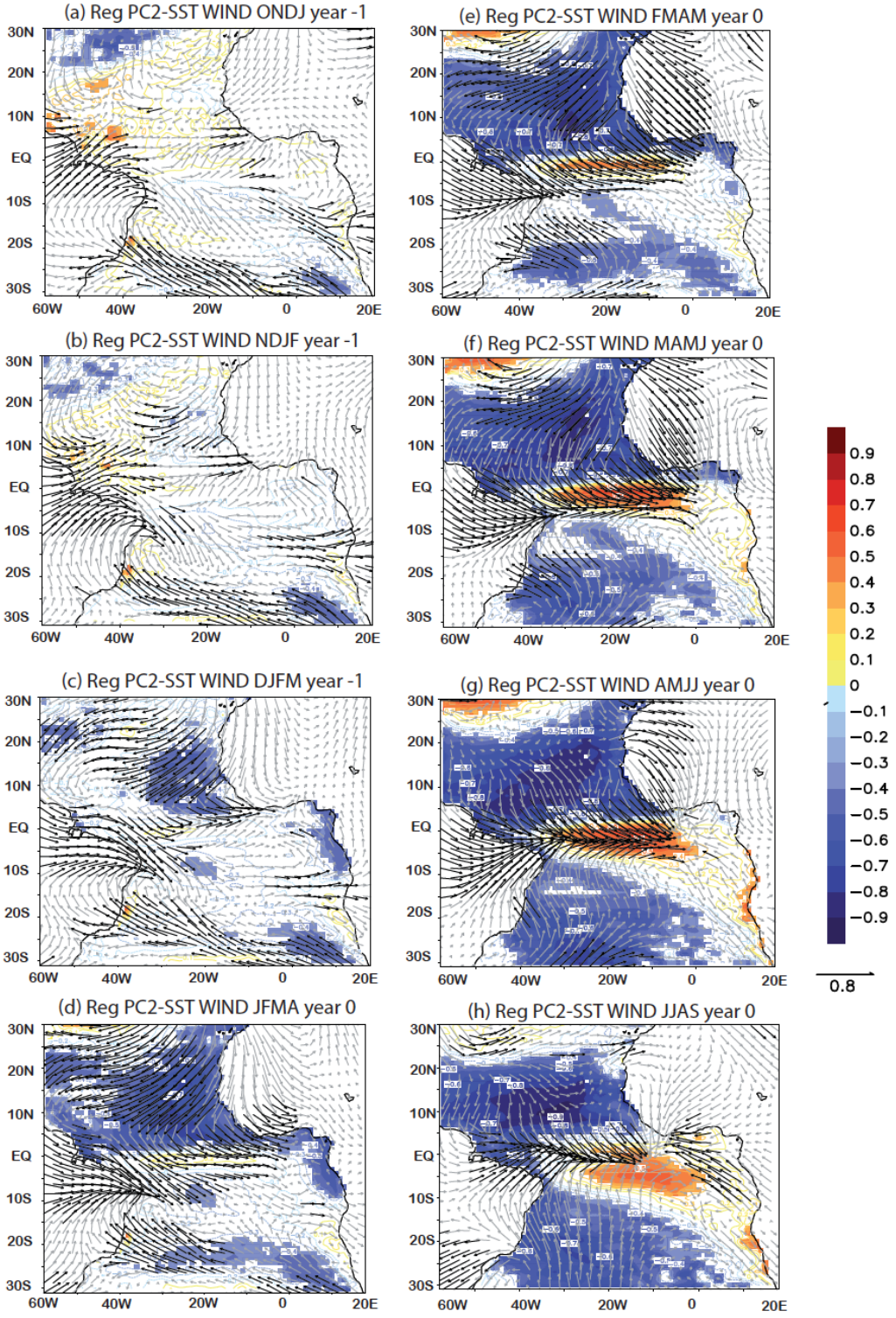

Figure 5. Canonical Atlantic Niño evolution: Same as Figure 4 but for the PC of the Canonical Atlantic Niño (PC2 for negative AMO periods).

These anomalous wind configurations seem to be part of a large-scale atmospheric patterns associated with the variability of the Subtropical atmospheric pressure systems. Thus, regression maps between the PCs of the BW- and C-Atlantic Niño and the SLP anomalies have been computed (Figure 6 and Figure 7). Figure 6 reveals that, the development of a BW-Atlantic Niño is preceded by an anomalous weakening of Sta Helena High in NDJF (Figure 6b), which is intensified and displaced northward from DJFM to FMAM (Figure 6c-e). These negative SLP anomalies produce the anomalous reduction of the south-eastern trades shown in Figure 4. Additionally, the Azores High is also weakened from FMAM, presenting a 4-month delay with respect to the alteration of Sta Helena High (Figure 6e). The simultaneous lower than normal SLP anomalies in north and south Atlantic from late winter (Figure 6e) induce the anomalous westerly winds in the entire tropical Atlantic shown in Figure 4. A center of negative SLP anomalies is located over the tropical Atlantic basin during summer months, related to the anomalous wind convergence and the maximum SST anomalies of the BW-Atlantic Niño (Figure 6h-i).

A different contribution of the Subtropical Highs is observed during the development of the C-Atlantic Niño event (Figure 7). Positive SLP anomalies in north and south Atlantic during previous autumn and winter (ONDJ-JFMA), suggest a strengthening of both Azores and Sta Helena High, contrasting to lower than normal SLP values in the tropical Atlantic (Figure 7a-d). This SLP configuration originates an intensification of the trades in NTA and STA and anomalous westerlies along the equator (Figure 5). During late winter and spring (FMAM-MJJA), this meridional pattern evolves into a zonal SLP gradient, with positive anomalies over South America and negative ones over the African continent (Figure 7e-i), reinforcing the anomalous equatorial westerly winds (Figure 5).

Different atmospheric forcing configurations related to the SST warming suggests that different oceanic processes could be involved in the development of the BW- and C-Atlantic Niño episodes. Thus, an analysis of the key variables at the equator and a detailed heat budget analysis of these two modes are presented in the following sections.

3.3 Equatorial Evolution of the SST anomalies for the *BW and C-Atlantic Niños*

For a BW-Atlantic Niño, anomalous westerly winds in the west equatorial Atlantic [60W-25W] from FMAM (black contours, Figure 8a) induce a deepening of the thermocline depth (D20) in the eastern side of the equatorial band (purple contours, Figure 8a). The anomalous deeper D20 inhibits the upwelling and vertical advection, contributing to warm the eastern equatorial Atlantic (shaded, Figure 8a). The positive SST anomalies are extended to the west covering the entire equatorial band, with maximum anomalies located around 10W. This zonal gradient of SST could induce an east-west SLP gradient (Figure 6e-f), which reinforces the westerly winds, establishing the Bjerknes feedback. Notice that, the eastern equatorial Atlantic shows an alteration of D20 from January, one month before the contribution of the westerly winds. It

could be caused by an anomalous convergence during JFMA (Figure 4) (although not significant) wind

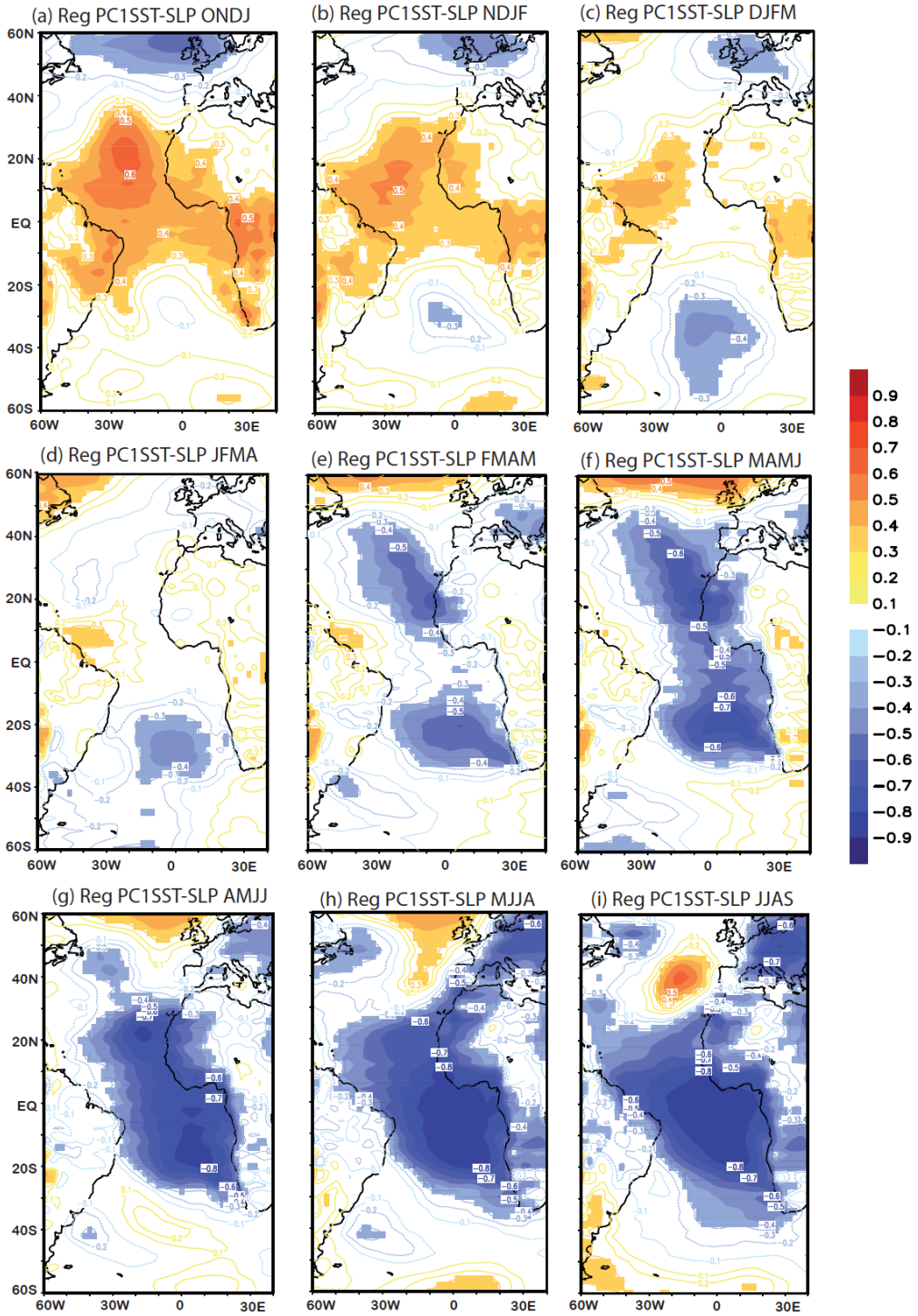

Figure 6. **SLP associated with Basin-Wide Atlantic Niño** (a-h) Regression maps between the PC of the Basin-Wide Atlantic Niño (PC1 for negative AMO periods) over the seasonal anomalies of observed Sea Level Pressure from ONDJ to JJAS. Only significant values exceeding 90% of the confidence level according to a t-test test are shown.

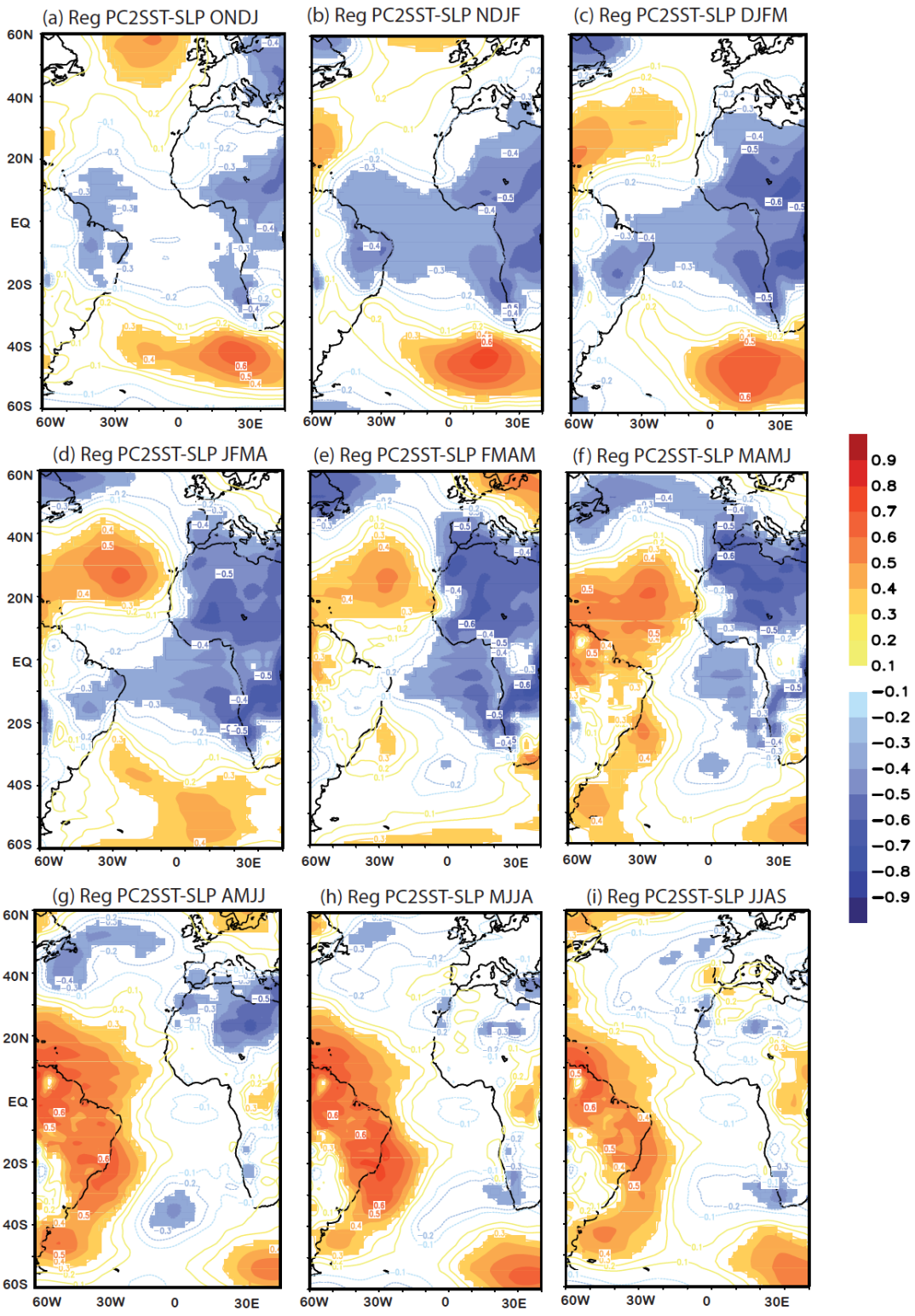

Figure 7. **SLP associated with Canonical Atlantic Niño** (a-h) Same as Figure 6 but for the PC of the Canonical Atlantic Niño (PC2 for negative AMO periods).

.

Regarding to the C-Atlantic Niño pattern, strong westerlies in the west-central equatorial Atlantic [60W-10W] from JFMA generate a deepening of the thermocline depth in the eastern side, favouring the warming of the central equatorial Atlantic from FMAM (Figure 8b). The thermocline becomes shallower in the west from MAMJ, establishing a zonal D20 gradient that reinforces the initial westerlies, contributing to create the see-saw SST pattern and activating in this way the Bjerknes feedback (Figure 8b). The C-Atlantic Niño shows a shorter duration than the BW-Atlantic Niño pattern, since its anomalous warm tongue after July (Figure 8b), contrasting to the persistent of the BW-Atlantic Niño SST anomalies until winter months (Figure 8a)

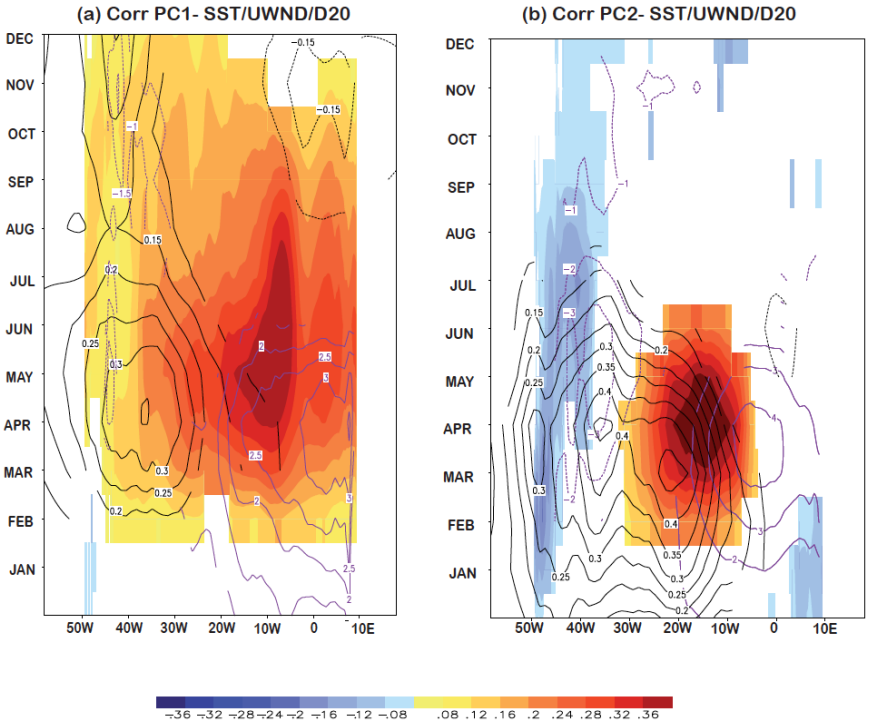

Figure 8. **Equatorial Atlantic Niños evolution:** Time-longitude diagram of the correlation between the PC of the BW-(a) and C-Atlantic Niño (b) over the seasonal modelled SST (shaded), observed zonal wind (black contours) and thermocline depth (D20, purple contours) along the equator from JFMA to DJFM. Significant values (90% confidence level) are shown.

3.4 Oceanic processes involved in the BW and C-Atlantic Niño development

<u>Basin wide Atlantic Niño development</u>

Regression maps between the PCs of the BW- and C-Atlantic Niño and the heat budget terms in the mixed layer: temperature trend (first row), net heat fluxes (second row), horizontal oceanic terms (third row) and vertical oceanic terms (fourth row) have been computed (Figure 9 and Figure 10). The main changes of the mixed layer temperature of these phenomena occur from DJFM to MAMJ, thus the heat budget analysis is focused on those seasons.

During the onset of the BW-Atlantic Niño pattern, SST anomalies appear south of 10S and also in the north-west of NTA [60W-30W,15N-30N] (contours, Figure 9a,e). This surface warming is associated with a positive temperature tendency in the mixed layer (shaded, Figure 9a,e), mainly due to the contribution of the net heat fluxes (Figure 9a-h). The anomalous weakening of the south-eastern trades during DJFM-JFMA reduces the latent heat loss, favouring the warming of STA (shaded, Figure 9b,f). Despite the important role of the net heat fluxes, the vertical terms also help to create the positive temperature trend in the subtropical regions (Figure 9d,h). As Sta Helena High is weakened (Figure 6), an anomalous anticyclonic circulation appears in STA, which produces an anomalous convergence of the Ekman transport (not shown), contributing to warm the STA basin (Figure 9d,h). Notice that, a strong warming appears along Angola-Namibian coast in JFMA, mainly attributed to horizontal terms (Figure 9e-h). The along-shore winds (Figure 9f) could generate an anomalous Ekman pumping that piles up the water to the coast (not shown), generating anomalous geostrophic currents (Figure 9g) that weaken the Benguela current through advection of heat from the equator.

The equatorial SST anomalies of the BW-Atlantic Niño pattern are developed during late winter and spring (FMAM-MAMJ, Figure 9i-p). Anomalous westerly wind generate an anomalous convergence of the zonal currents (not shown), deepening the thermocline depth and reducing the entrainment and vertical advection, contributing in this way to warm the equatorial Atlantic basin (Figure 9,i-l). Additionally, anomalous westward currents in the eastern equatorial Atlantic could pile up the warm waters to the east, weakening the Benguela current and creating the positive temperature trend shown along the south-African coast in MAMJ (Figure 9m-p).

Canonical Atlantic Niño development

The horseshoe pattern of the C-Atlantic Niño starts to develop during winter months, due to the contribution of the net heat fluxes (Figure 10a,e). As the north-east and south-east trades are reinforced, the evaporative cooling is enhanced, favouring the creation of negative SST anomalies in NTA and STA (Figure 10b,f). The strong westerly winds along the equator from JFMA to MAM produce an anomalous convergence of the zonal currents (figure 10g,k,o), deepening the thermocline depth and thus favouring to the warming of the equatorial band through vertical processes (Figure 10h,l,p). Notice that, a positive temperature trend is also shown along the Angola coast, driven by horizontal terms. The intensification of the eastward currents in the equatorial Atlantic and along the African coast could pile up warm waters, reducing the Benguela current and warming that area (Figure 10m-p). Finally, the atmosphere is always damping the SST anomalies at the equator throughout anomalous turbulent heat fluxes (figure 10j,n).

Comparative evolution of the two Niños at key regions:

We know summarized the relative contribution of the atmosphere and the horizontal and vertical oceanic terms for three different key regions: STA, NTA and the equator.

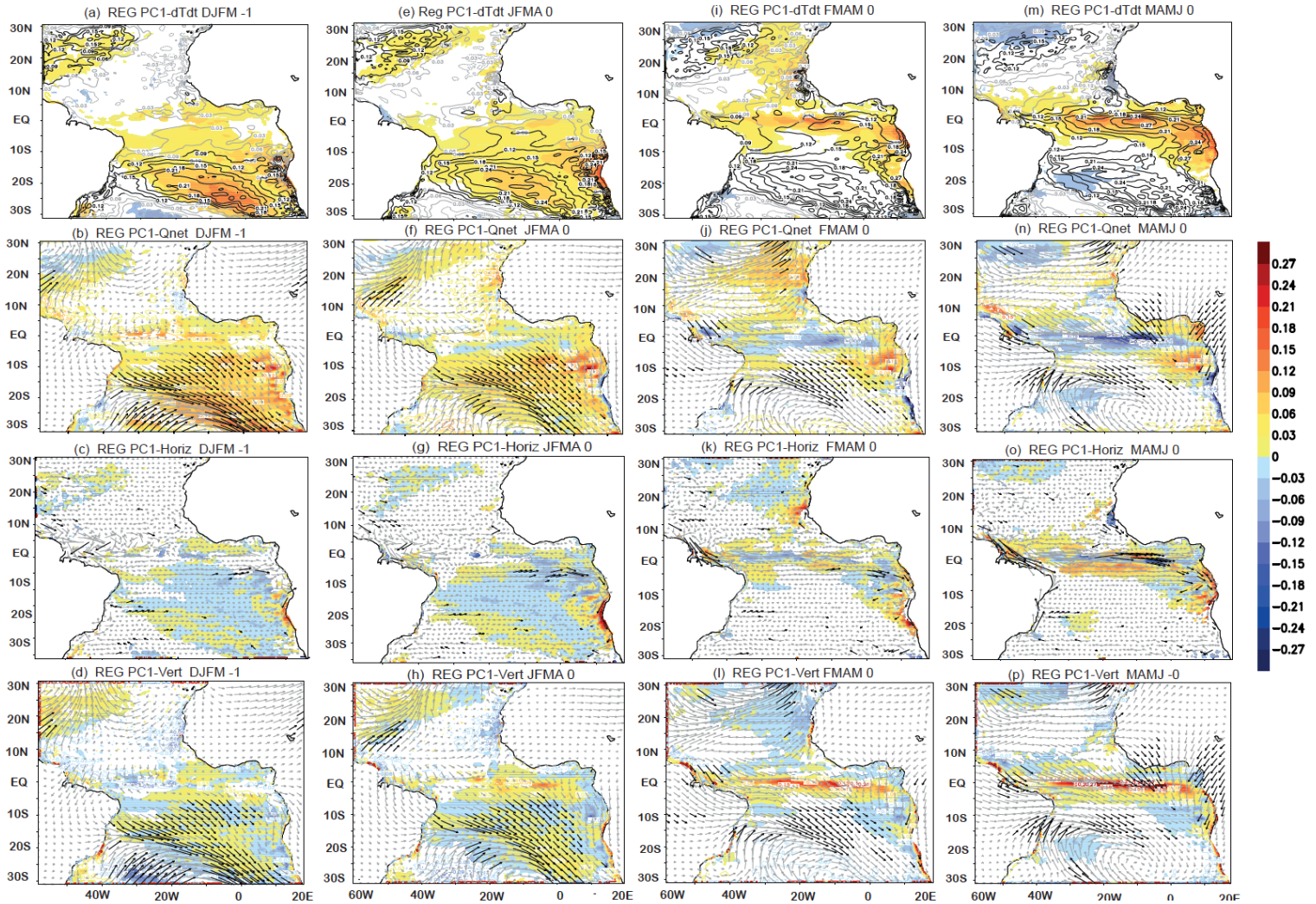

Figure 9. **Heat Budget for Basin-Wide Atlantic Niño:** Regression maps between the PC of the BW-Atlantic Niño over the seasonal anomalies of the temperature tendency integrated over the mixed layer (shaded, first row) and SST (contours, first row), net heat fluxes (shaded, second row) and the observed surfaced winds (vectors, second row), horizontal oceanic terms (shaded, third row) and oceanic horizontal currents (vectors, third row), vertical oceanic terms (shaded, fourth row) and the observed surfaced winds (vectors, fourth row) from DJFM to MAMJ from NEMO-INTER simulation. A t-test has been applied and significant values at 90% confidence level are presented.

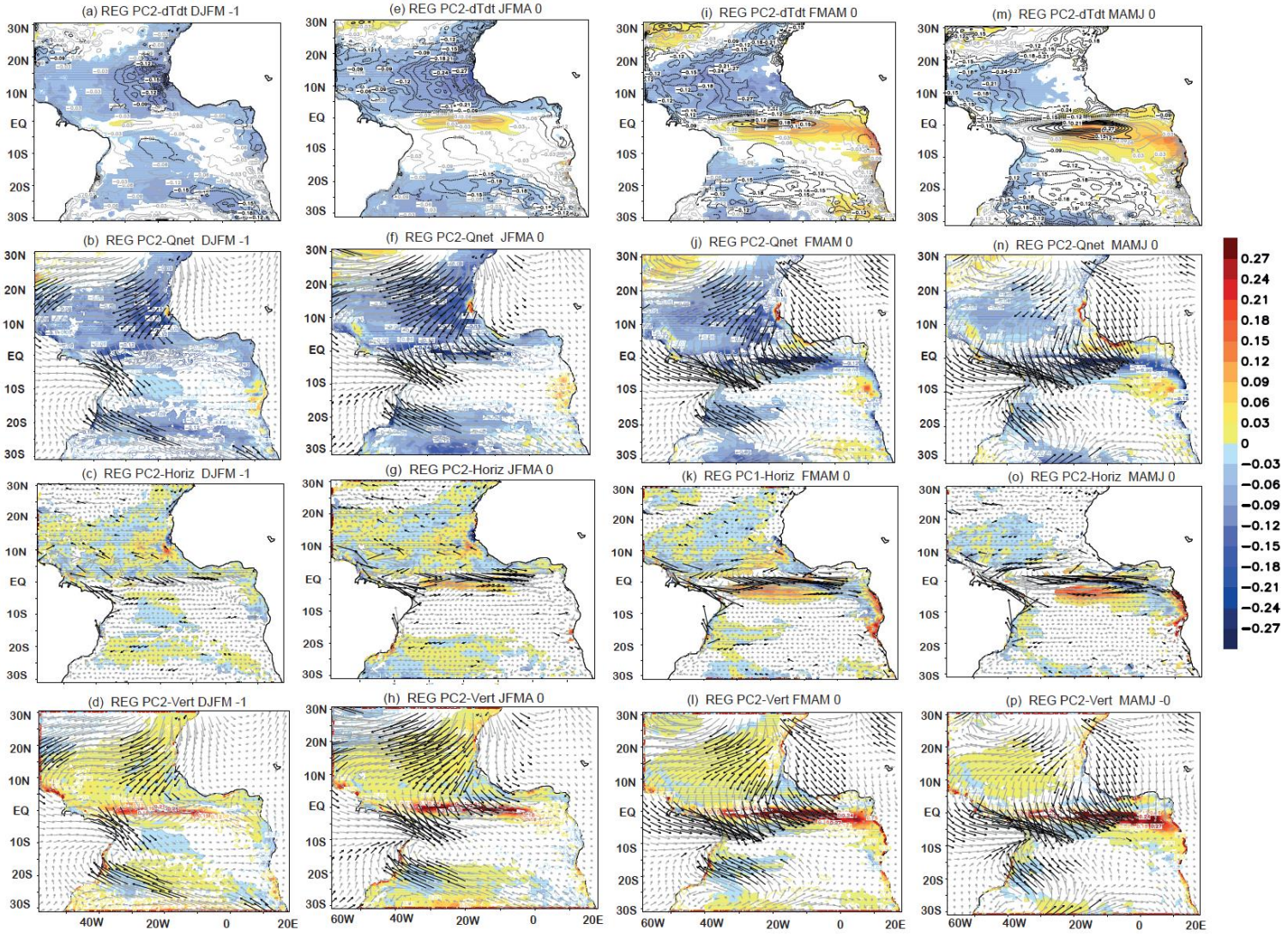

Figure 10. Heat Budget for Canonical Atlantic Niño: Same as Figure 9 but for the PC of the C-Atlantic Niño.

The development of the BW-Atlantic Niño pattern is driven by net heat fluxes in the subtropical regions, with the additional contribution of the vertical terms (Figure 11a,e). The vertical terms are the main responsible of the creation of the equatorial SST anomalies, although the horizontal terms could also help to warm the equatorial band (Figure 11c).

On the other hand, the creation of the cold horseshoe of the C-Atlantic Niño is mainly attributed to net heat fluxes (Figure 11b,f), while vertical terms create the equatorial warm tongue of this phenomenon with also a contribution of the horizontal terms. (Figure 11d).

Overall, the vertical terms are the most important terms driven equatorial SST for both types of Atlantic Niños. One important difference in the evolution of the SST tendency of both modes is that the heat fluxes are damping the SST anomalies over the equator from winter to summer in the C-Atlantic Niño (Figure 10d), while for the BW-Atlantic Niño the heat fluxes are contributing in the warming from late autumn to early spring (Figure 11c). This makes also a difference in the timing: the warming starts from previous NDJF in BW Atlantic Niño comparing with the warming of C-Atlantic Niño which starts in FMAM. However, both are peaking at MAMJ. The vertical terms are stronger in C-Atlantic Niño suggesting more thermocline (Bjekness) feedbacks than in BW Atlantic Niño. Horizontal terms are contributing to changes in the SST for both Niño types (figure 11c-d) suggesting that zonal advective feedbacks are also acting although to a less extent than the thermocline ones.

The anomalous horizontal currents could be an effect of equatorial waves (Hormann and Brandt, 2009), which in turn could affect thermocline depth [*Lübbecke et al*., 2010; *Polo et al*., 2008b]. In the following section, analysis of the oceanic waves is presented.

3.5 oceanic wave activity and its connection with the development of BW- and C-Atlantic Niños

Following methodologies and results from Polo et al (2008b) and in order to assess the oceanic waves activity over the equatorial Atlantic related to BW-Atlantic Niño, hövmoller diagrams between the correlation of BW-Atlantic Niño time series PC1 and 5-day SSH anomalies along 5N, the equator and South African coast and 5S are presented in Figure 12. Oceanic wave activity could exist from March to May in the equatorial Atlantic basin, which could influence the development of the BW-Atlantic Niño pattern (Figure 12b). The downwelling Kelvin wave propagating along the equator from March to May, seems to be reflected in 5N and 5S as Rossby waves displacing westward from May to November (Figure 12a,c). This intense Rossby wave activity is clarified after applying a 20–100 day band-pass filter to the SSH anomalies (Figure 12d,f). Nevertheless, there is not a pre-existence wave activity during late winter (January-February), suggesting that the Kelvin wave observed in March is mainly driven by the wind forcing (Figure 4). These results put forward that the anomalous equatorial Kelvin wave preceding the development of the BW-Atlantic Niño is unrelated with the

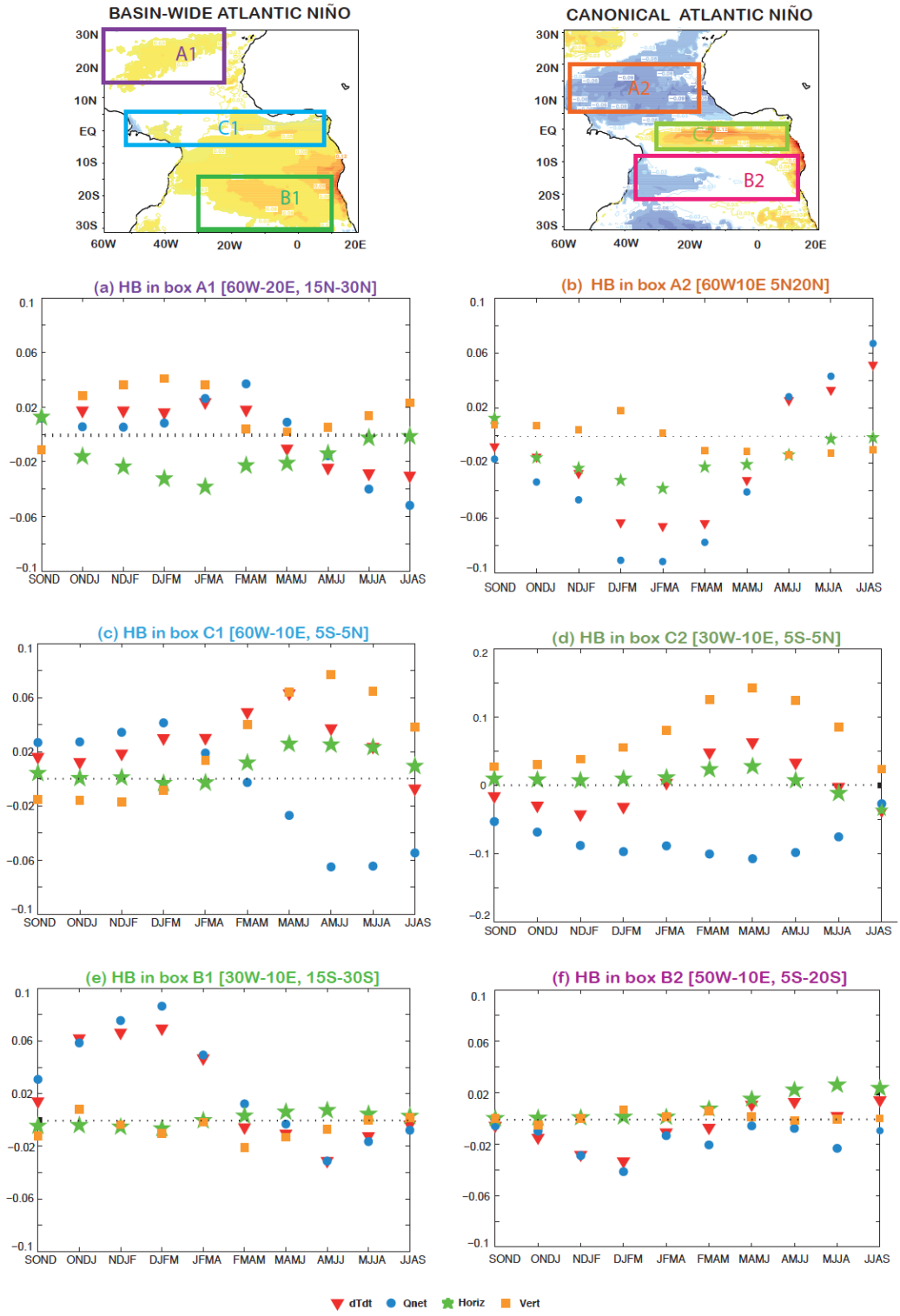

Figure 11. Heat Budget evolution for Atlantic Niños (a-f) Temporal evolution of the regression between the PC of the BW-Atlantic Niño (left column) and C-Atlantic Niño (right column) over the seasonal anomalies of the heat budget terms in the NTA (a-b), equatorial band (c-d) and STA (e-f) regions.

propagation of Rossby waves from the subtropical regions, in disagreement with suggestions from *Polo et al*. [2008a].

For the C-Atlantic Niño development, possible Kelvin wave-like propagations are shown during March-May along the equatorial band (Figure 13b). This activity is much more intense than for BW-Atlantic Niños which is coherent with more vertical and horizontal effects associated with the C- Atlantic Niños development (figure 10). Notice that the decay of the C-Atlantic Niño phenomenon seems to be attributed to an upwelling Kelvin, propagating along the equatorial band from August to September, damping the warmer SST anomalies (Figure 13b). This is in agreement with similar termination of the Atlantic Niño showed by Polo et al (2008a). This upwelling Kelvin wave could be the reflection of Rossby waves at 5N and 5S in May (figure 13a,c) which are in turn could be forced by wind stress curl off-equator close to the American continent (not shown). This intense Rossby wave propagation is clarified after filtering the signal (Figure 13, bottom panels). Moreover, a pre-existence wave activity in the west-central equatorial Atlantic is shown from February to May, which could also modify the vertical stratification of the equatorial Atlantic, favouring the creation of the C-Atlantic Niño pattern.

This preliminary wave analysis suggests that the propagation of equatorial Kelvin waves, triggered by equatorial wind forcing or by the reflection of subtropical Rossby waves could contribute to the development of the BW- and C- Atlantic Niño phenomena. Further research about the role of the equatorial and subtropical winds in triggering these waves and their impact in the development of the equatorial SST anomalies is required

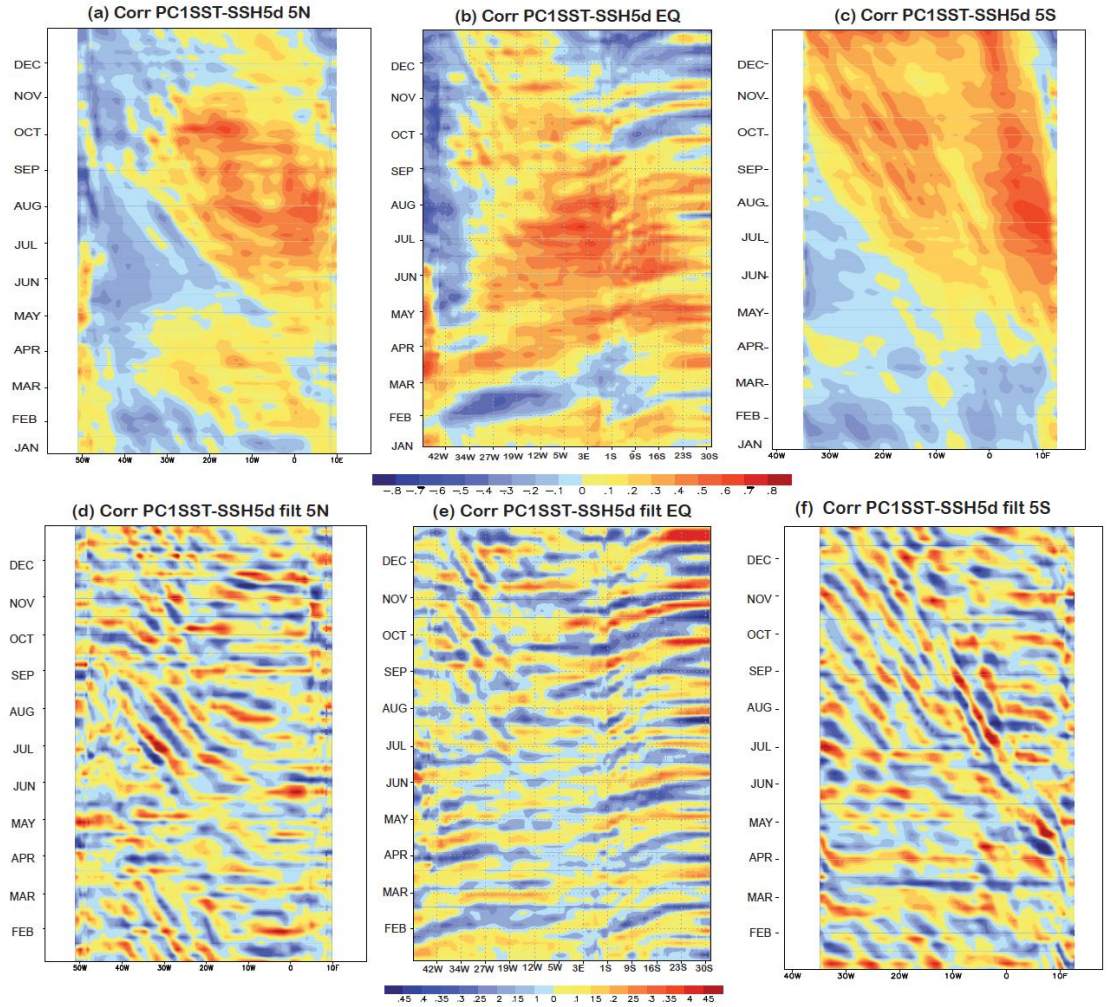

Figure 12. Oceanic wave activity related to BW-Atlantic Niños: Time-longitude diagram of the correlation between the PC of the BW-Atlantic Niño over the 5-day SSH anomalies along 5N (left panels), equatorial Atlantic and south African coast (middle panels) and 5S (right panels) from JFMA to DJFM. A 20-100 day Butterworth filter has been applied to the 5-day SSH anomalies in order to isolate the intra-seasonal variability (bottom panels).

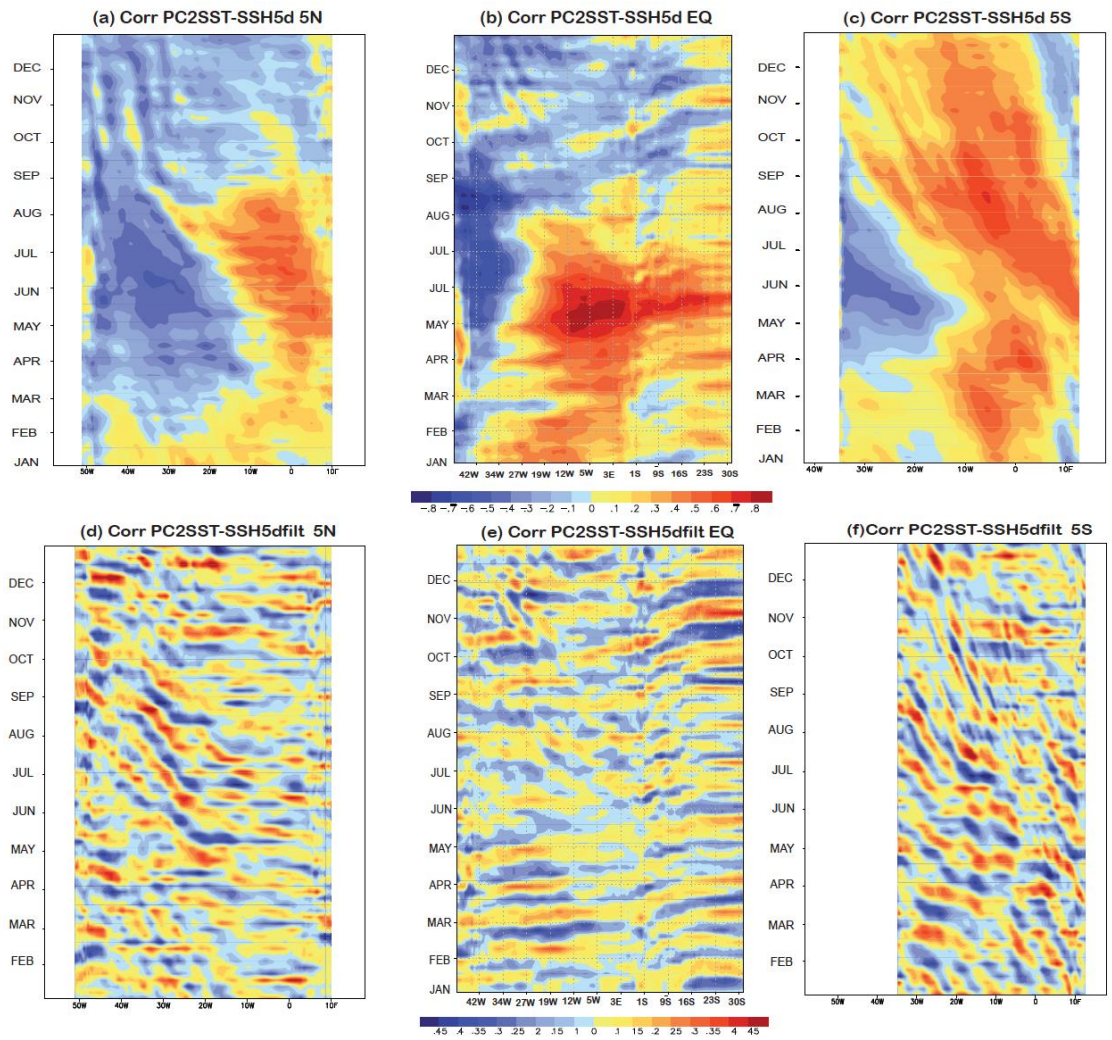

Figure 13. Oceanic wave activity related to C-Atlantic Niños Same as Figure 12 but for C-Atlantic Niño.

.

4.Discussion and conclusions

In the present study it has been demonstrated that:

- During positive AMO periods, a unique Atlantic Niño pattern appears, characterized by an anomalous warming in the central-east of the equatorial Atlantic.

- Under negative AMO phases, two different spatial patterns associated with the Atlantic Niño phenomenon emerge in the tropical Atlantic basin. The first mode presents an anomalous warming covering the entire tropical Atlantic basin, denoted as Basin-Wide (BW-) Atlantic Niño. The second mode shows positive SST anomalies restricted to the equatorial band and flanked by negative ones in north and south tropical Atlantic. It is named as Canonical (C-) Atlantic Niño. These two patterns coincide with those reported in previous studies associated with different Atlantic Niño teleconnections during last decades [*Rodríguez-Fonseca et al*., 2009; *Losada et al*., 2012a; *Martín-Rey et al*., 2014].

- The BW- and C-Atlantic Niño phenomena are associated with different wind forcings driven by the Subtropical High pressure systems. On the one hand, a weakening of both Azores and Sta Helena High produces a general reduction of the tropical trades and anomalous equatorial wind convergence, favouring the development of the BW-Atlantic Niño. On the other hand, an initial strengthening of both Subtropical Highs, evolving in a zonal SLP gradient, reinforces the northern and southern trades and originates anomalous westerlies along the equatorial band, triggering the development of the C-Atlantic Niño.

- A heat budget analysis reveals that, the subtropical SST anomalies are mainly due to net heat fluxes for the C- and BW-Atlantic Niño patterns, while an additional contribution of the vertical processes also is also shown for the BW-Atlantic Niño.

- The development of the equatorial warm tongue is attributed to the vertical processes in both phenomena, but activated by different atmospheric forcings: On the one hand, strong westerly winds along the equatorial band generate an anomalous convergence of the currents from winter months, warming the equatorial Atlantic for a C-Atlantic Niño event. On the other hand, an anomalous wind convergence from early spring, induces an anomalous convergence of the currents that deepens the thermocline, activating the vertical processes needed to develop the BW-Atlantic warm tongue. Equatorial warming in BW-Atlantic Niño has an additional contribution from turbulent fluxes from previous winter.

- Propagation of equatorial Kelvin waves triggered by equatorial wind anomalies or by the reflection of subtropical Rossby waves could play a role in the development of the BW- and C-Atlantic Niño SST patterns.

The present results put forward that two different configurations of the Atlantic Niño phenomenon co-exist during negative phases of the AMO associated with different wind forcings, which in turn activate diverse oceanic mechanisms. These wind configurations are driven by the Subtropical High pressure systems, nevertheless these anomalous SLP patterns could take part of a large-scale atmospheric structure. Thus global regression maps between the PC of the BW- and C-Atlantic Niño and the global seasonal SLP anomalies during previous autumn (ONDJ) are presented in Figure 14.

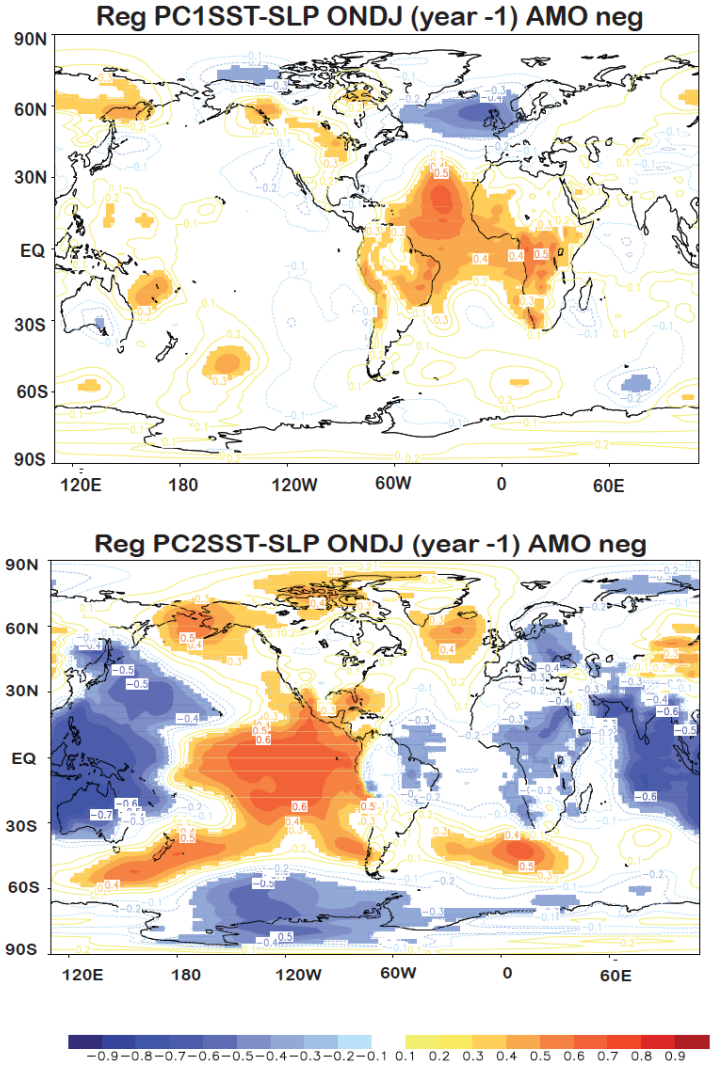

Figure 14. Global atmospheric forcing related to the Atlantic Niños: (a-b) Regression maps of the PC of the BW-Atlantic Niño (a) and C-Atlantic Niño (b) over the global seasonal SLP anomalies in ONDJ. Significant areas exceeding 90% confidence level according to a t-test are shown.

On the one hand, the weakening of Azores and Sta Helena High preceding the development of a BW-Atlantic Niño is associated with a North Atlantic Oscillation (NAO)-like pattern over the Atlantic Ocean during previous autumn (Figure 14a). On the other hand, the initial strengthening of Azores and Sta Helena High related to the triggering of the C-Atlantic Niño takes part of the atmospheric teleconnection of La Niña-like pattern (Figure 14b). This finding suggests that the origin of the BW-Atlantic Niño atmospheric forcing is confined to the Atlantic Ocean, while an atmospheric signal emanating from the Pacific basin is responsible of the development of the C-Atlantic Niño. Further research about the possible origins of this large-scale atmospheric forcings and the possible role of the multidecadal variability is carried already out by the authors.

References

Bjerknes, J. (1969), Atmospheric teleconnections from the equatorial Pacific, Monthly Weather Review, 97(3), 163-172.

Brodeau, L., B. Barnier, A. Treguier, T. Penduff, and S. Gulev (2010), An ERA40-based atmospheric forcing for global ocean circulation models, Ocean Modelling, 31, 88-104.

Butterworth, S. (1930), On the theory of filter amplifiers,, Experimental wireless and the wireless engineer 7, 536-541.

Carton, J., and B. Huang (1994), Warm Events in the Tropical Atlantic, Journal of Physical Oceanography, 24(5), 888-903.

Carton, J., X. Cao, B. Giese, and A. Da Silva (1996), Decadal and inter-annual SST variability in the Tropical Atlantic Ocean, Journal of Physical Oceanography, 26(7), 1165-1175.

Cassou, C., L. Terray, and A. S. Phillips (2005), Tropical Atlantic Influence on European Heat Waves, Journal of Climate, 18(15), 2805-2811.

Cassou, C., L. Terray, J. W. Hurrell, and C. Deser (2004), North Atlantic Winter Climate Regimes: Spatial Asymmetry, Stationarity with Time, and Oceanic Forcing, Journal of Climate, 17(5), 1055-1068.

Compo GP, J. W., PD Sardeshmukh, N Matsui, RJ Allan, X Yin, X., ... SJ Worley (2011), The Twentieth Century Reanalysis Project, Journal of the Royal Meteorological Society, 137(654), 1-28.

Ding, H., N. Keenlyside, and M. Latif (2012), Impact of the Equatorial Atlantic on the El Niño Southern Oscillation, Climate Dynamics, 38(9-10), 1965-1972.

Florenchie, P., J. R. E. Lutjeharms, C. J. C. Reason, S. Masson, and M. Rouault (2003), The source of Benguela Niños in the South Atlantic Ocean, Geophys. Res. Lett., 30(10), 1505, doi:10.1029/2003GL017172.

Hormann, V. and Brandt, P. (2009) Upper equatorial Atlantic variability during 2002 and 2005 associated with equatorial Kelvin waves Journal of Geophysical Research - Oceans, 114 . C03007. DOI: 10.1029/2008JC005101.

Hurrell, J. W., et al. (2006), Atlantic Climate Variability and Predictability: A CLIVAR Perspective, Journal of Climate, 19(20), 5100-5121.

Janicot, S. (1992), Spatiotemporal Variability of West African Rainfall. Part I: Regionalizations and Typings, Journal of Climate, 5(5), 489-497.

Joly, M., and A. Voldoire (2010), Role of the Gulf of Guinea in the inter-annual variability of the West African monsoon: what do we learn from CMIP3 coupled simulations?, International Journal of Climatology, 30(12), 1843-1856.

Keenlyside, N. S., and M. Latif (2007), Understanding Equatorial Atlantic Inter-annual Variability, Journal of Climate, 20(1), 131-142.

Kucharski, F., A. Bracco, J. H. Yoo, and F. Molteni (2008), Atlantic forced component of the Indian monsoon inter-annual variability, Geophysical Research Letters, 35(4), L04706.

Kucharski, F., A. Bracco, J. H. Yoo, A. M. Tompkins, L. Feudale, P. Ruti, and A. Dell'Aquila (2009), A Gill–Matsuno-type mechanism explains the tropical Atlantic influence on African and Indian monsoon rainfall, Quarterly Journal of the Royal Meteorological Society, 135(640), 569-579.

Kushnir, Y., M. Barreiro, P. Chang, J. Chiang, A. Lazar, and P. Malanotte-Rizzoli (2003), The role of the south Atlantic in the Variability of the ITCZ White paper for CLIVAR/IAI/OOPC.

Lamb, P. J. (1978), Case Studies of Tropical Atlantic Surface Circulation Patterns During Recent Sub-Saharan Weather Anomalies: 1967 and 1968, Monthly Weather Review, 106(4), 482-491.

Latif, M. (2001), Tropical Pacific/Atlantic Ocean interactions at multi-decadal time scales, Geophysical Research Letters, 28(3), 539-542.

Lopez-Parages, J., J. Villamayor, I. Gomara, T. Losada, M. Martín-Rey, E. Mohino, I. Polo, B. Rodríguez-Fonseca, and R. Suarez (2013), Nonstationary inter-annual teleconnections modulated by multidecadal variability, Fisica de la Tierra, 25, 11-39.

Losada, T., and B. Rodriguez-Fonseca (2015), Tropical Atmospheric Response to Decadal Changes in the Atlantic Equatorial Mode, Climate Dynamics (In press).

Losada, T., B. Rodríguez-Fonseca, and F. Kucharski (2012a), Tropical influence on the summer Mediterranean climate, Atmospheric Science Letters, 13(1), 36-42.

Losada, T., B. Rodríguez-Fonseca, S. Janicot, S. Gervois, F. Chauvin, and P. Ruti (2010a), A multi-model approach to the Atlantic Equatorial mode: impact on the West African monsoon, Climate Dynamics, 35(1), 29-43.

Losada, T., B. Rodríguez-Fonseca, I. Polo, S. Janicot, S. Gervois, F. Chauvin, and P. Ruti (2010b), Tropical response to the Atlantic Equatorial mode: AGCM multimodel approach, Climate Dynamics, 35(1), 45-52.

Losada, T., B. Rodriguez-Fonseca, E. Mohino, J. Bader, S. Janicot, and C. R. Mechoso (2012b), Tropical SST and Sahel rainfall: A non-stationary relationship, Geophysical Research Letters, 39(12), L12705.

Lübbecke, J. F., and M. J. McPhaden

(2013), A Comparative Stability Analysis of Atlantic and Pacific Niño Modes*, Journal of Climate, 26(16), 5965-5980.

Lübbecke, J. F., C. W. Böning, N. S. Keenlyside, and S.-P. Xie (2010), On the connection between Benguela and equatorial Atlantic Niños and the role of the South Atlantic Anticyclone, Journal of Geophysical Research: Oceans, 115(C9), C09015.

Madec, G. (2008), NEMO ocean engine, Note du Pole de mod`elisation, edited.

Martín-Rey, M., B. Rodriguez-Fonseca, and I. Polo (2015a), Atlantic opportunities for ENSO prediction, Geophysical Research Letters (under revision).

Martín-Rey, M., I. Polo, B. Rodríguez-Fonseca, and F. Kucharski (2012), Changes in the inter-annual variability of the tropical Pacific as a response to an equatorial Atlantic forcing, Scientia Marina, 76(S1), 105-116.

Martín-Rey, M., B. Rodríguez-Fonseca, I. Polo, and F. Kucharski (2014), On the Atlantic–Pacific Niños connection: a multidecadal modulated mode, Climate Dynamics, 43(11), 3163-3178.

Merle, J. (1980), Seasonal variation of heat-storage in the tropical Atlantic ocean, Oceanologica Acta, 3(4), 455-463.

Mohino, E., B. Rodríguez-Fonseca, T. Losada, S. Gervois, S. Janicot, J. Bader, P. Ruti, and F. Chauvin (2011), Changes in the inter-annual SST-forced signals on West African rainfall. AGCM intercomparison, Climate Dynamics, 37(9-10), 1707-1725.

North, G., T. Bell, F. Cahalan, and F. Moeng (1982), Sampling errors in the estimation of empirical orthogonal function, Mon. Wea. Rev. , 110 699–706.

Peter, A.-C., M. Le Hénaff, Y. du Penhoat, C. E. Menkes, F. Marin, J. Vialard, G. Caniaux, and A. Lazar (2006), A model study of the seasonal mixed layer heat budget in the equatorial Atlantic, Journal of Geophysical Research: Oceans, 111(C6), C06014.

Polo, I., B. Rodríguez-Fonseca, T. Losada, and J. García-Serrano (2008a), Tropical Atlantic Variability Modes (1979–2002). Part I: Time-Evolving SST Modes Related to West African Rainfall, Journal of Climate, 21(24), 6457-6475.

Polo, I., A. Lazar, B. Rodriguez-Fonseca, and S. Arnault (2008b), Oceanic Kelvin waves and tropical Atlantic intraseasonal variability: 1. Kelvin wave characterization, Journal of Geophysical Research: Oceans, 113(C7), C07009.

Polo, I., M. Martin-Rey, B. Rodriguez-Fonseca, F. Kucharski, and C. Mechoso (2015a), Processes in the Pacific La Niña onset triggered by the Atlantic Niño, Climate Dynamics, 44, 115–131.

Polo I., A. Lazar, B. Rodriguez-Fonseca and J. Mignot (2015b) Growth and decay of the Equatorial Atlantic SST mode by means of closed heat budget in a coupled General Circulation Model. Frontiers in Earth Science (Under revision)

Rayner, N. A., D. E. Parker, E. B. Horton, C. K. Folland, L. V. Alexander, D. P. Rowell, E. C. Kent, and A. Kaplan (2003), Global analyses of sea surface temperature, sea ice, and night marine air temperature since the late nineteenth century, Journal of Geophysical Research: Atmospheres, 108(D14), 4407.

Richter, I., S.-P. Xie, S. Behera, T. Doi, and Y. Masumoto (2014), Equatorial Atlantic variability and its relation to mean state biases in CMIP5, Climate Dynamics, 42(1-2), 171-188.

Richter, I., S. K. Behera, Y. Masumoto, B. Taguchi, N. Komori, and T. Yamagata (2010), On the triggering of Benguela Niños: Remote equatorial versus local influences, Geophysical Research Letters, 37(20), L20604.

Rodríguez-Fonseca, B., I. Polo, J. García-Serrano, T. Losada, E. Mohino, C. R. Mechoso, and F. Kucharski (2009), Are Atlantic Niños enhancing Pacific ENSO events in recent decades?, Geophysical Research Letters, 36(20), L20705.

Rodríguez-Fonseca, B., et al. (2011), Inter-annual and decadal SST-forced responses of the West African monsoon, Atmospheric Science Letters, 12(1), 67-74.

Rowell, D. P., C. K. Folland, K. Maskell, and M. N. Ward (1995), Variability of summer rainfall over tropical north Africa (1906–92): Observations and modelling, Quarterly Journal of the Royal Meteorological Society, 121(523), 669-704.

Ruiz-Barradas, A., J. A. Carton, and S. Nigam (2000), Structure of Inter-annual-to-Decadal Climate Variability in the Tropical Atlantic Sector, Journal of Climate, 13(18), 3285-3297.

Vauclair, F., and Y. du Penhoat (2001), Inter-annual variability of the upper layer of the tropical Atlantic Ocean from in situ data between 1979 and 1999, Climate Dynamics, 17(7), 527-546.

Vialard, J., C. Menkes, J.-P. Boulanger, P. Delecluse, E. Guilyardi, M. J. McPhaden, and G. Madec (2001), A Model Study of Oceanic Mechanisms Affecting Equatorial Pacific Sea Surface Temperature during the 1997–98 El Niño, Journal of Physical Oceanography, 31(7), 1649-1675.

Von Storch, H., and F. Zwiers (2001), Statistical Analysis in Climate Research, Cambridge University Press. , 484 pp.

Wagner, R. G., and A. M. da Silva (1994), Surface conditions associated with anomalous rainfall in the guinea coastal region, International Journal of Climatology, 14(2), 179-199.

Ward, M. N. (1998), Diagnosis and Short-Lead Time Prediction of Summer Rainfall in Tropical North Africa at Inter-annual and Multidecadal Timescales, Journal of Climate, 11(12), 3167-3191.

Zebiak, S. E. (1993), Air–Sea Interaction in the Equatorial Atlantic Region, Journal of Climate, 6(8), 1567-1586.

7. INTEGRATED DISCUSSION

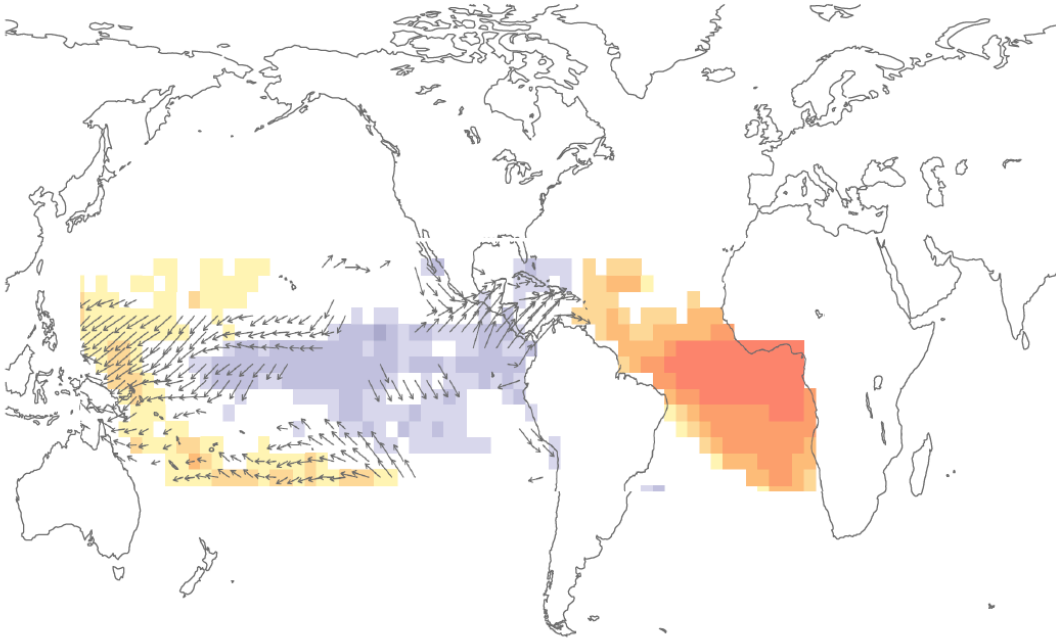

7. INTEGRATED DISCUSSION

Large uncertainties and drastic shifts have governed the present climate variability at multiple time scales [*Kosaka and Xie*, 2013; *Yao et al.*, 2015]. Thus, the scientific community has focused on understanding the causes of these changes through the determination of the role played by natural climate variability *vs* anthropogenic forcing.

On the one hand, natural decadal variability drives the changes in the background state of the global oceans through decadal SST patterns as the Atlantic Multidecadal Oscillation (AMO) and Pacific Decadal Oscillation (PDO). This modification of the tropical Atlantic and Pacific mean conditions has a strong impact on the inter-annual variability of both oceans. In this sense, the characteristics of ENSO have varied at decadal time scales [*Federov and Philander*, 2000; *Wang and An*, 2002; *Yeh and Kirtman*, 2005; *An et al.*, 2006; *Fang et al.*, 2008; *Borlace et al.*, 2013] associated with different phases of the PDO [*Yeh and Kirtman*, 2005; *Yeh et al.*, 2011; *Chung et al.*, 2013]. In relation to the AMO, model experiments have revealed how under a positive AMO phase, the ENSO variability is reduced [*Dong et al.*, 2006]. In this line, several authors have also demonstrated that a substantial weakening of the Atlantic Multidecadal Overturning Circulation, AMOC, is associated with a background state of cooler SSTs in the North Atlantic (strong negative AMO-like pattern) which originates an anomalous enhancement of the surface winds in the tropical Pacific, generating a shallower thermocline and increasing ENSO variability [*Dong and Sutton*, 2007; *Timmermann et al.*, 2007; *Kang et al.*, 2014]. Meanwhile, under the same negative AMO-like conditions, over the equatorial Atlantic the thermocline is anomalously deep, which decreases the inter-annual variability related to thermocline feedbacks [*Haarsma et al.*, 2008; *Polo et al.*, 2013]. However, the enhancement of ENSO in boreal winter increases the variance of equatorial Atlantic SST in boreal spring through heat fluxes [*Polo et al.*, 2013].

On the other hand, the anthropogenic forcing could also contribute to the changes in the Atlantic and Pacific Oceans during recent decades [*Yeh et al.*, 2009; *Kucharski et al.*, 2011; *McPhaden et al.*, 2011; *Tokinaga and Xie*, 2011]. *Tokinaga and Xie* [2011] have suggested that the Global Warming (GW) generates warmer SSTs in the western equatorial Atlantic, reducing the zonal gradient and thus the inter-annual variability during summer months. However, *Polo et al.* [2013] have pointed out that observed warmer SST conditions in South Atlantic (negative AMO phase in comparison with positive AMO phase) is associated with an increase of the eastern equatorial Atlantic variability during autumn season. *Thus, although the Atlantic background state has an impact on the tropical Atlantic climate, its influence over the inter-annual variability still remains unclear.*

The impacts of the changes in the background state can be noticed worldwide. In this way, some to the above-mentioned studies have shown how warmer conditions in the south Atlantic Ocean, associated with Global Warming [*Kucharski et al.*, 2011] or negative AMO phases [*Dong et al.*, 2006; *Dong and Sutton*, 2007; *Timmermann et al.*, 2007], enhance the convection over the tropical band, favouring the upper level divergent winds that are able to trigger atmospheric teleconnections [*Kucharski et al.*, 2008; 2009; *Losada et al.*, 2010a; *Losada et al.*, 2012b; *McGregor et al.*, 2013; *Kucharski et al.*, 2014].

According to these statements, a warming of the South Atlantic Ocean could be related to a reduction of its oceanic variability but also to an enhancement of the sources of teleconnections. Furthermore, this Atlantic warming is also associated with an increase of the equatorial Pacific oceanic variability. Under these circumstances, the recently discovered influence of the Atlantic Niños on ENSO phenomena [*Keenlyside and Latif*, 2007; *Polo et al.*, 2008a; *Rodríguez-Fonseca et al.*, 2009; *Ding et al.*, 2012] becomes reasonable.

The above mentioned changes in the inter-annual Atlantic and Pacific variability at multidecadal time scales, driven by the decadal oceanic patterns, could give rise to different modes of variability at inter-annual time scales. In this sense, it has been found that two different Atlantic Niño configurations co-exist in the tropical Atlantic basin

under negative AMO phases (*Martin-Rey et al.* [2015b]; Figure D1-D2). On the one hand, an Atlantic Niño characterized by an equatorial warming surrounded by a horseshoe-like shape of negative SST anomalies in north and south tropical Atlantic appears in the tropical Atlantic basin, associated with an intensification of the subtropical trades and anomalous westerly winds in the equatorial band (Figure D1). This mode resembles the Canonical Atlantic Niño pattern reported in previous studies [*Zebiak*, 1993; *Lübbecke et al.*, 2010; *Nnamchi et al.*, 2011a; *Richter et al.*, 2012a]. This canonical mode has been considered as the oceanic response for anomalous westerly winds in western equatorial Atlantic, which in turn are the drivers of the Bjerknes feedback [*Bjerknes*, 1969; *Keenlyside and Latif*, 2007; *Richter et al.*, 2013]. Although the wind anomalies in this region seem to be largely due to internal atmospheric variability [*I Richter et al.*, 2014], they can be also externally forced by changes in the Sta Helena High Pressure System [*Lübbecke et al.*, 2010; *Nnamchi et al.*, 2011a] or the influence of ENSO phenomena [*Latif and Grötzner*, 2000; *Saravanan and Chang*, 2000; *Münnich and Neelin*, 2005].

An analysis of the atmospheric forcings of these canonical Atlantic Niños, reveals that these events are preceded by an initial strengthening of Azores and Sta Helena High during autumn and winter months, which evolves in a zonal SLP gradient during late-winter and spring [*Martin-Rey et al.*, 2015b]. As a consequence of the SLP anomalies, the north-eastern and south-eastern trade winds are reinforced, enhancing the evaporation and cooling the subtropical regions through turbulent heat fluxes (Figure D1; *Martin-Rey et al.* [2015b].). The anomalous east-west SLP configuration during the spring season, generates strong westerly winds along the equator that produce an anomalous convergence of the currents, deepening the thermocline and warming the equatorial band through vertical processes [*Martin-Rey et al.*, 2015b]. These anomalous westerly winds could also activate the Bjerknes feedback in the tropical Atlantic basin [*Bjerknes*, 1969], contributing to amplify and maintain the canonical Atlantic Niño SST anomalies [*Bjerknes*, 1969; *Keenlyside and Latif*, 2007; *Richter et al.*, 2013]. Although some wind-evaporation-SST feedback [*Chang et al.*, 1997; *Okumura et al.*, 2001] could be expected

from the cross-equatorial wind pattern (Figure D1), the heat budget reveals no contribution from atmospheric fluxes at the equator [*Martin-Rey et al.*, 2015b].

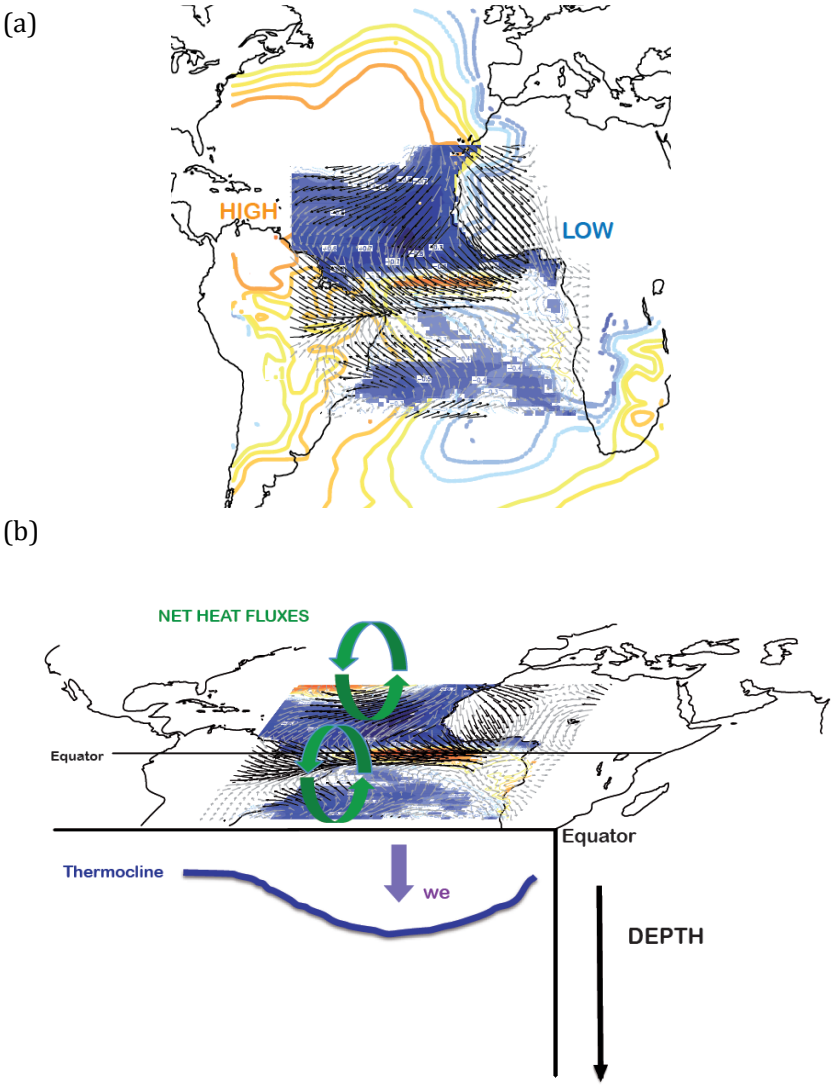

Figure D1. Scheme of the atmospheric (a) and oceanic processes (b) involved in the development of C-Atlantic Niños. [*Martín-Rey et al.* 2015b].Enhanced Azores high and weaken St Helena high induces eastward wind over western equatorial Atlantic.

On the other hand, a new Atlantic Niño pattern, characterized by a warming covering the whole basin, emerges in the tropical Atlantic during recent decades (Figure D2; *Martin-Rey et al.* [2015b].). This Basin-Wide Atlantic Niño co-exists with the Canonical mode, but it is associated with different atmospheric forcings and oceanic processes. A weakening of both Atlantic Subtropical High Pressure Systems during previous autumn and winter generates a reduction of the trades in the subtropical regions and anomalous wind convergence in the equatorial band (Figure D2). The weakened subtropical winds inhibit the evaporation and, thus, warm the north and south tropical Atlantic through turbulent heat fluxes. As a consequence of the anomalous subtropical cyclonic circulation, an anomalous convergence of the Ekman transport deepens the thermocline, also contributing to warm the subtropical areas [*Martin-Rey et al.*, 2015b]. Along the equatorial band, an anomalous wind convergence induces an anomalous convergence of the zonal currents, deepening the thermocline and activating the vertical processes responsible to the equatorial warming [*Martin-Rey et al.*, 2015b]. Besides, net heat fluxes seem to be active in warming the western equator during previous boreal winter and late-spring [*Martin-Rey et al.*, 2015b].

The different equatorial wind forcing in the BW-Atlantic Niño (anomalous wind convergence), respect to the Canonical mode (anomalous westerly winds) implies that different dynamical mechanisms could be operating in the development of these phenomena. In this sense, it is less clear the existence of the Bjerknes feedback in the onset of the BW-Atlantic Niño compared with the growth in the Canonical one. These results fit within the current scientific context of very recent studies, which put under debate the role of the Bjerknes feedback in the equatorial Atlantic [*Richter et al.*, 2012b; *Lübbecke and McPhaden*, 2013; *Nnamchi et al.*, 2015; *Richter et al.*, 2015]. For instance, some authors have indicated that there exist equatorial Atlantic warm events, different from the Canonical ones, that are forced by subtropical winds in north tropical Atlantic creating and anomalous warming that is consequently advected to the equatorial band [*Richter et al.*, 2012b; 2015]. The lack of anomalous winds in the western equatorial Atlantic implies that the Bjerknes feedback does not operate in these events [*Richter et al.*, 2015].

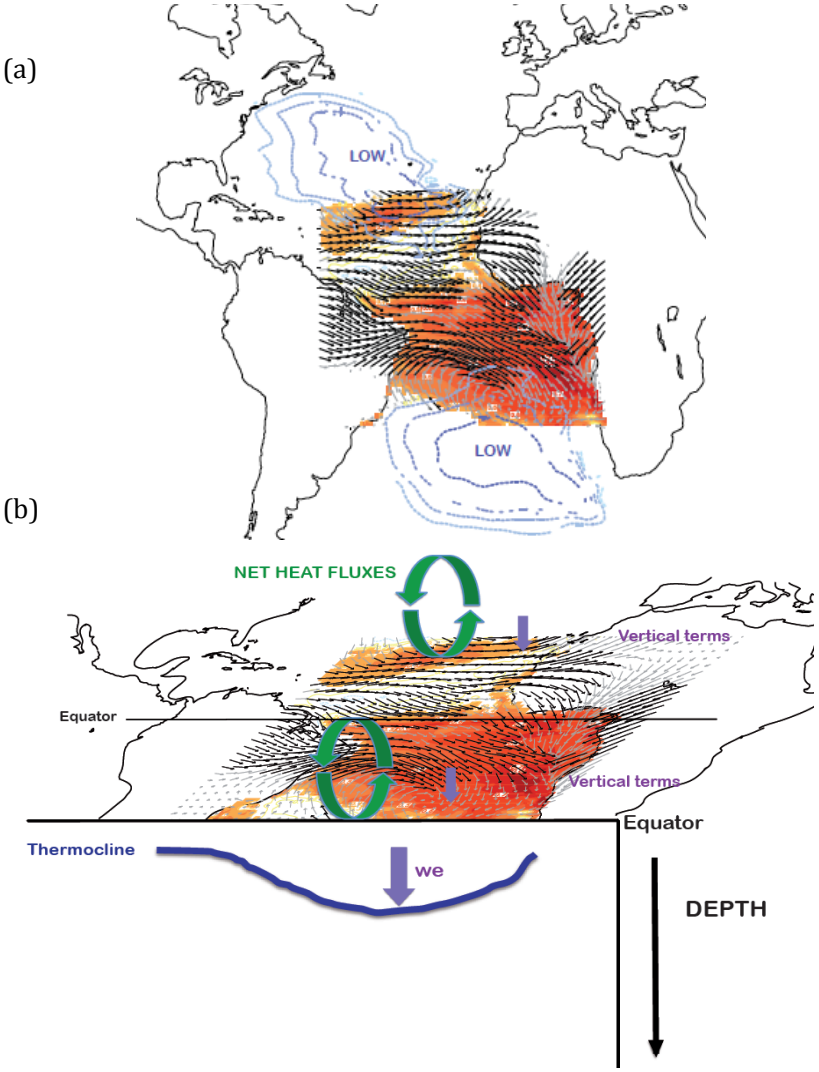

Figure D2. Scheme of the atmospheric (a) and oceanic processes (b) involved in the development of BW-Atlantic Niños. [*Martín-Rey et al.* 2015b]. Weakeningof both, Azores high and St Helena high induces wind convergence over western equatorial Atlantic.

The different equatorial wind forcing in the BW-Atlantic Niño (anomalous wind convergence), respect to the Canonical mode (anomalous westerly winds) implies that different dynamical mechanisms could be operating in the development of these phenomena. In this sense, it is less clear the existence of the Bjerknes feedback in the onset of the BW-Atlantic Niño compared with the growth in the Canonical one. These results fit within the current scientific context of very recent studies, which put under debate the role of the Bjerknes feedback in the equatorial Atlantic [*Richter et al.*, 2012b; *Lübbecke and McPhaden*, 2013; *Nnamchi et al.*, 2015; *Richter et al.*, 2015]. For instance, some authors have indicated that there exist equatorial Atlantic warm events, different from the Canonical ones, that are forced by subtropical winds in north tropical Atlantic creating and anomalous warming that is consequently advected to the equatorial band [*Richter et al.*, 2012b; 2015]. The lack of anomalous winds in the western equatorial Atlantic implies that the Bjerknes feedback does not operate in these events [*Richter et al.*, 2015].

In the same line of reasoning, despite the present Thesis evidences the crucial contribution of the vertical terms in the development of SST anomalies in the equatorial Atlantic (primarily in the C-Atlantic Niño) recent studies, using CGCMs with a slab-ocean configuration, have indicated that the inter-annual variability of the tropical Atlantic can be reproduced by thermodynamical processes without any thermocline feedbacks [*Nnamchi et al.*, 2015;]. Nevertheless, according to the above-mentioned studies, the air-sea interactions involved in the development of the Atlantic Niño phenomena could be highly-dependent on its spatial structure, which seems to vary at decadal time scales.

In this sense, the multidecadal changes of the Atlantic Niño pattern could be related to a modification in its teleconnections. Several authors have reported that the impact of the Atlantic Niño over the precipitation regime in WA [*Losada et al.*, 2010a; *Losada et al.*, 2010b; *Mohino et al.*, 2011; *Rodríguez-Fonseca et al.*, 2011], the Euro-Mediterranean sector [*Losada et al.*, 2012a] and the tropical Pacific variability [*Rodríguez-Fonseca et al.*, 2009; *Martín-Rey et al.*, 2012; *Martín-Rey et al.*, 2014; *Polo et al.*, 2015a] have changed in the last

part of the XX century. This modification coincides with the appearance of the BW-Atlantic Niño pattern as a variability mode clearly separated from the C-Atlantic Niño.

In particular, this BW-Atlantic Niño is able to influence the Pacific La Niña (and vice versa) during the next winter through an alteration of the Walker circulation (Figure D3; *Rodríguez-Fonseca et al.* [2009]; *Ding et al.* [2012]). The state of the art about the Atlantic-Pacific Niños connection presented a controversy about its stationarity. Some authors had proposed that this connection was stationary in time [*Ding et al.*, 2012], while other authors had reported that the Atlantic Niño impact on ENSO only occurred after the 1970s [*Keenlyside and Latif*, 2007; *Polo et al.*, 2008a; *Rodríguez-Fonseca et al.*, 2009]. The results of this Thesis shed light on the discussion, demonstrating that the Atlantic-Pacific connection is an air-sea coupled mode of tropical variability that only takes place at multidecadal time scales [*Martín-Rey et al.*, 2014].

Those periods in which the Atlantic-Pacific Niños connection occurs, during the first and last decades of the 20th century, coincide with negative phases of the AMO, suggesting its possible modulator role. In this way, a negative AMO could change the background state of the equatorial convection and enhance the divergence in upper levels over the western equatorial Atlantic [*Martín-Rey et al.*, 2014], as well as increasing the eastern equatorial Pacific SST variability [*Dong et al.* [2006], favouring in this way the inter-basin connection at multidecadal time scales (Figure D3).

However, apart from the AMO, other natural decadal patterns as the PDO or anthropogenic forcings (Global Warming, GW) could be suitable to contribute to changes in the mean state of the global oceans, and thus favouring the Atlantic-Pacific connection. For instance, the decades in which the Atlantic-Pacific mode emerges are also associated with positive phases of the PDO. Thus a global inter-hemispheric SST pattern, characterized by warmer conditions in the southern hemisphere, amplified by the GW during the last decades, could be responsible of the multidecadal modulation of the Atlantic-Pacific connection [*Kucharski et al.*, 2011].

Nevertheless, there are still many open questions which are in turn hot topics in the climate change and prediction scientific community: *Which is the role played by each decadal variability pattern in the inter-annual variability? Is there any interaction between the natural variability and the Global Warming?* To address these questions, the use of the current state-of-the-art climate models is required.

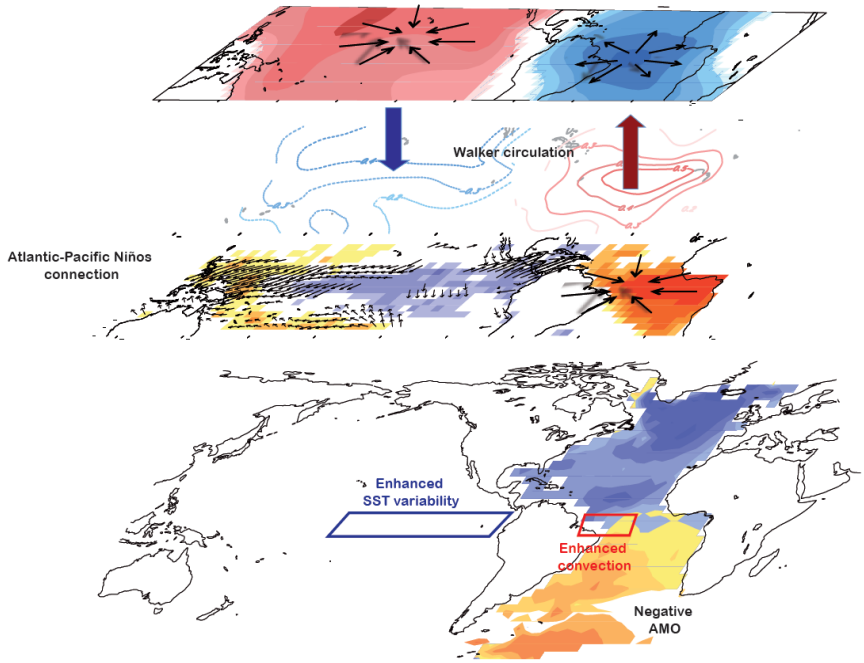

Figure D3. Scheme of the Atlantic-Pacific connection established at multidecadal time scales, which could be modulated by the AMO [*Rodríguez-Fonseca et al.* 2009; *Martín-Rey et al.* 2014; *Polo et al.* 2015a]. Under negative AMO, the convection over western equatorial Atlantic and SST over the eastern Pacific equator are enhanced. An Atlantic Nino increases the vertical ascends generates upper level divergence, which is able to impact the Pacific through anomalous walker circulation. Surface divergence over central Pacific and associated easterly wind over the west-central are responsible for La Niña onset.

Despite previous studies have proposed that the Atlantic Niño (Niña) could impact on the Pacific Niña (Niño) through an anomalous Walker circulation, the oceanic mechanisms involved in the development of these ENSO phenomena remained unclear at the beginning of this Thesis. It has been demonstrated how an Atlantic Niño is related to an ENSO phenomena developed by strong dynamical feedbacks, while ENSO events unrelated to the Atlantic forcing, are similar to those internally driven and seems to be led by thermodynamic processes [*Martín-Rey et al.*, 2012].

Furthermore, when a summer Atlantic Niño occurs, the convection over the tropical Atlantic basin is enhanced, altering the Walker circulation and giving rise to descending motions over the central Pacific (Figure D3; *Rodríguez-Fonseca et al.* [2009]; *Losada et al.* [2010b]). As a consequence of the anomalous subsidence over the central Pacific (around the dateline) imposed by the Atlantic Niño, easterly winds appears in western Pacific piling up the waters to the west and producing an alteration in the thermocline depth. This perturbation propagates eastward as a Kelvin wave from autumn to winter months and westward as off-equatorial Rossby waves (Figure D4;*Polo et al.* [2015a]). As the Kelvin wave propagates to the east, the thermocline depth gets shallower, favouring the cooling of the sea surface through temperature advection by anomalous zonal currents under a mean temperature gradient and by mean vertical upwelling velocity in an anomalous stratified ocean, in agreement with previous observational studies [*Jin and An*, 1999; *Dewitte et al.*, 2009]. These zonal advective and thermocline feedbacks reinforce the initial surface wind anomalies over the central-eastern Pacific setting up the oceanic conditions needed for the development of La Niña cold tongue (Figure D4; *Polo et al.* [2015a]). A similar air-sea mechanism, with the associated change in sign, would take place for an Atlantic Niña event.

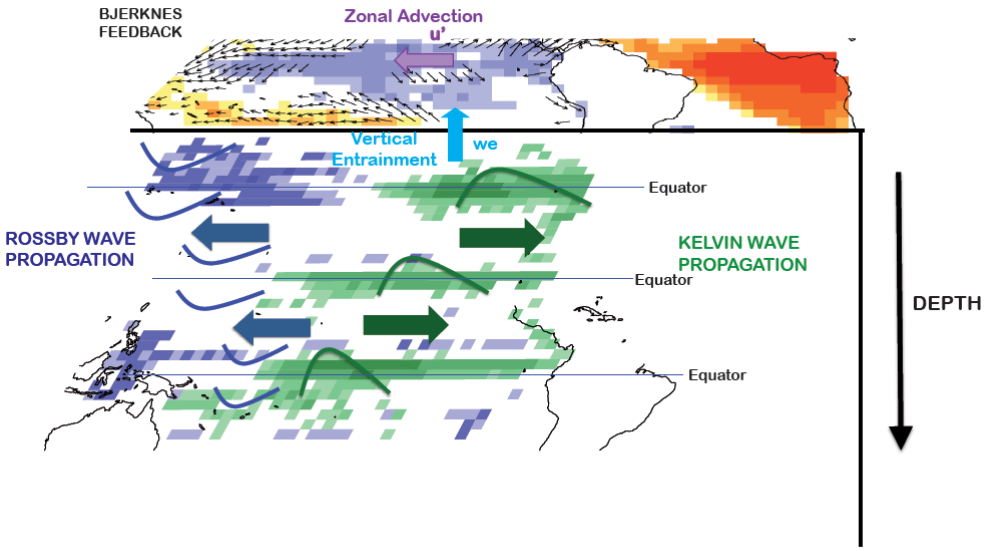

Figure D4. Scheme of the air-sea mechanisms involved in the Atlantic-forced ENSO phenomenon. [*Polo et al.* 2015a]. Easterly winds over the equatorial Pacific perturb the sea surface generating Rossby and Kelvin waves propagating westward and eastward respectively. Kelvin wave change the stratification, which is key in the thermocline feedback term.

These mechanisms were demonstrated with a reduced-gravity model similar to *Cane and Zebiak* [1985] but extended with a surface mixed-layer which allows prediction of SST [*Chang*, 1994]. They were also confirmed with additional numerical experiments with a continuously stratified ocean (NEMO).

This air-sea mechanism is in agreement with theoretical models as the "delayed-oscillator" scheme described by *Suarez and Schopf* [1988], primarily because it consider the oceanic waves as crucial in El Niño development. The mechanism described in *Polo et al.*, [2015a] could also verify the "recharge-oscillator" ENSO theory [*Jin*, 1997], since the anomalous surface winds in western Pacific are the key factor in triggering the Atlantic-forced ENSO. This information could be very useful to improve ENSO forecast, since the tropical Atlantic SSTs become a relevant precursor of ENSO.

The prediction of ENSO episodes stills remains a challenge for the scientific community. Although previous studies have predicted ENSO phenomena from its classic precursors, the western Indo-Pacific winds and tropical Pacific equatorial heat content [*Latif and Barnett*,

1994; *Clarke and Van Gorder*, 2003; *McPhaden et al.*, 2006a], obtaining good correlation skills, recent works have pointed out an enhancement of ENSO predictability when other tropical and extra-tropical regions are included [*Jansen et al.*, 2009; *Frauen and Dommenget*, 2012; *Boschat et al.*, 2013; *Dayan et al.*, 2013; *Keenlyside et al.*, 2013]. In this context, the role of the Atlantic SSTs in the enhancement of ENSO predictability has been already reported [*Jansen et al.*, 2009; *Frauen and Dommenget*, 2012; *Keenlyside et al.*, 2013]. Some authors, using a recharge-oscillator scheme, have demonstrated that the model skill is increased when the equatorial Atlantic SSTs are considered [*Jansen et al.*, 2009; *Frauen and Dommenget*, 2012]. This improvement in the ENSO prediction using the information of the tropical Atlantic Ocean is reasonable in the context of the Atlantic-Pacific connection. Nevertheless, these authors did not take into account the possible non-stationary influence of the Atlantic on ENSO phenomena.

The present Thesis have made a relevant statement for the prediction community by saying that tropical Atlantic could be important for ENSO forecast only in certain periods of time. A statistical cross-validated hindcast of ENSO along the 20th century, which considers the summer tropical Atlantic SSTs as the predictor field and the set of atmospheric and oceanic variables related to the Atlantic-Pacific mechanism as predictand field [*Martín-Rey et al.*, 2014; *Polo et al.*, 2015a], demonstrates that the ENSO prediction depends on the decades considered. During the first and last decades of the 20th century, the statistical hindcast is able to reproduce the Pacific variables involved in ENSO development, in agreement with the mechanism described in *Polo et al.* [2015a]. It is worth mentioning that for these periods, the statistical hindcast tends to predict larger SST anomalies in ENSO phenomena than in observations, showing a stronger signal in the SST, wind stress and thermocline depth fields. On the contrary, the cross-validated hindcast fails in simulating the ENSO-associated variables during the 1940s-1960s, putting forward the lack of ENSO predictability from the tropical Atlantic SST in that period.

Thus, it can be concluded that although the Atlantic SSTs seem to enhance the skill of the ENSO forecast, its prediction is strongly time-dependent. A good ENSO prediction will be only obtained, from the information of the tropical Atlantic SSTs during previous summer, in those decades in which the Atlantic-Pacific connection takes place. Moreover, those periods with predictive skill are also modulated at multidecadal time scales by changes in the background state of the tropical Atlantic and Pacific Oceans.

In this Thesis, it has been evidenced the important contribution of the inter-annual variability of the tropical Atlantic on the development of ENSO. Nevertheless, the correct simulation of the Atlantic variability remains a daunting task. Most of the Coupled General Circulation Models (CGCMs) suffer from large errors in reproducing the seasonal cycle and variability in the tropical Atlantic basin [*Mechoso et al.*, 1995; *Davey et al.*, 2002; *Richter et al.*, 2012b; *Wang et al.*, 2014; *Polo et al.*, 2015b]. In particular, the wrong simulation of the annual mean of the ITCZ, the equatorial surface winds and the eastern equatorial cold tongue in boreal summer, induce a non-realistic simulation of the tropical Atlantic climate [*Richter and Xie*, 2008].

These deficiencies in simulating the tropical Atlantic mean state and variability could influence the correct reproduction of the tropical Pacific inter-annual variability. In this sense, *Sasaki et al.* [2014] have shown that the suppression of the eastern tropical Atlantic bias induces a deeper thermocline and cooler conditions in south Pacific, reducing the ENSO variability. Nevertheless, a small bias in the tropical Atlantic could favour stronger teleconnections, as the Atlantic-Pacific connection [*Kucharski et al.*, 2014] or the impact over the Indian basin [*Barimalala et al.*, 2012]. *Thus, the results of the present Thesis highlight the need of improving the current simulation of the Atlantic mean state and variability, in order to achieve a realistic representation of the tropical and global climate.* Meanwhile sensitivity experiments are a useful tool to confirm the hypothesis infered in the observations.

7. DISCUSIÓN INTEGRADORA

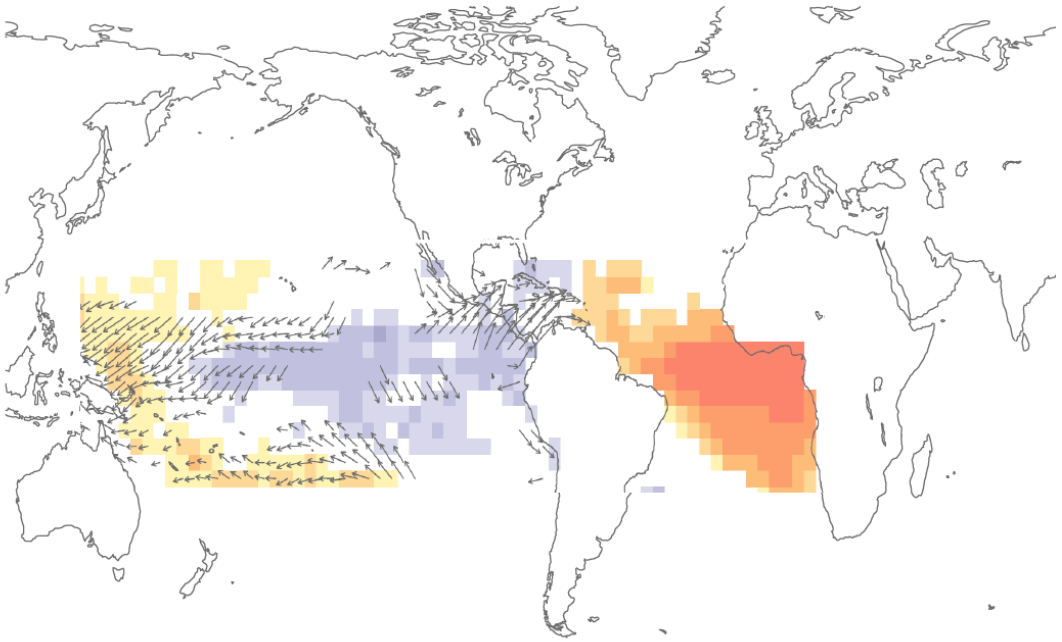

7.DISCUSIÓN INTEGRADORA

La variabilidad climática actual presenta grandes incertidumbres y cambios climáticos abruptos a distintas escalas temporales (Kosaka and Xie, 2013; Yao et al, 2015). Por eso, la comunidad científica está centrada en comprender las causas de dichos cambios, mediante la determinación del papel que juega la variabilidad climática natural *vs* el forzamiento antropogénico.

Por un lado, la variabilidad natural decadal controla los cambios del estado medio de los océanos globales mediante patrones decadales de SST como la Oscilación Multidecadal del Atlántico (AMO) y la Oscilación Decadal del Pacífico (PDO). Esta modificación de las condiciones medias del Atlántico y Pacífico tropical tiene un gran impacto en la variabilidad interanual de ambos océanos. En este sentido, las características de los fenómenos ENSO varian en escalas decadales [*Federov and Philander* 2000; *Wang and An* 2002; *An,* 2006; *Yeh and Hsieh* 2006; *Fang et al.* 2008; *Borlace et al.* 2013] asociadas con diferentes fases de la PDO [*Yeh and Kirtman* 2005; *Yeh et al.* 2011; *Chung and Li* 2013]. En relación con la AMO, experimentos con modelos han revelado como bajo una fase positiva de la AMO, la variabilidad del ENSO se reduce [*Dong et al.,* 2006]. En este sentido, ciertos autores han demostrado que una reducción substancial de la Circulación Multidecadal del Atlántico (AMOC) está asociada con un Atlantico Norte más frio (un patron de AMO negativa), el cual origina una intensificación anómala de los vientos en superficie en el Pacífico tropical, generando una termoclina más somera y aumentando la variabilidad del ENSO [*Dong and Sutton* 2007; *Timmermann et al.* 2007; *Kang et al.* 2014; Polo et al., 2013]. Mientras tanto, bajo las mismas condiciones de AMO negative, sobre el Atlántico ecuatorial, la termoclina se encuentra más profunda de lo normal, lo cual reduce la variabilidad interanual asociada con los procesos de realimentación de la termoclina [*Haarsma et al.,* 2008; *Polo et al.,* 2013]. Sin embargo, la intensificación del ENSO en el invierno boreal, aumenta la variabilidad de la SST del Atlántico ecuatorial durante la primavera boreal mediante flujos de calor [*Polo et al.,* 2013].

Por otro lado, el forzamiento antropogénico podría también contribuir a los cambios en los océanos Atlántico y Pacífico durante las últimas décadas [*Yeh et al.* 2009; *Kucharski et al.* 2011; *McPhaden et al.* 2011; *Tokinaga et al.* 2011]. Tokinaga et al. (2011) ha sugerido que el Calentamiento Global (GW) genera condiciones más cálidas de lo normal en el oeste del Atlántico ecuatorial, reduciendo el gradiente zonal y por tanto la variabilidad interanual durante los meses de verano. Sin embargo, *Polo et al.* [2013] ha indicado que SST más cálidas de lo normal en el Atlántico Sur (fase negativa de la AMO comparada con la fase positiva) se relacionan con un aumento de la variabilidad en el este del Atlántico ecuatorial durante el otoño. *Por tanto, aunque el estado medio del Atlántico tiene un impacto sobre el clima del Atlántico tropical, su influencia sobre la variabilidad interanual sigue sin aclararse.*

Los cambios en el estado medio presentan impactos globales. En este sentido, los estudios mencionados anteriormente han mostrado como bajo un Océano Atlántico Sur más cálido, asociado con el Calentamiento Global [*Kucharski et al.* 2011] o con fases negativas de la AMO [*Dong et al.* 2006; *Timmerman et al.* 2007; *Dong and Sutton* 2007], aumenta la convección sobre la banda tropical, favoreciendo los vientos divergentes en niveles altos, que son capaces de desencadenar las teleconexiones atmosféricas [*Kucharski et al.* 2007; 2008; *Losada et al.* 2010; 2012; *Kucharski et al.* 2011; 2014; *McGregor et al.* 2014].

De acuerdo con lo anteriormente expuesto, un calentamiento en el Océano Atlántico Sur podría relacionarse con una reducción de su variabilidad oceánica, pero con un aumento de las fuentes de teleconexión. Además, este calentamiento en el Atlántico está también relacionado con un incremento de la variabilidad oceánica del Pacífico ecuatorial. Bajo estas condiciones, es comprensible la conexión recientemente descubierta entre los Niños del Atlántico y los fenómenos ENSO [*Keenlyside and Latif* 2007; *Polo et al.* 2008; *Rodríguez-Fonseca et al.* 2009; *Ding et al*. 2012].

Los cambios en la variabilidad interanual del Atlántico y del Pacífico a escalas decadales, anteriormente mencionados, controlados por la variabilidad oceánica decadal, podrían dar lugar a la aparición de distintos modos de variabilidad a escalas interanuales. En este sentido, se ha encontrado que co-existen dos configuraciones del Niño Atlántico bajo fases negativas de la AMO [*Martín-Rey et al.* 2015b; Figure D1-D2]. Por un lado, un Niño Atlántico caracterizado por un calentamiento ecuatorial rodeado por una herradura de anomalías negativas de SST en el norte y sur del Atlántico tropical, aparece en cuenca Atlántica, asociado con una intensificación de los vientos alíseos subtropicales y vientos anómalos del oeste en la banda ecuatorial (Figure D1).

Este modo se asemeja al patron canónico del Niño Atlántico mostrado en estudios previos [*Zebiak* 1993; *Ritcher et al.* 2012; *Lübbecke et al.* 2010; *Nnamchi et al.* 2011]. Este modo Canónico es considerado como una respuesta oceánica a unos vientos anómalos del oeste en la parte occidental del Atlántico ecuatorial, los cuales desencadenan el mecanismo de realimentación de Bjerknes [*Bjerknes* 1969; *Keenlyside and Latif* 2007; *Ritcher et al.* 2012]. Aunque las anomalías de viento en esta region están asociadas en gran medida a la variabilidad interna atmosférica [*Ritcher et al.* 2014], pueden ser también forzadas externamente mediante cambios en el Anticiclón de Sta Helena [*Polo et al.* 2008; *Lübbecke et al.* 2010; *Nnamchi et al.* 2011] o mediante la influencia del fenómeno ENSO [*Saravanan and Chang* 2000; *Latif and Gröztner* 2001; *Munnich and Neelin* 2005].

Por otro lado, un nuevo patron del Niño Atlántico caracterizado por un calentamiento en toda la cuenca, aparece en el Atlántico tropical durante las últimas décadas (Figure D2; *Martín-Rey et al.* [2015b]). Este Niño Atlántico Extendido (Basin-Wide) co-existe con el modo canónico, pero está asociado con forzamientos atmosféricos y procesos oceánicos diferentes. Un debilitamiento de ambos Sistemas de Presión Subtropicales en el Atlántico durante el otoño e invierno previos, genera una reducción de los vientos alíseos en las regiones subtropicales y una convergencia anómala de viento en la banda ecuatorial (Figure D2).

(a)

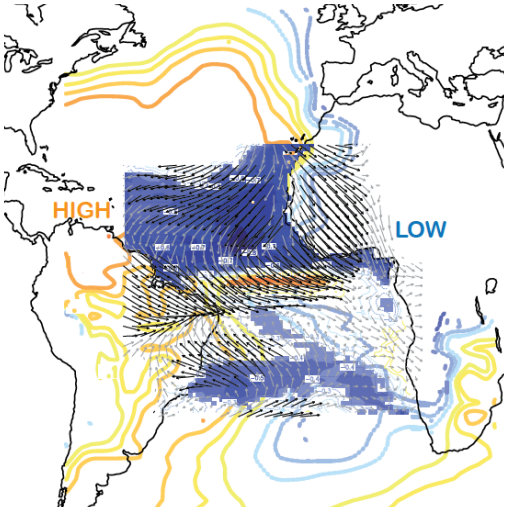

(b)

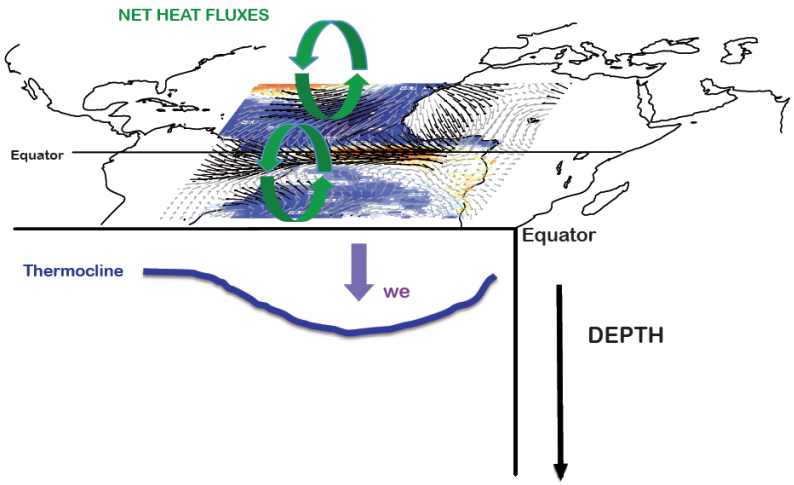

Figura D1. Esquema de los procesos atmosféricos (a) y oceánicos (b) involucrados en el desarrollo de los Niños Atlánticos. [*Martín-Rey et al.* 2015b]. Una intensificación del anticiclón de Azores y Sta genera un reforzamiento de los vientos alíseos subtropicales y vientos anómalos del oeste en la banda ecuatorial.

El debilitamiento de los vientos subtropicales inhibe la evaporación, y por tanto, calienta el norte y sur del Atlántico tropical a través de flujos turbulentos de calor. Debido a una circulación ciclónica anómala en los subtrópicos, se produce una convergencia del transporte de Ekman, hundiendo la termoclina y contribuyendo a calendar las regiones subtropicales *[Martín-Rey et al.* 2015b]. En la

banda ecuatorial, la convergencia anómala de viento genera una convergencia anómala de las corrientes zonales, hundiendo la termoclina y activando los procesos verticales reponsable de crear el calentamiento en el ecuador [Martín-Rey et al. 2015b]. Además, los flujos netos de calor parecen activar el calentamiento en el oeste del Atlántico ecuatorial durante el invierno y la primavera previos [*Martín-Rey et al.,* 2015b].

El diferente forzamiento de viento ecuatorial en el Niño Atlántico BW (convergencia anómala) respecto al modo Canónico (vientos anómalos del oeste) implica que existen diferentes mecanismos dinámicos que podrían estar operando en el desarrollo de estos eventos. En este sentido, no está tan clara la existencia del mecanismo de realimentación de Bjerknes en el comienzo del Niño Atlántico BW comparado con el desarrollo del modo Canónico. Estos resultados están de acuerdo con el contexto científico actual, puesto de manifiesto mediante trabajos recientes, que cuestionan el papel del mecanismo de realimentación de Bjerknes en el Atlántico ecuatorial [*Ritcher et al.* 2012; *Lübbecke and McPhaden*, 2013; *Ritcher et al.* 2015; *Nnamchi et al.,* 2015]. Por ejemplo, algunos autores han indicado que existen eventos cálidos en el Atlántico ecuatorial, diferentes a los modos canónicos, que están forzados por vientos subtropicales en el norte del Atlántico tropical, creando un calentamiento anómalo, que consecuentemente es advectado hacia la banda ecuatorial [*Ritcher et al.* 2012; 2015]. La no-existencia de vientos anómalos del oeste en la parte occidental del Atlántico ecuatorial implica que el mecanismo de realimentación de Bjerknes no está activo en estos fenómenos [Ritcher et al. 2015].

Siguiendo el mismo razonamiento, a pesar de que la presente Tesis demuestra la importante contribución de los terminos verticales en el desarrollo de las anomalías de SST del Atlántico ecuatorial (sobre todo en el Niño Atlántico Canónico), estudios recientes usando GCMs que consideran un modelo de océano de 1 sola capa, indican que se puede reproducir la variabilidad interanual del Atlántico tropical mediante procesos termodinámicos, sin necesidad de procesos de realimentación asociados con la termoclina [Nnamchi et al. 2015]. Sin embargo, de acuerdo con los estudios mencionados anteriormente,

los procesos de interacción aire-océano involucrado en el desarrollo del Niño Atlántico son altamente dependientes de su estructura espacial, la cual parece variar a escalas decadales.

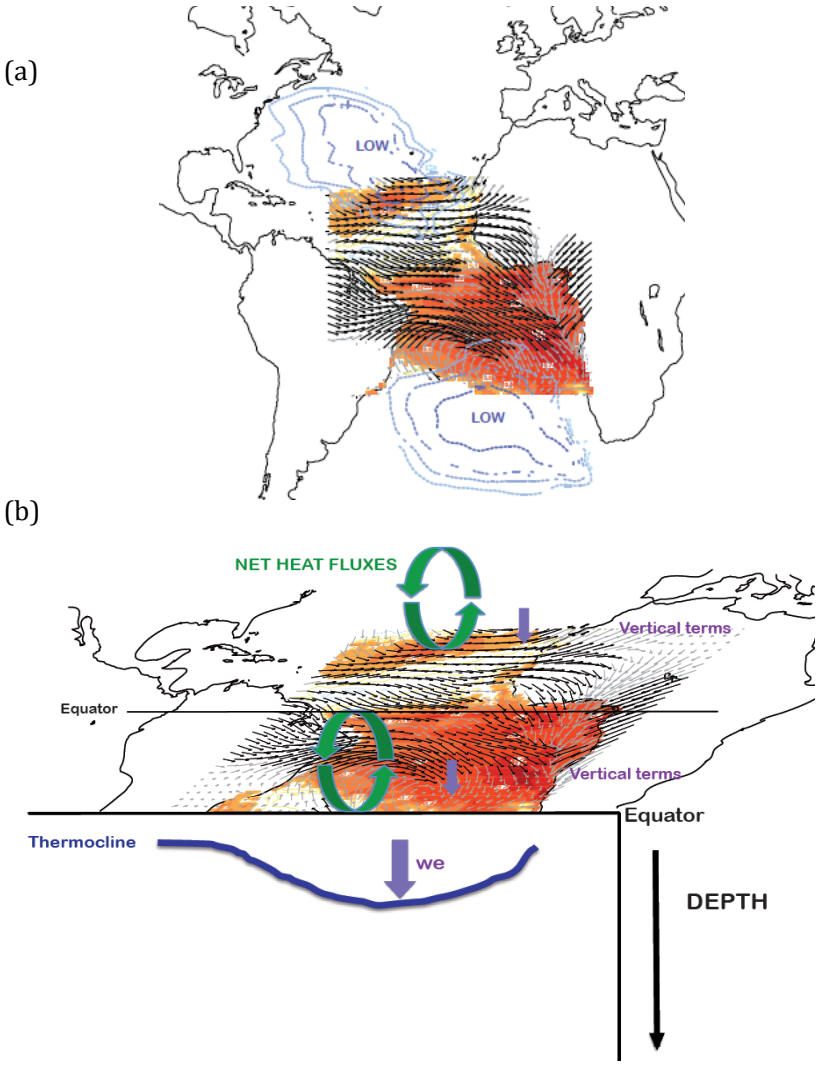

Figura D2. Esquema de los procesos (a) y oceánicos (b) involucrados en el desarrollo de los Niños Atlánticos BW. [*Martín-Rey et al.* 2015b]. Un debilitamiento de Azores y Sta Helena da lugar a una reducción de los vientos aliseos y una convergencia anómala de viento en la banda ecuatorial.

En este sentido, cambios multidecadales del patron del Niño Atlántico parecen estar relacionados con una modificación en sus teleconexiones. Ciertos autores han puesto de manifiesto que los impactos del Niño Atlántico sobre el regimen de precipitación del

Monzón de África Occidental (Losada et al. 2010ab; Rodríguez-Fonseca et al. 2010; Mohino et al. 2011), la región Euro-Atlántica (Losada et al. 2012a) y la variabilidad del Pacífico tropical (Rodríguez-Fonseca et al. 2009; Martín-Rey et al. 2012; 2014; Polo et al. 2015a) han cambiado en las últimas décadas del siglo XX. Esta modificación coincide con la aparición del Niño Atlántico BW como modo propio de variabilidad, claramente separado del Niño Atlántico Canónico.

En particular, el Niño Atlántico BW es capaz de influir en la Niña del Pacífico (y vice versa) durante el siguiente invierno mediante la alteración de la circulación de Walker (Figura D3; *Rodríguez-Fonseca et al.* [2009]; *Ding et al.* [2012]). El estado del arte sobre la estacionariedad de la conexión Atlántico-Pacífico, presenta gran controversia. Algunos autores propusieron que la conexión era estacionaria en el tiempo [*Ding et al.* 2012], mientras que otros autores sostenían que el Niño Atlántico impactaba en el ENSO solamente a partir de los 1970s [*Keenlyside and Latif* 2007; *Polo et al.* 2008a; *Rodríguez-Fonseca et al.* 2009]. Los resultados de la presente Tesis arrojan luz en esta discussion, demostrando que la conexión Atlántico-Pacífico es un modo acoplado aire-océano de variabilidad tropical que solamente aparece a escalas multidecadales [*Martín-Rey et al.* 2014].

Los periodos en los cuales la conexión Atlántico-Pacífico tiene lugar, las primeras y últimas décadas del siglo XX, coinciden con fases negativas de la AMO, sugiriendo su posible papel modulador. En este sentido, la AMO podría cambiar el estado medio de la convección ecuatorial e intensificar la divergencia en niveles altos sobre el oeste del Atlántico ecuatorial [*Martín-Rey et al.* 2014], además de aumentar la variabilida de la SST del este del Pacífico ecuatorial [*Dong et al.* 2006; *Martín-Rey et al.* 2014], favoreciendo de esta manera la conexión entre cuencas a escalas multidecadales (Figura D3).

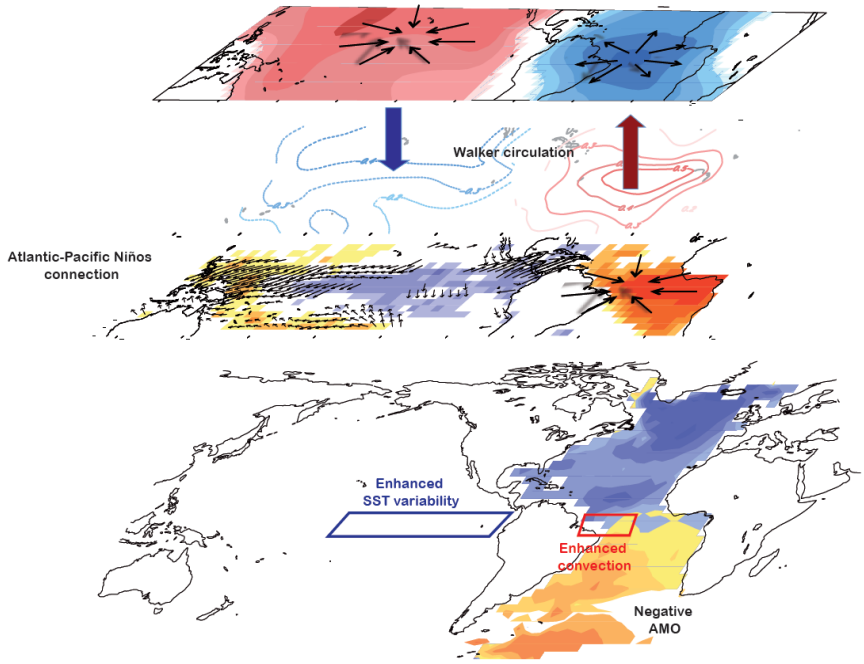

Figura D3. Esquema de la conexión Atlántico-Pacífico que se establece a escalas multidecadales, la cual podría estar modulada por la AMO [*Rodríguez-Fonseca et al.* 2009; *Martín-Rey et al.* 2014; *Polo et al.* 2015a]. Bajo fases negativas de la AMO, la convección sobre el oeste del Atlántico ecuatorial se intensifica. Un Niño Atlántico aumenta los movimientos ascendentes y genera divergencia en niveles altos, la cual es capaz de impactar en el Pacífico a traves de una circulación anómala de Walker. Una divergencia anómala en superficie está asociada con vientos del este sobre el centro y oeste del Pacífico, desencadenando el fenómeno de La Niña.

Sin embargo, aparte de la AMO, otros patrones de variabilidad natural decadal como la PDO o el forzamiento antropogénico (Calentamiento Global, GW) podrían contribuir a los cambios en el estado medio de los océanos globales, y por tanto favorecer la conexión Atlántico-Pacífico. Por ejemplo, las décadas en las que el modo Atlántico-Pacífico aparece, están asociadas con fases positivas de la PDO. Por tanto un patrón global inter-hemisférico de SST, caracterizado por un hemisferio sur más cálido, amplificado por el GW durante las últimas décadas, podría ser responsable de la modulación multidecadal de la conexión Atlántico-Pacífico [*Kucharski et al.* 2011].

Sin embargo, existen aun muchas preguntas abiertas que son los temas más candentes que existen actualmente en la comunidad científica en referencia al cambio climático y la predicción: ¿Cuál es el papel que juega cada patrón de variabilidad decadal en la interanual? ¿Existe alguna interacción entre la variabilidad natural y el Calentamiento Global? Para contester a estas preguntas es necesario hacer uso de los modelos climáticos actuales.

A pesar de que estudios previos han propuesto que el Niño (Niña) del Atlántico podría impactar en la Niña (Niño) del Pacífico a través de una circulación anómala de Walker, los mecanismos oceánicos involucrados en el desarrollo de estos fenómenos ENSO no habían sido aclarados al comienzo de esta Tesis. Se ha demostrado como un Niño Atlántico se relaciona con un fenómeno ENSO mediante fuertes mecanismos de realimentación dinámicos, mientras que los fenómenos ENSO que no están asociados con el forzamiento Atlántico, son similares a los generados internamente y parecen estar desarrollados por procesos termodinámicos [*Martín-Rey et al.* 2012].

Es más, cuando tiene lugar un Niño Atlántico durante el verano boreal, se aumenta la convección sobre el Atlántico tropical, alterándose la circulación de Walker y dando lugar a movimientos descentes sobre el Pacífico central (Figura D3; *Rodríguez-Fonseca et al.,* [2009]; *Losada et al.,* [2010a]; *Ding et al.,* [2011]). Como consecuencia de la subsidencia anómala sobre el centro de la cuenca, asociada con un el forzamiento de un Niño Atlántico, aparecen vientos del este en el Pacífico occidental que apilan las aguas en el oeste y producen una alteración la profundidad de la termoclina. Esta perturbación se propaga hacia el este en forma de onda de Kelvin de otoño a invierno, y hacia el oeste como dos ondas de Rossby fuera del ecuador (Figura D4; Polo et al. 2015a). A medida que la onda de Kelvin se propaga hacia el este, la termoclina se hace más somera, favoreciéndose el enfriamiento de la superficie del mar mediante advección de temperatura por corrientes zonales anómalas, bajo un gradiente medio de temperatura y mediante velocidad vertical media asociada con una estratificación anómala del océano, de acuerdo con estudios previos observacionales [*An et al.* 1999; *Jin and An*, 1999; *Dewitte et al.* 2009]. Estos mecanismos de realimentación de

advección zonal y asociados con la termoclina, refuerzan los vientos anómalos superficiales sobre el centro-este del Pacífico, precondicionando el océano para el desarrollo de la lengua fría de la Niña (Figura D4; *Polo et al.* [2015a]). Un mecanismo similar tendría lugar, con el correspondiente cambio de signo, para una Niña del Atlántico.

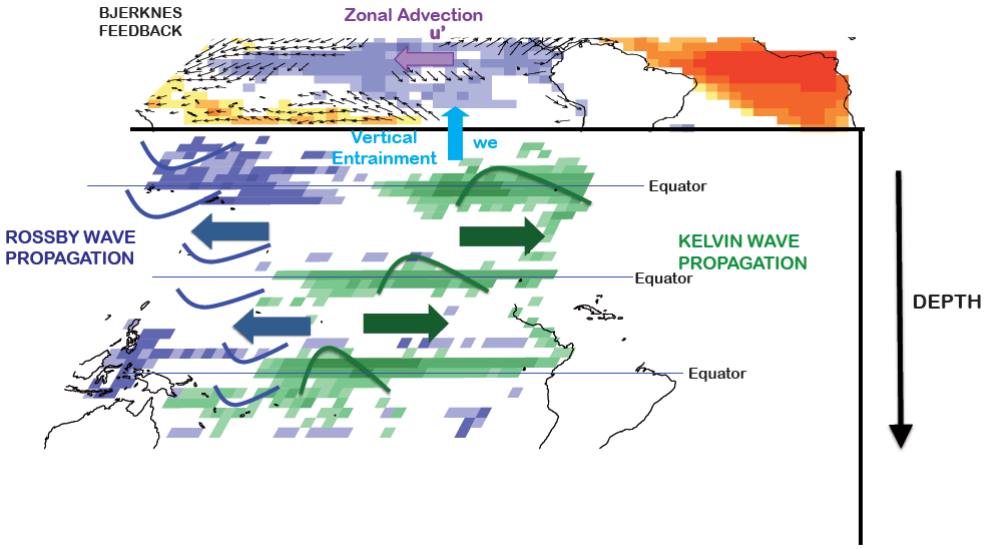

Figura D4. Esquema de los procesos de interacción aire-océano involucrados en el dearrollo del ENSO forzado por el Atlántico. [Polo et al. 2015a]. Vientos anómalos del este en el Pacífico ecuatorial perturban superficie del mar mediante la propagación de ondas de Rossby y de Kelvin hacia el oeste y este respectivamente. La onda de Kelvin modifica la estratificación, la cual es clave para el mecanismo de realimentación asociado con la termoclina.

Estos mecanismos se han demostrado a partir de un modelo de gravedad reducida similar al de *Cane and Zebiak* [1985] pero extendido a la capa de mezcla superficial, que permite predecir la SST [*Chang et al.*, 1994]. Estos mecanismos fueron confirmados con simulaciones realizadas por experimentos numéricos con un océano con una estratificación continua (NEMO).

Este mecanismo aire-océano está de acuerdo con el modelo teórico del "oscilador-retardado" descrito por *Suarez and Schopf* [1988], puesto que este considera que las ondas oceánicas son cruciales en el desarrollo del ENSO. El mecanismo descrito por Polo et al [2015a], podría también verificar la teoría del "oscilador-recargado" [Jin

1997], puesto que los vientos superficiales en el oeste del Pacífico son el factor clave en desencadenar los eventos ENSO forzados por el Atlántico. Esta información podría ser muy útil para mejorar la predicción del ENSO, ya que la SST del Atlántico tropical se convierte en precursor de dicho fenómeno.

La predicción de los fenómenos ENSO sigue suponiendo un desafío para la comunidad científica. Aunque estudios previos han predicho el ENSO mediante sus precursores clásicos, el viento en el oeste del Indo-Pacífico y el contenido de calor del Pacífico ecuatorial [*Latif et al.,* 1994; *Clarke and Van Gorder,* 2003; *McPhaden et al.,* 2006], obteniendo buenas correlaciones, trabajos recientes indican un aumento de la predictabilidad del ENSO cuando se incluyen otras regiones tropicales y extra-tropicales [*Jansen et al.,* 2009; *Frauen and Dommenget,* 2012; *Dayan et al.,* 2013; *Boschat et al.,* 2013; *Keenlyside et al.,* 2013]. En este contexto, se ha estudiado el papel de la SST del Atlántico en aumentar la predictabilidad del ENSO [*Jansen et al*. 2009; *Frauen and Dommenget* 2012; *Keenlyside et al.* 2013]. Algunos autores, usando el modelo del oscilador recargado, han demostrado que se mejora la predicción del ENSO cuando se considera la SST del Atlántico [*Jansen et al.* 2009; *Frauen and Dommenget* 2012; *Keenlyside et al.* 2013]. Esta mejora, a partir de considerar la información del Atlántico tropical, es entendible en el contexto de la reciente conexión Atlántico-Pacífico. Sin embargo, estos autores no tuvieron en cuenta la posible no-estacionariedad de la influencia del Atlántico sobre el ENSO.

La presente Tesis ha proporcionado una información relevante para la comunidad científica dedicada a la predicción, evidenciando la importancia del Atlántico tropical en la predicción del ENSO solamente durante ciertos periodos de tiempo. Se ha desarrollado un modelo estadístico de predicción del ENSO durante todo el siglo XX, considerando la SST del Atlántico tropical en verano como campo predictor, y el conjunto de variables atmosféricas y oceánicas relacionadas con la conexión Atlántico-Pacífico como campo a predecir [*Martín-Rey et al.* 2014; *Polo et al.* 2015a], demostrando que la predicción del ENSO depende de las décadas consideradas. Durante las primeras y últimas décadas del siglo XX, el modelo estadístico es

capaz de reproducir las variables del Pacífico tropical involucradas en el desarrollo del ENSO, de acuerdo con el mecanismo descrito en *Polo et al.* [2015a].

De debe mencionar que, para estos periodos, el modelo estadístico tiende a predecir mayores anomalías de SST en el fenómeno ENSO respecto de las observadas, mostrando una señal también más fuerte en el wind stress y la profundidad de la termoclina. Por el contrario, el modelo estadístico cros-validado falla a la hora de similar las variables asociadas con el ENSO en las décadas de los 1940s a los 1960s, poniendo de manifiesto la falta de predictabilidad el fenómeno ENSO a partir de la SST del Atlántico tropical en ese periodo.

Por tanto, se puede concluir que aunque la SST del Atlántico parece aumentar la predictabilidad del fenómeno ENSO, esta predicción tiene una gran dependencia del periodo de tiempo considerado. Solamente se obtiene una buena predicción del ENSO a partir de la información de la SST del Atlántico tropical, en las décadas en las cuales la conexión Atlántico-Pacifico tiene lugar. Es más, estos periodos donde existe una buena predicción son modulados a escalas multidecadales por cambios en el estado medio de los océanos del Atlántico y Pacífico tropical.

En esta tesis se ha demostrado la importante contribución de la variabilidad interanual del Atlántico tropical en el desarrollo del ENSO. Sin embargo, simular de manera correcta la variabilidad del Atlántico es una ardua tarea. La mayoría de los Modelos De Circulación General (GCMs) presentan grandes errors a la hora de reproducir el ciclo estacional y la variabilidad del Atlántico tropical [*Mechoso et al.* 1995; *Davey et al.* 2002; *Wang et al.* 2014; *Ritcher et al.* 2014; *Polo et al.,* 2015b]. En concreto, la deficiente simulación de la media annual de la ITCZ, los vientos ecuatoriales en superficie y la lengua fria en el este de la banda ecuatorial durante el verano boreal, son responsables de la mala simulación del clima del Atlántico tropical. En este sentido, *Sasaki et al.* [2014] ha mostrado como la eliminación del error en el este del Atlántico tropical genera una termoclina más profunda y condiciones más frías en el sur del Pacífico, que reducen la variabilidad del ENSO. Sin embargo,

pequeños errors en el Atlántico tropical podrían favorecer la generación de teleconexiones más fuertes, como la conexión Atlántico-Pacífico [*Kucharski et al.* 2014] o el impacto sobre la Cuenca del Indian [*Barimalala et al.* 2012]. *Por tanto, los resultados de la presente Tesis destacan la necesidad de mejorar la simulación actual del estado medio y la variabilidad del Atlántico, con el fin de conseguir una representación más realista del clima tropical y global.* Mientras tanto, es necesario el uso de experimentos de sensibilidad para confirmar las hipótesis que se infieren de las observaciones.

8. CONCLUSIONS

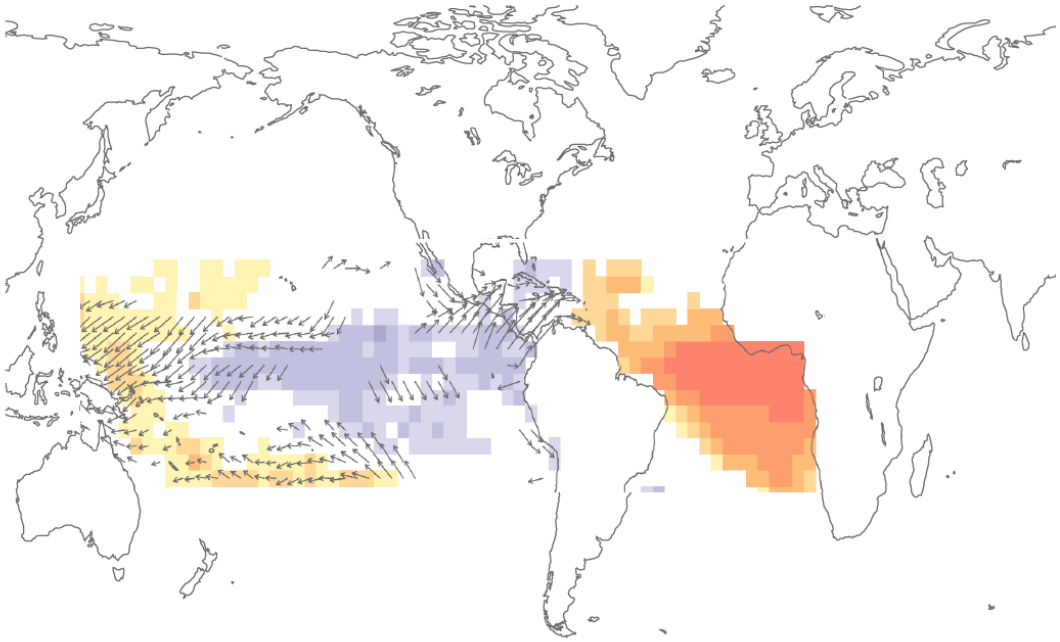

8. CONCLUSIONS

This thesis presents a study of the influence of the tropical Atlantic variability on ENSO phenomena. The air-sea interactions involved in ENSO development associated with the remote Atlantic forcing have been investigated. Furthermore, the non-stationary behaviour of this inter-basin connection and its possible multidecadal modulation has been also explored. Focusing on the tropical Atlantic basin, the Atlantic Niño pattern able to trigger ENSO episodes has been characterized, and the analysis of its atmospheric forcings and oceanic processes involved in its development is also investigated in this Thesis.

The main conclusions of this Thesis are presented as follows:

- Based on partially coupled experiments, different processes appear in the inter-annual tropical Pacific variability before and after the 1970s when considering only the variability in the Atlantic.

    - Before the 1970s, ENSO phenomena are characterized by a warming in the eastern tropical Pacific, without significant modifications in the wind stress or thermocline depth. These patterns are not related to the Atlantic forcing and are similar to internally driven ENSO episodes, which could be associated with thermodynamical mechanisms.

    - After the 1970s, ENSO phenomena are characterized by a an anomalous convergence during summer months which give rise to a stronger warming in the eastern tropical Pacific and a deepening of the thermocline depth during winter. These events are related to anomalous SSTs in the equatorial Atlantic during previous summer.

- The processes involved in the Atlantic Niño impact on the Pacific (the opposite for Atlantic Niña impact) are related to:

- An enhancement of the convection in the equatorial Atlantic, alteration of the Walker circulation and subsequent anomalous subsidence in central Pacific during boreal summer. As a consequence, anomalous surface divergence appears around the dateline, generating and intensification of the easterly winds in west Pacific.

- Wind anomalies over the Pacific pile up the water in western Pacific, producing a perturbation in the thermocline that propagates eastward as a Kelvin wave from autumn to winter and westward as an off-equatorial Rossby waves.

- Shallowing of the thermocline as the Kelvin wave propagates to the east, cooling the oceanic mixed layer through anomalous temperature advection by anomalous zonal currents and by mean vertical entrainment velocity.

- Reinforcement of the surface winds anomalies over the central eastern equatorial Pacific by zonal advection and thermocline feedbacks. This reinforcement establishes the Bjerknes feedback and sets up the conditions for La Niña cold tongue development.

- The Atlantic–Pacific Niños connection is a leading mode of tropical variability involving all the atmospheric and oceanic mechanisms associated with the Atlantic forcing.

- This Atlantic-Pacific mode is not stationary and it appears for certain decades. The mode emerges at multidecadal timescales coherently with negative phases of the Atlantic Multidecadal Oscillation (AMO). The AMO could modulate this inter-basin connection through changes in the western equatorial Atlantic convection and eastern Pacific SST variability.

- For these decades, a statistical hindcast for ENSO phenomena that considers the summer tropical Atlantic SSTs as the predictor field is able to predict the Pacific windstress and thermocline depth, which in turn trigger the processes involved in ENSO development.

    - The hindcast fails in simulating the Pacific variables during positive phases of the AMO, pointing out the lack of ENSO predictability from Tropical Atlantic SSTs during those decades.

    - The statistical hindcast confirms that surface wind in the western Pacific during boreal summer is the key variable in the development of ENSO events associated with the remote Atlantic forcing.

- Two different modes of inter-annual SST variability co-exist in the tropical Atlantic basin during negative phases of the AMO.

    - The leading mode presents an anomalous warming covering the entire tropical Atlantic basin. This mode, denoted as Basin-Wide (BW-) Atlantic Niño, is related to the development of a Pacific La Niña during next winter. The mode is preceded by a weakening of Azores and Sta Helena High during previous autumn and winter months, inducing a reduction of the tropical trades and anomalous wind convergence along the equatorial band.

    - The second mode is characterized by positive SST anomalies restricted to the equatorial band, flanked by negative ones in north and south tropical Atlantic. This mode, denoted as Canonical (C-) Atlantic Niño, is unrelated to the next winter ENSO phenomena. This mode is preceded by initial strengthening of Azores and Sta Helena High during previous autumn, evolving into a zonal SLP gradient at the Equator during late winter and spring. This SLP gradient intensifies the northern and southern trades and creates anomalous westerly winds along the equator.

- Different wind forcing of the BW- and C- Atlantic Niño patterns actives diverse oceanic mechanisms in the tropical Altantic basin, responsible of the development of the SST anomalies.

    - From the BW pattern, net heat fluxes and the vertical terms are the main processes in relation to a warming in north and south tropical. The weakening of the subtropical trades reduces the heat loss, favouring the warming of these regions. The anomalous cyclonic circulation in the subtropical areas also generates an anomalous convergence of the Ekman transport, which also contributes to create the positive SST anomalies. Over the equatorial band, the anomalous wind convergence induces an anomalous convergence of the surface currents (enhancing a deeper thermocline and downwelling processes), favouring the surface warming through vertical processes.

    - For a C-Atlantic Niño, the development of the subtropical negative SST anomalies is mainly attributed to net heat fluxes. The intensification of the north-east and south-east trades, enhances the evaporation and thus cools these areas. Over the equatorial band, the strong westerly winds produces a convergence of the currents deepening the thermocline and inhibiting the entrainment and advection of cold waters from the deep ocean, contributing in this way to the equatorial Atlantic warming.

8.CONCLUSIONES

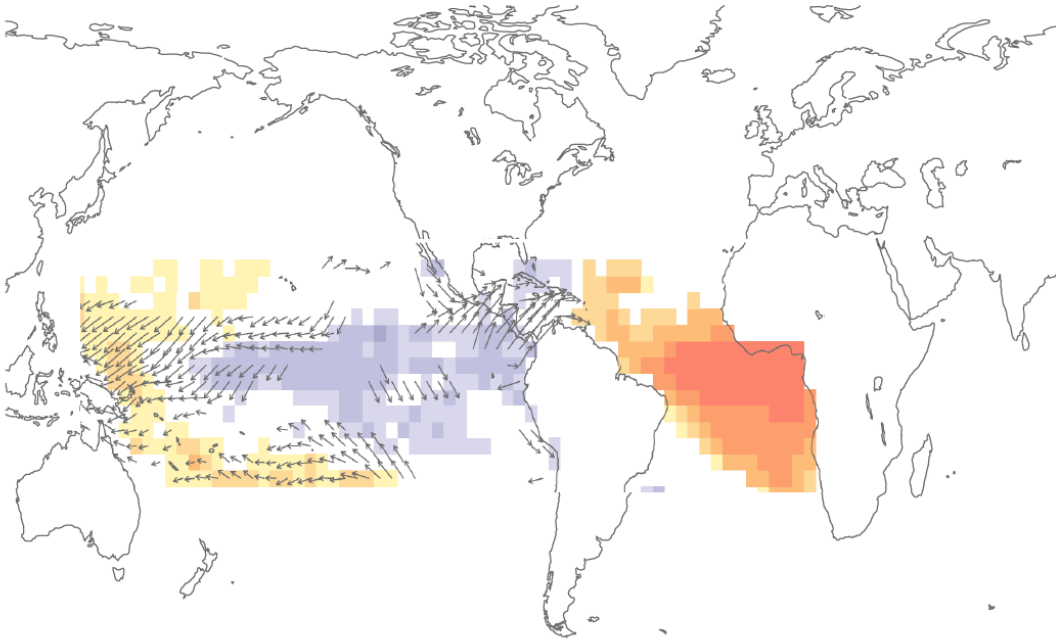

8. CONCLUSIONES

En esta Tesis se ha analizado la influencia de la variabilidad del Atlántico tropical sobre el fenómeno del ENSO. En concreto, se han investigado los procesos de interacción aire-océano involucrados en el desarrollo del ENSO, asociados con el forzamiento remoto del Atlántico. Además, se ha estudiado la no-estacionariedad de dicha conexión, así como su posible modulacion multidecadal. Los patrones de los Niños del Atlántico que son capaces de favorecer los episodios ENSO han sido caracterizados, mediante el análisis de sus forzamientos atmosféricos y de los procesos oceánicos involucrados en su desarrollo.

Las principales conclusiones de esta Tesis se muestran a continuación y se corresponden con los objetivos específicos que se han enumerado en la Sección 2.

- A partir de experimentos parcialmente acoplados que consideran solamente la variabilidad del océano Atlántico, se ha mostrado que existen distintos procesos involucrados en la variabilidad interanual del Pacifico tropical antes y después de la década de los 1970's.

    - Antes de los 70's, los fenómenos ENSO se caracterizan por un calentamiento en el este del Pacífico tropical, sin cambios significativos en el wind stress o en la profundidad de la termoclina. Estos patrones no están relacionados con un forzamiento del Atlántico, y son similares a los fénomenos ENSO generados por la variabilidad interna del sistema, los cuales parecen estar asociados con procesos termodinámicos.

    - Después de los 70's, los fenómenos ENSO se caracterizan por una convergencia anómala del wind stress durante el verano, que da lugar a un fuerte calentamiento en el este del Pacífico tropical y a una profundización de la termoclina durante los meses de invierno. Estos eventos se

relacionan con anomalías de temperatura en el Atlántico ecuatorial durante el verano anterior.

- Los procesos asociados con el impacto del Niño del Atlántico sobre el Pacífico (lo contrario ocurriría para una Niña del Atlántico) conllevan:

    - Un aumento de la convección en el Atlántico ecuatorial, una alteración de la circulación de Walker y la consecuente subsidencia anómala en el centro del Pacífico tropical durante el verano boreal. Como consecuencia, aparecen una divergencia anómala de viento en el centro de la cuenca que da lugar a una intensificación de los vientos del este en el Pacífico occidental.

    - Los vientos anómalos sobre el Pacífico apilan el agua en la oeste del la cuenca, generando una perturbación en la profundidad de la termoclina que se propaga hacia el este en forma de onda de Kelvin desde el otoño hasta el invierno, y hacia el oeste como una dos ondas de Rossby fuera del Ecuador.

    - El levantamiento de la termoclina se propaga en forma de onda de Kelvin hacia el este, favoreciendo el enfriamiento del Pacífico ecuatorial mediante los procesos de advección de temperatura a través de corrientes zonales anómalas y velocidad vertical media.

    - Los viento superficiales anómalos se intensifican en el centro-este del Pacífico ecuatorial debido a la advección zonal y a los procesos de realimentación asociados con la termoclina. Esta intensificación desencadena el proceso de realimentación de Bjerknes y favorece el desarrollo de la lengua fría de la Niña.

- La conexión entre los Niños del Atlántico y del Pacífico es el primer modo de variabilidad tropical e involucra los procesos atmósfericos y oceánicos asociados con el forzamiento del Atlántico.

- El modo Atlántico-Pacífico no es estacionario y aparece solamente durante ciertas décadas. Esta modulación multidecadal coincide con fases negativas de la Oscilación Multidecadal del Atlántico (AMO). La AMO podría modular esta conexión entre cuencas mediante cambios en la convección sobre el oeste del Atlántico ecuatorial y en la variabilidad de la Temperatura de la Superficie del Mar en el este del Pacífico.

- Durante esos periodos, un hindcast estadístico que considera la Temperatura de la Superficie del Mar en verano como predictor, es capaz de reproducir el windstress y la termoclina del Pacífico, los cuales desencadenan los procesos relacionados con el desarrollo del ENSO.

  - El hindcast no es capaz de simular las variables del Pacífico durante las fases positivas de la AMO, poniendo de manifiesto la falta de predictabilidad del ENSO a partir de la temperatura de la superficie del Atlántico tropical durante esas décadas.

  - El hindcast estadístico confirma que los vientos en superficie en el oeste del Pacífico durante el verano boreal son decisivos para el desarrollo de los fenómenos ENSO asociados con la influencia remota del Atlántico.

- Durante fases negativas de la AMO, co-existen dos modos de variabilidad interanual de la Temperatura de la superficie del Mar en el Atlántico tropical.

  - El modo principal se caracteriza por un calentamiento anómalo que cubre toda la cuenca del Atlántico tropical. Este modo se ha denominado Niño Atlántico extendido (BW), y esta relacionado con el desarrollo de una Niña en el Pacífico durante el invierno

siguiente. Este modo esta precedido por un debilitamiento del anticiclón de las Azores y de Sta Helena durante los meses previos de otoño e invierno, generando una reducción de los vientos aliseos y una convergencia anómala de viento en la banda ecuatorial.

- El segundo modo esta caracterizado por anomalías positivas de Temperatura de la Superficie del Mar en la banda ecuatorial, rodeadas de anomalías negativas en el norte y sur del Atlántico tropical. Este modo se ha denominado Nino Atlántico canónico (C) y no está relacionado con el fenómeno del ENSO durante el invierno siguiente. El Niño Atlántico canónico está precedido por un fortalecimiento del anticiclón de las Azores y de Sta Helena durante el otoño previo, que evoluciona en un gradiente zonal de anomalías de presión en superficie en el Ecuador durante el invierno y la primavera. Este gradiente de presión refuerza los vientos alíseos en el norte y sur del Atlántico tropical y genera vientos anómalos del oeste a lo largo de la banda ecuatorial.

o El diferente forzamiento atmosférico de los Niños Atlánticos BW y Canónicos, activa diferentes mecanismos oceánicos en el Atlántico tropical, responsables del desarrollo de las anomalías de Temperatura de la Superficie del Mar.

- En el desarrollo del patron de Niño Atlántico BW, los flujos de calor superficiales y los procesos verticales son los principales mecanismos que generan el calentamiento en el norte y sur del Atlántico tropical. El debilitamiento de los alíseos subtropicales reduce la pérdida de calor debida a procesos de evaporación, favoreciendo el calentamiento de dichas regiones. Además, la circulación ciclónica anómala en las areas subtropicales genera una convergencia anómala del transporte de Ekman, contribuyendo también a crear las anomalías positivas de Temperatura de la Superficie del Mar en dichas regiones. Sobre la banda ecuatorial, una convergencia anómala de viento da lugar a una convergencia anómala de las corrientes superficiales (hundiendo la termoclina e intensificando los procesos de

subducción), favoreciéndose el calentamiento de la superficie mediante los procesos verticales.

- En el caso del Niño Atlántico canónico, el desarrollo de las anomalías de Temperatura de la Superficie del Mar en las regiones subtropicales se debe fundamentalmente a los flujos de calor superficiales. La intensificacion de los vientos alíseos del noreste y sureste, aumenta la evaporación, enfriando dichas regiones. Sobre la banda ecuatorial, los fuertes vientos del oeste generan una convergencia de las corrientes, profundizando la termoclina e impidiendo el afloramiento de aguas frías del océano profundo, contribuyendo de esta manera al calentamiento del Atlántico ecuatorial.

FUTURE WORK

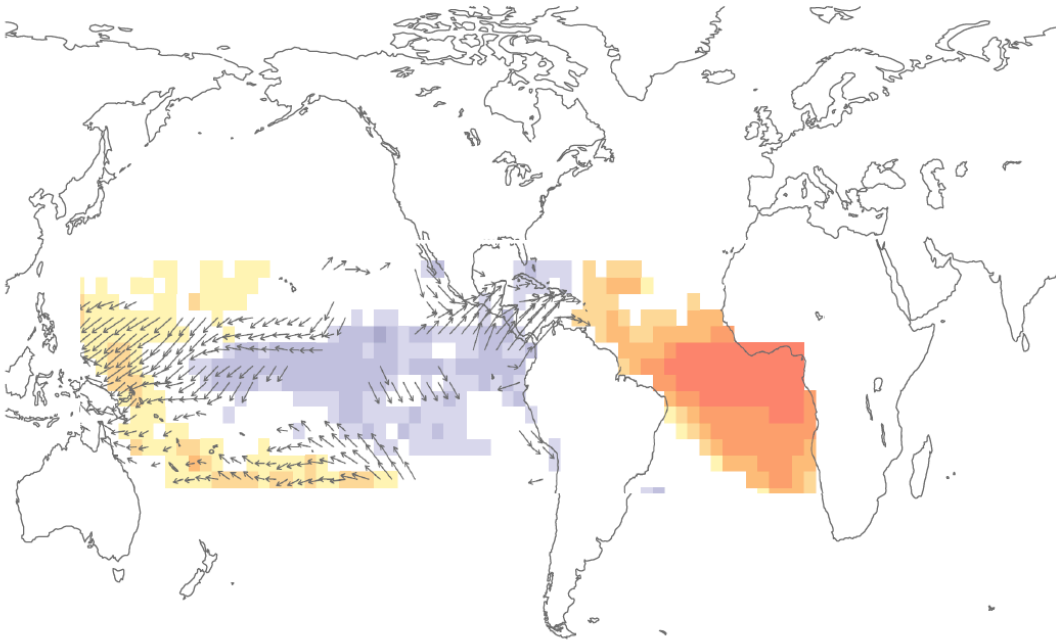

FUTURE WORK

- Preliminary results suggest the possible propagation of equatorial Kelvin waves (KW) during the onset and development of the BW- and C- Atlantic Niño patterns. These KW could be triggered by equatorial wind anomalies or by the reflection of subtropical Rossby waves. These results require a further analysis more in detail.

- Preliminary results suggest different atmospheric forcing for different Atlantic Niño events. Sensitivity ocean experiments following the different wind forcing associated with each of the configurations of the Atlantic Niños are needed to better understand the different processes involved. These experiments would also help to understand the connection between tropical and subtropical regions.

- The origin of the external forcing associated with each of the different configurations of the Atlantic Equatorial mode should be better clarified together with its predictability.

- The modulators of the Atlantic variability and its connection with the Pacific variabilty must be better determined and its contribution should also be better quantified.

TRABAJO FUTURO

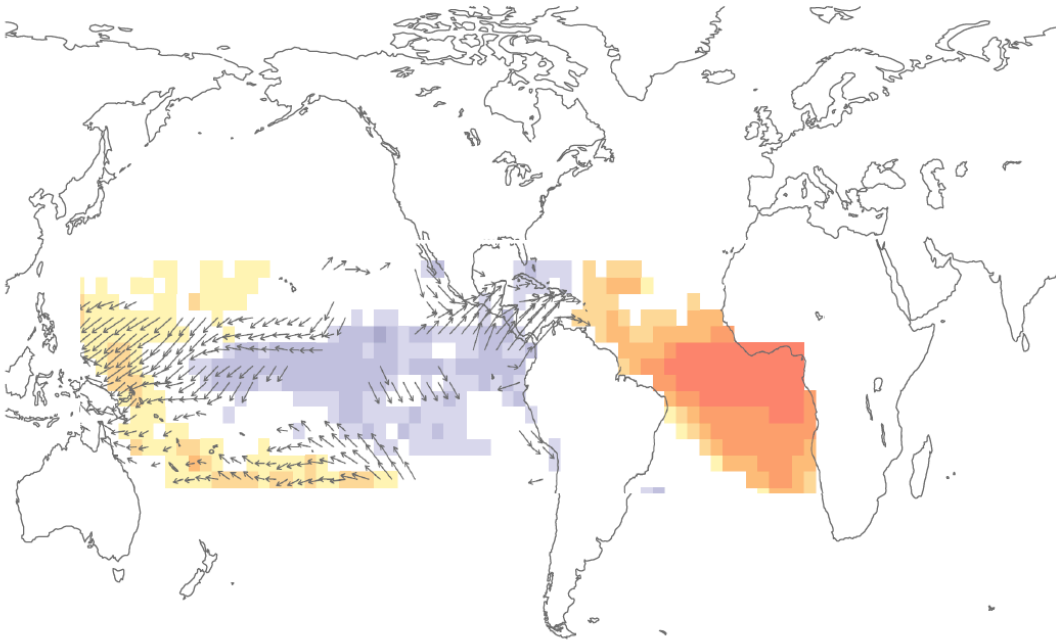

TRABAJO FUTURO

- Estudios previos sugieren una possible propagación de las ondas de Kelvin durante el comienzo y desarrollo del Niños Atlántico BW y Niño Atlántico Canónico. Estas ondas podrían ser generadas como consecuencia de los vientos anómalos ecuatoriales o por la reflexion de las ondas de Rossby subtropicales. Estos resultados requieren un análisis más detallado.

- Realizar experimentos de sensibilidad oceánicos que consideren los diferentes forzamientos de viento asociados con los diferentes patrones espaciales de Niño Atlántico, para comprender mejor los diferentes procesos asociados. Además, estos experimentos ayudarán también a entender la conexión entre las regiones tropicales y subtropicales.

- Se deben clarificar los forzamientos externos asociados a las diferentes configuraciones del Niño Atlántico, así como su predictabilidad.

- Se deben determinar los moduladores de la variabilidad del Atlántico y su conexión con la variabilidad del Pacífico, para poder diferenciar la contribución de los forzamientos externos frente a la variabilidad interna en la cuenca del Pacífico tropical.

REFERENCES

AchutaRao, K. and K. R. Sperber (2006), ENSO simulation in coupled ocean-atmosphere models: are the current models better? *Clim. Dyn.*, *27*(1), 1-15.

Alexander, M., I. Bladé, M. Newman, J. Lanzante, N. Lau, and J. Scott (2002), The Atmospheric Bridge: The Influence of ENSO Teleconnections on Air–Sea interaction over the Global Oceans, *J. Clim*, *15*(16), 2205-2231.

Amaya, D., and G. Foltz (2014), Impacts of canonical and Modoki El Niño on tropical Atlantic SST, *J Geophys Res: Oceans*.

An, Z. Ye, and W. Hsieh (2006), Changes in the leading ENSO modes associated with the late 1970s climate shift: Role of surface zonal current, *Geophys Res Lett*, *33*(L14609).

An, S., and F. Jin (2001), Collective Role of Thermocline and Zonal Advective Feedbacks in the ENSO Mode, *J Clim*, *14*(16), 3421-3432.

An, S., Z. Ye, and W. Hsieh (2006), Changes in the leading ENSO modes associated with the late 1970s climate shift: Role of surface zonal current, *Geophys Res Lett*, *33*(L14609).

Anderson, B., R. Perez, and A. Karspeck (2013), Triggering of El Niño Onset Through Trade-wind Induced Charging of the Equatorial Pacific, *Geophys Res Lett*, *40*(6), 1212-1216.

Annamalai, H., and J. M. Slingo (2001), Active/break cycles: diagnosis of the intraseasonal variability of the Asian summer monsoon. , *Clim Dyn*, *18*(1-2), 85-102.

Ashok, K., S. K. Behera, S. A. Rao, H. Weng, and T. Yamagata (2007), El Niño Modoki and its possible teleconnection., *J Geophys Res: Oceans (1978–2012), 112*(C11).

Baldi, M., Meneguzzo, G. A. Dalu, G. Maracchi, M. Pasqui, V. Capecchi, and F. Piani (2004), Guinea Gulf SST and Mediterranean summer climate: analysis of the interannual variability. , *In Proceedings of the 84th AMS Conference, Seattle, WA, USA.*

Barimalala, R., A. Bracco, and F. Kucharski (2012), The representation of the South Tropical Atlantic teleconnection to the Indian Ocean in the AR4 coupled models. *Clim dyn*, *38*(5-6), 1147-1166.

Barnston, A., and C. Ropelewski (1992), Prediction of ENSO episodes using canonical correlation analysis, *J Clim*, *5*(11), 1316-1345.

Barnston, A., M. Glantz, and H. Yuxiang (1999), Predictive Skill of Statistical and Dynamical Climate Models in SST Forecasts during the 1997–98 El Niño Episode and the 1998 La Niña Onset, *Bulletin of the American Meteorological Society*, *80*(2), 217-243.

Battisti, D. (1988), Dynamics and thermodynamics of a warming event in a coupled tropical atmosphere-ocean model, *J Atmos Sci*, *45*(20), 2889-2919.

Bellenger, H., E. Guilyardi, J. Leloup, M. Lengaigne, and J. Vialard (2013), ENSO representation in climate models: from CMIP3 to CMIP5, *Clim Dyn*, *42*(7-8), 1999-2018.

Bellucci, S. Gualdi, and A. Navarra (2012), The double-ITCZ syndrome in coupled general circulation models: the role of large-scale vertical circulation regimes, *J Clim,* , *23*(5), 1127-1145.

Bjerknes, J. (1921), The Meteorology of the Temperate Zone and the General Atmospheric circulation, *Mon Wea Rev*, *49*(1), 1-3.

Bjerknes, J. (1964), Advances in Geophysics., *Chapter, 1, 1-82.*

Bjerknes, J. (1969), Atmospheric teleconnections from the equatorial Pacific, *Mon Wea Rev*, *97*(3), 163-172.

Borlace, S., W. Cai, and A. Santoso (2013), Multidecadal ENSO Amplitude Variability in a 1000-yr Simulation of a Coupled Global Climate Model: Implications for Observed ENSO Variability, *J clim*, *10*(1), 138-161.

Boschat, G., P. Terray, and S. Masson (2013), Extratropical forcing of ENSO, *Geophys Res Lett*, *40*(8), 1605-1611.

Boulanger, J.-P., S. Cravatte, and C. Menkes (2003), Reflected and locally wind-forced interannual equatorial Kelvin waves in the western Pacific Ocean, *J Geophys Res: Oceans*, *108*(C10), 3311.

Box, G. E., and G. M. Jenkins (1976), Time series analysis: forecasting and control, , *revised ed. Holden-Day.*

Bretherton, C., C. Smith, and J. Wallace (1991), An intercomparison of methods for finding coupled patterns in climate data, *J Clim*, *5*(6), 541-560.

Breugem, W. P., W. Hazeleger, and R. J. Haarsma (2006), Multimodel study of tropical Atlantic variability and change. , *Geophysical Res Lett,* , *33*(23).

Breugem, W. P., P. Chang, C. J. Jang, J. Mignot, and W. Hazeleger (2008), Barrier layers and tropical Atlantic SST biases in coupled GCMs. , *Tellus A*, *60*(5), 885-897.

Brodeau, L., B. Barnier, A. Treguier, T. Penduff, and S. Gulev (2010), An ERA40-based atmospheric forcing for global ocean circulation models, *Ocean Modelling*, *31*, 88-104.

Brönnimann, S., S., E. Xoplaki, C. Casty, A. Pauling, and J. Luterbacher (2007), ENSO influence on Europe during the last centuries., *Clim Dyn, *, *28*(2-3), 181-197.

Butterworth, S. (1930), On the theory of filter amplifiers,, *Experimental wireless and the wireless engineer 7*, 536 - 541.

Cane, M. A. and E. S. Sarachik (1976), Forced baroclinic ocean motions. 1. Linear equatorial unbounded case., *J Mar Res 34* (4), 629-665.

Cane, M. A. and S. Zebiak (1985), A theory for El Niño and the Southern Oscillation. , *Science*, *228*(4703), 1085-1087.

Capotondi, A. Wittenberg, and S. Masina (2006), Spatial and temporal structure of tropical Pacific interannual variability in 20th century coupled simulations, *Ocean Modelling, *, *15*(3), 274-298.

Carton, J. A., and B. Huang (1994), Warm Events in the Tropical Atlantic, *J Phys Oce*, *24*(5), 888-903.

Carton, J. A., X. Cao, B. Giese, and A. Da Silva (1996), Decadal and interannual SST variability in the Tropical Atlantic Ocean, *J Phys Ocea*, *26*(7), 1165-1175.

Carton, J. A., G. Chepurin, X. Cao, and B. Giese (2000), A simple ocean data assimilation analysis of the global upper ocean 1950-95. Part I: Methodology, *J Phys Ocea*, *30*(2), 294-309.

Cassou, C., L. Terray, and A. S. Phillips (2005), Tropical Atlantic Influence on European Heat Waves, *J Clim*, *18*(15), 2805-2811.

Cassou, C., L. Terray, J. W. Hurrell, and C. Deser (2004), North Atlantic Winter Climate Regimes: Spatial Asymmetry, Stationarity with Time, and Oceanic Forcing, *J Clim*, *17*(5), 1055-1068.

Chakravorty, S., J. Chowdary, and C. Gnanaseelan (2014), Epochal changes in the seasonal evolution of tropical Indian Ocean warming associated with El Niño, *Clim Dyn*, *42*, 805-822.

Chang, P. (1994), A study of the seasonal cycle of sea surface temperature in the tropical Pacific Ocean using reduced gravity models, *J Geophys Res: Oceans*, *99*, 7725-7741.

Chang, P., L. Ji, and H. Li (1997), A decadal climate variation in the tropical Atlantic Ocean from thermodynamic air–sea interactions, *Nature*, *385*(516–518).

Chang, P., Saravanan, L. Ji, and G. Hegerl (2000), The effect of local sea surface temperatures on atmospheric circulation over the tropical Atlantic sector, *J Clim, 13*(13), 2195-2216.

Chang, P., Y. Fang, R. Saravanan, L. Ji, and H. Seidel (2006), The cause of the fragile relationship between the Pacific El Nino and the Atlantic Nino, *Nature*, *443*(7109), 324-328.

Chang, P., T. Yamagata, P. Schopf, S. K. Behera, J. Carton, W. S. Kessler, and S. P. Xie (2006b), Climate fluctuations of tropical coupled systems-the role of ocean dynamics, *J Clim*, *19*(20), 5122-5174.

Cherry, S. (1997), Some comments on singular value decomposition analysis, *J Clim*, *10*(7), 1759-1761.

Chiang, J. C. H. and Y. Kushnir (2000), Interdecadal changes in eastern Pacific ITCZ variability and its influence on the Atlantic ITCZ, *Geophys Res Lett*, *27*, 3687-3690.

Chiang, J. C. H., Y. Kushnir, and A. Giannini (2002), Deconstructing Atlantic Intertropical Convergence Zone variability: Influence of the local cross-equatorial sea surface temperature gradient and remote forcing from the eastern equatorial Pacific, *J Geophys Res: Oceans*, *107*.

Choi, J., S. An, J. Kug, and S. Yeh (2011), The role of mean state on changes in El Niño's flavor, *Clim Dyn*, *37*(5-6), 1205-1215.

Chung, C. T. Y. and T. Li (2013), Interdecadal Relationship between the Mean State and El Niño Types, *Journal of Climate*, *26*(2), 361-379.

Chung, C. T. Y., S. Power, J. Arblaster, H. Rashid, and G. Roff (2013), Nonlinear precipitation response to El Niño and global warming in the Indo-Pacific, *Clim Dyn*, *42*(7-8), 1837-1856.

Clarke, A., and L. Shu (2000), *Quasi-biennial winds in the far western equatorial Pacific phase-locking El Niño to the seasonal cycle*, American Geophysical Union, Washington, DC, ETATS-UNIS.

Clarke, A., and S. Van Gorder (2001), ENSO prediction using an ENSO trigger and a proxy for western equatorial Pacific warm pool movement, *Geophys Res Lett*, *28*, 579-582.

Clarke, A., and S. Van Gorder (2003), Improving El Niño prediction using a space-time integration of Indo-Pacific winds and equatorial Pacific upper ocean heat content, *Geophys Res Lett*, *30*(7), 1399.

Compo, G., J. S. Whitaker, and P. D. Sardeshmukh (2006), Feasibility of a 100-year reanalysis using only surface pressure data, *Bulletin of the American Meteorological Society, , 87*(2), 175-190.

Compo, G., J. Whitaker, P. Sardeshmukh, N. Matsui, R. Allan, X. Yin, and S. Worley (2011), The Twentieth Century Reanalysis Project, *J Royal Meteo Soc*, *137*(654), 1-28.

Czaja, A. (2004), Why is north tropical Atlantic SST variability stronger in boreal spring?, *J Clim*, *17*(15), 3017-3025.

Czaja, A., P. Van der Vaart, and J. Marshall (2002), A Diagnostic Study of the Role of Remote Forcing in Tropical Atlantic Variability, *J Clim*, *15*(22), 3280-3290.

d'Orgeville, M., and W. R. Peltier (2007), On the Pacific Decadal Oscillation and the Atlantic Multidecadal Oscillation: Might they be related?, *Geophys Res Lett*, *34*(23), L23705.

Davey, M., M. Huddleston, K. Sperber, P. Braconnot, F. Bryan, D. Chen, and S. Zebiak (2002), STOIC: A study of the coupled model climatology and variability in tropical ocean regions, *Clim Dyn*, *18*, 403-420.

Dayan, H., J. Vialard, T. Izumo, and M. Lengaigne (2013), Does sea surface temperature outside the tropical Pacific contribute to enhanced ENSO predictability?, *Clim Dyn,* 1-15.

De Szoeke, S. P. and S. Xie (2008), The Tropical Eastern Pacific Seasonal Cycle: Assessment of Errors and Mechanisms in IPCC AR4 Coupled Ocean-Atmosphere General Circulation Models*, *J Clim*, *21*(11), 2573-2590.

Delecluse, P., M. K. Davey, Y. Kitamura, S. G. H. Philander, and M. Suarez, & Bengtsson, L. (1998), Coupled general circulation modeling of the tropical Pacific. *J Geophys Res: Oceans* (1978–2012), *103*(C7), 14357-14373.

Delworth, T., and M. Mann (2000), Observed and simulated multidecadal variability in the Northern Hemisphere, *Clim Dyn*, *16*, 661-676.

Deser, C., A. Capotondi, R. Saravanan, and A. S. Phillips (2006b), Tropical Pacific and Atlantic climate variability in CCSM3, *J Clim, 19*(11), 2451-2481.

Dewitte, B., S Thual, SW Yeh, SI An, BK Moon, and B. Giese (2009), Low-Frequency Variability of Temperature in the Vicinity of the Equatorial Pacific Thermocline in SODA: Role of Equatorial Wave Dynamics and ENSO Asymmetry, *J Clim*, *22*(21), 5783-5795.

Diaz, H. F., M. P. Hoerling, and J. K. Eischeid (2001), ENSO variability, teleconnections and climate change, *International J Clim*, *21*(15), 1845-1862.

Ding, H., N. Keenlyside, and M. Latif (2012), Impact of the Equatorial Atlantic on the El Niño Southern Oscillation, *Clim Dyn*, *38*(9-10), 1965-1972.

Doi, T., G. A. Vecchi, A. J. Rosati, and T. L. Delworth (2012), Biases in the Atlantic ITCZ in seasonal-interannual variations for a coarse-and a high-resolution coupled climate model, *J Clim* , *25*(16), 5494-5511.

Dommenget, D., and M. Latif (2000), Interannual to Decadal Variability in the Tropical Atlantic, *J Clim*, *13*(4), 777-792.

Dong, B., and R. Sutton (2002), Adjustment of the coupled ocean–atmosphere system to a sudden change in the thermohaline circulation., *Geophys Res Lett*, *29(*(15), 18-11.

Dong, B., and R. Sutton (2007), Enhancement of ENSO Variability by a Weakened Atlantic Thermohaline Circulation in a Coupled GCM, *J Clim*, *20*(19), 4920-4939.

Dong, B., and T. Zhou (2014), The formation of the recent cooling in the eastern tropical Pacific Ocean and the associated climate impacts: A competition of global warming, IPO, and AMO, *J Geophys Res: Atmospheres*, *119*(19), 11-272.

Dong, B., R. Sutton, and A. Scaife (2006), Multidecadal modulation of El Niño–Southern Oscillation (ENSO) variance by Atlantic Ocean sea surface temperatures, *Geophys Res Lett*, *33*.

Eisenman, I., L. Yu, and E. Tziperman (2005), Westerly Wind Bursts: ENSO's Tail Rather than the Dog?, *J Clim*, *18*(24), 5224-5238.

Enfield, D. B. and D. Mayer (1997), Tropical Atlantic sea surface temperature variability and its relation to El Niño-Southern Oscillation, *J Geophys Res: Oceans*, *102*, 929-945.

Enfield, D. B., A. M. Mestas ‐ Nuñez, and P. J. Trimble (2001), The Atlantic multidecadal oscillation and its relation to rainfall and river flows in the continental US. , *Geophys Res Lett*, *28*(10), 2077-2080.

Fang, Y., J. C. H. Chiang, and P. Chang (2008), Variation of mean sea surface temperature and modulation of El Niño–Southern Oscillation variance during the past 150 years, *Geophys Res Lett*, *35*(14), L14709.

Federov, A., and S. Philander (2000), Is El Niño Changing?, *Science*, *288*.

Ferrel, W. (1856), Essay on the winds and ocean currents,, *Nashville J. Med. and Surg.,* , *11*, 287–301375–301389.

Florenchie, P., J. R. E. Lutjeharms, C. J. C. Reason, S. Masson, and M. Rouault (2003), The source of Benguela Niños in the South Atlantic Ocean, *Geophys Res Lett*, *30*(10), 1505.

Foltz, G. R., S. A. Grodsky, J. A. Carton, and M. J. McPhaden (2003), Seasonal mixed layer heat budget of the tropical Atlantic Ocean, *J Geophys Res: Oceans*, *108*(C5), 3146.

Fraedrich, K., and K. Müller (1992), Climate anomalies in Europe associated with ENSO extremes, *Int J Clim*, *12*(1), 25-31.

França, C., I. Wainer, A. De Mesquita, and G. Goñi (2003), Planetary equatorial trapped waves in the Atlantic Ocean from TOPEX/Poseidon altimetry, in: Goñi, G. J.; Malanotte- Rizzoli, P. (Ed.). Interhemispheric water exchange in the Atlantic Ocean. , *Elsevier Oceanography Series*, *68* 213-232.

Frauen, C., and D. Dommenget (2012), Influences of the tropical Indian and Atlantic Oceans on the predictability of ENSO, *Geophys Res Lett*, *39*(2), L02706.

Gaetani, M., B. Fontaine, P. Roucou, and M. Baldi (2010), Influence of the Mediterranean Sea on the West African monsoon: Intraseasonal variability in numerical simulations, *J Geophys Res: Atmospheres*, *115*(D24), D24115.

García-Serrano, J., T. Losada, B. Rodríguez-Fonseca, and I. Polo (2008), Tropical Atlantic Variability Modes (1979–2002). Part II: Time-Evolving Atmospheric Circulation Related to SST-Forced Tropical Convection, *J Clim, 21*(24), 6476-6497.

Gebbie, G., I. Eisenman, A. Wittenberg, and E. Tziperman (2007), Modulation of Westerly Wind Bursts by Sea Surface Temperature: A Semistochastic Feedback for ENSO, *J Atmos Sci*, *64*(9), 3281-3295.

Giannini, A., R. Saravanan, and P. Chang (2003), Oceanic forcing of Sahel rainfall on interannual to interdecadal time scales. , *Science*, *302*(5647), 1027-1030.

Giannini, A., J. C. H. Chiang, M. A. Cane, Y. Kushnir, and R. Seager (2001), The ENSO Teleconnection to the Tropical Atlantic Ocean: Contributions of the Remote and Local SSTs to Rainfall Variability in the Tropical Americas*, *J Clim*, *14*(24), 4530-4544.

Giese, B. S., and S. Ray (2011), El Niño variability in simple ocean data assimilation (SODA), 1871–2008, *J Geophys Res: Oceans*, *116*(C2), C02024.

Gill, A. E. (1980), Some simple solutions for heat-induced tropical circulation, *QJRMS*, *106*(449), 447-462.

Gill, A. E. (1982), Atmosphere-ocean dynamics, *Academic press*, *Vol. 30*.

Gouirand, I., V. Moron, Z.-Z. Hu, and B. Jha (2014), Influence of the warm pool and cold tongue El Niños on the following Caribbean rainy season rainfall, *Clim Dyn*, *42*(3-4), 919-929.

Graham, N. E. (1994), Decadal-scale climate variability in the tropical and North Pacific during the 1970s and 1980s: Observations and model results, *Clim Dyn*, *10*(3), 135-162.

Greatbatch, R. J., J. Lu, and K. A. Peterson (2004), Nonstationary impact of ENSO on Euro‐Atlantic winter climate, *Geophys Res Lett*, *31*(2).

Guilyardi, E., S. Gualdi, J. Slingo, A. Navarra, P. Delecluse, J. Cole, ..., and L. Terray (2004), Representing El Niño in coupled ocean-atmosphere GCMs: the dominant role of the atmospheric component., *J Clim*, *17*(24), 4623-4629.

Guilyardi, E. P. Braconnot, F. F. Jin, S. T. Kim, M. Kolasinski, T. Li, and I. Musat (2009), Atmosphere feedbacks during ENSO in a coupled GCM with a modified atmospheric convection scheme. , *J Clim*, *22*(21), 5698-5718.

Haarsma, R., E. Campos, W. Hazeleger, and C. Severijns (2008), Influence of the meridional overturning circulation on tropical Atlantic climate and variability, *J Clim*, *21*(6), 1403-1416.

Hadley, G. (1735), Concerning the cause of the general trade winds, *Phils. Trans. Roy. Soc., London*, *29*, 58-62.

Ham, Y.-G., J.-S. Kug, and J.-Y. Park (2013b), Two distinct roles of Atlantic SSTs in ENSO variability: North Tropical Atlantic SST and Atlantic Niño, *Geophys Res Lett*, *40*(15), 4012-4017.

Ham, Y.-G., J. S. Kug, J. Y. Park, and F. F. Jin (2013a), Sea surface temperature in the north tropical Atlantic as a trigger for El Niño/Southern Oscillation events, *Nature Geoscience,* , *6*(2), 112-116.

Handoh, I. C., A. J. Matthews, G. R. Bigg, and D. P. Stevens (2006a), Interannual variability of the tropical Atlantic independent of and associated with ENSO: Part I. The North Tropical Atlantic, *Int J Clim*, *26*(14), 1937-1956.

Handoh, I. C., G. R. Bigg, A. J. Matthews, and D. P. Stevens (2006b), Interannual variability of the Tropical Atlantic independent of and associated with ENSO: Part II. The South Tropical Atlantic, *Int J Clim*, *26*(14), 1957-1976.

Hartmann, D. (1994), Global physical climatology., *San Diego, Academic Press.* , 411

Hastenrath, S. (1991), Climate dynamics of the tropics *Kluwer Academic Publishers*.

Hastenrath, S. and L. Greischar (1993), Further work on the prediction of northeast Brazil rainfall anomalies., *J Clim, 6*(4), 743-758.

Hirota, N. and Y. Takayabu (2013), Reproducibility of precipitation distribution over the tropical oceans in CMIP5 multi-climate models compared to CMIP3, *Clim Dyn*, *41*(11-12), 2909-2920.

Hirota, N., Y. N. Takayabu, M. Watanabe, and M. Kimoto (2011), Precipitation reproducibility over tropical oceans and its relationship to the double ITCZ problem in CMIP3 and MIROC5 climate models, *J Clim, 24*(18), 4859-4873.

Hirst, A., and S. Hastenrath (1983), Atmosphere-ocean mechanisms of climate anomalies in the Angola-tropical Atlantic sector, *J Phys Ocea*, *13* (7), 1146-1157.

Holton, J. R. (2004), Introduction to Dynamical Meteorology, *Elsevier Academic Press, 4th Edition*.

Hormann, V., and P. Brandt (2009), Upper equatorial Atlantic variability during 2002 and 2005 associated with equatorial Kelvin waves, *J Geophys Res: Oceans*, *114*(C3), C03007.

Houghton, R., and Y. Tourre (1992), Characteristics of low-frequency sea surface temperature fluctuations in the tropical Atlantic. , *J Clim, 5*(7), 765-772.

Hovmöller, E. (1949), The Trough‐and‐Ridge diagram. , *Tellus*, *1*(2), 62-66.

Huang, B., P. S. Schopf, and Z. Pan (2002), The ENSO effect on the tropical Atlantic variability: A regionally coupled model study, *Geophys Res Lett*, *29*(21), 2044.

Hurrell, J. W. (1995), Decadal Trends in the North Atlantic Oscillation: Regional Temperatures and Precipitation, *Science*, *269*, 676-679.

Hurrell, J. W., Y. Kushnir, and M. Visbeck (2001), The north Atlantic oscillation. , *Science*, *291*(5504), 603-605.

Hurrell, J. W. et al. (2005), Atlantic Climate Variability and Predictability: A CLIVAR Perspective, *J Clim*, *19*(20), 5100-5121.

Hwang, and D. M. W. Frierson (2013), A new look at the double ITCZ problem: Connections to cloud bias over the Southern Ocean. , *Proc. Natl Acad. Sci. USA, , 110*, 4935-4940.

Izumo, T., J. Vialard, M. Lengaigne, C. de Boyer Montegut, S. K. Behera, J.-J. Luo, S. Cravatte, S. Masson, and T. Yamagata (2010), Influence of the state of the Indian Ocean Dipole on the following year's El Nino, *Nature Geosci*, *3*(3), 168-172.

Janicot, S. (1992), Spatiotemporal Variability of West African Rainfall. Part I: Regionalizations and Typings, *J Clim*, *5*(5), 489-497.

Janicot, S., V. Moron, and B. Fontaine (1996), Sahel droughts and ENSO dynamics., *Geophys Res Lett*, *23*(5), 515-518.

Janicot, S., S. Trzaska, and I. Poccard (2001), Summer Sahel-ENSO teleconnection and decadal time scale SST variations, *Clim Dyn*, *18* (3-4), 303-320.

Jansen, M. F., D. Dommenget, and N. Keenlyside (2009), Tropical Atmosphere–Ocean Interactions in a Conceptual Framework, *J Clim*, *22*(3), 550-567.

Jin, F. F. (1997), An Equatorial Ocean Recharge Paradigm for ENSO. Part I: Conceptual Model, *J Atmos Sci*, *54*(7), 811-829.

Jin, F. F. and S.-I. An (1999), Thermocline and Zonal Advective Feedbacks Within the Equatorial Ocean Recharge Oscillator Model for ENSO, *Geophys Res Lett*, *26*(19), 2989-2992.

Jin, E. K., et al. (2008), Current status of ENSO prediction skill in coupled ocean–atmosphere models, *Clim Dyn*, *31*(6), 647-664.

Joly, M., and Voldoire (2010), Role of the Gulf of Guinea in the inter-annual variability of the West African monsoon: what do we learn from CMIP3 coupled simulations?, *Int J Clim*, *30*(12), 1843-1856.

Joly, M., A. Voldoire, H. Douville, P. Terray, and J. Royer (2007), African monsoon teleconnections with tropical SSTs: validation and evolution in a set of IPCC4 simulations, *Clim Dyn*, *29*(1), 1-20.

Kang, I., H. No, and F. Kucharski (2014), ENSO amplitude modulation associated with the mean SST changes in the tropical central Pacific induced by Atlantic Multidecadal Oscillation. , *J Clim*, *27*(20), 7911-7920.

Kao, H.-Y., and J.-Y. Yu (2009), Contrasting Eastern-Pacific and Central-Pacific Types of ENSO, *J Clim*, *22*(3), 615-632.

Kaplan, A., Y. Kushnir, M. Cane, and M. Blumenthal, (1997), Reduced space optimal analysis for historical data sets: 136 years of Atlantic sea surface temperatures, *J. Geophys. Res, 102*, 2,835–827,860.

Keenlyside, N., and M. Latif (2007), Understanding Equatorial Atlantic Interannual Variability, *J Clim*, *20*(1), 131-142.

Keenlyside, N., H. Ding, and M. Latif (2013), Potential of equatorial Atlantic variability to enhance El Niño prediction, *Geophys Res Lett*, *40*(10), 2278-2283.

Kerr, R. A. (2000), A North Atlantic climate pacemaker for the centuries., *Science*, *288* 1984-1985.

Kim, W., and W. Cai (2014), The importance of the eastward zonal current for generating extreme El Niño, *Clim Dyn*, *42*(11-12), 3005-3014.

Klein, S., B. Soden, and N. Lau (1999), Remote sea surface temperature variations during ENSO: Evidence for a tropical atmospheric bridge. , *J. Clim 12*, 917-932.

Knight, J. R., C. K. Folland, and A. A. Scaife (2006), Climate impacts of the Atlantic Multidecadal Oscillation, *Geophys Res Lett*, *33*(17), L17706.

Kosaka, Y., and S. Xie (2013), Recent global-warming hiatus tied to equatorial Pacific surface cooling, *Nature*, *501*(7467), 403-407.

Kruk, M. C., K. R. Knapp, and D. H. Levinson (2010), A technique for combining global tropical cyclone best track data, *J Atmos Ocea Tech*, *27*(4), 680-692.

Kucharski, F., F. Molteni, and J. H. Yoo (2006b), SST forcing of decadal Indian Monsoon rainfall variability, *Geophys Res Lett 33,*.

Kucharski, F., A. Bracco, J. H. Yoo, and F. Molteni (2007), Low-frequency variability of the Indian monsoon-ENSO relationship and the tropical Atlantic: The "weakening" of the 1980s and 1990s. , *J Clim, 20*(16), 4255-4266.

Kucharski, F., A. Bracco, J. H. Yoo, and F. Molteni (2008), Atlantic forced component of the Indian monsoon interannual variability, *Geophys Res Lett*, *35*(4), L04706.

Kucharski, F., I. S. Kang, R. Farneti, and L. Feudale (2011), Tropical Pacific response to 20th century Atlantic warming, *Geophys Res Lett*, *38*(3), L03702.

Kucharski, F., F. S. Syed, A. Burhan, I. Farah, and A. Gohar (2014), Tropical Atlantic influence on Pacific variability and mean state in the twentieth century in observations and CMIP5, *Clim Dyn,* 1-16.

Kucharski, F., A. Bracco, J. H. Yoo, A. M. Tompkins, L. Feudale, P. Ruti, and A. Dell'Aquila (2009), A Gill–Matsuno-type mechanism explains the tropical Atlantic influence on African and Indian monsoon rainfall, *QJRM*, *135*(640), 569-579.

Kug, J. S., F.-F. Jin, and S.-I. An (2009), Two Types of El Niño Events: Cold Tongue El Niño and Warm Pool El Niño, *J Clim*, *22*(6), 1499-1515.

Kug, J. S., Y. Ham, F. Jin, and I. Kang (2010b), Scale interaction between tropical instability waves and low‐frequency oceanic flows, *Geophys Res Lett, , 37*(2).

Kushnir, Y., M. Barreiro, P. Chang, J. Chiang, A. Lazar, and P. Malanotte-Rizzoli (2003), The role of the south Atlantic in the Variability of the ITCZ *White paper for CLIVAR/IAI/OOPC*.

L'Heureux, M. L., S. Lee, and B. Lyon (2013), Recent multidecadal strengthening of the Walker circulation across the tropical Pacific, *Nature Clim. Change*, *3*(6), 571-576.

Lagrange, J. L. (1788), Oeuvres de Lagrange, Mécanique analytique, , *Gauthier-Villars, Paris (1889) tome XII*.

Lamb, P. J. (1978), Case Studies of Tropical Atlantic Surface Circulation Patterns During Recent Sub-Saharan Weather Anomalies: 1967 and 1968, *Mon Wea Rev*, *106*(4), 482-491.

Large, W. G., G. Danabasoglu, S. C. Doney, and J. C. McWilliams (1997), Sensitivity to surface forcing and boundary layer mixing in a global ocean model: Annual-mean climatology, *J Phys Oceay*, *27*(11), 2418-2447.

Larkin, N. and D. E. Harrison (2005a), On the definition of El Niño and associated seasonal average US weather anomalies. , *Geophys Res Lett, 32*(13).

Larkin, and D. E. Harrison (2005b), Global seasonal temperature and precipitation anomalies during El Niño autumn and winter, *Geophys Res Lett*, *32*(16).

Latif, M. and T. P. Barnett (1994), Causes of Decadal Climate Variability over the North Pacific and North America, *Science*, *266*(5185), 634-637.

Latif, M. and A. Grötzner (2000), The equatorial Atlantic oscillation and its response to ENSO, *Clim Dyn*, *16*(2-3), 213-218.

Lau, N. C. and M. J. Nath (1996), The Role of the "Atmospheric Bridge" in Linking Tropical Pacific ENSO Events to Extratropical SST Anomalies, *J Clim*, *9*(9), 2036-2057.

Lau, N. C. and M. Nath (2000), Impact of ENSO on the variability of the Asian-Australian monsoons as simulated in GCM experiments, *J Clim, 13*(24), 4287-4309.

Lau, N. C. and M. Nath (2003), Atmosphere-ocean variations in the Indo-Pacific sector during ENSO episodes, *J Clim*, *16*(1), 3-20.

Li, G. and S. Xie (2014), Tropical Biases in CMIP5 Multimodel Ensemble: The Excessive Equatorial Pacific Cold Tongue and Double ITCZ Problems*. *J Clim*, *27*(4), 1765-1780.

Lin, J. L. (2007), The double-ITCZ problem in IPCC AR4 coupled GCMs: Ocean-atmosphere feedback analysis, *J Clim*, *20*(18), 4497-4525.

Liu, P., and C.-H. Sui (2014), An observational analysis of the oceanic and atmospheric structure of global-scale multi-decadal variability, *Adv. Atmos. Sci.*, *31*(2), 316-330.

López-Parages, J., and B. Rodríguez-Fonseca (2012), Multidecadal modulation of El Niño influence on the Euro-Mediterranean rainfall, *Geophys Res Lett*, *39*(2), L02704.

López-Parages, J., B. Rodríguez-Fonseca, and L. Terray (2014), A mechanism for the multidecadal modulation of ENSO teleconnection with Europe. , *Clim Dyn, , 1-14.*

Lorenz, E. N. (1956), Empirical orthogonal functions and statistical weather prediction.

Losada, T., and B. Rodriguez-Fonseca (2015), Tropical Atmospheric Response to Decadal Changes in the Atlantic Equatorial Mode, *Clim Dyn*.

Losada, T., B. Rodríguez-Fonseca, and F. Kucharski (2012a), Tropical influence on the summer Mediterranean climate, *Atmos Sci Lett*, *13*(1), 36-42.

Losada, T., B. Rodríguez-Fonseca, S. Janicot, S. Gervois, F. Chauvin, and P. Ruti (2010b), A multi-model approach to the Atlantic Equatorial mode: impact on the West African monsoon, *Clim Dyn*, *35*(1), 29-43.

Losada, T., B. Rodriguez-Fonseca, E. Mohino, J. Bader, S. Janicot, and C. R. Mechoso (2012b), Tropical SST and Sahel rainfall: A non-stationary relationship, *Geophys Res Lett*, *39*(12), L12705.

Losada, T., B. Rodríguez-Fonseca, I. Polo, S. Janicot, S. Gervois, F. Chauvin, and P. Ruti (2010a), Tropical response to the Atlantic Equatorial mode: AGCM multimodel approach, *Clim Dyn*, *35*(1), 45-52.

Lübbecke, J. F., and M. J. McPhaden (2012), On the Inconsistent Relationship between Pacific and Atlantic Niños*, *J Clim*, *25*(12), 4294-4303.

Lübbecke, J. F., and M. J. McPhaden (2013), A Comparative Stability Analysis of Atlantic and Pacific Niño Modes*, *J Clim*, *26*(16), 5965-5980.

Lübbecke, J. F., C. W. Böning, N. S. Keenlyside, and S.-P. Xie (2010), On the connection between Benguela and equatorial Atlantic Niños and the role of the South Atlantic Anticyclone, *J Geophys Res: Oceans*, *115*(C9), C09015.

Madec, G. (2008), NEMO ocean engine, Note du Pole de modèlisation, edited.

Madec, G., P. Delecluse, M. Imbard, and C. Lévy (1998), OPA 8.1 ocean general circulation model reference manual. Note du Pôle de modélisation, , *Institut Pierre-Simon Laplace, 11, 91p.*

Magnusson, M. Alonso-Balmaseda, and F. Molteni (2013), On the dependence of ENSO simulation on the coupled model mean state. , *Clim Dyn*, *41*(5-6), 1509-1525.

Mantua, and S. Hare (2002), The Pacific Decadal Oscillation, *J Ocean*, *58*(1), 35-44.

Mantua, S. R. Hare, Y. Zhang, J. M. Wallace, and R. C. Francis (1997), A Pacific Interdecadal Climate Oscillation with Impacts on Salmon Production, *Bulletin of the American Meteorological Society*, *78*(6), 1069-1079.

Mariotti, A., N. Zeng, and K. M. Lau (2002), Euro ‐ Mediterranean rainfall and ENSO—a seasonally varying relationship. , *Geophys Res Lett, , 29*(12), 59-51.

Marshall, Y. Kushnir , D. Battisti, P. Chang, A. Czaja, R. Dickson, J. Hurrell, M. McCartney, R. Saravanan, and M. Visbeck (2001), North Atlantic climate variability: phenomena, impacts and mechanisms, , *Int. J. Climatol., , 21, ,* 1863-1898. .

Martín-Rey, M., I. Polo, B. Rodriguez-Fonseca, and A. Lazar (2015b), Two different configuration of the Atlantic Niño phenomenon under negative AMO phases, *to be submitted*.

Martín-Rey, M., B. Rodriguez-Fonseca, and I. Polo (2015a), Atlantic opportunities for ENSO prediction, *Geophys Res Lett*.

Martín-Rey, M., I. Polo, B. Rodríguez-Fonseca, and F. Kucharski (2012), Changes in the interannual variability of the tropical Pacific as a response to an equatorial Atlantic forcing, *Sci Mar*, *76*(S1), 105-116.

Martín-Rey, M., B. Rodríguez-Fonseca, I. Polo, and F. Kucharski (2014), On the Atlantic–Pacific Niños connection: a multidecadal modulated mode, *Clim Dyn*, *43*(11), 3163-3178.

Matsuno, T. (1966), Quasi-geostrophic motions in the equatorial area, , *J. Meteor. Soc. Japan*, *44*, 25–43.

McCreary, J. (1983), A model of tropical ocean-atmosphere interaction, *Mon Wea Rev*, *111*(2), 370-387.

McGregor, S., N. Ramesh, P. Spence, M. H. England, M. J. McPhaden, and A. Santoso (2013), Meridional movement of wind anomalies during ENSO events and their role in event termination, *Geophys Res Lett*, *40*(4), 749-754.

McPhaden, M. (1999), Genesis and Evolution of the 1997-98 El Niño, *Science*, *283*(5404), 950-954.

McPhaden, M. (2012), A 21st century shift in the relationship between ENSO SST and warm water volume anomalies, *Geophys Res Lett*, *39*(9), L09706.

McPhaden, M. and X. Yu (1999), Equatorial waves and the 1997–98 El Nino., *Geophys Res Lett*, *26*(19), 2961-2964.

McPhaden, S. E. Zebiak, and M. H. Glantz (2006a), ENSO as an integrating concept in earth science, *Science*, *314*(5806), 1740-1745.

McPhaden, M. T. Lee, and D. McClurg (2011), El Niño and its relationship to changing background conditions in the tropical Pacific Ocean, *Geophys Res Lett*, *38*(15), L15709.

Mechoso, C., A. Robertson, N. Barth, M. Davey, P. Delecluse, P. Gent, and O. Thual (1995), The seasonal cycle over the tropical

Pacific in coupled ocean–atmosphere general circulation models. , *Mon Wea Rev,* , *123*(9), 2825-2838.

Mélice, J. L., and J. Servain (2003), The tropical Atlantic meridional SST gradient index and its relationships with the SOI, NAO and Southern Ocean, *Clim Dyn*, *20*(5), 447-464.

Merle, J. (1980), Seasonal variation of heat-storage in the tropical Atlantic ocean, *Oceanologica Acta*, *3*(4), 455-463.

Miller, A. J., D.R. Cayan, T.P. Barnett, N.E. Graham, and J.M. Oberhuber. (1994), The 1976-77 climate shift of the Pacific Ocean. , *Oceanography 7*(1), 21-26.

Mitchell, T. P., and J. M. Wallace (1992), The Annual Cycle in Equatorial Convection and Sea Surface Temperature, *J Clim*, *5*(10), 1140-1156.

Mohino, E., B. Rodríguez-Fonseca, T. Losada, S. Gervois, S. Janicot, J. Bader, P. Ruti, and F. Chauvin (2011), Changes in the interannual SST-forced signals on West African rainfall. AGCM intercomparison, *Clim Dyn*, *37*(9-10), 1707-1725.

Molteni, F. (2003), Atmospheric simulations using a GCM with simplified physical parametrizations. I: Model climatology and variability in multi-decadal experiments. , *Clim. Dyn.* , *20*, 175-191.

Moore, D. W. (1968), Planetary-gravity waves in an equatorial ocean. , *PhD. thesis, Harvard University, Cambridge, Mass.*

Moore, P. Hisard, J. P. McCreary, J. Merle, J. J. O'Brien, J. Picaut, V. J., and C. Wunsch (1978), Equatorial adjustment in the eastern Atlantic, , *Geophys. Res. Lett.*, *5,* , 637-640.

Moron, V., and G. Plaut (2003), The impact of El Nino–southern oscillation upon weather regimes over Europe and the North Atlantic during boreal winter, *Int J Clim*, *23*(4), 363-379.

Moura, A. D. and J. Shukla (1981), On the dynamics of droughts in northeast Brazil: Observations, theory and numerical experiments with a general circulation model, *J Atmos Sci*, *38*(12), 2653-2675.

Münnich, M., and J. D. Neelin (2005), Seasonal influence of ENSO on the Atlantic ITCZ and equatorial South America, *Geophys Res Lett*, *32*(21), L21709.

Neelin, J. D., D. S. Battisti, A. C. Hirst, F.-F. Jin, Y. Wakata, T. Yamagata, and S. E. Zebiak (1998), ENSO theory, *J Geophys Res: Oceans*, *103*(C7), 14261-14290.

Nnamchi, H., and J. Li (2011b), Influence of the South Atlantic Ocean Dipole on West African Summer precipitation, *J Clim*, *24*(4), 1184-1197.

Nnamchi, H., J. Li, and R. Anyadike (2011a), Does a dipole mode really exist in the South Atlantic Ocean?, *J Geophys Res: Atmospheres (1984–2012),* , *116*(D15).

Nnamchi, H., J. Li, I. Kang, and F. Kucharski (2013), Simulated impacts of the South Atlantic Ocean Dipole on summer precipitation at the Guinea Coast, *Clim Dyn,* , *41*(3-4), 677-694.

Nnamchi, H., J. Li, F. Kucharski, K. Kang, N. Keenlyside, P. Chang, and R. Farneti (2015), Thermodynamic controls of the Atlantic Niño, *Nature, under review*.

Nobre, P., and J. Shukla (1996), Variations in sea surface temperatura, wind stress, and rainfall over the tropical Atlantic and South America, *J. Clim*, *9*, 2464-2479.

North, G. R. (1984), Empirical orthogonal functions and normal modes, *J Atmos Sci*, *41*(5), 879-887.

North, G. R., T. Bell, F. Cahalan, and F. Moeng (1982), Sampling errors in the estimation of empirical orthogonal function, *Mon. Wea. Rev.* , *110* 699–706.

Okumura, Y., S. Xie, A. Numaguti, and Y. Tanimoto (2001), Tropical Atlantic air‐sea interaction and its influence on the NAO. , *Geophys Res Lett,* , *28(8),* , 1507-1510.

Oueslati, B., and G. Bellon (2014), The double ITCZ bias in CMIP5 models: interaction between SST, large-scale circulation and precipitation, *Clim Dyn,* , *1-23*.

Peng, W. Robinson, S. Li, and M. Hoerling (2005), Tropical Atlantic SST forcing of coupled North Atlantic seasonal responses. , *J Clim*, *18*(3), 480-496.

Penland, C., and T. Magorian (1993), Prediction of Niño 3 Sea Surface Temperatures Using Linear Inverse Modeling, *J Clim*, *6*(6), 1067-1076.

Peter, A.-C., M. Le Hénaff, Y. du Penhoat, C. E. Menkes, F. Marin, J. Vialard, G. Caniaux, and A. Lazar (2006), A model study of the seasonal mixed layer heat budget in the equatorial Atlantic, *J Geophys Res: Oceans*, *111*(C6), C06014.

Philander, S. H. G. (1985), El Niño and La Niña, *J Atmos Sci*, *42*(23), 2652-2662.

Philander, S. H. G. (1990), El Niño, La Niña, and the Southern Oscillation, *International Geophysics Series,Academic Press*, *46,*, pp 293

Philander, S. H. G. and Fedorov (2003), Role of tropics in changing the response to Milankovich forcing some three million years ago. , *Paleoceanography*, *18*(2).

Philander, S. H. G., T. Yamagata, and R. C. Pacanowski (1984), Unstable air-sea interactions in the tropics. *J Atmos Sci,* , *41*(4), 604-613.

Picaut, J., F. Masia, and Y. du Penhoat (1997), An Advective-Reflective Conceptual Model for the Oscillatory Nature of the ENSO, *Science*, *277*(5326), 663-666.

Picaut, J., M. Ioualalen, C. Menkès, Delcroix, and M. McPhaden (1996), Mechanism of the zonal displacements of the Pacific warm pool: Implications for ENSO, *Science*, *274*(5292), 1486-1489.

Picaut, J., E. Hackert, A. J. Busalacchi, R. Murtugudde, and G. S. E. Lagerloef (2002), Mechanisms of the 1997–1998 El Niño–La Niña, as inferred from space-based observations, *J Geophys Res: Oceans*, *107*(C5), 5-1-5-18.

Pickard, and S. Pond (1983), Introductory dynamical oceanography. Elsevier.

Polo, I. (2008), Tropical Atlantic Variability: Ocean-Atmosphere interactions and climate impacts, *PhD Thesis, UCM.*

Polo, I., B. Rodríguez-Fonseca, and J. Sheinbaum (2005), Northwest Africa upwelling and the Atlantic climate variability, *Geophys Res Lett*, *32*(23), L23702.

Polo, I., B. Dong, and R. Sutton (2013), Changes in tropical Atlantic interannual variability from a substantial weakening of the meridional overturning circulation, *Clim dyn*, *41*(9-10), 2765-2784.

Polo, I., B. Rodríguez-Fonseca, T. Losada, and J. García-Serrano (2008a), Tropical Atlantic Variability Modes (1979–2002). Part I: Time-Evolving SST Modes Related to West African Rainfall, *J Clim*, *21*(24), 6457-6475.

Polo, I., A. Lazar, B. Rodriguez-Fonseca, and S. Arnault (2008b), Oceanic Kelvin waves and tropical Atlantic intraseasonal variability: 1. Kelvin wave characterization, *J Geophys Res: Oceans*, *113*(C7), C07009.

Polo, I., A. Lazar, B. Rodriguez-Fonseca, and J. Mignot (2015b), Growth and decay of the Equatorial-South Atlantic SST mode by means of closed heat budget in a coupled General Circulation Model, *Frontiers in Earth Science*, *under review*.

Polo, I., M. Martin-Rey, B. Rodriguez-Fonseca, F. Kucharski, and C. Mechoso (2015a), Processes in the Pacific La Niña onset triggered by the Atlantic Niño, *Clim Dyn*, 1-17.

Randall, R. A. Wood, S. Bony, R. Colman, T. Fichefet, J. Fyfe, ... , and B. P. Kirtman (2007), Climate models and their evaluation. In Climate Change 2007: The physical science basis. , *Contribution of Working Group I to the Fourth Assessment Report of the IPCC (FAR) (pp. 589-662). Cambridge University Press.*

Rayner, N. A., D. E. Parker, E. B. Horton, C. K. Folland, L. V. Alexander, D. P. Rowell, E. C. Kent, and A. Kaplan (2003), Global analyses of sea surface temperature, sea ice, and night marine

air temperature since the late nineteenth century, *Journal of Geophys Res: Atmospheres*, *108*(D14), 4407.

Reverdin, G., and M. J. McPhaden (1986), Near surface current and temperature variability observed in the equatorial Atlantic from drifting buoys, *J. Geophys. Res.*, *91*, 6569-6581.

Richter, I. and S. Xie (2008), On the origin of equatorial Atlantic biases in coupled general circulation models, *Clim Dyn*, *31*(5), 587-598.

Richter, I., S. Xie, A. Wittenberg, and Y. Masumoto (2012a), Tropical Atlantic biases and their relation to surface wind stress and terrestrial precipitation, *Clim Dyn*, *38*(5-6), 985-1001.

Richter, I., S. Behera, T. Doi, and B. Taguchi (2015), Rethinking the role of the Bjerknes feedback in the equatorial Atlantic, *Geophysical Research Abstracts, Vol. 17(EGU2015-9854,* 2015).

Richter, S. Xie, S. Behera, T. Doi, and Y. Masumoto (2012b), Equatorial Atlantic variability and its relation to mean state biases in CMIP5. , *Clim Dyn*, *42*(1-2), 171-188.

Richter, S. Behera, Y. Masumoto, B. Taguchi, N. Komori, and T. Yamagata (2010), On the triggering of Benguela Niños: Remote equatorial versus local influences, *Geophys Res Lett*, *37*(20), L20604.

Richter, S. Behera, Y. Masumoto, B. Taguchi, H. Sasaki, and T. Yamagata (2013), Multiple causes of interannual sea surface temperature variability in the equatorial Atlantic Ocean. , *Nature Geos*, *6*(1), 43-47.

Richter, I., S.-P. Xie, S. Behera, T. Doi, and Y. Masumoto (2014), Equatorial Atlantic variability and its relation to mean state biases in CMIP5, *Clim Dyn*, *42*(1-2), 171-188.

Roberts, A. Clayton, M. E. Demory, J. Donners, P. L. Vidale, W. Norton, and J. Slingo (2009), Impact of resolution on the tropical Pacific circulation in a matrix of coupled models. *J Clim*, *22*(10), 2541-2556.

Rodrigues, R. R., R. J. Haarsma, E. J. D. Campos, and T. Ambrizzi (2011), The Impacts of Inter–El Niño Variability on the Tropical Atlantic and Northeast Brazil Climate, *J Clim*, *24*(13), 3402-3422.

Rodríguez-Fonseca, B. (2001), Relación entre el Régimen de precipitación anómalo en la península Ibérica y la variabilidad de baja frecuencia del sistema climático en el Atlántico Norte, *PhD Thesis, UCM.*

Rodríguez-Fonseca, B., I. Polo, J. García-Serrano, T. Losada, E. Mohino, C. R. Mechoso, and F. Kucharski (2009), Are Atlantic Niños enhancing Pacific ENSO events in recent decades?, *Geophys Res Lett*, *36*(20), L20705.

Rodríguez-Fonseca, B., et al. (2011), Interannual and decadal SST-forced responses of the West African monsoon, *Atmos Sci Lett*, *12*(1), 67-74.

Rogers, J. C. (1984), The association between the North Atlantic Oscillation and the Southern Oscillation in the northern hemisphere., *Mon Wea Rev, , 112*(10), 1999-2015.

Rouault, M., P. Florenchie, N. Fauchereau, and C. J. C. Reason (2003), South east tropical Atlantic warm events and southern African rainfall, *Geophys. Res. Lett.*, *30*(8009).

Rouault, M., S. Illig, C. Bartholomae, C. J. C. Reason, and A. Bentamy (2007), Propagation and origin of warm anomalies in the Angola Benguela upwelling system in 2001, *J. Mar. Syst.*

Rowell, D. P. (2001), Teleconnections between the tropical Pacific and the Sahel, *QJR Met Soc*, *127*(575), 1683-1706.

Rowell, D. P., C. K. Folland, K. Maskell, and M. N. Ward (1995), Variability of summer rainfall over tropical north Africa (1906–92): Observations and modelling, *QJR Met Soc*, *121*(523), 669-704.

Ruiz-Barradas, A., J. A. Carton, and S. Nigam (2000), Structure of Interannual-to-Decadal Climate Variability in the Tropical Atlantic Sector, *J Clim*, *13*(18), 3285-3297.

Saravanan, R., and P. Chang (2000), Interaction between Tropical Atlantic Variability and El Niño–Southern Oscillation, *J Clim*, *13*(13), 2177-2194.

Sasaki, W., T. Doi, K. Richards, and Y. Masumoto (2014), Impact of the equatorial Atlantic sea surface temperature on the tropical Pacific in a CGCM, *Clim Dyn*, *43*(9-10), 2539-2552.

Servain, J. Picaut, and J. Merle (1982), Evidence of remote forcing in the equatorial Atlantic Ocean, *J Phys Ocean*, *12*(5), 457-463.

Servain, J., I. Wainer, J. P. McCreary, and A. Dessier (1999), Relationship between the equatorial and meridional modes of climatic variability in the tropical Atlantic, *Geophysical Research Letters*, *26*(4), 485-488.

Shannon, A. J. Boyd, G. B. Brundrit, and T. Taunton-Clark (1986), On the existence of an El Niño-type phenomenon in the Benguela System,, *J. Mar. Res.*, *44*(495-520).

Slingo, J., and H. Annamalai (2000), 1997: The El Niño of the century and the response of the Indian summer monsoon. , *Mon Wea Rev*, *128*(6), 1778-1797.

Stephenson, D. B., V. Pavan, and R. Bojariu (2000), Is the North Atlantic Oscillation a random walk?, *Int J Clim*, *20*(1), 1-18.

Sterl, A., and W. Hazeleger (2003), Coupled variability and air-sea interaction in the South Atlantic Ocean, *Clim Dyn*, *21*(7-8), 559-571.

Steward, R. (2008), Introduction to Physical Oceanography, *Texas A & M University.*

Stockdale, M. A. Balmaseda, and A. Vidard (2006), Tropical Atlantic SST prediction with coupled ocean-atmosphere GCMs. , *J Clim,* , *19*(23), 6047-6061.

Suarez, M. J., and P. S. Schopf (1988), A Delayed Action Oscillator for ENSO, *J Atmos Sci*, *45*(21), 3283-3287.

Sun, C., J. Li, F. F. Jin, and R. Ding (2013), Sea surface temperature inter-hemispheric dipole and its relation to tropical precipitation, *Env Res Lett*, *8(4),* (044006.).

Sutton, R. T., and D. L. R. Hodson (2007), Climate Response to Basin-Scale Warming and Cooling of the North Atlantic Ocean, *J Clim*, *20*(5), 891-907.

Sutton, R. T., S. P. Jewson, and D. P. Rowell (2000), The Elements of Climate Variability in the Tropical Atlantic Region, *J Clim*, *13*(18), 3261-3284.

Svendsen, L., N. Kvamstø, and N. Keenlyside (2014), Weakening AMOC connects Equatorial Atlantic and Pacific interannual variability, *Climate Dynamics*, *43*(11), 2931-2941.

Taschetto, A. S., A. S. Gupta, N. C. Jourdain, A. Santoso, C. C. Ummenhofer, and M. H. England (2014), Cold Tongue and Warm Pool ENSO Events in CMIP5: Mean State and Future Projections, *J Clim*, *27*(8), 2861-2885.

Terray, P. (2011), Southern Hemisphere extra-tropical forcing: a new paradigm for El Niño-Southern Oscillation, *Clim Dyn 36*(11-12), 2171-2199.
Terray, P., and S. Dominiak (2005), Indian Ocean Sea Surface Temperature and El Niño–Southern Oscillation: A New Perspective, *J Clim, 18*(9), 1351-1368.

Thompson, C. J., and D. S. Battisti (2001), A Linear Stochastic Dynamical Model of ENSO. Part II: Analysis, *J Clim*, *14*(4), 445-466.

Timmermann, A., S. I. An, U. Krebs, and H. Goosse (2005), ENSO Suppression due to Weakening of the North Atlantic Thermohaline Circulation*. , *J Clim*, *18*(16), 3122-3139.

Timmermann, A., et al. (2007), The Influence of a Weakening of the Atlantic Meridional Overturning Circulation on ENSO, *J Clim, 20*(19), 4899-4919.

Tokinaga, H., and S. Xie (2011), Weakening of the equatorial Atlantic cold tongue over the past six decades. , *Nature Geos*, *4*(4), 222-226.

Trenberth, K. E. (1997), The Definition of El Niño, *Bulletin of the American Meteorological Society*, *78*(12), 2771-2777.

Trzaska, S., A. W. Robertson, J. D. Farrara, and C. R. Mechoso (2007), South Atlantic Variability Arising from Air–Sea Coupling: Local Mechanisms and Tropical–Subtropical Interactions, *J Clim*, *20*(14), 3345-3365.

Uppala, S., P. Kallberg, A. J. Simmons, U. Andrae, V. Bechtold, Fiorino, M., Gibson, J. K., Haseler, J.,, A. Hernandez, Kelly, G. A., Li, X., Onogi, K., Saarinen, S., Sokka, N., Allan, R. P., Andersson, E.,, K. Arpe, Balmaseda, M. A., Beljaars, A. C. M., van de Berg, L., Bidlot, J., Bormann, N., Caires, S.,, F. Chevallier, Dethof, A., Dragosavac, M., Fisher, M., Fuentes, M., Hagemann, S., Holm, E.,, and B. J. Hoskins, Isaksen, L., Janssen, P. A. E. M., Jenne, R., McNally, A. P., Mahfouf, J. F., Morcrette, J. J., Rayner, N. A., Saunders, R. W., Simon, P., Sterl, A., Trenberth, K. E., Untch, A., Vasiljevic, D., Viterbo, P. y Woollen, J. (2005), The ERA-40 Reanalysis. , *Quat. J. Roy. Meteor. Soc.* , *131*, 2961-3012,
.

Van Oldenborgh, G. J., S. Y. Philip, and M. Collins (2005), El Niño in a changing climate: a multi-model study. *Ocean Science*, *1*(2), 81-95.

Vauclair, F., and Y. du Penhoat (2001), Interannual variability of the upper layer of the tropical Atlantic Ocean from in situ data between 1979 and 1999, *Clim Dyn*, *17*(7), 527-546.

Venzke, S., M. Latif, and A. Villwock (2000), The coupled GCM ECHO-2. Part II: Indian ocean response to ENSO. , *Journal of Climate, 13*(8), 1371-1383.

Vialard, J., C. Menkes, J.-P. Boulanger, P. Delecluse, E. Guilyardi, M. J. McPhaden, and G. Madec (2001), A Model Study of Oceanic

Mechanisms Affecting Equatorial Pacific Sea Surface Temperature during the 1997–98 El Niño, *J Phys Ocean*, *31*(7), 1649-1675.

Villamayor, J. and E. Mohino (2015), Robust Sahel drought due to the Interdecadal Pacific Oscillation in CMIP5 simulations. , *Geophys. Res. Lett.,* , *42:* , 1214–1222. .

Vimont, D. J., Battisti, and Hirst (2001), Footprinting: A seasonal connection between the tropics and mid‐latitudes. , *Geophy Res Lett,* , *28*(20), 3923-3926.

Vimont, D. J., J. M. Wallace, and D. S. Battisti (2003), The Seasonal Footprinting Mechanism in the Pacific: Implications for ENSO*, *J Clim*, *16*(16), 2668-2675.

Von Storch, H. and C. Frankignoul (1998), Empirical modal decomposition in coastal oceanography. The global coastal ocean: processes and methods, *1*(419).

Von Storch, H. and F. Zwiers (2001), Statistical Analysis in Climate Research. , *Cambridge University Press.* , 484 pp.

Wagner, R. G., and A. M. da Silva (1994), Surface conditions associated with anomalous rainfall in the guinea coastal region, *IntJ Clim*, *14*(2), 179-199.

Walker, G. (1924), Correlation in seasonal variations of weather IX: A further study of world weather, *Mem.Indian Meteor. Dept.* , *24*, 275–332.

Wallace, J. M. and D. S. Gutzler (1981), Teleconnections in the geopotential height field during the Northern Hemisphere winter, *Mon Wea Rev*, *109*(4), 784-812.

Wang, C. (2005), ENSO, Atlantic climate variability, and the Walker and Hadley circulations., *InThe Hadley Circulation: Present, Past, and Future. H. F. Diaz and R. S. Bradley, Eds.,Kluwer Academic Publishers*, 173-202.

Wang, C. (2006), An overlooked feature of tropical climate: Inter-Pacific-Atlantic variability, *Geophys Res Lett*, *33*(12), L12702.

Wang, B. and A. Zhang (2002), Pacific-East Asian Teleconnection. Part II: How the Philippine Sea Anomalous Anticyclone is Established during El Niño Development*. , *J Clim* , *15*(22), 3252-3265.

Wang, B. and S. An (2002), A mechanism for decadal changes of ENSO behavior: roles of background wind changes, *Clim Dyn*, *18*(6), 475-486.

Wang, C. and P.C. Fiedler (2006), ENSO variability and the eastern tropical Pacific: A review, *Progress in Oceanography*, *69*(2–4), 239-266.

Wang, L. Zhang, S. Lee, L. Wu, and C. Mechoso (2014), A global perspective on CMIP5 climate model biases., *Nature Climate Change*, *4*(3), 201-205.

Ward, M. N. (1998), Diagnosis and Short-Lead Time Prediction of Summer Rainfall in Tropical North Africa at Interannual and Multidecadal Timescales, *J Clim*, *11*(12), 3167-3191.

Weisberg, R. H. and C. Wang (1997), A Western Pacific Oscillator Paradigm for the El Niño‐Southern Oscillation, *Geophys Res Lett*, *24* (7), 779-782.

Whitaker, J. S., and T. M. Hamill (2002), Ensemble data assimilation without perturbed observations, *Mon Wea Rev*, *130*(7), 1913-1924.

Whitaker, J. S., G. P. Compo, X. Wei, and T. M. Hamill (2004), Reanalysis without radiosondes using ensemble data assimilation, *Mon. Wea. Rev.*, *132*, 1190–1200.

Wilks, D. S. (2005), Statistical Methods in the Atmospheric Sciences, *2nd Edition, vol 91,International Geophysics Series, Academic Press*.

Wittenberg, A. T., A. Rosati, N. C. Lau, and J. J. Ploshay (2006), GFDL's CM2 global coupled climate models. Part III: Tropical Pacific climate and ENSO, *J Clim*, *19*(5), 698-722.

Woodruff, S. D. et al. (2010), ICOADS release 2.5: Extensions and enhancements to the surfacemarine meteorological archive. , *Int. J. Climatol.* .

Wright, R. (1986), The redistributive roles of unemployment insurance and the dynamics of voting, *J Pub Econ, 31*(3), 377-399.

Wyrtki, K. (1975), El Niño—The Dynamic Response of the Equatorial Pacific Oceanto Atmospheric Forcing, *J Phys Ocean, 5*(4), 572-584.

Wyrtki, k. (1985), Water displacements in the Pacific and the genesis of El Niño cycles, *J Geophys Res: Oceans (1978–2012)*, *90*(C4), 7129-7132.

Xie, S. and S. Philander (1994), A coupled ocean-atmosphere model of relevance to the ITCZ in the eastern Pacific, *Tellus*, *46-A*(4), 340-350.

Xie, P. and P. Arkin (1996), Analysis of global monthly precipitation using gauge observations, satellite estimates and numerical model predictions, *J. Clim*, *9*, 840-858.

Xie, S. P. and Y. Tanimoto (1998), A pan‐Atlantic decadal climate oscillation, *Geophys Res Lett, 25*(12), 2185-2188.

Yao, S., G. Huang, R. Wu, and X. Qu (2015), The global warming hiatus—a natural product of interactions of a secular warming trend and a multi-decadal oscillation, *Theor Appl Climatol*, *1-12.*

Ye, Z. and W. Hsieh (2006), The influence of climate regime shift on ENSO, *Clim Dyn 26*, 823-833.

Yeh, S. and B. Kirtman (2005), Pacific decadal variability and decadal ENSO amplitude modulation, *Geophys Res Lett*, *32*(5), L05703.

Yeh, S., B. Kirtman, J. Kug, W. Park, and M. Latif (2011), Natural variability of the central Pacific El Niño event on multi-centennial timescales, *Geophys Res Lett*, *38*(2), L02704.

Yeh, S., J. S. Kug, B. Dewitte, M. Kwon, B. Kirtman, and F. Jin (2009), El Nino in a changing climate, *Nature*, *461*(7263), 511-514.

Yeh, S., B. Kirtman, J. Kug, W. Park, and M. Latif (2011), Natural variability of the central Pacific El Niño event on multi-centennial timescales, *Geophys Res Lett*, *38*(2), L02704.

Yin, X., B. E. Gleason, G. P. Compo, N. Matsui, and R. S. Vose (2008), The International Surface Pressure Databank (ISPD) land component version 2.2. National Climatic Data Center:

Asheville, NC. Available from ftp://ftp. ncdc. noaa. gov/pub/data/ispd/doc/ISPD2, 2.

Yu, J. Y., and C. R. Mechoso (1999), A discussion on the errors in the surface heat fluxes simulated by a coupled GCM, *J Clim*, *12*(2), 416-426.

Yu, W., W. Han, E. D. Maloney, D. Gochis, and S.-P. Xie (2011), Observations of eastward propagation of atmospheric intraseasonal oscillations from the Pacific to the Atlantic, *J Geophys Res: Atmospheres*, *116*(D2), D02101.

Zanchettin, D., S. W. Franks, P. Traverso, and M. Tomasino (2008), On ENSO impacts on European wintertime rainfalls and their modulation by the NAO and the Pacific multi‐decadal variability described through the PDO index, *International J Clim*, *28*(8), 995-1006.

Zebiak, S. E. (1993), Air–Sea Interaction in the Equatorial Atlantic Region, *J Clim*, *6*(8), 1567-1586.

Zhang, R. and T. L. Delworth (2005), Simulated tropical response to a substantial weakening of the Atlantic thermohaline circulation, *J Clim, , 18*(12), 1853-1860.

GLOSSARY

ABA: Angola Benguela Area
AGCM: Atmospheric General Circulation Model
AMO: Atlantic Multidecadal Oscillation
AMOC: Atlantic Multidecadal Overturning Circulation
BW: Basin-Wide
C: Canonical
CGCM: Coupled General Circulation Model
CMIP: Coupled Model Intercomparison Project
CP: Central Pacific
CT: Cold Tongue
CLIVAR: Climate Variability and Predictability
ECMWF: European Centre for Medium-Range Weather Forecasts
EM: Equatorial Mode
EMMCA: Extended Multiple Maximum Covariance Analysis
ENSO: El Niño and the Southern Oscillation
EOF: Empirical Orthogonal Function
EP: Eastern Pacific
ERA: ECMWF Re-Analysis
EUC: Equatorial Under Current
FT: Fourier Transform
GCM: General Circulation Model
GG: Gulf of Guinea
GW: Global Warming
HadISST: Hadley Center Sea Ice and Sea Surface Temperature
ICOADS: International Comprehensive Ocean-Atmosphere Data Set
IOD: Indian Ocean Dipole
IPO: Interdecadal Pacific Oscillation
ITCZ: Inter-Tropical Convergence Zone
KW: Kelvin wave
MCA: Maximum Covariance Analysis
MJO: Madden Julian Oscillation
ML: Mixed Layer
MM: Meridional Mode
NAO: North Atlantic Oscillation
NCAR: National Center for Atmospheric Research
NEC: North Equatorial Current
NEMO: Nucleus for European Modelling of the Ocean
NOAA: National Oceanic and Atmospheric Administration
NTA: North Tropical Atlantic

OAFlux: Objective Analyzed air-sea Fluxes
OGCM: Ocean General Circulation Model
PC: Principal Component
PCA: Principal Component Analysis
PDO: Pacific Decadal Oscillation
PIRATA: PIlot Research Atmosphere Tropical Atlantic
PNA: Pacific North American
PREFACE: Enhancing PREdiction oF tropical Atlantic ClimatE and its teleconnections
PSA: Pacific South American
RGO: Reduced Gravity Ocean
RMSE: Root Mean Square Error
RW: Rossby wave
SAOD: South Atlantic Ocean Dipole
SEC: South Equatorial Current
SLA: Sea Level Anomalies
SLP: Sea Level Pressure
SO: Southern Oscillation
SOI: Southern Oscillation Index
SODA: Simple Ocean Data Assimilation
SPEEDY: Simplified Parameterizations primtivE Equation DYnamics.
SSH: Sea Surface Height
SST: Sea Surface Temperature
STA: South Tropical Atlantic
SVD: Singular Value Decomposition
TA: Tropical Atlantic
TAV: Tropical Atlantic Variability
TROPA: TROpical Atlantic group
WA: West Africa
WAM: West African Monsoon
WES: Wind- Evaporation-Sea Surface Temperature